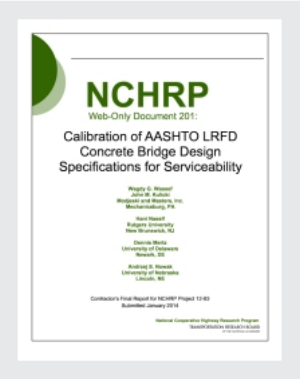

Calibration of AASHTO LRFD Concrete Bridge Design Specifications for Serviceability

DETAILS

0 pages | 8.5 x 11 | PAPERBACK
ISBN 978-0-309-43362-4 | DOI 10.17226/22407

AUTHORS

Wassef, Wagdy G.; Kulicki, John M.; Nassif, Hani; Mertz, Dennis; and Nowak, Andrzej S.

ACKNOWLEDGMENT

This work was sponsored by the American Association of State Highway and Transportation Officials (AASHTO), in cooperation with the Federal Highway Administration, and was conducted in the National Cooperative Highway Research Program (NCHRP), which is administered by the Transportation Research Board (TRB) of the National Academies.

THE NATIONAL ACADEMIES

Advisers to the Nation on Science, Engineering, and Medicine

The **National Academy of Sciences** is a private, nonprofit, self-perpetuating society of distinguished scholars engaged in scientific and engineering research, dedicated to the furtherance of science and technology and to their use for the general welfare. On the authority of the charter granted to it by the Congress in 1863, the Academy has a mandate that requires it to advise the federal government on scientific and technical matters. Dr. Ralph J. Cicerone is president of the National Academy of Sciences.

The **National Academy of Engineering** was established in 1964, under the charter of the National Academy of Sciences, as a parallel organization of outstanding engineers. It is autonomous in its administration and in the selection of its members, sharing with the National Academy of Sciences the responsibility for advising the federal government. The National Academy of Engineering also sponsors engineering programs aimed at meeting national needs, encourages education and research, and recognizes the superior achievements of engineers. Dr. C. D. Mote, Jr., is president of the National Academy of Engineering.

The **Institute of Medicine** was established in 1970 by the National Academy of Sciences to secure the services of eminent members of appropriate professions in the examination of policy matters pertaining to the health of the public. The Institute acts under the responsibility given to the National Academy of Sciences by its congressional charter to be an adviser to the federal government and, on its own initiative, to identify issues of medical care, research, and education. Dr. Harvey V. Fineberg is president of the Institute of Medicine.

The **National Research Council** was organized by the National Academy of Sciences in 1916 to associate the broad community of science and technology with the Academy's purposes of furthering knowledge and advising the federal government. Functioning in accordance with general policies determined by the Academy, the Council has become the principal operating agency of both the National Academy of Sciences and the National Academy of Engineering in providing services to the government, the public, and the scientific and engineering communities. The Council is administered jointly by both Academies and the Institute of Medicine. Dr. Ralph J. Cicerone and Dr. C. D. Mote, Jr., are chair and vice chair, respectively, of the National Research Council.

The **Transportation Research Board** is one of six major divisions of the National Research Council. The mission of the Transportation Research Board is to provide leadership in transportation innovation and progress through research and information exchange, conducted within a setting that is objective, interdisciplinary, and multimodal. The Board's varied activities annually engage about 7,000 engineers, scientists, and other transportation researchers and practitioners from the public and private sectors and academia, all of whom contribute their expertise in the public interest. The program is supported by state transportation departments, federal agencies including the component administrations of the U.S. Department of Transportation, and other organizations and individuals interested in the development of transportation. **www.TRB.org**

www.national-academies.org

TABLE OF CONTENTS

LIST OF FIGURES

LIST OF TABLES

ACKNOWLEDGEMENTS

The research reported herein was performed by Modjeski and Masters, Inc. supported by the University of Nebraska at Lincoln, Dr. Dennis R. Mertz of the University of Delaware, and Rutgers University.

Because of the close relationship between this project and the Strategic Highway Research Program 2 (SHRP 2) Project R19B, information and report sections were freely exchanged between the two projects. Dr. John M. Kulicki of Modjeski and Masters was the Principal Investigator of the SHRP2 R19B project.

The following graduate students contributed to this project at different times:

- Dan Su — Rutgers University
- Marek Kozikowski — University of Nebraska
- Przemyslaw Rakoczy — University of Nebraska
- Krzysztof Waszczuk — University of Nebraska
- Anna Maria Rakoczy — University of Nebraska
- Dustin M. Schopen — University of Delaware
- Benjamin Berwick — University of Delaware

ABSTRACT

The notion of limit state is fundamental in the *AASHTO LRFD Bridge Design Specifications* (AASHTO LRFD) (AASHTO 2012). A limit state is defined as the boundary between acceptable and unacceptable performance of the structure or its component.

The strength, or ultimate, limit states (ULS) of the AASHTO LRFD are calibrated through structural-reliability theory to achieve a certain level of safety. Exceeding the strength limit state results in a collapse or failure, an event that should not occur any time during the lifetime of the structure. Therefore, there is a need for an adequate safety margin expressed in the form of a target reliability index, β_T. For bridge girders, the target reliability is taken as, $\beta_T = 3.5$ (Nowak 1999; Kulicki et al., 2007). The strength limit states do not consider the integration of the daily, seasonal, and long-term service stresses that directly affect long-term bridge performance and subsequent service life.

The current service limit states (SLS) of the AASHTO LRFD are intended to ensure a serviceable bridge for the design life; assumed to be 75 years in AASHTO LRFD. When the SLS is exceeded, repair or replacement of components may be needed, repeatedly exceeding SLS can lead to deterioration and eventually collapse or failure (ULS). In general, SLS can be exceeded but the frequency and magnitude have to be within acceptable limits.

The current service limit states are based upon the traditional serviceability provisions of the *Standard Specifications for Highway Bridges* (AASHTO 2002). They are formulated to achieve component proportions similar to those of the *Standard Specifications*. However, these service limit states were not calibrated using reliability theory to truly achieve uniform probability of exceedence as the tools and data necessary to accomplish this calibration were not available to the code writers when AASHTO LRFD was developed. Currently, the development of calibrated service limit states remains a difficult task due to the lack of clear consequences of exceeding the SLS. This report presents the work performed on calibrating the service limit states related to concrete bridges in AASHTO LRFD.

EXECUTIVE SUMMARY

The current service limit states (SLS) of the AASHTO LRFD are intended to ensure a serviceable bridge for the design life; assumed to be 75 years in AASHTO LRFD. When the SLS is exceeded, repair or replacement of components may be needed, repeatedly exceeding SLS can lead to deterioration and eventually collapse or failure (ULS). In general, SLS can be exceeded but the frequency and magnitude have to be within acceptable limits.

The current service limit states were not statistically calibrated; rather, they are based upon the traditional serviceability provisions of the *Standard Specifications for Highway Bridges* (AASHTO 2002). The lack of tools and data necessary to accomplish the statistical calibration precluded the statistical calibration when the AASHTO LRFD was originally developed. Currently, the development of calibrated service limit states remains a difficult task due to the lack of clear consequences of exceeding the SLS. Very little useful information exists in the literature.

This report presents the work performed on calibrating the service limit states related to concrete bridges in AASHTO LRFD. To accomplish the SLS calibration, the main steps performed were:

- Available literature was reviewed to identify information on the existing service limit states
- Existing service limit states in AASHTO LRFD and in other design specifications were identified
- Current service limit-state design practices and the need for additional service limit states were investigated through a questionnaire to major bridge owners across the US
- Sources of information and databases needed for calibration were identified
- Limit states amenable to calibration were identified and the limit state function; i.e. the criteria that determines whether the limit state was exceeded, were determined
- A large set of Weigh in Motion (WIM) data was analyzed to determine the live-load model to be used for service limit-state calibration
- A calibration process for service limit states was developed
- The calibration process was applied to the selected limit states and the load and resistance factors that resulted in uniform reliability, and the associated reliability indices, were determined
- Revisions to existing design specifications were developed

The limit states that were found amenable to statistical calibration using the information currently available are:

- Cracking of reinforced concrete components
- Tensile stresses in concrete in prestressed concrete components
- Fatigue of concrete and reinforcement

The results of the work indicated that the main problem in calibrating the service limit states is the lack of clear consequences to exceeding the limit state and the ability to define more than one limit state function to address the same phenomenon.

In the absence of reasons to increase or decrease the reliability inherent in the designs performed using the current specifications, the goal of the calibration was to achieve uniform reliability with an average reliability similar to that inherent in current designs.

The study of the Weigh-In-Motion (WIM) data indicated that the number of incidences of heavy vehicles existing in adjacent traffic lanes is very small. Therefore, for most limit states, the live loads used on the load side of the service limit state calibration were assumed to occupy a single traffic loads.

The calibration of the limit state for Cracking of Reinforced Concrete Decks through the Distribution of Reinforcement indicated that the existing provisions produce uniform reliability and no revisions to the specifications were proposed. The calibration for the limit state for Tension in Prestressed Concrete Beams indicated that, for most cases, an increase of the load factor for live load from 0.8 to 1.0 is necessary to improve the uniformity of the reliability and to maintain the average level of reliability inherent in existing bridges. The calibration of the fatigue limit state indicated that an increase in the load factor for the Fatigue I limit state from 1.5 to 2.0 is needed along with revisions to the constant amplitude fatigue threshold for reinforcing steel.

1 BACKGROUND AND RESEARCH APPROACH

1.1 Background

The *AASHTO LRFD Bridge Design Specifications* (*AASHTO LRFD*) represented a refinement of bridge design practices as compared to past American Association of State Highway and Transportation Officials (AASHTO) specifications. A primary goal of using the Load and Resistance Factor Design (LRFD) philosophy is to achieve uniform reliability which can be achieved through statistical calibration. However, during the development of *AASHTO LRFD* the service and fatigue limit states were not statistically calibrated. These limit states were calibrated against previous AASHTO design requirements to achieve component proportions comparable to past practices. This process does not achieve uniform reliability.

This project was initiated to address the lack of statistical calibration of the service and fatigue limit states for the design of concrete structures in the *AASHTO LRFD*.

1.2 Special Challenges Related to Service Limit States

The Strength Limit States (ULSs) of the *AASHTO LRFD* are calibrated through structural-reliability theory to achieve a certain level of safety. They are intended to achieve similar component proportions to those of the *Standard Specifications for Highway Bridges*. These ULSs consider the extreme loads the bridge is expected to be subjected to during its design life. They do not consider the integration of the daily, seasonal, and long-term service stresses that directly affect long-term bridge performance and subsequent service life.

The current Service Limit States (SLSs) of the *AASHTO LRFD* are intended to ensure a serviceable bridge for the specified 75-year design life. These limit states are based upon the traditional serviceability provisions of the *Standard Specifications for Highway Bridges*. These SLSs are not calibrated using reliability theory to truly achieve a determined life with a specific level of certainty as the tools and data to accomplish this calibration were not available to the *AASHTO LRFD* code writers.

The background on the current *AASHTO LRFD* SLSs are presented in Chapter 2 and in Appendix A. Some of these SLSs may relate to a specified design life; others do not. Many are presently very deterministic, such as some owners' wish to limit the tensile stresses in prestressed concrete components to a level which is thought to result in a crack-free component. This SLS could be calibrated to achieve a certain probability of a crack-free component, but this calibration would include a service life only in the determination of the live load the component must resist, for example, a 75-year live load.

To achieve the objective of developing the appropriate tools, candidate SLSs have to be evaluated against a set of criteria. This applies both to the retention of some of the existing SLSs in the *AASHTO LRFD*, as well as any new limit states which may be developed as part of this project or in the future. The criteria include:

- **Is the limit state quantitatively and qualitatively meaningful?** – Does the limit states tell something that can be used to maintain a structure in service and continue or extend its service life?

- **Can the limit state be calibrated?** – Can limit state functions be developed and can a means be developed to determine the data necessary to perform a calibration? Where no such data exists, expert elicitation (Delphi process) may be useful in at least determining a range of data and the relative importance of certain characteristics in the data, including uncertainty, so that some calibration can proceed.

Consideration of SLSs requires a different input data than the ULSs. In ULSs, the limit state function is defined with two variables, resistance, which was considered constant in time, and loads. For SLSs, a different approach is needed because:

- The definition of resistance can be very difficult.
- Defining the acceptance criteria is difficult as exceeding the set limits for the service limit state does not necessary lead to immediate change in the resistance or the performance.
- Acceptable performance can be subjective (full life-cycle analysis is required).
- Resistance and load effects can be and often are correlated.
- Load is to be considered as a function of time, described by magnitude and frequency of occurrence.
- Resistance and loads can be strongly affected by quality of workmanship, operation procedures and maintenance.
- Resistance can be subject to changes in time, mostly but not only deterioration, with difficult to predict initiation time and time-varying rate of deterioration (e.g. corrosion, accumulation of debris, cracking).
- Resistance can depend on geographical location (climate, exposure to industrial pollution, exposure to salt as deicing or proximity to the ocean).

In general, the consequences of exceeding SLSs are an order, or even several orders, of magnitude smaller than those associated with ULSs. Therefore, an acceptable probability of exceeding a SLS is much higher than for a ULS. If the target reliability index for ULS is β_T = 3.5 to 4.0, then for SLS, β_T = 0.0 to 1.0 might be quite acceptable.

Further to special challenges, it may be found that changes to materials or construction practices are the more effective way to deal with what appears to be a serviceability issue. This could be the case, for example, with deck cracking where changes to mix proportions and/or curing practices designed to reduce shrinkage may be as effective as limit states based on strain calculations.

1.3 Problem Statement and Research Objective

The objectives of this research, as stated in the project's Request for Proposals (RFP), are to develop new concrete service and fatigue limit states as needed, calibrate new and existing concrete service and fatigue limit states, and prepare specifications and commentary for consideration for adoption by the AASHTO Highway Subcommittee on Bridges and Structures.

1.4 Scope of the Study

The scope of the study was generally determined by the tasks identified in the RFP as the tasks anticipated to be encompassed by the research. The task description, copied from the RFP, is provided below.

Task 1. Collect and summarize information on design practices and research findings related to concrete bridge serviceability, including fatigue. Review and evaluate state Department of Transportations' (DOTs') technical issues pertaining to application of the *AASHTO LRFD Bridge Design Specifications* to serviceability. The details of owner-specified special design and permit vehicles shall also be collected. This information shall be assembled from technical literature; case histories; and unpublished experiences of engineers, bridge owners, and others. Review pertinent serviceability criteria in structural design specifications from other countries and disciplines.

Task 2. Review the relevance of existing service and fatigue limit states and identify any new limit states needed to accommodate loading and performance criteria. Provide recommendations on new limit states to be developed and calibrated and the existing limit states to be calibrated.

Task 3. Identify concrete bridge member designs used by state DOTs and select representative designs for calibration. Consider the variability in design and construction practices in the design cases.

Task 4. Define the calibration procedure to be used for concrete bridge service and fatigue limit states.

Task 5. Identify statistical data needed for calibration of the limit states (type, quantity, and quality). Identify data sources and assess their applicability to reliability-based calibration for the limit states.

Task 6. Develop an updated and detailed work plan to complete Tasks 8 through 11.

Task 7. Submit an interim report describing the findings of Tasks 1 through 6 for panel review. National Cooperative Highway Research Program (NCHRP) review and approval of the interim report will be required before proceeding with the remaining tasks. The contractor should anticipate meeting with the project panel to discuss the proposed work plan.

Task 8. Following approval of the work plan submitted in Task 7, assemble the databases and determine the statistical parameters required for the calibration.

Task 9. Determine target reliability indices for each of the service and fatigue limit states. Submit the recommended values with justification in a letter report for NCHRP review and approval.

Task 10. Using the approved target reliability indices and calibration procedure, calculate service and fatigue limit state load and resistance factors for concrete bridges.

Task 11. Draft specifications and commentary with complete details for panel review and comment. Prepare design examples that demonstrate the application of the proposed specifications.

Task 12. Revise the specifications, commentary, and examples consistent with panel review comments.

Task 13. Prepare a final report documenting the entire research effort. The recommended specifications, the calibration procedure, calculations and data, and the design examples shall be included as appendices to the report.

1.5 Relationship to Project SHRP R19B

Several members of the research team were also involved with the Strategic Highway Research Program (SHRP) project SHRP R19B; Bridges for Service Life Beyond 100 Years: Service Limit State Design. The two projects were running concurrently. The goal of the SHRP R19B project is to develop framework for calibration of the service and fatigue limit states in the *AASHTO LRFD*. SHRP R19B scope included applying the calibration procedures to the existing service limit states and, where need exists, develop new calibrated limit states for incorporation in the *AASHTO LRFD* for a variety of bridge materials, foundations, joints and bearings. With the broader scope of R19B, significant overlap exists between the area of concrete structures in SHRP2 R19B and this project. All aspects of the development of the live load models, calibration processes and the application of the calibration process to concrete-related limit states are fully applicable to both projects. The work on the live load model and the basic calibration process were developed jointly by the two projects. Significant portions of the calibration process for the fatigue limit state were originally developed in SHRP R19B and were incorporated herein.

1.6 Research Approach

To accomplish the stated objectives of the research and to cover the work on the tasks of the project, the following approach was followed:

- Existing AASHTO LRFD and some other major bridge design specifications were reviewed to identify existing service and fatigue limit states.
- To determine the current state of practice of design for the SLSs, a questionnaire was developed and sent to major bridge owners across North America including all 50 states Departments of Transportation and other major authorities. The questionnaire included questions covering design loads, design provisions and general questions related to the performance of bridge structures in service.
- An extensive literature search was performed to identify and review relevant past research and the background of existing service and fatigue limit states.
- An extensive set of weigh-in-motion (WIM) data was assembled and analyzed to determine the live load model appropriate for use for fatigue and SLSs.
- The SLSs appropriate for calibration and the variables to be included in the statistical calibration for each limit state were identified.
- Databases of existing and simulated bridges were developed for use in the calibration.
- A calibration process was developed.
- The inherent reliability indices of existing and simulated bridges were determined and a target reliability index was selected for each limit state.
- The calibration process was refined and the load and resistance factors required to produce the target reliability indices were determined.
- Proposed revisions to the design specifications were developed.

2 SERVICE LIMIT STATES IN CURRENT PRACTICES AND AVAILABLE LITERATURE

2.1 State-of-the-Art Summary

Two different approaches were used to collect data on the state-of-the-art of current practices with regard to service limit states. First, a questionnaire was sent to major bridge owners to collect data on current practices and to determine if there are new service limit states that bridge owners desire to be included in the design specifications. Second, a literature search was performed to review the service limit states used by *AASHTO LRFD* and other international bridge design specifications and to review the background of relevant design provisions.

A summary of the results of these studies is presented below. The details of the state of practice and the literature search are presented in Appendix A and B, respectively.

2.1.1 Questionnaire of Bridge Owners

To determine the current state of practice of design for the Service Limit State, a questionnaire was developed and sent to major bridge owners across North America including the Departments of Transportation in all 50 US states, Ministry of Transport in all Canadian Provinces, District of Columbia and many turnpike authorities, bridge authorities and commissions.

The survey included twenty questions covering the following topics:

- Modifications to the specification loading (HL93 Loading) for Service Limit states
- Checking SLSs under the effects of legal loads as part of the normal design procedure
- Revisions to the SLS stress limits for prestressed concrete components
- Revisions to existing SLSs for concrete structures
- Method used for designing for Control of Cracking by Distribution of Reinforcement
- Checking concrete superstructure and substructures for any additional service load combinations beyond those in *AASHTO LRFD*
- Checking concrete structures for SLSs under overloads
- Cracking of pre-tensioned concrete beams immediately after prestressing force release
- Cracking of prestressed concrete beams in service?
- Damage to ends of end of prestressed beams under expansion joints
- Use of the deck empirical design method and the performance of these decks in service
- Observations of deck cracking
- Type of reinforcement bars used in newer decks (i.e., black bars, epoxy coated, galvanized, stainless steel, etc.)
- Average life span of concrete decks and the main reasons decks are replaced
- Types of concrete superstructures in use
- Problems with bearings in concrete structures
- Cracking of abutments and piers
- Average service life span of the concrete substructures

- Fatigue problems in concrete superstructures
- Use of coatings in concrete substructures

Twenty nine responses to the questionnaire were received and analyzed. The following conclusions were drawn from the responses to the questionnaire:

- The majority of bridge owners use the HL-93 loading for service limit states without modifications to the load. Where changes are made, the changes appear to address issues related to state-specific weight limits and vehicle configurations.
- During the design process, about half the respondents indicated that they routinely check the design for strength for legal loads as an additional design case. Half of those doing so also check the service limit state design requirements under legal loads, however, it is not clear whether the same limits are used for HL-93 and legal loads.
- About one-third of the respondents indicated that they use a lower tensile stress limit for prestressed concrete components.
- Some bridge owners use modified deflection limits or load factors for some service limits.
- The majority of bridge owners check the control of cracking through the distribution of reinforcement using the method specified in the *AASHTO LRFD* albeit some bridge owners modify the requirements to be more stringent.
- Only one respondent indicated that they check for an additional service limit state that does not exist in *AASHTO LRFD*. This limit state relates to limiting the reinforcement stresses under dead load. The lack of widespread use of additional limit states indicated that bridge owners do not see a great need for adding new service limit states to the design specifications.
- About one-fourth of the respondents indicated that they check some service limit states when analyzing structures for permit vehicles.
- More than half the respondents indicating observing early age cracking near the ends of prestressed beams. Two-thirds of the cracking was inclined and the remaining was vertical cracking.
- About two-thirds of the respondents indicated observing cracking of prestressed concrete in service. However, the frequency cracking was observed was low (one-third reporting observing cracking indicated frequency less than 1% of bridges, one-third indicating frequency between 1 to 5% and one-third indicating frequency 5 to 10%).
- About one-fourth of the respondents indicated using the empirical deck design method for some bridges. In one case the respondent indicated that decks designed using this method developed more cracks than decks designed using the conventional method.
- Deck cracking was reported to have been observed in about 80% of the responses. More than half of the reported cracking is in the transverse direction with the remaining split between longitudinal and map cracking. About 60% of the reported deck cracking was observed immediately after curing.
- About two-thirds of respondents indicated using epoxy-coated rebar in almost all new decks, one-fourth of respondents indicated the use of black bars and the remaining use galvanized bars. Other types of bars, such as MMFX bars, are in few cases.
- The average concrete deck life span given by respondents varied from 25 years to full bridge life. Most respondents indicated the decks are replaced due to the corrosion of the reinforcement or the concrete itself with fewer cases replaced due to extensive cracking.
- About 60% of the respondents indicated observing cracking of concrete piers and abutments. The lack of a pattern of the observed cracking indicated that the reported

problems are associated more with workmanship and detailing practice more than the design provisions.
- All respondents indicated that no damage was observed due to fatigue of reinforcement bars, prestressing steel or concrete.
- The responses to the questionnaire indicated that most bridge owners apply the service limit states included in *AASHTO LRFD* with no, or with few, revisions. The additional limit states used by bridge owners appeared to be related either to owner-specified vehicles, or to address a specific issue that does not seem to be shared by other bridge owner as evident by the lack of use of these additional limit states by other owners.

A copy of the questionnaire and a detailed breakdown of the responses are included in Appendix A.

2.1.2 Literature Review

A comprehensive literature review was performed to locate information on calibrating the service limit states and to determine the background of service limit states currently existing in the design specifications.

Generally, no significant information specific to the calibrating of the service limit states was found. Much of the information located was found to be too general to be useful. Many of the methods discussed for reducing serviceability issues related to non-structural aspects of the design process, which would not be useful in calibrating limit states. Some of the sources, however, provided useful methods of anticipating and determining the effects of serviceability issues such as crack width, crack spacing, and prestressed concrete fatigue.

Several design specifications were reviewed to determine the service limit states included in the design. These specifications include *AASHTO LRFD*, the Canadian National Code and the Eurocode. The service limit states in each code are detailed in Appendix A including the background of the provisions. A complete list of the service limit states in the Eurocode is included as Appendix B.

2.1.3 Overarching Characteristics of Other Specifications

2.1.3.1 Reversible versus Irreversible Limit States

The SLSs may be categorized as reversible and irreversible. Reversible SLSs are those for which no consequences of load exceeding the specified service requirement remain once the load is removed. Irreversible SLSs are those for which consequences remain. For example, for concrete structures, a crack-width limit state with limited width is a reversible limit state as the crack will close once the driving load is removed. On the other hand, a crack-width limit state defined by a high width (such as 0.02 inches or 0.5 mm) is irreversible as the crack will not fully close once the load is removed.

Due to their lesser safety implications, irreversible SLSs, which do not concern the safety of the traveling public, are calibrated to a higher probability of failure and a corresponding lower reliability index than the strength limit states. Reversible SLSs would typically be calibrated to an even lower reliability index.

2.1.3.2 Load-Driven versus Non-Load-Driven Limit States

Difference between load-driven and non-load-driven limit states is basically in the degree of involvement of externally-applied load components in the formulation of the limit state function. In the load-driven limit states, the damage occurs due to accumulated applications of external loads, usually live load (trucks). Examples of load-driven limit states include: decompression and cracking of prestressed concrete and vibrations or deflection. The damage caused by exceeding SLSs may be reversible or irreversible and, therefore, the cost of repair may vary significantly. On the other hand, in non-load-driven SLSs, the damage occurs due to deterioration or degradation as a function of time and aggressive environment or as inherent behavior due to certain material properties cause the damage. Examples of non-load-driven SLS include penetration of chlorides leading to corrosion of reinforcement, leaking joints leading to corrosion under the joints and shrinkage cracking of concrete components. In these examples, the external load occurrence plays a secondary role.

2.1.4 Lessons Learned from Review of Existing Design Specifications

Review of existing design specifications revealed that the service limit states covered by different specifications are somewhat similar. It was concluded that the information reviewed suggests that other specifications do not include what can be termed as "new" service limit states that need to be added to *AASHTO LRFD*. However, the review resulted in some concepts that may be of interest. These concepts include:

- The target reliability index for service limit states may have different value for different limit states. Furthermore, the target reliability for a certain limit state may vary depending on the consequences of exceeding the limit state.
- To differentiate between different limit states based on the consequences of exceeding the limit state, the following factors may be considered:
  - Whether the limit state is reversible or irreversible: Irreversible limit states may have higher target reliability than reversible limit states.
  - Relative cost of repairs: Limit states that have the potential to cause damage that will be costly to repair may have higher target reliability than limit states that have the potential of causing only minor damage.
- Generally, the calibration of the SLS in other specifications is lagging behind the calibration for ULS. Many of the requirements in other specifications relate to general concepts and expert opinion rather than to actual calibration

2.1.5 Search for Concrete SLSs Not Yet Implemented

Several reports were reviewed in an effort to determine whether any additional concrete SLSs should be considered when designing bridges. The additional information was meant to supplement the literature review and the bridge owners' survey. Reports were gathered from sources such as the NCHRP, the Federal Highway Administration (FHWA), *American Concrete Institute* (*ACI) Structural Journal*, ACI committee documents, and conference proceedings of the Structures Congress and the American Society of Civil Engineers (ASCE).

The investigated reports pertained to establishing concrete cracking of beams and bridge decks, concrete shrinkage, fatigue of prestressed concrete members. Each report was reviewed to determine the usefulness of the information. Any information that could potentially be used in creating new SLSs were noted and investigated further. The search did not lead to any totally new limit states.

2.1.6 SLSs to be Considered in this Report

Potential limit states and possible calibration approaches for service limit states related to concrete structures and some general limit states that are not material-dependent have been reviewed. Some of the potential limit states have since been determined to be uncalibrateable. For example, some are deterministic or are based on judgment and experience. The SLSs still thought to be calibrateable are listed in Table 2-1 along with whether the phenomena being addressed are reversible or irreversible and whether the live load will involve single lane loading or multiple lane loading (see Chapter 4 for live load models). A complete list of all service limit states in *AASHTO LRFD* is included in Appendix A.

Note that SLS references to partial prestressing have been removed. AASHTO no longer accepts partial prestressing as a design strategy.

Table 2-1 SLSs Identified for Development

LRFD Article	Reversible	Lanes	Multiple Presence Factor (MPF)
3.4.1 - Load Factors and Load Combinations for Fatigue	No	Single	-
5.5.3.1 - General - Compressive Stress Limit for Concrete - A Fatigue Criterion	No	Single	No
5.5.3.2 - Fatigue of Reinforcing Bars	No	Single	-
5.5.3.4 - Fatigue of Welded or Mechanical Splices of Reinforcement	No	Single	-
5.6.3.6 - Crack Control Reinforcement - Deemed to Satisfy *	No	-	-
5.7.3.4 - Control of Cracking by Distribution of Reinforcement	No	N/A**	No
5.9.3 - Stress Limitations for Prestressing Tendons (no revisions required)***	No	Multiple	Yes
5.9.4.2.2 - Tension Stresses in Precompressed Prestressed Concrete	Yes	Single	No

* The available information on this limit state does not provide a quantifiable way of assessing the provided margin of adequacy such as safety or reliability. Based on past performance, it was considered "deemed to satisfy". See Section 3.3 for the application of "deemed to satisfy"

** Decks are affected by axle loads not full trucks or lanes loaded

*** This limit state is irreversible and as such the case of multiple lanes loaded is appropriate to minimize the possibility of strand yielding under service loads

3 OVERVIEW OF CALIBRATION PROCESS

3.1 Introduction

The new generation of bridge design codes is based on probabilistic methods. Load and resistance (load carrying capacity) parameters are treated as random variables, and structural performance is quantified in terms of the reliability index (Nowak and Collins, 2013). This approach allows for a rational comparison of different materials and load combinations. Increased degree of uncertainty causes a reduction in the reliability and strict control of structural parameters results in a safer structure. The probabilistic analysis requires statistical models of load and resistance parameters. The load models for bridges can be based on truck surveys and other field tests. Resistance models for structural components (e.g. bridge girders) can be derived from material tests, lab tests, and analytical simulations.

With the advent of limit states design methodology in North American design specifications, there has been increasing demand to obtain statistical data to assess the reliability of designs. Reliability depends on load and resistance factors that are determined through calibration procedures using available statistical data. Methodologies that can be used to determine load and resistance factors are described in *NCHRP Report 368* (Nowak, 1999) and *Transportation Research Board* (*TRB) Circular E-C079* (Allen, et al., 2005), including the basic reliability concepts and detailed procedures that can be used to characterize data to develop the statistics and functions needed for reliability analysis.

The code calibration procedure can include closed-form solutions for estimating load and resistance factors that can be used for simple cases, as well as more rigorous probabilistic analysis methods such as the Monte Carlo method which is described in Section 3.2.3. There are three levels of probabilistic design: Levels I, II, and III (Nowak and Collins, 2013). The Level I method is the least accurate while Level III is the only fully probabilistic method. However, Level III requires complex statistical data beyond what is generally available in engineering practice. Level I and Level II probabilistic methods are more viable approaches for structural design. In Level I design methods, safety is measured in terms of a safety factor, or the ratio of nominal (design) resistance to nominal (design) load. In Level II, safety is expressed in terms of the reliability index, β. The Level II approach generally requires iterative techniques best performed using computer algorithms. For simpler cases, closed-form solutions to estimate β are available. Closed-form analytical procedures to estimate load and resistance factors should be considered approximate, with the exception of very simple cases where an exact closed-form solution exists. Alternatively, spreadsheet programs can be used to estimate load and resistance factors using the more rigorous and adaptable Monte Carlo simulation technique, which in turn can be used to accomplish a Level II probabilistic analysis.

The goal of Level I or II analyses is to develop factors that increase the nominal load or decrease the nominal resistance to give a design with an acceptable and consistent reliability. To accomplish this, an equation that incorporates and relates all of the variables that affect the potential for failure of the structure or structural component must be developed for each limit state.

For LRFD calibration purposes, statistical characterization should focus on the prediction of load or resistance relative to what is actually measured in a structure. Therefore, this statistical characterization is typically applied to the bias, the ratio of the measured to predicted value. The predicted (nominal) value is calculated using the design model being investigated.

The degree of variation is measured in terms of the coefficient of variation, which is the ratio of standard deviation to the mean value.

Regardless of the level of probabilistic design used to perform LRFD calibration, the steps needed to conduct a calibration are as follows:

- Develop the limit state equation to be evaluated, so that the correct random variables are considered. Each limit state equation must be developed based on a prescribed failure mechanism. The limit state equation should include all the parameters that describe the failure mechanism and that would normally be used to carry out a deterministic design of the structure or structural component.
- Statistically characterize the data upon which the calibration is based (i.e., the data that statistically represent each random variable in the limit state equation being calibrated). Key parameters include the mean, standard deviation, and coefficient of variation (COV) as well as the type of distribution that best fits the data (i.e. often normal or lognormal).
- Select a target reliability value based on the margin of safety implied in current designs, considering the need for consistency with reliability values used in the development of other *AASHTO LRFD* specifications, the consequence of exceeding the limit state, cost and the levels of reliability for design as reported in the literature for similar structures. If the performance of existing structures that were designed using the current code provisions is acceptable, then there is no need to increase safety margin in the newly developed code. Furthermore, the acceptable safety level can be taken as corresponding to the lower tail of distribution of betas.
- Determine load and resistance factors using reliability theory consistent with the selected target reliability.

It is recognized that the accuracy of the results of a reliability theory analysis is directly dependent on the adequacy, in terms of quantity and quality, of the input data used. The final decision made regarding the magnitude of the load and resistance factors selected for a given limit state must consider the adequacy of the data. If the adequacy of the input data is questionable, the final load and resistance factor combination selected should be weighted toward a level of safety that is consistent with past successful design practice, using the reliability theory results to gain insight as to whether or not past practice is conservative or unconservative.

The calibration procedure can be different depending on the type of limit state. In the case of serviceability limit states, it is much more complex mostly due to difficulties in formulation of the limit state equation. The parameters of load and resistance are determined not only by magnitude, as is the case with strength limit states, but also frequency of occurrence (e.g. crack opening) and as a function of time (e.g. corrosion rate, chloride penetration rate). Acceptability criteria are not well defined as they are subjective (e.g. deflection limit, allowable tensile stress) and the code-specified limit state function does not necessarily have a physical meaning (e.g. allowable compression stress in concrete).

3.2 Calibration by Determination of Reliability Indices

3.2.1 Basic Framework

Expanding on the four basic steps outlined above, the framework for calibration of SLS using reliability indices is summarized as follows:

Step 1: Formulate the Limit State Function and Identify Basic Variables. Identify the load and resistance parameters and formulate the limit state function. For each considered limit state, the acceptability criteria were established. In most cases, it was not possible to select a deterministic boundary between what is acceptable and unacceptable. Some of the code-specified limit state functions do not have a physical meaning (e.g. allowable compression stress in concrete).

Step 2: Identify and Select Representative Structural Types and Design Cases. Select the representative components and structures to be considered in the development of code provisions for the SLSs.

Step 3: Determine Load and Resistance Parameters for the Selected Design Cases. Identify the design parameters based on typical structural types, loads, and locations (climate, exposure to harsh environment). For each considered element and structure, values of typical load components must be determined.

Step 4: Develop Statistical Models for Load and Resistance. Gather statistical information about the performance of the considered types and models, in selected representative locations and traffic. Gather statistical information about quality of workmanship. Ideally, for given location, and traffic, the required data includes: general assessment of performance, assumed time to initiation of deterioration, assumed deterioration rate as a function of time, maintenance, and repair (frequency and extent). Develop statistical load and resistance models (as a minimum, determine the bias factors and coefficients of variation). The parameters of load and resistance are determined not only by magnitude, as is the case with strength limit states, but also frequency of occurrence (e.g. crack opening) and as a function of time (e.g. corrosion rate, chloride penetration rate). The available statistical parameters were utilized. However, the database is rather limited and for some serviceability limit states, there is a need to assess, develop, and/or derive the statistical parameters.

The parameters of time-varying loads were determined for various time periods. The analyses were performed for various traffic parameters (average daily truck traffic (ADTT), legal loads, multiple presence, traffic patterns). The load frequencies serve as a basis for determination of acceptability criteria.

Step 5: Develop the Reliability Analysis Procedure. The reliability can be calculated using either a closed-form formula or Monte Carlo method. The reliability index for each case can be calculated using closed-formulas available for particular types of probability distribution functions (PDFs) in the literature or Monte Carlo method. In this study, all of the reliability calculations were based on Monte Carlo analysis. The Monte Carlo method is a stochastic technique that is based on the use of random numbers and probability statistics to simulate a large number of computer-based experiments. The outcome of the simulation is a large number of solutions that takes into account all the random variables in the resistance equation.

Step 6: Calculate the Reliability Indices for Current Design Code and Current Practice. Calculate the reliability indices for selected representative bridge components corresponding to current design and practice.

Step 7: Review the Results and Select the Target Reliability Index, β_T. Based on the calculated reliability indices, select the target reliability index, β_T. Select the acceptability criteria, i.e., performance parameters, that are acceptable, and performance parameters that are not acceptable.

Step 8: Select Potential Load and Resistance Factors. Prepare a recommended set of load and resistance factors. The objective is that the design parameters (load and resistance factors) have to meet the acceptability criteria for the considered design situations (location and traffic). The design parameters should provide reliability that is consistent, uniform, and conceivably close to the target level.

Step 9: Calculate Reliability Indices. Calculate the reliability indices corresponding to the recommended set of load and resistance factors for verification. If the design parameters do not provide consistent safety levels, modify the parameters and repeat Step 8.

Figure 3-1 presents the flowchart for the basic calibration framework described above.

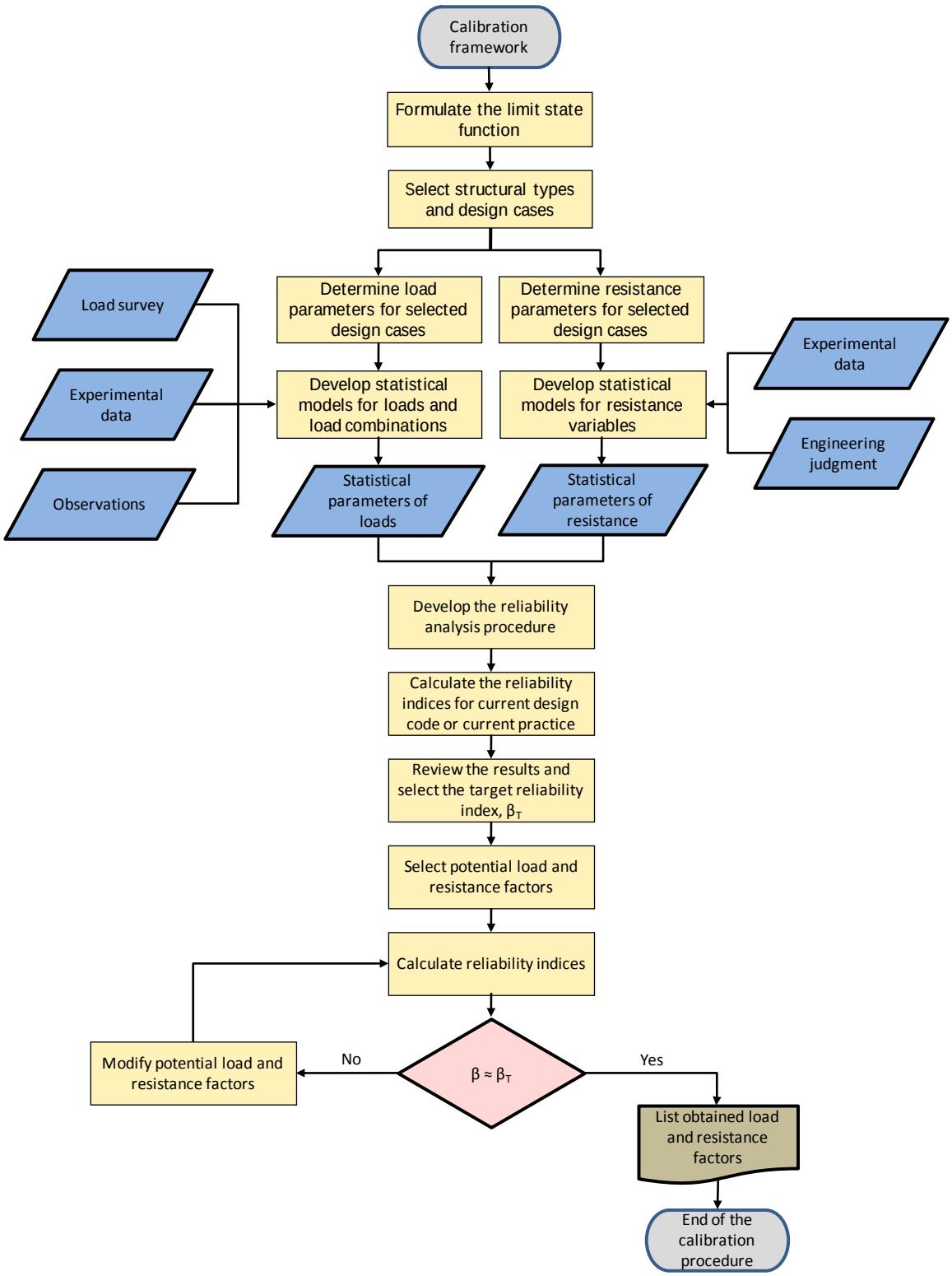

Figure 3-1 Basic calibration framework – flowchart.

Step 4 above requires the analysis of data describing load and resistance. Normal probability paper is a special scale that facilitates the statistical interpretation of data. The

horizontal axis represents the variable for which the cumulative distribution function (CDF) is plotted, e.g. gross vehicle weight (GVW), mid-span moment or shear. The vertical axis represents the number of standard deviations from the mean value. This is often referred to as the Standard Normal Variable" or the "Z-Score." The vertical axis can also be interpreted as probability of being exceeded and, for example, one standard deviation corresponds to 0.159 probability of being exceeded. The most important property of normal probability paper is that the CDF of a normal random variable is represented by a straight line. The straighter the plot of data, the more accurately it can be represented as a normal distribution. In addition, the curve representing the CDF of any other type of random variable can be evaluated and its shape can provide an indication about the statistical parameters such as the maximum value, type of distribution for the whole CDF or, if needed, only for the upper or lower tail of the CDF. Furthermore, the intersection of the CDF with horizontal axis (zero on vertical scale), corresponds to the mean. The slope of CDF determines the standard deviation, σ_x as shown in Figure 3-2. A steeper CDF on probability paper indicates a smaller standard deviation. Further information about construction and use of the probability paper can be found in textbooks (e.g. Nowak and Collins, 2013).

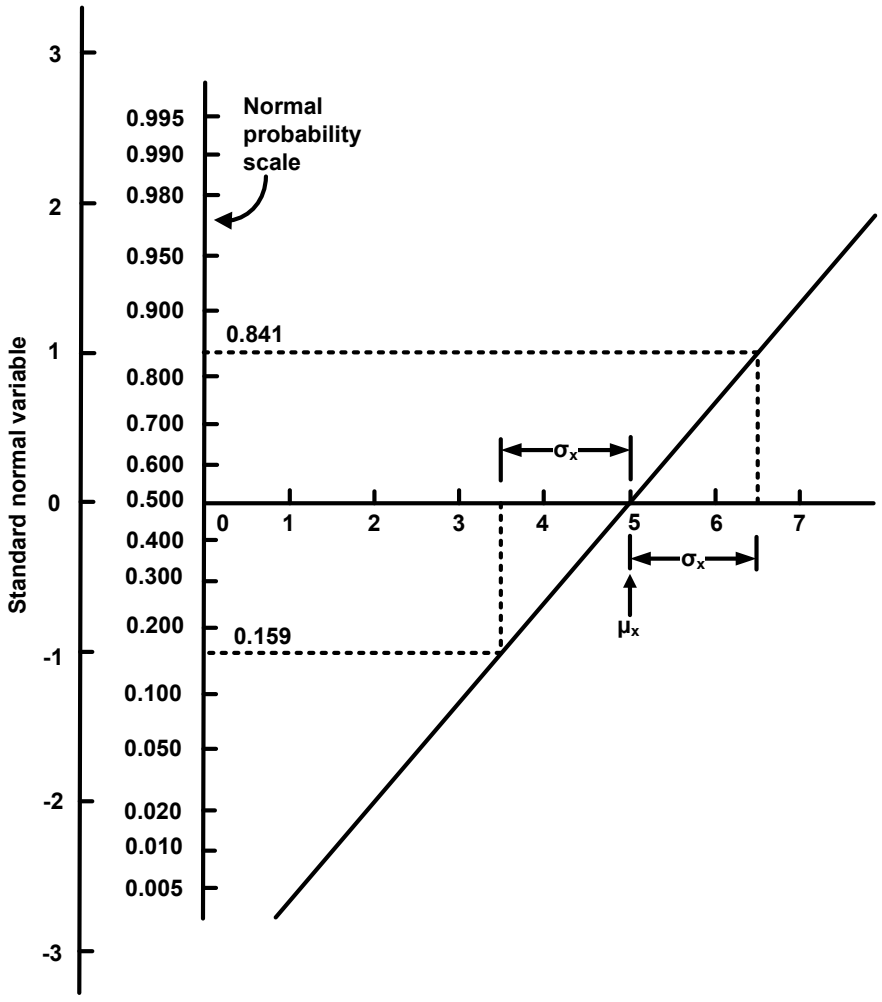

Figure 3-2 Use of normal probability paper.

3.2.2 Closed-form Solutions

The reliability index, β, is defined as

$$\beta = \Phi^{-1}\left(P_f\right) \tag{3-1}$$

where Φ^{-1} is the inverse of the standard normal distribution and P_f is the probability of failure.

If the limit state function can be expressed in terms of two random variables, *R* representing the resistance and *Q* representing the load effect,

$$g = R - Q \tag{3-2}$$

then the probability of failure is

$$P_f = \text{Prob}\ (g < 0) \tag{3-3}$$

Then, the reliability index, β, can be calculated using a closed-form formula in two cases: when both *R* and *Q* are normal random variables or when both *R* and *Q* are lognormal random variables. In all other cases, the available procedures produce approximate results.

In the case of *R* and *Q* both being normal random variables, the reliability index, β, can be calculated using the following formula,

$$\beta = \frac{\overline{R} - \overline{Q}}{\sqrt{\sigma_R^{\,2} + \sigma_Q^{\,2}}} \tag{3-4}$$

where

$\overline{R}$ = mean or expected value of the distribution of resistance
$\overline{Q}$ = mean or expected value of the distribution of load
σ_R = standard deviation of the distribution of resistance
σ_Q = standard deviation of the distribution of load

Sometimes, $R - Q$ is termed M, the margin of safety. Using this terminology the equation becomes,

$$\beta = \frac{\overline{M}}{\sigma_M} \tag{3-5}$$

For the case when both distributions are lognormally distributed, a more complete derivation of the closed-form solutions and how they can be applied to LRFD calibration is shown by Allen, et al. (2005). While closed-form solutions are useful for illustrative purposes, in practice either load or resistance or both are not normally distributed which limits the use of closed-form solutions in code calibration.

3.2.3 Using Monte Carlo Simulation in the Calibration Process

The typical application of Monte Carlo simulation, referenced in Step 5 above for bridge-structural reliability, as reported in the literature (Allen, et al., 2005; Nowak and Collins, 2013) is well known. Application of Monte Carlo simulation follows the steps below:

- It is assumed that dead load is normally distributed and live load CDF is as shown on the probability paper (directly from WIM data). The statistical parameters of live load depend on the time period. For longer time period the statistical parameters are obtained by extrapolation of the available WIM data. The total load is a sum of dead load and live load and, therefore, in practice it can be treated as a normal variable. This assumption is partly justified by the Central Limit Theorem, and is acceptable if the load components are of similar magnitude (Nowak and Collins 2013).
- Resistance is assumed to have lognormal distribution. The resistance side of the LRFD equation is a product of terms.
- The minimum statistical parameters needed for each random variable are the coefficient of variation, V, and the bias, λ. Using the reported statistics of load and resistance along with computer-generated random numbers, the distributions of load and resistance are developed and values chosen randomly from these distributions. For example for the simple load combination of dead load plus live load, random values of dead load and live load are chosen from the normal distributions fitted in the region of interest. A random value of resistance is chosen from the lognormal distribution of resistance.
- The simulation is run by selecting random values from both the load and resistance distributions. The limit state function, $R_i - (D_i + L_i)$ is calculated for each set of random variables. If the value is equal to or greater than zero, the function is satisfied and the individual case is safe. If the value is negative, the criterion is not satisfied and the case represents a failure.
- After a large number of iterations, the failures are counted and the failure rate determined. For the sampling to be significant at least ten failures should be observed, otherwise, more iteration is necessary. If the expected probability of failure is very low, then the number of iterations can be prohibitively large. Therefore, an alternative way to determine the reliability index is to generate a smaller number of limit state function values, plot the results on the normal probability paper, and extrapolate the obtained lower tail of the distribution function. The extrapolated lower tail will then allow for assessment of the reliability index and probability of failure (or failure rate).
- Using the failure rate, the reliability index is determined as the inverse of the standard normal cumulative distribution.

3.2.4 Statistical Parameters for Resistance and Other Loads (Excerpted from Kulicki, et al. 2007)

3.2.4.1 Resistance Models

The resistance was considered as a product of a nominal resistance, R_n, and three factors: M = material factor (strength of material, modulus of elasticity), F = fabrication factor (geometry, dimensions), and P = professional factor (use of approximate resistance models, e.g. the Whitney stress block, idealized stress and strain distribution model).

$$R = R_n \cdot M \cdot F \cdot P \tag{3-6}$$

The mean value, μ_R, and the coefficient of variation, V_R, of resistance, R, may be approximated by the following accepted equations for the range of values that were considered:

$$\mu_R = R_n \cdot \mu_M \cdot \mu_F \cdot \mu_P \tag{3-7}$$

$$V_R = \sqrt{V_M^2 + V_F^2 + V_P^2} \tag{3-8}$$

The statistical parameters of resistance of reinforced concrete and prestressed concrete were determined using the test results available prior to 1990, special simulations, and engineering judgment. They were developed for reinforced concrete T-beams and prestressed concrete AASHTO-type girders. Bias factors and coefficients of variation were determined for material factor, *M,* fabrication factor, *F*, and analysis factor, *P*. Factors *M* and *F* were combined.

For concrete components, the material parameters were taken from Ellingwood, et al. (1980). Only the statistical parameters were obtained but no raw test data. The basis for these parameters was research by Mirza and MacGregor (1979), The data included mean value and coefficient of variation for the compressive strength of concrete, yield strength of reinforcing bars, and prestressing strands. In addition, the data included the statistical parameters of fabrication factor and professional factor.

The material data, combined with statistical parameters of the fabrication factor and professional factor, were used in Monte Carlo simulations that resulted in the statistical parameters of resistance for reinforced concrete T-beams and prestressed concrete girders, for moment and shear, as shown in Table 3-1 (Nowak, 1999). The statistical parameters include three factors representing uncertainty in materials, dimensions and geometry, and analytical model.

It was assumed that resistance is a lognormal random variable.

Table 3-1 Statistical Parameters of Component Resistance (Used with permission of the Transportation Research Board of the National Academies)

Type of Structure	Material and Fabrication factors, *FM*		Professional factor, *P*		Resistance, *R*	
	λ	*V*	λ	V	λ	*V*
Reinforced concrete						
Moment	1.12	0.12	1.02	0.06	1.14	0.13
Shear w/steel	1.13	0.12	1.075	0.10	1.20	0.155
Shear no steel	1.165	0.135	1.20	0.10	1.40	0.17
Prestressed concrete						
Moment	1.04	0.045	1.01	0.06	1.05	0.075
Shear w/steel	1.07	0.10	1.075	0.10	1.15	0.14

3.2.4.2 Statistics of Loads Other Than Live Load

The data presented below were developed in support of strength calibrations but are equally applicable to load calculations related to SLS calibration.

The bias factors for DL_1 and DL_2 were provided by the Ontario Ministry of Transportation based on surveys of actual bridges in conjunction with calibration of the *Ontario Highway Bridge Design Code* (*OHBDC*) (*OHBDC*, 1979; Lind and Nowak, 1978). The coefficients of variation provided by the Ministry of Transportation for dead load were 0.04 and 0.08 for DL_1 and DL_2, respectively (Lind and Nowak, 1978). However, there is no report available to support this data. The coefficients of variation used in calibration were taken from the *National Bureau of Standards (NBS) Special Publication 577* (Ellingwood, et al. 1980) and include other uncertainties (also human error).

The parameters of DL_3 are calculated using the survey data provided by the Ontario Ministry of Transportation in conjunction with calibration of the *OHBDC* (1979).

Table 3-2 Statistical Parameters of Dead Load

Dead Load Component	Bias Factor	Coefficient of Variation
Factory made members, DL_1	1.03	0.08
Cast-in-place, DL_2	1.05	0.10
Wearing surface, DL_3	1.00 (for 3 in. mean thickness)	0.25
Miscellaneous, DL_4	1.03 ~ 1.05	0.08 ~ 0.10

3.3 "Deemed to Satisfy"

"When you can measure what you are speaking about, and express it in numbers, you know something about it, when you cannot express it in numbers, your knowledge is of a meager and unsatisfactory kind; it may be the beginning of knowledge, but you have scarcely, in your thoughts advanced to the stage of science." William Thomson, Lord Kelvin

The least rigorous process for establishing design requirements, and load and resistance factors in particular, is referred to as "deemed to satisfy." In this process, experience and empirical observations are used to define the boundary between satisfactory performance and unsatisfactory performance. It provides no quantifiable way of assessing the provided margin of adequacy such as safety or reliability. Since there is no way to quantify the performance margin, there is no way to assess the benefit of a change in requirement other than a general knowledge that changing a certain parameter should move in the direction of higher performance. The obvious corollary is that cost/benefit cannot be quantified. An example of "Deemed to Satisfy" is the specification of concrete cover requirements in U.S. practice which is based only on experience and has no consistent mathematical basis.

The above notwithstanding, "deemed to satisfy" has a place in the pantheon of engineering tools. It is often the basis of detailing requirements and may serve as the beginning of design specification development as in "experience shows that if we do (or don't do) this or that the results are generally acceptable." Expert elicitation (Delphi Process) or an experimental program may provide insight into the adequacy of deemed to satisfy.

4 LIVE LOAD FOR CALIBRATION

4.1 Development of Live Load Models for Service Limit States

4.1.1 Introduction

The consideration of limit states, both ultimate (strength) and serviceability, requires the knowledge of loads. The objective of this task is to determine the statistical parameters of live load for the limit states considered in *AASHTO LRFD* (2012). For Strength Limit States, the live load statistics were determined in NCHRP 12-33 and documented in the Calibration Report (*NCHRP Report 368*) (Nowak, 1999). The emphasis was placed on prediction of the extreme expected live load effects in the 75 year lifetime of a bridge. The database at that time was a truck survey carried out by the Ontario Ministry of Transportation in Canada. The basic statistical parameters of the maximum 75 live load effect (moment and shear force) were determined by extrapolation of the truck survey data. It was assumed that the survey represented two weeks of heavy traffic. The procedure is described in *NCHRP Report 368* (Nowak, 1999).

The Serviceability Limit States require additional statistical parameters, not only the maximum values but also load spectra, i.e. frequency of occurrence of loads. The maximum values are needed for shorter time periods, such as day, week, month, or year. At present, a considerable amount of WIM truck data is available and the research team had access to two sources: NCHRP Project 12-76 (*NCHRP Report 683*) (Sivakumar, et al., 2011) and FHWA files. This chapter provides documentation on the development of the statistical parameters of live load for service limit states and fatigue.

The analysis includes consideration of the WIM database from NCHRP 12-76 and FHWA. The obtained data included over 65 million vehicles. Out of that number, about 10 million were deleted/filtered because of obvious errors in the WIM records, leaving about 55 million. Then, data from New York (about 7.8 million records) and Indiana other than site SPS-6 (about 13 million records) were also removed. The New York data was not considered because it included a considerable number of extremely heavy vehicles. It was decided that this data would have a strong effect on the statistical parameters and the remaining states would be unnecessarily penalized. Indiana data could not be considered because the format was not compatible with the other states. Therefore, the considered database included about 35 million vehicles.

The obtained WIM data includes the following information for each location and each recorded vehicle: number of axles, spacing between axles, axle loads, gross vehicle weight, vehicle speed, and exact time of measurement. Statistical parameters are determined for the GVW and moment caused by the vehicles, including a CDF, bias factor, λ, that is equal to the mean-to-nominal ratio, i.e. the ratio of the mean value and the nominal (or design) value, and coefficient of variation, COV, equal to the ratio of standard deviation to the mean.

The CDFs for the WIM data for each site were plotted on normal probability paper which was described in Section 3.2.1.

4.1.2 WIM Database

The truck survey includes WIM truck measurements from 52 sites obtained from NCHRP 12-76 and FHWA.

The data obtained from FHWA is summarized herein and includes trucks recorded from:

- Arizona (SPS 1 – Special Pavement Study, Location 1) – data recorded continuously from January 2008 until December 2008
- Arizona (SPS 2 – Special Pavement Study, Location 2) – data recorded continuously from January 2008 until December 2008
- Arkansas (SPS 2 – Special Pavement Study, Location 2) – data recorded continuously from January 2008 until December 2008
- Colorado (SPS 2 – Special Pavement Study, Location 2) – data recorded continuously from January 2008 until December 2008
- Delaware (SPS 1 – Special Pavement Study, Location 1) – data recorded continuously from January 2008 until December 2008
- Illinois (SPS 6 – Special Pavement Study, Location 6) – data recorded continuously from January 2008 until December 2008
- Indiana (SPS 6 – Special Pavement Study, Location 6) – data recorded continuously from July 2008 until December 2008
- Kansas (SPS 2 – Special Pavement Study, Location 2) – data recorded continuously from January 2008 until December 2008
- Louisiana (SPS 1 – Special Pavement Study, Location 1) – data recorded continuously from January 2008 until December 2008
- Maine (SPS 5 – Special Pavement Study, Location 5) – data recorded continuously from January 2008 until December 2008
- Maryland (SPS 5 – Special Pavement Study, Location 5) – data recorded continuously from January 2008 until December 2008
- Minnesota (SPS 5 – Special Pavement Study, Location 5) – data recorded continuously from January 2008 until December 2008
- New Mexico (SPS 1 – Special Pavement Study, Location 1) – data recorded continuously from May 2008 until December 2008
- New Mexico (SPS 5 – Special Pavement Study, Location 5) – data recorded continuously from May 2008 until December 2008
- Pennsylvania (SPS 6 – Special Pavement Study, Location 6) – data recorded continuously from January 2008 until December 2008
- Tennessee (SPS 6 – Special Pavement Study, Location 6) – data recorded continuously from January 2008 until December 2008
- Virginia (SPS 1 – Special Pavement Study, Location 1) – data recorded continuously from January 2008 until December 2008
- Wisconsin (SPS 1 – Special Pavement Study, Location 1) – data recorded continuously from January 2008 until December 2008

Data obtained from NCHRP projects is also summarized herein, and includes trucks recorded from:

California:

- Lodi – Site 003 – data recorded continuously from June 2006 until March 2007

- Antelope East Bound – Site 003 – data recorded almost continuously from April 2006 until March 2007 (107 days missing)
- Antelope West Bound – Site 003 – data recorded almost continuously from April 2006 until March 2007 (109 days missing)
- LA 710 South Bound – Site 059 – data recorded continuously from April 2006 until March 2007
- LA 710 North Bound – Site 060 – data recorded almost continuously from April 2006 until March 2007 (32 days missing)
- Bowman – Site 072 – data recorded almost continuously from April 2006 until February 2007 (139 days missing)

Florida:
- US29 – Site 9916 – data recorded continuously from January 2005 until December 2005 (11 days missing)
- I-95 – Site 9919 – data recorded continuously from January 2005 until December 2005 (16 days missing)
- I-75 – Site 9926 – data recorded almost continuously from January 2005 until December 2005 (100 days missing)
- I-10 – Site 9936 – data recorded almost continuously from January 2005 until December 2005 (100 days missing)
- State Route – Site 9927 – data recorded almost continuously from January 2004 until December 2004 (5 days missing)

Indiana:
- Site 9511 – data recorded continuously from January 2006 until December 2006
- Site 9512 – data recorded continuously from January 2006 until December 2006
- Site 9532 – data recorded continuously from January 2006 until December 2006
- Site 9534 – data recorded continuously from January 2006 until December 2006
- Site 9552 – data recorded continuously from January 2006 until December 2006

Mississippi:
- I-10 – Site 3015 – data recorded continuously from January 2006 until December 2006 (28 days missing)
- I-55 – Site 2606 – data recorded continuously from January 2006 until December 2006 (16 days missing)
- I-55 – Site 4506 – data recorded almost continuously from March 2006 until December 2006 (39 days missing)
- US49 – Site 6104 – data recorded continuously from January 2006 until December 2006 (5 days missing)
- US61 – Site 7900 – data recorded almost continuously from January 2006 until December 2006 (49 days missing)

New York:
- I-95 North Bound – Site 0199 – data recorded continuously from March 2006 until December 2006
- I-95 South Bound – Site 0199 – data recorded continuously from July 2006 until November 2006
- I-495 West Bound – Site 0580 – data recorded continuously from January 2006 until December 2006

- I-495 East Bound – Site 0580 – data recorded continuously from January 2006 until December 2006
- Highway 12 – Site 2680 – data recorded continuously from January 2005 until December 2005
- I-84 (East Bound and West Bound) – Site 8280 – data recorded continuously from January 2006 until December 2006
- I-84 (East Bound and West Bound) – Site 8382 – data recorded continuously from January 2005 until December 2005
- I-81 (North Bound and South Bound) – Site 9121 – data recorded continuously from January 2005 until December 2005
- Highway 17 (East Bound and West Bound) – Site 9631 – data recorded continuously from February 2006 until December 2006

4.1.3 WIM Data Filtering

It was observed that the WIM data both from NCHRP 12-76 and FHWA include a number of vehicle records that appear to be incorrect. There are various reasons for questioning the data, for example GVW is too low, unrealistic geometry, and so on. Therefore, the data was filtered first to eliminate questionable vehicles using the following criteria:

- Weight per axle <2 kips or >70 kips, based upon NCHRP 12-76
- Record where the first axle spacing is less than 5 feet, based upon NCHRP 12-76
- Record where any axle spacing is less than 3.4 feet, based upon NCHRP 12-76
- Record where GVW varies from the sum of the axle weights by more than 10%, based upon NCHRP 12-76
- Record where the length of the truck varies from the sum of the axle spacings by more than 1ft, based upon NCHRP 12-76
- Record which has a GVW less than a threshold. At various times the threshold was 10 kips or 12 kips
- Record where the steering axle is less than 6 kips, based upon NCHRP 12-76
- Record where the sum of the axle spacing lengths is less than 7 ft., based upon Pelphrey, et al. (2008)
- Record where the sum of axle spacing is greater than the length of truck by more than 1 ft
- Class of the vehicle according to FHWA – 3 – 14, to filter out passenger vehicles, motorcycles, etc.
- Speed – 10 mph – 100 mph, based upon NCHRP 12-76

The filtering process is illustrated in the flowchart in Figure 4-1. A heavy vehicle meeting all of the conditional filters involving GVW would pass the filters. Therefore, the research team reviewed exceptionally heavy vehicles to check if their configuration resembled permit vehicles, such as cranes and garbage trucks. The data was divided into two sets. The first set contains regular truck traffic. This data is used for the live load model for Service Limit States. The remaining set of data includes permit vehicles and illegally overloaded vehicles that occur relatively infrequently. The latter data is used along with the regular truck traffic for live load analysis including effect of heavy vehicles. The heavy vehicles are assumed to be permit vehicles or illegally loaded vehicles. The GVW criteria of 20 kips in Step 3 is a traditional, albeit arbitrary cutoff used in virtually all previous fatigue studies to reduce the calculation effort by not considering light traffic which will not contribute significantly to cumulative damage.

Vehicles considered to be permit vehicles and illegally loaded trucks were filtered using the following criteria:

- Total number of axles less than 3 and GVW is more than 50 kips
- Steering axle weight is more than 35 kips
- Individual axle weight is more than 45 kips

Vehicles used to calibrate for the fatigue limit state were determined by filtering out trucks with GVW less than 20 kips from the trucks used for the service limit states. This follows the process historically used to perform fatigue analysis.

The filtering process is illustrated in the flowchart below shown as Figure 4-1.

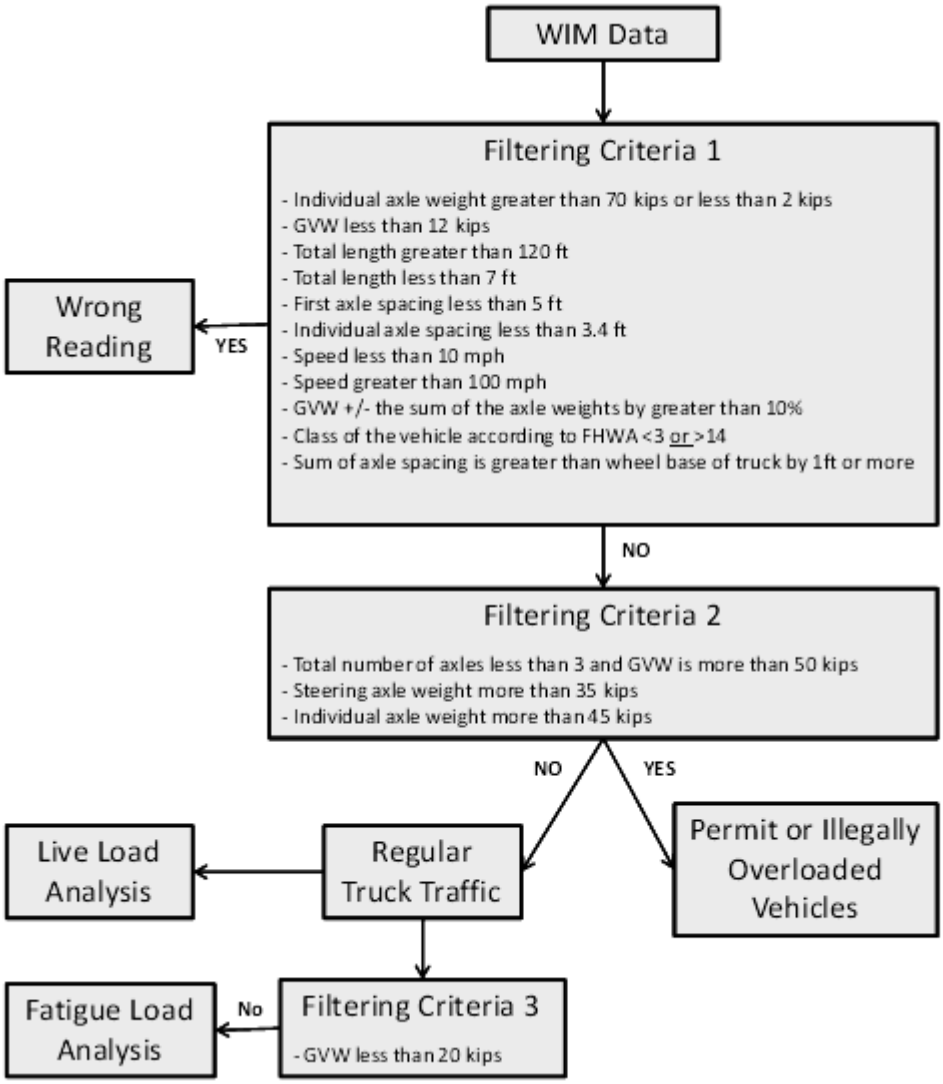

Figure 4-1 Flowchart of the Filtering Process.

The CDFs of GVWs were plotted on the probability paper and examples are shown in Figure 4-2 through Figure 4-5. The live load model used in calibration for strength limit states based on the Ontario truck survey is also shown. Trucks included in the Ontario study were selected by observing traffic and stopping trucks that appeared to be heavy. This is the reason

for the position of the Ontario curve relative to the other curves. At the upper tail of the curve, the Ontario data does not indicate that the heaviest vehicles in the Ontario study are heavier that those represented by other curves.

Figure 4-3 represents CDF of the GVW of trucks from the FHWA sites plotted on probability paper. Data collected from fourteen sites represent one year of traffic, data from Indiana sites represents six months of traffic and data from New Mexico sites represent eight months of traffic. The maximum truck GVW is 220 kips. Mean values range from 20 to 65 kips.

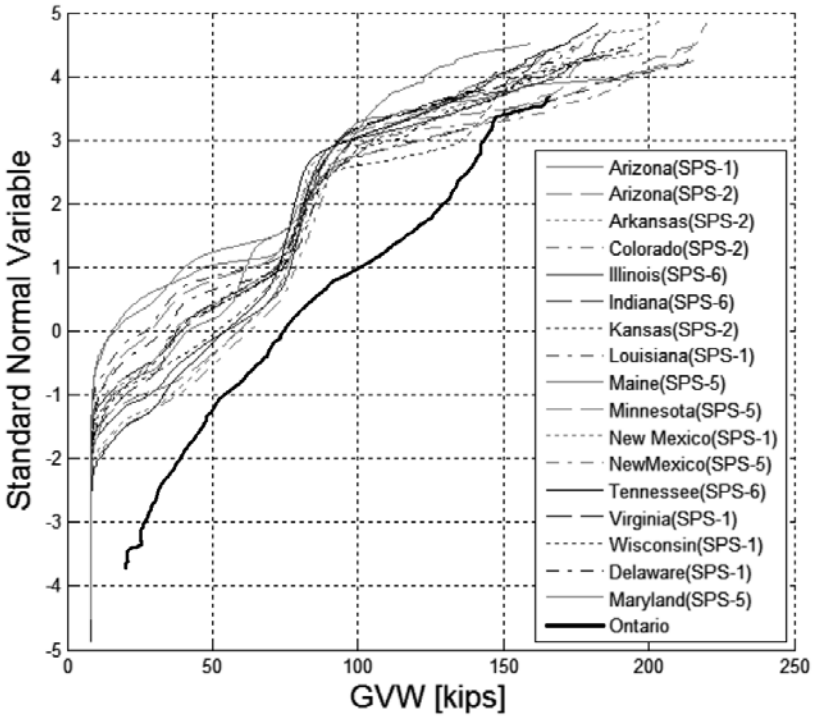

Figure 4-2 CDF of GVW - FHWA Data and Ontario.

Figure 4-2 through Figure 4-5 represent CDFs of the GVWs for Oregon, Florida, Indiana, Mississippi, California and New York, respectively, i.e. the NCHRP 12-76 data. The corresponding traffic data from these figures is given in Table 4-1.

Table 4-1 Summary of State Sites and Their Traffic Data for Figure 4-2 through Figure 4-5

Figure Number	State	Number of Sites	Months of Data	Maximum GVW (kips)	Mean-Value Range (kips)
Figure 4-2	Oregon	4	4	200	43 - 52
	Florida	5	12	250	20 - 50
Figure 4-3	Indiana	5	12	250	25 - 57
	Mississippi	5	12	260	38 - 57
Figure 4-4	California	2	8.7	250	40 - 50
		1	7		
	New York	7	12	380	35 - 50

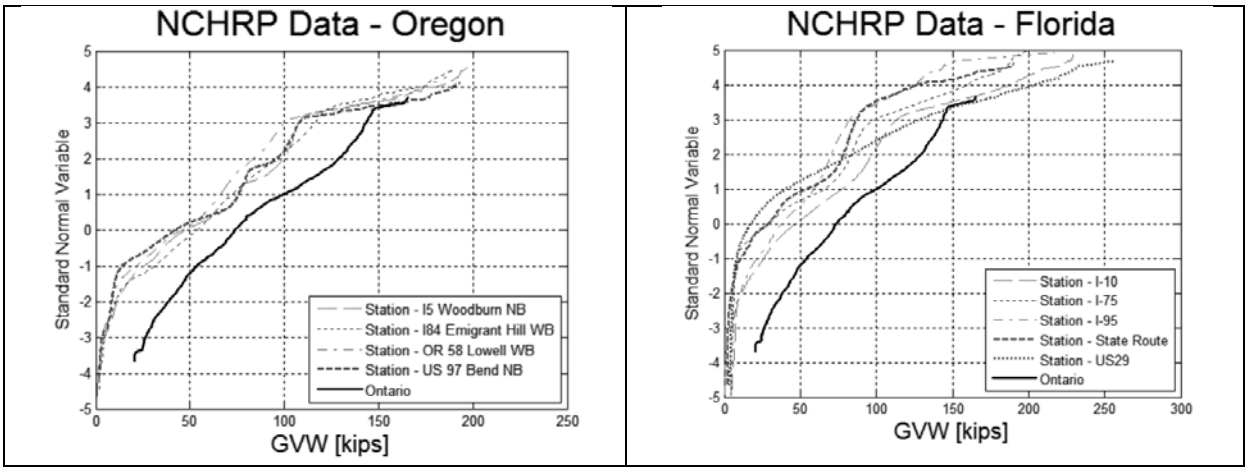

Figure 4-3 CDF of GVW – Oregon, Florida and Ontario.

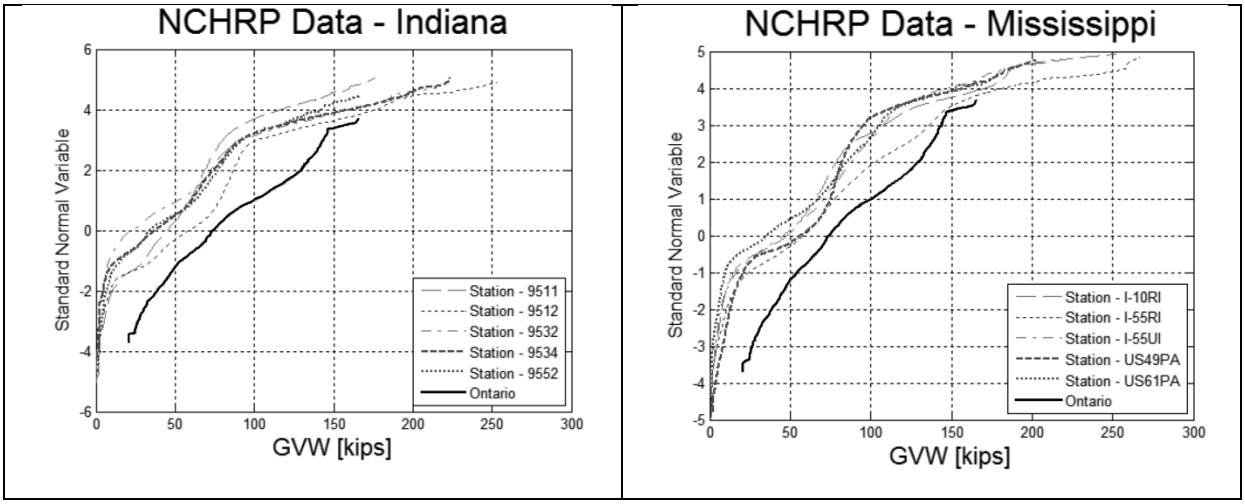

Figure 4-4 CDF of GVW – Indiana, Mississippi and Ontario.

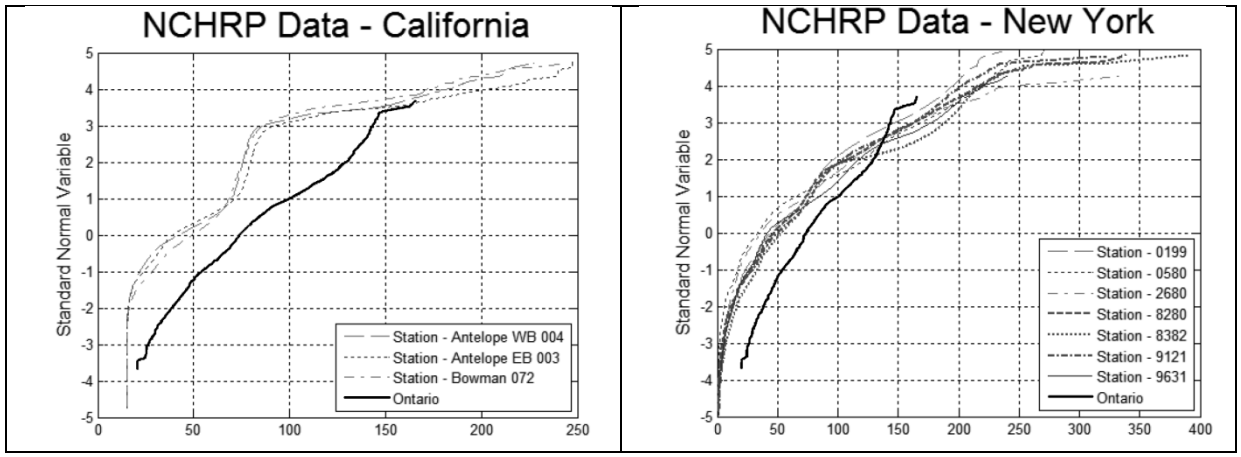

Figure 4-5 CDF of GVW – California, New York and Ontario.

As an initial observation, the data shown in Figure 4-2 through Figure 4-5 is generally consistent for the majority of the sites (The word “consistent” refers to the similarity of the general shape of the curves, i.e., the CDFs.). Exceptions are the heavily loaded sites from New York identified below:

- Site 9121 – on I-81 by Whitney Point
- Site 8382 – on I-84 by Port Jervis
- Site 8280 – on I-84 by Fishkill
- Site 0580 – on I-495 – Queens New York City

Since these sites were so exceptional, it was decided not to include the New York WIM data in developing a national, notional SLS live load. Additionally, several sites for which the recording format differed or had considerably less than one tier of data were eliminated from consideration. A summary of the remaining 32 sites and filtered data including the WIM locations, number of records and ADTT is shown in Table 4-2. Approximately 35 million records are represented by these sites.

Table 4-2 WIM Locations and Number of Recorded Vehicles

Site	Number of Days in Data	Total Number of Truck Records, N	Lane ADTT
AZ SPS-1	365	35,572	97
AZ SPS-2	365	1,430,461	3919
AR SPS-2	365	1,675,349	4590
CO SPS-2	365	343,603	941
DE SPS-1	365	201,677	553
IL SPS-6	365	854,075	2340
IN SPS-6	214	185,267	508
KS SPS-2	365	477,922	1309
LA SPS-1	365	85,702	235
ME SPS-5	365	183,576	503
MD SPS-5	365	164,389	450
MN SPS-5	365	55,572	152
NM SPS-1	245	117,102	321
NM SPS-5	245	608,280	1667
PA SPS-6	365	1,495,741	4098
TN SPS-6	365	1,622,320	4445
VA SPS-1	365	259,190	710
WI SPS-1	365	226,943	622
CA Antelope EB	258	837,667	2192*
CA Antelope WB	256	943,147	2258*
CA Bowman	134	651,090	2018*
CA LA-710 NB	333	4,092,484	6380*
CA LA-710 SB	365	4,661,287	8366*
CA Lodi	304	3,298,499	5186*
FL I-10	354	1,641,480	2207*
FL I-95	349	2,112,518	2558*
FL US-29	354	389,164	606*
MS I-10	337	1,965,022	2967*
MS I-55UI	268	1,232,223	2054*
MS I-55R	349	1,333,268	1790*
MS US-49	359	1,225,138	1475*
MS US-61	319	159,299	254*
Total		**35,856,898**	

* NCHRP data is for multilane cases, lane with maximum ADTT is listed.

The CDFs of GVWs and moment are plotted as separate curves for each location. The legend for all CDFs is shown in Figure 4-6.

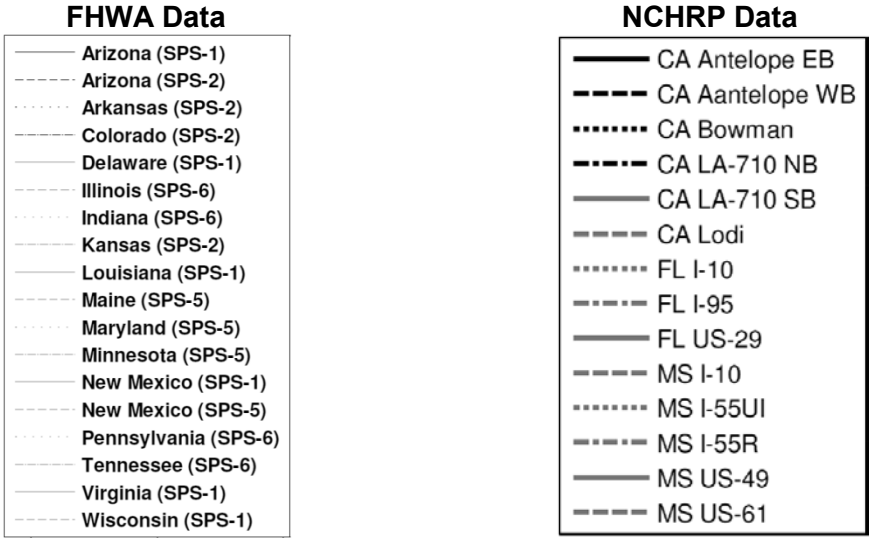

Figure 4-6 Legend for All Graphs.

4.2 Initial Data Analysis

4.2.1 Gross Vehicle Weight (GVW)

The CDFs for the GVWs from the remaining FHWA and NCHRP sites are plotted on probability paper in Figure 4-7. Each of the 32 curves represents a different location. The resulting curves indicate that the distribution of GVW is not normal. Irregularity of the CDFs is a result of different types of vehicles in the WIM data such as long and short, fully loaded and empty, or loaded by volume only, and so on. For the considered locations, the mean gross vehicle weights are between 25 and 65 kips. The upper tails of the CDF curves show a similar trend, but there is a considerable spread of the maximum values, from 150 to over 250 kips.

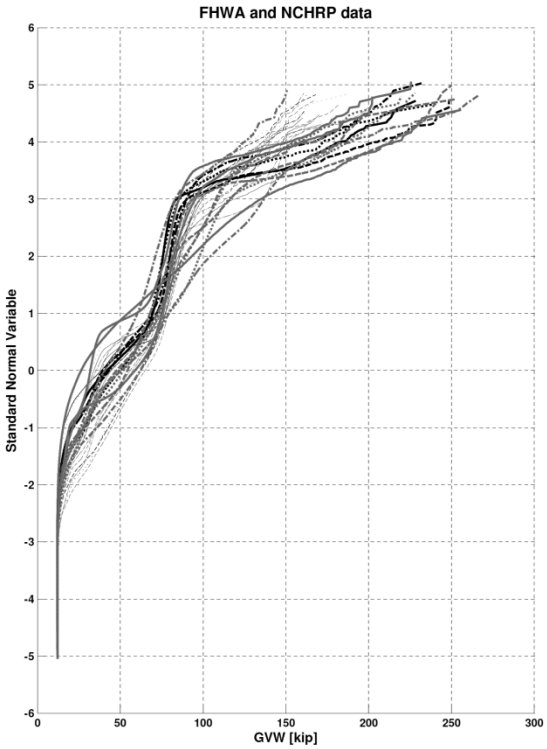

Figure 4-7 CDF of Gross Vehicle Weight (GVW).

4.2.2 Moments from the WIM Data

The distribution of simple span moments due to WIM trucks was obtained by calculating the maximum bending moment for each vehicle in the database. Each vehicle was run over influence lines to determine the maximum moment using a specially developed computer program. The calculations were carried out for spans from 30 through 200 ft. For easier interpretation and comparison of results, the calculated WIM data moments were then divided by the corresponding HL-93 moment. Normalizing the data to a common reference makes the data easier to interpret. HL-93 was just a convenient reference and ties this work to the original strength limit state calibration and associated published information.

The CDFs for the ratio of the WIM truck moment to HL-93 moment are plotted on normal probability paper in Figure 4-8 and Figure 4-12. The shape of the CDF curves is similar to that of GVW. The mean WIM moments are between 0.2 and 0.4 of the HL-93 moments, for all span lengths considered. The maximum values of the WIM moment are between 1.0 and 1.4 of HL-93 moment in most cases.

The obtained results served as basis for determining the statistical parameters of live load needed for the reliability analysis of the serviceability limit states.

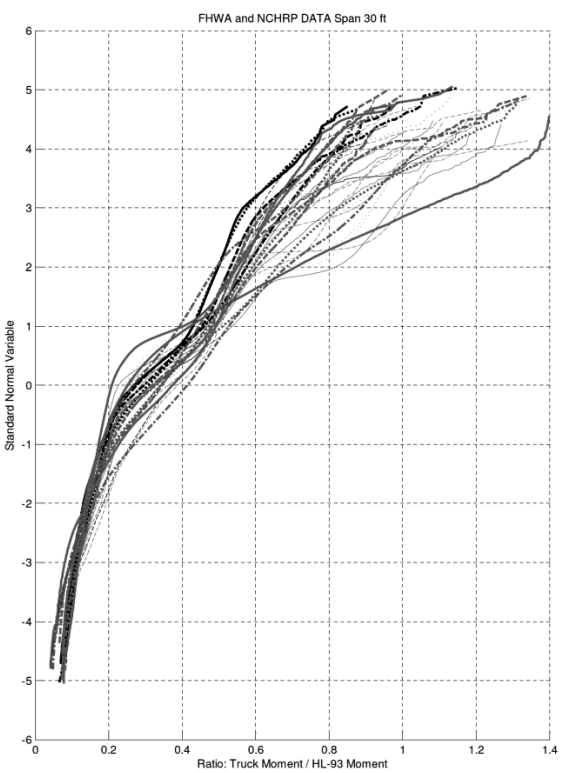

Figure 4-8 CDFs of WIM Moment and HL-93 Moment Ratio, Span = 30 ft.

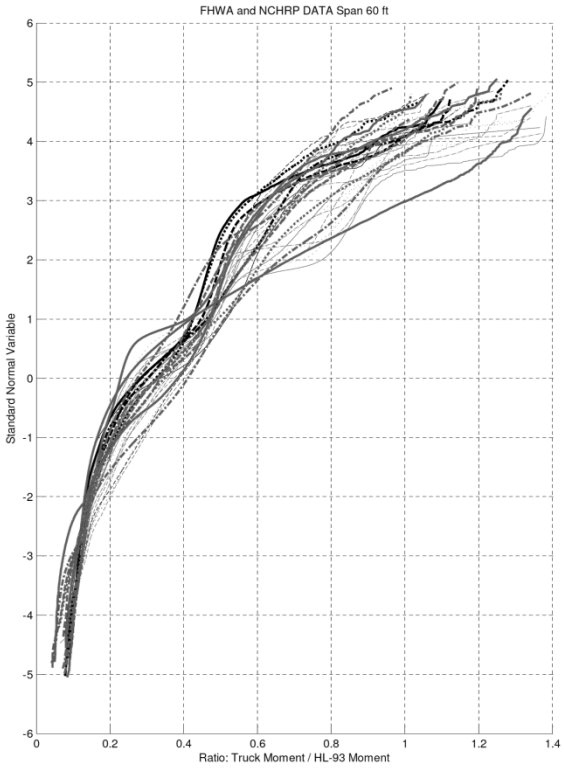

Figure 4-9 CDFs of WIM Moment and HL-93 Moment Ratio, Span = 60 ft.

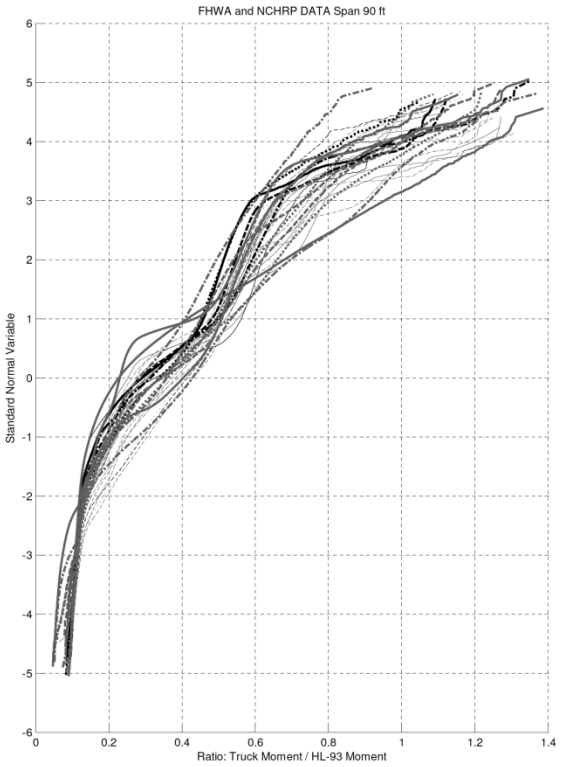

Figure 4-10 CDFs of WIM Moment and HL-93 Moment Ratio, Span = 90 ft.

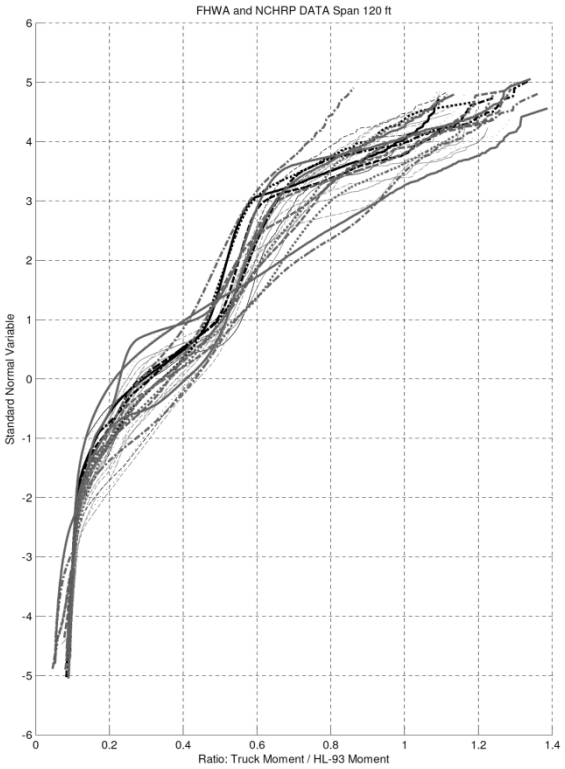

Figure 4-11 CDFs of WIM Moment and HL-93 Moment Ratio, Span = 120 ft.

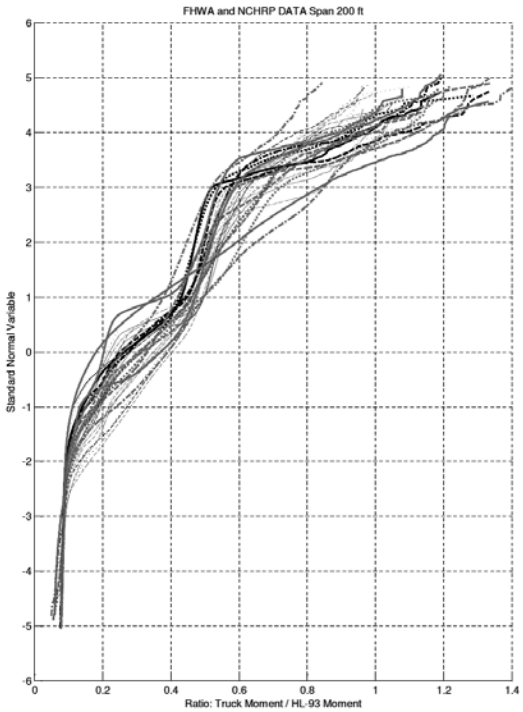

Figure 4-12 CDFs of WIM Moment and HL-93 Moment Ratio, Span = 200 Ft.

4.2.3 Filtering of Presumed Illegal Overloads and Special Permit Loads

The goal of this analysis was to observe the change in the very top tail of the distribution after removing a number of the heaviest vehicles from the database. These extremely heavy vehicles seem to be either permit vehicles which should either be included in the design process, as some states do, or reviewed for permit issuance using the Strength II limit state load combination, or they are illegal overloads. An example of the heaviest truck in the WIM data is presented in Figure 4-13. This truck was recorded at site 8382 located near Port Jervis, NY. The total length of the truck is 100.6 ft. The GVW is 391.4 kips. The position of the twelve axles, their weight and its length suggest that the vehicle should be categorized as a permit vehicle. WIM equipment captures each vehicle, including permit vehicles, as a string of axles and an FHWA designation is given based on the best FHWA category that fits the detected configuration. Heavy vehicles are assumed to be permit vehicles or illegally loaded vehicles.

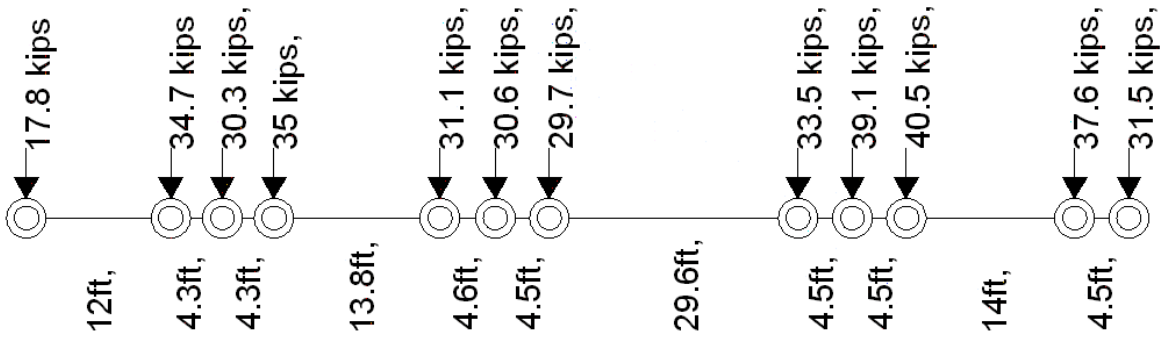

Figure 4-13 Configuration of Extremely Loaded Truck.

The initial study indicated that the removal of a very small number of the heaviest vehicles drastically changes the upper tail of the CDF of moments and shears. It was decided to explore this by investigating the number of vehicles that exceed an upper value of 1.35, which corresponds to the maximum bias ratio obtained from the Ontario measurements.

The results of the analysis for sites from New York and Mississippi were plotted on probability paper, in Figure 4-14 through Figure 4-16. It can be observed that, as expected, the very upper tail of the distribution changes drastically by removal of only a very small percentage of vehicles.

For example in Figure 4-15 New York 8382, considering 90 ft spans if only the six largest moment ratios (corresponding to the six heaviest trucks including the 391-kip vehicle shown above) out of 1.55 million data records remaining after application of the additional filter to remove moments less than 15% of the corresponding HL-93 moment, the bias changes from approximately 2.35 to approximately 1.65. Even for the WIM sites which demonstrated very extreme tails, these extreme trucks constituted only the upper 0.01% to 0.22% of the truck population. For most of the locations reviewed, the percentage was lower (see Table 4-3). The heaviest loads may have an important impact on calibration of the ULSs, however, in the case of SLS, the upper tail of the CDF of the live load is not important, as it is the main body of CDF that affects the SLS performance. Therefore, for SLS calibration, it was decided to ignore the upper tip of the CDF of live load.

Table 4-3 Removal of the Heaviest Vehicles for 90 ft Spans

Figure Number	State	Location	Number of trucks before filtering	Number of trucks after filtering	Number of removed trucks	Percent of removed trucks
Figure 4-14	NY	0580	2,474,407	2,468,952	5455	0.22%
Figure 4-14	NY	2680	89,286	89,250	36	0.04%
Figure 4-15	NY	8280	1,717,972	1,717,428	544	0.03%
Figure 4-15	NY	8382	1,551,454	1,550,914	540	0.03%
Figure 4-16	NY	9121	1,235,963	1,235,886	77	0.01%
Figure 4-16	MS	I-10	2,103,302	2,103,300	2	0.00%

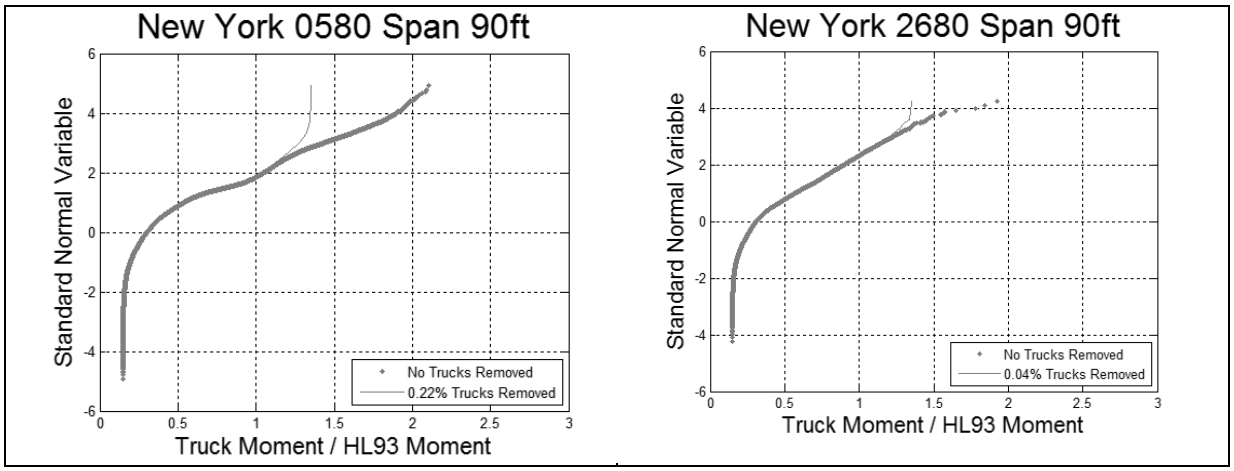

Figure 4-14 Data Removal New York 0580 and 2680.

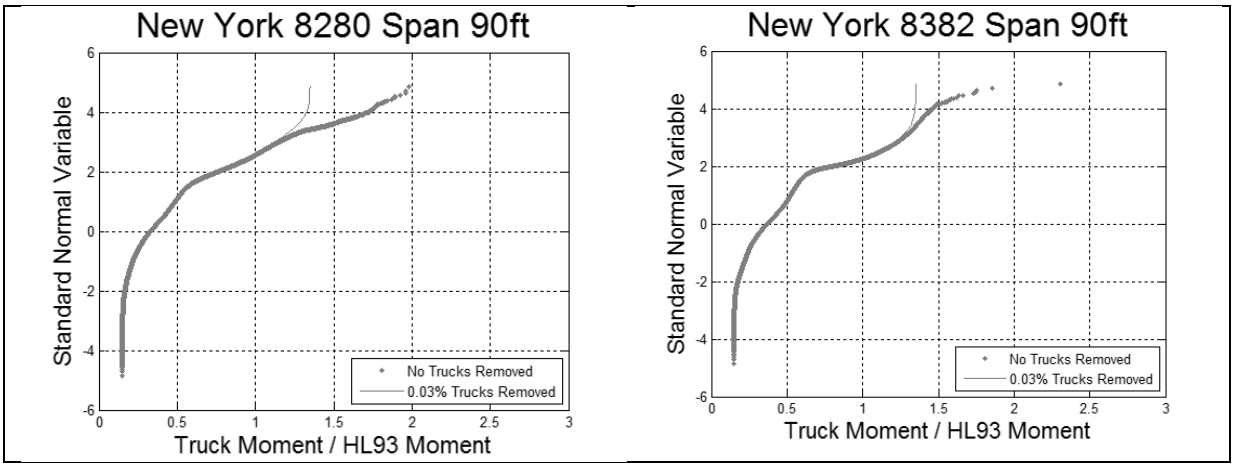

Figure 4-15 Data Removal New York 8280 and 8382.

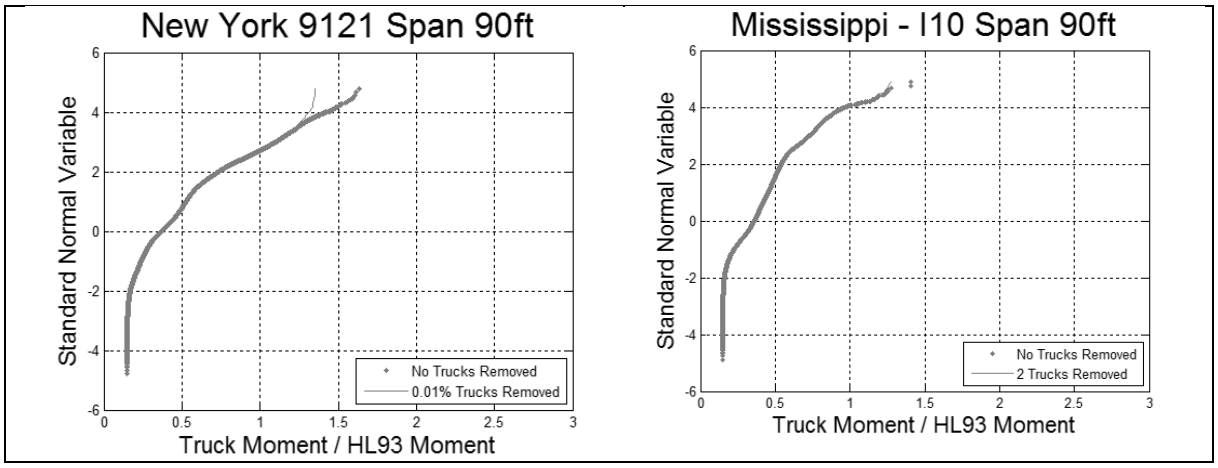

Figure 4-16 Data Removal New York 9121 and Mississippi I-10.

4.2.4 Multiple Presence Analysis

Multiple presence was investigated by a correlation analysis of the WIM data sets. The objective of the correlation analysis was to select two trucks within the group of vehicles that simultaneously occurred on the bridge positioned as shown in Figure 4-17, and which satisfy the following requirements:

Both trucks have the same number of axles
GVWs of the trucks are within +/- 5%
All corresponding spacings between axles are within +/- 10%

The maximum load effect is often caused by a simultaneous occurrence of two or more trucks on the bridge. The statistical parameters of these effects are influenced by the degree of correlation. In calibration for the strength limit states, certain probabilities of occurrence of correlated trucks were assumed based on engineering judgment applied to limited observations of multiple presence of trucks of unknown weight. The available WIM data allows for verification of these assumptions.

A special program was developed to filter the data using the time of a record and the speed of the truck to find instances when either of the events shown in Figure 4-17 occurred involving similar trucks. The filter resulted in selecting the observed cases of two trucks with the headway distance less than 200 ft in either the same lane or two adjacent lanes, as illustrated in Figure 4-17.

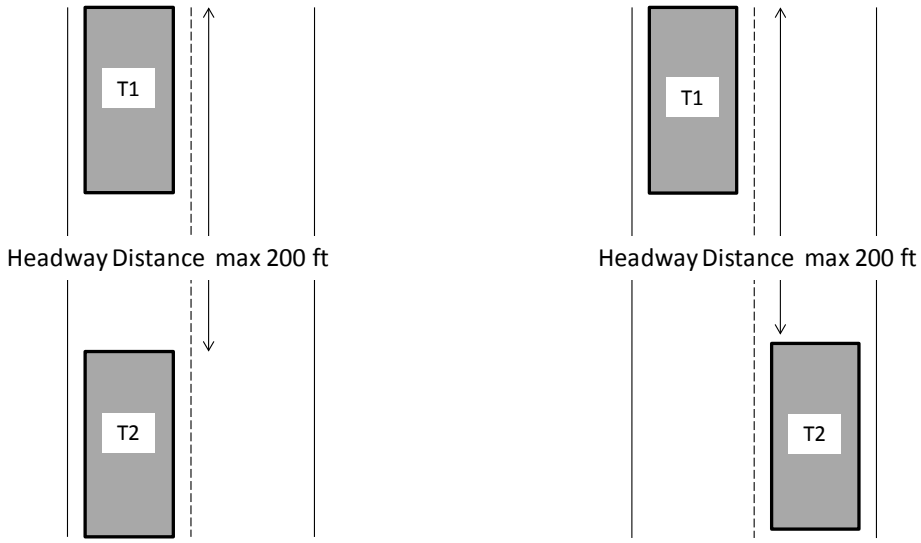

Figure 4-17 Two Cases of The Simultaneous Occurrence.

Two Trucks – Side-by-Side

The analysis of the degree of correlation was performed for Site 9936 in Florida along I-10 and 8382 in New York with a total number of records equal to 1,654,004 and 1,594,674, respectively. The filtering of the data resulted in selection of 2518 fully correlated trucks in adjacent lanes in Florida and selection of 3748 fully correlated trucks in adjacent lanes in New York. Histograms of GVW of the fully correlated side-by-side trucks identified are shown in Figure 4-18.

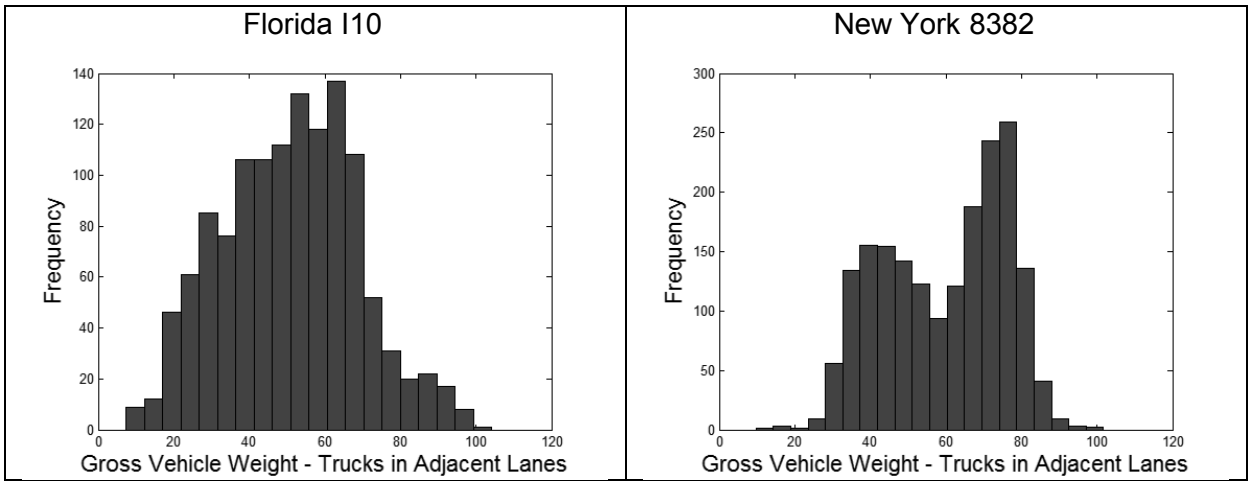

Figure 4-18 Histogram – Trucks Side-by-Side – Florida I-10 and New York 8382.

The selected trucks were plotted on probability paper and compared with all recorded vehicles. The GVW of both of the correlated trucks were added together and divided by two to obtain the average GVW. (Note that the correlation criteria assure that the average is similar to the two selected trucks in each pair.) The comparison of the mean correlated GVW of the trucks recorded in adjacent lanes with the GVW of the whole population from Florida and New York are shown in Figure 4-19.

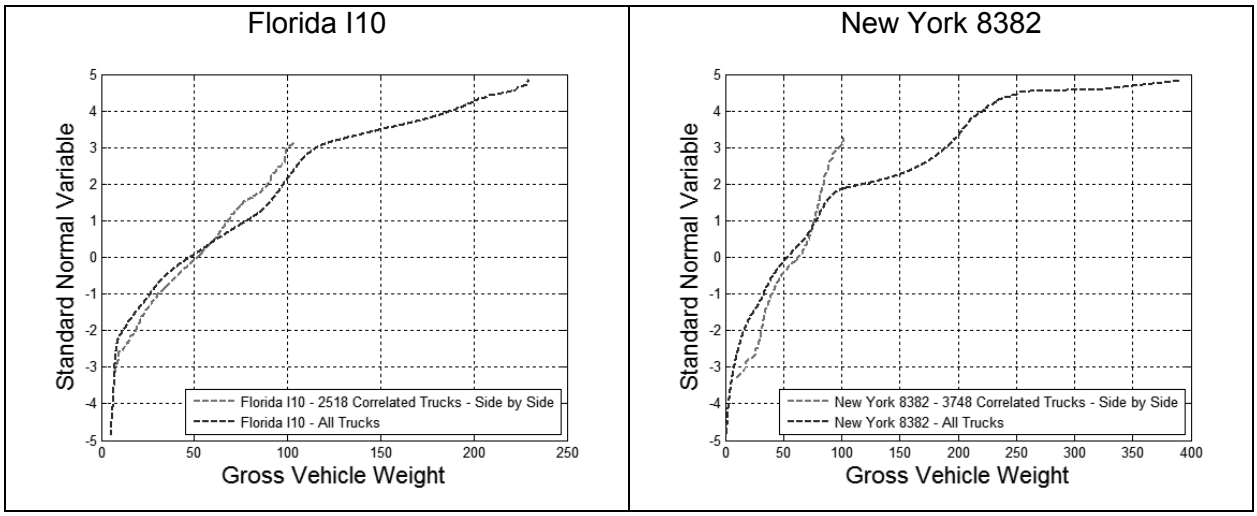

Figure 4-19 Comparison of the Mean GVW and GVW of the Whole Population – Florida and New York.

Two Trucks – One After Another

The filtering of the data resulted in selection of 8380 fully correlated trucks in one lane in Florida and 9868 fully correlated trucks in one lane in New York. Histograms of these trucks are shown in Figure 4-20. The comparison of the mean correlated GVW of the trucks recorded in one lane with the GVW of the whole data from Florida and New York are shown in Figure 4-21.

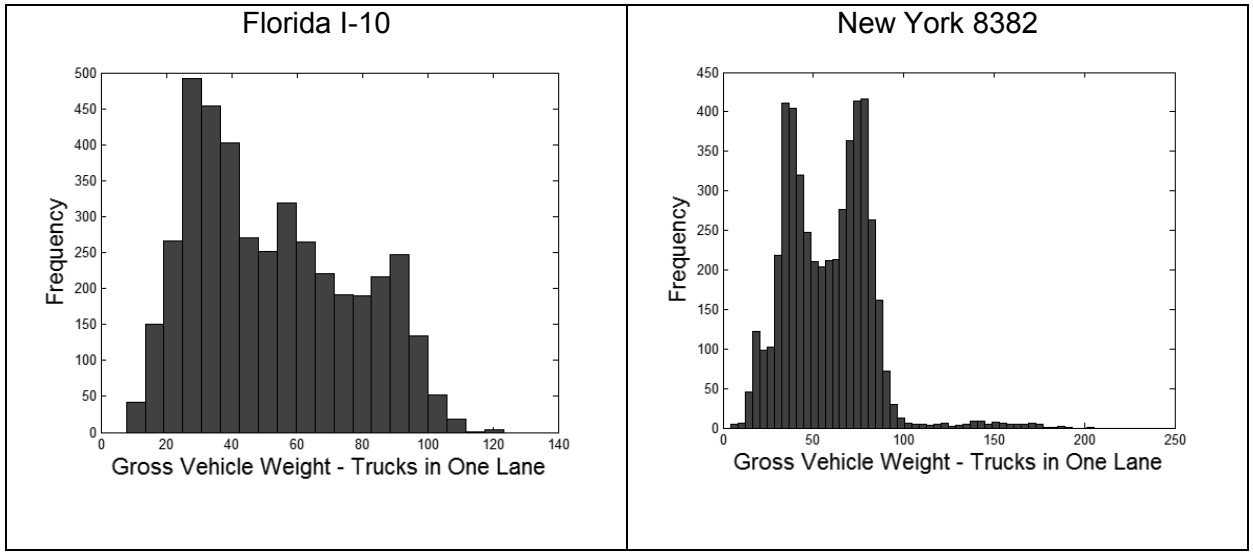

Figure 4-20 Histogram – Trucks One After Another – Florida I-10 and New York 8382.

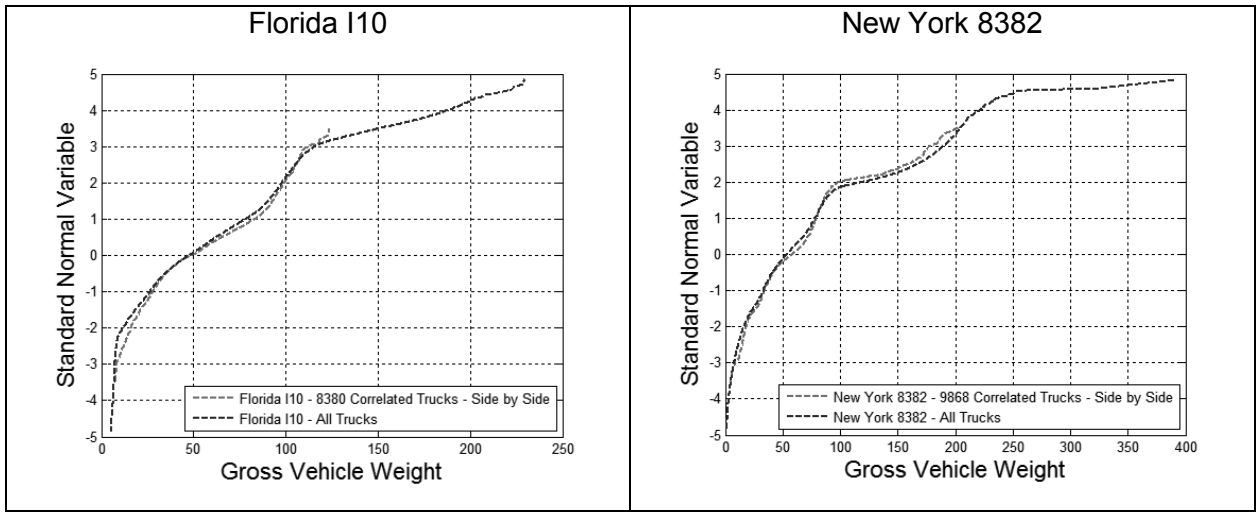

Figure 4-21 Comparison of the Mean GVW and GVW of the Whole Population – Florida and New York.

Implications for Specification Development

This study of multiple presence based on WIM data indicated that the vehicles representing the extreme tails of the CDF need not be considered to occur simultaneously in multiple lanes. The implication is that, for the SLS, only a single-lane live-load model need be considered on the load side, Q, of limit state functions. The resistance side of limit state functions, R, should represent the requirements of the applicable design requirement, even if that is a multiple lane loading.

The issue of multiple load lanes was considered in the development of HL-93 for AASHTO LRFD Strength Limit States, and the conclusion was that extreme truck load does not occur simultaneously with another, fully correlated, extreme truck, but was considered to occur simultaneously with a somewhat lighter truck—about 15% to 20% lighter truck. This 2-lane loading was correlated to the design loading of two lanes of HL-93 with a load factor of 1.75 and a multiple presence factor of 1.0. (Note that the multiple presence factor for a single lane loading is 1.20 to account for the occasional truck that creates more force effect than the family of configurations used to develop the HL-93 load configuration.)

4.2.5 Project Guidelines Regarding Live Load

The following guidelines are based on live load bias factors and coefficients of variation determined from the preliminary analysis of WIM measurements and some previous work by the research team (Nowak, 1999).

- It is recommended to use dynamic load as 10% of live load, with COV = 80%
- Generally use a single loaded lane (no multiple loaded lanes)
- The national load, i.e. notional load, should not try to encompass all WIM records. Some of the extremely heavy vehicles are permit loads and some are illegal overloads. A relatively small number of loads were excluded for most of the service limit state studies, but they were included for overload limit state.

- Different probabilities of exceedance may be used for various limit states based on consequences. Different probabilities of exceedance may also be used when calibrating the same limit state for components in different environment.
- Some jurisdictions may need exceptions based on their legal loads and extent of enforcement, and
- Basic HL-93 load model, scaled by calibrated load factors, is appropriate for SLS

With these recommendations, the evaluation of numerical live load models continued. The processes used and results obtained are summarized herein. Further details and extensive graphical presentations are contained in Rakoczy (2011).

4.3 Statistical Parameters for Service Limit States Other Than Fatigue

4.3.1 Maximum Moments for Different Time Periods

The maximum moment is a random variable. It depends on the period of time, ADTT and distribution of traffic (e.g. CDF of WIM moments). For a given CDF of WIM moments, F(x), period of time, T, and ADTT, the mean value of the maximum moment can be determined as follows. The total number of vehicles, N, expected during the considered time period, T (days), is T times ADTT. The expected or mean value of the maximum moment, Mmax(T) for time T is equal to the moment corresponding to probability {1 – F[1/N(T)]}, where F(x) is the CDF of WIM moments, which is $F^{-1}[1 - 1/N(T)]$ where F^{-1} is the inverse of CDF.

The objective is to determine the mean maximum moment for different time periods, i.e. 1 day, 2 weeks, 1 month, 2 months, 6 months, 1 year, 5 years, 50 years, 75 years and 100 years. The number of recorded vehicles for each location is given in Table 4-2. The data was collected over different time periods, in most cases about one year, but the number of vehicles varies because of different ADTT. Each CDF in Figure 4-8 through Figure 4-12 includes the number of data points equal to the corresponding number of vehicles, N. For each CDF, the vertical coordinate of the maximum moment, z_{max}, is equal to,

$$z_{max} = -\Phi^{-1}(1/N) \tag{4-1}$$

where Φ^{-1} is the inverse standard normal distribution function. For example, if N = 1 million, then z_{max} = 4.75.

In further analysis, five single lane ADTT's are considered: 250, 1,000, 2,500, 5,000 and 10,000. The calculations were performed separately for each ADTT. To determine the mean maximum moments corresponding to the considered time periods, the vertical coordinates are found first.

Starting with ADTT = 250, the vertical coordinate of the mean maximum 1 day moment, z, is

$$z = -\Phi^{-1}(1/250) = 2.65 \tag{4-2}$$

because the number of trucks per 1 day is 250.

For the mean maximum 2 week moment, z, is

$$z = -\Phi^{-1}(1/3500) = 3.44 \quad (4\text{-}3)$$

because the number of trucks per 2 weeks is (250 trucks)(14 days) = 3500 trucks.

Finally, for the mean maximum 100 year moment, z, is

$$z = -\Phi^{-1}(1/9{,}125{,}000) = 5.18 \quad (4\text{-}4)$$

because the number of trucks per 100 years is (250 trucks)(365 days)(100 years) = 9,125,000 trucks.

Similarly, for ADTT = 1000, the vertical coordinate of the mean maximum 1 day moment, z, is

$$z = -\Phi^{-1}(1/1000) = 3.09 \quad (4\text{-}5)$$

because the number of trucks per 1 day is 1000.

For the mean maximum 2 week moment, z, is

$$z = -\Phi^{-1}(1/14{,}000) = 3.8 \quad (4\text{-}6)$$

because the number of trucks per 2 weeks is (1000 trucks)(14 days) = 14,000 trucks.

Finally, for the mean maximum 100 year moment, z, is

$$z = -\Phi^{-1}(1/36{,}500{,}000) = 5.67 \quad (4\text{-}7)$$

because the number of trucks per 100 years is (1000 trucks)(365 days)(100 years) = 36,500,000 trucks.

Values of z for the considered ADTTs and time periods from 1 day to 100 years are summarized in Table 4-4.

Table 4-4 Vertical Coordinates for the Mean Maximum Moment.

	ADTT				
	250	**1,000**	**2,500**	**5,000**	**10,000**
1 Day	2.65	3.09	3.35	3.54	3.72
2 Weeks	3.44	3.08	4.02	4.18	4.33
1 Month	3.65	4.00	4.20	4.35	4.50
2 Months	3.82	4.15	4.35	4.50	4.65
6 Months	4.09	4.39	4.59	4.73	4.87
1 Year	4.24	4.55	4.73	4.87	5.01
5 Years	4.59	4.87	5.05	5.18	5.31
50 Years	5.05	5.31	5.47	5.60	5.72
75 Years	5.13	5.38	5.55	5.67	5.78
100 Years	5.18	5.44	5.60	5.72	5.83

For example, for the WIM moments in Figure 4-11 (span 120 ft.), the vertical coordinates corresponding to different time periods are shown in Figure 4-22 for ADTT = 1000.

There are 32 WIM locations and, therefore, 32 curves in each Figure 4-8 through Figure 4-12, representing CDFs of WIM moment. The mean maximum moment can be obtained directly from the graph by reading the moment ratio (horizontal axis) corresponding to the vertical coordinate representing the considered time period. For example, from Figure 4-22, the mean maximum 1 day moment ratio for FL-US29 is 0.95, and the mean maximum 1 year moment ratio is 1.39. Values for longer time periods were projected or interpolated as appropriate.

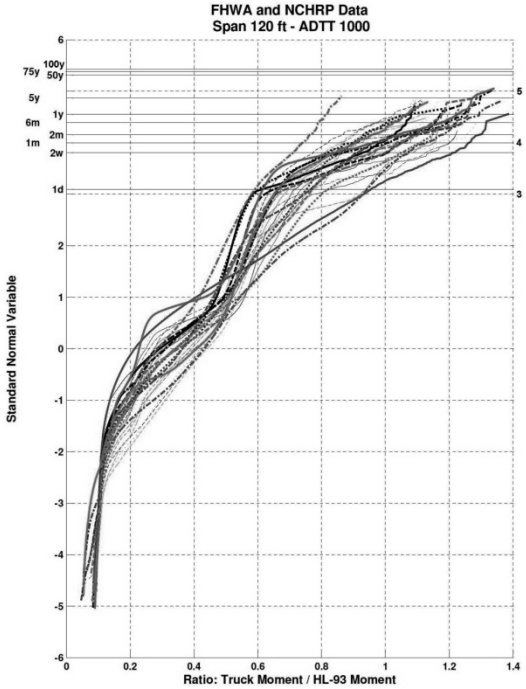

Figure 4-22 Vertical Coordinates for Different Time Periods, ADTT = 1000 and Span = 120 ft.

In the results for each ADTT and span length, there are 32 values of the mean maximum 1 day moment, 32 values of the mean maximum 2 week moment, and so on. For easier review and comparison, cumulative distribution functions of these 32 values obtained from Figure 4-22, are plotted on the normal probability paper in Figure 4-23. There is one CDF for 1 day values, one for 2 weeks, and so on. These are CDFs of extreme variables, as each of the 32 values is the maximum moment for a WIM location. The obtained CDFs are almost parallel, in particular this applies to the upper part. Because of regularity, it is easier to determine the statistical parameters. Each data point represents the mean of maximum value for one of 32 WIM locations, therefore, the CDF's in Figure 4-23 are extreme value distributions rather than hypothetical curves.

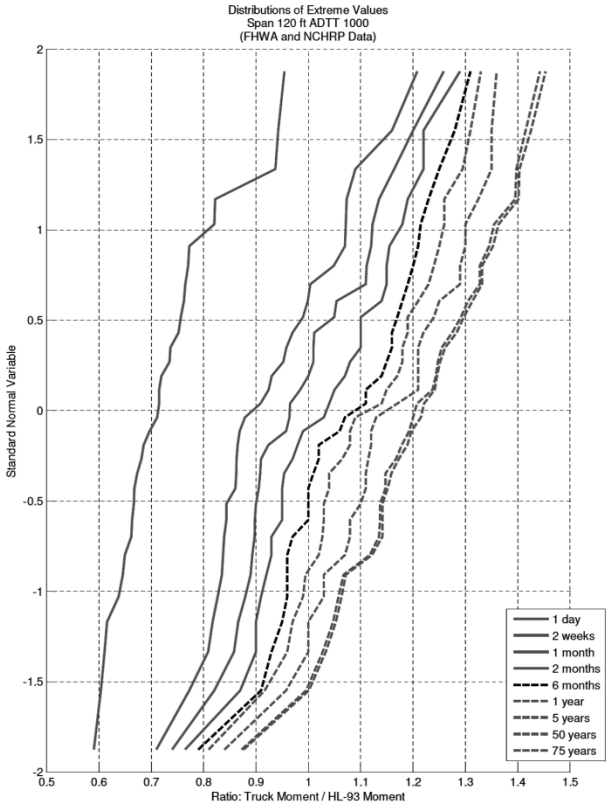

Figure 4-23 CDFs of Mean Maximum Moment Ratios for ADTT = 1000 and Span Length 120 ft.

4.3.2 Statistical Parameters of Live Load

It is assumed that the considered 32 WIM locations are representative for the truck traffic in the United States. The statistical parameters (the mean maximum and coefficient of variation of the maximum live load) were determined for each WIM location. The cumulative distribution functions (CDF) of the mean maximum values were plotted on probability paper. This is an extreme value distribution. The mean of these mean maximum values can be considered as the mean maximum national live load. The standard deviation of the mean maximum values can be determined from the graphs (slope of the CDF). However, the WIM locations were not selected randomly, but the selection was based on availability of WIM stations with truck data and credibility of the measured data (truck records). If the considered WIM locations are biased (non-representative), then the processed database can underestimate or overestimate the statistical parameters of the national live load. Therefore, for the purpose of further reliability analysis, it is conservatively assumed that the calculated mean maximum live load is increased by 1.5 standard deviation. The probability of exceeding this value (mean plus 1.5 standard deviation) is about 5%, so that it will be exceeded by 5% out of 32 WIM locations (i.e. in one or two WIM locations).

The upper parts of the CDFs are almost straight lines, therefore, the fitting by normal distributions is justified. The mean values can be read directly from the graph, as the intersection of CDFs (represented by straight lines) and the horizontal axis at zero on the vertical scale. This process is depicted in Figure 4-24. The visual comparison of how the actual CDF fits a straight line is much better than any curve fitting formula because we are mostly

interested in some parts of the CDF only. Different curves can have different slope and this is reflected in the standard deviations.

Calculations were carried out for all considered cases of ADTT and span length. The results were extrapolated to 100 years and span length of 300 ft. and are summarized in Table 4-5 through Table 4-9. Statistical parameters were calculated for a variety of ADTT's (500, 1000, 2500, 5000, 10,000) but AASHTO LRFD is based on 5000 (consistent with strength limit states). Live load data for other values of ADTT other than 5000 are tabulated so owners can repeat the calibration process with other data. For a given bridge, use of a lower ADTT should lead to a higher reliability index.

Bias factors vary depending on ADTT for shorter time periods, however for longer time periods it is about 1.4.

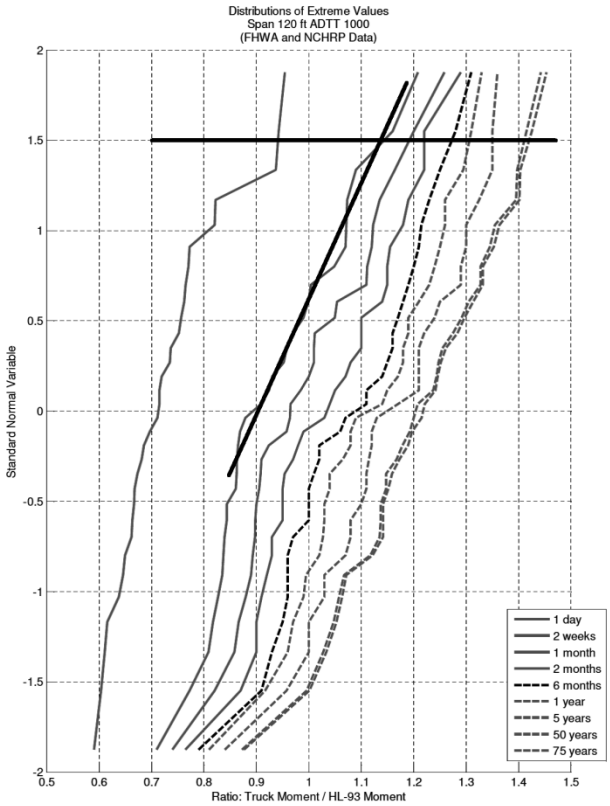

Figure 4-24 Determination of Mean Values at 1.5 σ.

4.3.3 Reactions

Tables of statistics for reactions of simply supported spans were developed for the same spans, time periods and ADTTs as previously presented for bending moments using an analogous methodology as presented in Section 4.3.2. The results are shown in Table 4-10 to Table 4-14. Graphical representations are presented in Rakoczy (2011).

4.3.4 Axle Loads

Decks are typically designed for axle loads, not truck loads. Therefore, statistical parameters for axle loads for various time periods and ADTTs are developed using methodology analogous to the methodology used for moments (see in Section 4.3.2) are presented in Table 4-15.

Table 4-5 Statistical Parameters of Live Load Moments for ADTT 250, $\lambda = \mu + 1.5\sigma$

ADTT 250																		
Span	30 ft			60 ft			90 ft			120 ft			200 ft			300 ft		
	λ	μ	COV	λ	μ	COV	λ	μ	COV	λ	μ	COV	λ	μ	COV	λ	μ	COV
1 Day	0.92	0.65	0.28	0.82	0.64	0.23	0.80	0.66	0.17	0.79	0.65	0.15	0.71	0.56	0.18	0.61	0.48	0.18
2 Weeks	1.06	0.80	0.21	1.05	0.80	0.16	1.01	0.80	0.18	1.02	0.80	0.16	0.93	0.73	0.16	0.84	0.67	0.16
1 Month	1.12	0.85	0.21	1.09	0.85	0.19	1.08	0.85	0.18	1.08	0.85	0.17	1.01	0.78	0.19	0.90	0.73	0.16
2 Months	1.14	0.90	0.18	1.15	0.91	0.17	1.14	0.90	0.18	1.14	0.90	0.17	1.05	0.85	0.15	0.95	0.77	0.15
6 Months	1.19	0.95	0.17	1.23	0.96	0.19	1.20	0.97	0.15	1.19	0.98	0.14	1.12	0.91	0.15	1.04	0.85	0.15
1 Year	1.23	1.00	0.15	1.27	0.98	0.19	1.24	1.00	0.16	1.22	1.04	0.12	1.15	0.94	0.15	1.08	0.88	0.15
5 Years	1.31	1.07	0.15	1.35	1.09	0.16	1.31	1.13	0.11	1.31	1.14	0.10	1.25	1.02	0.15	1.18	0.97	0.15
50 Years	1.37	1.17	0.11	1.39	1.16	0.13	1.39	1.25	0.07	1.37	1.19	0.10	1.32	1.06	0.16	1.25	1.02	0.15
75 Years	1.38	1.20	0.10	1.40	1.19	0.12	1.41	1.27	0.07	1.39	1.21	0.10	1.34	1.08	0.16	1.27	1.04	0.15
100 Years	1.39	1.22	0.09	1.43	1.21	0.12	1.42	1.28	0.07	1.41	1.22	0.10	1.35	1.09	0.16	1.29	1.05	0.15

Table 4-6 Statistical Parameters of Live Load Moments for ADTT 1,000, $\lambda = \mu + 1.5\sigma$

ADTT 1,000																		
Span	30 ft			60 ft			90 ft			120 ft			200 ft			300 ft		
	λ	μ	COV	λ	μ	COV	λ	μ	COV	λ	μ	COV	λ	μ	COV	λ	μ	COV
1 Day	0.99	0.72	0.28	0.89	0.71	0.20	0.90	0.72	0.17	0.89	0.71	0.17	0.81	0.63	0.19	0.71	0.55	0.19
2 Weeks	1.14	0.87	0.21	1.13	0.90	0.16	1.13	0.89	0.18	1.14	0.91	0.16	1.06	0.85	0.16	0.97	0.77	0.16
1 Month	1.18	0.95	0.16	1.19	0.95	0.16	1.19	0.95	0.17	1.19	0.96	0.16	1.11	0.91	0.14	1.01	0.83	0.14
2 Months	1.23	0.99	0.16	1.26	0.99	0.18	1.26	1.00	0.17	1.23	1.03	0.13	1.16	0.96	0.14	1.07	0.89	0.14
6 Months	1.27	1.04	0.14	1.31	1.05	0.16	1.30	1.10	0.12	1.27	1.09	0.11	1.22	0.99	0.15	1.15	0.93	0.15
1 Year	1.33	1.07	0.16	1.34	1.08	0.16	1.32	1.15	0.10	1.31	1.14	0.10	1.25	1.01	0.16	1.18	0.95	0.16
5 Years	1.37	1.11	0.15	1.37	1.14	0.13	1.36	1.21	0.08	1.35	1.17	0.10	1.30	1.06	0.15	1.24	1.01	0.15
50 Years	1.38	1.24	0.07	1.42	1.21	0.12	1.41	1.26	0.08	1.41	1.21	0.11	1.35	1.11	0.14	1.28	1.05	0.14
75 Years	1.40	1.26	0.07	1.42	1.23	0.11	1.42	1.28	0.07	1.41	1.23	0.10	1.36	1.13	0.13	1.29	1.07	0.13
100 Years	1.40	1.27	0.07	1.44	1.24	0.11	1.43	1.29	0.07	1.43	1.24	0.10	1.37	1.14	0.13	1.30	1.09	0.13

Table 4-7 Statistical Parameters of Live Load Moments for ADTT 2,500, $\lambda = \mu + 1.5\sigma$

ADTT 2,500																		
Span	30 ft			60 ft			90 ft			120 ft			200 ft			300 ft		
	λ	μ	COV	λ	μ	COV	λ	μ	COV	λ	μ	COV	λ	μ	COV	λ	μ	COV
1 Day	1.03	0.80	0.19	0.97	0.79	0.18	0.97	0.77	0.17	0.98	0.78	0.17	0.90	0.70	0.19	0.80	0.62	0.19
2 Weeks	1.20	0.93	0.19	1.20	0.96	0.17	1.20	0.96	0.17	1.20	0.97	0.15	1.12	0.92	0.14	1.02	0.84	0.14
1 Month	1.23	0.99	0.16	1.25	0.99	0.17	1.26	1.00	0.17	1.22	1.04	0.12	1.16	0.95	0.15	1.09	0.89	0.15
2 Months	1.28	1.04	0.15	1.31	1.04	0.17	1.29	1.11	0.11	1.27	1.12	0.09	1.21	0.98	0.15	1.12	0.91	0.15
6 Months	1.31	1.07	0.15	1.34	1.07	0.17	1.32	1.15	0.10	1.31	1.14	0.10	1.25	1.01	0.16	1.18	0.95	0.16
1 Year	1.34	1.11	0.14	1.35	1.11	0.14	1.36	1.19	0.09	1.34	1.17	0.09	1.28	1.04	0.15	1.21	0.98	0.15
5 Years	1.36	1.15	0.12	1.39	1.18	0.12	1.39	1.24	0.08	1.38	1.20	0.10	1.33	1.07	0.16	1.26	1.01	0.16
50 Years	1.40	1.25	0.08	1.42	1.22	0.11	1.43	1.29	0.07	1.43	1.23	0.11	1.37	1.11	0.15	1.29	1.05	0.15
75 Years	1.40	1.26	0.07	1.43	1.24	0.10	1.43	1.30	0.07	1.44	1.24	0.10	1.37	1.13	0.14	1.29	1.06	0.14
100 Years	1.40	1.27	0.07	1.44	1.25	0.10	1.44	1.31	0.07	1.44	1.25	0.10	1.39	1.14	0.14	1.32	1.09	0.14

Table 4-8 Statistical Parameters of Live Load Moments for ADTT 5,000, $\lambda = \mu + 1.5\sigma$

ADTT 5,000																		
Span	30 ft			60 ft			90 ft			120 ft			200 ft			300 ft		
	λ	μ	COV	λ	μ	COV	λ	μ	COV	λ	μ	COV	λ	μ	COV	λ	μ	COV
1 Day	1.08	0.85	0.18	1.02	0.82	0.17	1.03	0.82	0.17	1.03	0.82	0.17	0.95	0.75	0.17	0.84	0.67	0.17
2 Weeks	1.24	0.98	0.17	1.26	1.00	0.17	1.24	1.00	0.16	1.24	1.04	0.13	1.16	0.96	0.14	1.06	0.88	0.14
1 Month	1.28	1.04	0.15	1.32	1.03	0.18	1.30	1.12	0.11	1.26	1.11	0.09	1.20	0.99	0.14	1.13	0.93	0.14
2 Months	1.31	1.07	0.15	1.34	1.07	0.17	1.32	1.15	0.10	1.31	1.14	0.10	1.23	1.02	0.14	1.16	0.96	0.14
6 Months	1.34	1.11	0.14	1.35	1.11	0.14	1.34	1.19	0.08	1.32	1.17	0.09	1.28	1.04	0.15	1.23	1.00	0.15
1 Year	1.35	1.14	0.12	1.38	1.14	0.14	1.38	1.21	0.09	1.36	1.19	0.09	1.31	1.07	0.15	1.25	1.02	0.15
5 Years	1.39	1.16	0.13	1.40	1.19	0.12	1.40	1.25	0.08	1.41	1.21	0.11	1.34	1.10	0.15	1.28	1.05	0.15
50 Years	1.41	1.21	0.11	1.44	1.24	0.10	1.44	1.27	0.09	1.46	1.23	0.12	1.39	1.13	0.15	1.30	1.06	0.15
75 Years	1.42	1.22	0.11	1.45	1.25	0.10	1.45	1.29	0.08	1.46	1.25	0.11	1.40	1.14	0.15	1.31	1.07	0.15
100 Years	1.42	1.23	0.11	1.45	1.26	0.10	1.47	1.30	0.08	1.47	1.26	0.11	1.40	1.15	0.15	1.33	1.08	0.15

Table 4-9 Statistical Parameters of Live Load Moments for ADTT 10,000, $\lambda = \mu + 1.5\sigma$

ADTT 10,000																		
Span	30 ft			60 ft			90 ft			120 ft			200 ft			300 ft		
	λ	μ	COV	λ	μ	COV	λ	μ	COV	λ	μ	COV	λ	μ	COV	λ	μ	COV
1 Day	1.17	0.88	0.22	1.09	0.89	0.16	1.11	0.87	0.18	1.13	0.87	0.20	1.02	0.81	0.17	0.91	0.75	0.17
2 Weeks	1.29	1.02	0.18	1.31	1.04	0.17	1.29	1.11	0.11	1.27	1.12	0.09	1.22	0.98	0.16	1.16	0.93	0.16
1 Month	1.32	1.06	0.16	1.34	1.08	0.16	1.32	1.15	0.10	1.29	1.14	0.09	1.25	1.01	0.16	1.20	0.97	0.16
2 Months	1.35	1.09	0.16	1.35	1.11	0.14	1.35	1.18	0.09	1.32	1.17	0.09	1.28	1.04	0.15	1.23	1.00	0.15
6 Months	1.35	1.12	0.13	1.37	1.14	0.13	1.37	1.20	0.09	1.34	1.19	0.08	1.30	1.06	0.15	1.25	1.02	0.15
1 Year	1.37	1.17	0.11	1.39	1.16	0.13	1.39	1.24	0.08	1.38	1.20	0.10	1.32	1.08	0.15	1.27	1.04	0.15
5 Years	1.39	1.24	0.08	1.41	1.21	0.11	1.42	1.27	0.08	1.42	1.22	0.11	1.37	1.11	0.15	1.30	1.06	0.15
50 Years	1.40	1.28	0.06	1.45	1.24	0.11	1.45	1.30	0.08	1.46	1.25	0.11	1.40	1.14	0.15	1.31	1.07	0.15
75 Years	1.41	1.29	0.06	1.46	1.26	0.10	1.47	1.32	0.08	1.47	1.26	0.11	1.40	1.16	0.14	1.32	1.09	0.14
100 Years	1.42	1.30	0.06	1.47	1.27	0.10	1.49	1.33	0.08	1.48	1.27	0.11	1.42	1.17	0.14	1.33	1.10	0.14

Table 4-10 Statistical Parameters of Live Load Reactions for ADTT 250, $\lambda = \mu + 1.5\sigma$

ADTT 250																		
Span	30 ft			60 ft			90 ft			120 ft			200 ft			300 ft		
	μ+1.5σ	μ	COV	μ+1.5σ	μ	COV	μ+1.5σ	μ	COV	μ+1.5σ	μ	COV	μ+1.5σ	μ	COV	μ+1.5σ	μ	COV
1 Day	1.02	0.85	0.13	0.88	0.74	0.12	0.88	0.74	0.12	0.86	0.72	0.13	0.73	0.61	0.13	0.57	0.48	0.13
2 Weeks	1.22	1.02	0.13	1.08	0.91	0.12	1.11	0.94	0.12	1.08	0.90	0.13	0.97	0.80	0.14	0.82	0.68	0.14
1 Month	1.28	1.07	0.13	1.14	0.96	0.13	1.17	0.99	0.12	1.15	0.97	0.12	1.06	0.88	0.14	0.93	0.77	0.14
2 Months	1.32	1.11	0.13	1.19	1.01	0.12	1.22	1.04	0.12	1.20	1.02	0.12	1.12	0.92	0.14	0.98	0.81	0.14
6 Months	1.37	1.16	0.12	1.27	1.07	0.12	1.32	1.11	0.13	1.30	1.10	0.12	1.18	0.97	0.14	1.08	0.89	0.14
1 Year	1.41	1.20	0.12	1.31	1.10	0.13	1.37	1.14	0.13	1.35	1.12	0.13	1.22	1.01	0.14	1.12	0.93	0.14
5 Years	1.49	1.26	0.12	1.38	1.15	0.13	1.46	1.22	0.13	1.44	1.20	0.13	1.35	1.11	0.14	1.24	1.02	0.14
50 Years	1.54	1.30	0.12	1.49	1.23	0.14	1.52	1.28	0.13	1.52	1.28	0.13	1.45	1.18	0.15	1.36	1.11	0.15
75 Years	1.55	1.31	0.12	1.50	1.24	0.14	1.55	1.29	0.13	1.55	1.29	0.13	1.46	1.19	0.15	1.37	1.12	0.15
100 Years	1.56	1.32	0.12	1.50	1.25	0.14	1.55	1.30	0.13	1.55	1.30	0.13	1.47	1.20	0.15	1.38	1.12	0.15

Table 4-11 Statistical Parameters of Live Load Reactions for ADTT 1,000, λ = μ + 1.5σ

ADTT 1000																		
Span	30 ft			60 ft			90 ft			120 ft			200 ft			300 ft		
	μ+1.5σ	μ	COV	μ+1.5σ	μ	COV	μ+1.5σ	μ	COV	μ+1.5σ	μ	COV	μ+1.5σ	μ	COV	μ+1.5σ	μ	COV
1 Day	1.14	0.94	0.14	0.95	0.80	0.13	0.94	0.80	0.11	0.91	0.79	0.10	0.84	0.70	0.13	0.74	0.62	0.13
2 Weeks	1.31	1.10	0.13	1.17	0.99	0.12	1.19	1.02	0.11	1.19	1.02	0.11	1.09	0.91	0.13	0.97	0.81	0.13
1 Month	1.35	1.15	0.12	1.23	1.03	0.13	1.26	1.08	0.11	1.25	1.07	0.11	1.17	0.97	0.13	1.06	0.88	0.13
2 Months	1.38	1.18	0.11	1.26	1.08	0.11	1.31	1.11	0.12	1.31	1.11	0.12	1.22	1.01	0.14	1.11	0.92	0.14
6 Months	1.42	1.22	0.11	1.29	1.11	0.11	1.38	1.15	0.13	1.37	1.16	0.12	1.28	1.05	0.14	1.18	0.97	0.14
1 Year	1.45	1.25	0.11	1.32	1.14	0.11	1.40	1.19	0.12	1.40	1.19	0.12	1.32	1.09	0.14	1.21	1.00	0.14
5 Years	1.50	1.29	0.11	1.40	1.20	0.11	1.49	1.26	0.12	1.50	1.26	0.13	1.38	1.14	0.14	1.28	1.06	0.14
50 Years	1.56	1.33	0.11	1.46	1.25	0.11	1.56	1.30	0.13	1.57	1.30	0.14	1.47	1.20	0.15	1.35	1.10	0.15
75 Years	1.57	1.34	0.11	1.47	1.26	0.11	1.57	1.31	0.13	1.58	1.31	0.14	1.48	1.21	0.15	1.36	1.11	0.15
100 Years	1.57	1.35	0.11	1.48	1.27	0.11	1.57	1.32	0.13	1.59	1.32	0.14	1.49	1.22	0.15	1.36	1.12	0.15

Table 4-12 Statistical Parameters of Live Load Reactions for ADTT 2,500, λ = μ + 1.5σ

ADTT 2500																		
Span	30 ft			60 ft			90 ft			120 ft			200 ft			300 ft		
	μ+1.5σ	μ	COV	μ+1.5σ	μ	COV	μ+1.5σ	μ	COV	μ+1.5σ	μ	COV	μ+1.5σ	μ	COV	μ+1.5σ	μ	COV
1 Day	1.18	1.00	0.12	1.02	0.88	0.10	1.07	0.90	0.12	1.04	0.89	0.11	0.93	0.78	0.13	0.79	0.66	0.13
2 Weeks	1.35	1.14	0.12	1.23	1.05	0.11	1.29	1.09	0.12	1.29	1.09	0.12	1.19	0.99	0.13	1.06	0.89	0.13
1 Month	1.38	1.17	0.12	1.26	1.08	0.11	1.35	1.14	0.12	1.34	1.13	0.12	1.23	1.02	0.14	1.12	0.93	0.14
2 Months	1.41	1.20	0.12	1.29	1.11	0.11	1.40	1.17	0.13	1.38	1.17	0.12	1.29	1.06	0.14	1.17	0.96	0.14
6 Months	1.47	1.24	0.12	1.34	1.14	0.11	1.44	1.20	0.13	1.44	1.20	0.13	1.33	1.09	0.15	1.22	1.00	0.15
1 Year	1.49	1.25	0.13	1.36	1.16	0.11	1.47	1.23	0.13	1.48	1.24	0.13	1.38	1.12	0.15	1.25	1.02	0.15
5 Years	1.55	1.29	0.13	1.44	1.21	0.12	1.55	1.29	0.13	1.54	1.28	0.13	1.43	1.17	0.15	1.31	1.08	0.15
50 Years	1.59	1.33	0.13	1.53	1.27	0.13	1.58	1.32	0.13	1.59	1.32	0.14	1.50	1.21	0.16	1.38	1.11	0.16
75 Years	1.60	1.34	0.13	1.54	1.28	0.13	1.59	1.33	0.13	1.60	1.33	0.14	1.51	1.22	0.16	1.39	1.12	0.16
100 Years	1.60	1.35	0.13	1.54	1.29	0.13	1.59	1.34	0.13	1.61	1.34	0.14	1.51	1.23	0.16	1.40	1.13	0.16

Table 4-13 Statistical Parameters of Live Load Reactions for ADTT 5,000, $\lambda = \mu + 1.5\sigma$

ADTT 5000																		
Span	**30 ft**			**60 ft**			**90 ft**			**120 ft**			**200 ft**			**300 ft**		
	μ+1.5σ	**μ**	**COV**	**μ+1.5σ**	**μ**	**COV**	**μ+1.5σ**	**μ**	**COV**	**μ+1.5σ**	**μ**	**COV**	**μ+1.5σ**	**μ**	**COV**	**μ+1.5σ**	**μ**	**COV**
1 Day	1.25	1.05	0.12	1.09	0.94	0.11	1.14	0.96	0.13	1.12	0.94	0.13	1.02	0.84	0.14	0.90	0.74	0.14
2 Weeks	1.42	1.19	0.13	1.30	1.10	0.12	1.36	1.13	0.13	1.36	1.13	0.13	1.26	1.03	0.15	1.13	0.93	0.15
1 Month	1.46	1.22	0.13	1.34	1.13	0.12	1.39	1.16	0.13	1.40	1.17	0.13	1.30	1.06	0.15	1.18	0.96	0.15
2 Months	1.48	1.24	0.13	1.36	1.15	0.12	1.43	1.20	0.13	1.44	1.20	0.13	1.33	1.09	0.15	1.21	0.99	0.15
6 Months	1.51	1.27	0.13	1.39	1.18	0.12	1.47	1.23	0.13	1.48	1.24	0.13	1.39	1.13	0.15	1.27	1.03	0.15
1 Year	1.54	1.28	0.13	1.41	1.20	0.12	1.50	1.26	0.13	1.51	1.27	0.13	1.41	1.15	0.15	1.29	1.06	0.15
5 Years	1.58	1.32	0.13	1.48	1.25	0.12	1.54	1.30	0.12	1.56	1.30	0.13	1.46	1.19	0.15	1.34	1.09	0.15
50 Years	1.62	1.36	0.13	1.53	1.29	0.12	1.59	1.35	0.12	1.61	1.35	0.13	1.52	1.23	0.15	1.40	1.14	0.15
75 Years	1.63	1.37	0.12	1.54	1.30	0.12	1.60	1.36	0.12	1.62	1.36	0.13	1.53	1.24	0.15	1.41	1.15	0.15
100 Years	1.63	1.38	0.12	1.55	1.31	0.12	1.61	1.37	0.12	1.62	1.37	0.13	1.53	1.25	0.15	1.42	1.15	0.15

Table 4-14 Statistical Parameters of Live Load Reactions for ADTT 10,000, $\lambda = \mu + 1.5\sigma$

ADTT 10000																		
Span	**30 ft**			**60 ft**			**90 ft**			**120 ft**			**200 ft**			**300 ft**		
	μ+1.5σ	**μ**	**COV**	**μ+1.5σ**	**μ**	**COV**	**μ+1.5σ**	**μ**	**COV**	**μ+1.5σ**	**μ**	**COV**	**μ+1.5σ**	**μ**	**COV**	**μ+1.5σ**	**μ**	**COV**
1 Day	1.31	1.10	0.13	1.20	1.00	0.13	1.23	1.03	0.13	1.21	1.01	0.13	1.11	0.91	0.14	0.98	0.81	0.14
2 Weeks	1.45	1.21	0.13	1.35	1.12	0.13	1.40	1.17	0.13	1.41	1.18	0.13	1.31	1.07	0.15	1.19	0.97	0.15
1 Month	1.48	1.24	0.13	1.39	1.16	0.13	1.43	1.20	0.13	1.45	1.21	0.13	1.36	1.10	0.15	1.24	1.00	0.15
2 Months	1.50	1.26	0.13	1.42	1.19	0.13	1.46	1.23	0.12	1.48	1.24	0.13	1.39	1.13	0.15	1.27	1.03	0.15
6 Months	1.52	1.28	0.13	1.45	1.21	0.13	1.48	1.25	0.12	1.52	1.26	0.13	1.41	1.15	0.15	1.31	1.07	0.15
1 Year	1.55	1.29	0.13	1.46	1.22	0.13	1.51	1.28	0.12	1.54	1.28	0.13	1.44	1.17	0.15	1.33	1.08	0.15
5 Years	1.60	1.34	0.13	1.50	1.26	0.13	1.55	1.31	0.12	1.59	1.33	0.13	1.49	1.22	0.15	1.37	1.12	0.15
50 Years	1.64	1.37	0.13	1.56	1.30	0.13	1.62	1.36	0.13	1.62	1.35	0.13	1.54	1.25	0.15	1.43	1.16	0.15
75 Years	1.65	1.38	0.13	1.57	1.31	0.13	1.63	1.37	0.12	1.63	1.36	0.13	1.55	1.26	0.15	1.44	1.17	0.15
100 Years	1.66	1.39	0.13	1.57	1.32	0.13	1.63	1.38	0.12	1.64	1.37	0.13	1.55	1.27	0.15	1.45	1.18	0.15

Table 4-15 Statistical Parameters for Axle Loads, $\lambda = \mu + 1.5\sigma$

Time period	ADTT=250		ADTT=1000		ADTT=2500		ADTT=5000		ADTT=10 000	
	λ	COV [%]	λ	COV [%]	λ	COV [%]	λ	COV [%]	λ	COV [%]
1 day	0.91	0.17	1.00	0.17	1.07	0.16	1.11	0.16	1.15	0.16
2 weeks	1.09	0.16	1.17	0.16	1.24	0.15	1.29	0.15	1.32	0.15
1 month	1.14	0.16	1.23	0.15	1.28	0.15	1.32	0.14	1.36	0.14
2 months	1.18	0.15	1.27	0.15	1.32	0.14	1.36	0.14	1.38	0.14
6 months	1.24	0.15	1.32	0.14	1.37	0.14	1.40	0.14	1.42	0.13
1 year	1.30	0.14	1.37	0.14	1.41	0.13	1.42	0.13	1.45	0.13
5 years	1.38	0.14	1.43	0.13	1.46	0.13	1.47	0.13	1.49	0.13
50 years	1.45	0.13	1.48	0.13	1.50	0.13	1.51	0.13	1.53	0.12
75 years	1.45	0.13	1.48	0.12	1.50	0.12	1.51	0.12	1.53	0.12
100 years	1.46	0.13	1.49	0.12	1.51	0.12	1.52	0.12	1.53	0.12

4.4 Development of Statistical Parameters of Fatigue Load

4.4.1 Objective

Fatigue is one of the major causes of distress in steel highway bridges. Cracking or rupture of components and connections calls for costly repairs or replacements. The durability of affected structures can be enhanced by applying reliability theory to this limit state. The limit state of fatigue is reached when accumulated load spectra exceed the fatigue resistance of material. Therefore, a rational approach to evaluation of existing bridges and design for new bridges requires the knowledge of the load carrying capacity and accumulated loads as shown on Figure 4-25. A considerable effort was directed toward tests of materials under cyclic loading, to establish the so called S-N curves, where S is the applied stress and N is number of load applications to failure. However knowledge about the real fatigue stress caused by the current truck traffic was limited and outdated, based on research done in the 1980's.

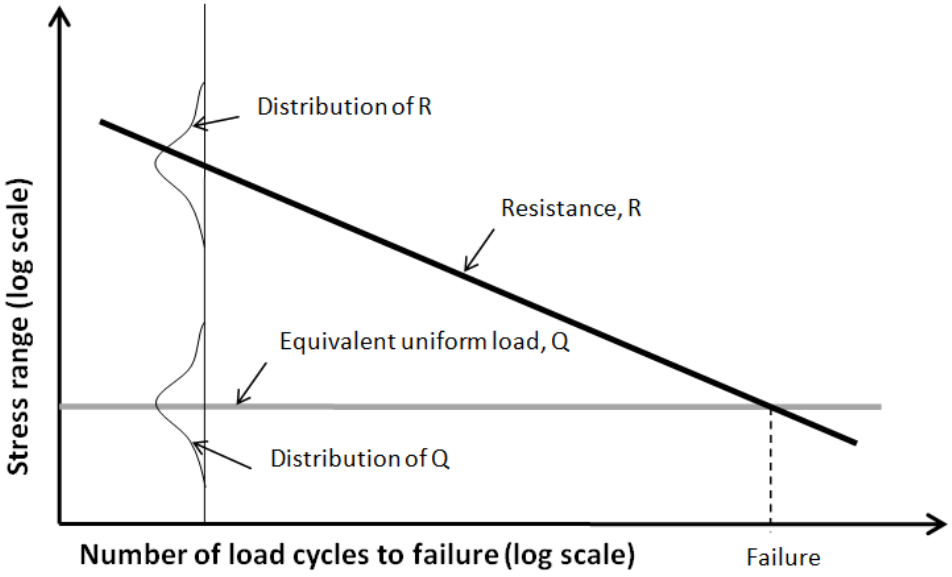

Figure 4-25 Fatigue Failure on S-N Curve.

The current *AASHTO LRFD* (2012) has two different Fatigue Limit States. Fatigue Limit State I is related to infinite load-induced fatigue life. The fatigue load in this limit state reflects the load levels found to be representative of the maximum stress range of the truck population for infinite fatigue-life design. Fatigue Limit State II is related to finite load-induced fatigue life. The fatigue load in this limit state is intended to reflect a load level found to be representative of the effective stress range of the truck population with respect to the induced number of load cycles and their cumulative damage effects on the bridge components. Only Fatigue I applies to fatigue of concrete and the considered types of reinforcement.

The focus of this section is to develop statistical models of fatigue load based on the WIM truck survey data. The fatigue load is intended to be used in calibration of the design provisions in the *AASHTO LRFD* (2012). The WIM measurements provide an unbiased data set. The 15 WIM sites provided by the Federal Highway Administration are considered as representative for the United States for this analysis. Only sites with one full year of constant reading were used for fatigue analysis.

Three cases are considered: mid-span moment for a simply supported bridge, moment at the interior support of a two span continuous bridge and moment at 0.4 span of a continuous bridge. The surveyed vehicles were run over influence lines as traffic streams to determine the number and magnitude of moment cycles for a wide range of span lengths for each case. The fatigue load time history was then developed for the bending moment as shown in Kulicki et. al (2013). The Fatigue II (finite life) load was calculated as an equivalent moment using the linear damage rule first proposed by A. Palmgren (1924) and later popularized by Miner (1945) as the Palmgren-Miner rule. The Fatigue I (infinite life) load for each location was determined by finding the highest 0.01% of the load cycles and using the smallest of them as the fatigue load for the considered location. The obtained results combined with fatigue resistance models served as the basis for the development of calibrated criteria for service limit state in *AASHTO LRFD*.

4.4.2 WIM Data Used for Fatigue Calculation

To be consistent with previous research done by Fisher (1977), in addition to filters used for live load, filter 3 was used to remove light trucks with GVW under 20 kips because light vehicles cause relatively low fatigue damage. A summary of the data used for fatigue analysis including WIM locations, number of records and ADTT is shown in Table 4-16.

Table 4-16 WIM Locations and Number of Vehicles Used for Fatigue Analysis

Site	Number of Days in Data	Total Number of Truck Records, N	Lane ADTT
AZ SPS-1	365	26,501	97
AZ SPS-2	365	1,391,098	3919
AR SPS-2	365	1,642,334	4590
CO SPS-2	365	326,017	941
DE SPS-1	365	175,889	553
IL SPS-6	365	821,809	2340
KS SPS-2	365	456,881	1309
LA SPS-1	365	70,831	235
ME SPS-5	365	172,333	503
MD SPS-5	365	124,474	450
MN SPS-5	365	47,794	152
PA SPS-6	365	1,458,818	4098
TN SPS-6	365	1,583,151	4445
VA SPS-1	365	237,804	710
WI SPS-1	365	209,239	622

4.4.3 Fatigue Limit State II – Finite Fatigue Life

Live load on bridges is caused mainly by moving trucks. As a truck moves across a bridge, the stress at any point varies. Determining the accumulated fatigue damage due to traffic loads involves the conversion of the live load effects to an equivalent constant stress amplitude and an associated number of cycles. This is done using the rain flow method and the Palmgren-Miner's formula for equivalent load. This process is used to determine the accumulated fatigue damage and how it compares to the fatigue damage observed in similar details during laboratory testing. Based on the comparison, the remaining fatigue life of a certain detail can be determined. The development of the design load for the Fatigue Limit State II is documented in Kulicki et. al. (2013) (SHRP R19B Report).

For concrete and reinforcement fatigue, Fatigue Limit State II is not used.

4.4.4 Fatigue Limit State I – The Maximum Moment Range Ratio

Fatigue limit state I is related to an infinite load-induced fatigue life. The fatigue load in this limit state reflects the load levels found to be representative of the maximum stress range of the truck population for an infinite fatigue-life design (*AASHTO LRFD,* 2012). In other words, if the majority of stress cycles is below a threshold magnitude, $(\Delta F)_{TH}$, failure will require so many load cycles that the considered detail will have an infinite fatigue life. The threshold stress, $(\Delta F)_{TH}$, is a boundary between the finite and infinite fatigue life, as shown in Figure 4-26.

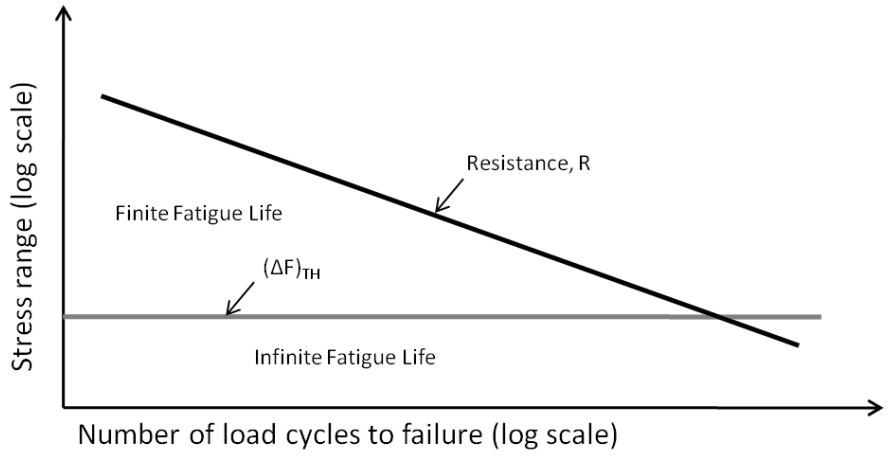

Figure 4-26 The Threshold Stress $(\Delta F)_{TH}$ on S-N Curve.

Fatigue limit state I refers to the stress value that has 1/10,000 probability of being exceeded. It is assumed that the distribution of stress has the same shape of the CDF as that of the corresponding moments. Therefore, the fatigue load analysis is performed using the developed CDFs for moments for various considered sites, cases and spans from 30 to 200 ft. The moment corresponding to the upper 0.01% is determined as a percentile corresponding to the probability of 0.9999 or 3.8 on the vertical axis in Figure 4-27. This moment represents the maximum stress range corresponding to an unlimited fatigue life. For example, for the WIM data from Arkansas (SPS-1) the moment for span of 120 ft corresponding to the upper 0.01% is 2505.5 k-ft, as shown in Figure 4-27.

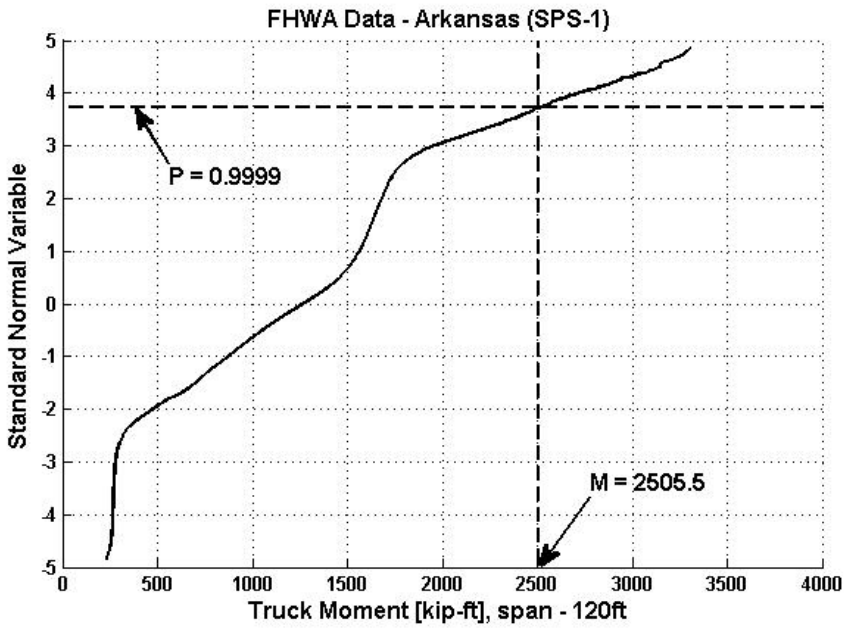

Figure 4-27 Moment Corresponding to the Upper 0.01%, Span = 120 ft.

The calculations were performed for the considered locations, cases and span lengths. The obtained values of moment were divided by the corresponding AASHTO fatigue truck moment. The results are summarized in Table 4-17 through Table 4-19.

Table 4-17 The Maximum Moment Range for Simply Supported Bridges at the Mid-Span

Simple Support - mid-span	# of Vehicles	"1/10000 Moment Cycle"					"1/10000 Moment" / HS20 Fatigue Moment				
		30	60	90	120	200	30	60	90	120	200
Arizona (SPS-1)	26501	424	1003	1761	2754	5640	1.74	1.84	1.63	1.70	1.84
Arizona (SPS-2)	1391098	308	765	1416	2246	4711	1.26	1.41	1.31	1.38	1.54
Arkansas (SPS-2)	1642334	352	860	1526	2460	5066	1.44	1.58	1.41	1.52	1.65
Colorado (SPS-2)	326017	336	814	1497	2409	4854	1.38	1.50	1.38	1.48	1.58
Delaware (SPS-1)	175889	454	1257	2302	3212	5735	1.86	2.31	2.12	1.98	1.87
Illinois (SPS-6)	821809	350	844	1480	2408	5033	1.43	1.55	1.37	1.48	1.64
Kansas (SPS-2)	456881	411	1018	1989	3112	6083	1.69	1.87	1.84	1.92	1.99
Louisiana (SPS-1)	70831	460	1237	2126	3332	6616	1.89	2.27	1.96	2.05	2.16
Maine (SPS-5)	172333	397	964	1722	2726	5549	1.63	1.77	1.59	1.68	1.81
Maryland (SPS-5)	124474	412	1038	1802	2599	5061	1.69	1.91	1.66	1.60	1.65
Minnesota (SPS-5)	47794	392	1111	2220	3316	6225	1.61	2.04	2.05	2.04	2.03
Pennsylvania(SPS-6)	1458818	402	1003	1730	2623	5291	1.65	1.84	1.60	1.62	1.73
Tennessee (SPS-6)	1583151	419	1020	1652	2387	4906	1.72	1.88	1.52	1.47	1.60
Virginia (SPS-1)	237804	369	946	1709	2562	5055	1.51	1.74	1.58	1.58	1.65
Wisconsin (SPS-1)	209239	393	968	1712	2717	5396	1.61	1.78	1.58	1.67	1.76

Table 4-18 The Maximum Moment Range for Continuous Bridges at the Middle Support

Continuous - Middle Support	# of Vehicles	"1/10000 Moment Cycle"					"1/10000 Moment" / HS20 Fatigue Moment				
		30	60	90	120	200	30	60	90	120	200
Arizona (SPS-1)	26501	-266	-701	-1026	-1608	-3089	1.45	1.95	1.94	2.11	2.30
Arizona (SPS-2)	1391098	-211	-549	-968	-1526	-3019	1.15	1.52	1.83	2.00	2.25
Arkansas (SPS-2)	1642334	-213	-643	-995	-1522	-3187	1.16	1.78	1.88	2.00	2.38
Colorado (SPS-2)	326017	-231	-579	-877	-1312	-2813	1.25	1.61	1.66	1.72	2.10
Delaware (SPS-1)	175889	-248	-650	-1173	-1643	-3303	1.35	1.80	2.21	2.16	2.46
Illinois (SPS-6)	821809	-207	-640	-1005	-1506	-3093	1.13	1.78	1.90	1.98	2.31
Kansas (SPS-2)	456881	-294	-755	-1015	-1469	-2937	1.60	2.10	1.92	1.93	2.19
Louisiana (SPS-1)	70831	-278	-815	-1128	-1539	-3255	1.51	2.26	2.13	2.02	2.43
Maine (SPS-5)	172333	-251	-694	-970	-1418	-2967	1.37	1.93	1.83	1.86	2.21
Maryland (SPS-5)	124474	-240	-592	-1049	-1564	-3281	1.31	1.64	1.98	2.05	2.45
Minnesota (SPS-5)	47794	-292	-695	-1034	-1487	-2753	1.59	1.93	1.95	1.95	2.05
Pennsylvania(SPS-6)	1458818	-245	-638	-1067	-1588	-3131	1.33	1.77	2.01	2.09	2.33
Tennessee (SPS-6)	1583151	-222	-628	-1025	-1559	-2977	1.21	1.74	1.93	2.05	2.22
Virginia (SPS-1)	237804	-223	-603	-973	-1477	-3010	1.21	1.67	1.84	1.94	2.24
Wisconsin (SPS-1)	209239	-250	-671	-953	-1394	-2892	1.36	1.86	1.80	1.83	2.16

Table 4-19 The Maximum Moment Range for Continuous Bridges at 0.4 of the Span Length

Continuous - 0.4L	# of Vehicles	"1/10000 Moment Cycle"					"1/10000 Moment" / HS20 Fatigue Moment				
		30	60	90	120	200	30	60	90	120	200
Arizona (SPS-1)	26501	399	976	1764	2769	5542	1.62	1.67	1.61	1.71	1.83
Arizona (SPS-2)	1391098	293	761	1431	2228	4636	1.19	1.30	1.30	1.37	1.53
Arkansas (SPS-2)	1642334	338	849	1527	2416	4914	1.37	1.45	1.39	1.49	1.62
Colorado (SPS-2)	326017	319	805	1528	2428	4857	1.30	1.38	1.39	1.50	1.60
Delaware (SPS-1)	175889	439	1279	2243	3141	5635	1.78	2.19	2.04	1.94	1.86
Illinois (SPS-6)	821809	334	814	1508	2399	4893	1.36	1.39	1.37	1.48	1.61
Kansas (SPS-2)	456881	394	1049	1983	3088	5988	1.60	1.79	1.81	1.90	1.98
Louisiana (SPS-1)	70831	458	1126	2174	3349	6486	1.86	1.92	1.98	2.06	2.14
Maine (SPS-5)	172333	377	937	1811	2768	5525	1.53	1.60	1.65	1.71	1.82
Maryland (SPS-5)	124474	406	1036	1817	2618	4941	1.65	1.77	1.65	1.61	1.63
Minnesota (SPS-5)	47794	382	1142	2134	3223	6065	1.55	1.95	1.94	1.99	2.00
Pennsylvania(SPS-6)	1458818	395	1020	1726	2608	5243	1.61	1.74	1.57	1.61	1.73
Tennessee (SPS-6)	1583151	416	1012	1636	2379	4868	1.69	1.73	1.49	1.47	1.61
Virginia (SPS-1)	237804	356	955	1704	2509	4947	1.45	1.63	1.55	1.55	1.63
Wisconsin (SPS-1)	209239	375	958	1705	2662	5326	1.53	1.64	1.55	1.64	1.76

4.4.5 Statistical Parameters of Fatigue Live Load

The objective was to determine the statistical parameters of fatigue load for the Fatigue I limit state (LS) that can be considered as representative for a national load. The ratios of "1/10000 Moment" to “HL-93 Fatigue Moment” were plotted on normal probability paper in Figure 4-28 through Figure 4-30. Each point on the graphs represents one of 15 sites considered.

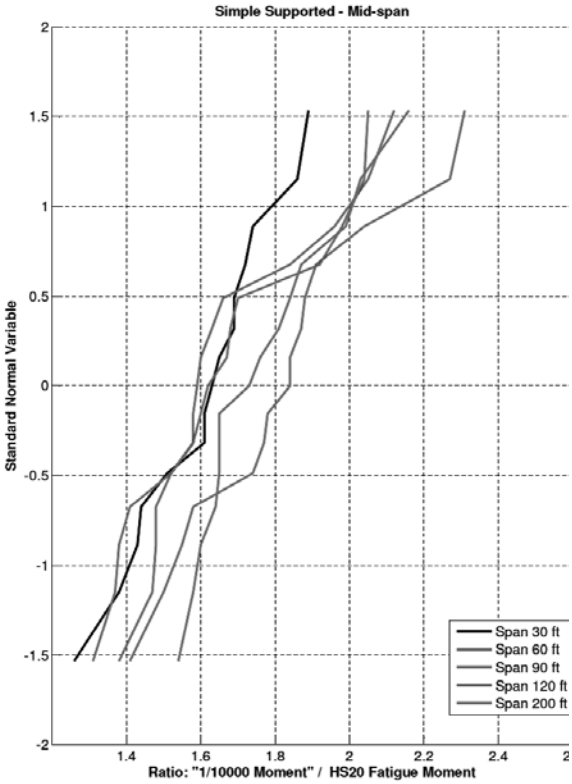

Figure 4-28 The Maximum Moment Range Ratio (Fatigue LS I) for Simple Supported Bridges at the Mid-Span.

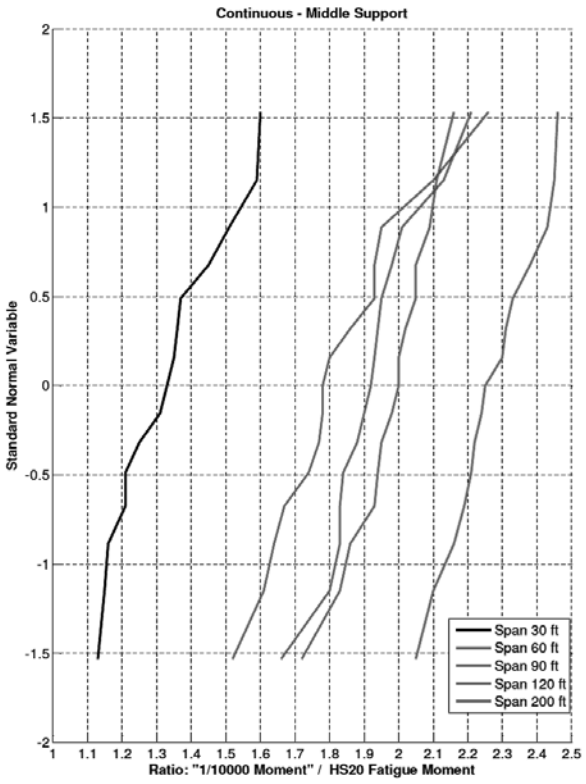

Figure 4-29 The Maximum Moment Range Ratio (Fatigue LS I) for Continuous Bridges at the Middle Support.

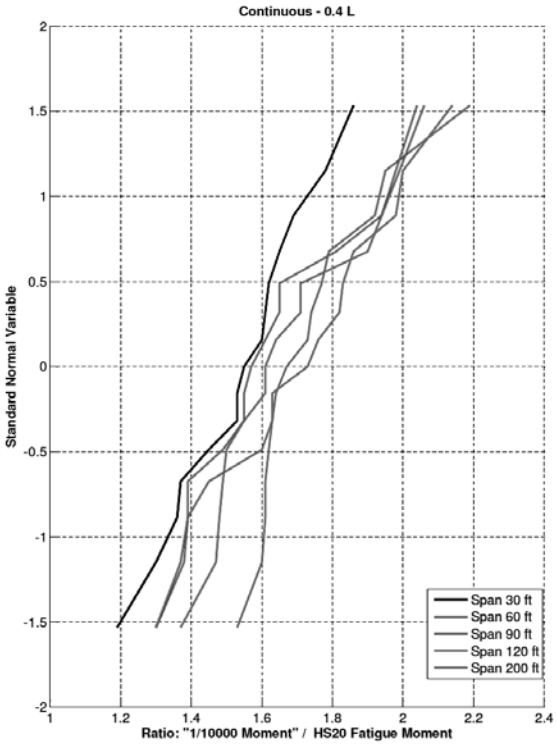

Figure 4-30 The Maximum Moment Range Ratio (Fatigue LS I) for Continuous Bridges at 0.4 of the Span Length.

To determine the statistical parameters from the graphs, a straight line was fitted for each distribution. A straight line corresponds to the normal distribution on the normal probability paper. The intersection of the straight line with the horizontal axis is at the mean value. The standard deviation is determined from the slope of the straight line. The statistical parameters of fatigue load based on 15 considered sites, i.e. mean, μ, and COV, calculated as the ratio of standard deviation, σ to the mean, μ, are listed in Table 4-20.

It is assumed that the considered 15 WIM locations are representative for truck traffic in the United States. For the purpose of further reliability analysis, it is recommended to assume that the mean fatigue load is equal to the mean for 15 WIM locations plus 1.5 standard deviations, 1.5 σ. The probability of exceeding this value is about 5%; 95% of sites in the United States are below this value as is shown on Figure 4-31. The moment ratios corresponding to the mean plus 1.5 standard deviations for Fatigue I limit state are also listed in Table 4-20.

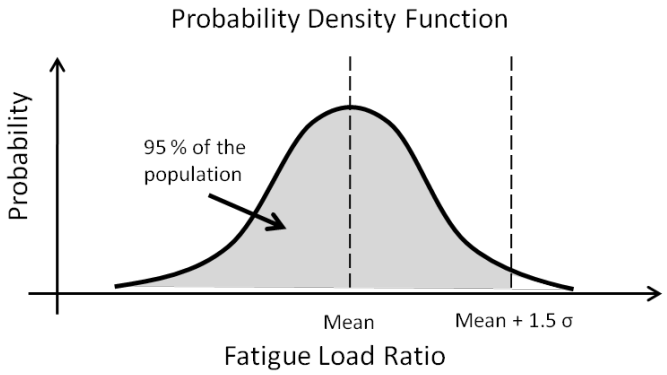

Figure 4-31 Probability Density Function of the National Fatigue Load.

The statistical parameters were calculated for all considered cases and span length.

Table 4-20 The Maximum Moment Range Ratio for Fatigue I LS

The Maximum Moment Range Ratio for Fatigue I LS				
	Span	**Mean**	**Mean+1.5 σ**	**COV**
Simple Supported Mid-span	30 ft	1.6	1.90	0.13
	60 ft	1.83	2.24	0.15
	90 ft	1.6	1.96	0.15
	120 ft	1.64	1.88	0.10
	200 ft	1.7	2.15	0.18
Continuous Middle Support	30 ft	1.35	1.61	0.13
	60 ft	1.81	2.13	0.12
	90 ft	1.92	2.18	0.09
	120 ft	1.97	2.17	0.07
	200 ft	2.27	2.47	0.06
Continuous 0.4 L	30 ft	1.54	1.86	0.14
	60 ft	1.67	2.06	0.16
	90 ft	1.6	1.92	0.13
	120 ft	1.65	1.97	0.13
	200 ft	1.72	2.11	0.15

The values at the middle support are expected to be lower than shown in Table 4-20 due to fanning of the reaction force through the height of the beams and because the actual support is not a knife edge support. This was taken into account when recommending a revised load factor for Fatigue I limit state.

4.4.6 Recommendations

The analysis resulted in the relatively tightly clustered moment range ratios shown in Table 4-20 for the Fatigue I limit state. As with previous live load recommendations herein, the values to be considered for calibration are the moment ratios at the “mean plus 1.5 standard deviations” and the COVs. Therefore, for simplicity, the recommended values for the calibration of the fatigue limit states are further simplified into single values independent of span length. For Fatigue I limit state, it is recommended to use stress ranges (loads) based on 2.0 HL-93 and a COV=0.12.

The calibration of the fatigue limit state for concrete and reinforcement is detailed in Chapter 5.

4.5 Development of Overload and Permit Load Parameters

4.5.1 Based on WIM Data

4.5.1.1 Load Model

Heavy vehicles in the WIM data are assumed to be either permit vehicles or illegally overloaded vehicles. WIM data was used as the basis for estimating how often a given design moment (or shear) is exceeded. Table 4-21 shows the number of times the live load moment exceeded 100% of HL-93, 110% of HL-93, 120% of HL-93 and 130% of HL-93 for 32 WIM sites. One of the sites clearly has a unique traffic pattern – Florida Route 29. The Florida Department of Transportation was contacted about this site and it was determined that truck traffic from several other highways were being directed onto this road and that undoubtedly accounted for the relatively large number of times the HL-93 was exceeded for the various percents indicated. Additionally, the total number of times the various ratios of HL-93 were exceeded, excluding Florida Route 29, are shown in the table, as well as the average number per site.

Notice that data was collected for most, but not all, sites for a full year. The data was scaled to one year and the scaled data is shown in Table 4-22. The average rate of exceedance in Table 4-23 is higher than Table 4-22 because the data was collected for less than one year at a number of sites. These sites are those showing increased number incidents in Table 4-23 than in Table 4-22.

Figure 4-32 shows the average accumulative rate of exceedance for the 31 remaining WIM sites by HL-93 ratio for each span length considered. Figure 4-33 shows the same information by span for each HL-93 ratio considered. The reduction in the rate of exceedance with increasing HL-93 ratio is clear.

Table 4-21 Number of Times WIM Moments Exceeded a Factored HL-93 Loadings

	MOMENT														
	Ratio Truck/HL-93 >= 1.1					Ratio Truck/HL-93 >= 1.2					Ratio Truck/HL-93 >= 1.3				
Site	**30 ft**	**60 ft**	**90 ft**	**120 ft**	**200 ft**	**30 ft**	**60 ft**	**90 ft**	**120 ft**	**200 ft**	**30 ft**	**60 ft**	**90 ft**	**120 ft**	**200 ft**
AZ SPS-1	1	0	0	0	0	0	0	0	0	0	0	0	0	0	0
AZ SPS-2	0	0	1	1	0	0	0	0	0	0	0	0	0	0	0
AR SPS-2	2	7	3	0	0	0	3	0	0	0	0	0	0	0	0
CO SPS-2	0	2	5	4	0	0	0	2	0	0	0	0	0	0	0
DE SPS-1	36	33	22	11	0	10	22	10	1	0	1	11	1	0	0
IL SPS-6	0	0	1	0	0	0	0	0	0	0	0	0	0	0	0
IN SPS-6	3	11	11	10	2	2	4	5	4	0	0	0	1	0	0
KS SPS-2	16	33	35	31	2	7	16	17	7	0	6	7	6	0	0
LA SPS-1	44	6	12	14	7	26	6	7	7	0	6	6	5	4	0
ME SPS-5	4	4	5	2	0	0	4	2	0	0	0	2	0	0	0
MD SPS-5	5	6	2	2	0	0	1	1	0	0	0	1	0	0	0
MN SPS-5	7	5	6	5	0	4	2	2	1	0	2	1	1	0	0
NM SPS-1	0	1	1	1	0	0	0	0	0	0	0	0	0	0	0
NM SPS-5	3	1	1	2	0	2	0	0	0	0	0	0	0	0	0
PA SPS-6	32	22	17	14	1	13	17	13	1	0	3	13	2	0	0
TN SPS-6	53	4	4	0	0	5	1	0	0	0	1	0	0	0	0
VA SPS-	0	0	1	1	0	0	0	0	0	0	0	0	0	0	0
WI SPS-1	1	0	3	3	1	0	0	1	1	0	0	0	0	0	0
CA Antelope EB	0	1	0	0	5	0	0	0	0	0	0	0	0	0	0
CA Antelope WB	0	5	4	13	28	0	0	0	1	9	0	0	0	0	1
CA Bowman	0	0	0	1	1	0	0	0	0	1	0	0	0	0	0
CA LA-710 NB	1	31	50	51	15	0	6	24	19	0	0	0	4	1	0
CA LA-710 SB	1	17	45	48	14	0	3	18	19	0	0	0	1	1	0
CA Lodi	0	4	16	46	140	0	0	1	2	32	0	0	0	0	2
FL I-10	79	40	46	75	37	22	16	14	17	5	10	5	4	5	2
FL I-95	0	0	0	0	0	0	0	0	0	0	0	0	0	0	0
FL US-29	653	495	322	245	106	360	266	174	119	51	177	160	82	59	21
MS I-10	24	22	31	33	22	7	2	10	19	2	2	2	2	2	1
MS I-55UI	0	0	0	1	2	0	0	0	0	0	0	0	0	0	0
MS I-55R	19	30	48	58	32	7	8	16	21	19	2	3	5	8	9
MS US-49	0	0	2	1	0	0	0	0	0	0	0	0	0	0	0
MS US-61	0	0	1	2	1	0	0	1	1	0	0	0	0	0	0
	Ratio Truck/HL-93 >= 1.1					**Ratio Truck/HL-93 >= 1.2**					**Ratio Truck/HL-93 >= 1.3**				
	30 ft	**60 ft**	**90 ft**	**120 ft**	**200 ft**	**30 ft**	**60 ft**	**90 ft**	**120 ft**	**200 ft**	**30 ft**	**60 ft**	**90 ft**	**120 ft**	**200 ft**
Total W/O FL 29	331	285	373	430	310	105	111	144	121	68	33	51	32	21	15
Average per site	10.7	9.2	12.0	13.9	10.0	3.4	3.6	4.6	3.9	2.2	1.1	1.6	1.0	0.7	0.5

Table 4-22 Exceedances Per Year

	MOMENT – Exceedances Per Year																			
	Ratio Truck/HL-93 >= 1.0					Ratio Truck/HL-93 >= 1.1					Ratio Truck/HL-93 >= 1.2					Ratio Truck/HL-93 >= 1.3				
Site	30 ft	60 ft	90 ft	120 ft	200 ft	30 ft	60 ft	90 ft	120 ft	200 ft	30 ft	60 ft	90 ft	120 ft	200 ft	30 ft	60 ft	90 ft	120 ft	200 ft
AZ SPS-1	4	0	0	1	0	1	0	0	0	0	0	0	0	0	0	0	0	0	0	0
AS SPS-2	0	2	6	5	0	0	0	1	1	0	0	0	0	0	0	0	0	0	0	0
AR SPS-2	14	10	17	10	0	2	7	3	0	0	0	3	0	0	0	0	0	0	0	0
CO SPS-2	0	5	6	6	2	0	2	5	4	0	0	0	2	0	0	0	0	0	0	0
DE SPS-1	140	48	33	27	1	36	33	22	11	0	10	22	10	1	0	1	11	1	0	0
IL SPS-6	1	3	4	4	1	0	0	1	0	0	0	0	0	0	0	0	0	0	0	0
IN SPS-6	27	32	24	19	14	5	19	19	17	3	3	7	9	7	0	0	0	2	0	0
KS SPS-2	42	47	80	96	10	16	33	35	31	2	7	16	17	7	0	6	7	6	0	0
LA SPS-1	76	16	25	30	13	44	6	12	14	7	26	6	7	7	0	6	6	5	4	0
ME SPS-5	6	7	8	7	1	4	4	5	2	0	0	4	2	0	0	0	2	0	0	0
MD SPS-5	25	8	8	2	1	5	6	2	2	0	0	1	1	0	0	0	1	0	0	0
MN SPS-5	9	8	18	19	2	7	5	6	5	0	4	2	2	1	0	2	1	1	0	0
NM SPS-1	1	1	1	3	0	0	1	1	1	0	0	0	0	0	0	0	0	0	0	0
NM SPS-5	12	7	7	9	4	4	1	1	3	0	3	0	0	0	0	0	0	0	0	0
PA SPS-6	155	45	22	21	1	32	22	17	14	1	13	17	13	1	0	3	13	2	0	0
TN SPS-6	2085	29	8	7	0	53	4	4	0	0	5	1	0	0	0	1	0	0	0	0
VA SPS-1	7	10	1	2	1	0	0	1	1	0	0	0	0	0	0	0	0	0	0	0
WI SPS-1	6	3	5	4	2	1	0	3	3	1	0	0	1	1	0	0	0	0	0	0
CA Antelope EB	0	13	25	31	25	0	1	0	0	7	0	0	0	0	0	0	0	0	0	0
CA Antelope WB	0	30	71	100	84	0	7	6	19	40	0	0	0	1	13	0	0	0	0	1
CA Bowman	0	3	3	8	16	0	0	0	3	3	0	0	0	0	3	0	0	0	0	0
CA LA-710 NB	10	99	150	153	85	1	34	55	56	16	0	7	26	21	0	0	0	4	1	0
CA LA-710 SB	3	62	105	111	54	1	17	45	48	14	0	3	18	19	0	0	0	1	1	0
CA Lodi	0	110	137	281	417	0	5	19	55	168	0	0	1	2	38	0	0	0	0	2
FL I-10	279	141	159	264	152	81	41	47	77	38	23	16	14	18	5	10	5	4	5	2
FL I-95	0	0	0	0	0	0	0	0	0	0	0	0	0	0	0	0	0	0	0	0
MS I-10	41	48	53	53	44	26	24	34	36	24	8	2	11	21	2	2	2	2	2	1
MS I-55UI	0	4	5	11	8	0	0	0	1	3	0	0	0	0	0	0	0	0	0	0
MS I-55R	142	100	255	349	89	20	31	50	61	33	7	8	17	22	20	2	3	5	8	9
MS US-49	0	3	11	13	7	0	0	2	1	0	0	0	0	0	0	0	0	0	0	0
MS US-61	0	1	5	8	6	0	0	1	2	1	0	0	1	1	0	0	0	0	0	0
FL US-29	1291	995	651	496	204	673	510	332	253	109	371	274	179	123	53	183	165	85	61	22
Annual Average	99.6	28.9	40.4	53.4	33.6	11.0	9.8	12.8	15.1	11.7	3.5	3.7	4.9	4.2	2.6	1.1	1.7	1.1	0.7	0.5

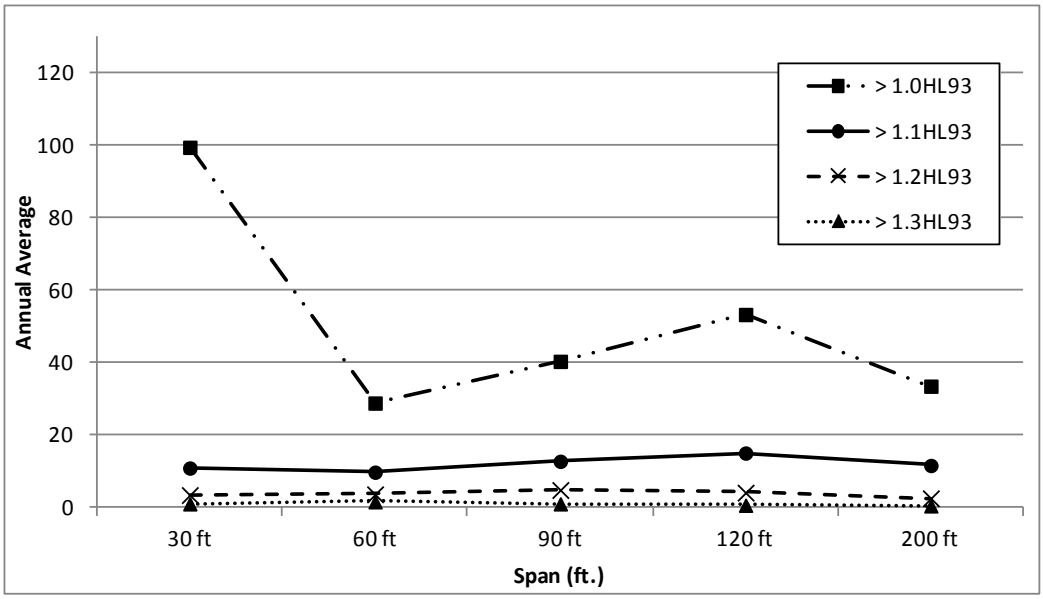

Figure 4-32 Annual Average Exceedances Versus Span.

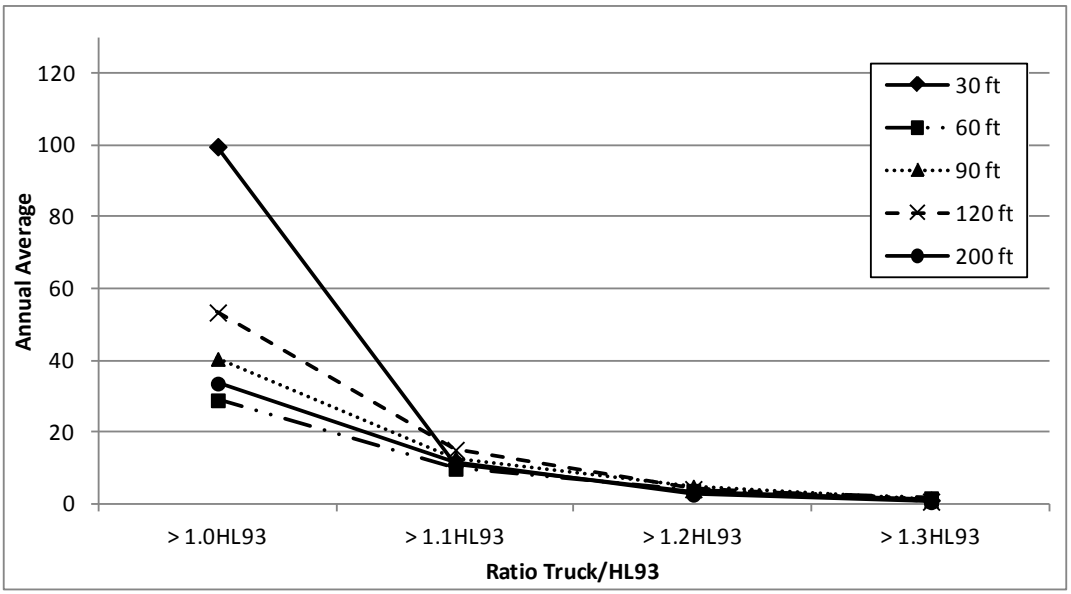

Figure 4-33 Annual Average Exceedances Versus Ratio Truck/HL-93.

A more meaningful assessment of the exceedance rate is presented in Table 4-23 and Figure 4-34 and Figure 4-35. In this case, the exceedance data has been scaled for a number of vehicles based on a single lane ADTT of 2500 at each site assuming that the distribution of trucks is the same, i.e. the data is scalable. The average rate of exceedance in Table 4-23 is higher than Table 4-22 because many of the WIM sites were on roads with single lane ADTTs less than 2500. Nevertheless, the rate at which 1.3 HL-93 is exceeded is quite low. The values in Table 4-23 can be scaled for locations with a single lane ADTT other than 2500 with the same assumption of scalability.

Table 4-23 Events Per Year Scaled to ADTT = 2500

	MOMENT – Events Per Year Scaled to ADTT = 2500																			
	Ratio Truck/HL-93 >= 1.0					Ratio Truck/HL-93 >= 1.1					Ratio Truck/HL-93 >= 1.2					Ratio Truck/HL-93 >= 1.3				
Site	**30 ft**	**60 ft**	**90 ft**	**120 ft**	**200 ft**	**30 ft**	**60 ft**	**90 ft**	**120 ft**	**200 ft**	**30 ft**	**60 ft**	**90 ft**	**120 ft**	**200 ft**	**30 ft**	**60 ft**	**90 ft**	**120 ft**	**200 ft**
AZ SPS-1	103	0	0	26	0	0	0	0	0	0	0	0	0	0	0	0	0	0	0	0
AS SPS-2	0	1	4	3	0	0	0	1	1	0	0	0	0	0	0	0	0	0	0	0
AR SPS-2	8	5	9	5	0	1	4	2	0	0	0	2	0	0	0	0	0	0	0	0
CO SPS-2	0	13	16	16	5	0	5	13	11	0	0	0	5	0	0	0	0	0	0	0
DE SPS-1	633	217	149	122	5	163	149	100	50	0	45	100	45	5	0	5	50	5	0	0
IL SPS-6	1	3	4	4	1	0	0	1	0	0	0	0	0	0	0	0	0	0	0	0
IN SPS-6	79	94	69	54	39	15	54	54	49	10	10	20	25	20	0	0	0	5	0	0
KS SPS-2	80	90	153	183	19	31	63	67	59	4	13	31	32	13	0	11	13	11	0	0
LA SPS-1	808	170	266	319	138	468	64	128	149	74	277	64	74	74	0	64	64	53	43	0
ME SPS-5	30	35	40	35	5	20	20	25	10	0	0	20	10	0	0	0	10	0	0	0
MD SPS-5	139	44	44	11	6	28	33	11	11	0	0	6	6	0	0	0	6	0	0	0
MN SPS-5	148	131	296	312	33	115	82	99	82	0	66	33	33	16	0	33	16	16	0	0
NM SPS-1	8	8	8	16	0	0	8	8	8	0	0	0	0	0	0	0	0	0	0	0
NM SPS-5	45	/	/	*	8	8	2	2	3	0	3	0	0	0	0	0	0	0	0	0
PA SPS-6	95	27	13	13	1	20	13	10	9	1	8	10	8	1	0	2	8	1	0	0
TN SPS-6	1173	16	4	4	0	30	2	2	0	0	3	1	0	0	0	1	0	0	0	0
VA SPS-1	25	35	4	7	4	0	0	4	4	0	0	0	0	0	0	0	0	0	0	0
WI SPS-1	24	12	20	16	8	4	0	12	12	4	0	0	4	4	0	0	0	0	0	0
CA Antelope EB	0	10	20	24	20	0	1	0	0	5	0	0	0	0	0	0	0	0	0	0
CA Antelope WB	0	20	48	68	57	0	5	4	13	27	0	0	0	1	9	0	0	0	0	1
CA Bowman	0	1	1	4	8	0	0	0	1	1	0	0	0	0	1	0	0	0	0	0
CA LA-710 NB	2	20	31	31	17	0	7	11	11	3	0	1	5	4	0	0	0	1	0	0
CA LA-710 SB	1	12	21	22	11	0	3	9	9	3	0	1	4	4	0	0	0	0	0	0
CA Lodi	0	25	32	65	96	0	1	4	13	39	0	0	0	1	9	0	0	0	0	1
FL I-10	151	76	86	142	82	44	22	26	42	21	12	9	8	9	3	6	3	2	3	1
FL I-95	0	0	0	0	0	0	0	0	0	0	0	0	0	0	0	0	0	0	0	0
MS I-10	0	2	3	6	4	0	0	0	1	1	0	0	0	0	0	0	0	0	0	0
MS I-55UI	0	2	3	6	4	0	0	0	1	1	0	0	0	0	0	0	0	0	0	0
MS I-55R	93	66	167	229	58	13	21	33	40	22	5	5	11	14	13	1	2	3	5	6
MS US-49	0	2	8	10	5	0	0	1	1	0	0	0	0	0	0	0	0	0	0	0
MS US-61	0	6	23	40	29	0	0	6	11	6	0	0	6	6	0	0	0	0	0	0
FL US-29	2922	2252	1473	1122	462	1524	1155	751	572	247	840	621	406	278	119	413	373	191	138	49
Annual Average	117.0	37.8	50.6	58.7	21.7	32.0	18.4	20.8	19.8	7.5	14.3	9.7	9.1	5.8	1.2	4.0	5.6	3.2	**1.7**	0.3

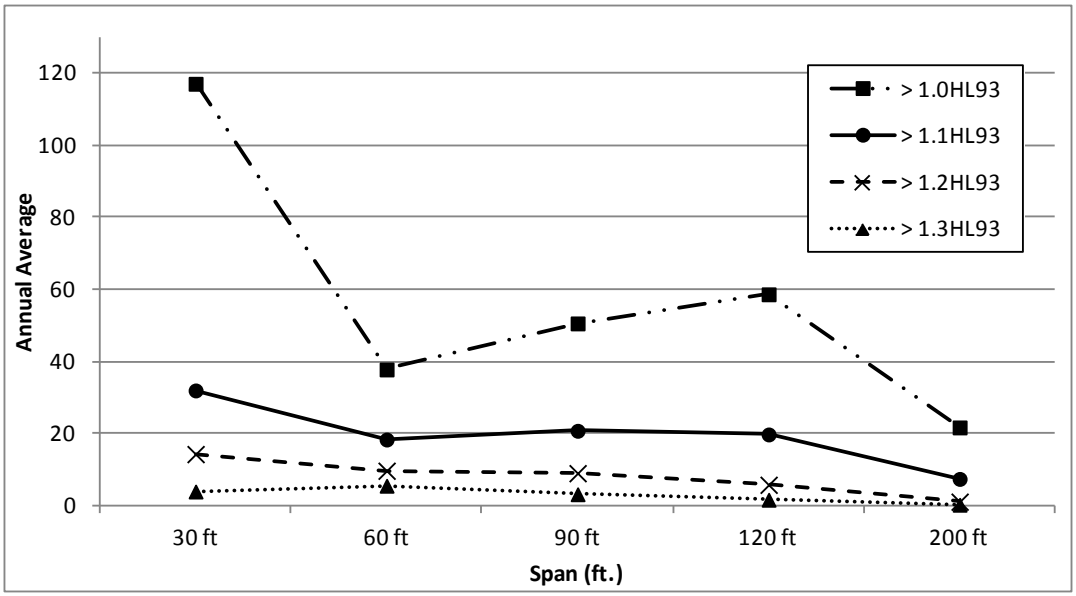

Figure 4-34 Annual Average Events Scaled to ADTT = 2500 Versus Span.

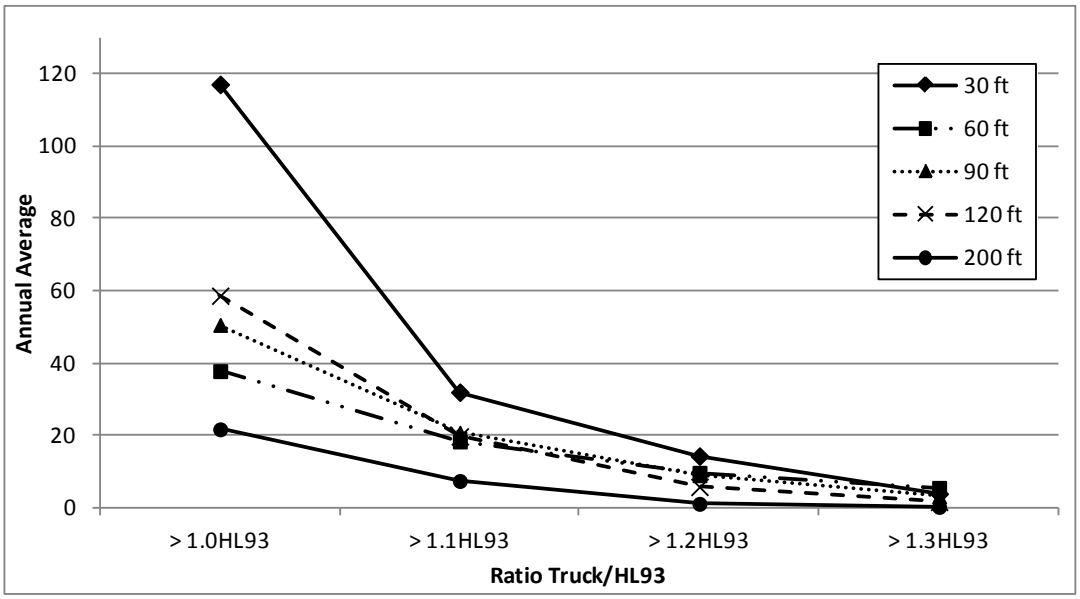

Figure 4-35 Annual Average Events Scaled to ADTT = 2500 Versus Ratio Truck/HL-93.

The issue of number of loaded lanes was discussed in Section 4.2.4. For the WIM sites where data was recorded in two lanes, and given the definition of correlated events in that discussion, it was shown that the number of events of multiple lanes loaded with correlated trucks was quite small, and the histograms of GVW showed that the number of events of two heavy trucks was even smaller. It was concluded that multiple lanes of heavy trucks need not be considered for the service limit states. Thus it is concluded that in most cases design for multiple lanes of overload is not necessary. Furthermore, no MPF needs to be applied on the load side of the limit state function when calibrating for overloads.

To summarize, based on a review of the WIM data:

- Site-specific consideration of sites with unusually high volumes of heavy trucks is warranted
- Design for a single lane loading is justified by this study
- Elimination of the single lane MPF of 1.20 when investigating service limit states under overload vehicles is justified by this study

4.5.2 Based on Louisiana Permit Load Citations

Louisiana DOTD provided a compilation of truck citations issued in the state in 2009. Due to missing needed information, the data was not sufficient for calibration. Nevertheless, the data was analyzed to provide insight into the nature of permit vehicles.

The data includes information about the vehicle class according to the Louisiana Regulations for Trucks, actual and permitted GVW, number of axle sets, number of axles for each axle set, axle set scale weight and axle set legal weight. Vehicles classified as Type 9999 are considered to be permit vehicles. It was observed that most of the violations were due to incorrect load distribution resulting in violation of the allowable axle set weight rather than exceeding of the gross vehicle weight.

The data did not include the weight of individual axles or axle spacing. This limited the value of the data to investigating the statistical parameters of the vehicle GVW and precluded determining the statistical parameters of the load effects by running the trucks across spans of different length. It is also important to note that while the vehicles stopped represent a sample of the entire population of legal and permit vehicles; the vehicles in the database only represent those that were cited.

The original data included 50,257 records. A number of records were eliminated from the set as they included no axle set loads (1456) or included obvious errors, e.g. two records included axle loads below 100 pounds. The remaining number of records was 48,799. These records included both permit and legal loads. Out of these, 869 records were designated as Type 9999 which indicates they were permit vehicles.

Each vehicle had two different permitted GVWs listed; one for interstate highways and one for non-interstate routes. For all vehicles, the non-interstate GVW was equal to or higher than the interstate GVW. The permitted individual axle set weight was the same for both the interstate and non-interstate roads. For many trucks, the sum of the permitted individual axle weights exceeded the permitted GVW which indicated that when the truck reaches its permitted GVW, some axle sets will have to be lower than their permitted weight.

Table 4-24 gives a statistics of the violations when all permit vehicles are considered (869 records).

Table 4-25 shows the statistics when only permit vehicles with a legal load above 80,000 lbs are considered (680 records). As the data did not classify the type of road, the analyses were performed once assuming all vehicles were on interstate roads and then were repeated assuming all vehicles were on non-interstate roads.

When all records are considered:

- About 39.9% and 40.7% of the citations considering interstate and non-interstate roads, respectively, were for reasons other than GVW or axle group weights. No reason was given for non-load-related citations but it is assumed that the citations are related to the geometric characteristics of the trucks including axle spacing and tire width.
- The GVW exceeded the permitted in 31.1% and 30.0% of the records for interstate and non-interstate roads, respectively
- For both interstate and non-interstate roads, one or more axle group exceeded the permitted axle group weight in 46.4% of the records, while the GVW was not exceeded
- About 13.7% and 12.9% of the citations considering interstate and non-interstate roads, respectively, indicated the permitted GVW was exceeded while none of the permitted axle group weights were exceeded

Table 4-24 Statistics of Cited Vehicles When All Permit Vehicles are Considered

	Total Number of Records	No of violators (Interstate)	No of violators (Non-Interstate)
No of violations not related to axle group weight or GVW	869	347	354
Steering axle (axle set 1)(*)	869	85	85
Axle set 2 (*)	864	233	233
Axle set 3 (*)	816	183	183
Axle set 4 (*)	168	33	33
Axle set 5 (*)	54	7	7
GVW exceeding permitted	869	270	261
GVW exceeding permitted with no axle group exceeding permitted	869	119	112
One or more axle group exceeding permitted with GVW exceeding permitted	869	151	149
Vehicles with one or more axle groups exceeding permitted	869	403	403
Vehicles with one or more axle groups exceeding permitted with GVW less than permitted	869	252	254
Axle groups exceeding permitted	2771 axle groups	541	541

(*) Number of axle groups in each record varied from 1 to 5. Five records represented one-axle-group dollies. These records showed one axle group instead of a steering axle.

Table 4-25 Statistics of Cited Permit Vehicles When Only Vehicles with GVW Greater Than 80,000 lbs are Considered

	Interstate		Non-Interstate	
	Total Number of Records	No of violators	Total Number of Records	No of violators
Steering axle (axle set 1)	680	78	681	78
Axle set 2 (*)	676	180	677	180
Axle set 3 (*)	640	165	641	165
Axle set 4 (*)	141	31	142	31
Axle set 5 (*)	49	7	49	7
GVW exceeding permitted	680	162	681	154
GVW exceeding permitted with no axle group exceeding permitted	680	42	681	36
One or more axle group exceeding permitted with GVW exceeding permitted	680	120	681	118
Vehicles with one or more axle groups exceeding permitted	680	336	681	336
Vehicles with one or more axle groups exceeding permitted with GVW less than permitted	680	216	681	218
Axle groups exceeding permitted	2186 axle groups	461	2190 axle groups	461

(*) Number of axle groups in each record varied from 1 to 5. Four records represented one-axle-group dollies. These records showed that the vehicle contain one axle group instead of listing a steering axle followed by other axle groups.

When only records with permitted GVW greater than 80,000 lbs are considered:

- About 44.4% and 45.4% of the citations considering interstate and non-interstate roads, respectively, were for reasons other than GVW or axle group weights.
- The GVW exceeded the permitted in 23.8% and 22.6 of the records for interstate and non-interstate roads, respectively
- One or more axle group exceeded the permitted axle group weight 31.7% and 32.0% of the records for interstate and non-interstate roads, respectively, while the GVW was not exceeded
- The permitted GVW was exceeded while none of the permitted axle group weights were exceeded in 6.2% and 5.3% of the records for interstate and non-interstate roads, respectively

Comparing the results for all the records to those for records of vehicles with permitted GVW greater than 80,000 lbs indicates that the latter are slightly more likely to be cited for reasons other than weight-related issues. In other words, heavier vehicles are less likely to violate the permitted axle group weights and GVW.

The gross vehicle weight (GVW) of Louisiana permit trucks (Type 9999) from citation data was plotted on normal probability paper. For comparison, the CDF's of the GVW of the vehicles in the WIM data from Louisiana (LA SPS-1) and GVW of the permit vehicles were

plotted in Figure 4-36. The shape of CDF of permit vehicles is similar to the upper tail of the WIM data from Louisiana; the part representing heavier vehicles.

Ratio of axle set scale weight and allowable axle set weight for axle sets with different number of axles was calculated and plotted on the normal probability paper as shown on Figure 4-37.

Ratio of GVW and allowable GVW for all permit vehicles was calculated and plotted on the normal probability paper as shown on Figure 4-38. The relationship between GVW and the ratio of GVW and allowable GVW is shown in Figure 4-39.

The Louisiana violation data did not include any information about the axle spacing, therefore, the load effect (moment or shear) due to a permit truck passage cannot be calculated. However, Laman and Nowak (Laman 1993) observed that the GVW and load effect due to a truck passage (moment) are highly correlated as shown in Figure 4-40. For longer spans, such as 120 and 200 ft, the correlation is almost perfectly linear. For shorter spans, the correlation is also linear for a significant range of truck weights but with a higher degree of variation for heavier vehicles. For shorter spans, the maximum moment due to a truck passage is often caused by a group of axles rather than the GVW of the truck.

Therefore, the shape of the cumulative distribution function of the load effect (moment) is very similar to the CDF of GVW due to the correlation between the two.

The statistical parameters of permit vehicles in the database are determined by considering the distribution of ratio of actual GVW and allowable GVW, as shown on Figure 4-38. From this figure, the bias factor is taken as 1.0 and the coefficient of variation is 10%. However, for shorter span lengths, below 90 ft, where axle set weight governs, the coefficient of variation is taken as 20% due to a higher variation in ratio of axle set scale weight and permitted axle set weight. These values are based on analyzing the curves in Figure 4-37.

Figure 4-39 shows the relationship between the permitted GVW and the actual GVW. Out of 869 vehicles, 162 had a permitted GVW between 70 kips and 80 kips, inclusive, and 133 vehicles had a permitted GVW between 80.01 kips and 85 kips. Figure 4-39 indicates that the worst violators are concentrated in these two groups. When the GVW is violated, heavier vehicles tend to exceed the permitted value by a smaller percentage than lighter vehicles.

Table 4-26 shows the total number of vehicles and the number of vehicles with scale GVW exceeding the permitted GVW. A breakdown of the ratio of scale GVW to permitted GVW is also included. The results in Table 4-26 and in Figure 4-37 indicate that the worst violators are the vehicles with permitted GVW between 70 kips and 85 kips, inclusive. The heavier the permitted GVW, the lower the percentage of vehicles with scale GVW exceeding the permitted GVW. In addition, when in violation, the maximum ratio of scale GVW to permitted GVW is typically lower for heavier vehicles. For example:

- For the 295 vehicles with permitted GVW between 70 kips to 85 kips, inclusive, 47 vehicles (15.9%) has a ratio greater than 1.25.
- For the 105 vehicles with permitted GVW between 85.01 kips to 100 kips, inclusive, two vehicles (1.9%) has a ratio greater than 1.25 (1.55 and 1.27). The next highest ratio is 1.14.

- For the 147 vehicles with permitted GVW between 100.01 kips to 125 kips, inclusive, one vehicle (0.68%) has a ratio greater than 1.25 (1.257). The next highest ratio is 1.16.
- For the 295 vehicles with permitted GVW above 125 kips the highest ratio is 1.07 with no ratio above 1.02 for vehicles with permitted GVW above 150 kips.

The tendency of haulers to violate the permitted weights is dependent on the level of enforcement, the amount of the fine for the violation and the availability of a permit legally covering the load they need to move, i.e. the maximum loads allowed by the issuing state. Therefore, the analysis of the Louisiana violations data can only be generalized to other states with similar level of enforcement, level of fines and similar collection of permit vehicles.

In addition, the total number of vehicles that were stopped but were found in conformance with the permits is not known. Therefore, the statistics of the entire population of permit vehicles, in conformance and in violation of the permits, could not be determined using the available information.

Table 4-26 Number of GVW Violations Per Weight Class for Louisiana Permit Vehicles

	Total No. of Records	No. of GVW violations	Ratio of actual GVW/Permitted GVW					
			R < 1.0	1.0 < R ≤ 1.25	1.25 < R ≤ 1.5	1.5 < R ≤ 1.75	1.75 < R ≤ 2.0	R>2.0
Permitted GVW < 70	27	8	19	6	0	1	0	1
70 ≤ Permitted GVW ≤ 80	162	100	62	80	9	4	4	3
80 < Permitted GVW ≤ 85	133	96	37	69	10	9	7	1
85 < Permitted GVW ≤ 100	105	14	91	12	1	1	0	0
100 < Permitted GVW ≤ 125	147	24	123	23	1	0	0	0
125 < Permitted GVW ≤ 150	159	14	145	14	0	0	0	0
150 < Permitted GVW ≤ 175	92	13	79	13	0	0	0	0
175 < Permitted GVW ≤ 200	24	0	24	0	0	0	0	0
200 < Permitted GVW ≤ 250	19	0	19	0	0	0	0	0
Permitted GVW >250	1	1	0	1	0	0	0	0
Total	869	270						

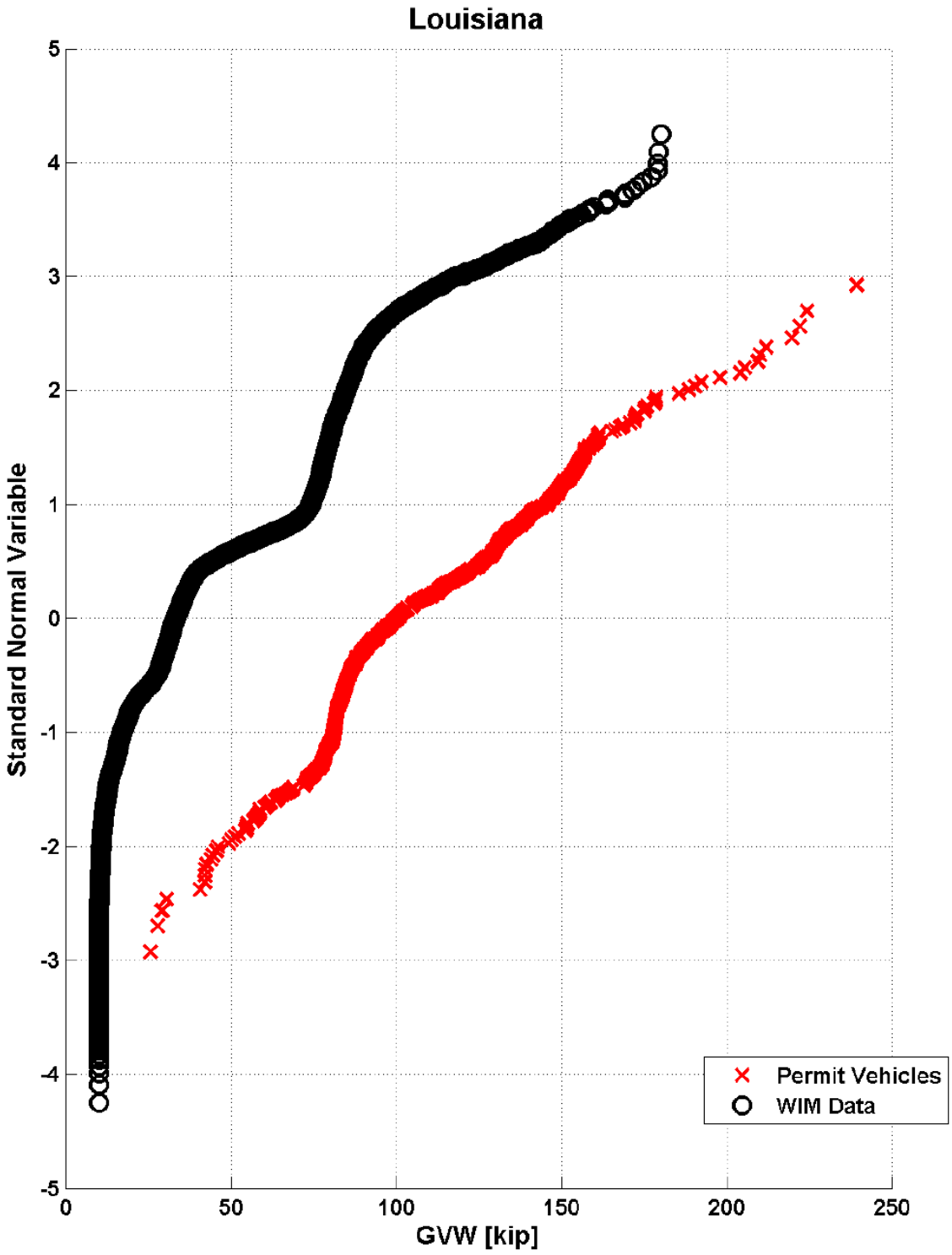

Figure 4-36 Gross Vehicle Weight of Louisiana Permit and WIM Trucks

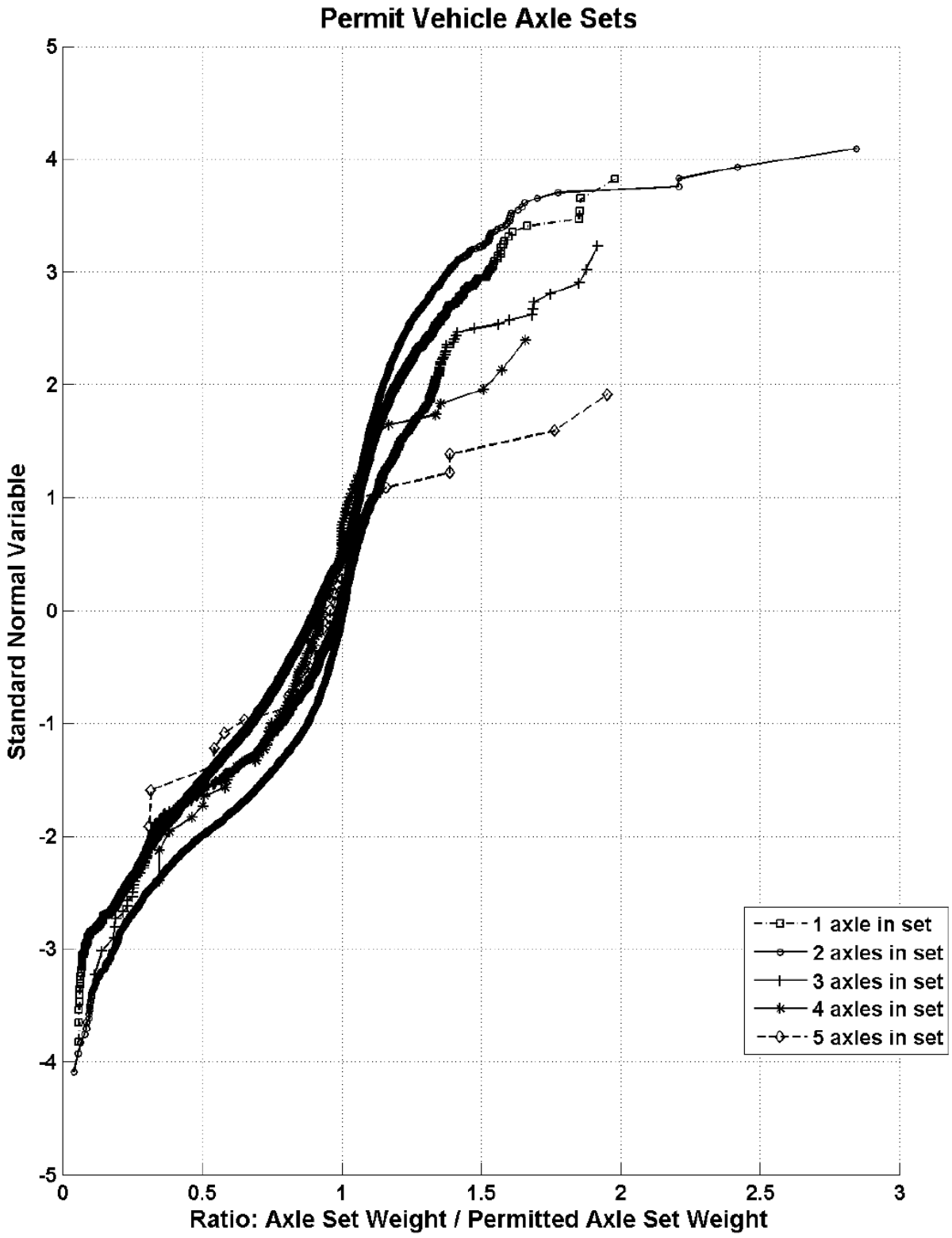

Figure 4-37 Ratio of Axle Group Scale Weight and Permitted Axle Set Weight for Axle Sets with Different Number of Axles

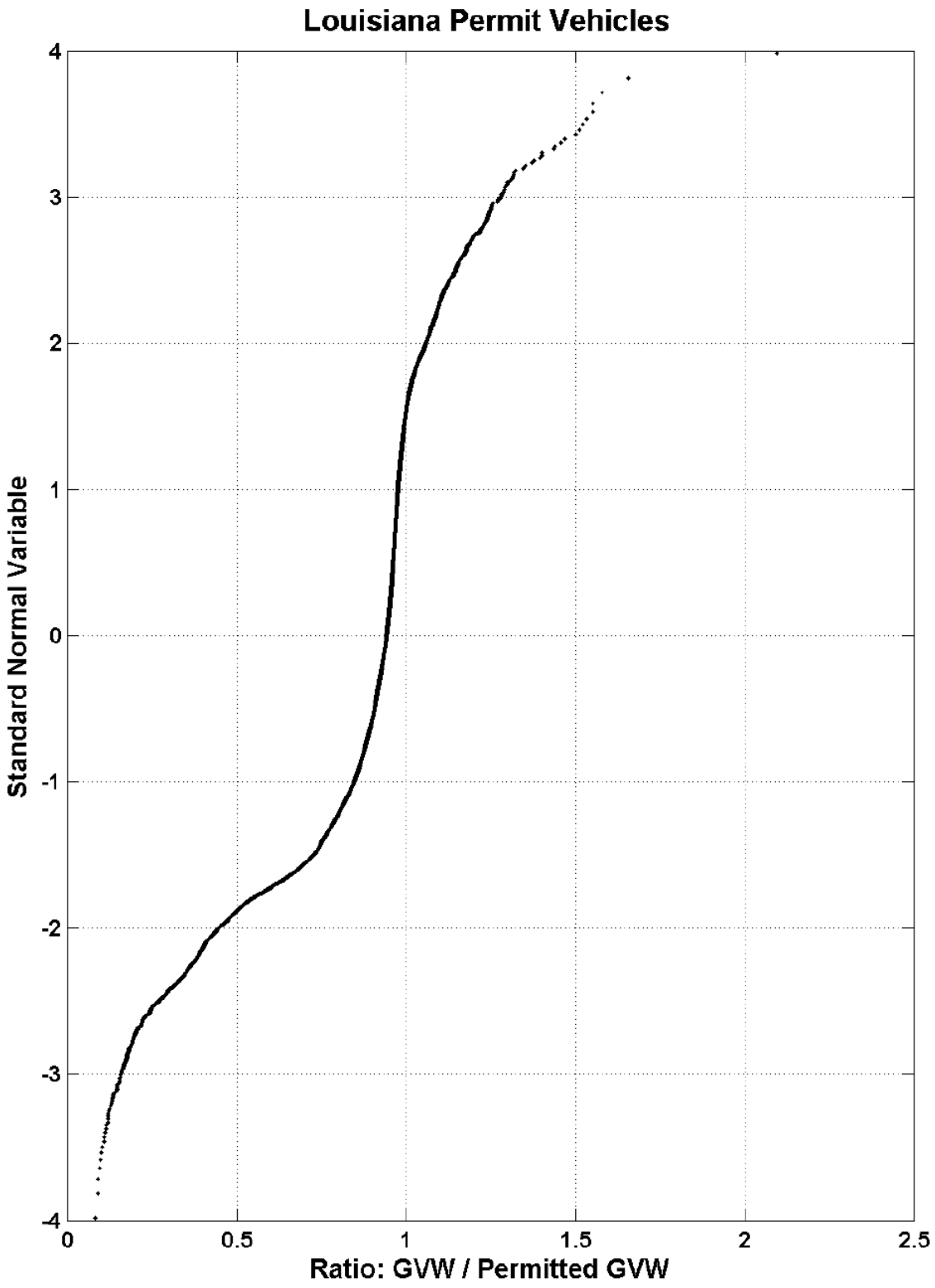

Figure 4-38 Ratio of GVW and Permitted GVW for Permit Vehicles

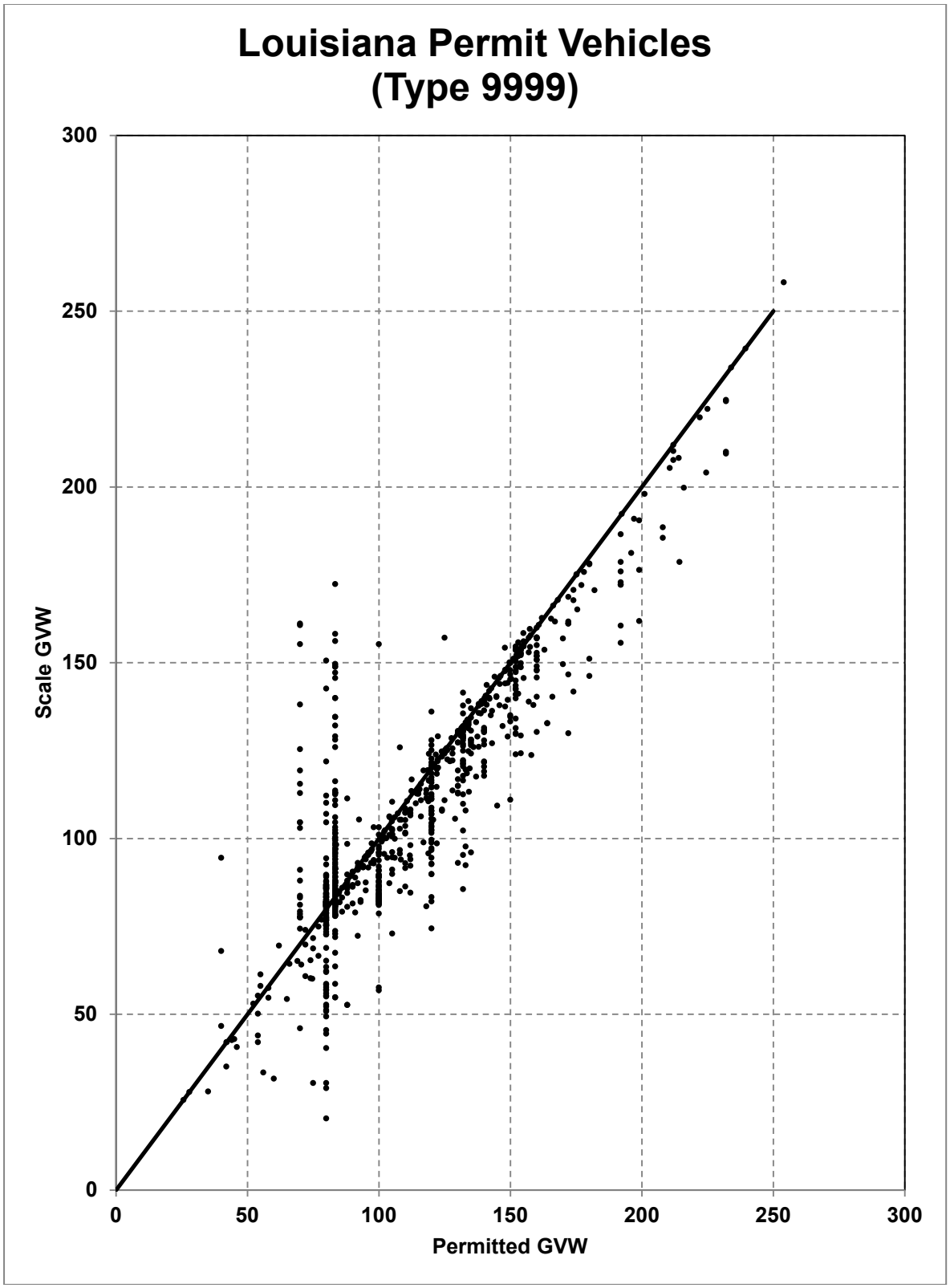

Figure 4-39 Correlation of GVW to Ratio of GVW and Permitted GVW

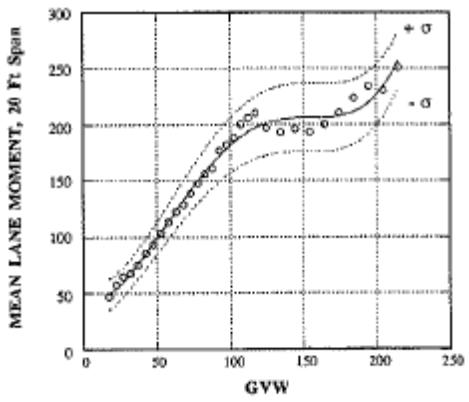

a) 20 Foot Mean Lane Moment v GVW

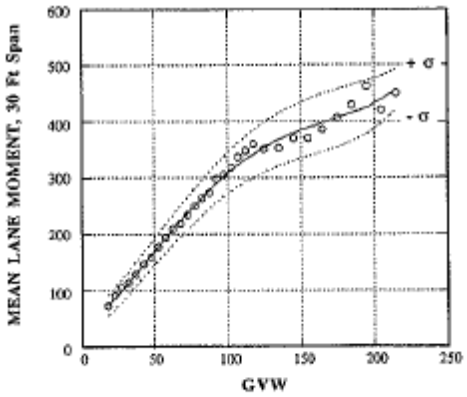

b) 30 Foot Mean Lane Moment v GVW

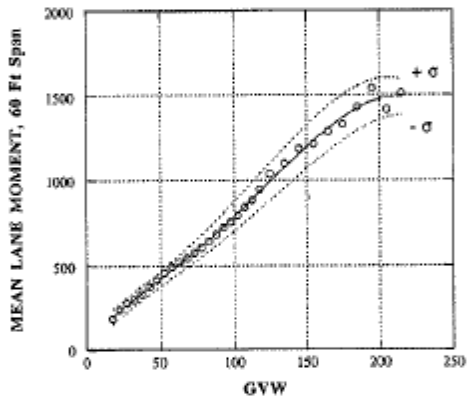

c) 60 Foot Mean Lane Moment v GVW

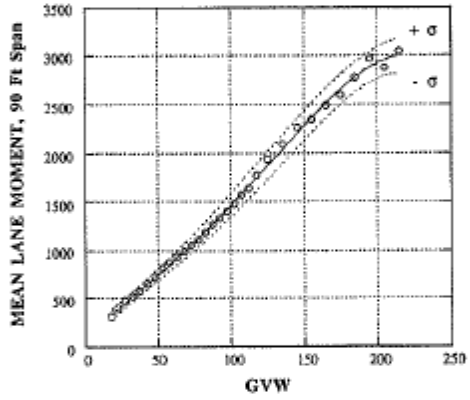

d) 90 Foot Mean Lane Moment v GVW

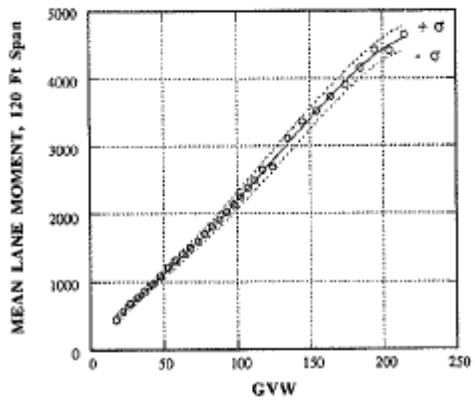

e) 120 Foot Mean Lane Moment v GVW

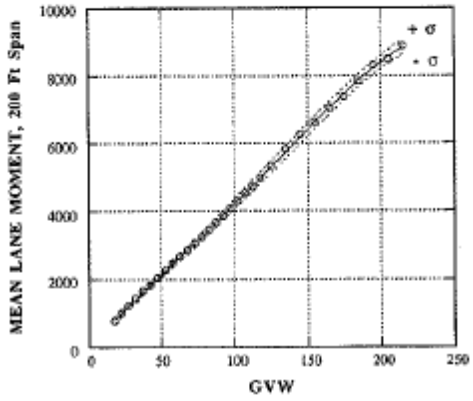

f) 200 Foot Mean Lane Moment v GVW

Figure 4-40 Correlation of GVW and Lane Moment for Various Span Lengths. (Laman 1993)

The research team also obtained a database of the permits issued by New Jersey Department of Transportation from 8/16/10 through 11/30/2011. No information about the actual trucks or violations was available which diminished the value of this database. Nevertheless, the statistics of the NJ permits were compared to those of Louisiana violations.

Table 4-27 shows the distribution of the New Jersey Permitted GVW's and Louisiana permitted and actual GVW's is shown in Table 4-27 and Figure 4-41. The analysis of the data indicates that the majority of permits in New Jersey (83%) are for permitted GVW between 85 and 150 kips. This compares to 47 % for the same GVW group in Louisiana. On the other hand, vehicles permitted for GVW up to 85 kips represent 6% of the permits in New Jersey and 37% of the permits in Louisiana. The percentage is comparable for the vehicles permitted for GVW higher than 150 kips is also higher in Louisiana, 11% for New Jersey Verses 16% in Louisiana.

The statistics of the actual GVW are closer to New Jersey Permit data. With no information available on New Jersey actual GVW's, it is not possible to extend the statistics of Louisiana actual GVW's to New Jersey Permit data.

Table 4-27 Statistics for Different GVW Categories

GVW Category (kips)	NJ Permit Data		Louisiana (Permitted GVW)		Louisiana (Actual GVW)	
	Count of Trucks	Percentage	Count of Trucks	Percentage	Count of Trucks	Percentage
<70	284	0.60%	27	3.11%	69	7.94%
70~80	902	1.90%	162	18.64%	54	6.21%
80~85	1610	3.39%	133	15.30%	114	13.12%
85~100	11136	23.46%	105	12.08%	179	20.60%
100~125	15544	32.75%	147	16.92%	174	20.02%
125~150	12858	27.09%	159	18.30%	172	19.79%
150~175	3267	6.88%	92	10.59%	74	8.52%
175~200	990	2.09%	24	2.76%	18	2.07%
200~250	592	1.25%	19	2.19%	14	1.61%
>250	282	0.59%	1	0.12%	1	0.12%
Total	47465		869		869	

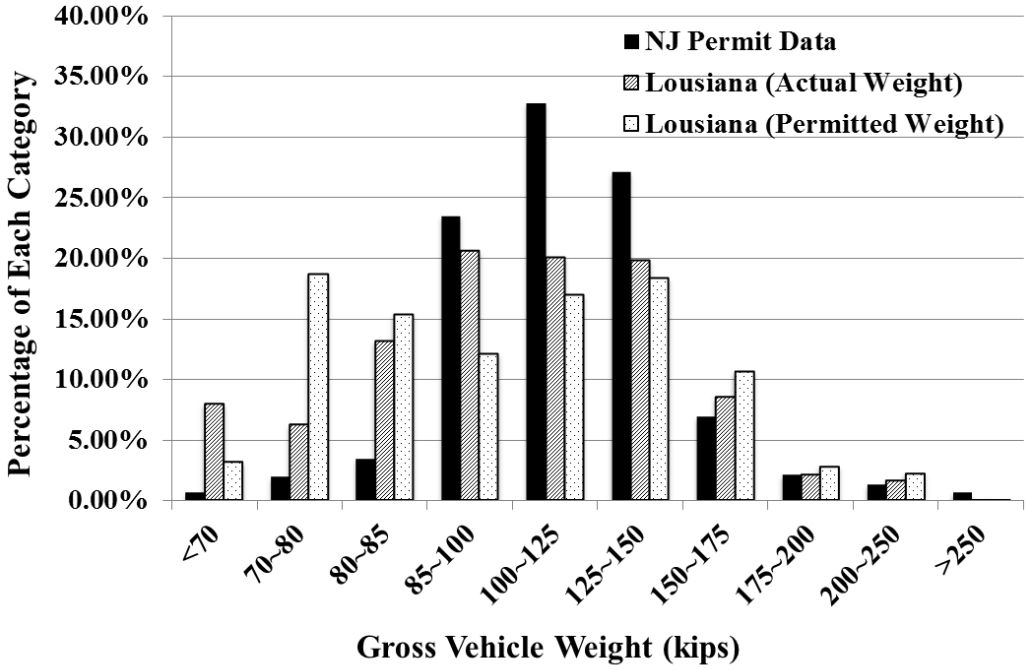

Figure 4-41 Histograms for NJ Permit Data and Louisiana Violation Records

The significant difference between the distribution of the vehicles in different load categories in New Jersey permits as compared to the vehicles in Louisiana's permit vehicles violations indicated that generalizing the relationship between the permitted and scale weights in Louisiana's permit vehicle violations to New Jersey data is unjustifiable.

4.5.3 Conclusions Regarding Overloads and Permit Loads

The analyses of WIM data led to the following conclusions:

- Site-specific consideration of sites with unusually high volumes of heavy trucks is warranted
- Design for a single lane loading is justified by this study
- Elimination of the single lane MPF of 1.20 on the HL-93 loading when considering the effects of overload and permit vehicles for service limit state is justifiable

The analyses of Louisiana permit load citations and comparing the data to New Jersey Permit data led to the following conclusions:

- Heavier permit vehicles are less likely to violate the permitted axle group weights and GVW
- When the GVW is violated, heavier vehicles tend to exceed the permitted value by a smaller percentage than lighter vehicles.
- Due to difference in permit weight limits in different states, the weight and geometry characteristics of permit vehicles are state-specific or at best regional

Generally, it is expected that the tendency of haulers to violate the permitted weights is dependent on the level of enforcement, the amount of the fine for the violation and the availability of a permit legally covering the load they need to move, i.e. the maximum loads allowed by the issuing state. Therefore, the analysis of permit vehicles will tend to be jurisdiction-specific or at best regional.

5 CALIBRATION RESULTS

5.1 Cracking of Reinforced Concrete Components Service I Limit State – Annual Probability

Traditionally, reinforced concrete components are designed to satisfy the requirements of the strength limit state and then they are checked for the Service I limit state load combination to ensure that the crack width under service conditions does not exceed a certain value. However, the specifications provisions are written in a form emphasizing reinforcement details, i.e. limiting bar spacing rather than crack width. Satisfying the Service I limit state for crack control through the distribution of reinforcement may require a reduction in the reinforcement spacing. This may require the use of smaller bar diameters or, if the smallest allowed bar diameters are already being used, an increase in the number of reinforcement bars leading to an increase in the reinforcement area.

Two exposure classifications exist in *AASHTO LRFD*: Class 1 exposure condition and Class 2 exposure condition. Class 1 relates to an estimated maximum crack width of 0.017 in. while Class 2 relates to an estimated maximum crack width of 0.01275 in. Class 2 is typically used for situations where the concrete is subjected to severe corrosion conditions such as bridge decks exposed to deicing salts and substructures exposed to water. Class 1 is used for less corrosive conditions and could be thought of as an upper bound in regards to crack width for appearance and corrosion. Previous research indicates that there appears to be little or no correlation between crack width and corrosion. However, the different classes of exposure conditions have been so defined in the design specifications in order to provide flexibility in the application of these provisions to meet the needs of the bridge owner.

The load factors for dead load (DL) and live load (LL) specified for the Service I load combination are as follows:

DL load factor = 1.0
LL load factor = 1.0

When designing reinforced concrete bridge decks using the conventional design method, most designers follow a similar approach in selecting the deck thickness and reinforcement. The thickness is typically selected as the minimum acceptable thickness, often based on the owner's standards. The choice of main reinforcement bar diameter is typically limited to #5 and #6 bars and the designer does not switch to #6 bars unless #5 bars result in bar spacing less than the minimum spacing allowed. This limits the number of possible variations and allows the development of a deck database that can be used in the calibration.

For decks designed using the empirical method, not determined based on a calculated design load, the reinforcement does not change with the change in girder spacing resulting in varying crack resistance. As the statistical parameters for both the load effect and the resistance are required to perform the calibration, a meaningful calibration of decks designed using the empirical design method could not be performed.

For other components, including prestressed decks, designers may select different member dimensions resulting in different reinforcement area. Even for the same reinforcement area, the designer may use bars or strands of different diameter and spacing and, consequently, result in different crack resistance and a different reliability index for each

possible variation. The variation in the cracking behavior of the same component with the change in the selected reinforcement prohibits the performance of a meaningful calibration for such components.

Due to the reasons indicated above, the calibration for Service I limit state for crack control through the distribution of reinforcement was limited to reinforced concrete decks designed using the conventional design method. The decks are assumed to be supported on parallel longitudinal girders.

5.1.1 Live Load Model

Reinforced concrete decks designed using the conventional method are designed for the heavy axles of the design truck. This required developing the statistical parameters of the axle loads of the trucks in the WIM data. The statistical parameters for the axle loads are presented in Section 4.3.4. Statistical parameters corresponding to a one year return period were assumed in the reliability analysis. ADTTs of 1000, 2500, 5000, and 10,000 were considered, however, an ADTT of 5000 was used as the basis for the calibration.

5.1.2 Target Reliability Index

5.1.2.1 Limit State Function

For the control of cracking of reinforced concrete through the distribution of reinforcement, the limiting criteria are the calculated crack widths, assumed to be 0.017 in. and 0.01275 in for Class 1 and Class 2, respectively. Due to the lack of clear consequences for violating the limiting crack width, there was no basis to change the nature or the limiting values of the limit state function, i.e. the crack width criteria. The work was based on maintaining the current crack width values and calibrating the limit state to produce a uniform reliability index similar to the average reliability index produced by the current designs.

5.1.2.2 Statistical Parameters of Variables Included in the Design

Several variables affect the resistance of prestressed components. Table 5-1 shows a list of variables that were considered to be random variables during the performance of the reliability analyses. These variables represent a summary of the information based on previous research studies by Siriaksorn and Naaman (1980) and Nowak (2008).

Table 5-1 Summary of Statistical Information for Variables used in the Calibration of Service I Limit State for Crack Control

Variable	Distribution	Mean	COV	Remarks
A_s	normal	$0.9\,A_s$	0.015	Siriaksorn and Naaman (1980)
b	normal	b_n	0.04	Siriaksorn and Naaman (1980)
C_{E_c}	normal	33.6	0.1217	Siriaksorn and Naaman (1980)
d	normal	$0.99\,d_n$	0.04	Nowak (2008)
d_c	normal	d_{cn}	0.04	Nowak (2008)
E_s	normal	E_{sn}	0.024	Siriaksorn and Naaman (1980)
f_c'	lognormal $E_c = C_{E_c}\,\gamma_c^{1.5}\sqrt{f_c'}$	(psi) 3000:1.31 f_{cn}' 3500:1.27 f_{cn}' 4000:1.24 f_{cn}' 4500:1.21 f_{cn}' 5000:1.19 f_{cn}'	3000:0.17 3500:0.16 4000:0.15 4500:0.14 5000:0.135	Siriaksorn and Naaman (1980)
f_y	lognormal	$1.13\,f_{yn}$	0.03	Nowak (2008)
h	normal	h_n	$1/(6.4\mu)$	Siriaksorn and Naaman (1980)
γ_c	normal	150	0.03	Siriaksorn and Naaman (1980)

A_s = area of steel rebar, in^2
b = the width of equivalent transverse strip of concrete deck, in.
C_{Ec} = constant parameter for concrete elasticity modulus.
d = effective depth of concrete section, in.
d_c = bottom cover measured from center of lowest bar, in
E_s = modulus of elasticity of steel reinforcement, psi
f_c' = specified compressive strength of concrete, psi
f_y = yield strength of steel reinforcement, psi
h = the thickness of the deck, in.
γ_c = unit weight of concrete, pcf

5.1.2.3 Database of Reinforced Concrete Decks

A database consisting of 15 reinforced concrete decks designed using the conventional method of deck design was developed. As typical in deck design, #5 bars were used unless they resulted in bar spacing less than 5 in.; the minimum spacing many jurisdictions allow in

deck design. If #5 bars result in a bar spacing less than 5 in., #6 bars were used. No maximum bar spacing was considered in the design to ensure that all decks produced a calculated crack width equal to the maximum allowed crack width allowed by the specifications. The designs were not checked for other limit states as the purpose was to calibrate the Service I limit state. The design of the 15 decks was repeated twice, once assuming Class 1 exposure conditions and another time assuming Class 2 exposure conditions.

Table 5-2 presents the summary information of 15 designed bridge decks. The top and bottom concrete cover assumed in the design were 2.5 in. and 1.0 in., respectively.

Table 5-2 Summary Information of 15 Bridge Decks Designed using *AASHTO LRFD* Conventional Deck Design Method

Deck Group #	Girder Spacing (ft.)	Deck Thickness (in.)
1	6	7.0
		7.5
		8.0
2	8	7.5
		8.0
		8.5
3	10	8.0
		8.5
		9.0
		9.5
4	12	8.0
		8.5
		9.0
		9.5
		10.0

5.1.2.4 Selection of the Target Reliability Index

Monte Carlo simulation was used to obtain the statistical parameters of resistance (or capacity) and dead load while the statistical parameters for live load were taken from Section 4.3.4. The reliability indices for various ADTTs and exposure conditions for the 15 decks are summarized in Table 5-3. Due to the difference in positive and negative moment (bottom and top) reinforcement of the deck, the reliability index was calculated separately for the positive and negative moment reinforcement.

Table 5-3 Summary of Reliability Indices for Concrete Decks Designed According to *AASHTO LRFD* (2012)

ADTT	Positive Moment Region		Negative Moment Region	
	Reliability Index (Class 1)	Reliability Index (Class 2)	Reliability Index (Class 1)	Reliability Index (Class 2)
1000	2.44	1.54	2.37	1.77
2500	1.95	1.07	1.79	1.27
5000	1.66	0.85	1.61	1.05
10000	1.39	0.33	1.02	0.5
Avg.	1.86	0.95	1.70	1.15
Max.	2.44	1.54	2.37	1.77
Min.	1.39	0.33	1.02	0.50
Std Dev.	0.45	0.50	0.56	0.53
COV	24%	53%	33%	46%

It should be noted that even though the design for Class 2 resulted in more reinforcement than for Class 1 exposure conditions, the reliability index for Class 2 is lower than that for Class 1 due to the more stringent limiting criteria (narrower crack width).

Current practices rarely result in the deck positive moment reinforcement being controlled by the Service I limit state due to the smaller bottom concrete cover. When Strength I limit state is considered, more positive moment reinforcement is typically required than by Service I. The additional reinforcement results in actual reliability indices for the positive moment region higher than those shown in Table 5-3.

For the negative moment region, the design is often controlled by the Service I limit state. Thus, the reliability indices shown for the negative moment region in Table 5-3 are considered representative of the actual reliability indices that would be calculated when all limit states, including Strength I, are considered in the design.

Therefore, it is recommended that the target reliability index be based on the reliability index for the negative moment region. Since the Class 2 case is the more common case for negative moment reinforcement of decks, the reliability index for Class 2 was used as the basis for selecting the target reliability index. The reliability index for Class 1 was assumed to represent a relaxation of the base requirements. The case of ADTT=5000 was also considered as the base case on which the reliability analysis was performed. Table 5-4 shows the inherent reliability indices for the negative moment region of decks designed for the current *AASHTO LRFD Specifications*. Based on the values shown in Table 5-4, target reliability indices of 1.6 and 1.0 were selected for Class 1 and Class 2, respectively, based on ADTT=5000.

Table 5-4 Reliability Indices of Existing Bridges based on 1-year Return Period

ADTT	Reliability Index	
	Current Practice (Class 1, Negative)	Current Practice (Class 2, Negative)
1000	2.37	1.77
2500	1.79	1.27
5000	1.61	1.05
10,000	1.02	0.50

5.1.3 Calibration Result

The basic steps of the calibration process are shown below as they relate to the Service I calibration.

5.1.3.1 Step 1: Formulate the Limit State Function and Identify Basic Variables

The limit state function considered is the limit on the estimated crack width. In the absence of information suggesting that the current criteria based on a crack width of 0.017 in. and 0.01275 in. for Class 1 and Class 2, respectively, is not adequate, the current crack widths were maintained as the limiting criteria. A discussion of crack width equations in the literature is included in Appendix A.

5.1.3.2 Step 2: Identify and Select Representative Structural Types and Design Cases

The database of decks used in this study is described in Section 5.1.2.3.

5.1.3.3 Step 3: Determine Load and Resistance Parameters for the Selected Design Cases

The variables include the dimension of the cross-section and the material properties. The statistical information includes the probability distribution and statistical parameters such as mean, μ, and standard deviation, σ.

5.1.3.4 Step 4: Develop Statistical Models for Load and Resistance

The variables affecting the load and resistance were identified. These include live load, and resistance including the dimensions of the cross-section, the material properties, etc. The statistical information includes the probability distribution and statistical parameters for axle loads presented in Section 4.3.4 and for other variables affecting the resistance presented in Section 5.1.2.2.

5.1.3.5 Step 5: Develop the Reliability Analysis Procedure

The statistical information of all the required variables is used to determine the statistical parameters of the resistance by using Monte Carlo simulation.

For each deck, Monte Carlo simulation was performed for each random variable associated with the calculation of the resistance and dead load. One thousand simulations were performed. For each random variable 1000 values were generated independently based on the statistics and distribution of that random variable. For each simulation, the dead load

and the resistance were calculated using one of the 1000 sets of values of the random variable, i.e. the n^{th} simulation used the n^{th} value of each random variable where n varied from 1 to 1000. This process resulted in 1000 values of the dead load and the resistance. The mean and standard deviation of the dead load and the resistance were then calculated based on the 1000 simulations.

5.1.3.6 Step 6: Calculate the Reliability Indices for Current Design Code and Current Practice

Using the statistics of the dead load and the resistance, calculated from the Monte Carlo simulation as described above, and the statistics of the live load as derived from the WIM data as described in Chapter 4, the reliability index was calculated for each deck.

The reliability index was calculated using the following equation:

$$\beta = \frac{\mu_R - \mu_Q}{\sqrt{\sigma_R^2 + \sigma_Q^2}} \tag{5-1}$$

where

β = reliability index.

μ_R = mean value of the resistance

μ_Q = mean value of the applied loads

σ_R = standard deviation of the resistance

σ_Q = standard deviation of the applied loads.

The calculated reliability indices of the decks in the database are shown in Table 5-3 for both positive and negative moment reinforcement and for Class 1 and Class 2 exposure conditions.

5.1.3.7 Step 7: Review the Results and Select the Target Reliability Index, β_T

The initial target reliability index was determined as shown in Table 5-4.

5.1.3.8 Step 8: Select Potential Load and Resistance Factors for Service I, Crack Control through the Distribution of Reinforcement

The load factors for dead loads and live loads for Service I limit state in the *AASHTO LRFD* (2012) are 1.0. The existing specifications do not explicitly include a resistance factor for the distribution of the control of cracking through the distribution of reinforcement. This results in an implied resistance factor of 1.0. The load and resistance factors were maintained for the initial reliability index calculations.

For Class 1 exposure condition (maximum crack width of 0.017 in), Figure 5-1 and Figure 5-2 present the reliability indices for the bridge decks in the database designed using a live load factor of 1.0 over a one year period for an ADTT of 5000. As indicated in Table 5-3,

the average values of the reliability index are 1.66 and 1.61 for positive and negative moment regions, respectively.

Figure 5-1 Reliability Indices of Various Bridge Decks Designed Using a 1.0 Live Load Factor Over A 1 Year Return Period (ADTT=5000), Positive Moment Region, Class 1 Exposure

Figure 5-2 Reliability Indices Of Various Bridge Decks Designed Using A 1.0 Live Load Factor Over A 1 Year Return Period (ADTT=5000), Negative Moment Region, Class 1 Exposure

For Class 2 exposure condition (maximum crack width of 0.01275 in), Figure 5-3 and Figure 5-4 present the reliability indices for the bridge decks in the database designed using a live load factor of 1.0 over one year period for an ADTT of 5000. As indicated in Table 5-3, the

average values of the reliability index are 0.85 and 1.05 for positive and negative moment regions, respectively.

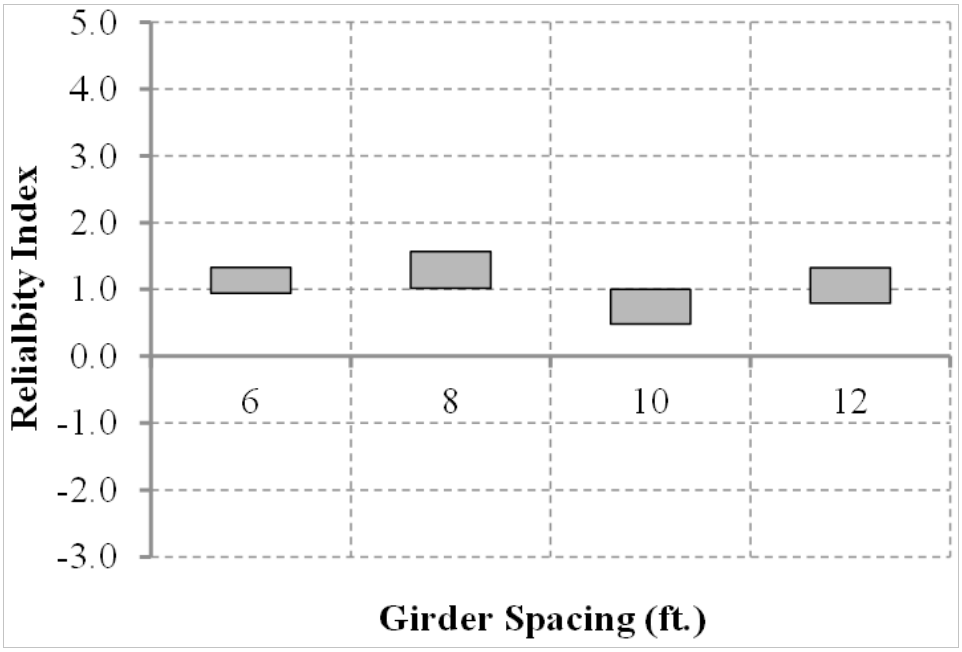

Figure 5-3 Reliability Indices Of Various Bridge Decks Designed Using A 1.0 Live Load Factor Over A 1 Year Return Period (ADTT=5000), Positive Moment Region, Class 2 Exposure

Figure 5-4 Reliability Indices Of Various Bridge Decks Designed Using A 1.0 Live Load Factor Over A 1 Year Return Period (ADTT=5000), Negative Moment Region, Class 2 Exposure

As discussed in Section 5.1.2.4, for positive moment (bottom) reinforcement, Strength I limit state requirements typically result in more reinforcement than needed to satisfy Service I

requirements and the reliability index for cracking at the bottom will be higher than shown in Figure 5-1 and Figure 5-3. This resulted in the recommendation that the reliability index should be based on the negative moment (top) reinforcement.

5.1.3.9 Step 9: Calculate Reliability Indices

As shown in Figure 5-2 and Figure 5-4, the reliability index associated with cracking at the top of the deck appears to be very uniform across the range of girder spacings considered. It was concluded that there was no need to redesign the decks for different load and/or resistance factors to improve the uniformity of the results. With this conclusion, the reliability indices are the same as shown in Table 5-3 and Table 5-4 and in Figure 5-2 and Figure 5-4.

5.1.3.10 Summary and Recommendations for Service I Limit State, Crack Control through the Distribution of Reinforcement

The following conclusions are drawn based on the reported reliability analyses:

- Assessment of current practice leads to recommended target reliability indices of 1.6 proposed for the base case (Class 1 exposure) and 1.0 for the enhanced requirements, i.e. smaller maximum crack width, for Class 2 exposure conditions. These values correspond to an ADTT of 5000.
- The current requirements in the specifications produce uniform reliability across the range of girder spacing considered, so there is no need to change the load or the resistance factors.

5.1.4 Proposed AASHTO LRFD Revisions

As indicated above, no revisions to applicable *AASHTO LRFD* provisions related to control of cracking by distributed reinforcement in reinforced concrete components are warranted by the results of this research.

5.2 Tension in Prestressed Concrete Beams Service III Limit State – Annual Probability

Traditionally, prestressed concrete beams are proportioned for the service limit state such that the concrete tensile and compressive stresses immediately after transfer and at the final stage are within certain stress limits defined in the specifications. Under the current *AASHTO LRFD Specifications* (2012), two service limit state load combinations are used to calculate the stresses in prestressed concrete components: the Service Load I and Service Load III load combinations. The two service load combinations are described as:

- Service I—Load combination relating to the normal operational use of the bridge with a 55 mph wind and all loads taken at their nominal values. Also related to deflection control in buried metal structures, tunnel liner plate, and thermoplastic pipe, to control crack width in reinforced concrete structures, and for transverse analysis relating to tension in concrete segmental girders. This load combination should also be used for the investigation of slope stability.
- Service III—Load combination for longitudinal analysis relating to tension in prestressed concrete superstructures with the objective of crack control and to the principal tension in the webs of segmental concrete girders.

The load factors for DL and LL specified for the two load combinations are as follows:

Service I:	DL load factor	=	1.0
	LL load factor	=	1.0
Service III:	DL load factor	=	1.0
	LL load factor	=	0.8

Based on the definition of the two limit states, Service I limit state is used for calculating all service stresses in the superstructure and substructure components at all stages except that Service III limit state is used to calculate the tensile stresses in the superstructure components under full service loads and the principal tension in webs of segmental concrete.

Stresses immediately after transfer are independent of the live loads. At the final stage, typically the design is controlled by the tensile stress in the concrete and not by the compressive stresses on the opposite side of the girders. As such, the calibration for prestressed concrete superstructures was performed for Service III limit state and no calibration was performed for Service I limit state.

In addition to designing prestressed concrete components for the service limit state, all prestressed components are also checked for the strength limit state. For typical precast prestressed superstructure beams, e.g. I-shapes, bulb tees and adjacent and spread box beams, the controlling case of the design is usually the service limit state.

The service limit state stresses are calculated assuming an uncracked section. As such, the concrete is assumed to be subjected to tensile stresses. However, due to the relatively low load factors used for the service limit states, it is highly probable that the structure is subjected to heavy trucks that produce live load effects higher than those produced by the design factored service loads. When a heavy truck causes the tensile stress in the concrete to exceed the modulus of rupture, the concrete is expected to crack. Once the load passes, the prestressing force will cause the crack to close and it will remain closed as long as the concrete at the crack location remains under compression. However, if a truck heavy enough to cause the concrete stress calculated based on the uncracked section basis to be tensile, the crack will reopen.

Successful past performance of prestressed concrete components suggests that past design requirements result in a frequency of the crack opening sufficiently small so as to not produce adverse strand fatigue problems at crack locations.

5.2.1 History of Major Relevant Design Provisions and Revisions to AASHTO LRFD Specifications

5.2.1.1 Load Factor for Live Load in Service III Load Combination

During the early stages of the development of the *AASHTO LRFD Specifications* in the early 1990s, only Service I load combination was considered for calculating all stresses in prestressed concrete components. The load factor for live load was 1.0 which is the same load factor used for service loads under the *AASHTO Standard Specifications*; the predecessor to the *AASHTO LRFD Specifications*.

The design live load specified in the *AASHTO LRFD Specifications* produces higher unfactored, undistributed load effects than that specified in the *AASHTO Standard*

Specifications. The girder distribution factors, particularly for interior girders, for many typical girder systems in the *AASHTO LRFD Specifications* are lower than that in the *Standard Specifications* thus reducing the difference between the unfactored distributed load effects in the two specifications. Even with the smaller distribution factor, the unfactored distributed load effects from the *AASHTO LRFD Specifications* were higher for most girder systems. Using the same load factor for service limit state (1.0) resulted in higher design factored load effects for the *AASHTO LRFD* designs than for those designed to the *AASHTO Standard Specifications*. The results from the trial designs conducted during the development of the *AASHTO LRFD Specifications* indicated a larger number of strands than required by the *AASHTO Standard Specifications*. This would suggest that designs performed under the *AASHTO Standard Specifications* resulted in under-designed components that should have shown signs of cracking. In the absence of widespread cracking, the load factor for live load was decreased to 0.8 and the Service III load combination was created and was specified for tension in prestressed concrete components. This resulted in a similar number of strands for the designs conducted using both *AASHTO Standard* and *AASHTO LRFD Specifications*.

5.2.1.2 Method of Calculating Prestressing Losses

The AASHTO LRFD Bridge Design Specifications (2012) includes three methods for determining the time-dependent prestressing losses. These three methods are:

- Approximate method: Currently, this method is termed: “Approximate Estimate of Time-Dependent Losses”. and is the least-detailed. It requires limited calculations to estimate the time-dependent losses. Prior to 2005, the specifications included a simpler approximate method which was termed: “Approximate Lump Sum Estimate of Time-Dependent Losses”. The lump-sum method allowed selecting a value for the time-dependent losses from a table. The value varied based on the type of girders and the type and grade of prestressing steel. Some concrete compressive strength requirements were required to be allowed to use this method.
- Refined Estimates of Time-Dependent Losses: This method is more detailed than the approximate method. More details on this method are presented below.
- Time-Step method: This method is highly detailed and is based on tracking the changes in the material properties with time. The loss calculations are based on the time of the application of loads and the material properties at the time of the load application. This method is required to be used in the design of post-tensioned segmental bridges. It may also be used for other types of bridges; however, due to the level of effort required, it is typically limited to segmental bridges.

Throughout the remainder of Section 5.2, unless explicitly indicated otherwise, the time-dependent losses are calculated using the “Refined Estimates of Time-Dependent Losses” in AASHTO LRFD.

Originally, the method of calculating prestressing force losses in *AASHTO LRFD Specifications* (the “pre-2005” method) was the same method used in *AASHTO Standard Specifications*. A new method of loss calculations (the “post-2005” method) first appeared in the 2005 Interim to the Third Edition of *AASHTO LRFD Specifications*. The post-2005 method is thought to produce a more accurate estimate of the losses. The post-2005 method has new equations for calculating the time-dependent prestressing losses and it also introduced the concept of “elastic gain.” After the initial prestressing loss at transfer, when load components

that produce tensile stresses in the concrete at the strand locations are applied to the girder, the strands are subjected to an additional tensile strain equal to the strain in the surrounding concrete due to the application of the loads. This results in an increase in the force in the strands. The increase in the force in the strands was termed "elastic gain" and the post-2005 prestressing loss method allows including the elastic gain to be used to offset some of the losses.

When the "elastic gain" was considered, the post-2005 prestress loss method produced lower prestressing force losses than the earlier method. The reduction in prestressing losses resulted in fewer strands than what was required under the *AASHTO Standard Specifications* and under earlier editions of *AASHTO LRFD Specifications*. This raised some concern as some practitioners and researchers thought that the higher prestressing losses calculated using the pre-2005 loss method compensated for the lower live load effects caused by the lower design live load used in the *AASHTO Standard Specifications* or the lower load factor used for Service III load combination of *AASHTO LRFD Specifications*. Some of the work presented in the following sections was intended to investigate the effect of different loss methods and different design specifications on the reliability index for Service III load combination.

5.2.2 Live Load Model

Traditionally, prestressed concrete components are designed for the number of traffic lanes, including multiple presence factors, that produces the highest load effects. This was assumed to continue in the future and all sections designed as part of this study utilized this approach.

However, as indicated in Section 4.2.4, the presence of heavy loads in adjacent traffic lanes simultaneously is not likely. As such, the load side of the limit state function in the reliability analysis was calculated assuming the live load existed in only one lane and no multiple presence factor was included. The design truck, tandem, and uniform lane load specified in the *AASHTO LRFD* were used unless otherwise noted. The live load distribution factors specified in the *AASHTO LRFD Specifications* were used in distributing the design loads. The dynamic load allowance used in the original calibration of the strength limit state in *AASHTO LRFD* (10%) was applied to the load side.

The return period considered in the calibration of the Service III limit state was one year. This return period was selected due to the fact that the live load statistics were developed based on 1 year of reliable WIM data from various WIM sites. Furthermore, since only 3 out of 32 WIM sites have an ADTT larger than 5000 and only 1 out of 32 WIM sites have an ADTT larger than 8000, an ADTT of 5000 was used for the bulk of the calibration. The bias and COV of live load were taken as shown in Table 5-5 through Table 5-9.

5.2.3 Methods of Analysis for Study Bridges

Unless explicitly indicated otherwise, the methods of analysis used in designing and analyzing the study bridges throughout Section 5.2.4 through Section 5.2.6 are as follows:

For bridges designed or analyzed using the post-2005 prestressing loss method:

- The time-dependent prestressing loss method used is the method designated in the *AASHTO LRFD* (2012) as the "Refined Estimates of Time-Dependent Losses,"

- The section properties used in the analysis are based on the gross section of the concrete, and
- The calculations of prestressing losses consider the effects of the "elastic gain" as allowed by the current design provisions.

Regardless of the method of design used in designing a girder, the stresses in the girder used as part of the reliability index calculations were determined by analyzing the girder using the above assumptions.

For bridges designed using the pre-2005 prestressing loss method:

- The time-dependent prestressing loss method used is the method designated in the *AASHTO LRFD* editions prior to 2005 as the "Refined Estimates of Time-Dependent Losses,"
- The section properties used in the analysis are based on the gross section of the concrete, and
- The calculations neglect the effects of the "elastic gain."

5.2.4 Target Reliability Index

In the development of the *AASHTO LRFD Specifications*, the target reliability index for the strength limit states was 3.5. The limit state was assumed to be violated when the applied load effects exceeded the resistance which was in turn assumed to be equal to the design factored load. The definition of "failure" under the strength limit state is well defined as it relates to a certain criteria related to the properties of the materials used, such as steel yield stress or concrete compressive strength, or a behavior criteria where violation may lead to the instability of the component, such as local or global buckling. Due to the lack of clear consequences for violating the limiting stress specified for the concrete in a prestressed concrete component, selecting the limit state function required investigating different possible alternatives.

5.2.4.1 Limit State Functions Investigated

The following three different limit state functions were investigated:

- Decompression Limit State: This limit state assumes that the "failure" occurs when the stress in the concrete on the tension face calculated based on the uncracked section under the combined effect of factored dead load and live load ceases to be compression.
- Stress Limit State: This limit state assumes that the "failure" occurs when the tensile stress in the concrete on the tension face calculated based on the uncracked section under the combined effect of factored dead load and live load exceeds a certain tensile stress limit calculated based on the uncracked section properties regardless of whether the section has been previously cracked or not. Stress limits of $f_t = 0.0948\sqrt{f_c'}$, $f_t = 0.19\sqrt{f_c'}$ and $f_t = 0.25\sqrt{f_c'}$ were initially considered in the reliability analysis, however, a stress limit of $f_t = 0.19\sqrt{f_c'}$ was used for the final calibration.
- Crack Width Limit State: This limit state assumes that the "failure" occurs when the previously formed crack in the concrete opens and the crack width reaches a certain pre-specified crack width. Crack widths of 0.008, 0.012, and 0.016 inches

were initially considered in the reliability analysis, however, none produced uniform reliability. The bulk of the calibration was performed using a crack width of 0.016 inches. The differentiation between different environments is accounted for in the calibration through the use of different reliability indices in association with the same crack width.

For each girder, the design was performed based on certain stress limits as is conventionally done and the girder section and number of strands were determined. The reliability index was determined for each of the three limit state functions described above using the same girder design, i.e. the same girder section and same number of strands.

Each of the limit state functions requires a different level of loading before the criteria is violated. As such, the frequency at which any of the three limit states is violated and the corresponding reliability index depend on the level of loading required to cause the limit state to be violated. For a specific cross-section with a specific prestressing steel area and force, reaching the decompression limit state requires less applied load than reaching a specified tensile stress which in turn requires less load than that required to reach a specific crack width. Requiring higher load to violate a specific limit state means that the section resistance is higher and this results in higher reliability index. Table 5-5 shows the required load and the corresponding reliability index for the three limit states relative to each other.

Table 5-5 Relation Between Limiting Criteria and Reliability Index for a Given Girder

Limiting Criteria	Live Load required to violate the limiting criterion	Frequency of exceeding the limiting criterion	Reliability Index
Decompression	Lowest	Highest	Lowest
Maximum allowable tensile stress limit	Middle	Middle	Middle
Maximum allowable crack width limit state	Highest	Lowest	Highest

With the target reliability index depending on the definition of the limit state, selecting the target reliability index required investigating all three criteria and selecting the one which provides more uniform reliability across a wide range of bridge geometrical characteristics.

The process of calibration is illustrated for prestressed I-beams sections in Section 5.2.4.3 through Section 5.2.6. The final results for other types of sections are shown in Section 5.3.5. More details on the work on all types of sections are given in Appendix C and Appendix D.

5.2.4.2 Statistical Parameters of Variables Included in the Design

Several variables affect the resistance of prestressed components. Table 5-6 shows a list of variables that were considered to be random variables during the performance of the reliability analyses. These variables represent a summary of the information based on previous research studies by Siriaksorn and Naaman (1980) and Nowak, et al. (2008).

Table 5-6 Random Variables and the Value of Their Statistical Parameters

Variables	Distribution	Mean, μ	COV, Ω	Remarks
A_s	normal	$0.9A_{sn}$*	0.015	Siriaksorn and Naaman (1980)
A_{ps}	normal	$1.01176A_{psn}$	0.0125	Siriaksorn and Naaman (1980)
b, b_0, b_1, b_w	normal	b_n	0.04	Siriaksorn and Naaman (1980)
C_{E_c}	normal	33.6	0.1217	Siriaksorn and Naaman (1980), nominal=33 $C_{E_c} = E_c / \left(\gamma_c^{1.5} \cdot \sqrt{f'_c} \right)$
$C_{f_{ci}}$	normal	0.6445	0.073	nominal=0.8 $C_{f_{ci}} = f_{ci} / f'_c$
d_p, d_s	normal	d_{pn}, d_{sn}	0.04	Siriaksorn and Naaman (1980)
e_1	normal	e_{0n}	0.04	Siriaksorn and Naaman (1980)
E_{ps}	normal	$1.011E_{psn}$	0.01	Siriaksorn and Naaman (1980) E_{psn} = 29000 ksi
E_s	normal	E_{sn}	0.024	Siriaksorn and Naaman (1980)
f'_c	lognormal	$1.11f'_{cn}$	0.11	Nowak (2008)
f_{pu}	lognormal	$1.03f_{pun}$	0.015	Nowak (2008) f_{pun} = 270 ksi
f_{si}	normal	$0.97f_{sin}$	0.08	developed based on Gross and Burns (2000)
f_y	lognormal	$1.13f_{yn}$	0.03	Nowak (2008)
h, h_f, h_{f1}, h_{f2}	normal	h_n, h_{fn}, h_{f1n}, h_{f2n}	0.025	Siriaksorn and Naaman (1980)
I	normal	I_n	11 / (32μ)	Siriaksorn and Naaman (1980)
γ_c	normal	γ_{cn} = 150	0.03	Siriaksorn and Naaman (1980)
Δf_s	normal	$1.05\Delta f_{sn}$	0.10	developed based on Gross and Burns (2000) and Tadros, et al. (2003)
Σ0	normal	$\Sigma 0_n$	0.03	Siriaksorn and Naaman (1980)

*Subscript of "*n*" refers to nominal values

Notations:

A_s = area of non-prestressing steel, in^2
A_{ps} = area of prestressing steel in tension zone, in^2
b = prestressed beam top flange width, in.
b_0 = deck width transformed to the beam material, in.
b_1 = prestressed beam bottom flange width, in.
b_w = web thickness, in.
c = depth of neutral axis from the extreme compression fiber, in
$C_{f_{ci}}$ = f_{ci} / f'_c
d_p = distance from extreme compression fiber to centroid of prestressing steel, in.
d_s = distance from extreme compression fiber to centroid of non-prestressing steel, in.
e_1 = eccentricity of the prestressing force with respect to the centroid of the section at mid-span, in.
E_{ps} = modulus of elasticity of prestressing steel, psi
E_s = modulus of elasticity of non-prestressing steel, psi

f'_c = specified compressive strength of concrete, psi
f_{pu} = specified tensile strength of prestressing steel, psi
f_{si} = initial stress in prestressing steel, psi
f_y = yield strength of non-prestressing steel, psi
h = girder depth, in.
h_f = deck thickness, in.
h_{f1} = top flange thickness, in.
h_{f2} = bottom flange thickness, in.
l = clear span length of the beam members, ft.
γ_c = unit weight of concrete, pcf
Σ0 = sum of reinforcing element circumferences, in.
Δf_s = prestress losses, psi

5.2.4.3 Database of Existing Bridges

A database of existing prestressed concrete girder bridges was extracted from the database of bridges used in the NCHRP 12-78 project (Mlynarski, et al. 2011). The database used in this study included 30 I- and bulb-T girder bridges, 31 adjacent box girder bridges, and 36 spread box girder bridges. The geometric characteristics of the bridges are included in Appendix C.

Depending on the environmental exposure conditions, both the *AASHTO Standard Specifications* and the *AASHTO LRFD Specifications* allow designing conventional prestressed components for maximum concrete tensile stress of $f_t = 0.0948\sqrt{f'_c}$ or $f_t = 0.19\sqrt{f'_c}$ for severe corrosion conditions or no worse than moderate corrosion conditions, respectively. When either specifications are applied without owner's exceptions, most bridges are designed for $f_t = 0.19\sqrt{f'_c}$ with a small number of bridges in coastal areas designed for $f_t = 0.0948\sqrt{f'_c}$. It was not known what stress limit each bridge in the database was designed for. As the percentage of bridges designed for severe corrosive conditions is small, it was assumed that most bridges in the database were likely designed for the higher limit.

Based on the construction date of these bridges, it is likely that all existing bridges considered were designed using the prestressing loss provisions method that existed in both the *AASHTO Standard Specifications* and in the pre-2005 *AASHTO LRFD*.

The database of existing bridges was used to estimate the reliability index inherent in the existing bridge system and used this as a starting point for the calibration.

5.2.4.4 Estimated Reliability Index of Existing Bridges

Table 5-7 summarizes the average reliability indices for the existing I- and bulb T girder bridges database. For example, the average reliability indices at decompression level, maximum allowable tensile stress limit under service loads of $f_t = 0.19\sqrt{f'_c}$, and maximum allowable crack width limit of 0.016 inches are 0.74, 1.05, and 2.69, respectively, for an ADTT of 5000 and a return period of one year.

Table 5-7 Summary of Reliability Indices for Existing I- and Bulb T Girder Bridges with One Lane Loaded and Return Period of 1 Year

Performance Levels		ADTT			
		ADTT=1000	ADTT=2500	ADTT=5000	ADTT=10000
Decompression		0.95	0.85	0.74	0.61
Maximum Tensile Stress Limit	$f_t = 0.0948\sqrt{f_c'}$	1.15	1.01	0.94	0.82
	$f_t = 0.19\sqrt{f_c'}$	1.24	1.14	1.05	0.95
	$f_t = 0.25\sqrt{f_c'}$	1.40	1.27	1.19	1.07
Maximum Crack Width	0.008 in	2.29	2.21	1.99	1.85
	0.012 in	2.65	2.60	2.37	2.22
	0.016 in	3.06	2.89	2.69	2.56

5.2.4.5 Database of Simulated Bridges

A database of simulated simple span bridges was designed using AASHTO I-girder sections for four different cases. The simulated bridges have span lengths of 30, 60, 80, 100, and 140 ft. and girder spacing of 6, 8, 10, and 12 ft. This database was analyzed to determine the effect of the change in the method of estimating prestressing losses (pre-2005 and post-2005 methods) and the design environment ("severe corrosive conditions" and "normal" or "not worse than moderate corrosion conditions"). The two environmental conditions are signified by the maximum concrete tensile stress limit ($f_t = 0.0948\sqrt{f_c'}$ or $f_t = 0.19\sqrt{f_c'}$) used in the design. The four cases of design considered were:

Case 1: *AASHTO LRFD* with maximum concrete tensile stress of $f_t = 0.0948\sqrt{f_c'}$ and pre-2005 prestress loss method

Case 2: *AASHTO LRFD* with maximum concrete tensile stress of $f_t = 0.0948\sqrt{f_c'}$ and post-2005 prestress loss method

Case 3: *AASHTO LRFD* with maximum concrete tensile stress of $f_t = 0.19\sqrt{f_c'}$ and pre-2005 prestress loss method

Case 4: *AASHTO LRFD* with maximum concrete tensile stress of $f_t = 0.19\sqrt{f_c'}$ and post-2005 prestress loss method

Table 5-8 and Table 5-9 show the span length and girder spacing along with the calculated reliability indices for I-girder bridges designed for maximum concrete tensile stress $f_t = 0.0948\sqrt{f_c'}$ (Case 1 and Case 2) and $f_t = 0.19\sqrt{f_c'}$ (Case 3 and Case 4), respectively, for ADTT=5000.

In performing the design, the cases using post-2005 prestress loss method (Case 2 and Case 4) were designed using the smallest possible AASHTO girder size. To facilitate the comparisons, where possible, Case 1 and Case 3 were then designed using the same AASHTO section used for Case 2 and Case 4, respectively. For the cases where the section used for Case 2 or Case 4 was too small to be used for the corresponding Case 1 or Case 3, no design

is shown in Table 5-8 and Table 5-9 for Case 1 and Case 3. For the 140 ft. span bridges with 12 ft. girder spacing, no AASHTO I-girder section was sufficient.

Bridges designed for Case 1 and Case 3 are also thought to be similar to those designed using AASHTO Standard specifications for the two environmental conditions. The reliability indices calculated for Case 1 and Case 3 represent the inherent reliability of bridges currently on the system as most of them were designed before 2005. Case 2 and Case 4 generally represent the inherent reliability of newer bridges designed using the 2005 and later versions of AASHTO LRFD for severe and normal environmental conditions, respectively.

Comparing Case 1 to Case 2 and Case 3 to Case 4 shows the effect of changing the prestressing loss method.

Using the post-2005 prestress loss method resulted in smaller number of strands than the pre-2005 loss method. As shown in Table 5-8 and Table 5-9, the lower number of strands resulted in lower reliability index for bridges designed using the post-2005 prestress loss method.

As shown in Table 5-8 and Table 5-9, regardless of the loss method and/or the limit state used, the reliability indices for each case varied significantly. This suggested the need to calibrate the limit state to develop a combination of load and resistance factors that produce a more uniform reliability index across the range of different span lengths and girder spacings.

Table 5-8 Summary of the Reliability Indices of Simulated Bridges Designed Using AASHTO Girders with ADTT=5000 and $f_t = 0.0948\sqrt{f_c'}$

Cases	Section Type	Span Length (ft.)	Spacing (ft.)	Case 1 Designed Using Pre-2005 Loss Method			Case 2 Designed Using Post-2005 Loss Method		
				Decomp.	Max. Tensile	Max. Crack	Decomp.	Max. Tensile	Max. Crack
1	AASHTO I	30	6	1.05	1.49	2.92	1.03	1.51	2.55
2	AASHTO I	30	8	0.90	0.94	2.41	0.93	1.00	2.32
3	AASHTO I	30	10	1.16	1.68	2.87	1.28	1.67	2.82
4	AASHTO I	30	12	1.28	1.67	2.91	0.63	0.97	2.29
Average for 30 ft. Span				**1.10**	**1.45**	**2.78**	**0.97**	**1.29**	**2.50**
5	AASHTO II	60	6	0.66	1.01	3.35	0.23	0.61	2.47
6	AASHTO II	60	8	—	—	—	0.73	1.04	2.42
7	AASHTO III	60	10	1.22	1.62	3.01	0.43	0.76	1.97
8	AASHTO III	60	12	1.57	1.96	3.68	0.73	0.99	2.51
Average for 60 ft. Span				**1.15**	**1.53**	**3.35**	**0.53**	**0.85**	**2.34**
9	AASHTO III	80	6	1.35	1.66	4.1	0.61	0.92	3.07
10	AASHTO III	80	8	1.8	2.14	5.23	0.82	1.13	3.64
11	AASHTO III	80	10	—	—	—	0.90	1.19	2.93
12	AASHTO IV	80	12	2.2	2.49	5.11	0.83	1.17	3.32
Average for 80 ft. Span				**1.78**	**2.10**	**4.81**	**0.79**	**1.10**	**3.24**
13	AASHTO III	100	6	—	—	—	1.45	1.85	3.51
14	AASHTO IV	100	8	1.86	2.00	3.86	1.33	1.43	3.44
15	AASHTO IV	100	10	—	—	—	1.33	1.65	3.37
16	AASHTO V	100	12	1.68	1.99	4.08	0.93	1.24	3.33
Average for 100 ft. Span				**1.77**	**2.00**	**3.97**	**1.26**	**1.54**	**3.41**
17	AASHTO IV	120	6	—	—	—	1.32	1.76	3.81
18	AASHTO V	120	8	1.54	2.05	3.65	0.92	1.4	3.14
19	AASHTO V	120	10	—	—	—	0.95	1.46	3.02
20	AASHTO VI	120	12	1.82	2.26	3.88	0.9	1.35	3.38
Average for 120 ft. Span				**1.68**	**2.16**	**3.77**	**1.02**	**1.49**	**3.34**
21	AASHTO VI	140	6	1.48	1.99	3.91	0.86	1.36	2.32
22	AASHTO VI	140	8	—	—	—	0.99	1.47	2.79
23	AASHTO VI	140	10	—	—	—	1.05	1.53	3.22
24	—	140	12	—	—	—	—	—	—
Average for 140 ft. Span				**1.48**	**1.99**	**3.91**	**0.97**	**1.45**	**2.78**
Average for All Spans				**1.44**	**1.80**	**3.66**	**0.92**	**1.28**	**2.94**

Table 5-9 Summary of the Reliability Indices of Simulated Bridges Designed Using AASHTO Girders with ADTT=5000 and $f_t = 0.19\sqrt{f_c'}$

Cases	Section Type	Span Length (ft.)	Spacing (ft.)	Case 3 Designed Using Pre-2005 Loss Method			Case 4 Designed Using Post-2005 Loss Method		
				Decomp.	Max. Tensile	Max. Crack	Decomp.	Max. Tensile	Max. Crack
1	AASHTO I	30	6	1.00	1.55	2.39	0.97	1.55	2.46
2	AASHTO I	30	8	0.94	0.92	2.35	0.91	1.00	2.16
3	AASHTO I	30	10	1.29	1.66	2.91	1.18	1.66	2.79
4	AASHTO I	30	12	1.30	1.72	3.02	1.26	1.70	2.91
Average for 30 ft. Span				**1.13**	**1.46**	**2.67**	**1.08**	**1.48**	**2.58**
5	AASHTO II	60	6	0.74	1.13	3.11	0.18	0.58	2.41
6	AASHTO II	60	8	1.04	1.39	2.82	0.28	0.66	1.91
7	AASHTO III	60	10	0.42	0.79	2.05	0.42	0.78	2.07
8	AASHTO III	60	12	0.66	1.00	2.5	0.68	0.96	2.53
Average for 60 ft. Span				**0.72**	**1.08**	**2.62**	**0.39**	**0.75**	**2.23**
9	AASHTO III	80	6	0.56	0.97	3.13	0.13	0.51	2.53
10	AASHTO III	80	8	1.06	1.46	3.43	0.42	0.78	3.2
11	AASHTO III	80	10	1.58	1.84	3.65	0.37	0.65	2.72
12	AASHTO IV	80	12	0.83	1.15	3.72	0.51	0.87	3.11
Average for 80 ft. Span				**1.01**	**1.36**	**3.48**	**0.36**	**0.70**	**2.89**
13	AASHTO III	100	6	—	—	—	0.82	1.23	3.44
14	AASHTO IV	100	8	1.31	1.42	3.60	0.69	0.76	2.76
15	AASHTO IV	100	10	1.80	1.98	3.67	0.75	1.04	3.12
16	AASHTO V	100	12	1.08	1.37	3.43	0.40	0.72	2.55
Average for 100 ft. Span				**1.40**	**1.59**	**3.57**	**0.67**	**0.94**	**2.97**
17	AASHTO IV	120	6	1.53	1.98	3.71	0.70	1.28	3.10
18	AASHTO V	120	8	0.90	1.30	3.31	0.46	0.85	2.55
19	AASHTO V	120	10	1.25	1.65	3.35	0.26	0.78	2.68
20	AASHTO VI	120	12	1.19	1.66	3.37	0.47	0.91	2.69
Average for 120 ft. Span				**1.22**	**1.65**	**3.44**	**0.47**	**0.96**	**2.76**
21	AASHTO VI	140	6	0.84	1.41	3.23	0.28	0.82	2.41
22	AASHTO VI	140	8	1.22	1.68	3.30	0.53	0.98	3.04
23	AASHTO VI	140	10	—	—	—	0.62	1.08	2.46
24	—	140	12	—	—	—	—	—	—
Average for 140 ft. Span				1.03	1.55	3.27	0.48	0.96	2.64
Average for All Spans				**1.07**	**1.43**	**3.15**	**0.58**	**0.96**	**2.68**

5.2.4.6 Selection of the Target Reliability Index

The target reliability indices were selected based on the calculated average values of the reliability levels of existing bridges and previous practices with some consideration given to experiences from other Codes (*Eurocode* and International Organization for Standardization (ISO) 2394 Document). As indicated earlier, a return period of 1 year was selected and an ADTT equal to 5000 was used.

Table 5-10 shows the target reliability indices selected in this study as well as the reliability indices for the existing and simulated bridge databases. Notice that the environmental condition for existing bridges was not known and that the two columns showing the reliability indices of the simulated bridges are for cases where the pre-2005 prestressing loss method was used as these are thought to better represent the bridges currently on the system.

For example, the reliability index of existing bridges, simulated bridges designed for severe environments, and simulated bridges designed for normal environments, at the decompression performance level is around 0.74, 1.44 and 1.07, respectively (See Table 5-7 through Table 5-10). Therefore, a target reliability index of 1.2 and 1.0 was selected for the decompression performance level for bridges designed for severe environments and bridges designed for normal environments, respectively. The reliability index of 1.0 means that 15 out of 100 bridges will probably have the bottom of the girder decompress in any given year.

Table 5-10 Reliability Indices for Existing and Simulated Bridges (Return Period of 1 Year and ADTT 5000)

Performance Level	Reliability Index				
	Average β for Existing Bridges in the NCHRP 12-78	Average β for Simulated bridges designed for $f_t = 0.0948\sqrt{f_c'}$ and pre-2005 loss method	Average β for Simulated bridges designed for $f_t = 0.19\sqrt{f_c'}$ and pre-2005 loss method	Proposed Target β for bridges in severe environment	Proposed Target β for bridges in normal environment
Decompression	0.74	1.44	1.07	1.20	1.00
Maximum Allowable Tensile Stress of $f_t = 0.19\sqrt{f_c'}$	1.05	1.80	1.43	1.50	1.25
Maximum Allowable Crack Width of 0.016 in.	2.69	3.68	3.15	3.30	3.10

5.2.5 Calibration Result

The basic steps of the calibration process are shown below as they relate to the Service III calibration.

5.2.5.1 Step 1: Formulate the Limit State Function and Identify Basic Variables

The three limit state functions that were investigated are listed in Section 5.2.4.1. The limit state function is formulated by deriving an expression for the resistance prediction

equation. For the decompression and tensile stress limits, the stress in the concrete is calculated as it is usually done for the design of prestressed concrete components. For the crack width limit state, Appendix E presents a detailed derivation of the resistance prediction equation for a typical prestressed concrete bridge girder. The derived equation considers uncracked and cracked section behavior in a general format by including the crack width equation. In lieu of setting the stress to zero, the resistance for the decompression limit state can also be derived by setting the crack width to zero in the general equation for crack width.

The majority of the equations for the prediction of the maximum crack width are given in terms of the stress in the steel. Various maximum crack width prediction equations were evaluated using test data available in the literature. Appendix F presents a comparison and evaluation of maximum crack width prediction equations for prestressed concrete members.

5.2.5.2 Step 2: Identify and Select Representative Structural Types and Design Cases

Various design cases for span lengths ranging from 30 to 140 ft. were designed as shown in Section 5.2.4.5. For maximum crack width limit state, a crack width of 0.016 in. is considered. For the maximum allowable stress limit state, the stress considered is as stated in the discussion included in the following sections.

5.2.5.3 Step 3: Determine Load and Resistance Parameters for the Selected Design Cases

The variables include the dimension of the cross-section and the material properties. The statistical information includes the probability distribution and statistical parameters such as mean, μ, and standard deviation, σ.

5.2.5.4 Step 4: Develop Statistical Models for Load and Resistance

The variables affecting the load and resistance were identified. These include live load; those affecting resistance include the dimensions of the cross-section, the material properties, etc. The statistical information includes the probability distribution and statistical parameters for live load presented in Section 4.3.2 and for other variables affecting the resistance presented in Section 5.2.4.2.

5.2.5.5 Step 5: Develop the Reliability Analysis Procedure

The statistical information of all the required variables is used to determine the statistical parameters of the resistance by using Monte Carlo simulation. Monte Carlo simulation is useful in generating a large number of random cases that are used in defining the mean and standard deviation of the resistance.

For each girder, Monte Carlo simulation was performed for each random variable associated with calculation of the resistance and dead load. One thousand simulations were performed. For each random variable, 1000 values were generated independently based on the statistics and distribution of that random variable. For each simulation, the dead load and the resistance were calculated using one of the 1000 sets of values of each random variable resulting in 1000 values of the dead load and the resistance. The mean and standard deviation of the dead load and the resistance were then calculated based on the 1000 simulations.

5.2.5.6 Step 6: Calculate the Reliability Indices for Current Design Code and Current Practice

Using the statistics of the dead load and the resistance, calculated from Monte Carlo simulation as described above, and the statistics of the live load as derived from the WIM data as described in Section 4, the reliability index was calculated for each girder.

The reliability index was calculated using the following equation:

$$\beta = \frac{\mu_R - \mu_Q}{\sqrt{\sigma_R^2 + \sigma_Q^2}} \tag{5-2}$$

where

β = reliability Index

μ_R = mean value of the resistance

μ_Q = mean value of the applied loads

σ_R = standard deviation of the resistance

σ_Q = standard deviation of the applied loads

The calculated reliability indices of existing and simulated bridges are shown in Table 5-7 through Table 5-9.

5.2.5.7 Step 7: Review the Results and Select the Target Reliability Index β_T

The initial target reliability index was determined as shown in Table 5-10.

5.2.5.8 Step 8: Select Potential Load and Resistance Factors for Service III

For all steps, the resistance factor was assumed to be the same as in the current *AASHTO LRFD Specifications* (2012), i.e. equal to 1.0.

The Service III limit state resistance is affected by the tensile stress limit used in the design. Therefore, in addition to trying different load factors, different stress limits for the design were also investigated. Maximum concrete design tensile stress of $f_t = 0.0948\sqrt{f_c'}$, $f_t = 0.19\sqrt{f_c'}$ and $f_t = 0.25\sqrt{f_c'}$ were considered. In addition, the simulated bridge database used in determining the target resistance factor was further expanded to allow longer spans.

Due to having three different concrete tensile stress limits, Step 8 is repeated three times below and are designated 8a, 8b, and 8c. For this step, the range of span lengths was increased to 220 feet.

5.2.5.8.1 Step 8a: Select Potential Load and Resistance Factors for Service III - Bridges Designed for Maximum Concrete Tensile Stress of $f_t = 0.0948\sqrt{f'_c}$

In this section, the calibration for a selected bridge database (shown in Table 5-11) was performed assuming an ADTT of 5000 and maximum concrete design tensile stress of $f_t = 0.0948\sqrt{f'_c}$.

1. Calculate the reliability level of designs according to *AASHTO LRFD Specifications* (2012) (Figure 5-5 through Figure 5-7)

Figure 5-5 through Figure 5-7 show the reliability indices for the bridges designed using AASHTO-type girders according to *AASHTO LRFD Specifications* (2012), including a load factor of 0.8 for Service III limit state, and assuming a maximum concrete tensile stress of $f_t = 0.0948\sqrt{f'_c}$. The geometric characteristics of the bridges are shown in Table 5-11. It was observed that the average reliability index for the decompression limit state, maximum allowable tensile stress limit state, and maximum allowable crack width limit state are 0.97, 1.31, and 3.06, respectively. Since the reliability indices are lower than the target reliability indices and that the reliability indices are not uniform across different spans, modifications to the load factor are applied in the next step in an attempt to achieve higher, and more uniform, reliability indices.

Table 5-11 Summary Information of Bridges Designed with γ_{LL}=0.8, ($f_t = 0.0948\sqrt{f'_c}$)

Cases	Section Type	Span Length (ft.)	Girder Spacing (ft.)	A_{ps} (in^2)	# of Strands
1	AASHTO I	30	6	1.224	8
2	AASHTO I	30	8	1.530	10
3	AASHTO I	30	10	1.836	12
4	AASHTO I	30	12	2.142	14
5	AASHTO II	60	6	2.448	16
6	AASHTO II	60	8	3.366	22
7	AASHTO III	60	10	3.060	20
8	AASHTO III	60	12	3.672	24
9	AASHTO III	80	6	3.672	24
10	AASHTO III	80	8	4.590	30
11	AASHTO III	80	10	5.508	36
12	AASHTO IV	80	12	5.202	34
13	AASHTO III	100	6	6.120	40
14	AASHTO IV	100	8	6.426	42
15	AASHTO IV	100	10	7.344	48
16	AASHTO V	100	12	7.038	46
17	AASHTO IV	120	6	7.956	52
18	AASHTO V	120	8	7.956	52
19	AASHTO V	120	10	9.180	60
20	AASHTO VI	120	12	8.874	58
21	AASHTO VI	140	6	8.262	54
22	AASHTO VI	140	8	9.792	64
23	AASHTO VI	140	10	11.322	74
24	AASHTO VI	140	12	-	-
25	FIB-96	160	6	5.508	36
26	FIB-96	160	8	6.426	42
27	FIB-96	160	10	7.344	48
28	FIB-96	160	12	-	-
29	FIB-96	180	6	7.344	48
30	Mod. BT-72	180	9	16.218	106
31	Mod. AASHTO VI	180	9	15.912	104
32	Mod. AASHTO VI	200	9	20.502	134
33	Mod. NEBT-2200	200	9	16.830	110
34	Mod. W95PTMG	200	9	16.830	110
35	Mod. NEBT-2200	220	9	20.808	136

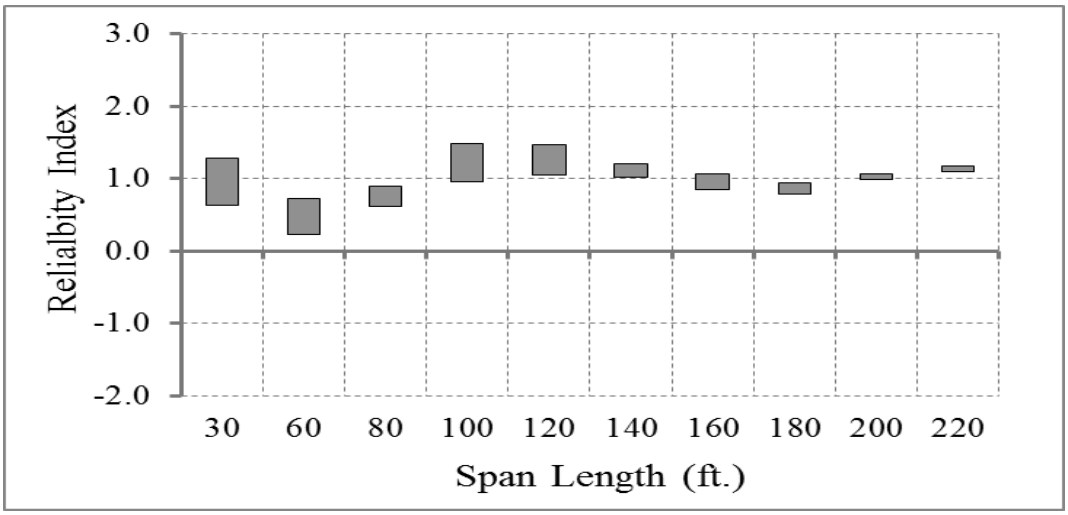

Figure 5-5 Reliability indices for bridges at decompression limit state (ADTT=5000), γ_{LL}=0.8, ($f_t = 0.0948\sqrt{f_c'}$).

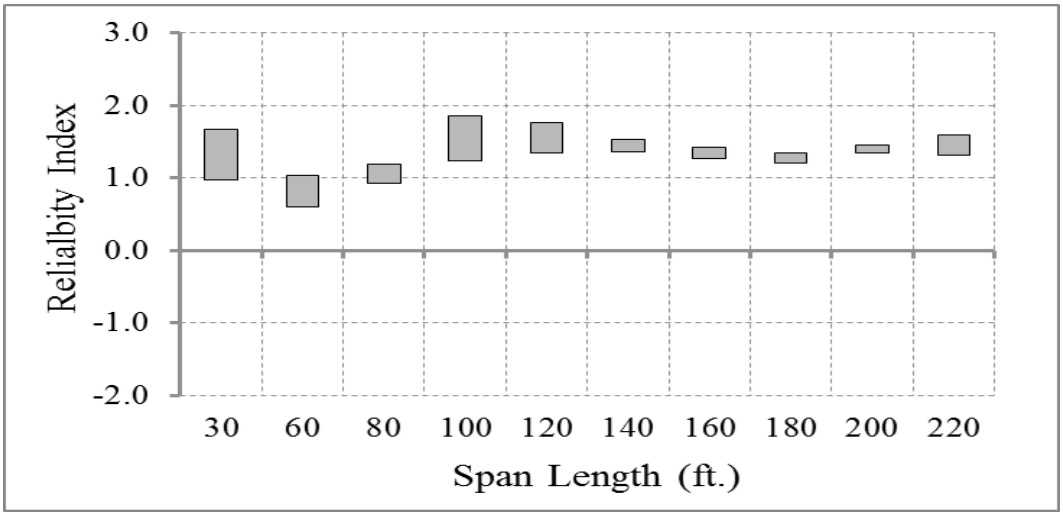

Figure 5-6 Reliability indices for bridges at maximum allowable tensile stress limit state (ADTT=5000), γ_{LL}=0.8, ($f_t = 0.0948\sqrt{f_c'}$).

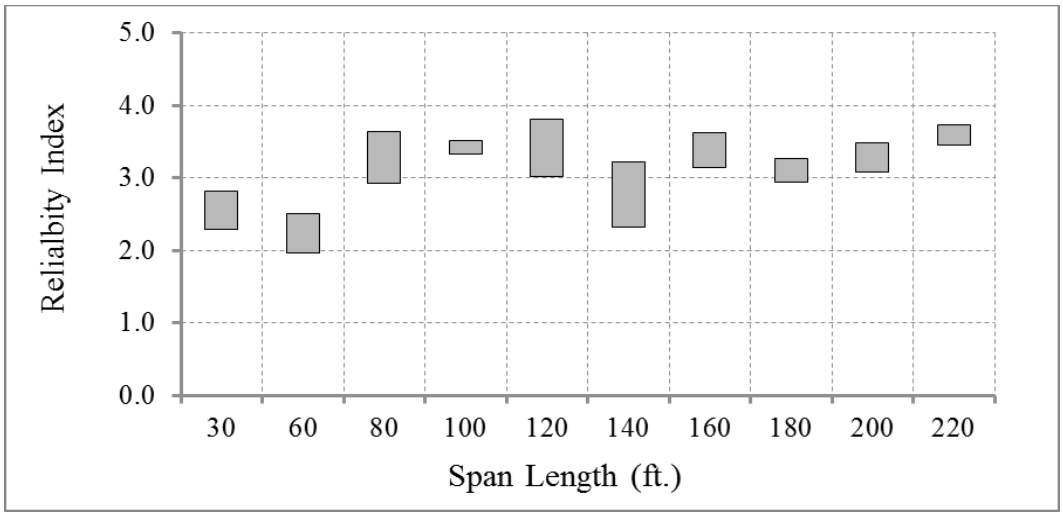

Figure 5-7 Reliability Indices for bridges at maximum allowable crack width limit state (ADTT=5000), γ_{LL}=0.8, ($f_t = 0.0948\sqrt{f_c'}$).

2. Redesign the bridges with live load factor of 1.0

In this step, the bridges have been redesigned using a live load factor of 1.0 and the dead load and resistance factors were kept the same during the redesign. Table 5-12 shows the design geometric characteristics of the redesigned bridges.

Figure 5-8 through Figure 5-10 show the reliability indices for the redesigned bridges using a live load factor of 1.0. The average reliability index for the decompression limit state, the maximum allowable tensile stress limit state, and the maximum allowable crack width limit state are 1.33, 1.70, and 3.32, respectively. It was observed that the reliability level of bridges became more uniform than for the case of using a live load factor of 0.8, particularly for the decompression and maximum tensile stress limit states. Therefore, a live load factor of 1.0 was proposed to be used if the tensile stress is limited to $f_t = 0.0948\sqrt{f_c'}$.

Table 5-12 Summary Information of Bridges Designed with γ_{LL}=1.0, ($f_t = 0.0948\sqrt{f'_c}$)

	Section Type	Span Length (ft.)	Girder Spacing (ft.)	A_{ps} (in^2)	# of Strands
1	AASHTO I	30	6	1.224	8
2	AASHTO I	30	8	1.530	10
3	AASHTO I	30	10	1.836	12
4	AASHTO I	30	12	2.142	14
5	AASHTO II	60	6	3.06	20
6	AASHTO II	60	8	3.978	26
7	AASHTO III	60	10	3.366	22
8	AASHTO III	60	12	4.284	28
9	AASHTO III	80	6	4.284	28
10	AASHTO III	80	8	5.202	34
11	AASHTO III	80	10	6.120	40
12	AASHTO IV	80	12	5.814	38
13	AASHTO III	100	6	7.038	46
14	AASHTO IV	100	8	7.038	46
15	AASHTO IV	100	10	8.262	54
16	AASHTO V	100	12	7.650	50
17	AASHTO IV	120	6	8.874	58
18	AASHTO V	120	8	8.874	58
19	AASHTO V	120	10	10.404	68
20	AASHTO VI	120	12	9.792	64
21	AASHTO VI	140	6	8.874	58
22	AASHTO VI	140	8	10.710	70
23	AASHTO VI	140	10	-	-
24	AASHTO VI	140	12	-	-
25	FIB-96	160	6	5.814	38
26	FIB-96	160	8	7.344	48
27	FIB-96	160	10	7.956	52
28	FIB-96	160	12	-	-
29	FIB-96	180	6	7.956	52
30	Mod. BT-72	180	9	17.442	114
31	Mod. AASHTO VI	180	9	17.442	114
32	Mod. AASHTO	200	9	22.032	144
33	Mod. NEBT-2200	200	9	18.360	120
34	Mod. W95PTMG	200	9	18.360	120
35	Mod. NEBT-	220	9	22.338	146

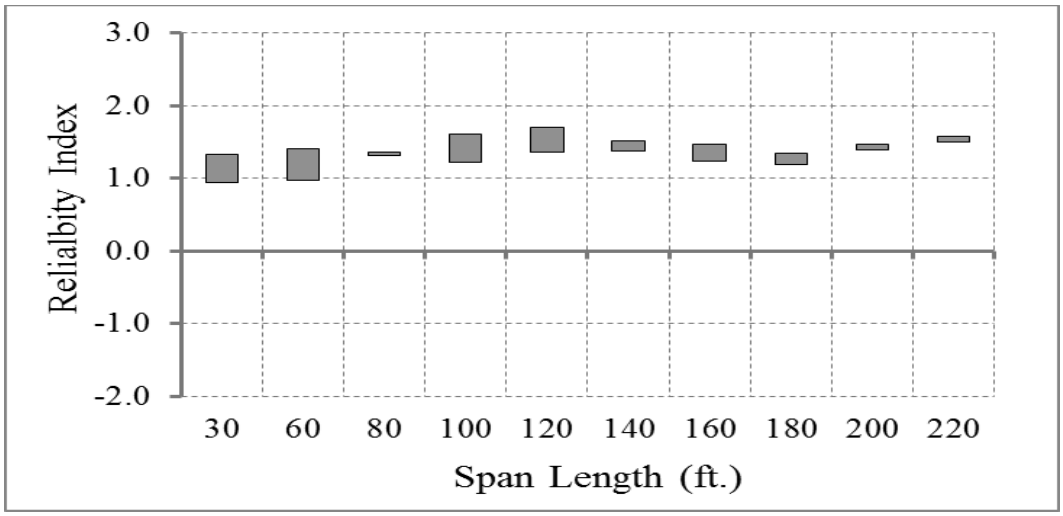

Figure 5-8 Reliability indices for bridges at decompression limit state (ADTT=5000), γ_{LL}=1.0 ($f_t = 0.0948\sqrt{f_c'}$).

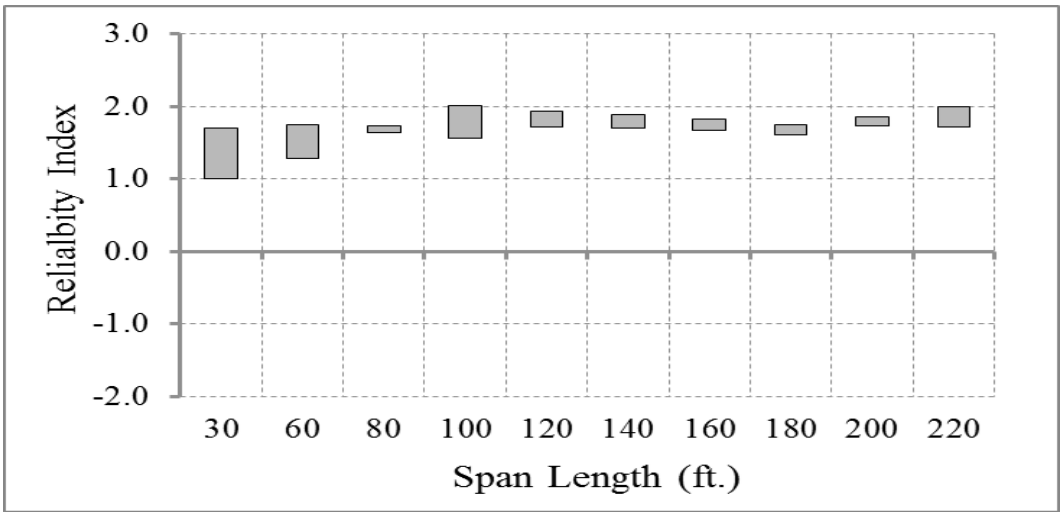

Figure 5-9 Reliability indices for bridges at maximum allowable tensile stress limit state (ADTT=5000), γ_{LL}=1.0 ($f_t = 0.0948\sqrt{f_c'}$).

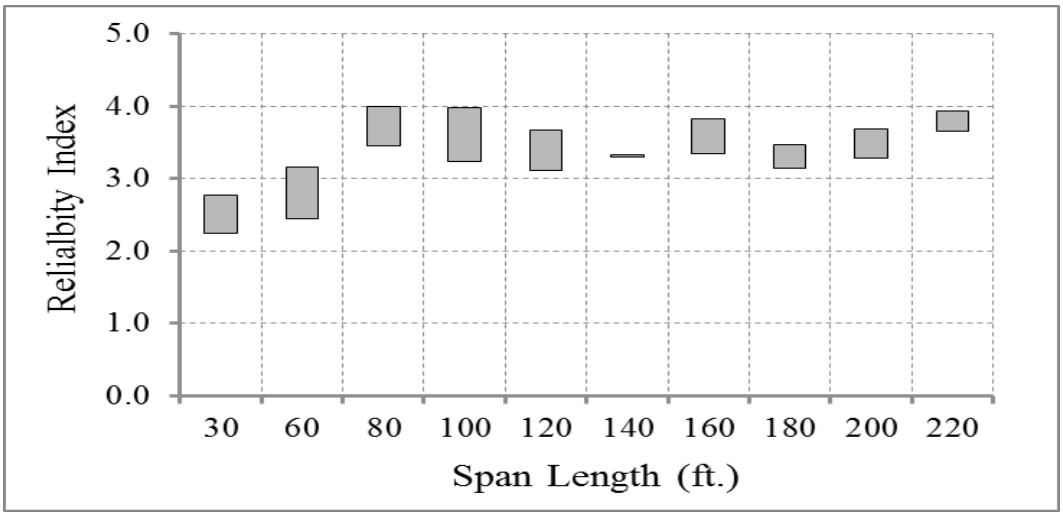

Figure 5-10 Reliability indices for bridges at maximum allowable crack width limit state (ADTT=5000), γ_{LL}=1.0 ($f_t = 0.0948\sqrt{f'_c}$).

5.2.5.8.2 Step 8b: Select Potential Load and Resistance Factors for Service III - Bridges Designed for Maximum Concrete Tensile Stress of $f_t = 0.19\sqrt{f'_c}$

In this section, the work described under Step 8a above was repeated except that the girders were redesigned assuming maximum concrete tensile stress of $f_t = 0.19\sqrt{f'_c}$.

1. Calculate the reliability level of designs according to *AASHTO LRFD Specifications* (2012) with maximum concrete tensile stress for design $f_t = 0.19\sqrt{f'_c}$ (Figure 5-11 through Figure 5-13).

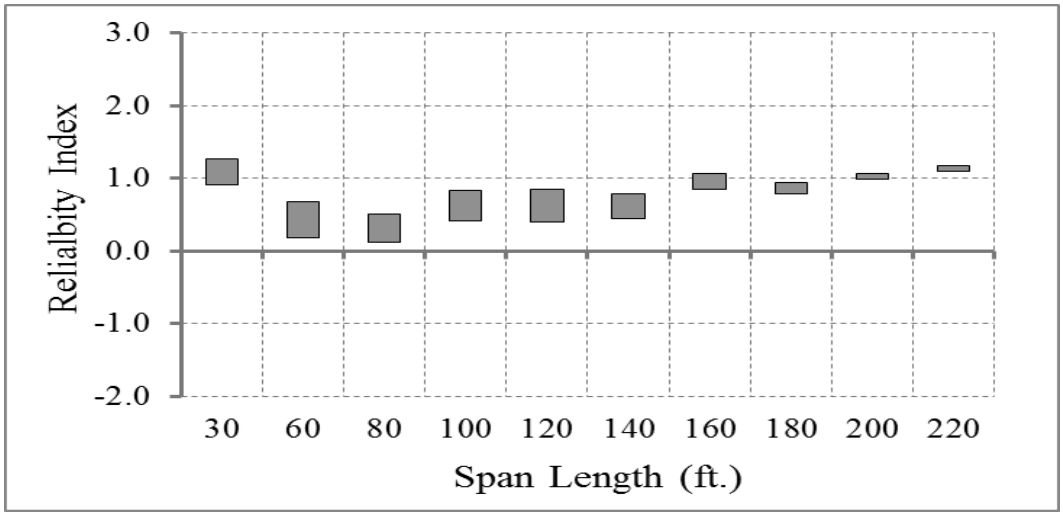

Figure 5-11 Reliability indices for bridges at decompression limit state (ADTT=5000), γ_{LL}=0.8 ($f_t = 0.19\sqrt{f'_c}$).

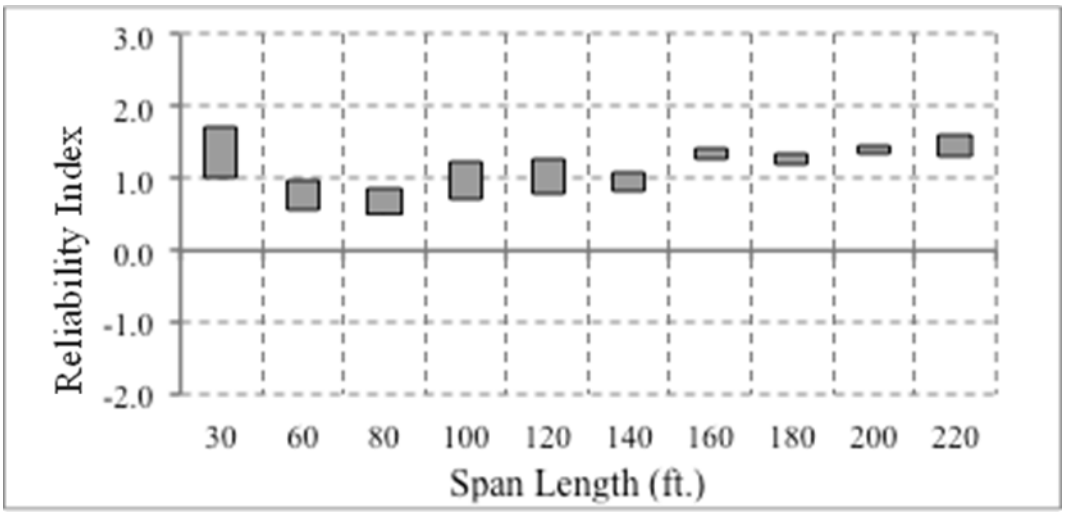

Figure 5-12 Reliability indices for bridges at maximum allowable tensile stress limit state (ADTT=5000), γ_{LL}=0.8 ($f_t = 0.19\sqrt{f'_c}$).

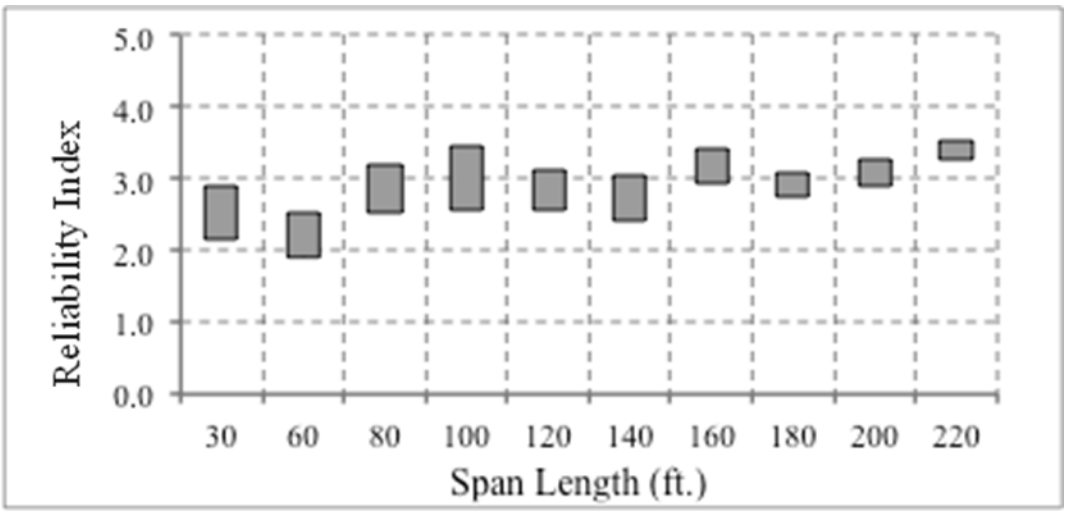

Figure 5-13 Reliability indices for bridges at maximum allowable crack width limit state (ADTT=5000), γ_{LL}=0.8 ($f_t = 0.19\sqrt{f'_c}$).

2. Redesign the bridges with live load factor of 1.0

Figure 5-14 through Figure 5-16 show the reliability indices for the redesigned bridges using a live load factor of 1.0 and $f_t = 0.19\sqrt{f'_c}$. Similar to bridges designed for maximum concrete tensile stress of $f_t = 0.0948\sqrt{f'_c}$, it was observed that the reliability level of bridges became more uniform than the case of using a live load factor of 0.8, particularly for the decompression and maximum tensile stress limit states. Therefore, a live load factor of 1.0 was proposed to be used if the maximum tensile stress is limited to $0.19\sqrt{f'_c}$.

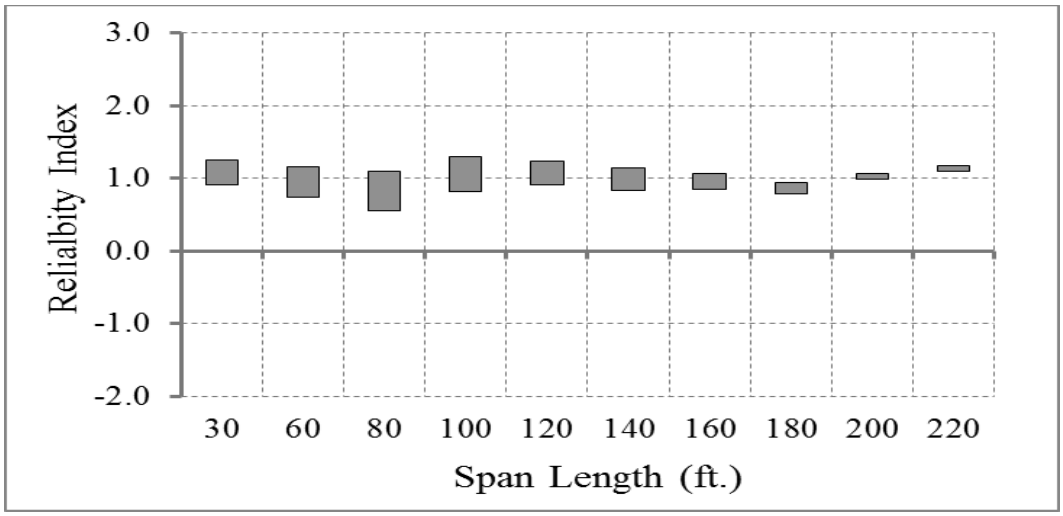

Figure 5-14 Reliability indices for bridges at decompression limit state (ADTT=5000), γ_{LL}=1.0 ($f_t = 0.19\sqrt{f'_c}$).

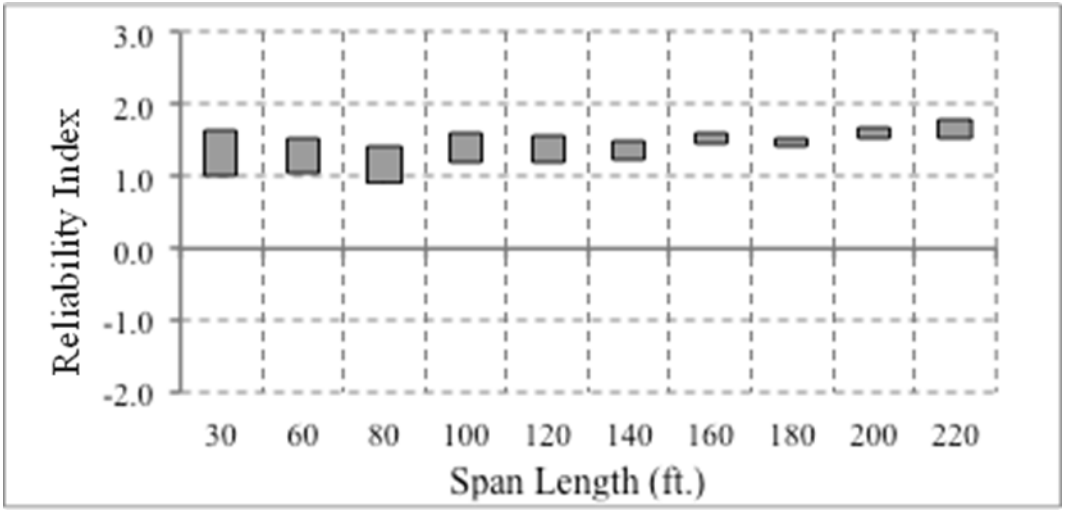

Figure 5-15 Reliability indices for bridges at maximum tensile stress limit state (ADTT=5000), γ_{LL}=1.0 ($f_t = 0.19\sqrt{f'_c}$).

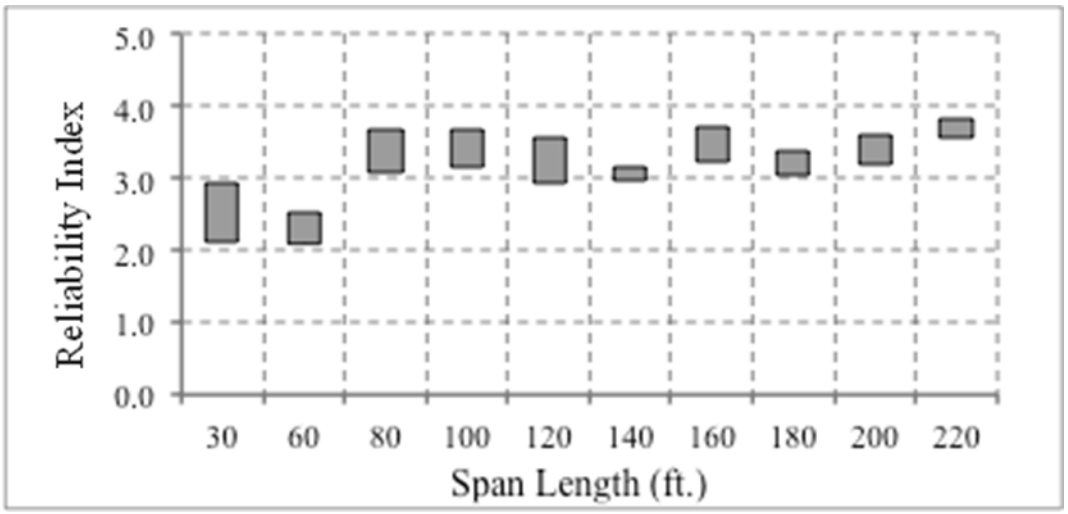

Figure 5-16 Reliability indices for bridges at maximum crack width limit state (ADTT=5000), γ_{LL}=1.0 ($f_t = 0.19\sqrt{f_c'}$).

5.2.5.8.3 Step 8c: Select Potential Load and Resistance Factors for Service III – Bridges Designed for Maximum Concrete Tensile Stress of $f_t = 0.25\sqrt{f_c'}$

In this section, the work described under Step 8a and Step 8b above was repeated except that the girders were redesigned assuming maximum concrete tensile stress of $f_t = 0.25\sqrt{f_c'}$.

1. Calculate the reliability level of designs according to *AASHTO LRFD Specifications* (2010) with maximum concrete tensile stress for design $f_t = 0.25\sqrt{f_c'}$ (Figure 5-17 through Figure 5-19.

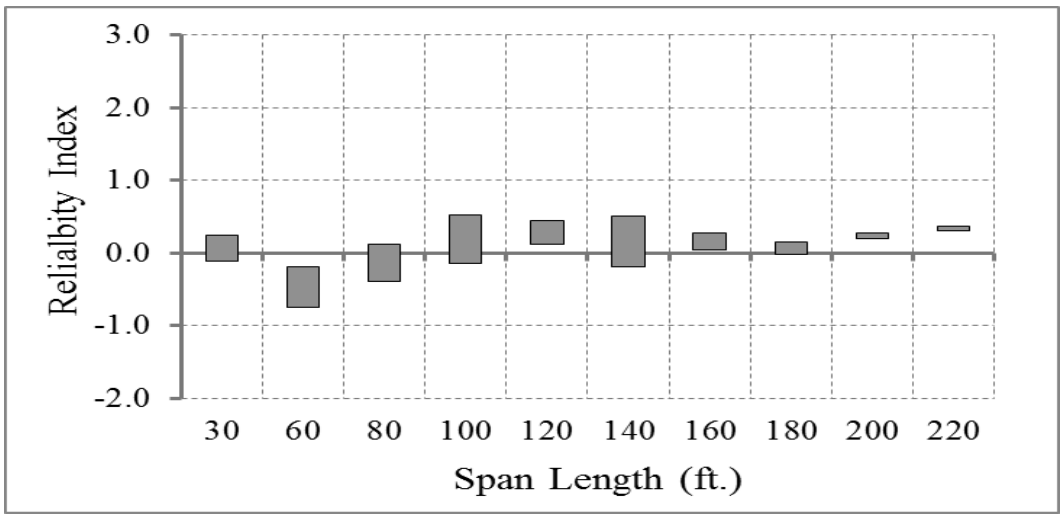

Figure 5-17 Reliability indices for bridges at decompression limit state (ADTT=5000), γ_{LL}=0.8 ($f_t = 0.25\sqrt{f_c'}$).

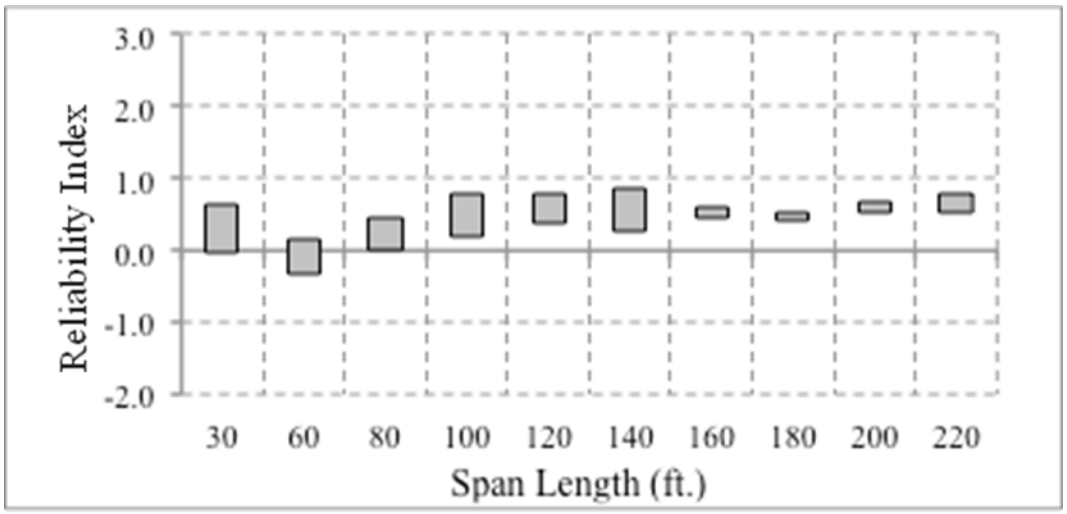

Figure 5-18 Reliability indices for bridges at maximum allowable tensile stress limit state (ADTT=5000), γ_{LL}=0.8 ($f_t = 0.25\sqrt{f_c'}$).

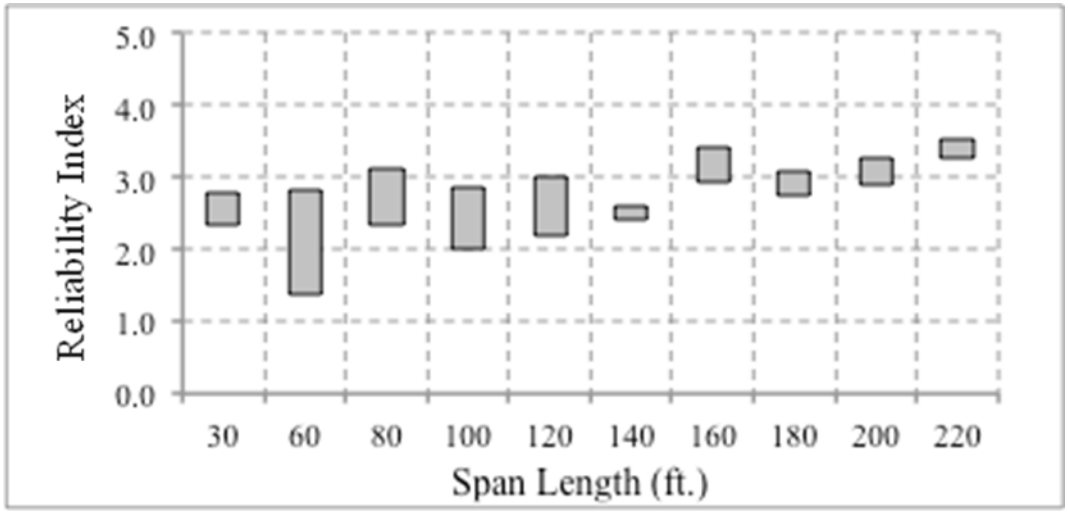

Figure 5-19 Reliability indices for bridges at maximum allowable crack width limit state (ADTT=5000), γ_{LL}=0.8 ($f_t = 0.25\sqrt{f_c'}$).

2. Redesign the bridges with live load factor of 1.0

Figure 5-20 through Figure 5-22 show the reliability indices for the redesigned bridges using a live load factor of 1.0 and $f_t = 0.25\sqrt{f_c'}$. Similar to bridges designed for maximum concrete tensile stress of $f_t = 0.0948\sqrt{f_c'}$ and $f_t = 0.16\sqrt{f_c'}$, it was observed that the reliability level of bridges became more uniform than the case of using a live load factor of 0.8, particularly for the decompression and maximum tensile stress limit states. Therefore, a live load factor of 1.0 was proposed to be used if the maximum tensile stress is limited to $f_t = 0.25\sqrt{f_c'}$.

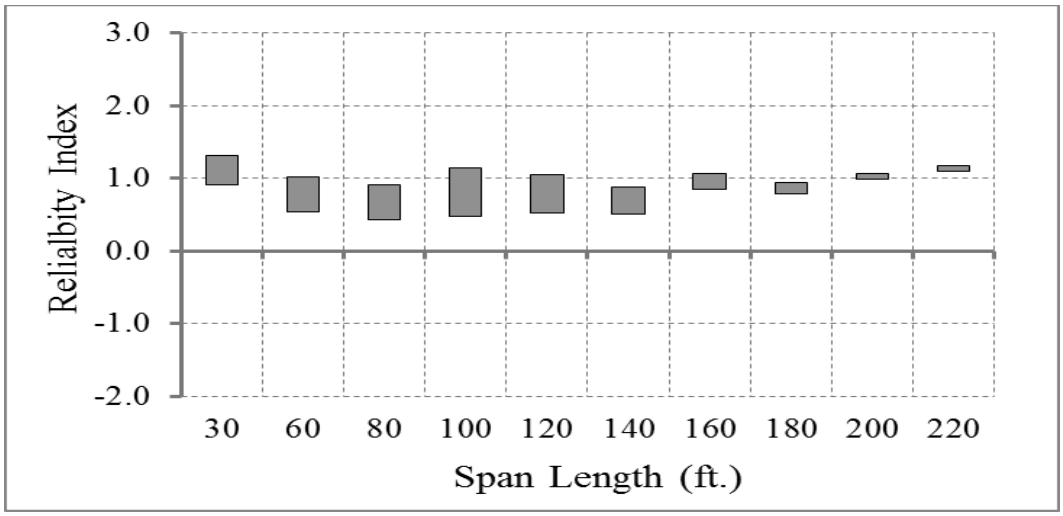

Figure 5-20 Reliability indices for bridges at decompression limit state (ADTT=5000), γ_{LL}=1.0 ($f_t = 0.25\sqrt{f_c'}$).

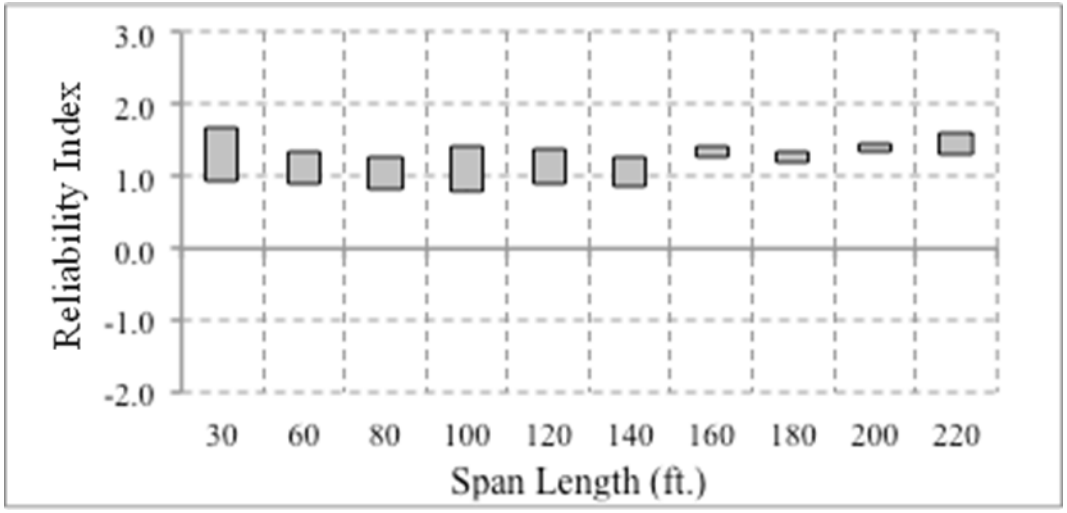

Figure 5-21 Reliability indices for bridges at maximum tensile stress limit state (ADTT=5000), γ_{LL}=1.0 ($f_t = 0.25\sqrt{f_c'}$).

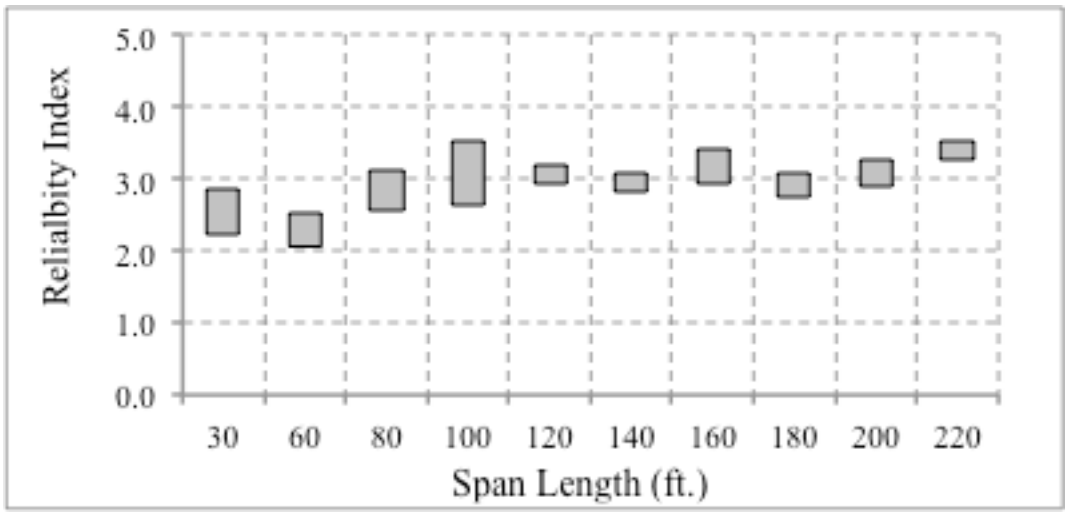

Figure 5-22 Reliability indices for bridges at maximum crack width limit state (ADTT=5000), γ_{LL}=1.0 ($f_t = 0.25\sqrt{f_c'}$).

5.2.5.9 Step 9: Calculate Reliability Indices

The reliability indices were calculated for three different cases as shown in Step 8 above. In Step 9, the calculated values were reviewed to determine whether they are close to the target reliability index and whether they are uniform across the range of spans considered. If they are not, the load factors, resistance factors, and/or the concrete tensile stress limit used for design would need to be changed and Step 8 would be repeated. The limit state function to be used as the basis for the calibration is also determined in Step 9.

5.2.5.10 Summary of Target Reliability Indices for Different Design and Performance Levels

A summary of the average reliability indices calculated for the different cases is given in Table 5-13 through

Table 5-15. Regardless of the maximum tensile stress limit used in the design, the limiting criteria for the maximum tensile stress when determining the reliability index was taken as $f_t = 0.19\sqrt{f_c'}$.

Table 5-13 Summary of Reliability Indices for Simulated Bridges Designed for $f_t = 0.0948\sqrt{f_c'}$

ADTT	Live Load Factor=0.8			Live Load Factor=1.0		
	Decompression	Max Tensile Stress Limit	Crack Width	Decompression	Max Tensile Stress Limit	Crack Width
1000	1.05	1.41	3.16	1.42	1.79	3.36
2500	1.01	1.35	3.11	1.38	1.75	3.33
5000	0.97	1.31	3.06	1.33	1.70	3.32
10000	0.94	1.30	3.00	1.32	1.66	3.28

Table 5-14 Summary of Reliability Indices for Simulated Bridges Designed for $f_t = 0.19\sqrt{f'_c}$

ADTT	Live Load Factor=0.8			Live Load Factor=1.0		
	Decompression	Max Tensile Stress Limit	Crack Width	Decompression	Max Tensile Stress Limit	Crack Width
1000	0.84	1.27	2.92	1.11	1.53	3.25
2500	0.70	1.15	2.87	1.04	1.46	3.17
5000	0.68	1.10	.82	1.00	1.41	3.14
10000	0.64	1.07	2.78	0.98	1.34	3.11

Table 5-15 Summary of Reliability Indices for Simulated Bridges Designed for $f_t = 0.25\sqrt{f'_c}$

ADTT	Live Load Factor=0.8			Live Load Factor=1.0		
	Decompression	Max Tensile Stress Limit	Crack Width	Decompression	Max Tensile Stress Limit	Crack Width
1000	0.20	0.55	2.83	0.93	1.29	3.03
2500	0.08	0.49	2.77	0.89	1.27	2.95
5000	0.06	0.44	2.72	0.85	1.23	2.92
10000	0.02	0.41	2.66	0.82	1.20	2.88

As indicated earlier, the calibration of the specifications are based on an ADTT of 5000. It was observed that for this ADTT, the reliability indices obtained assuming the bridges are designed for maximum stress limit of $f_t = 0.0948\sqrt{f'_c}$ and $f_t = 0.19\sqrt{f'_c}$ (see the outlined cells Table 5-13 and Table 5-14) are very close to the target reliability indices shown in Table 5-10.

5.2.5.11 Effect of Proposed Changes on Design

To investigate the effect of the proposed change in the load factor, the number of strands required for different design cases was compared (see Table 5-16). The comparison indicated that when a live load factor of 0.8 is used in both cases, the post-2005 prestress loss method results in smaller number of strands than when the pre-2005 prestress loss method is used. It also indicated that when the post-2005 loss method is used with a load factor of 1.0, the required number of strands is similar to that required when a load factor of 0.8 is used in conjunction with the pre-2005 prestress loss method, i.e. designs similar between pre-2005 and post-2005 methods.

5.2.5.12 Summary and Recommendations for Service III Limit State

For typical I-girders designed using the post-2005 prestress loss method and the assumptions listed in Section 5.2.3, comparing the target reliability indices shown in Table 5-10 and the calculated reliability indices for different design criteria, load factors, and design live load as shown in Table 5-13 through

Table 5-15 and Figure 5-5 through Figure 5-22, the following conclusions were drawn and summarized:

1. For a specific girder of known cross-section and specific number and arrangement of prestressing strands, the reliability index varies based on:

- The design maximum concrete tensile stress (a maximum tensile stress of $f_t = 0.0948\sqrt{f_c'}$ and $f_t = 0.19\sqrt{f_c'}$ is currently shown in *AASHTO LRFD* (2012) and is proposed to remain the same),
- The limit state function, i.e. decompression, tensile stress of a certain value (assumed to be $f_t = 0.19\sqrt{f_c'}$ in the work shown above), or a crack width of a certain value (assumed to be 0.016 in.), and
- ADTT.

The effect of different factors can be deduced from Table 5-13 through Table 5-15.

2. The target reliability index can be achieved uniformly across various span lengths using the load factor developed following the proposed calibration procedure. The level of uniformity varies with the limiting criteria. The decompression limit state showed the highest level of uniformity and is recommended to be used as the basis for the reliability analysis, i.e. the determination of the load and resistance factors and associated design criteria.

3. It is recommended that the reliability indices corresponding to ADTT of 5000 be used as the basis for the calibration. The reliability index is not highly sensitive to changes in the ADTT so there is no need to use different load factor for ADTTs up to 10000.

Table 5-16 Comparison of number of strands required for different design assumptions

Cases	Section Type	Span Length (ft.)	Girder Spacing (ft.)	$f_t = 0.0948\sqrt{f'_c}$, γLL=0.8, Pre-2005 losses	$f_t = 0.0948\sqrt{f'_c}$, γLL=0.8, Post-2005 losses	$f_t = 0.0948\sqrt{f'_c}$, γLL=1.0, Post-2005 losses	$f_t = 0.19\sqrt{f'_c}$, γLL=0.8, Pre-2005 losses	$f_t = 0.19\sqrt{f'_c}$, γLL=0.8, Post-2005 losses	$f_t = 0.19\sqrt{f'_c}$, γLL=1.0, Post-2005 losses
1	AASHTO I	30	6	8	8	8	8	8	8
2	AASHTO I	30	8	10	10	10	10	10	10
3	AASHTO I	30	10	12	12	12	12	12	12
4	AASHTO I	30	12	14	14	14	14	14	14
5	AASHTO II	60	6	20	16	20	18	16	16
6	AASHTO II	60	8	-	22	26	24	20	22
7	AASHTO III	60	10	22	20	22	20	20	20
8	AASHTO III	60	12	28	24	28	24	24	24
9	AASHTO III	80	6	28	24	28	24	22	24
10	AASHTO III	80	8	38	30	34	32	28	30
11	AASHTO III	80	10	-	36	40	42	32	38
12	AASHTO IV	80	12	40	34	38	34	32	34
13	AASHTO III	100	6	-	40	46	-	38	42
14	AASHTO IV	100	8	50	42	46	44	38	42
15	AASHTO IV	100	10	-	48	54	56	44	50
16	AASHTO V	100	12	56	46	50	48	42	46
17	AASHTO IV	120	6	-	52	58	58	48	52
18	AASHTO V	120	8	62	52	58	54	48	52
19	AASHTO V	120	10	-	60	68	68	54	60
20	AASHTO VI	120	12	74	58	64	64	54	58
21	AASHTO VI	140	6	62	54	58	54	48	52
22	AASHTO VI	140	8	-	64	70	68	58	64
23	AASHTO VI	140	10	-	74	-	-	68	74
24		140	12	-	-	-	-	-	-

4. With satisfactory past performance of prestressed beams, the target reliability index is selected to be similar to the average inherent reliability index of the bridges on the system. There is no scientific reason to substantiate targeting a different, higher or lower, reliability index.

5. The recommended target reliability index for the decompression limit state is 1.0 for bridges designed for no worse than moderate corrosion conditions and 1.2 for bridges designed for severe corrosion conditions. Based on the study of WIM data, the reliability index is determined assuming live load exists in single lane and without applying the multiple presence factor. This would appear on the "load side" of the limit state function.

6. Based on the reliability indices calculated for different design and load scenarios, to achieve the target reliability index, it is recommended that the following be used for designing for Service III limit state:

- Live load factor of 1.0.
- Maximum concrete tensile stress of $f_t = 0.0948\sqrt{f_c'}$ and $f_t = 0.19\sqrt{f_c'}$ for bridges in severe corrosion conditions and for bridges in no worse than moderate corrosion conditions, respectively.
- Girders to be designed following conventional design methods and assuming the live loads exist in single lane or multiple lanes, whichever produces higher load effects. The appropriate multiple presence factor applies.

These design parameters would appear on the "resistance side" of the limit state function during calibration.

7. The results of the calibration demonstrated that girders designed using the conventional design methods and the controlling number of loaded traffic lanes produce uniform reliability approximately equal to the target reliability index provided that the load factor is based on a reliability index calculated using the decompression criteria and assuming one lane of traffic.

5.2.6 Results for Adjacent Box Beams, Spread Box Beams, and American Segmental Box Institute (ASBI) Boxes

Work similar to that described above for I-beams was performed for adjacent box beams, spread box beams, and ASBI box beams. The details of the work are shown in Appendix D. The final results assuming the decompression limit state, ADTT of 5000, return period of 1 year, and a load factor of 1.0 for live load are shown in Figure 5-23 through Figure 5-28. Table 5-17 shows the average reliability indices represented graphically in Figure 5-23 through Figure 5-28.

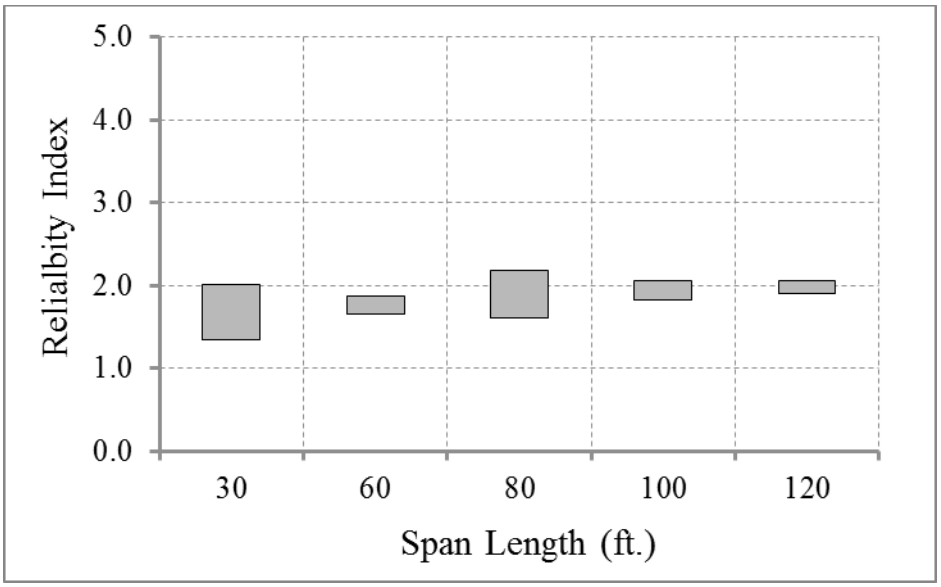

Figure 5-23- Adjacent box beams, reliability indices for bridges at decompression limit state (ADTT=5000), γ_{LL}=1.0 ($f_t = 0.0948\sqrt{f'_c}$).

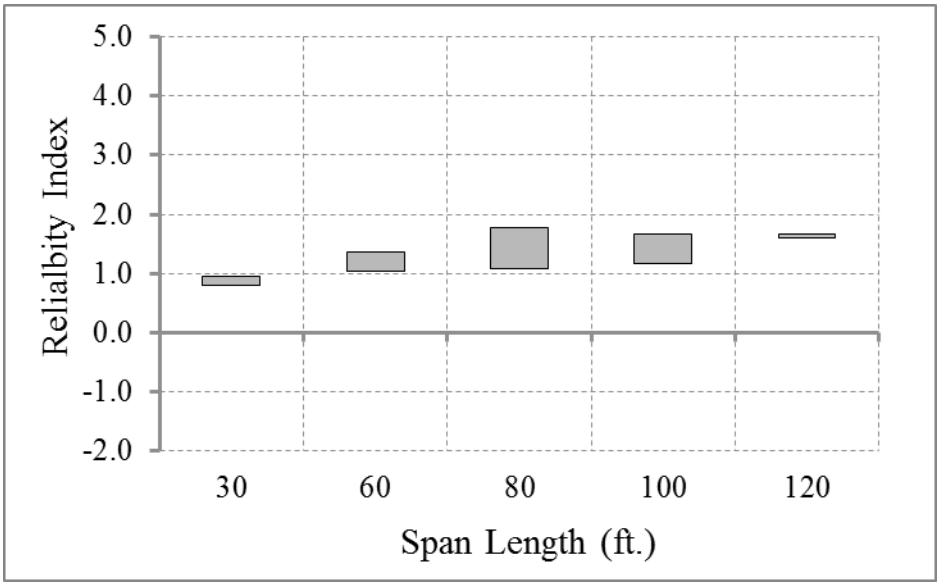

Figure 5-24 Adjacent box beams, reliability indices for bridges at decompression limit state (ADTT=5000), γ_{LL}=1.0 ($f_t = 0.19\sqrt{f'_c}$).

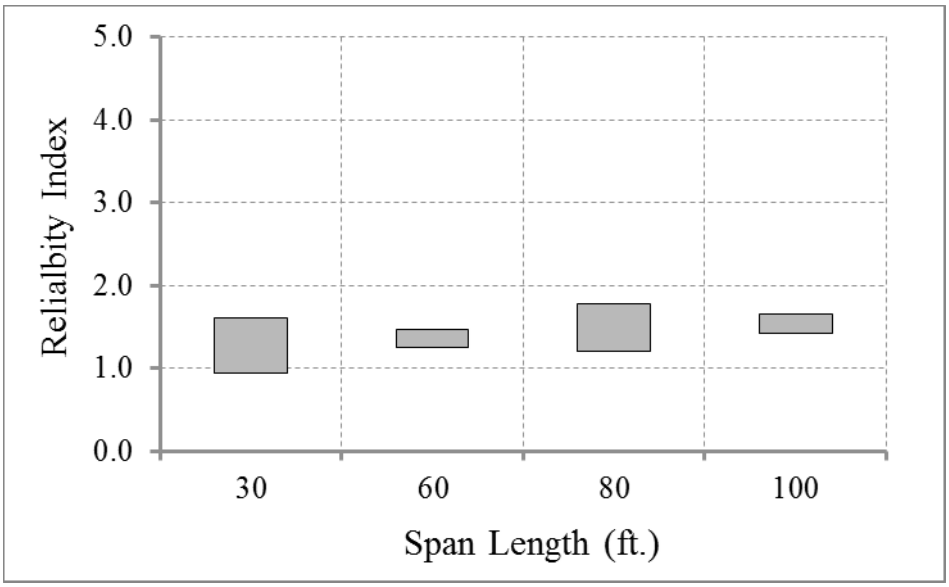

Figure 5-25 Spread box beams, reliability indices for bridges at decompression limit state (ADTT=5000), γ_{LL}=1.0 ($f_t = 0.0948\sqrt{f_c'}$).

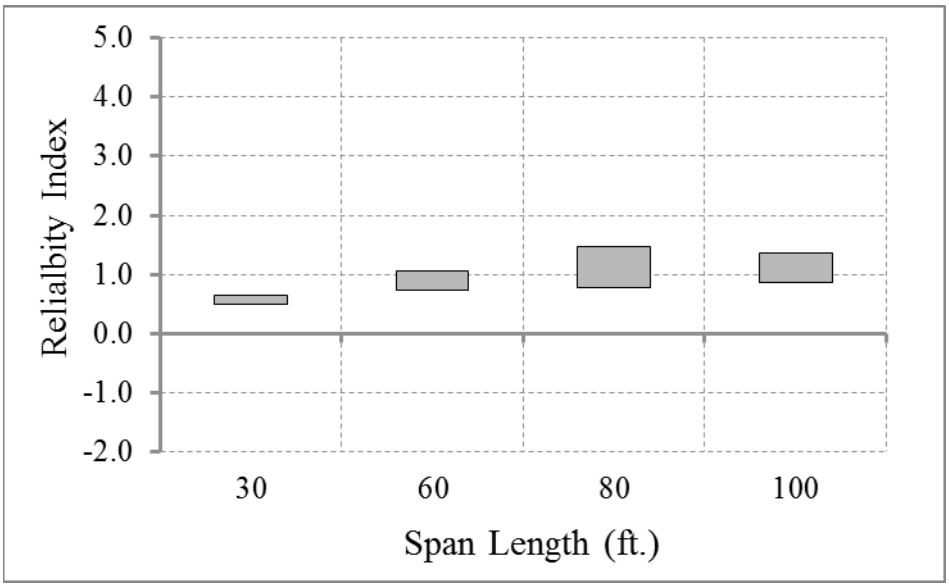

Figure 5-26 Spread box beams, reliability indices for bridges at decompression limit state (ADTT=5000), γ_{LL}=1.0 ($f_t = 0.19\sqrt{f_c'}$).

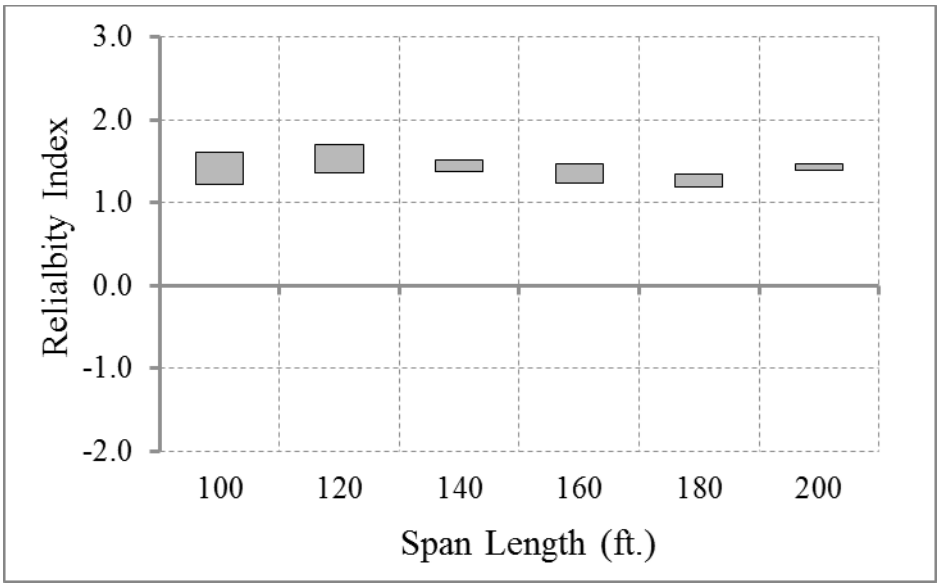

Figure 5-27 ASBI box beams, reliability indices for bridges at decompression limit state (ADTT=5000), γ_{LL}=1.0 ($f_t = 0.0948\sqrt{f_c'}$).

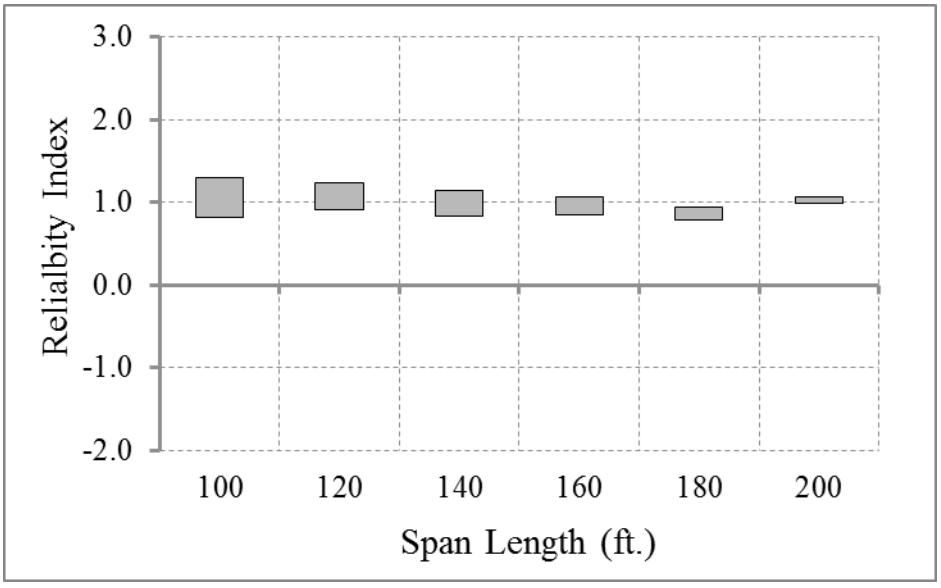

Figure 5-28 ASBI box beams, reliability indices for bridges at decompression limit state (ADTT=5000), γ_{LL}=1.0 ($f_t = 0.19\sqrt{f_c'}$).

Table 5-17 Average Reliability Indices for Different Types of Girders

Type of Section	Maximum tensile stress used in design (ksi)	
	$f_t = 0.0948\sqrt{f'_c}$	$f_t = 0.19\sqrt{f'_c}$
I- and Bulb T Girders	1.33	1.00
Adjacent Box Beams	1.85	1.31
Spread Box Beams	1.45	1.01
ASBI Box Beams	1.41	1.00

The results shown in Figure 5-23 through Figure 5-28 indicate that the reliability indices for each type of girder is reasonably uniform across the range of spans considered. With the exception of the adjacent box beams, the average reliability index for other section types is very close to each other and to the target reliability index. For adjacent box beams, the average reliability index is slightly higher. However, the difference does not warrant incorporating measures to reduce the resistance of the beams such as revising the distribution factor equations or use of lower load factors for adjacent box beams.

5.2.7 Sections Designed Using Other Methods of Determining Prestressing Time-Dependent Losses and/or Section Properties

As indicated in Section 5.2.3, the calibration of Service III limit states presented above assumes that the sections are designed using the "Refined Estimates of Time-Dependent Losses". *AASHTO LRFD* requires the time-dependent losses for segmental bridges to be determined using detailed time step methods. As such, the 2005 revisions to the "Refined Estimates of Time-Dependent Losses" did not affect the time-dependent prestressing loss calculations for segmental bridges. Historically, segmental bridges have also been designed using gross-section properties, not transformed section properties, and neglected the effects of the "elastic gain". The time step method may also be used to design prestressed concrete components other than segmental bridges if approved by the owner. However, the level of effort required to perform time step analysis typically precluded this method for non-segmental construction.

The proposed increase in the load factor for live load for Service III limit state from 0.8 to 1.0 is based on comparing sections designed using the *AASHTO LRFD* pre-2005 provisions and the post-2005 provisions without making any exceptions to the specifications requirements and assuming that the method termed in the *AASHTO LRFD* as the: "Refined Estimates of Time-Dependent Losses" was used for calculating the time-dependent losses.

The development of the method termed as the "Approximate Estimate of Time-Dependent Losses" in *AASHTO LRFD* was based on producing prestress losses similar results to those produced by the method termed "Refined Estimates of Time-Dependent Losses". Therefore, the change in the load factor should also be applied to the former method.

The changed in the prestress loss methods in 2005 did not affect the time step method. Therefore, the increase in the load factor should not be applied to sections designed using the time step method. These sections have to satisfy the following conditions to continue using the 0.8 load factor for live load:

- Time-dependent losses are determined using time step method,

- Gross sections properties are used for the calculations, and
- The calculations of the force in the prestressing steel neglects the effects of the elastic gain.

5.2.8 Proposed AASHTO LRFD Revisions

In AASHTO (2012), Article 5.9.4.2.2 ("Tension Stresses" for stresses in fully prestressed components at service limit state after losses) is the Article containing the design stress limits that are affected by the calibration of the Service III limit state. Due to the lack of changes to the design stress limits, no revisions to this section are required.

The only required revisions to the specifications based on the calibration of the limit state for tension in prestressed concrete presented above are those in Article 3.4.1 to specify the load factor for live load as 0.8 or 1.0 depending on the design procedure used.

5.3 Fatigue Limit State – Lifetime

5.3.1 Formulate the Limit State Function

While two limit states for load-induced fatigue are defined in *AASHTO LRFD* Article 3.4.1; only Fatigue I, related to infinite load-induced fatigue life; is applicable to concrete members as they are always designed for infinite life.

For load-induced fatigue considerations, according to *AASHTO LRFD* Article 5.5.3.1, concrete members shall satisfy:

$$\gamma\left(\Delta f\right) \le \left(\Delta F\right)_n \tag{5-3}$$

where

γ = load factor
(Δf) = force effect, live load stress range due to the passage of the fatigue load
$(\Delta F)_{TH}$ = constant-amplitude fatigue threshold

This general limit state function is used for the calibration of the fatigue limit states for concrete members.

The fatigue load of *AASHTO LRFD* Article 3.7.1.4 and the fatigue live-load load factors of *AASHTO LRFD* Table 3.4.1-1 are based upon extensive research of structural-steel highway bridges. The fatigue load is the *AASHTO LRFD* design truck (HS20-44 truck of AASHTO *Standard Specifications*, 2002), but with a fixed rear-axle spacing of 30 feet. The live-load load factors for the fatigue limit state load combinations are summarized in Table 5-18.

Table 5-18 Current Fatigue Load Factors

Fatigue Limit State	LL Load Factor
Fatigue I	1.5
Fatigue II (used for steel structures only)	0.75

The load factor for the Fatigue I load combination reflects load levels found to be representative of the maximum stress range of the truck population for infinite fatigue-life design. The factor was chosen on the assumption that the maximum stress range in the random variable spectrum is twice the effective stress range caused by Fatigue II load combination.

The load factor for the Fatigue II load combination reflects a load level found to be representative of the effective stress range of the truck population with respect to a small number of stress range cycles and to their cumulative effects in steel elements, components, and connections for finite fatigue-life design.

Information on the Fatigue II Limit state is included for reference and they were based on work done on steel components by Kulicki et. al. (2013)

The resistance factors for the fatigue limit states, ϕ, are inherently taken as unity and hence do not appear in Eq. (5-3).

5.3.1.1 Select Structural Types and Design Cases

The available data suggested that two fatigue limit states for concrete members could be rationally calibrated based upon current practice and the available data: steel reinforcement in tension (AASHTO LRFD Article 5.5.3.2) and concrete in compression (AASHTO LRFD Article 5.5.3.1).

5.3.1.2 Determine Load and Resistance Parameters for Selected Design Cases

5.3.1.2.1 Steel Reinforcement in Tension

Steel reinforcement considered herein includes straight reinforcing bars and welded-wire reinforcement. *AASHTO LRFD* Article 5.5.3.2 specifies the fatigue resistance of these types of reinforcement.

The fatigue resistance of straight reinforcing bars and welded-wire reinforcement without a cross weld in the high-stress region (defined as one-third of the span on each side of the section of maximum moment) is specified as:

$$\left(\Delta F\right)_{TH} = 24 - 0.33 f_{min} \quad (5\text{-}4)$$

where

f_{min} is the minimum stress.

For welded-wire reinforcement with a cross weld in the high-stress region, the fatigue resistance is specified as:

$$(\Delta F)_{TH} = 16 - 0.33 f_{min} \quad (5\text{-}5)$$

Both of these equations implicitly assume a ratio of radius to height (in other words, *r*/*h*) of the rolled-in transverse bar deformations of 0.3.

These fatigue resistances are defined as constant-amplitude fatigue thresholds in *AASHTO LRFD*. ACI Committee Report ACI 215R-74 and the supporting literature indicate that steel reinforcement exhibits a constant-amplitude fatigue threshold. ACI 215R-74 suggests that the resistances are "a conservative lower bound of all available test results." In other words, a horizontal constant-amplitude threshold has been drawn beneath all of the curves.

The studies used to define the fatigue resistance of steel reinforcement (Fisher and Viest, 1961; Pfister and Hognestad, 1964; Burton and Hognestad, 1967; Hanson et al., 1968; Helgason et al., 1976; Lash, 1969; MacGregor et al., 1971; Amorn et al., 2007) were reanalyzed to estimate constant-amplitude fatigue thresholds for every case that can be identified in the research to determine their uncertainty, in terms of bias, mean, and COV. The various thresholds were grouped together to make design practical.

5.3.1.2.2 Concrete in Compression

The compressive stress limit of 0.40 f_c' for fully prestressed components in other than segmentally constructed bridges of *AASHTO LRFD* Article 5.5.3.1 applies to a combination of the live load specified in the Fatigue I limit state load combination plus one-half the sum of the effective prestress and permanent loads after losses, i.e. a load combination derived from a modified Goodman diagram. This suggests that it represents an infinite-life check as the Fatigue I limit state load combination corresponds with infinite fatigue life.

For this study, the research used to define these S-N curves, Hilsdorf and Kesler (1966) was re-evaluated to estimate the constant-amplitude fatigue threshold, the infinite-life fatigue resistance. The uncertainty of the fatigue resistance was quantified in terms of bias, mean, and coefficient of variation.

5.3.1.3 Develop Statistical Models for Loads and Resistances

5.3.1.3.1 Load Uncertainties

Based on the analysis of WIM data discussed in Chapter 4, it is suggested that the current load factor of 1.5 for the Fatigue I limit state be increased to 2.0 to account for current and projected truck loads. Similarly, based on work by Kulicki et. al. (2013), it is proposed that the load factor of 0.75 for the Fatigue II limit state, which is not used for concrete structures and is mentioned here for reference only, be increased to a value of 0.80. The mean values and COV's from Chapter 4 are tabulated in Table 5-19.

Table 5-19 Load Uncertainties

Limit State	Mean	COV
Fatigue I	2.0	0.12
Fatigue II (used for steel structures only)	0.8	0.07

5.3.1.3.2 Resistance Uncertainties

The collection of the fatigue data was statistically analyzed using normal probability plots as the data best fits the normal distribution which is explained in further detail later. The normal probability plot is a graphical technique used in determining the statistical parameters of a normally distributed data set. The data points are plotted against a theoretical normal distribution and form an approximate straight line. Points that deviate from the straight line indicate deviation from normality. In other words if the observed data is normally distributed the points should form a straight line.

The horizontal axis of the normal probability plot represents the values of the data set while the vertical axis is the set of standard normal values or Z-scores. These standard normal values are representative of the cumulative distribution function of the standard normal distribution. Thus an ordered pair plotted within the normal probability plots of this project has an abscissa of the new fatigue parameter and an ordinate of the corresponding standard normal value.

The fatigue data was then filtered to include the data that most accurately reflects the fatigue behavior of each type of component, i.e. reinforcement in tension or concrete in compression. In other words, the data was truncated based on the nature of the curve within each normal probability plot to include the pertinent fatigue data. In general, the majority of the lower portion of each curve was selected for each detail category. This lower tail of the data was selected because it is the portion of the curve that fits the normal distribution, as it is the straight portion of the normal probability plot. Moreover, the lower portion of the fatigue data represents the range of values that fatigue cracking is expected to occur within when analyzed for the fatigue limit states load combinations using the Monte Carlo simulation approach.. Failure occurs when the load exceeds the resistance; thus the higher portions of the fatigue data sets represent fatigue resistance data that are very unlikely to be exceeded by the fatigue loads used within this study and therefore are insignificant.

Different approaches for selecting the cutoff values in which different cutoff values were used for each category were investigated to determine the sensitivity of the resulting reliability indices. It was determined that the relative difference of the results determined from the different techniques were negligible. Other techniques used to determine the cutoff values included the use of constant cutoff values for all of the various components, i.e. reinforcement in tension and concrete in compression as well as manually inserting best-fit lines by different analysts.

Determining the statistical parameters of the data is relatively straightforward once the data was filtered and fitted with a line of best fit using Microsoft Excel software. The mean value is simply the intersection of the best fit line with the horizontal axis. The standard deviation of the data is taken as the inverse of the slope of the best fit line. More simply stated it is the change in horizontal coordinates divided by the change in the vertical coordinates. Moreover, the COV is the ratio of the standard deviation divided by the mean of the data. The resulting

statistical parameters can be seen in Table 5-20. The probability plots of the fatigue data and corresponding truncated data for steel reinforcement in tension and concrete in compression can be seen in Appendix G. Figure 5-29 and Figure 5-30 show the normal probability plots of the full fatigue data set and the truncated data fatigue resistance of steel reinforcement in tension, respectively.

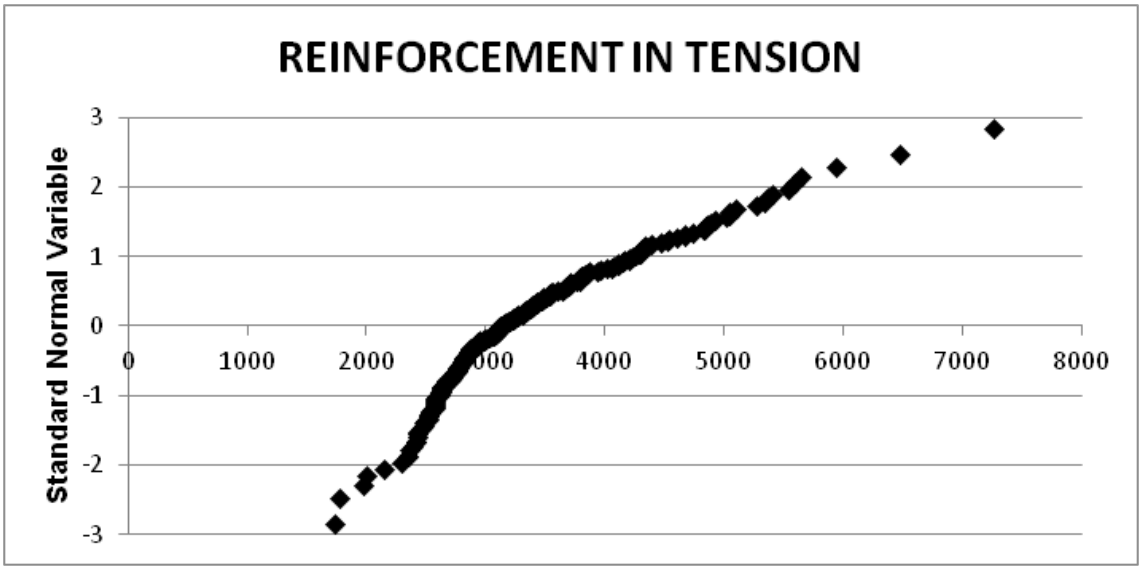

Figure 5-29 Normal Probability Plot of Fatigue Resistance Data for Steel Reinforcement in Tension

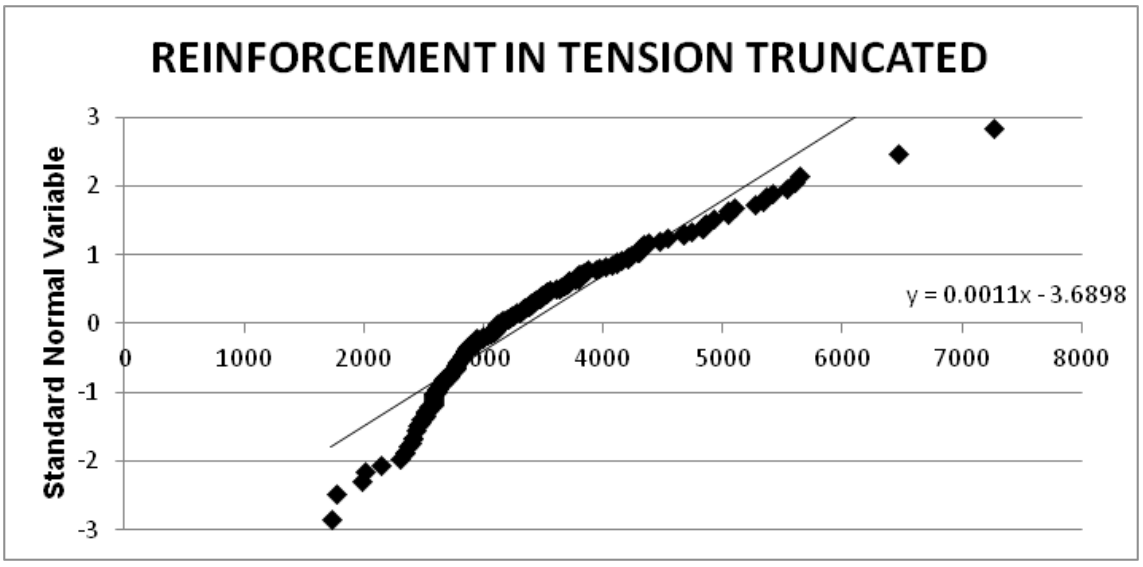

Figure 5-30 Normal Probability Plot of Truncated Fatigue Resistance Data with Best-Fit Line for Steel Reinforcement in Tension

Table 5-20 Resistance Uncertainties

Resistance	Standard Deviation	COV	Bias	Mean	Nominal	Cutoff Standard Normal Variable
steel reinforcement in tension	769.23	0.24	1.94	3261.54	1681.21	2
concrete in compression	117.65	0.45	1.74	260.35	149.66	2

5.3.1.4 Develop the Reliability Analysis Procedure

5.3.1.4.1 General

In the code calibration it is necessary to develop a process by which to express the structural reliability or the probability of the loads on the member being greater than its resistance; in other words, failure of the criteria. The reliability analysis performed within this project is an iterative process that consists of Monte Carlo simulations to select load and resistance factors that achieve reliability close to the target reliability index. The Monte Carlo technique samples load and resistance parameters from selected statistical distributions, such as a normal distribution. The reliability is measured in terms of a reliability index, or safety index, β. β is defined as a function of the probability of failure, PF, using the following equation. Thus β is the number of standard deviations that the mean safety margin falls on the safe side. The higher the β value, the higher the reliability.

$$\beta = - \Phi^{-1}(PF)$$

where

Φ^{-1} = the inverse standard normal distribution function

5.3.1.4.2 Monte Carlo Simulation

The following is a description of the calibration procedure applied to bridge structures. The distribution of loads is typically assumed to be normally distributed as the loads are a summation of force effects. The fatigue resistance has also been assumed to follow normal distributions. These distributions for load and resistance are developed using determined statistical parameters from the available data. The minimum statistical parameters needed for each random variable is the COV and the bias (λ). The COV is a measure of the scatter of the variable and the bias is the ratio of the mean to the nominal value. The simulation is then run by selecting random values from both the load and resistance distributions and comparing them using the appropriate limit-state function. If the result from the evaluation of the limit-state function is equal to or greater than zero, the function is satisfied and no failure results. Conversely, if the result is negative then a failure is recorded. This process is repeated over a large number of iterations and the number of failures is counted to determine the failure rate. Finally the reliability index is determined by taking the inverse of the standard normal cumulative distribution function using the determined failure rate.

5.3.1.5 Calculate the Reliability Indices for Current Design Code or Current Practice

Monte Carlo simulation was used to estimate the current inherent reliability indices by comparing the distribution of fatigue load with the distribution of fatigue resistance, based upon the uncertainties of load and resistance.

The simulations for both limit states were completed using a total of 10,000 replicates to achieve a sufficient number of failures.

For steel reinforcement in reinforced concrete members, the inherent β is approximately 2.0, but the inherent β for compression of concrete members is approximately 1.0. Both of these fatigue limit states are based upon the Fatigue I limit state and design for infinite life. The calculated inherent β's are given below in Table 5-21.

Table 5-21 Current Reliability Indices for the *AASHTO LRFD* Fatigue I Limit States

Resistance	β
Steel reinforcement in tension	1.9
Concrete in compression	0.9

5.3.1.6 Select the Target Reliability Index, β_T

Philosophically, the target reliability index should be identical for all members and all fatigue limit states. As such, the work on reinforcement and concrete fatigue was performed concurrently with, and is compared to, the work on structural steel fatigue.

As such, we propose a constant target reliability index, β_T, of 1.0 for steel reinforcement in tension, concrete in compression and structural steel members. This proposed target reflects the inherent reliability of the current Fatigue I limit state for concrete in compression and the Fatigue I and II limit states for structural steel members shown in Table 5-22 for comparison. This proposed target reduces the reliability of steel reinforcement in tension to levels consistent with the other calibrated fatigue limit states for which unity was chosen as the target reliability index.

Table 5-22 Current Reliability Indices for Steel Members Using AASHTO Fatigue I and Fatigue II Limit States

Detail Category	β	
	Fatigue I	Fatigue II
A	1.2	1.0
B	1.1	0.9
B'	1.5	1.0
C	1.2	0.9
C'	1.2	0.9
D	2.0	1.3
E	0.9	0.7
E'	1.7	1.4

5.3.1.7 Select Potential Load and Resistance Factors

Proposed resistance factors for the Fatigue I limit state are given in Table 5-23. Resistance factors other than the current values of unity are shown in boldface.

Table 5-23 Proposed Fatigue I Limit-State Resistance Factors

Resistance	Proposed Resistance Factor, Φ	Reliability Index, β
Steel reinforcement in tension	**0.8**	1.1
Concrete in compression	1.0	0.9

5.3.1.8 Calculate Reliability Indices

With the proposed resistance factors, the reliability indices are all within ± 0.1 of the target reliability index of 1.0.

The resultant reliability indices tabulated above can also be achieved by revising the *AASHTO LRFD* constant-amplitude fatigue thresholds for steel reinforcement in tension. This may be a better solution than including a resistance factor other than unity for only one of the concrete member fatigue limit states. The required revision to the *AASHTO LRFD* equations for the thresholds are given below.

The revised fatigue resistance of straight reinforcing bars and welded-wire reinforcement without a cross weld in the high-stress region would be specified as:

$$(\Delta F)_{TH} = 19 - 0.26 f_{min} \quad (5\text{-}6)$$

where

f_{min} is the minimum stress.

For welded-wire reinforcement with a cross weld in the high-stress region, the fatigue resistance would be specified as:

$$(\Delta F)_{TH} = 13 - 0.26 f_{min} \quad (5\text{-}7)$$

5.3.2 Proposed AASHTO LRFD Revisions

In *AASHTO LRFD* (2012), the Fatigue Limit State applicable to concrete structures is addressed in Sections 3 and 5. The Articles that will require modification to implement the revisions recommended herein are indicated in Table 5-24.

Table 5-24 Summary of Relevant Articles in AASHTO LRFD for Fatigue

Article (See Note)	Title	Relates To
3.4.1, Table 3.4.1-1	Load Factors and Load Combinations	Fatigue I and II*
5.5.3.2	Reinforcing Bars	Fatigue Threshold
5.5.3.3	Prestressing Tendons	Fatigue Threshold

* All concrete-related fatigue issues utilize Fatigue I limit state. Other revisions related to Fatigue II limit state for use in designing steel structures are detailed in Kulicki et. al. (2013) SHRP R19B report

The proposed revisions are detailed in Chapters 6 and 7.

5.4 Service Design for Overload

One of the goals of this project was to develop a service limit state for permit (overload) vehicles for concrete structures akin to Service II limit state in the current AASHTO LRFD which is applicable only to steel structures. The Service II limit state is intended to prevent changes in ride quality and appearance of steel structures resulting from permanent deflections due to yielding under service loads.

For steel structures, the limit state function and the consequences are well defined; the yielding of the steel component and the permanent deformations associated with yielding. For all concrete structures service limit states, the limit state function and the consequences of exceeding the limit state are not well defined. For service limit states discussed above for concrete structures, the calibration was based on obtaining uniform reliability at a level similar to the average reliability inherent in past designs. The consequence of exceeding the limit state was not part of the calibration as it was not possible to quantify. In the absence of past requirements for designing concrete components for service level overloads, there is no basis to what might be a reasonable level of reliability under overloads.

With the reliability indices selected for the service limit states are the range of 1.0 to 1.6 (15.9% and 5.5% probability of exceeding the limit state during one year, respectively), it is expected that the service limit states calibrated earlier will be exceeded when heavy permit vehicles cross a bridge. The question changes from the frequency of exceeding the limit state to the consequences of significantly exceeding the limit state.

For a meaningful calibration under overloads, the following needs to be available:

- Adequate information on the frequency of permit vehicles on the highways in comparison to other vehicles.
- Adequate information on the actual weights of permit vehicles and how these weights compare to the permitted loads.
- Quantifying the consequences of exceeding the limit states (required for all service limit states calibrated in this report other than fatigue for which the consequences are known) and quantifying the consequences of significantly exceeding the limit states. For example, in addition to quantifying the consequences of exceeding the compression limit state for prestressed

components under normal service loads, the consequences of significantly exceeding the decompression, i.e. opening a wide crack, also need to be quantified. The latter can then be used for calibration under permit loads.

The following conclusions were drawn from the study of heavy vehicles in the WIM data, the Louisiana truck citation data and New Jersey Permit data (see Section 4):

- The frequency of vehicles producing load effects exceeding HL-93 varies significantly from one site to another. Generally, the average frequency of vehicles producing load effects exceeding HL-93 is small and is dependent on the span length. Vehicles producing load effects exceeding HL-93 are generally assumed to be permit vehicles.
- The available information on how actual loads compare to the permitted loads is limited. This information is from one source (Louisiana) and is incomplete in that the truck configuration and individual axle loads are not given.
- The percentage of vehicles in each GVW category based on the permitted GVW's varies significantly between New Jersey and Louisiana. With no information on the actual GVW's in New Jersey and how they compare to the permitted GVW's, it is not known how the actual GVW's in New Jersey compare to those in Louisiana. The lack of correlation between the two states also indicates that variation between states exist and makes any assumption regarding other states' permit vehicles unjustifiable.

It was concluded that the available information is not adequate to produce meaningful calibration for the concrete limit states under overloads.

6 PROPOSED CHANGES TO *AASHTO LRFD*

Various articles of *AASHTO LRFD* which would need to be modified to implement the calibrated SLS resulting from this research were identified. This Chapter contains the suggested modifications formatted in a form suitable for consideration by the affected Technical Committees as potential Agenda Items for the Highway Subcommittee on Bridges and Structures (HSCOBS). Since the various SLS revisions are independent of each other and could be implemented individually, the suggested provisions are presented in separate subsections for each SLS. The article numbering system used in *AASHTO LRFD* has been preserved. The proposed revisions are underlined and deletions are shown as strikethrough.

6.1 Cracking of Prestressed Concrete – Currently Service III

6.1.1 Proposed Revisions to Section 5

5.7.3.4—Control of Cracking by Distribution of Reinforcement

The provisions specified herein shall apply to the reinforcement of all concrete components, except that of deck slabs designed in …….

.
.
.
.
.
.
.
.
.
.
.

Such reinforcement may be included in strength computations if a strain compatibility analysis is made to determine stresses in the individual bars or wires.

C5.7.3.4

All reinforced concrete members are subject to cracking under any load condition, including thermal effects and restraint……..

.
.
.
.
.

The requirements for skin reinforcement are based upon ACI 318-95. For relatively deep flexural members, some reinforcement should be placed near the vertical faces in the tension zone to control cracking in the web. Without such auxiliary steel, the width of the cracks in the web may greatly exceed the crack widths at the level of the flexural tension reinforcement.

The reliability index for control of cracking by distribution of reinforcement in reinforced concrete decks using the conventional design methods and using Equation 5.7.3.4 was investigated in Wassef et. al. (2014). It was found that the equation gives a fairly uniform reliability index.

6.2 Cracking of Prestressed Concrete

6.2.1 Proposed Revisions to Section 3

3.4—LOAD FACTORS AND COMBINATIONS

3.4.1—Load Factors and Load Combinations
The total factored force effect shall …….

Service I—Load combination relating to the normal operational use of the bridge with a 55 mph wind and all loads taken at their nominal values. Also related to deflection control in buried metal structures, tunnel liner plate, and thermoplastic pipe, to control crack width in reinforced concrete structures, and for transverse analysis relating to tension in concrete segmental girders. This load combination should also be used for the investigation of slope stability.

Service II—Load combination intended to control yielding of steel structures and slip of slip-critical connections due to vehicular live load.

Service III—Load combination for longitudinal analysis relating to tension in prestressed concrete superstructures with the objective of crack control and to principal tension in the webs of segmental concrete girders.

C3.4.1

The background for the load factors……..

Compression in prestressed concrete components and tension in prestressed bent caps are investigated using this load combination. Service III is used to investigate tensile stresses in prestressed concrete components.

This load combination corresponds to the overload provision for steel structures in past editions of the AASHTO Specifications, and it is applicable only to steel structures. From the point of view of load level, this combination is approximately halfway between that used for Service I and Strength I Limit States.
Prior to 2014, the longitudinal analysis relating to tension in prestressed concrete superstructures was investigated using a load factor for live load of 0.8. ~~The live load specified in these specifications~~ This load factor reflected, among other things, the then-current exclusion weight limits mandated by various jurisdictions at the time of the development of the specifications in 1993. Vehicles permitted under these limits have been in service for many years prior to 1993. It was concluded at that time that, for longitudinal loading, there is no nationwide physical evidence that these vehicles have caused cracking in existing prestressed concrete components. The 0.8 load factor was applied regardless of the method used for determining the loss of prestressing. ~~The statistical significance of the 0.80 factor on live load is that the event is expected to occur about once a year for bridges with two traffic lanes, less often for bridges with more than two traffic lanes, and about once a day for bridges with a single traffic lane.~~
The calibration of the service limit states for concrete components (Wassef et. al. 2014) concluded that typical components designed using the Refined Estimates of Time-Dependent Losses method incorporated in the specifications in 2005 have a lower reliability index against flexural cracking in prestressed components than components designed using the prestress loss calculation method specified prior to 2005. For

components designed using the currently-specified methods for instantaneous prestressing losses and the currently-specified Refined Estimates of Time-Dependent Losses method, an increase in the load factor for live load from 0.8 to 1.0 was required to maintain the level of reliability against cracking of prestressed concrete components inherent in the system.

Components which design satisfies all of the following conditions:

- A refined time step method is used for calculating the time-dependent prestressing losses
- The section properties are determined based on the concrete gross section, and,
- The force in prestressing steel is determined without taking advantage of the elastic gain, were not affected by the changes in the prestressing loss calculation method introduced in 2005. For these components, a load factor for live load of 0.8 was maintained.

Service I should be used for checking tension related to transverse analysis of concrete segmental girders.

The principal tensile stress check is introduced in order to verify the adequacy of webs of segmental concrete girder bridges for ~~longitudinal shear and torsion~~ axial load, longitudinal moment, longitudinal shear and torsion.

Service IV—Load combination relating only to tension in prestressed concrete columns with the objective of crack control.

Table 3.4.1-1—Load Combinations and Load Factors

Load Combination Limit State	*DC DD DW EH EV ES EL PS CR SH*	*LL IM CE BR PL LS*	*WA*	*WS*	*WL*	*FR*	*TU*	*TG*	*SE*	Use One of These at a Time				
										EQ	*BL*	*IC*	*CT*	*CV*
Strength I (unless noted)	γ_p	1.75	1.00	—	—	1.00	0.50/1.20	γ_{TG}	γ_{SE}	—	—	—	—	—
Strength II	γ_p	1.35	1.00	—	—	1.00	0.50/1.20	γ_{TG}	γ_{SE}	—	—	—	—	—
Strength III	γ_p	—	1.00	1.40	—	1.00	0.50/1.20	γ_{TG}	γ_{SE}	—	—	—	—	—
Strength IV	γ_p	—	1.00	—	—	1.00	0.50/1.20	—	—	—	—	—	—	—
Strength V	γ_p	1.35	1.00	0.40	1.0	1.00	0.50/1.20	γ_{TG}	γ_{SE}	—	—	—	—	—
Extreme Event I	γ_p	γEQ	1.00	—	—	1.00	—	—	—	1.00	—	—	—	—
Extreme Event II	γ_p	0.50	1.00	—	—	1.00	—	—	—	—	1.00	1.00	1.00	1.00
Service I	1.00	1.00	1.00	0.30	1.0	1.00	1.00/1.20	γ_{TG}	γ_{SE}	—	—	—	—	—
Service II	1.00	1.30	1.00	—	—	1.00	1.00/1.20	—	—	—	—	—	—	—
Service III	1.00	~~0.80~~ γ_{LL}	1.00	—	—	1.00	1.00/1.20	γ_{TG}	γ_{SE}	—	—	—	—	—
Service IV	1.00	—	1.00	0.70	—	1.00	1.00/1.20	—	1.0	—	—	—	—	—
Fatigue I—*LL*, *IM* & *CE* only	—	1.50	—	—	—	—	—	—	—	—	—	—	—	—
Fatigue II—*LL*, *IM* & *CE* only	—	0.75	—	—	—	—	—	—	—	—	—	—	—	—

Table 3.4.1-4—Load Factors for Live Load for Service III Load Combination, γ_{LL}

Component	γ_{LL}
Prestressed concrete components designed using a refined time step method to determine the time-dependent prestressing losses in conjunction with the gross section properties and without taking advantage of the elastic gain	0.8
All other prestressed concrete components	1.0

6.3 Fatigue

Only Fatigue I Limit State is applicable to concrete and reinforcement. Information on the Fatigue II Limit state is included for reference and they were based on work done on steel components by Kulicki et al. (2013).

6.3.1 Proposed Revisions to Section 3

3.4—LOAD FACTORS AND COMBINATIONS

Table 3.4.1-1—Load Combinations and Load Factors

Load Combination Limit State	*DC DD DW EH EV ES EL PS CR SH*	*LL IM CE BR PL LS*	*WA*	*WS*	*WL*	*FR*	*TU*	*TG*	*SE*	Use One of These at a Time				
										EQ	*BL*	*IC*	*CT*	*CV*
Strength I (unless noted)	γ_p	1.75	1.00	—	—	1.00	0.50/1.20	γ_{TG}	γ_{SE}	—	—	—	—	—
Strength II	γ_p	1.35	1.00	—	—	1.00	0.50/1.20	γ_{TG}	γ_{SE}	—	—	—	—	—
Strength III	γ_p	—	1.00	1.40	—	1.00	0.50/1.20	γ_{TG}	γ_{SE}	—	—	—	—	—
Strength IV	γ_p	—	1.00	—	—	1.00	0.50/1.20	—	—	—	—	—	—	—
Strength V	γ_p	1.35	1.00	0.40	1.0	1.00	0.50/1.20	γ_{TG}	γ_{SE}	—	—	—	—	—
Extreme Event I	γ_p	γEQ	1.00	—	—	1.00	—	—	—	1.00	—	—	—	—
Extreme Event II	γ_p	0.50	1.00	—	—	1.00	—	—	—	—	1.00	1.00	1.00	1.00
Service I	1.00	1.00	1.00	0.30	1.0	1.00	1.00/1.20	γ_{TG}	γ_{SE}	—	—	—	—	—
Service II	1.00	1.30	1.00	—	—	1.00	1.00/1.20	—	—	—	—	—	—	—
Service III	1.00	0.80	1.00	—	—	1.00	1.00/1.20	γ_{TG}	γ_{SE}	—	—	—	—	—
Service IV	1.00	—	1.00	0.70	—	1.00	1.00/1.20	—	1.0	—	—	—	—	—
Fatigue I— *LL, IM & CE* only	—	~~1.50~~ 2.0	—	—	—	—	—	—	—	—	—	—	—	—
Fatigue II— *LL, IM & CE* only	—	~~0.75~~ 0.80	—	—	—	—	—	—	—	—	—	—	—	—

6.3.2 Proposed Revisions to Section 5

5.5.3.2—Reinforcing Bars

The constant-amplitude fatigue threshold, $(\Delta F)_{TH}$, for straight reinforcement and welded wire reinforcement without a cross weld in the high-stress region shall be taken as:

~~$(\Delta F)_{TH} = 24 - 0.33 f_{min}$~~ ~~(5.5.3.2-1)~~

$(\Delta F)_{TH} = 19 - 0.26 f_{min}$ (5.5.3.2-1)

The constant-amplitude fatigue threshold, $(\Delta F)_{TH}$, for straight welded wire reinforcement with a cross weld in the high-stress region shall be taken as:

~~$(\Delta F)_{TH} = 16 - 0.33 f_{min}$~~ ~~(5.5.3.2-2)~~

$(\Delta F)_{TH} = 13 - 0.26 f_{min}$ (5.5.3.2-2)

where:

f_{in}_ = minimum live-load stress resulting from the Fatigue I load combination, combined with the more severe stress from either the permanent loads or the permanent loads, shrinkage, and creep-induced external loads; positive if tension, negative if compression (ksi)

The definition of the high-stress region for application of Est. 5.5.3.2-1 and 5.5.3.2-2 for flexural reinforcement shall be taken as one-third of the span on each side of the section of maximum moment.

C5.5.3.2

Bends in primary reinforcement should be avoided in regions of high-stress range.

Structural welded wire reinforcement has been increasingly used in bridge applications in recent years, especially as auxiliary reinforcement in bridge I- and box beams and as primary reinforcement in slabs. Design for shear has traditionally not included a fatigue check of the reinforcement as the member is expected to be uncracked under service conditions and the stress range in steel minimal. The stress range for steel bars has existed in previous editions. It is based on Hansen et al. (1976). The simplified form in this edition replaces the (r/h) parameter with the default value 0.3 recommended by Hansen et al. Inclusion of limits for WWR is based on recent studies by Hawkins et al. (1971, 1987) and Tadros et al. (2004). Coefficients in Equations 5.5.3.2-1 and 5.5.3.2-2 have been updated based on calibration reported in Kulicki et al (2013).

Since the fatigue provisions were developed based primarily on ASTM A615 steel reinforcement, their applicability to other types of reinforcement is largely unknown. Consequently, a cautionary note is added to the Commentary.

7 CONCLUSIONS AND SUGGESTED FUTURE RESEARCH

7.1 Conclusions

7.1.1 General Conclusions Related to the Calibration of Service Limit States

- The main problem in calibrating the service limit states is the lack of clear consequences to exceeding the limit state.

- The target reliability index used in the calibration of any limit state is a measure of the frequency this limit state is expected to be violated during the period assumed in the calibration. Due to the lack of clear consequences, the target reliability index for each service limit state has to be selected taking into consideration the reliability inherent in past designs. At this time, there are no justifiable reasons to select target reliability indices that are higher or lower than those inherent in past designs.

- Basing the target reliability index for each service limit state on the reliability inherent in this limit state in past designs results in different target reliability indices applied to different service limit states.

- For the same phenomenon being addressed, more than one limiting criteria may be used as the limit state function. Each limiting criterion results in a different reliability index.

- For the same service limit state and same limiting criterion, the target reliability index may vary depending on the environmental conditions.

7.1.2 Conclusions Related to the Live Load Model for Service Limit States

- The probability of heavy correlated trucks existing in two adjacent lanes is very low. For the service limit states calibrated in this report for concrete structures, assuming that the live load only exists in a single traffic lane with no multiple presence factors applied is appropriate
- The design load for SLS, i.e. notional load, should not try to encompass all WIM records. Some of the extremely heavy vehicles are permit loads and some are illegal overloads
- Some jurisdictions may need to make exceptions based on their legal loads and extent of enforcement
- Basic HL-93 load model, scaled by calibrated load factors, is appropriate for SLS
- Available information on the scale weights of permit loads, how the actual loads compare to the conditions of the permits and the frequency of permit loads on the highways is insufficient to perform calibration that is meaningful and can be generalized to other locations

7.1.3 General Conclusions Related to the Specific Limit States Calibrated

7.1.3.1 Cracking of Reinforced Concrete Decks through the Distribution of Reinforcement

- Assessment of current practice leads to a recommended target reliability indices of 1.6 for the base case (Class 1 exposure) and 1.0 for situations when there is increased concern of appearance and/or corrosion (Class 2 exposure). These values correspond to a single lane ADTT of 5000 and annual probability.
- The current requirements in the specifications produce uniform reliability across the range of girder spacing considered, so there is no need to change the load or resistance factors.
-

7.1.3.2 Tension in Prestressed Concrete Beams

For sections designed using conventional methods:

- Among several limit state functions investigated, decompression produced the most uniform results and is recommended as the basis for the calibration
- For a specific girder of known cross-section and specific number and arrangement of prestressing strands, the reliability index varies based on the design maximum concrete tensile stress, the limiting criteria, e.g. decompression, and ADTT
- A uniform reliability index can be achieved uniformly across various span lengths using the load factor developed following the proposed calibration procedure and assuming the decompression limit state
- The reliability index is not highly sensitive to changes in the ADTT. While the bulk of the work assumed an ADTT of 5000, based on the analysis of selected cases, using ADDT's as high as 10000 essentially resulted in essentially the same load and resistance factors
- The recommended target reliability index for the decompression limit state is 1.0 for bridges designed for no worse than moderate corrosion conditions and 1.2 for bridges designed for severe corrosion conditions
- Based on the reliability indices calculated for different design and load scenarios, to achieve the target reliability index, it is recommended that the following be used for designing for Service III limit state:
  - Live load factor of 1.0.
  - Maximum concrete tensile stress of $f_t = 0.0948\sqrt{f_c'}$ and $f_t = 0.19\sqrt{f_c'}$ for bridges in severe corrosion conditions and for bridges in no worse than moderate corrosion conditions, respectively.
  - Girders to be designed following conventional design methods and assuming the live loads exist in single lane or multiple lanes, whichever produces higher load effects. The appropriate multiple presence factor applies.
- The results of the calibration demonstrated that girders designed using the conventional design methods and the controlling number of loaded traffic lanes produce uniform reliability approximately equal to the target reliability index provided that the load factor is based on a reliability index calculated using the decompression

criteria and assuming one lane of traffic on the load side of the reliability index calculation.

For sections satisfying the following conditions:

- Time-dependent losses are determined using time step method,
- Gross sections properties are used for the calculations, and
- The calculations of the force in the prestressing steel neglects the effects of the elastic gain.

A load factor for live load of 0.8 may be used.

7.1.3.3 Fatigue of Steel Reinforcement in Tension and Concrete in Compression

- The proposed load factor for the infinite fatigue life is 2.0; up from 1.5 in the current specifications.
- The target reliability index for fatigue of steel reinforcement in tension and concrete in compression is taken as 1.0; the same as it is currently implied in the specifications for structural steel components, steel reinforcement in tension and concrete in compression.
- The current limit on stresses on concrete in compression that is meant to control concrete fatigue results in a reliability index close to the target reliability index. No revisions to the stress limit are required.
- The current threshold on the constant-amplitude fatigue for steel reinforcement results in a reliability index higher than the target reliability index. Reducing the reliability index can be achieved using either of the following approaches:
  - Maintain the current equation used to calculate the constant-amplitude threshold and apply a resistance factor of 0.8, or,
  - Multiply the current equation used to calculate the constant-amplitude threshold by a factor of 0.8 and apply a resistance factor of 1.0 which matches the resistance factor for all other fatigue cases

The latter approach is recommended which results in revising the constant fatigue threshold equations to:

For straight reinforcing bars and welded-wire reinforcement without a cross weld in the high-stress region:

$$(\Delta F)_{TH} = 19 - 0.26 f_{min}$$

For welded-wire reinforcement with a cross weld in the high-stress region:

$$(\Delta F)_{TH} = 13 - 0.26 f_{min}$$

7.2 Suggested Future Research

- Research on quantifying the consequences of exceeding different service limit states is needed. This quantification needs also to consider the degree of severity the limit states are exceeded to allow a better understanding of the effect of heavier vehicles on the serviceability of different components.

- Instrumentation of a prestressed concrete girder bridge on one of the heavily travelled roads to confirm the assumption that prestressed concrete beams may actually crack in service under heavy loads is needed. The bridge should be located in a jurisdiction that uses the HL-93 loading without jurisdiction-specific heavy vehicles for design.
- Data is needed on the distribution of actual weights and configurations of permit vehicles and how they relate to the permitted weights and configurations. The data needs to be collected from several jurisdictions to investigate whether the same trends exist at different locales.
- Data on the frequency of permit vehicles on different roads needs to be developed.
- Research is needed to investigate whether the deck shrinkage restraint by the girders and the relative stiffness of the deck to the supporting members have an effect on deck cracking.

REFERENCES

AASHTO LRFD Bridge Design Specifications, 6th ed. 2012. AASHTO, Washington, DC.

Allen, T., A. Nowak, and R. Bathurst. 2005. *Transportation Research Circular E-C079: Calibration to Determine Load and Resistance Factors for Geotechnical and Structural Design*. Transportation Research Board of the National Academies, Washington, DC. http://onlinepubs.trb.org/onlinepubs/circulars/ec079.pdf.

Amorn, W., J. Bowers, A. Girgis, and M. Tadros. 2007. Fatigue of Deformed Welded-Wire Reinforcement. *Journal, Precast/Prestressed Concrete Institute*, Vol. 52, No. 1, pp. 106–120.

Barker, M., and K. Barth. 2007. *Live Load Deflection Serviceability of HPS Composite Steel Girder Bridges*. 2007 World Steel Bridge Symposium Papers, New Orleans, LA.

Burton, K., and E. Hognestad. 1967. Fatigue Test of Reinforcing Bars-Tack Welding of Stirrups. *Journal, American Concrete Institute*, Vol. 64, No. 5, pp. 244–252.

Ellingwood, B., J. Galambos, J. MacGregor, and C. Cornell. 1980. *Development of a Probability Based Load Criterion for American National Standard A58*. NBS Special Publication 577. U.S. Department of Commerce, National Bureau of Standards, Washington, DC.

EN 1990 (Eurocode 0): Basis of Structural Design. 2002. European Committee for Standardization, Brussels, Belgium.

EN 1991-1-6 (Eurocode 1): Actions on Structures - Part 1-6: General Actions - Actions during Execution. 2005. European Committee for Standardization, Brussels, Belgium.

EN 1991-2 (Eurocode 1): Actions on Structures - Part 2: Traffic Loads on Bridges. 2003. European Committee for Standardization, Brussels, Belgium.

EN 1992-2 (Eurocode 2): Design of Concrete Structures - Part 2: Concrete Bridges - Design and Detailing Rules. 2005. European Committee for Standardization, Brussels, Belgium.

EN 1998-2 (Eurocode 8): Design of Structures for Earthquake Resistance - Part 2: Bridges. 2005. European Committee for Standardization, Brussels, Belgium.

Fisher, J., and I. Viest. 1961. *Fatigue Tests of Bridge Materials of the AASHO Road Test*. Special Report 66. American Association of State Highway Officials, Highway Research Board, Washington, DC.

Gross, S., and S. Burns. 2000. *Field Performance of Prestressed High Performance Concrete Bridges in Texas*. FHWA/TX-05/9-580/589-2. Center for Transportation Research at the University of Texas at Austin, Texas Department of Transportation, FHWA, Austin, TX.

Hanson, J., K. Burton, and E. Hognestad. 1968. Fatigue Tests of Reinforcing Bars-Effect of Deformation Pattern. *Journal of the Portland Cement Association Research and Development Laboratories*, Vol. 10, No. 3, pp. 2–13.

Helgason, T., J. Hanson, N. Somes, W. Corley, and E. Hognestad. 1976. *NCHRP Report 164: Fatigue Strength of High Yield Reinforcing Bars*. TRB, National Research Council, Washington, DC.

Hilsdorf, H., and C. Kesler. 1966. Fatigue Strength of Concrete under Varying Flexural Stresses. *Journal Proceedings, American Concrete Institute*, Vol. 63, No. 10, pp. 1059–1076.

ISO 2394: General Principles on Reliability for Structures, 3rd ed. 1998. International Organization for Standardization, Geneva, Switzerland.

Kulicki, J., W. Wassef, D. Mertz, A. Nowak, N. Samtani, and H. Nassif. 2013. *Service Load Design for 100-Year Life*. SHRP2, R19B. Transportation Research Board of the National Academies, Washington, DC (Under Preparation).

Kulicki, J., Z. Prucz, C. Clancy, D. Mertz, and A. Nowak. 2007. *Updating the Calibration Report for AASHTO LRFD Code*. Report on NCHRP 20-7/186. Transportation Research Board of the National Academies, Washington, DC.

Lash, S. 1969. Can High-Strength Reinforcement be used in Highway Bridges. In *First International Symposium on Concrete Bridge Design*. SP-23. American Concrete Institute, Detroit, MI, pp. 283–300.

Lind, N., and A. Nowak. 1978. *Calculation of Load and Performance Factors*. Report submitted to the Ontario Ministry of Transportation and Communications, Ontario, Canada.

MacGregor, J., I. Jhamb, and N. Nuttall. 1971. Fatigue Strength of Hot Rolled Deformed Reinforcing Bars. *Journal Proceedings, American Concrete Institute*, Vol. 68, No. 3, pp. 169–179.

Mirza, S., and J. MacGregor. 1979. Variability of Mechanical Properties of Reinforcing Bars. *ASCE Journal of the Structural Division*, Vol. 105, No. 5, pp. 921–937.

Mirza, S., and J. MacGregor. 1979. Variations in Dimensions of Reinforced Concrete Members. *ASCE Journal of the Structural Division*, Vol. 105, No. 4, pp. 751–766.

Mlynarski, M., W. Wassef, and A. Nowak. 2011. *NCHRP Report 700: A Comparison of AASHTO Bridge Load Rating Methods*. Transportation Research Board of the National Academies, Washington, DC.

Nowak, A. 1999. *NCHRP Report 368: Calibration of LRFD Bridge Design Code*. TRB, National Research Council, Washington, DC.

Nowak, A., and K. Collins. 2013. *Reliability of Structures*. McGraw-Hill, New York, NY.

Nowak, A., E. Szeliga, and M. Szerszen. 2008. Reliability-Based Calibration for Structural Concrete, Phase 3. *Portland Cement Association, Research and Development Serial No. 2849*, pp. 1–110.

Ontario Highway Bridge Design Code. 1979. Ontario Ministry of Transportation, Toronto, ON, Canada.

Pfister, J., and E. Hognestad. 1964. High Strength Bars as Concrete Reinforcement, Part 6 - Fatigue Tests. *Journal of the Portland Cement Association Research and Development Laboratories*, Vol. 6, No. 1, pp. 65–84.

Rakoczy, P. 2011. WIM Based Load Models for Bridge Serviceability Limit States. PhD Dissertation. University of Nebraska-Lincoln, Lincoln, NE.

Roeder, C., K. Barth, and A. Bergman. 2002. *NCHRP Web Document 46: Improved Live Load Deflection Criteria for Steel Bridges*. Transportation Research Board of the National Academies, Washington, DC.

Siriaksorn, A., and A. Naaman. 1980. *Reliability of Partially Prestressed Beams at Serviceability Limit States*. University of Illinois at Chicago Circle, Department of Materials Engineering, Chicago, IL.

Sivakumar, B., M. Ghosn, and F. Moses. 2011. *NCHRP Report 683: Protocols for Collecting and Using Traffic Data in Bridge Design*. Transportation Research Board of the National Academies, Washington, DC.

Standard Specifications for Highway Bridges, 17th ed. 2002. AASHTO, Washington, DC.

Tadros, M., N. Al-Omaishi, S. Seguirant, and J. Gallt. 2003. *NCHRP Report 496: Prestress Losses in Pretensioned High-Strength Concrete Bridge Girders*. Transportation Research Board of the National Academies, Washington, DC.

ABBREVIATIONS, ACRONYMS, INITIALISMS, AND SYMBOLS

AASHTO	American Association of State Highway and Transportation Officials
ACI	American Concrete Institute
ADTT	Average Daily Truck Traffic
ASBI	American Segmental Bridge Institute
ASCE	American Society of Civil Engineers
CC	Consequence Class
CDF	Cumulative Distribution Function
CEB	Euro-International Committee for Concrete (Comité Euro-International du Béton)
CHBDC	*Canadian Highway Bridge Design Code*
COV	Coefficient of Variation
DL	Dead Load
DOT	Department of Transportation
FHWA	Federal Highway Administration
FIP	International Federation for Prestressing (Fédération Internationale de la Précontrainte)
GVW	Gross Vehicle Weight
HSCOBS	Highway Subcommittee on Bridges and Structures
ISO	International Organization for Standardization
LL	Live Load
LR	Low Relaxation
LRFD	Load and Resistance Factor Design
LS	Limit State
MPF	Multiple Presence Factor
NBS	National Bureau of Standards
NCHRP	National Cooperative Highway Research Program
OHBDC	*Ontario Highway Bridge Design Code*
PDF	Probability Distribution Function
PS	Prestressed Segmental
RFP	Request for Proposal
RC	Reliability Class
RMC	Root Mean Cube
SHRP	Strategic Highway Research Program
SLS	Service Limit State(s)
SPS	Special Pavement Study
SR	Stress Relieved
TRB	Transportation Research Board
ULS	Strength or Ultimate Limit State(s)
WIM	Weigh-in-Motion

APPENDIX A – CURRENT STATE OF THE ART

Table of Contents

List of Tables

List of Figures

A.1 Approach

As part of Phase I of the project an assessment of the current state of the art related to service limit states was conducted as follows:

- A survey of Bridge owners was conducted and is presented in Section A2.
- A review of technical literature is summarized in Section A.3.
- A survey was made of the requirements for SLSs in several modern bridge design specifications including *AASHTO LRFD*. The requirements of the *Eurocode* and the *Canadian Highway Bridge Design Code* (*CHBDC*) (2006) were also reviewed and significant clauses are summarized herein.

A.2 Questionnaire of Bridge Owners

A.2.1 Introduction

To determine the current state of practice of design for the Service Limit State, a questionnaire was developed and sent to major bridge owners across North America. In addition to the 50 US states and the District of Columbia, the questionnaire was also sent to the following bridge owners:

Alberta Transportation
Delaware River and Bay Authority
Delaware River Joint Toll Bridge Commission
Delaware River Port Authority
Kansas Turnpike
Maryland Transportation Authority - FSK Bridge
New Brunswick Department of Transportation
New Jersey Transit Authority
New Jersey Turnpike Authority
New Jersey Turnpike Authority
New York City Transit Authority - New York
New York State Bridge Authority
New York State Thruway Authority
Nova Scotia Department of Transportation and Infrastructure Renewal
Ohio Turnpike
Oklahoma Turnpike Authority
Ontario Ministry of Transportation
Pennsylvania Turnpike Commission
Port Authority of New York and New Jersey
Rhode Island Turnpike and Bridge Authority
Saskatchewan Ministry of Highways and Infrastructure

The questionnaire included 20 questions covering design loads, design provisions and general questions related to the performance of bridge structures.

Twenty nine responses were received. These responses came from:

Alabama Department of Transportation
Alaska Department of Transportation
Arizona Department of Transportation
Arkansas Department of Transportation
California Department of Transportation
Florida Department of Transportation
Hawaii Department of Transportation
Kansas Department of Transportation
Kentucky Department of Transportation
Louisiana Department of Transportation
Michigan Department of Transportation
Minnesota Department of Transportation
Mississippi Department of Transportation
Missouri Department of Transportation
Montana Department of Transportation
New Mexico Department of Transportation
New York Department of Transportation
North Carolina Department of Transportation
Oklahoma Department of Transportation
Pennsylvania Department of Transportation
South Carolina Department of Transportation
South Dakota Department of Transportation
Texas Department of Transportation
Virginia Department of Transportation
Washington Department of Transportation
Wisconsin Department of Transportation
Wyoming Department of Transportation
Kansas Turnpike Authority
Ontario Ministry of Transport

Most responses included answering all questions. However, as some respondents skipped one or more questions, the total number of responses cited in some of the following sections is less than the total number of questionnaires returned to us.

A.2.2 Analysis of Questionnaire Responses

Shown below is a copy of the questionnaire questions with the number of responses and comments and explanations received. Shown also are the research team's analysis of the responses.

1. Some agencies modify the HL93 loading. Please specify what load your agency use for the design of **concrete structures**:

   _23_ Unmodified HL93 loading

   __4_ Modified HL93 Loading: (please specify):

   __1_ Other (please specify):

The modifications to the HL 93 loading included:

California: *The application of the tandem load for negative moment near, and reaction of, interior supports is modified. 100% of two tandems spaced 26 to 40 ft. in the same lane is used.*

Kentucky: *The HL93 load is increased by 25%*

Michigan: *The HL93 load is increased by 20% and the load case involving two tandems in the same lane was revised to replace the two axles (25 kips each) with one 60 kip load. A load factor of 1.2 is applied to the 60 kip load.*

Minnesota: *MNDOT load rating is currently done by LFR. Because there have been some low ratings for continuous steel superstructures designed by LRFD, the double truck plus lane load is increased for all continuous superstructures (including concrete) when the longest span is greater than 100 ft. MNDOT Bridge Office Memo to Designers (2005-01) states:*

- *For bridges with longest span below 100 feet: 90% of the HL-93 double truck with DLA plus lane load (same as in LRFD 3.6.1.3)*
- *For bridges with longest span between 100 and 200 feet:(90 + (span - 100) x 0.2)% of the HL-93 double truck with DLA plus lane load*
- *For bridges with longest span above 200 feet: 110% of the HL-93 double truck with DLA plus lane load*

Ontario: *Canadian Highway Bridge Design Code loading*

Pennsylvania: *The tandem load increased by 25%. The dynamic load allowance for deck design was increased from 33% to 50%*

It is clear that revisions to the HL93 by bridge owners are kept to a minimum. These revisions appear to address issues related to state-specific weight limits and vehicle configurations.

2. In addition to the HL93 loading (or its replacement as indicated in the answer to question 1 above), does your agency routinely check bridge structures for the effects of legal permit loads as part of the normal design procedure?

   Yes 13 No 15

   If Yes, does your agency check concrete components for the service limit states under these legal loads?

   Yes 5 No 6

   If Yes:

   Please provide the configuration of the legal loads used

Only New York and Pennsylvania provided the configuration of their permit vehicles used for service limit state. Following is the description of the two vehicles and their use:

New York: *The New York Permit Vehicle is an eleven-axle vehicle. The total weight of the vehicle is 220 kips and the distance between the front and rear axles is 51 ft. (axle weights are: 10, 18, 18, 23, 23, 23, 21, 21, 21, 21, 21 and axle spacings, in ft., are 9, 4, 4, 4, 4, 10, 4, 4, 4, 4). The permit vehicle is used in checking the Strength II limit state and in checking prestressed components under Service III Limit State.*

Pennsylvania: *The Pennsylvania P-82 vehicle is an eight-axle vehicle. The total weight of the vehicle is 204 kips and the distance between the front and rear axles is 55 ft. The truck consists of a front axle weighing 15 kips followed by seven axles weighing 27 kips each. The axle spacings are: 11, 4, 4, 24, 4, 4, 4 (ft). The permit vehicle is used in checking the Strength II limit state and in checking prestressed components under two state-specific revised Service III limit states. The load for both limit states is 100% of the dead load plus 100% of the live load. Service IIIA is used for checking that the stress in the reinforcement does not exceed 0.9 the yield strength under the specified load combination and Service IIIB is used to ensure that prestressed concrete members do not reach the cracking moment under the specified loads.*

Indicate whether the same service stress limits are used for both the HL93 and the legal loads

Four respondents answered Yes and another one answered No. Other respondents skipped this question.

Indicate whether the permit vehicle is applied to:

__3_ Multiple lane

__5__ Single lane with normal traffic in other lanes

__1__ Single lane with no traffic in other lanes

Owners are nearly equally split on the issue of checking new designs for legal loads as part of the design procedures. Furthermore, the owners who check new designs for legal loads are split on whether these legal loads should be used in conjunction with service limit states.

3. Did your agency revise the stress limits for prestressed concrete components under Service limit states as shown in Articles 5.9.4 of the AASHTO LRFD bridge design specifications? (for example: design for no tension under all loads)

Yes 12 No 16

The responses indicate that revisions to the specifications' stress limits under service load combinations are not widely used. Revisions pointed out by respondents include:

Alaska: *No tensile stresses in concrete under Service I Load combination.*

Arizona: *Tensile stress limit of $0.0948\sqrt{f'_c}$ (ksi) in the precompressed tension zone.*

California: *No tensile stresses in concrete under final conditions in areas with bonded reinforcement under service loads*

Hawaii: *No tensile stresses allowed in precompressed tensile zone after all losses have occurred except when computing load capacity ratings at the operating level and for Legal and permit loads*

Kansas: *Allowed tensile stress in concrete is $0.0948\sqrt{f'_c}$ (ksi) for inventory rating and $0.19\sqrt{f'_c}$ (ksi) for operating rating*

Minnesota: *Zero tension in post-tensioned slabs and in top slabs of post-tensioned boxes.*

North Carolina: *Article 5.9.4.2 Allowable Stresses: Stress at Service Limit State After Losses Tension in the Precompressed Tensile Zone,*

- *Box beams and cored slabs at all sites: no tension at mid span*
- *Girders at corrosive sites: no tension*
- *For other girders and panels, the tension is limited to $0.19\sqrt{f'_c}$ (ksi)*

Pennsylvania: *A table with stress limits for different situations is included in the design specifications*

South Dakota: *No tensile stresses in concrete after losses and under full service loading for Interstate and high truck traffic routes and one-half the allowable tensile stress for all other state route structures.*

Washington: *Differences include:*

- *Temporary tension in areas with bonded reinforcement sufficient to resist the tensile force in the concrete Limit is 0.19 instead of $0.24\ \sqrt{f'_c}$ except during shipping where the $0.24\ \sqrt{e'_c}$ applies*
- *Final tensile stress in precompressed tensile zone: No tension*
- *Final compression under LL + ½ DL + Effective P/S = $0.4f'_c$*

4. With the exception of issues covered under Question 3 above, did your agency revise any other service limit states (design requirements specified to be checked under service load combinations)?

   Yes 12 No 16

The responses indicate that the majority of jurisdictions do not apply any revisions to the service limit states in the AASHTO LRFD specifications. Revisions pointed out by respondents include:

Arizona: *The steel stress is limited to $0.6f_y$ and for bridge deck design steel stress is limited to $0.4f_y$*

Kansas: *Deflection limits were revised*

Louisiana: *Design for 1.0 LL factor (rather than 0.80) under Service III*

Michigan: *Check cantilevers for reinforcement dead load service stress < 22 ksi*

Minnesota: *Use a maximum value of 2 inches for concrete cover*

Pennsylvania: *LL Load Factor for Service III revised to 0.65 for load cases containing both pedestrian live loads and vehicular load together.*

Texas: *Limit dead load stress in main reinforcement of pier caps to 22 ksi.*

5. What method of Control of Cracking by Distribution of Reinforcement (AASHTO LRFD Article 5.7.3.4) is used by your jurisdiction:

   _15__ Current requirements **without** modifications

__7__ Current requirements **with** modifications (Please specify revisions below)

__2__ Pre-2005 Interim requirements (the Z equation) **without** modifications

__0__ Pre-2005 Interim requirements (the Z equation) **with** modifications (please specify revisions below)

__7__ Other, please specify below

The responses indicate that the great majority of jurisdictions are using the provisions included in AASHTO LRFD for Control of Cracking by Distribution of Reinforcement. The revisions applied by some jurisdictions mostly relate to the application of the provisions to certain components. Respondents indicating using "other methods" indicated the following revisions:

Alaska: *The computer program Response 2000 is used to check the design of some members*
Florida: *Tensile stresses in longitudinal reinforcing steel for all mildly reinforced pier columns, pier caps and bent caps under construction loading and Service III Loading are limited to 24 ksi for Grade 60 reinforcement*
Kansas: *Use maximum cover of 2" for deck design*
Minnesota: *Use maximum cover of 2"*
Missouri: *Use Pre-2005 Interims for crack control reinforcement in decks; current provisions used for all other components*
New York: *Crack control requirements are not applied to footings*
Ontario: *Use CHBDC CAN/CSA S6-06, Clause 8.12*
Virginia: *Crack control not applied to concrete decks on prestressed concrete or steel stringers*
Washington: *Only Exposure Class 2 is used*

6. Do you check concrete structures, including concrete substructures, for any additional service load combinations beyond that in the LRFD Specifications?

Yes 3 No 23

If Yes, please provide the additional load combinations below or provide relevant pages of your agency's design manual

Michigan: *Check cantilevers for reinforcement dead load service stress < 22 ksi.*
Missouri: *Gross concrete section of beams in multi-column bents, without contribution from reinforcement, shall not rupture under service dead loads (1.0DC + 1.0DW).*
Pennsylvania: *A table of load factors is provided in the design manual*

7. When analyzing structures for overloads (i.e. trucks with special permits), do you check concrete components for the service limit state under these trucks?

Yes 6 No 20

If Yes, are the same service stress limits used for both the HL93 and the overloads.

Yes 3 No 3

If Yes, please specify:

Among the six responses indicating checking bridges under overloads for the service limit state, only one response indicated which limit states the bridges are checked for: In Kansas, bridges are checked for fatigue and crack control under overloads.

8. Have you observed cracking of pretensioned concrete beams immediately after prestressing force release and before removing the beam from the precasting bed?

Yes 17 No 12

If Yes, please state typical locations:

__16_ Near the end of the beams (__5__ Vertical cracks ___15__ Inclined cracks)

___1_ Near midspan of the beam (_____ Vertical cracks ____1__ Inclined cracks)

Among the 17 responses indicating observing early-age cracking of prestressed concrete beams in service, two responses did not indicate the location and type of cracking while the remaining 16 responses indicated cracking near the ends of the beams. Among the latter 16 responses, one response indicated only vertical cracking, 11 responses indicated only inclined cracking, four responses indicated both vertical and inclined cracking and one response did not indicate the orientation of cracking.

The frequency of cracking was cited by only two responses. One response indicated the frequency is "rare" and the other indicated that cracking is not routinely observed and indicated that is mostly related to precasting yard procedures.

The responses to this question suggest that a study of the cause of cracking should be considered by the bridge community.

9. Have you observed cracking of prestressed concrete beams in service?

Yes 21 No 7

If Yes:

Approximately, what is the percentage of prestressed beams in your inventory in which you observed cracking?

__8__ Less than 1%

__7__ 1 to 5%

__5__ 5 to 10%

__1_ More than 10%, Please state __15_____%_

When are the cracks typically first observed?

__1__ Immediately after construction

__5__ Within 1 year of construction

__3__ 2 to 5 years after construction

_____ More than 5 years after construction

_13__ Not sure

What type of cracks and in bridges of what age group (e.g. bridges constructed before 1970's)? (please mark all applicable):

_14__ Shear cracks (typically inclined cracks near the end of the girders)

Age group this was observed in: _____

__2__ Flexural cracks (typically vertical cracks near max. moment regions)

Age group this was observed in: _____

__6__ Vertical cracks near the end of pretensioned girders

Age group this was observed in: _____

__2__ Anchorage zone of post-tensioned girders

Age group this was observed in: _____

__5__ Other, Please describe:

Age group this was observed in: _____

The responses to this question suggest the following:

Even though approximately 75% of the respondents to this question indicated that they observed cracking of prestressed concrete beams in service, it appears that the percentage of bridges where cracking is observed is typically small. Among 21 jurisdictions indicating that cracks have been observed, eight (38%) indicated cracking observed in less than 1% of bridges, seven (33%) indicated cracking observed in 1% to 5% of bridges, and, five (24%) indicated cracking observed in 5% to 10% of bridges.

Most of the cracking occurs at a relatively young age. Out of 22 respondents answering the question related to the time cracking was observed six respondents (27%) indicated cracking observed within two years of construction, three respondents (14%) indicated cracking observed 2 to 5 years from construction and the remaining thirteen respondents (59%) were not sure of the time of cracking.

The most common form of cracking is shear cracking (48% of responses indicating cracking observed) followed by vertical cracking (21%). Only Florida and Wisconsin indicated anchorage zone cracking (this is probably because Florida uses post-tensioning more extensively than most other owners and, thus, are more likely to observe problems related to post-tensioning)

Most reported cracking took place in older bridges (pre-1970's). in only one case cracking was reported in bridges in the 2 to 5 year age group.

Other types of reported cracking included:

Arkansas: *Vertical cracks over piers of simple spans made continuous for bridges from between 1973 and 2005.*

Florida: *Insignificant longitudinal cracks in upper/lower flanges predominately over bearing areas, Hairline diagonal cracks in the web, running from the top of the web near beam end diagonally 3 to 4 feet in length. In all age groups*

Michigan: *Cracking observed in beams of bridges on highly skewed alignments*

Missouri: *Diagonal cracking observed but in opposing orientation to shear cracks; occurs in all age groups.*

Pennsylvania: Cracking in adjacent non-composite P/S box beams under open joints in parapets

Texas: *Anchorage zone of pretensioned girders.*

The responses to this question indicate that newer bridges designed under the current specifications did not show wide spread cracking. However, it is not clear whether more cracking will start appearing once these bridges continue to age.

10. Have you observed end of prestressed beam damage under expansion joints?

Yes 12 No 16

If Yes,

Did it affect serviceability?

Yes 6 No 5

Have you tried to repair the damage?

Yes 9 No 2

If repaired, what repair technique was used?

Even though 40% of the respondents to this question indicated observing damage to ends of prestressed concrete beams under expansion joints, none of the responses indicated that it was a significant concern. Methods of repair indicated are: patching, chipping and over-casting, fiber wrap, mortar repair and expansion of the beam seat to provide support further from the beam end.

11. Is the deck empirical design method used in your jurisdiction?

Yes 5 No 23

If Yes,

What percentage of new decks (defined as decks designed in the last 5 years) are designed using the empirical method

0%	23 Responses
1%-20%	1 Response
20% to 40%	1 Response
40% to 60%	
60% to 80%	
80% to 99%	2 Response
100%	

Did decks designed using the empirical design method perform as good as traditionally designed decks?

Yes 4 No 1

If No, please explain in what way:

More cracking than conventional decks was cited as the reason for the negative answer above.

Are the minimum reinforcement ratios specified in AASHTO LRFD for empirical deck design used?

Yes 2 No 3

If No, Please indicate the limits used:

The revisions to reinforcement requirements include using the following reinforcement:

Michigan: #4 @ 12" top mat longitudinal and transverse, #4 @ 8" bottom mat longitudinal and transverse, and, extra bars under barrier and at corners of bridges with skew angle greater than 25 deg

Louisiana: Use #5@12 each direction at top and bot. Later the spacing was reduced to 7" (Notice that Louisiana's response indicated that currently they do not construct decks using the empirical method)

Is the maximum reinforcement spacing of 18" specified in AASHTO LRFD for empirical deck design used?

Yes 1 No 4

If No, Please indicate the maximum spacing used:

If a tighter spacing is used, what is the reason?

__2_ Maximum reinforcement spacing accepted by your jurisdiction is generally <18"

____ Spacing dictated by crack control requirements is used

__1_ Other, please specify

Generally, it appears that the 12" maximum reinforcement spacing allowed by most jurisdictions for a wide range of concrete components is enforced for decks designed using the empirical method. It also appears that tighter reinforcement spacing is sometimes used in an attempt to minimize deck cracking problems.

12. Has deck cracking been widely observed in bridges under your agency's jurisdiction?

Yes 21 No 7

If Yes,

What types of deck cracks have you observed in bridges under your agency's jurisdiction?

_10__ Longitudinal cracking

_20_ Transverse cracking

_10_ Map cracking

When cracking was first observed?

__9__ After exposure to service traffic

__8__ After exposure to construction live loads

_19__ During/Immediately after curing.

If the latter, was there a correlation between ambient conditions and early cracking:

Yes 3 No. 6 If Yes, please explain:

Minnesota indicated that a significant temperature differential between the girder and deck during curing may cause early cracking. Mississippi indicated that while cracking of the deck was not widely observed, shrinkage cracking was observed in decks when concrete was cast during hot weather. New York reported correlation between deck cracking and low air and beam temperature at the time the deck is cast.

Was there any correlation between deck cracking and traffic (traffic counts and percentage of trucks)?

Yes 4 No 17

If Yes, please explain below.

Positive responses to this question indicated higher tendency of deck cracking for bridges with high ADTT and for more flexible steel girders.

Is the deck cracking type and extent in decks designed using the empirical design method different from cracking in decks designed using the traditional method?

Yes 1 No 3 Not Applicable 23 (Empirical deck design not used)

If yes, how does the performance of decks designed using the empirical compare to that of standard decks?

One respondent indicated that decks designed using the empirical method tends to develop more cracks than conventionally designed deck. The response also indicated that the empirically designed decks tend to develop more cracks parallel to the girders while conventionally designed decks tend to develop cracks transverse to the girders.

13. What type of reinforcement do you use in newer (designed in the last 5 years) concrete decks?

_14_ Epoxy-coated rebar (used in approximately see (a) below % of newer decks)

__9_ Black rebar (used in approximately see (b) below % of newer decks)

__3_ Galvanized rebar (used in approximately see (c) below % of newer decks)

____ Stainless steel rebar (used in approximately _____ % of newer decks)

____ Stainless steel clad rebar (used in approximately _____ % of newer decks)

__2__ Other (see (d) below)

(a) *Out of the 14 relevant responses, 12 responses indicated using epoxy-coated bars almost exclusively. One response gave the percentage to be 70% another 80%.*

(b) *Out of the 9 relevant responses, 6 responses indicated using black bars almost exclusively. 20%, 75% and 80% were given by one respondent each.*

(c) *All three relevant responses indicated use in 5% of decks with the balance being epoxy-coated rebar in New York and Pennsylvania and black rebar in South Carolina.*

(d) *New Mexico reported using MMFX rebar in 5% of new decks. Virginia started using the MMFX rebar in 2008 and was planning on using it in all new decks starting January 2010.*

Generally, epoxy-coated rebar is the most-used type of deck reinforcement. The use of black bars is limited to southern states where the use of deicing chemicals is limited or nonexistent (California, Hawaii, Louisiana, Mississippi and South Carolina).

14. What is the average life span of concrete decks under your agency's jurisdiction

____ Years

Range of deck life span from 25 years to full bridge life was given. No general trend could be deduced. Some northern states indicated deck life span longer than that given by some southern states.

And,

What is the main reason decks are replaced

_19_ Deterioration of the concrete itself

_15_ Corrosion of reinforcement

__9_ Extensive cracking

__4_ Other, Please state:_____

There was no clear correlation between the reason for deck replacement and the climate (use of deicing chemicals).

15. What type of **new concrete superstructures** (bridges designed in the last five years) typically used in your jurisdiction and what is the **approximate** percentage of each type of the total number of **concrete** bridges?

___% Prestressed I-beam and bulb tees

___% Prestressed adjacent prestressed box beams

___% Prestressed spread prestressed box beams

___% Slab bridges

___% Segmental concrete

___% Reinforced concrete

___% Others, Please specify

Out of 27 responses to this question, 21 responses indicated that prestressed I and Bulb Tees are the most-used types varying in percentage from 100% to 40%. Respondents showing different types of construction to be the dominant types are as follows:

Arkansas: *Reinforced concrete accounts for 75% of bridges*

California: *Cast-in-Place post-tensioned box-girders account for 69% of bridges (85% of bridge area)*

Louisiana: *Bridges are split equally between reinforced concrete slab bridges and prestressed precast beams (I beams and bulb tees combined)*

Michigan: *Prestressed precast spread box beams account for 50% of concrete bridges while prestressed precast beams account for 40%*

New York: *Prestressed precast adjacent box beams account for 45% of concrete bridges while prestressed precast beams account for 20%*

North Carolina: *Prestressed precast adjacent box beams account for 40% of concrete bridges while prestressed precast I and Bulb Tees account for 35%.*

Virginia: *The response stated that reinforced concrete bridges account for 38% of concrete bridges while prestressed precast beams account for 26%. It is not*

clear whether culverts are counted in determining reinforced concrete bridges causing them to appear the dominant type..

It appears that the type of construction is mostly a function of past practice and the sections produced by local/regional precasters.

16. Have you observed problems with bearings in concrete bridges?

Yes 13 No 15

If Yes:

What type of problems?

Types of problems cited include:

Hawaii:	*Bulging elastomeric bearing pads. Unseated roller bearings.*
Louisiana:	*Lack of anchor bolt cover (riser concrete), resulting in loss of restraint. Bolt shear, resulting in lateral movement of bearing pads. Excessive movement resulting in shear or distortion of bearing pads. Bad detailing, corrosion.*
North Carolina:	*Freezing of steel bearings; tearing, deformation, and "walking" of elastomeric bearings*
Michigan:	*Bulging, splitting of neoprene*
Minnesota:	*Locking of sliding plate type bearings, "walking" of elastomeric bearings, and leaking of elastomer in pot bearings.*
Mississippi:	*Older steel sliding bearings tend to lock-up over time*
Missouri:	*"Walking" of elastomeric bearings*
Pennsylvania:	*Uneven bearing*
South Dakota:	*Shifting of neoprene/rubber bearings and hardness inconsistency.*
Texas:	*Occasional pad slippage.*
Washington:	*Steel-reinforced elastomeric bearings have "walked"*

Did the problems cause significant unintended forces to develop?

Yes 4 No 9

Did the problems result in damage to the concrete beams?

Yes 2 No 11

If Yes, please state what type of damage

In two responses, the locking of steel sliding bearings tend to cause cracks or spalling in the bottom flange at the beam end or cracking and spalling of substructures. Another response cited cracking near the ends of reinforced concrete T-beams without specifying the type of bearings, if any, used.

Generally, it appears that problems with bearings on concrete bridges are not wide spread. Except for the steel sliding bearings cited above, when bearing problems arise, they do not seem to cause significant damage to the girders.

17. Have you observed cracking of abutments and piers?

Yes 20 No 8

If Yes, please state what type of cracks

Substructure cracking problems cited include:

Alaska:	*Problems appear to be related to providing too much heat during cold weather concrete construction.*
Arkansas:	*Cracking and deflection of abutment backwalls at top of cap*
Florida:	*Typically due to time effects, shrinkage or creep.*
Kansas:	*Tension cracks*
Louisiana:	*Longitudinal, vertical and inclined cracks and spalling*
Michigan:	*On rare occasions - Various Causes - settlement, pull out from bearing anchors, corroded steel, shear cracking in hammerhead piers etc.*
Minnesota:	*Settlement or shrinkage cracks, shear cracks, diagonal cracks in abutment wingwalls.*
Missouri:	*Horizontal cracks along beam edge due to inadequate cover and water ponding, vertical cracks due to thermal movement of superstructure, and diagonal shear cracks*
New Mexico:	*Problems mostly observed with the steel expansion bearing devices that locked up and caused spalling of the vertical faces of the pier caps. Replacing the steel expansion bearing devices with elastomeric bearing pads and patching the pier caps appear to have eliminated the problems.*
New York:	*Vertical cracking in abutments, corrosion related cracking in piers*
North Carolina:	*Horizontal cracks where deicing salt has reached horizontal reinforcing steel. Spalling of pier caps when steel bearings are frozen.*
Oklahoma:	*Cracks between wingwalls and backwalls*
Pennsylvania:	*Shrinkage cracks.*
South Dakota:	*There has been some minor spalling of integral backwall/diaphragm concrete around the embedded ends of concrete beams (mostly on skewed structures). Also, cracks developed on local road double tee structures where the beam ends were welded to anchor plates embedded into the abutment/pier caps.*
Texas:	*Flexural, shear and corrosion related.*
Virginia:	*Flexural cracks in concrete pier caps. Settlement cracks in abutments Temperature and shrinkage cracks.*
Wisconsin:	*Wingwall body cracks*
Wyoming:	*Cracks of different orientation in 53% of abutments (including pedestals on abutments), 34% of bent caps and 20% of concrete columns..*

The lack of a pattern of the observed problems indicate that these problems are associated more with workmanship and detailing practice more than the design provisions.

18. What is the average service life span of the concrete substructures under your agency's jurisdiction

    ____ Years

    One respondent cited a life span of 40 years for substructures in salt water. Other responses indicated a range of substructure life span from 45 years to bridge life span. One respondent indicated that the goal for new substructures is 100 years.

19. Have you observed problems that you think are related to fatigue in:

Rebar	Yes	0	No	28
Prestressing strand	Yes	0	No	28
Concrete	Yes	2	No	25

    It does not appear that fatigue of concrete and reinforcement represents a concern to most bridge owners. The only two responses indicating problems with concrete fatigue were those from California and Hawaii. The latter indicated that they are speculating that observed spalling deck problems may be related to fatigue of concrete in addition to cover issues rather than corrosion of rebar.

20. Does your agency specify coatings for concrete substructures?

    Yes 9 No 19

    If Yes, please state what type

Types of coatings cited include:

Kansas: *Mastic system below grade and epoxy above grade*
Michigan: *When specified in the special provisions: acrylic based concrete surface coating.*
Minnesota: *A gray colored cementitious based surface finish or acrylic paint is applied for aesthetic reasons but it also supplies some level of sealing protection.*
Missouri: *Epoxy or urethane protective coating on substructures under deck joints*
New Mexico: *Penetrating Water Repellent Treatment. Other coatings used on exposed concrete surfaces include: special surface finish (color) and permanent anti-graffiti protective coatings*
New York: *Occasionally silane or epoxy coating*
Oklahoma: *Water repellant on pier caps and beam seats*
Pennsylvania: *Penetrating sealer at expansion joints & substructure within 14' of traffic lanes*
Washington: *Pigmented sealer for architectural reasons.*

Generally, the responses indicate that the use of concrete coatings does not follow any trend.

A.2.3 Lessons Learned from the Questionnaire

The responses to the questionnaire indicated that most bridge owners apply the service limit states included in AASHTO LRFD with no, or with few, revisions. The additional limit states used by bridge owners appeared to be related either to owner-specified vehicles, or to address a specific issue that does not seem to be shared by other bridge owner as evident by the lack of use of these additional limit states by other owners. It is expected that some of the other agencies that have not responded to the questionnaire also use permit vehicles in checking some aspects of the design under service loads. The use of permit vehicles to check some service conditions, the desire expressed by some bridge designers to have guidance on applying permit vehicles to service conditions, and, the requirements of the Request For Proposals (RFP) of the NCHRP 12-83 project which included a requirement to consider the treatment of owner-specified vehicles, suggest a need exists for a service load combination for concrete structures that is akin to the Service II limit state used for steel structures. The load factors for live load for such load combination can be determined using the same principles that will be used for calibrating limit states under other service limit states. However, the statistical parameters to be used for permit vehicles will be different from those for random traffic. More detailed discussions on the statistical parameters for permit vehicles are presented in Section 4.

A.3 Concrete Serviceability Requirements in Several Modern Bridge Design Specifications

A.3.1 AASHTO LRFD

The existing *AASHTO LRFD Bridge Design Specifications* (AASHTO LRFD) was reviewed to identify the service limit states in the specifications. In addition, these limit states were compared to those in the Canadian Highway Bridge Design Code (CHBDC) and the Eurocode to identify any service limit states that does not have an equivalent in AASHTO LRFD; which would represent a potential additional limit states.

Table A-1 lists the existing limit states in *AASHTO LRFD* specifications and the relevant specifications articles.

Table A-1 Existing Service Limit States in *AASHTO LRFD*

AASHTO LRFD Article	Basic Provision
2.5.2.6.2 Criteria for Deflection	In the absence of other criteria, the following deflection limits may be considered for steel, aluminum, and/or concrete construction: Vehicular load, general - Span/800, Vehicular and/or pedestrian loads - Span/1000, Vehicular load on cantilever arms - Span/300, and Vehicular and/or pedestrian loads on cantilever arms - Span/375.
3.4.1 and 3.6.1.4 Fatigue	Fatigue truck and load factors in Table 3.4.1-1.
5.5.3.1 General	"Fatigue need not be investigated for concrete deck slabs in multi-girder applications."
	"Fatigue of the reinforcement need not be checked for fully prestressed components designed to have extreme fiber tensile stress due to Service III Limit State within the tensile stress limit specified in Table 5.9.4.2.2-1."
5.5.3.2 Reinforcing Bars	"The stress range in straight reinforcement and welded wire reinforcement without a cross weld in the high-stress region resulting from the fatigue load combination, specified in Table 3.4.1-1, shall satisfy: $f_f \leq 24 - 0.33 f_{min}$" "The stress range in straight welded wire reinforcement with a cross weld in the high-stress region resulting from the fatigue load combination, specified in Table 3.4.1-1, shall satisfy: $f_f \leq 16 - 0.33 f_{min}$"
5.5.3.3 Prestressing Tendons	"The stress range in prestressing tendons shall not exceed: • 18.0 ksi for radii of curvature in excess of 30.0 ft., and • 10.0 ksi for radii of curvature not exceeding 12.0 ft."

AASHTO LRFD Article	Basic Provision
5.5.3.4 Welded or Mechanical Splices of Reinforcement	"For welded or mechanical connections that are subject to repetitive loads, the range of stress, f_f, shall not exceed the nominal fatigue resistance given in Table 1."
5.6.3.6 Crack Control Reinforcement	"The ratio of reinforcement area to gross concrete area shall not be less than 0.003 in each direction."
5.7.3.4 Control of Cracking by Distribution of Reinforcement	"The spacing s of mild steel reinforcement in the layer closest to the tension face shall satisfy the following: $s \le \frac{700\gamma_e}{\beta_s f_{ss}} - 2d_c$ "
	"If the effective depth, de, of nonprestressed or partially prestressed concrete members exceeds 3.0 ft., longitudinal skin reinforcement shall be uniformly distributed along both side faces of the component for a distance de/2 nearest the flexural tension reinforcement. The area of skin reinforcement Ask in in.2/ft. of height on each side face shall satisfy: $A_{sk} \ge 0.012(d_c - 30) \le \frac{A_s + A_{ps}}{4}$ "
5.8.5 Principal Stresses in Webs of Segmental Concrete Bridges	"The principal tensile stress resulting from the long-term residual axial stress and maximum shear and/or maximum shear combined with shear from torsion stress at the neutral axis of the critical web shall not exceed the tensile stress limit of Table 5.9.4.2.2-1 at the Service III Limit State of Article 3.4.1 at all stages during the life of the structure, excluding those during construction. When investigating principal stresses during construction, the tensile stress limits of Table 5.14.2.3.3-1 shall apply."

AASHTO LRFD Article	Basic Provision
5.9.3 Stress Limitations for Prestressing Tendons	"The tendon stress due to prestress or at the service limit state shall not exceed the values: • Specified in Table 1, or • Recommended by the manufacturer of the tendons or anchorages."
5.9.4.1.1 Compression Stresses	"The compressive stress limit for pretensioned and post-tensioned concrete components, including segmentally constructed bridges, shall be 0.60 f'_{ci} (ksi)."
5.9.4.1.2 Tension Stresses	"The limits in Table 1 shall apply for tensile stresses."
5.9.4.2.1 Compression Stresses	"Compression shall be investigated using the Service Limit State Load Combination I specified in Table 3.4.1-1. The limits in Table 1 shall apply."
5.9.4.2.2 Tension Stresses	"For service load combinations that involve traffic loading, tension stresses in members with bonded or unbonded prestressing tendons should be investigated using Load Combination Service III specified in Table 3.4.1-1. The limits in Table 1 shall apply."
5.9.4.3 Partially Prestressed Components AASHTO is considering eliminating partial prestressing	"Compression stresses shall be limited as specified in Articles 5.9.4.1.1 and 5.9.4.2.1 for fully prestressed components."
	"Tensile stress in reinforcement at the service limit state shall be as specified in Article 5.7.3.4, in which case f_s shall be interpreted as the change in stress after decompression."

AASHTO LRFD Article	Basic Provision
5.10.8 Shrinkage and Temperature Reinforcement	"For bars or welded wire fabric, the area of reinforcement per foot, on each face and in each direction, shall satisfy: $A_s \geq \frac{1.30bh}{2(b+h)f_y}$ $0.11 \leq A_s \leq 0.60$ „
5.10.10.1 Splitting Resistance	"The splitting resistance of pretensioned anchorage zones provided by reinforcement in the ends of pretensioned beams shall be taken as: $P_r = f_s A_s$ with the stress in steel not to exceed 20 ksi
5.14.2.3.3 Construction Load Combinations at the Service Limit State	"Flexural tension and principal tension stresses shall be determined at service limit states as specified in Table 1, for which the following notes apply: • Note 1: equipment not working, • Note 2: normal erection, and • Note 3: moving equipment. Stress limits shall conform to Article 5.9.4."
5.14.2.6.2 Construction Load Combinations	"Tensile stresses in segmental substructures during construction shall be computed for applicable load combinations of Table 5.14.2.3.3-1."
5.14.1.4.9c Positive Moment Connection Using Prestressing Strand	"The stress in the strands used for design, as a function of the total length of the strand, shall not exceed: $f_{psl} = \frac{(\ell_{dsh} - 8)}{0.228}$ $f_{pul} = \frac{(\ell_{dsh} - 8)}{0.163}$ "

Some of the limit states are deterministic or represent detailing requirements. The literature search did not yield information on the background of these limit states and they were

deemed uncalibrateable or "deemed to satisfy". The literature search yielded information on the following limit states and the information is summarized in the following sections::

- live load deflection of structures,
- fatigue of rebar and prestressing strands,
- cracking of reinforced concrete components,
- tensile stresses of prestressed concrete components,
- compressive stresses of prestressed concrete components,

As stated in Chapter 1, these limit states and the associated load and resistance factors for SLS are based on apparent successful past practice and have not been subject to a reliability-based calibration. There are no consistent performance levels associated with these limit states although some are associated with differences in environmental or traffic exposure.

A.3.1.1 Limitations on the Live Load Deflection of Bridge Structures

The current requirements for deflection limits in the *AASHTO LRFD* have their roots in the corresponding provisions of the *Standard Specifications for Highway Bridges*, 17th Edition (2002). These provisions have been reviewed repeatedly. Summaries by Wright and Walker (1972), Roeder, et al. (2002), and Barker and Barth (2007) are often referenced.

Historically, deflection limits were treated as an issue specific to steel bridges. The ASCE Committee on Deflection Limitations of Bridges of the Structural Division (1958) reported on their examination of the live load deflection limits and depth-to-span ratios in the 1953 American Association of State Highway Officials (AASHO) *Standard Specifications for Highway Bridges*. A comprehensive review of the deflection limits and depth-to-span ratios and their evolution was completed. The earliest deflection limits were adopted in 1871 by the Phoenix Bridge Company which limited deflection to 1/1200 of the span length for a train moving 30 miles per hour. The American Railway Engineering Association (AREA) adopted depth-to-span ratios in the early 1900's though the limits were without basis. Depth-to-span ratios for highway bridges were initially set forth in 1913 and adopted by AASHO in 1924. Vibrations became an issue in the 1930's and the Bureau of Public Roads attempted to provide a correlation between the bridges with vibration problems and bridge properties. The result was limiting deflections to L/800 for simple and continuous spans without pedestrians, L/1000 for simple and continuous spans with pedestrians, and L/300 for cantilevered spans. The ASCE Committee surveyed state highway departments to obtain data on the behavior of bridges and the views of experienced bridge designers. The conclusions of the survey include: maximum oscillations occur with passage of medium weight vehicles not heavy vehicles, reports of objectionable vibrations came from continuous span bridges more often than simple span bridges, and there is no defined level of vibration which constitutes being undesirable. The vibration of the bridge is affected by the following quantities:

- Bridge flexibility and associated natural frequency
- Flexibility of vehicle suspension and associated natural frequency
- Relative weight of vehicles and bridge
- Vehicle speed
- Profile of approach roadway and bridge deck
- Frequency of load application
- Motion caused by loads in adjacent spans of continuous span structures

- Damping characteristics of bridge and vehicle

The use of depth-to-span ratios began in the early 1900's with the American Railway Engineering and Maintenance of Way Association (AREMA) specification (at that time AREA) stating that pony trusses and plate girders should have a depth not less than 1/10 of the span length. These ratios have changed little over the years. The current depth-to-span limits are 1/10 for trusses and 1/12 for steel rolled shapes and plate girders. At the time, railroads did not use concrete bridges of any significant length.

The early specifications for highway bridges adopted with some modification the depth-span ratios from AREMA for use in steel highway bridges.

Deflection limits in the American Association of State Highway Officials (AASHO) *Standard Specifications for Highway Bridges* was limited to steel composite and noncomposite bridges. No limits or method of calculation of deflections of concrete structures specified. Starting in 1977, provisions related to deflections of concrete bridges were incorporated in the AASHTO *Standard Specifications for Highway Bridges*:

- A method of calculating deflections of concrete structures was introduced in the 1977 Twelfth Edition of AASHTO *Standard Specifications for Highway Bridges,* however, no deflection limits were specified.
- Superstructure depth limitations for continuous structures were introduced in the 1983 Thirteenth Edition of AASHTO *Standard Specifications for Highway Bridges,* with a requirement that simple spans should have about 10 percent greater depth. Still no deflection limits were specified for concrete structures.
- The 1989 Fourteenth Edition of AASHTO *Standard Specifications for Highway Bridges* contained superstructure depth limitations for both simple and continuous spans as shown in Table A-2. In addition, deflection limits of 1/1000 and 1/800 span length were specified for bridges with and without pedestrian traffic, respectively. For cantilevered arms, deflection limits of 1/375 and 1/300 of cantilever length were specified for bridges with and without pedestrian traffic, respectively. These are the same limits historically specified for steel bridges in AASHTO.

Table A-2 Recommended Minimum Depth of Concrete Structures in 1989 AASHTO

Superstructure Type	Minimum depth in feet	
	Simple spans*	Continuous spans*
Bridge slabs with main reinforcement parallel to traffic	1.2(S+10)/30	(S+10)/30
T-Girders	0.070S	0.065S
Box-Girders	0.060S	0.055S
Pedestrian Structure girders	0.033S	0.033S

*S = Span length

The available research on deflection deals largely with the deflection of steel bridges and the deck cracking which is thought by some to be exacerbated by the flexibility of steel girders. Deflection of concrete bridges is usually investigated as part of the comparison to steel bridge deflections. The available literature indicates that transverse deck cracking can be affected by many different items. Additionally there is disagreement on whether limiting static live load deflection (girder flexibility) is a satisfactory method to prevent deck cracking. Researchers are

equally divided between those that concluded that girder flexibility affects deck cracking and those that concluded that girder flexibility does not affect deck cracking. As indicated by some of the studies, concrete material factors may be more important to reduce the formation of early-age deck cracks.

Some modern specifications such as the *Ontario Highway Bridge Design Code* (*OHBDC*) and its successor the *CHBDC* utilize a combination of frequency, perception levels and deflection limits to distinguish between acceptable and unacceptable response. Figure A-1, taken from the 2006 Edition of the *CHBDC*, illustrated this approach which has the benefit of directly addressing the design issue, vibration control. This is similar to the procedure for building design developed by Murphy.

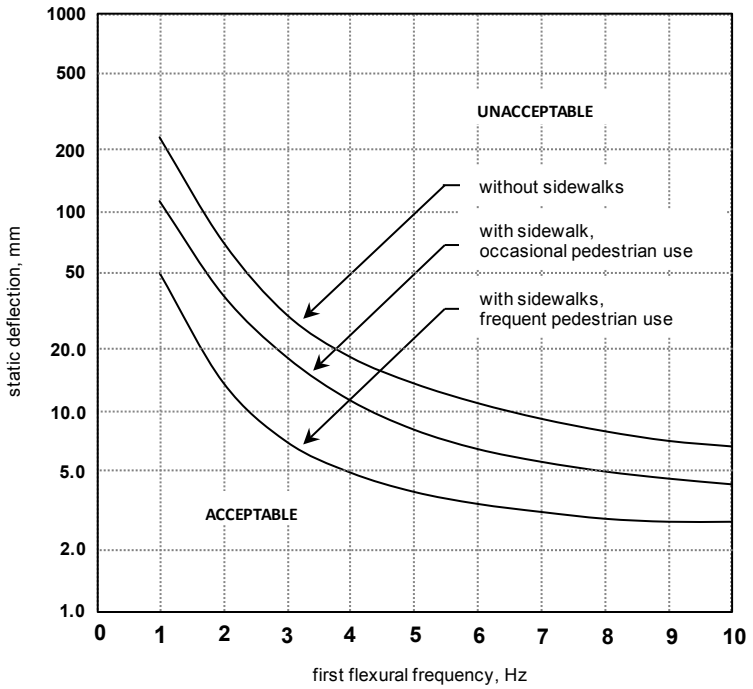

Figure A-1 Deflection provisions in 2006 edition of *CHBDC*.

In the *Eurocode* live loads include a "vibration factor" to account for stresses caused by vibration, no checks for frequency or displacement are required (*EN 1990, 2002*). In New Zealand vertical velocity is limited to 0.055 m/s (2.2 in/s) under two 120 kN (27 kip axles) of one HN unit if a bridge carries significant pedestrian traffic or where cars are likely to be stationary. Previous versions included span-to-depth ratios and deflection limits, but these have now been removed.

To date, specifications based on determining the frequency have not received wide acceptance in U.S. practice. There has been a perceived difficulty in determining the first fundamental frequency of the bridge. Equations for simple span structures have been available for decades, e.g. Biggs (1964). Similarly, formulas for frequency have been developed for continuous structures of regular geometry. Historically, frequencies could be calculated using the Rayleigh method typically implemented through Newmark's numerical integration. Roeder, et al. (2002) summarized empirical equations that are based not only on theoretical structural

dynamics but also have adjustments for apparent behavior in the field. Modern refined computational methods make the determination of frequencies and mode shapes relatively straightforward. Thus there does not seem to be impediments to adoption of an approach similar to that specified by the *CHBDC*.

A.3.1.2 Fatigue-and-fracture Limit States

A.3.1.2.1 General

The fatigue-and-fracture limit state is divided into two load combinations: Fatigue I for infinite-life fatigue resistance and Fatigue II for finite-life fatigue resistance. These relatively new provisions appeared in the 2009 interim changes to load provisions in Section 3 of the *AASHTO LRFD* published in early 2009. The fatigue resistance provisions of both concrete and steel bridges in Sections 5 and 6 of the *AASHTO LRFD*, respectively, were modified accordingly.

A.3.1.2.2 Loads

General

The fatigue load of *AASHTO LRFD* Article 3.6.1.4 and the fatigue live-load load factors of *AASHTO LRFD* Table 3.4.1-1 are based upon extensive research on structural-steel highway bridges. The use of this load was extended to fatigue of concrete, reinforcement and prestressing strand. As the origin of fatigue load is in the design of steel bridges, frequent references are made to steel bridges in the discussion below.

The fatigue load is the *AASHTO LRFD* design truck (HS20-44 truck of the *Standard Specifications for Highway Bridges*) but with a fixed rear-axle spacing of 30 feet. The live-load load factors for the fatigue limit-state load combinations are summarized in Table A-3.

Table A-3 Fatigue Live-Load Load Factors

Fatigue Limit-State Load Combination	LL Load Factor
Fatigue I	1.50
Fatigue II	0.75

Infinite-life Fatigue

The Fatigue I load factor of 1.50, used to design highway bridges with higher traffic volumes for infinite fatigue life, is based upon a 1-in-10,000 rate of exceedance (Dexter and Fisher 2000). This stress range is the stress range below which the inherent flaws in steel do not propagate to significant crack sizes during the design life of the bridge. If all of the stress ranges experienced by a detail are below this value, the detail is assumed to have infinite life. Thus, this stress range represents a maximum limit to achieve infinite life. This value was revisited in this study through simulation using weigh-in-motion (WIM) data.

Finite-life Fatigue

This limit state is not used for concrete structures and, therefore, is not discussed in this report. Limited information related to revisions to the finite-life fatigue (Fatigue II limit state) provisions in AASHTO LRFD are provided for information only as they are parallel to the revisions to Fatigue I provisions that are applicable to concrete components. The development of the information on Fatigue II limit state can be found in Kulicki et. al. (2013).

Recommendations

The stress ranges represented by both of these load factors (the RMC and the exceedance of 1 in 10,000) are based upon observations on steel highway bridges and structural-steel laboratory specimens. Extending these stress ranges to steel reinforcement, both non-prestressed and prestressed, is quite appropriate as the stress ranges represent fatigue-damage accumulation in steel. It is assumed that these fatigue-damage accumulation models apply to concrete in compression as well as steel reinforcement. This approach is proposed for this study as well. A validation of these principles for concrete highway bridges is far beyond the scope and funding of this study.

A.3.1.2.3 Fatigue Resistance of Concrete Structures

The fatigue resistance of concrete, non-prestressed reinforcement and prestressing tendons in the *AASHTO LRFD* is based upon ACI Committee Report ACI 215R-74(92), *Considerations for Design of Concrete Structures Subjected to Fatigue Loading* (1997). This reference includes an extensive bibliography on fatigue resistance of concrete and its reinforcement.

Concrete

The compressive stress limit of $0.40f_c'$ for fully prestressed components in other than segmentally constructed bridges of *AASHTO LRFD* Article 5.5.3.1 applies to a combination of the Fatigue I limit-state load combination (which includes only live load) plus one-half the sum of the effective prestress and permanent loads after losses (a load combination derived from a modified Goodman diagram). This suggests that it represents an infinite-life check as the Fatigue I limit-state load combination corresponds with infinite fatigue life.

ACI 215R-74(92) indicates that the fatigue resistance of concrete in the form of an S-N curve (stress range versus number of cycles) is approximately linear between 100 and 10 million cycles. It does not exhibit a constant-amplitude fatigue threshold up to that point (would be indicated by a horizontal S-N curve). Further, it suggests that the compression stress limit of $0.4f_c'$ is based upon a target fatigue life of 10 million cycles. For highway bridges, a target fatigue life of 10 million cycles is significantly less than the design life. A highway bridge with an ADTT of 2,000 trucks per day would experience over 50 million cycles during its 75-year design life.

For this study, the research used to define these S-N curves, Ople and Hulsbos (1966), was re-evaluated to estimate the fatigue resistance to about 10^8 cycles (100 million), a practical upper bound for highway bridges. The uncertainty of the fatigue resistance will be quantified in terms of bias, mean, and coefficient of variation (COV).

For this study, the research used to define these S-N curves, Ople and Hulsbos (1966), was re-evaluated to estimate the fatigue resistance to about 10^8 cycles (100 million), a practical upper bound for highway bridges. The uncertainty of the fatigue resistance will be quantified in terms of bias, mean and coefficient of variation (COV).

Non-prestressed Reinforcement

As used herein, non-prestressed reinforcement includes straight reinforcing bars and welded-wire reinforcement. *AASHTO LRFD* Article 5.5.3.2 specifies the fatigue resistance of these types of reinforcement.

The fatigue resistance of straight reinforcing bars and welded-wire reinforcement without a cross weld in the high-stress region (defined as one-third of the span on each side of the section of maximum moment) is specified as:

$$\left(\Delta F\right)_{TH} = 24 - 0.33 f_{\min} \quad \text{(A-1)}$$

where f_{min} is the minimum stress.

For welded-wire reinforcement with a cross weld in the high-stress region, the fatigue resistance is specified as:

$$\left(\Delta F\right)_{TH} = 16 - 0.33 f_{\min} \quad \text{(A-2)}$$

Equations (A-1) and (A-2) implicitly assume a ratio of radius to height (in other words, r/h) of the rolled-in transverse bar deformations of 0.3.

These fatigue resistances are defined as constant-amplitude fatigue thresholds in *AASHTO LRFD*. ACI Committee Report *ACI 215R-74(92)* and the supporting literature indicate that non-prestressed reinforcement exhibits a constant-amplitude fatigue threshold yet it is unclear that these equations are in fact the threshold values. *ACI 215R-74(92)* suggests that the resistances are "a conservative lower bound of all available test results." In other words, a horizontal constant-amplitude threshold has been drawn beneath all of the curves.

The studies used to define the fatigue resistance of non-prestressed reinforcement (Fisher and Viest, 1961; Pfister and Hognestad, 1964; Burton and Hognestad, 1967; Hanson, et al., 1968; Helgason, et al., 1976; Lash, 1969; MacGregor, et al., 1971; Amorn, et al., 2007) were re-analyzed to estimate constant-amplitude fatigue thresholds for steel reinforcement in tension and concrete in compression and to determine their uncertainty, in terms of bias, mean and coefficient of variation. The various thresholds were grouped together to make design practical and more rational than the single threshold currently defined.

The *AASHO Road Test* (1962) demonstrated that a bridge does not necessarily collapse due to fracture subsequent to fatigue of non-prestressed reinforcement. Such non-prestressed-reinforcement fracture yields distress such as excessive deflection and wide cracks which facilitates detection and subsequent repair. This consequence suggests that a target reliability index less than that for strength limit states would be acceptable (in other words, $\beta_T < 3.5$).

Prestressing Tendons

Fully prestressed components satisfying the tensile stress limits specified in *AASHTO LRFD* Table 5.9.4.2.2-1 at the Service III limit-state load combination are exempt from fatigue considerations. (The Service III limit-state load combination and its calibration is discussed in other sections of this report) This exemption acknowledges that tendons in uncracked prestressed concrete components designed to the requirements of Article 5.9.4 of AASHTO LRFD do not experience stress ranges which result in fatigue cracking. Most prestressed concrete bridge members are covered by this exemption.

For segmentally constructed bridges, *AASHTO LRFD* Article 5.5.3.3 specifies the fatigue resistance of prestressing tendons as given in Table A-4. Reductions in stress range limits for fretting fatigue are not included in the tabulated values.

Table A-4 Prestressing-Tendon Fatigue Resistance

Radius of Curvature (Feet)	Constant-Amplitude Fatigue Threshold (Ksi)
> 30	18
≤ 30 and > 12	Linear Interpolation Between 18 and 10
≤ 12	10

No in-service fatigue cracking of prestressing tendons has been observed, thus justifying the exemption. The majority of the research on fatigue cracking of prestressing strands is based upon testing of tendons in air. Application of the resultant fatigue resistance to concrete members with prestressing tendons is questionable (Hanson, et al., 1970; Tachau, 1971; Warner and Hulsbos, 1966). Thus, the uncertainty of the fatigue resistance of prestressing tendons in concrete members is not well documented. Further, the determination of stress ranges in cracked prestressed concrete members is complicated and beyond the normal prestressed concrete member design procedure (Abeles, et al., 1969; Abeles and Brown, 1971; Abeles, et al., 1974). The uncertainty of this determination is also not well defined. As such, it is proposed that this fatigue limit state not be calibrated.

Welded and Mechanical Splices of Reinforcement

In *AASHTO LRFD* Article 5.5.3.4, constant-amplitude fatigue thresholds are given in Table 5.5.3.4-1. These values are used in the general fatigue limit state equation (*AASHTO LRFD* Equation 5.5.3.1-1) for the design of welded or mechanical splices of reinforcement for infinite fatigue life.

Review of the available test data in *NCHRP Research Results Digest 197* (1994) suggests that any splice capable of developing 125 percent of the yield strength of the bar will sustain 1 million cycles of a 4 ksi constant-amplitude stress range. This fatigue limit is a close lower bound for the splice fatigue data obtained in *NCHRP Research Results Digest 197* (1994).

NCHRP Research Results Digest 197 (1994) found that there is substantial uncertainty in the fatigue performance of different types of welds and connectors much as structural-steel details. However, all types of splices appeared to exhibit a constant-amplitude fatigue limit for repetitive loading exceeding about 1 million cycles. The stress ranges for over 1 million cycles of loading given in *AASHTO LRFD* Table 5.5.3.4-1 are based on statistical tolerance limits to constant-amplitude staircase test data, such that there is a 95 percent level of confidence that 95 percent of the data would exceed the given values for 5 million cycles of loading. These values may, therefore, be regarded as a fatigue limit below which fatigue damage is unlikely to occur during the design lifetime of the structure. This is the same basis used to establish the fatigue design provisions for unspliced reinforcing bars in *AASHTO LRFD* Article 5.5.3.2, which is based on fatigue tests reported in *NCHRP Report 164* (Helgason, et al., 1976).

Table A-5 Constant-Amplitude Fatigue Threshold of Splices from *AASHTO LRFD* Table 5.5.3.4-1

Type of Splice	$(\Delta F)_{TH}$ for greater than 1,000,000 cycles
Grout-filled sleeve, with or without epoxy-coated bar	18 ksi
Cold-swaged coupling sleeves without threaded ends and with or without epoxy-coated bar; Integrally-forged coupler with upset NC threads; Steel sleeve with a wedge; One-piece taper-threaded coupler; and Single V-groove direct butt weld	12 ksi
All other types of splices	4 ksi

.

A.3.1.3 Cracking of Reinforced Concrete Structures

Cracking in reinforced concrete structures is controversial but must be controlled for aesthetic purposes, durability, and corrosion resistance. Cracking is primarily caused by flexural and tensile stresses, but also from temperature, shrinkage, shear, and torsion. Although researchers do not agree on any single crack width equation, the most significant parameters to control cracking are widely agreed upon. The most sensitive factor is the reinforcing steel stress, followed by concrete cover, bar spacing, and the area of concrete surrounding each bar. It has been agreed upon that the bar diameter is not a major variable. For engineering practice, equations in the ACI 318-08 Code (ACI Committee 318, 2008) and *AASHTO LRFD* (2012) are used to control cracking. The corresponding provisions are discussed below.

A.3.1.3.1 Crack Control Reinforcement

This section reviews previous research studies on control of cracking as well as predicting crack width in concrete members. A significant amount of research has been conducted to investigate crack control in concrete members. The research resulted in the development of numerous equations to predict the crack width on the tension surface and the side faces at the level of reinforcement. Equations available to predict crack width were developed for the concrete members with cover less than 2.5 in. and are not applicable for beams with larger concrete cover. Different equations have been adopted by different codes.

However, for calibration purposes, these equations were evaluated with regard to accuracy and applicability. The results from various equations were compared and validated using data collected from available literature.

One of the early studies by Clark (1956) included testing 58 specimens and collecting over 105 crack width readings. Clark concluded that the average crack width is closely related to the following parameters: 1) the diameter of the reinforcing bar, 2) the total reinforcement ratio, 3) area of the beam section, and 4) the distance from the bottom reinforcement to the beam bottom surface. Moreover, Clark stated that the average width was also proportional to the stresses in the reinforcing bars beyond the cracking stress. He suggested that the width of the cracks can be reduced by using a large number of small diameter bars and by increasing the amount of the steel reinforcement. Based on these results, Equation (A-3) was developed to predict the average crack width of the concrete beams. The maximum crack width was estimated by multiplying the average crack width by 1.64 (Clark 1956).

$$w_{ave} = C_1 \frac{D}{p}\left[f_s - C_2\left(\frac{1}{p} + n\right)\right] \quad \text{(A-3)}$$

where

A_e = bd, in²
b = width of component, in.
C_1, C_2 = coefficients that depend on distribution of bond stress, bond strength, and tensile strength of concrete, for Clark's study; $C_1 = 2.27 \times 10^{-8}\left(h - d\right)/d$, $C_2 = 56.6$
d = distance from compressive face of beam/slab to centroid of longitudinal tensile reinforcement, in.
D = diameter of reinforcing bar, in.
f_s = computed stress in reinforcement, psi
h = overall depth of beam/slab, in.
n = ratio of modulus of elasticity of steel to concrete (assumed to be 8 in Clark's study)
p = A_s / A_e = cross-sectional area of reinforcement/cross-sectional area of concrete
w_{ave} = average width of cracks, in.

Kaar and Mattock (1963) also developed a well-known crack width equation for bottom face cracking as follows:

$$w_b = 0.115 \beta f_s \sqrt[4]{A} \quad \text{(A-4)}$$

where

A = average effective concrete area around reinforcing bar, having same centroid as reinforcement, in²

f_s = steel stress calculated by elastic crack section theory, ksi

w_b = maximum crack width, 0.001 in.

β = ratio of distances to neutral axis from extreme tension fiber and from centroid of reinforcement

Broms (1965) conducted tests on 37 tension and 10 flexural members to analyze crack width and crack spacing. Broms observed that the crack spacing decreased rapidly with increasing load and a number of primary tensile cracks formed on the surface of flexural and tension members. Secondary tensile cracks were confined to the surrounding area of reinforcement. The study concluded that the absolute minimum visible crack spacing is the same as the distance from the surface to the center of the reinforcing bar located nearest to the surface of the member. Thus, the theoretical minimum crack spacing is equal to the thickness of the concrete cover (Broms, 1965).

Gergely and Lutz (1968) developed an equation to predict the crack width based on a detailed statistical assessment of experimental data available in the literature at the time. Gergely and Lutz identified various parameters, such as reinforcing bar locations, stresses in the reinforcement, concrete cover depth, and spacing of the reinforcement, as the controlling factors affecting the crack width. The Gergely and Lutz equation is presented as follows:

$$w_b = 0.076\beta f_s \sqrt[3]{Ad_c} \quad \text{(A-5)}$$

where

A = average effective concrete area around reinforcing bar, having same centroid as reinforcement, in²

d_c = bottom cover measured from center of lowest bar, in.

f_s = steel stress calculated by elastic crack section theory, ksi

w_b = maximum crack width, 0.001 in.

β = ratio of distances to neutral axis from extreme tension fiber and from centroid of reinforcement

The maximum concrete cover tested in this study was 3.31 in. However, only three test specimens over 2.5-in. cover were tested in the study.

In the study by Frosch (1999), the crack widths were determined from an equation developed based on a physical model. Results were compared with the test data used in Kaar and Mattock (1963) and Gergely and Lutz (1968). The crack width model developed in this study showed that the crack spacing and width are functions of the distance between the reinforcing steel. Crack control can be achieved by limiting the spacing of these reinforcing bars. Based on the research findings, Frosch (1999) suggested that limiting the maximum bar spacing would prevent large cracks in the concrete beams.

Based on the physical model, the equation to calculate the maximum crack width for uncoated reinforcement was developed as shown below (Frosch, 1999):

$$w_c = \frac{2 f_s}{E_s} \beta \sqrt{\left(d_c^2 + \left(\frac{s}{2} \right)^2 \right)} \quad \text{(A-6)}$$

where

E_s = elastic modulus of steel reinforcement (can be taken as 29000 ksi)
d_c = bottom cover measured from center of lowest bar, in.
f_s = stress in steel reinforcement, ksi
s = maximum permissible bar spacing, in.
w_c = limiting crack width, in. (0.016 in, based on *ACI 318-95* (ACI Committee 318, 1995))
β = 1.0 + 0.08 d_c

Frosch (1999) suggested that for epoxy-coated reinforcement, the above equation for uncoated reinforcement should be multiplied by a factor of 2. Equation (A-6) is rearranged to solve for the allowable bar spacing as follows:

$$s = 2 \sqrt{\left(\left(\frac{w_c E_s}{2 f_s \beta} \right)^2 - d_c^2 \right)} \quad \text{(A-7)}$$

Based on the physical model, the following design recommendation that addresses the use of the both uncoated and coated reinforcement was presented. The equation to calculate the maximum spacing of reinforcement was given as follows (Frosch, 1999):

$$s = 12 \alpha_s \left[2 - \frac{d_c}{3 \alpha_s} \right] \leq 12 \alpha_s \quad \text{(A-8)}$$

where

$$\alpha_s = \frac{36}{f_s} \gamma_c$$

d_c = thickness of concrete cover measured from extreme tension fiber to center of bar or wire located closest thereto, in.
f_s = calculated stress in reinforcement at service load, ksi. It shall be computed as the moment divided by the product of steel area and internal moment arm. f_s shall not exceed 60 percent of the specified yield strength f_y.

s = maximum spacing of reinforcement, in.

α_s = reinforcement factor

γ_c = reinforcement coating factor: 1.0 for uncoated reinforcement; 0.5 for epoxy-coated reinforcement, unless test data can justify a higher value

Frosch (2001) summarized the physical model for cracking, and illustrated the development and limitations of the proposed design method. He recommended formulas for calculating the maximum crack width for uncoated and epoxy-coated reinforcement as well as the design recommendation for their use similar to those in Frosch's paper published in 1999.

In general, largest crack widths are expected at the extreme tensile face of the beam. However, Beeby (1979) conducted studies that showed the largest crack widths occurring in the web along the beam side face occurred at about mid-height. Frosch (2002) conducted research on the modeling and control of cracking in side face of the concrete beams. The study showed that to provide adequate crack control the maximum skin reinforcement spacing is a function of the side concrete cover. It was also shown that a maximum bar spacing of 12 in. provides reasonable crack control up to 3 in. of concrete cover. The crack model developed by Frosch (2002) allows for the calculation of the crack width at any location along the cross section. A profile of the crack width through the depth of the section is more easily created and allows for information regarding optimum locations for placing skin reinforcement for the purpose of controlling side face cracks.

Frosch (2002) showed that the crack spacing and crack width along the side face are functions of the distance from the reinforcement, so the crack can be controlled by adding skin reinforcement and limiting the reinforcement spacing. Since the maximum crack width was observed at halfway between the reinforcement and neutral axis, the following equation can be used to solve for the crack width at $x = (d - c)/2$:

$$w_c = \varepsilon_s \sqrt{d_s^2 + \left(\frac{1}{2}(d-c)\right)^2} \tag{A-9}$$

where

c = depth of neutral axis from compression face, in.

d_s = concrete cover for skin reinforcement, in.

d = effective depth, in.

ε_s = reinforcing strain = f_s / E_s

The study of the physical model showed that sections with effective depth of 36 in. and covers up to 3 in. can be designed without skin reinforcement. For thicker covers, the maximum effective depth not requiring skin reinforcement should be decreased. Additionally, maximum effective depth decreases for covers thicker than 3 in. for Grade 60 reinforcement resulting in the maximum depth, *d* = 36 in.

In order to prevent excessive cracks throughout the depth of the section, maximum spacing of the reinforcement should be determined. According to Frosch (2002), the placement of the first bar is the most critical for the spacing of the skin reinforcement. The maximum crack width was calculated halfway between the primary reinforcement and the first skin reinforcement bar at a distance $x = s/2$, yielding the following equation:

$$w_s = 2\frac{f_s}{E_s}\sqrt{d_s^2 + \left(\frac{s}{2}\right)^2} \tag{A-10}$$

For sections where skin reinforcement exists, it is necessary to determine the location in the section where the reinforcement can be discontinued. Since crack widths are controlled by skin reinforcement below its end point, it is required to calculate the maximum distance s_{na} where the skin reinforcement can be eliminated. The maximum crack width will occur approximately halfway between the neutral axis and the location of the first layer of skin reinforcement at a distance $x = s_{na}/2$ from the neutral axis (Frosch, 2002). The maximum crack width, w_s, can be calculated with the following equation based on the physical model developed by Frosch (2002):

$$w_s = s_{na}\left(\frac{\varepsilon_s}{d-c}\right)\sqrt{d_s^2 + \left(\frac{s_{na}}{2}\right)^2} \tag{A-11}$$

where

s_{na} = maximum distance where the skin reinforcement can be eliminated.

Frosch (2002) recommended that the design formula should be based on a physical model to address the control of cracking in reinforced concrete structures and to unify the design criteria for controlling cracking in side and bottom faces. Frosch (2002) recommended the maximum spacing of flexural tension reinforcement as follows:

$$s = 12\alpha_s\left[2 - \frac{d_c}{3\alpha_s}\right] \le 12\alpha_s \tag{A-12}$$

where

$$\alpha_s = \frac{36}{f_s}$$

d_c = thickness of concrete cover, in., for bottom-face reinforcement, measured from extreme tension fiber to center of bar, and for skin reinforcement, measured from side face to center of bar

f_s = calculated stress in reinforcement at service load, ksi. It shall be computed as the moment divided by the product of steel area and internal moment arm. It shall be

permitted to take f_s as not more than 60 percent of the specified yield strength f_y.

s = maximum spacing of reinforcement, in.

α_s = reinforcement factor

Skin reinforcement shall be required along both side faces of a member for a distance d/2 from the nearest flexural tension reinforcement if the effective depth exceeds the depth calculated by Equation (A-12) shown below:

$$d = 42\alpha_s - 2d_c \leq 36\alpha_s \quad \text{(A-13)}$$

Epoxy-coated reinforcement is widely used to increase the durability of structures. The epoxy coating has been shown to decrease bond strength which can decrease crack spacing and increase crack widths when compared to uncoated reinforcement (Blackman and Frosch, 2005). Blackman and Frosch investigated crack width of the concrete beams with epoxy-coated reinforcement. The primary variables used in the study include epoxy coating thickness and reinforcing bar spacing. Blackman and Frosch designed ten slab specimens in order to examine the effect of epoxy coating on cracks. It was concluded that the epoxy coating thickness does not affect the concrete crack significantly. Frosch (1999), Frosch (2001), Frosch (2002), and Blackman and Frosch (2005) presented an equation to compare the average measured crack spacing for the uncoated and epoxy-coated bars with the calculated values:

$$S_c = \psi_s d^* \quad \text{(A-14)}$$

where

S_c = crack spacing, in.

d^* = controlling cover distance, in.

Ψ_s = crack spacing factor: 1.0 for minimum crack spacing; 1.5 for average crack spacing; 2.0 for maximum crack spacing

Cracking of structures is rather common and is not always damaging to the structure. However, when considering a bridge deck, moderately sized cracks can be detrimental to the longevity of the structure due to the exposure to harsh environments. Recently, increased concrete cover, coupled with the use of high-performance concrete, are becoming increasingly popular because of their durability. This results in unrealistically small bar spacing and prevents the use of contemporary crack control practices that are based on statistical studies. Therefore, it is desirable to develop methods to predict average and maximum crack widths of reinforced concrete members with thicker concrete covers at various locations.

Choi and Oh (2009) studied the crack width for transversely post-tensioned concrete deck slabs in box girder bridges. They tested four full-scale concrete box girder segments, and then derived the maximum crack width equation from the testing data as follows:

$$w_{\max} = 3\times10^{-6}\left(f_s - f_0\right)\phi_s\left(\frac{A_{t,eff}}{A_{st}+\xi A_{pt}}\right)^{0.75}\frac{h-x}{d-x} \quad \text{(A-15)}$$

$$\xi = \sqrt{\frac{\tau_{ap}}{\tau_{as}}\frac{\pi+(n-1)}{n\pi}\frac{\phi_s}{\phi_p}} \quad \text{(A-16)}$$

where

A_{st} = total area of reinforcing bars, mm^2
A_{pt} = total area of prestressing tendons, mm^2
$A_{t,eff}$ = effective tensile concrete area, mm^2
d = effective depth, mm
f_s = increment of reinforcing bar stress after decompression, MPa
f_0 = steel stress at the initial occurrence of crack, MPa
h = height of cross section, mm
n = number of strands in a flat duct.
x = depth of neutral axis, mm
$w_{\max}$ = predicted maximum crack width, mm
ϕ_s = diameter of reinforcing bar, mm
ϕ_p = diameter of prestressing tendons, mm
$\frac{\tau_{ap}}{\tau_{as}}$ = 0.465 for grouted post-tensioned tendons

A.3.1.3.2 Control of Cracks in Current Specifications Provisions

The code provisions specifying the distribution of reinforcement are reviewed in this section.

ACI requirements for flexural crack control in beams and thick one-way slabs are based on the statistical analysis of maximum crack width data from several sources (Gergely and Lutz, 1968). ACI maintains that crack control is particularly important when reinforcement with yield strength over 40,000 psi is used. Good detailing practices such as concrete cover and spacing of reinforcement should lead to adequate crack control even when reinforcement with yield strength 60,000 psi is used. *ACI 318-08 (ACI Committee 318, 2008)* Article 10.6 does not distinguish between interior and exterior exposure since corrosion is not clearly correlated with surface crack widths in the range normally found at service load levels. *ACI 318-08* only requires that the spacing of reinforcement closest to the tension face, s, shall not exceed that given by:

$$s = 15\left(\frac{40,000}{f_s}\right) - 2.5c_c \quad \text{(A-17)}$$

but not greater than $12\left(\frac{40,000}{f_s}\right)$, where c_c is the least distance from surface of reinforcement or prestressing steel to the tension face. If there is only one bar or wire nearest to the extreme tension face, *s* used in Equation (A-17) is the width of the extreme tension face. These provisions are not sufficient for structures subject to very aggressive exposure or designed to be watertight.

Special investigation is required for structures subject to very aggressive exposure or designed to be watertight. *ACI 318-99* (ACI Committee 318, 1999) limited the maximum spacing to 12 in., but this limitation was removed in *ACI 318-08* (ACI Committee 318, 2008). *ACI 318-08* also recommends the use of several bars at moderate spacing rather than fewer bars at larger spacing to control cracking. These provisions were updated recently to reflect the higher service stresses that occur in flexural reinforcement with the use of the load combinations introduced in *ACI 318-02* (ACI Committee 318, 2002). The maximum bar spacing is specified to directly control cracking. Similar recommendations have been stated for deep beams with the requirement of skin reinforcement.

AASHTO LRFD (2012) also provides provisions of reinforcement spacing to control flexural cracking. Similar to the equation adopted in ACI, AASHTO emphasizes the importance of reinforcement detailing and that smaller bars at moderate spacing tend to be more effective than an equivalent area of larger bars. *AASHTO LRFD* also agrees with *ACI 318-08* on the most important parameters affecting crack width and specifies a formula for distribution of reinforcement to control cracking. The equation in *AASHTO LRFD* (2008) is based on the physical crack model of Frosch (2001) rather than on the statistically-based model used in previous editions. The equation limits bar spacing rather than crack width as follows:

$$s \le \frac{700\gamma_e}{\beta_s f_{ss}} - 2d_c \qquad \text{(A-18)}$$

where

d_c = thickness of concrete cover measured from extreme tension fiber to center of the flexural reinforcement located closest thereto (in.)

f_{ss} = tensile stress in steel reinforcement at the SLS (ksi)

h = overall thickness of depth of the component (in.)

$\beta_s = 1 + \frac{d_c}{0.7(h - d_c)}$ (geometric relationship between crack width at tension face versus crack width at reinforcement level)

γ_e = exposure factor = 1.00 for Class 1 exposure, 0.75 for Class 2 exposure

As shown above, unlike ACI, AASHTO specifies exposure conditions to meet the needs of the authority having jurisdiction. Class 1 exposure condition is based on a maximum crack width of 0.017 in. and applies when cracks can be tolerated due to reduced concerns of appearance and/or corrosion. This exposure class can be thought of as an upper bound in regards to crack width for appearance and corrosion. Class 2 exposure condition generally applies to decks and substructures exposed to water and any other components exposed to

corrosive environments. *AASHTO LRFD* (2008) also specifies requirements for skin reinforcement based on *ACI 318-11* (ACI Committee 318, 2011). AASHTO LRFD Equation 5.7.3.4-1, or Equation (A-18) above, also applies to both reinforced and prestressed concrete, with specifications on the steel stresses used. In general, if AASHTO Class 2 exposure condition is used, all AASHTO spacings were less than those derived by the ACI equation. However, if Class 1 exposure condition is used, ACI spacing becomes more conservative.

A.3.1.4 Principal Stresses in Webs of Segmental Concrete Bridges

Recently, Okeil (2006) studied the allowable tensile stress for webs of prestressed segmental (PS) concrete bridges using a reliability-based approach. In this study, six PS concrete bridge designs were analyzed. Okeil states that by complying with the allowable tensile stresses, flexural cracking at the top and bottom fibers is controlled. However, for the webs, cracks might develop due to a biaxial stress state resulting from a combination of shear and normal stresses. Controlling shear cracking requires that the principal stress be limited to an allowable tensile stress, $f_{t,all}$. This issue has been addressed by the Florida Department of Transportation (*Structures Manual*, 2013) and produced a recommendation for the allowable tensile stresses to be used in checking web tensile principal stress, σ_1. However, the recommendation ignored the accompanying compressive principal stress, σ_2, which has a significant effect on the tensile strength of concrete. The objective of Okeil's study was to develop an allowable stress limit under which cracking in webs of PS bridges under service load conditions can be controlled.

Three equations were considered: ACI (ACI Committee 318, 2005), Kupfer and Gerstle (1973), and Oluokun (1991), as shown in Equations (A-19) through (A-21), respectively:

$$f_{tu} = 6.7(f_c')^{0.5}, \text{ in psi} \quad \text{(A-19)}$$

$$f_{tu} = 1.59(f_c')^{0.67}, \text{ in psi} \quad \text{(A-20)}$$

$$f_{tu} = 1.38(f_c')^{0.69}, \text{ in psi} \quad \text{(A-21)}$$

where

f_c' = concrete compressive strength, psi
f_{tu} = uniaxial tensile strength of concrete, psi

Okeil concluded that Equation (A-21) provides better estimate of the tensile strength over a wider range of concrete compressive strength. Using a biaxial state of stress and regression analysis, Okeil (2006) developed a relationship between the tensile strength and the corresponding compressive strength as follows:

$$\frac{\sigma_{tu}}{f_{tu}} = 1 + 0.85\frac{\sigma_{cu}}{f_c'} \quad \text{(A-22)}$$

where

σ_{cu} , σ_{tu} = ultimate strengths of concrete under compression-tension biaxial state of stress

Equation (A-23) is obtained by combining Equation (A-21) and Equation (A-22):

$$\sigma_{tu} = 1.38(f_c^{'})^{0.69}(1 + 0.85\frac{\sigma_{cu}}{f_c^{'}}) \text{ , in psi} \quad \text{(A-23)}$$

After a detailed parametric study and reliability analysis, Okeil (2006) recommended an expression for estimating the allowable tensile stress in webs of post-tensioned segmental bridges under biaxial stresses as follows:

$$f_{ct} = 0.60(f_c')^{0.7}(1 + 0.85\frac{\sigma_2}{f_c'}) \quad \text{(A-24)}$$

where

σ_2 = principal stresses in centroidal stress block in web of PS bridge, ksi

It should be noted that the findings of this study are limited to the range of concrete compressive strength between 5 to 8 ksi.

A.3.1.5 Stress Limitations for Prestressing Tendons

AASHTO LRFD (2012) provides stress limits for prestressing tendons at various service conditions. The stress limit values are listed in Table A-6.

ACI 318-08 provides similar limits on the tensile stress in prestressing tendons and rebar (ACI Committee 318, 2008). Major revision of the limits was made in the 1983 version of *ACI 318* to incorporate the higher yield strength of low-relaxation wire and strand (ACI Committee 318, 1983). The *ACI 318-08* stress limits in prestressing steel are listed as follows (ACI Committee 318, 2008):

Due to prestressing steel jacking force: $0.94 f_{py}$ but not greater than the lesser of $0.80 f_{pu}$ and the maximum value recommended by the manufacturer of prestressing steel or anchorage devices.

Immediately after prestress transfer: $0.82 f_{py}$ but not greater than $0.74 f_{pu}$.

Post-tensioning tendons, at anchorage devices and couplers, immediately after force transfer: $0.70 f_{pu}$.

EN1992-2 (Eurocode 2): Design of Concrete Structures (*EN1992-2*, 2003) restricts inelastic deformation of the steel in concrete structures at the SLS to prevent large, permanently open cracks. In *EN1992-2*, at the SLSs, the stress limit for prestressing steel is $0.75 f_{pk}$ after

allowance for losses, where f_{pk} is characteristic tensile strength of prestressing steel. The exact meaning of "characteristic" tensile strength is not defined in *EN1992-2* and is interpreted herein as the specified strength. This limit of $0.75 f_{pk}$ is listed in *EN1992-2*, Section 7.

Table A-6 Stress Limits for Prestressing Tendons (AASHTO LRFD, 2012)

Condition	Tendon Type		
	Stress-Relieved Strand and Plain High-Strength Bars	Low Relaxation Strand	Deformed High-Strength Bars
Pretensioning			
Immediately prior to transfer (f_{pbt})	$0.70 f_{pu}$	$0.75 f_{pu}$	–
At SLS after all losses (f_{pe})	$0.80 f_{py}$	$0.80 f_{py}$	$0.80 f_{py}$
Post-Tensioning			
Prior to seating - short-term f_{pbt} may be allowed	$0.90 f_{py}$	$0.90 f_{py}$	$0.90 f_{py}$
At anchorages and couplers immediately after anchor set	$0.70 f_{pu}$	$0.70 f_{pu}$	$0.70 f_{pu}$
Elsewhere along length of member away from anchorages and couplers immediately after anchor set	$0.70 f_{pu}$	$0.74 f_{pu}$	$0.70 f_{pu}$
At SLS after losses (f_{pe})	$0.80 f_{py}$	$0.80 f_{py}$	$0.80 f_{py}$

A.3.1.6 Concrete Tension Stresses

The early discussion of cracking control is diverse. At the First United States Conference on Prestressed Concrete in 1951, some experts opined that a completely crackless concrete member is only better for a specific purpose, but others thought that cracking of prestressed concrete beams is as important as yielding. In 1958, the "Tentative Recommendations for Prestressed Concrete" proposed by ACI-ASCE Joint Committee 323 suggested that prestressed concrete before losses due to creep and shrinkage should meet the following limits (note unit in the following provisions is psi for the allowable tensile stress):

$3\sqrt{f'_{ci}}$ for members without non-prestressed reinforcement;

$6\sqrt{f'_{ci}}$ for members with non-prestressed reinforcement provided to resist the tensile force in concrete; computed on the basis of an uncracked section.

The 1963 *Building Code Requirements for Reinforced Concrete* (ACI Committee 318, 1963) included the recommendation for the tensile stress limits, in psi, as proposed by ACI-ASCE Joint Committee 323 (1958), with some modifications, as follows:

$3\sqrt{f'_{ci}}$ for members without auxiliary reinforcement in the tension zone;

When the calculated tension stress exceeds $3\sqrt{f'_{ci}}$, reinforcement shall be provided to resist the total tension force in the concrete computed on the assumption of uncracked section.

The 1977 *Building Code Requirements for Reinforced Concrete* modified the allowable tensile stress limit, in psi, as follows (ACI Committee 318, 1977):

$6\sqrt{f'_{ci}}$ for the extreme fiber stress in tension at ends of simply supported members;

$3\sqrt{f'_{ci}}$ for the extreme fiber stress in tension at other locations.

In the current *ACI 318-11*, Section 18.4.1 specifies the allowable tensile stress in concrete immediately after prestress transfer (before time-dependent prestress losses) as follows (ACI Committee 318, 2011):

Where computed concrete tensile strength, f_t, exceeds $6\sqrt{f'_{ci}}$ at ends of simply supported members, or $3\sqrt{f'_{ci}}$ at other locations, additional bonded reinforcement shall be provided in the tensile zone to resist the total tensile force in concrete computed with the assumption of an uncracked section.

The AASHTO *Standard Specifications for Highway Bridges* (1992) specified the allowable tensile stresses, before losses due to creep and shrinkage, as follows:

200 psi or $3\sqrt{f'_{ci}}$ for members in tension areas with no bonded reinforcement;

Where the calculated tensile stress exceeds this value, reinforcement shall be provided to resist the total tension force in the concrete computed on the assumption of uncracked section. The maximum tensile stress shall not exceed $7.5\sqrt{f'_{ci}}$.

Table A-7 shows the tensile stress limits and provisions by the *AASHTO LRFD* (2012).

Table A-7 Tensile Stress Limits in Prestressed Concrete at SLS after Losses, Fully Prestressed Components (AASHTO LRFD, 2012, Table 5.9.4.2.2-1)

Bridge Type	Location	Stress Limit
Other Than Segmentally Constructed Bridges	Tension in the precompressed Tensile Zone Bridges, Assuming Uncracked Sections	
	For components with bonded prestressing tendons or reinforcement that are subjected to not worse than moderate corrosion condition.	$0.19\sqrt{f_c'}(ksi)$
	For components with bonded prestressing tendons or reinforcement that are subjected to severe corrosive conditions	$0.0948\sqrt{f_c'}(ksi)$
	For components with unbonded prestressing tendons	No tension
Segmentally Constructed Bridges	Longitudinal Stresses Through Joints in the Precompressed Tensile Zone	
	Joints with minimum bonded auxiliary reinforcement through the joints sufficient to carry the calculated longitudinal tensile force at a stress of 0.5 fy; internal tendons or external tendons	$0.0948\sqrt{f_c'}(ksi)$
	Joints without the minimum bonded auxiliary reinforcement through joints	No tension
	Transverse Stress Through Joints	
	Tension in the transverse direction in precompressed tensile zone	$0.0948\sqrt{f_c'}(ksi)$
	Principal Tensile Stress at Neutral Axis in Web	
	All types of segmental concrete bridges with internal and/or external tendons, unless the Owner imposes other criteria for critical structures.	$0.110\sqrt{f_c'}(ksi)$

A.3.1.7 Existing Limit States that are Deterministic or Represent Detailing Requirements

The following limit states exist in *AASHTO LRFD*. Reviewing the background of these limit states revealed that they are either deterministic or represent detailing requirements that cannot be calibrated. No calibration is anticipated for these limit states.

Fatigue in Concrete Deck Slabs and Culvert Top Slabs (*AASHTO LRFD* Article 5.5.3.1)

Stresses measured in concrete deck slabs of bridges and top slabs of box culverts in service are far below infinite fatigue life, most probably due to internal arching action.

AASHO *Standard Specifications for Highway Bridges* (1974 and 1975 Interims) include the background that led to waiving fatigue requirements for these components

Fatigue of Reinforcement of Fully Prestressed Components (*AASHTO LRFD*, Article 5.5.3.1)

For fully prestressed components designed to have extreme fiber tensile stress due to Service III Limit State within the tensile stress limit specified in the *AASHTO LRFD* Table 5.9.4.2.2-1, the fatigue limit-state load factors, the girder distribution factors, and dynamic load allowance cause fatigue limit-state stress to be considerably less than the corresponding value determined from SLS III. For fully prestressed components, the net concrete stress is usually significantly less than the concrete tensile stress limit specified in AASHTO LRFD Table 5.9.4.2.2-1. Therefore, the calculated flexural stresses are significantly reduced. For this situation, the calculated steel stress range, which is equal to the modular ratio times the concrete stress range, is almost always less than the steel fatigue stress range limit specified in Article 5.5.3.3.

Fatigue of Prestressing Tendons (*AASHTO LRFD*, Article 5.5.3.3)

With fatigue in fully prestressed components waived, see above, these provisions are only applicable to segmental bridges. Little data is available on the uncertainty of load and resistance of segmental bridges. There is no evidence of fatigue damage on these structures so no changes are recommended and calibration was not necessary.

Crack Control Reinforcement for Components Designed using Strut and Tie Model (*AASHTO LRFD*, Article 5.6.3.6)

Birrcher, et. al., (2009) proposed the new provisions regarding the crack control reinforcement as follows:

"The spacing of the bars in these grids shall not exceed the smaller of d/4 and 12.0 in"
"The reinforcement in the vertical and horizontal direction shall satisfy the following:

$$\frac{A_v}{b_w s_v} \geq 0.003, \frac{A_h}{b_w s_h} \geq 0.003 \quad \text{(A-25)}$$

where

A_v, A_h = total area of vertical and horizontal crack control reinforcement within spacing s_v and s_h, respectively, in^2

b_w = width of member web, in.

s_v, s_h = spacing of vertical and horizontal crack control reinforcement, respectively, in.

"Crack control reinforcement shall be distributed evenly near the side faces of the strut. Where necessary, interior layers of crack control reinforcement may be used."

A.3.2 Eurocode

The *Eurocode* contains the following sections to which reference is made in some other sections of this report.

EN 1990 (*Eurocode 0): Basis of Structural Design*
EN 1991 (*Eurocode 1): Actions on Structures*
EN 1992 (*Eurocode 2): Design of Concrete Structures*
EN 1993 (*Eurocode 3): Design of Steel Structures*
EN 1994 (*Eurocode 4): Design of Composite Steel and Concrete Structures*
EN 1995 (*Eurocode 5): Design of Timber Structures*
EN 1996 (*Eurocode 6): Design of Masonry Structures*
EN 1997 (*Eurocode 7): Geotechnical Design*
EN 1998 (*Eurocode 8): Design of Structures for Earthquake Resistance*
EN 1999 (*Eurocode 9): Design of Aluminum Structures*

These sections allow the user countries to incorporate country-specific requirements through the incorporation of a National Annex.

The *Eurocode* replaced most previous country specifications, such as the German Institute for Standardization (DIN) and the British BS5400 and is expected to eventually replace all other European Union member country specifications. It is assumed that the requirements of the *Eurocode* encompass those of the previous specifications and, thus, no other European specifications were reviewed.

A.3.2.1 Definition of SLS

The *Eurocode* defines the SLSs as those concerning (*EN 1990*, 2002):

- The functioning of the structure or structural members under normal use;
- The comfort of users;
- The appearance of the construction works.

The *Eurocode* (*EN 1990*, 2002) includes requirements calling for:

- The serviceability requirements to be agreed upon for each individual project.
- A distinction to be made between reversible and irreversible serviceability limit states.
- The verification of SLS based on criteria concerning the following aspects:
  a) Deformations that affect
     – The appearance,
     – The comfort of users, or
     – The functioning of the structure (including the functioning of machines or services), or that cause damage to finishes or non-structural members.
  b) Vibrations
     – That cause discomfort to people, or
     – That limit the functional effectiveness of the structure.
  c) Damage that is likely to adversely affect
     – The appearance,

- The durability, or
- The functioning of the structure.

In the context of serviceability, the *Eurocode* considers the term "appearance" to be concerned with such criteria as high deflection and extensive cracking, rather than aesthetics (*EN 1990*, 2002).

A.3.2.2 Background on the *Eurocode's* Reliability Basis

The *Eurocode* specifies that structures be designed for a particular design working life, T_u (*EN 1990*, 2002). The design working life is defined as the period for which a structure is assumed to be usable for its intended purpose with anticipated maintenance but without major repair being necessary. Examples of the selection of the design working life are given in Table A-8.

Table A-8 Design Working Lives (EN 1990, 2002, adapted from Table (2.1))

Design Working Life Category	Design Working Life (Years)	Examples
1	10	Temporary structures
2	10 to 25	Replaceable structural parts, e.g. gantry girders, bearings
3	15 to 30	Agricultural and similar structures
4	50	Building structures and other common structures
5	100	Monumental building structures, bridges and other civil engineering structures

The levels of reliability relating to the ULS and SLS (In the *Eurocode*, the ULS and SLS are termed the ultimate and serviceability limit states, respectively.) can be achieved by suitable combinations of protective measures (e.g. protection against fire, protection against corrosion, etc.), measures relating to design calculations (e.g. choice of partial factors), measures relating to quality management, measures aimed to reduce errors in design (e.g., project supervision) and execution (construction) of the structure (e.g., inspection during execution) and other kinds of measures.

The *Eurocode* defines three different levels of consequences classes (CC), CC1, CC2 and CC3, as defined in Table A-9. Three reliability classes (RC); RC1, RC2, RC3; may be associated with the three consequence classes; CC1, CC2 and CC3.

Table A-9 Eurocode Consequence Classes (EN 1990, 2002, adapted from Table (B1))

Consequence Class	Description Related To Consequences	Reliability Class
CC1	Low consequence for loss of human life; economic, social or environmental consequences small or negligible	RC1
CC2	Moderate consequence for loss of human life; economic, social or environmental consequences considerable	RC2
CC3	Serious consequences for loss of human life, or for economic, social or environmental concerns	RC3

The vast majority of bridges are designed to CC2 with CC3 a possibility only for those bridges with very high consequences of failure, such as a signature bridge.

The provisions of the *Eurocode*, specifically *EN 1990* (2002) with the partial factors given in Annex A1 and *EN 1991* to *EN 1999*, yield designs consistent with reliability class RC2. The *Eurocode* uses the multiplication factors, K_{F1}, given in Table A-10 applied to load factors to differentiate the three reliability classes. Other measures (differing levels of quality control, for example) in lieu of modifying the load factors are sometimes preferred.

Table A-10 Multiplication Factor, KF1, for Reliability Differentiation

Reliability Class	K_{F1}
RC1	0.9
RC2	1.0
RC3	1.1

Table A-11 below summarizes the probabilities of failure, p_F, inherent to the *Eurocode* and the *AASHTO LRFD* for strength, along with the corresponding reliability indices, β, below them in italics. The defining probabilities of failure in the case of the *Eurocode* and the defining reliability indices for the *AASHTO LRFD* are shown in boldface.

Table A-11 Target Probabilities of Failure (p_F) and Reliability Indices (β_T)

Code		Reference Period (years)				
		1	**50**	**75**	**100**	**120**
Eurocode	CC2 (K_{F1} = 1.0)	**1.00E-06**	5.00E-05	7.50E-05	1.00E-04	1.20E-04
		4.75	*3.89*	*3.79*	*3.72*	*3.67*
	CC3 (K_{F1} = 1.1)	**1.00E-07**	5.00E-06	7.50E-06	1.00E-05	1.20E-05
		5.20	*4.42*	*4.33*	*4.26*	*4.22*
AASHTO LRFD	typical bridges (η_I = 1.0)	2.67E-06	1.33E-04	2.00E-04	2.67E-04	3.20E-04
		4.55	*3.65*	***3.50***	*3.46*	*3.41*
	important bridges (η_I = 1.05)	9.60E-07	4.80E-05	7.20E-05	9.60E-05	1.15E-04
		4.76	*3.90*	***3.80***	*3.73*	*3.68*

SLS Reliability

The SLSs of the *Eurocode* are categorized as reversible and irreversible. Reversible SLSs are those for which no consequences remain once the load exceeding the specified SLS load is removed. Irreversible SLSs are those for which consequences remain. For example, a crack-width limit state with limited width is a reversible limit state, whereas one defined by a large width (such as 0.5 mm) is irreversible because, if the crack width is high enough, once the live load is removed the crack does not close completely.

The irreversible SLSs, which do not concern the safety of the traveling public, are calibrated to a lower probability of failure and corresponding reliability index than the strength limit states, as shown in Table A-12.

Table A-12 Irreversible SLS Target Probabilities of Failure and Corresponding Reliability Indices (*EN 1990*, 2002, adapted from Table (C2))

Reliability Class	Reference Period (Years)	
	1	**50**
RC2	1.00E-03	1.00E-01
	2.9	1.5

SLS Load Combinations

EN 1990 (2002) includes three different types of load combinations for the SLSs: characteristic combination, frequent combination and quasi-permanent combination. Table A-13 summarizes the *Eurocode's* service limit-state load combinations.

Table A-13 SLS Combinations

SLS		Load Combinations		
Type	**Description**	**Type**	**Acceptance of Infringement**	**Example**
Reversible	those limit states that will not be exceeded when the actions which caused the infringement are removed	frequent	specified duration and frequency of infringements are accepted	the crack-width limit state of a prestressed concrete beam with bonded tendons characterized by a 0.2 mm crack width
		quasi-permanent	specified long-term infringement is accepted	the crack-width limit state for a reinforced concrete or prestressed concrete beam with unbonded tendons characterized by a 0.3 mm crack width
Irreversible	those limit states that remain permanently exceeded even when the actions which caused the infringement are removed	characteristic (5% probability of exceedance)	no infringement accepted	the crack-width limit state characterized by a 0.5 mm crack width, because such a wide crack cannot completely close once the loads that caused it are removed

A.3.2.3 Serviceability Design Basic Approach

A.3.2.3.1 Basic Equation

The basic equation in the *Eurocode* (*EN 1990*, 2002) for verifying that a SLS is satisfied is:

$E_d \leq C_d$

where

C_d = the limiting design value of the relevant serviceability criterion.
E_d = the design value of the effects of actions specified in the serviceability criterion, determined on the basis of the relevant combination.

A.3.2.3.2 Serviceability Criteria

Specific serviceability criteria such as crack width, stress or strain limitation and slip resistance exist in separate sections (*EN 1991* to *EN 1999*). In addition to these requirements, project specific deformations to be considered in relation to serviceability requirements are required to be as detailed in relevant code annexes in accordance to the type of construction works, or agreed with the client or the National authority.

A.3.2.3.3 Combination of Actions (Load Combinations)

The combinations of actions (load combination) for serviceability limit states in the *Eurocode* are defined symbolically by the following expressions:

a) Characteristic (rare) Combination:

$$E_d = E\left\{\sum_{j\geq 1} G_{k,j} + P_k + Q_{k,1} + \sum_{i>1} \psi_{0,i} \cdot Q_{k,i}\right\} \quad \text{(A-26)}$$

The characteristic combination is normally used for irreversible limit states.

b) Infrequent Combination:

$$E_d = E\left\{\sum_{j\geq 1} G_{k,j} + P_k + \psi'_{1,1} \cdot Q_{k,1} + \sum_{i>1} \psi_{1,i} \cdot Q_{k,i}\right\} \quad \text{(A-27)}$$

c) Frequent Combination:

$$E_d = E\left\{\sum_{j\geq 1} G_{k,j} + P_k + \psi_{1,1} \cdot Q_{k,1} + \sum_{i>1} \psi_{2,i} \cdot Q_{k,i}\right\} \quad \text{(A-28)}$$

The frequent combination is normally used for reversible limit states.

d) Quasi-permanent Combination:

$$E_d = E\left\{\sum_{j\geq 1} G_{k,j} + P_k + \sum_{i>1} \psi_{2,i} \cdot Q_{k,i}\right\} \quad \text{(A-29)}$$

where:

Effect of Action (*E*)
Effect of actions (or action effect) on structural members, (e.g. internal force, moment, stress, strain) or on the whole structure (e.g. deflection, rotation)

Permanent Action (*G*)
Action that is likely to act throughout a given reference period and for which the variation in magnitude with time is negligible, or for which the variation is always in the same direction (monotonic) until the action attains a certain limit value

Variable Action (*Q*)
Action for which the variation in magnitude with time is neither negligible nor monotonic

Combination Value of a Variable Action ($\Psi_0 Q_k$)
Value chosen - in so far as it can be fixed on statistical bases - so that the probability that the effects caused by the combination will be exceeded is approximately the same as by the characteristic value of an individual action. It may be expressed as a determined part of the characteristic value by using a factor ($\Psi_0 \leq 1.0$)

Frequent Value of a Variable Action ($\Psi_1 Q_k$)
Value determined - in so far as it can be fixed on statistical bases - so that either the total time, within the reference period, during which it is exceeded is only a small given part of the reference period, or the frequency of it being exceeded is limited to a given value. It may be expressed as a determined part of the characteristic value by using a factor ($\Psi_1 \leq 1.0$)

Quasi-permanent Value of a Variable Action ($\Psi_2 Q_k$)
Value determined so that the total period of time for which it will be exceeded is a large fraction of the reference period. It may be expressed as a determined part of the characteristic value by using a factor ($\Psi_2 \leq 1.0$)

$G_{k,j}$	=	characteristic (extreme) value of permanent action j
$G_{kj,sup}/G_{kj,inf}$	=	upper/lower value of permanent action j
P	=	relevant prestressing value of prestressing action
$Q_{k,l}$	=	characteristic value of the leading (dominant) variable action l
$Q_{k,l}$	=	characteristic value of the accompanying variable action i
Ψ_0	=	factor for combination value of a variable action
Ψ_1	=	factor for frequent value of a variable action
Ψ_2	=	factor for quasi-permanent value of a variable action

The *Eurocode* allows some of the above expressions to be modified and gives detailed rules in relevant sections of the code (Parts of *EN 1991* to *EN 1999*). As each of the *Eurocode* countries has its own National Annex where the country-specific requirements are placed, the *Eurocode* allows that the serviceability criteria desired by each country to be specified in the National Annex. Recommended values of the Ψ factors for different types of structures (e.g. buildings, highway bridges or railway bridges) are tabulated in the *Eurocode*.

Table A-14 shows the recommended values for highway bridges.

Table A-14 Recommended Values of Ψ Factors for Highway Bridges in the Eurocode (EN 1990, 2002, adapted from Table A2.1)

Action	Symbol		Ψ_0	Ψ_1	Ψ_2
Traffic Loads (*EN 1991-2, 2003*, Table 4.4)	gr1a (LM1+pedestrian or cycle-track loads)[1]	TS	0,75	0,75	0
		UDL	0,40	0,40	0
		Pedestrian+cycle-track loads[2]	0,40	0,40	0
	gr1b (Single Axle)		0	0,75	0
	gr2 (Horizontal Forces)		0	0	0
	gr3 (Pedestrian Loads)		0	0	0
	gr4 (LM4 – Crowd Loading)		0	0,75	0
	gr5 (LM3 – Special Vehicles)		0	0	0
Wind Forces	F_{wk} - Persistent Design Situations - Execution		 0,6 0,8	 0,2 -	 0 0
	F^*_W		1,0	-	-
Thermal Actions	T_k		0,6[3]	0,6	0,5
Snow Loads	Q_{snk} (During Execution)		0,8	-	-
Construction Loads	Q_c		1,0	-	1,0

1) The recommended values of Ψ_0, Ψ_1, Ψ_2, for gr1a and gr1b are given for roads with traffic corresponding to adjusting α_{Qi}, α_{qi}, α_{qr}, and β_Q equal to 1. Those relating to UDL correspond to the most common traffic scenarios, in which an accumulation of lorries can occur, but not frequently. Other values may be envisaged for other classes of routes, or of expected traffic, related to the choice of the corresponding α factors. For example, a value of Ψ_2 other than zero may be envisaged for the UDL system of LM1 only, for bridges supporting a severe continuous traffic. See also *EN 1998-2 (2005)*.

2) The combination value of the pedestrian and cycle-track load, mentioned in Table 4.4a of *EN 1991-2* (2003), is a "reduced" value. Ψ_0 and Ψ_1 factors are applicable to this value.

3) The recommended Ψ_0 value for thermal actions may in most cases be reduced to 0 for ultimate limit states EQU, STR and GEO. See also the design *Eurocodes*.

NOTE 1: The Ψ values may be set by the National Annex. Recommended values of Ψ factors for the groups of traffic loads and other more common actions are given in:

- Table A2.1 for road bridges
- Table A2.2 for foot bridges
- Table A2.3 for railway bridges

NOTE 2: When the National Annex refers to the infrequent combination of actions for some serviceability limit states of concrete bridges, the National Annex may define the values of Ψ_{1infq}. The recommended values of Ψ_{1infq} are:

- 0,80 for gr1a (LM1), gr1b (LM2), gr3 (pedestrian loads), gr4 (LM4, crowd loading) and T (thermal actions)
- 0,60 for F_W in persistent design situations
- 1,00 in other cases (i.e. the characteristic value is substituted for the infrequent value)

NOTE 3: The characteristic values of wind actions and snow loads during execution are defined in *EN 1991-1-6 (2005)*. Where relevant, representative values of water forces (F_{wa}) may be defined for the individual project.

A.3.2.4 Existing Limit State

A summary of the SLS requirements in the *Eurocode* is attached as Appendix B.

A.3.3 Canadian Highway Bridge Design Code (CHBDC)

A.3.3.1 Background

The *CHBDC* (2006) and earlier *OHBDC* (1991) cover Strength Limit States (ULS) and SLS. The serviceability limit states in the *CHBDC* include fatigue, deflection, cracking and compressive stress in concrete. The SLS acceptability criteria were determined by reference to past practice.

As an example of this process, special consideration was given to the tensile stress limit state in prestressed concrete girders. The acceptability criterion was formulated in terms of the minimum return time period between exceeding the decompression moment. It was assumed that the girders will crack anyway due to shrinkage prior to installation, or under exceptionally heavy trucks, and then the crack will reopen each time the decompression moment is exceeded. An open crack, even for a fraction of a second, is assumed to allow water with salt or other pollutants to penetrate, and eventually reach the rebar and prestressing steel, resulting in corrosion, delamination, spalling of concrete, and, eventually, girder failure. The minimum acceptable return time period for decompression moment was then determined by a group of experts invited by the Code Control Committee using a process of expert elicitation (Delphi process). The group was asked to provide their expert opinion. They deliberated and came to a conclusion that a return period of three weeks is acceptable. However, the group did not feel strongly about it, so they agreed that the target probability of exceeding this limit state is 50%, which corresponds to the target reliability index $\beta_T = 0$.

A.3.3.2 Existing Limit States

In general, the SLSs in the *CHBDC* are very parallel to the SLSs currently specified in *AASHTO LRFD*. There are some differences in application, but the general phenomena being treated are basically the same. Based on the 2006 *CHBDC*, no new limit states that do not exist in *AASHTO LRFD* were found in the *CHBDC*.

Clause 3.5.1 and Table 3.1 in particular, contain the requirements for load factors and load combinations. Table 3.6.1(a) lists only two load combinations for serviceability limit states. Service load combinations use a load factor of 0.9 for the live load based on the CL-W-625 truck (140.5 kips, 59 ft long) or lane loading. This unfactored live load is considerably larger than the

HL93 truck, alone, i.e., without the Unified Distribution Load (UDL). Load Combination 2 applies to superstructure vibration only. The CHBDC also specifies a lane load which consists of 80% of the axles of the CL-W truck superimposed on a UDL of 9 kN/m which is similar to the UDL used with the HL93 loading.

Clause 8.5.1 states that cracking, deformation, stress and vibrations SLS should be considered.

Clause 8.5.2 specifies serviceability limit states for concrete structures and it indicates that these are cracking, deformations, stress, and vibration.

Clause 8.5.2.2 deals with a cross-reference to Clause 8.12 with some limits on earth cover.

Clause 8.5.2.3 deals with deformation provisions and indicates that short-term and long-term deformations may affect the function of the structure.

Clause 8.5.2.4 deals with stresses in the component not exceeding certain values of Clauses 8.7.1, 8.8.4.6, and 8.23.7.

Clause 8.5.2.5 deals with vibrations and refers back to clauses in Section 3 on loads.

The commentary for Clause 8.5.2.1 speaks to the fact that, in general, nonprestressed and partially prestressed components are expected to crack under the service loads and indicates that it is generally a good practice to provide sufficient prestress so that under the permanent loads any cracks previously caused due to the application of live load will be closed under the permanent loads. This is to enhance durability.

Clause 8.12 deals with control of cracking by specifying distribution requirements and a tensile strain limitation.

Clause 8.12.3.1 specifies limits on crack width for non-prestressed and prestressed components for several types of exposure.

Clause 8.12.3.2 provides guidance on calculating the crack width and spacing based on parameters which include the average strain in the reinforcing. A distinction is made for epoxy-coated reinforcement for which the calculated crack width is increased 20%.

A.4 Search for SLSs Not Yet Implemented

Several reports were reviewed in an effort to determine whether any additional concrete SLSs should be considered when designing bridges. The additional information was meant to supplement the literature review and the bridge owners' survey. Reports were gathered from sources such as the NCHRP, the FHWA, *ACI Structural Journal*, ACI Committee documents, and conference proceedings of the Structures Congress and the American Society of Civil Engineers (ASCE).

The investigated reports pertained to establishing concrete cracking of beams and bridge decks, concrete shrinkage, fatigue of prestressed concrete members. Each report was

reviewed to determine the usefulness of the information. Any methods that could potentially be used in creating new SLSs were noted and investigated further.

Much of the information was found to be too general to be useful. Many of the methods discussed for reducing serviceability issues related to non-structural aspects of the design process, which would not be useful in calibrating limit states. Some of the sources, however, provided useful methods of anticipating and determining the effects of serviceability issues such as crack width, crack spacing, and prestressed concrete fatigue.

Bridge related research problem statements are reviewed annually by Technical Committee 11 of the HSCOBS. It was thought that a review of these documents could show a need for additional SLSs that were not approved for funding but which might still be worthwhile in the context of this project. However, there is apparently no archive of old research problem statements.

A.5 References

AASHO Road Test: Report 4 - Bridge Research. 1962. Special Report 61D. AASHO, Highway Research Board, Washington, DC.

AASHTO LRFD Bridge Design Specifications, 4th ed. 2008. Including 2008 Interim. AASHTO, Washington, DC.

AASHTO LRFD Bridge Design Specifications, 6th ed. 2012. AASHTO, Washington, DC.

Abeles, P., and E. Brown, II. 1971. Expected Fatigue Life of Prestressed Concrete Highway Bridges as Related to the Expected Load Spectrum. In *Second International Symposium on Concrete Bridge Design*. SP-26. American Concrete Institute, Detroit, MI, pp. 962–1010.

Abeles, P., E. Brown, II, and C. Hu. 1974. Fatigue Resistance of Under-Reinforced Prestressed Beams Subjected to Different Stress Ranges; Miner's Hypothesis. In *Abeles Symposium: Fatigue of Concrete*. SP-41. American Concrete Institute, Detroit, MI, pp. 279–300.

Abeles, P., F. Barton, and E. Brown, II. 1969. Fatigue Behavior of Prestressed Concrete Bridge Beams. In *First International Symposium on Concrete Bridge Design*. SP-23. American Concrete Institute, Detroit, MI, pp. 579–599.

ACI Committee 215. 1974. *Considerations for Design of Concrete Structures Subjected to Fatigue Loading*. ACI 215R-74. American Concrete Institute, Detroit, MI.

ACI Committee 318. 1963. *Building Code Requirements for Reinforced Concrete*. ACI 318-63. American Concrete Institute, Detroit, MI.

ACI Committee 318. 1977. *Building Code Requirements for Reinforced Concrete*. ACI 318-77. American Concrete Institute, Detroit, MI.

ACI Committee 318. 1983. *Building Code Requirements for Reinforced Concrete*. ACI 318-83. American Concrete Institute, Detroit, MI.

ACI Committee 318. 1995. *Building Code Requirements for Structural Concrete and Commentary*. ACI 318-95/318R-95. American Concrete Institute, Farmington Hills, MI.

ACI Committee 318. 1999. *Building Code Requirements for Structural Concrete and Commentary*. ACI 318-99/318R-99. American Concrete Institute, Farmington Hills, MI.

ACI Committee 318. 2002. *Building Code Requirements for Structural Concrete and Commentary*. ACI 318-02/318R-02. American Concrete Institute, Farmington Hills, MI.

ACI Committee 318. 2005. *Building Code Requirements for Structural Concrete and Commentary*. ACI 318-05. American Concrete Institute, Farmington Hills, MI.

ACI Committee 318. 2008. *Building Code Requirements for Structural Concrete and Commentary*. ACI 318-08. American Concrete Institute, Farmington Hills, MI.

ACI Committee 318. 2011. *Building Code Requirements for Structural Concrete and Commentary*. ACI 318-11. American Concrete Institute, Farmington Hills, MI.

ACI-ASCE Joint Committee 323. 1958. Tentative Recommendations for Prestressed Concrete. *Journal, American Concrete Institute*, Vol. 54, No. 1, pp. 545–578.

Amorn, W., J. Bowers, A. Girgis, and M. Tadros. 2007. Fatigue of Deformed Welded-Wire Reinforcement. *Journal, Precast/Prestressed Concrete Institute*, Vol. 52, No. 1, pp. 106–120.

Barker, M., and K. Barth. 2007. *Live Load Deflection Serviceability of HPS Composite Steel Girder Bridges*. 2007 World Steel Bridge Symposium Papers, New Orleans, LA.

Beeby, A. 1979. The Prediction of Crack Widths in Hardened Concrete. *The Structural Engineer*, Vol. 57A, No. 1, pp. 9.

Biggs, J. 1964. *Introduction to Structural Dynamics*. McGraw-Hill, New York, NY.

Birrcher, D., R. Tuchscherer, M. Huizinga, O. Bayrak, S. Wood, and J. Jirsa. 2009. *Strength and Serviceability Design of Reinforced Concrete Deep Beams*. FHWA/TX-09/0-5253-1. Center for Transportation Research at the University of Texas at Austin, Texas Department of Transportation, FHWA, Austin, TX.

Blackman, D., and R. Frosch. 2005. Epoxy Coated Reinforcement and Crack Control. In *Serviceability of Concrete: A Symposium Honoring Dr. Edward G. Nawy*. SP-225. American Concrete Institute, Farmington Hills, MI, pp. 163–178.

Broms, B. 1965. Crack Width and Crack Spacing In Reinforced Concrete Members. *Journal, American Concrete Institute*, Vol. 62, No. 10, pp. 1237.

Burton, K., and E. Hognestad. 1967. Fatigue Test of Reinforcing Bars-Tack Welding of Stirrups. *Journal, American Concrete Institute*, Vol. 64, No. 5, pp. 244–252.

Canadian Highway Bridge Design Code. 2006. Includes Supplement 1, Supplement 2, and Supplement 3. Canadian Standards Association International, Toronto, ON, Canada.

Choi, Y., and B. Oh. 2009. Crack Width Formula for Transversely Post-Tensioned Concrete Deck Slabs on Box Girder Bridges. *Structural Journal, American Concrete Institute*, Vol. 106, No. 6, pp. 753–761.

Clark, A. 1956. Cracking in Reinforced Concrete Flexural Members. *Journal Proceedings, American Concrete Institute*, Vol. 52, No. 4, pp. 851.

Committee on Deflection Limitations of Bridges of the Structural Division. 1958. Deflection Limitations. *ASCE Journal of the Structural Division*, Vol. 84, No. 3, pp. 1633.1–1633.20.

Dexter, R., and J. Fisher. 2000. Fatigue and Fracture. In *Bridge Engineering Handbook*. Chen and Duan (Eds). CRC Press, New York, NY, pp. 53.1–53.23.

EN 1990 (Eurocode 0): Basis of Structural Design. 2002. European Committee for Standardization, Brussels, Belgium.

EN 1991-1-6 (Eurocode 1): Actions on Structures - Part 1-6: General Actions - Actions during Execution. 2005. European Committee for Standardization, Brussels, Belgium.

EN 1991-2 (Eurocode 1): Actions on Structures - Part 2: Traffic Loads on Bridges. 2003. European Committee for Standardization, Brussels, Belgium.

EN 1992-2 (Eurocode 2): Design of Concrete Structures - Part 2: Concrete Bridges - Design and Detailing Rules. 2005. European Committee for Standardization, Brussels, Belgium.

EN 1998-2 (Eurocode 8): Design of Structures for Earthquake Resistance - Part 2: Bridges. 2005. European Committee for Standardization, Brussels, Belgium.

Fisher, J., and I. Viest. 1961. *Fatigue Tests of Bridge Materials of the AASHO Road Test*. Special Report 66. American Association of State Highway Officials, Highway Research Board, Washington, DC.

Frosch, R. 1999. Another Look at Cracking and Crack Control in Reinforced Concrete. *Structural Journal, American Concrete Institute*, Vol. 96, No. 3, pp. 437–442.

Frosch, R. 2001. Flexural Crack Control in Reinforced Concrete. In *Design and Construction Practices to Mitigate Cracking*. SP-204. American Concrete Institute, Farmington Hills, MI, pp. 135–154.

Frosch, R. 2002. Modeling and Control of Side Face Beam Cracking. *Structural Journal, American Concrete Institute*, Vol. 99, No. 3, pp. 376–385.

Gergely, P., and L. Lutz. 1968. Maximum Crack Width in Reinforced Concrete Members. In *Causes, Mechanisms and Control of Cracking in Concrete*. SP-20. American Concrete Institute, Detroit, MI, pp. 87–117.

Hanson, J., K. Burton, and E. Hognestad. 1968. Fatigue Tests of Reinforcing Bars-Effect of Deformation Pattern. *Journal of the Portland Cement Association Research and Development Laboratories*, Vol. 10, No. 3, pp. 2–13.

Helgason, T., J. Hanson, N. Somes, W. Corley, and E. Hognestad. 1976. *NCHRP Report 164: Fatigue Strength of High Yield Reinforcing Bars*. TRB, National Research Council, Washington, DC.

Kaar, P., and A. Mattock. 1963. High Strength Bars as Concrete Reinforcement, Part 4 - Control of Cracking. *Portland Cement Association Development Department Bulletin D59*, pp. 15–38.

Kupfer, H., and K. Gerstle. 1973. Behavior of Concrete under Biaxial Stress. *ASCE Journal of the Engineering Mechanics Division*, Vol. 99, No. 4, pp. 853–866.

Lash, S. 1969. Can High-Strength Reinforcement be used in Highway Bridges. In *First International Symposium on Concrete Bridge Design*. SP-23. American Concrete Institute, Detroit, MI, pp. 283–300.

MacGregor, J., I. Jhamb, and N. Nuttall. 1971. Fatigue Strength of Hot Rolled Deformed Reinforcing Bars. *Journal Proceedings, American Concrete Institute*, Vol. 68, No. 3, pp. 169–179.

Manning, D. G. 1994. *NCHRP Research Results Digest 197: Fatigue Behavior of Welded and Mechanical Splices in Reinforcing Steel*. TRB, National Research Council, Washington, DC.

Okeil, A. 2006. Allowable Tensile Stress for Webs of Prestressed Segmental Concrete Bridges. *Structural Journal, American Concrete Institute*, Vol. 103, No. 4, pp. 488–495.

Oluokun, F. 1991. Prediction of Concrete Tensile Strength from its Compressive Strength: Evaluation of Existing Relations for Normal Weight Concrete. *Materials Journal, American Concrete Institute*, Vol. 88, No. 3, pp. 302–309.

Ontario Highway Bridge Design Code. 1979. Ontario Ministry of Transportation, Toronto, ON, Canada.

Ople, F., and C. Hulsbos. 1966. Probable Fatigue Life of Plain Concrete with Stress Gradient. *Journal Proceedings, American Concrete Institute*, Vol. 63, No. 1, pp. 59–82.

Pfister, J., and E. Hognestad. 1964. High Strength Bars as Concrete Reinforcement, Part 6 - Fatigue Tests. *Journal of the Portland Cement Association Research and Development Laboratories*, Vol. 6, No. 1, pp. 65–84.

Roeder, C., K. Barth, and A. Bergman. 2002. *NCHRP Web Document 46: Improved Live Load Deflection Criteria for Steel Bridges*. TRB, National Research Council, Washington, DC.

Standard Specifications for Highway Bridges, 11th ed. 1975. Including 1974 and 1975 Interims. AASHO, Washington, DC.

Standard Specifications for Highway Bridges, 12th ed. 1977. AASHTO, Washington, DC.

Standard Specifications for Highway Bridges, 13th ed. 1983. AASHTO, Washington, DC.

Standard Specifications for Highway Bridges, 14th ed. 1989. AASHTO, Washington, DC.

Standard Specifications for Highway Bridges, 15th ed. 1992. AASHTO, Washington, DC.

Standard Specifications for Highway Bridges, 17th ed. 2002. AASHTO, Washington, DC.

Standard Specifications for Highway Bridges, 6th ed. 1953. AASHO, Washington, DC.

Structures Manual. 2013. Florida Department of Transportation, Tallahassee, FL.

Tachau, H., C. Hulsbos, and D. VanHorn. 1971. Discussion of Fatigue Tests on Prestressed Concrete I-Beams. *ASCE Journal of the Structural Division*, Vol. 97, No. 9, pp. 2429–2431.

Warner, R., and C. Hulsbos. 1966. Probable Fatigue Life of Prestressed Concrete Beams. *Journal, Precast/Prestressed Concrete Institute*, Vol. 11, No. 2, pp. 16–39.

Wright, R., and W. Walker. 1972. Vibration and Deflection of Steel Bridges. *Engineering Journal, American Institute of Steel Construction*, Vol. 9, No. 1, pp. 20–31.

APPENDIX B – SLS REQUIREMENTS IN THE EUROCODE

Table of Contents

List of Tables

B.1 Introduction

B.1.1 General Information

The Structural Eurocode program provides comprehensive information for the structural design and verification of buildings and civil engineering works (including geotechnical aspects). It comprises the following standards – each one consisting of a number of parts. [Often only a limited number of parts of each standard may be relevant to bridge structures]:

EN 1990 Eurocode 0: Basis of Structural Design
EN 1991 Eurocode 1: Actions on structures
EN 1992 Eurocode 2: Design of concrete structures
EN 1993 Eurocode 3: Design of steel structures
EN 1994 Eurocode 4: Design of composite steel and concrete structures
EN 1995 Eurocode 5: Design of timber structures
EN 1996 Eurocode 6: Design of masonry structures
EN 1997 Eurocode 7: Geotechnical design
EN 1998 Eurocode 8: Design of structures for earthquake resistance
EN 1999 Eurocode 9: Design of aluminum structures

Following is a description of the SLS requirements in sections relevant to bridges.

B.1.2 Structural Eurocodes

The Structural Eurocode standards provide common structural design rules for everyday use for the design of whole structures and component products of both a traditional and an innovative nature. Unusual forms of construction or design conditions are not specifically covered and additional expert consideration is required by the designer in such cases.

The Eurocodes are being implemented by each member country of the European Union through National Standards which comprise the full text of each Eurocode (including any annexes), and may be followed by a National Annex.

The National Annex only contains information on those parameters which are left open in the Eurocode for national choice, (known as Nationally Determined Parameters). They are to be used for the design of buildings and civil engineering works to be constructed in the country concerned, and are usually one or more of the following:

- Values and/or classes where alternatives are given in the Eurocode,
- Values to be used where a symbol only is given in the Eurocode,
- Country specific data (geographical, climatic, etc.), *e.g.* snow map,
- The procedure to be used where alternative procedures are given in the Eurocode.

The National Annex may also contain:

- Decisions on the application of informative annexes,

- References to non-contradictory complementary information to assist the user to apply the Eurocode.

This summary does not include any numeric values presented in any National Annex.

The following sections address some of the Structural Eurocodes in turn, and summarize the relevant articles relating to the serviceability limit state used in bridge design.

B.2 EN 1990 Eurocode 0: Basis of Structural Design

Eurocode 0 (Basis of structural design) is the lead document in the Eurocode suite. It describes the principles and requirements for safety, serviceability and durability of structures. It is based on the limit state concept used in conjunction with a partial factor method. It provides the basis and general principles for the structural design and verification of buildings and civil engineering works (including geotechnical aspects).

EN 1990:2002 should be used in conjunction with all the other Eurocodes (EN 1991 to EN 1999) for design.

NOTE For the design of special construction works (*e.g.* nuclear installations, dams, etc.), other provisions than those in EN 1990 to EN 1999 might be necessary.

EN 1990 also gives guidelines for the aspects of structural reliability relating to safety, serviceability, and durability:

– for design cases not covered by EN 1991 to EN 1999 (other actions, structures not treated, other materials);
– to serve as a reference document for other European Committee for Standardization Technical Committees (CEN/TCs) concerning structural matters.

EN 1990 is also applicable as a guidance document for the design of structures where other materials or other actions outside the scope of EN 1991 to EN 1999 are involved.

EN 1990 is applicable for the structural appraisal of existing construction, in developing the design of repairs and alterations, or in assessing changes of use.

NOTE Additional or amended provisions might be necessary where appropriate.

EN 1990 is intended for use by:

– committees drafting standards for structural design and related product, testing, and execution standards,
– clients (*e.g.* for the formulation of their specific requirements on reliability levels and durability),
– designers and constructors, and
– relevant authorities.

The general assumptions of EN 1990 are:

- The choice of the structural system and the design of the structure is made by appropriately qualified and experienced personnel,
- Execution is carried out by personnel having the appropriate skill and experience,
- Adequate supervision and quality control is provided during execution of the work, i.e. in design offices, factories, plants, and on site,
- The construction materials and products are used as specified in EN 1990 or in EN 1991 to EN 1999 or in the relevant execution standards, or reference material or product specifications,
- The structure will be adequately maintained, and
- The structure will be used in accordance with the design assumptions.

NOTE: There may be cases when the above assumptions need to be supplemented.

It should be noted that clauses are listed and enumerated within each article of the Eurocodes and that distinction is made between clauses that present Principles and those that present Application Rules. This distinction is preserved in the summaries given in this report.

The Principles comprise:

- General statements and definitions for which there is no alternative, as well as
- Requirements and analytical models for which no alternative is permitted unless specifically stated.

The Principles are identified by the letter P following the paragraph number. [e.g. (2)P]

The Application Rules [identified by a number in brackets e.g. (2)], are generally recognized rules which comply with the Principles and satisfy their requirements.

It is permissible to use alternative design rules different from the Application Rules given in EN 1990 for works, provided that it is shown that the alternative rules accord with the relevant Principles and are at least equivalent with regard to the structural safety, serviceability, and durability which would be expected when using the Eurocodes.

The clauses relating to serviceability limit state design presented in Eurocode 0 are summarized in Table B-1.

Table B-1 Summary of clauses relating to serviceability limit state design in Eurocode 0

Eurocode Article	Basic Provision	Discussion
Eurocode 0 **3.4 Serviceability limit states**	(1)P The limit states that concern : – the functioning of the structure or structural members under normal use; – the comfort of people; – the appearance of the construction works, shall be classified as serviceability limit states. NOTE 1: In the context of serviceability, the term "appearance" is concerned with such criteria as high deflection and extensive cracking, rather than aesthetics. NOTE 2: Usually the serviceability requirements are specific to each individual project. (2)P A distinction shall be made between reversible and irreversible serviceability limit states. [NOTE: 'Reversible' = where no consequences of actions exceeding the specified service requirement will remain when the actions are removed. 'Irreversible' = where some consequences of actions will remain when the actions are removed] (3) The verification of serviceability limit states should be based on criteria concerning the following aspects: a) deformations that affect: – the appearance, – the comfort of users, or – the functioning of the structure (including the functioning of machines or services), or that cause damage to finishes or non-structural members; b) vibrations – that cause discomfort to people, or – that limit the functional effectiveness of the structure; c) damage that is likely to adversely affect – the appearance, – the durability, or – the functioning of the structure. NOTE: Additional provisions related to serviceability criteria are given in the relevant EN 1992 to EN 1999.	
Eurocode 0 **6.5.1 Verifications**	(1)P It shall be verified that : $E_d \leq C_d$ (6.13) where: C_d is the limiting design value of the relevant serviceability criterion. E_d is the design value of the effects of actions specified in the serviceability criterion, determined on the basis of the relevant combination.	
Eurocode 0 **6.5.2 Serviceability criteria**	(1) The deformations to be taken into account in relation to serviceability requirements should be as detailed in the relevant Annex A according to the type of construction works, or agreed with the client or the National authority. NOTE: For other specific serviceability criteria such as crack width, stress or strain limitation, slip resistance, see EN 1991 to EN 1999.	
Eurocode 0 **6.5.3**	(1) The combinations of actions to be taken into account in the relevant design situations should be appropriate for the serviceability requirements and performance criteria being verified.	

Combination of actions	(2) The combinations of actions for serviceability limit states are defined symbolically (see also 6.5.4) : NOTE: It is assumed, in these expressions, that all partial factors are equal to 1. See Annex A and EN 1991 to EN 1999. a) Characteristic combination: (equation given at 6.14a) NOTE: The characteristic combination is normally used for irreversible limit states. b) Frequent combination: (equation given at 6.15a) NOTE: The frequent combination is normally used for reversible limit states. c) Quasi-permanent combination: (equation given at 6.16a) NOTE: The quasi-permanent combination is normally used for long-term effects and the appearance of the structure. (3) For the representative value of the prestressing action (i.e. *P*k or *P*m), reference should be made to the relevant design Eurocode for the type of prestress under consideration. (4)P Effects of actions due to imposed deformations shall be considered where relevant. NOTE: In some cases expressions (6.14) to (6.16) require modification. Detailed rules are given in the relevant Parts of EN 1991 to EN 1999.	
Eurocode 0 **6.5.4 Partial factors for materials**	(1) For serviceability limit states the partial factors γM for the properties of materials should be taken as 1.0 except if differently specified in EN 1992 to EN 1999.	
Eurocode 0 Annex A2 **A2.1 Field of application**	(1) This Annex A2 to EN 1990 gives rules and methods for establishing combinations of actions for serviceability and ultimate limit state verifications (except fatigue verifications) with the recommended design values of permanent, variable and accidental actions and ψ factors (applied to actions) to be used in the design of road bridges, footbridges and railway bridges. It also applies to actions during execution. Methods and rules for verifications relating to some material-independent serviceability limit states are also given. NOTE 1: Symbols, notations, Load Models and groups of loads are those used or defined in the relevant section of EN 1991-2. NOTE 2: Symbols, notations and models of construction loads are those defined in EN 1991-1-6. NOTE 3: Guidance may be given in the National Annex with regard to the use of Table 2.1 (design working life – for UK bridges this is normally 120 years). NOTE 4: Most of the combination rules defined in clauses A2.2.2 to A2.2.5 are simplifications intended to avoid needlessly complicated calculations. They may be changed in the National Annex or for the individual project as described in A2.2.1 to A2.2.5. NOTE 5: This Annex A2 to EN 1990 does not include rules for the determination of actions on structural bearings (forces and moments) and associated movements of bearings or give rules for the analysis of bridges involving ground-structure interaction that may depend on movements or deformations of structural bearings. (2) The rules given in this Annex A2 to EN 1990 may not be sufficient for: - bridges that are not covered by EN 1991-2 (for example bridges under an airport runway, mechanically-moveable bridges, roofed bridges, bridges carrying water, etc.),	

	- bridges carrying both road and rail traffic, and - other civil engineering structures carrying traffic loads (for example backfill behind a retaining wall).	
Eurocode 0 Annex A2 **A2.2 Combination of actions** **A2.2.1 General**	(1) Effects of actions that cannot occur simultaneously due to physical or functional reasons need not be considered together in combinations of actions. (2) Combinations involving actions which are outside the scope of EN 1991 (e.g. due to mining subsidence, particular wind effects, water, floating debris, flooding, mud slides, avalanches, fire and ice pressure) should be defined in accordance with EN 1990, 1.1(3). NOTE 1: Combinations involving actions that are outside the scope of EN 1991 may be defined either in the National Annex or for the individual project. NOTE 2: For seismic actions, see EN 1998. NOTE 3: For water actions exerted by currents and debris effects, see also EN 1991-1-6. (4) The combinations of actions given in expressions 6.14a to 6.16b should be used when verifying serviceability limit states. Additional rules are given in A2.4 for verifications regarding deformations and vibrations.	
Eurocode 0 Annex A2 **A2.2 Combination of actions** **A2.2.2 Combination rules for road bridges**	(1) The infrequent values of variable actions may be used for certain serviceability limit states of concrete bridges. NOTE: The National Annex may refer to the infrequent combination of actions. (6) Wind actions and thermal actions need not be taken into account simultaneously unless otherwise specified for local climatic conditions. NOTE: Depending upon the local climatic conditions a different simultaneity rule for wind and thermal actions may be defined either in the National Annex or for the individual project.	
Eurocode 0 Annex A2 **A2.4 Serviceability and other specific limit states** **A2.4.1 General**	(2) The serviceability criteria should be defined in relation to the serviceability requirements in accordance with 3.4 and EN 1992 to EN 1999. Deformations should be calculated in accordance with EN 1991 to EN 1999 by using the appropriate combinations of actions according to expressions (6.14a) to (6.16b) (see Table A2.6) taking into account the serviceability requirements and the distinction between reversible and irreversible limit states. NOTE: Serviceability requirements and criteria may be defined as appropriate in the National Annex or for the individual project.	
Eurocode 0 Annex A2 **A2.4.2 Serviceability criteria regarding deformation and vibration for road bridges**	(1) Where relevant, requirements and criteria should be defined for road bridges concerning: - uplift of the bridge deck at supports, - damage to structural bearings. NOTE: Uplift at the end of a deck can jeopardize traffic safety and damage structural and non-structural elements. Uplift may be avoided by using a higher safety level than usually accepted for serviceability limit states. (2) Serviceability limit states during execution should be defined in accordance with EN 1990 to EN 1999 (3) Requirements and criteria should be defined for road bridges concerning deformations and vibrations, where relevant. NOTE 1: The verification of serviceability limit states concerning deformation and vibration needs to be considered only in exceptional cases for road bridges. The frequent combination of actions is recommended for the assessment of deformation.	

	NOTE 2: Vibrations of road bridges may have various origins, in particular traffic actions and wind actions. For vibrations due to wind actions, see EN 1991-1-4. For vibrations due to traffic actions, comfort criteria may have to be considered. Fatigue may also have to be taken into account.	
Eurocode 0 Annex A2 **A2.4.3.2 Pedestrian comfort criteria (for serviceability)**	(1) The comfort criteria should be defined in terms of maximum acceptable acceleration of any part of the deck. NOTE The criteria may be defined as appropriate in the National Annex or for the individual project. The following accelerations (m/s2) are the recommended maximum values for any part of the deck: i) 0.7 for vertical vibrations, ii) 0.2 for horizontal vibrations due to normal use, iii) 0.4 for exceptional crowd conditions. (2) A verification of the comfort criteria should be performed if the fundamental frequency of the deck is less than: - 5 Hz for vertical vibrations, - 2.5 Hz for horizontal (lateral) and torsional vibrations. NOTE: The data used in the calculations, and therefore the results, are subject to very high uncertainties. When the comfort criteria are not satisfied with a significant margin, it may be necessary to make provision in the design for the possible installation of dampers in the structure after its completion. In such cases the designer should consider and identify any requirements for commissioning tests.	
Eurocode 0 Annex A2 **A2.4.4.3 Limiting values for the maximum vertical deflection for passenger comfort** A2.4.4.3.1 Comfort criteria	(1) Passenger comfort depends on the vertical acceleration *b*v inside the coach during travel on the approach to, passage over and departure from the bridge. (2) The levels of comfort and associated limiting values for the vertical acceleration should be specified. NOTE: These levels of comfort and associated limiting values may be defined for the individual project. Recommended levels of comfort are given in Table A2.9.	
Eurocode 0 Annex A2 **A2.4.4.3 Limiting values for the maximum vertical deflection for passenger comfort** A2.4.4.3.3 Requirements for a dynamic vehicle/bridge interaction analysis for checking passenger comfort	(1) Where a vehicle/bridge dynamic interaction analysis is required the analysis should take account of the following behaviors: iv) a series of vehicle speeds up to the maximum speed specified, v) characteristic loading of the real trains specified for the individual project in accordance with EN1991-2, 6.4.6.1.1, vi) dynamic mass interaction between vehicles in the real train and the structure, vii) the damping and stiffness characteristics of the vehicle suspension, viii) a sufficient number of vehicles to produce the maximum load effects in the longest span, ix) a sufficient number of spans in a structure with multiple spans to develop any resonance effects in the vehicle suspension. NOTE: Any requirements for taking track roughness into account in the vehicle/bridge dynamic interaction analysis may be defined for the individual project.	

B.3 EN 1991 Eurocode 1: Actions on Structures

Eurocode 1 - (Actions on structures) provides information on all actions that should normally be considered in the design of buildings and civil engineering works. It is in four main parts. The first part is divided into seven sub-parts which cover densities, self-weight and imposed loads; actions due to fire; snow; wind; thermal actions; loads during execution and accidental actions. The remaining three parts cover traffic loads on bridges, actions by cranes and machinery and actions for silos and tanks.

The second part (EN 1991-2: 2003) concerns the design of bridges. Sections from this standard relating to the serviceability limit state are summarized in the table below.

For the design of bridges, EN 1991-2 defines imposed loads (models and representative values) associated with road traffic, pedestrian actions and rail traffic which include, when relevant, dynamic effects and centrifugal, braking and acceleration actions and actions for accidental design situations. For the design of new bridges, EN 1991-2 is intended to be used, for direct application, together with Eurocodes EN 1990 to 1999. The bases for combinations of traffic loads with non-traffic loads are given in EN 1990, A2.

A summary of clauses relating to loads and actions in Eurocode EN 1991-2 is presented in Table B-2.

Table B-2 Summary of clauses relating to loads and actions in Eurocode EN 1991-2

Eurocode Article	Basic Provision	Discussion
Eurocode 1 **1.3 Distinction between Principles and Application Rules**	(5) It is permissible to use alternative design rules different from the Application Rules given in EN 1991-2 for works, provided that it is shown that the alternative rules accord with the relevant Principles and are at least equivalent with regard to the structural safety, serviceability and durability which would be expected when using the Eurocodes.	
Eurocode 1 **Section 2 Classification of actions** **2.2 Variable actions**	(1) For normal conditions of use (*i.e.* excluding any accidental situation), the traffic and pedestrian loads (dynamic amplification included where relevant) should be considered as variable actions. (2) The various representative values are: – characteristic values, which are either statistical, *i.e.* corresponding to a limited probability of being exceeded on a bridge during its design working life, or nominal, see EN 1990, 4.1.2(7); – frequent values; – quasi-permanent values. (3) For calculation of fatigue lives, separate models, associated values and, where relevant, specific requirements are given in 4.6 for road bridges, in 6.9 for railway bridges, and in the relevant annexes.	
Eurocode 1 **Section 4 Road traffic actions and other actions specifically for road bridges** **4.1 Field of**	(1) Load models defined in this section should be used for the design of road bridges with loaded lengths less than 200 m. NOTE 1: 200 m corresponds to the maximum length taken into account for the calibration of Load Model 1 (see 4.3.2). In general, the use of Load Model 1 is safe-sided for loaded lengths over 200 m. NOTE 2: Load models for loaded lengths greater than 200 m may be defined in the National Annex or for the individual project.	

application	(2) The models and associated rules are intended to cover all normally foreseeable traffic situations (*i.e.* traffic conditions in either direction on any lane due to the road traffic) to be taken into account for design (see however (3) and the notes in 4.2.1). (3) The effects of loads on road construction sites (*e.g.* due to scrapers, lorries carrying earth, etc.) or of loads specifically for inspection and tests are not intended to be covered by the load models and should be separately specified, where relevant.	
Eurocode 1 **4.2 Representation of actions** **4.2.1 Models of road traffic loads**	(1) Loads due to the road traffic, consisting of cars, lorries and special vehicles (*e.g.* for industrial transport), give rise to vertical and horizontal, static and dynamic forces. NOTE 1: The load models defined in this section do not describe actual loads. They have been selected and calibrated so that their effects (with dynamic amplification included where indicated). NOTE 2: The National Annex may define complementary load models, with associated combination rules where traffic outside the scope of the load models specified in this section needs to be considered. NOTE 3: The dynamic amplification included in the models (except for fatigue), although established for a medium pavement quality (see annex B) and pneumatic vehicle suspension, depends on various parameters and on the action effect under consideration. Therefore, it cannot be represented by a unique factor. In some unfavorable cases, it may reach 1,7 (local effects), but still more unfavorable values can be reached for poorer pavement quality, or if there is a risk of resonance. These cases can be avoided by appropriate quality and design measures. Therefore, an additional dynamic amplification may have to be taken into account for particular calculations (see 4.6.1.(6)) or for the individual project.	
Eurocode 1 **4.3 Vertical loads – Characteristic values** **4.3.1 General and associated design situations**	(1) Characteristic loads are intended for the determination of road traffic effects associated with ultimate limit state verifications and with particular serviceability verifications (see EN 1990 to EN 1999). NOTE: There are 4 load models described in detail to cover most of the effects of the traffic of lorries and cars, special vehicles and pedestrian crowd loading. They are used for general and local verifications. One of these models is used to represent dynamic effects on short structural members.	
Eurocode 1 **4.6 Fatigue load models** **4.6.1 General**	(1) Traffic running on bridges produces a stress spectrum which may cause fatigue. The stress spectrum depends on the geometry of the vehicles, the axle loads, the vehicle spacing, the composition of the traffic and its dynamic effects. NOTE: There are 5 load models described in detail. The first two are intended to be used to check whether the fatigue life may be considered unlimited when a constant stress amplitude fatigue limit is given. Therefore they are appropriate for steel constructions and may be inappropriate for other materials. The remaining 3 load models are intended to be used for fatigue life assessment. Each of these last three models is more accurate than its predecessor culminating in the last model which is based on actual traffic data.	

B.4 EN 1992 Eurocode 2: Design of Concrete Structures

Eurocode 2 - (Design of concrete structures) is concerned with the requirements for resistance, serviceability, durability and fire resistance of concrete structures. (Other requirements, e.g. concerning thermal or sound insulation, are not considered). It applies to the design of buildings and civil engineering works in plain, reinforced and prestressed concrete.

EN 1992 is presented in three main parts. The first part has two sub-parts covering buildings and structural fire design. The last two main parts cover concrete bridges and liquid retaining and containing structures, as listed below: Those underlined have been reviewed in the compilation of this report.

EN 1992-1.1:2004	Design of concrete structures. General rules and rules for buildings
EN 1992-1.2:2004	Design of concrete structures. Fire design
EN 1992-2:2005	Design of concrete structures. Concrete bridges. Design and detailing rules
EN 1992-3:2006	Design of concrete structures. Liquid retaining and containing structures

Note also:
PD 6687:2006 Background paper to the UK National Annexes to BS EN 1992-1
PD 6687-2:2008 Recommendations for the design of structures to BS EN 1992-2

The second part, EN 1992-2: 2005 *(Design of concrete structures. Concrete bridges – Design and detailing rules)* is relevant for the design of concrete bridges. Sections from this standard relating to the serviceability limit state are summarized in the table below. (It should be noted that EN 1992-2 draws heavily from the general clauses presented in EN 1992-1.1 *(Design of concrete structures. General rules and rules for buildings)* where relevant, these clauses are also included in the summaries given in the table below).

EN 1992-2 describes the principles and requirements for safety, serviceability and durability of concrete structures, together with specific provisions for bridges. For the design of new bridges, EN 1992-2 is intended to be used, for direct application, together with other parts of EN 1992, Eurocodes EN 1990, 1991, 1997 and 1998.

A summary of clauses relating to the serviceability limit state design of concrete bridges Eurocode EN 1992-1 is presented in Table B-3.

Table B-3 Concrete Design Provisions

Eurocode Article	Basic Provision	Discussion
Eurocode 2 **Section 2 Basis of Design** **2.1 Requirements** **2.1.1 Basic requirements**	(3) The basic requirements of EN 1990 Section 2 are deemed to be satisfied for concrete structures when the following are applied together: - limit state design in conjunction with the partial factor method in accordance with EN 1990, - actions in accordance with EN 1991, - combination of actions in accordance with EN 1990 and - resistances, durability and serviceability in accordance with this Standard. NOTE: Requirements for fire resistance (see EN 1990 Section 5 and EN 1992-1.2) may dictate a greater size of member	

	than that required for structural resistance at normal temperature.	
Eurocode 2 **2.3.1.2 Thermal effects**	(1) Thermal effects should be taken into account when checking serviceability limit states. (2) Thermal effects should be considered for ultimate limit states only where they are significant (e.g. fatigue conditions, in the verification of stability where second order effects are of importance, etc). In other cases they need not be considered, provided that the ductility and rotation capacity of the elements are sufficient. (3) Where thermal effects are taken into account they should be considered as variable actions and applied with a partial factor and ψ factor. NOTE: The ψ factor is defined in the relevant annex of EN 1990 and EN 1991 -1.5.	
Eurocode 2 **2.3.1.3 Differential settlements /movements**	(2) The effects of differential settlements should generally be taken into account for the verification for serviceability limit states.	
Eurocode 2 **2.3.2 Material and product properties** **2.3.2.1 General** **2.3.2.2 Shrinkage and creep**	(1) Shrinkage and creep are time-dependent properties of concrete. Their effects should generally be taken into account for the verification of serviceability limit states. (3) When creep is taken into account its design effects should be evaluated under the quasi-permanent combination of actions irrespective of the design situation considered i.e. persistent, transient or accidental. *NOTE:* In most cases the effects of creep may be evaluated under permanent loads and the mean value of prestress.	
Eurocode 2 **2.4.2 Design values** **2.4.2.4 Partial factors for materials**	(2) The values for partial factors for materials for serviceability limit state verification should be taken as those given in the particular clauses of this Eurocode. NOTE: The values of γ_C and γ_S in the serviceability limit state for use in a Country may be found in its National Annex. The recommended value for situations not covered by particular clauses of this Eurocode is 1.0.	
Eurocode 2 **SECTION 3 MATERIALS** **3.1 Concrete** **3.1.1 General**	(1)P The following clauses give principles and rules for normal and high strength concrete. (2) Rules for lightweight aggregate concrete are given in Section 11.	
Eurocode 2 **3.3 Prestressing steel** **3.3.1 General**	(I)P This clause applies to wires, bars and strands used as prestressing tendons in concrete structures. (2)P Prestressing tendons shall have an acceptably low level of susceptibility to stress corrosion. (3) The level of susceptibility to stress corrosion may be assumed to be acceptably low if the prestressing tendons comply with the criteria specified in EN 10138 or given in an appropriate European Technical Approval.	
Eurocode 2 **SECTION 4 Durability and cover**	(I)P A durable structure shall meet the requirements of serviceability, strength and stability throughout its design working life, without significant loss of utility or excessive unforeseen maintenance (for general requirements see also EN	

to reinforcement **4.1 General**	1990). (2)P The required protection of the structure shall be established by considering its intended use, design working life (see EN 1990), maintenance program and actions. (3)P The possible significance of direct and indirect actions, environmental conditions (4.2) and consequential effects shall be considered. Note: Examples include deformations due to creep and shrinkage (see 2.3.2).	
Eurocode 2 **SECTION 5 STRUCTURAL ANALYSIS** **5.2 Geometric imperfections**	(3) Imperfections need not be considered for serviceability limit states.	
Eurocode 2 **5.4 Linear elastic analysis**	(1) Linear analysis of elements based on the theory of elasticity may be used for both the serviceability and ultimate limit states. (3) For thermal deformation, settlement and shrinkage effects at the ultimate limit state (ULS), a reduced stiffness corresponding to the cracked sections, neglecting tension stiffening but including the effects of creep, may be assumed. For the serviceability limit state (SLS) a gradual evolution of cracking should be considered.	
Eurocode 2 **5.6 Plastic analysis** **5.6.4 Analysis with strut-and-tie models**	(2) Verifications in SLS may be carried out using strut-and-tie models, e.g. verification of steel stresses and crack width control, if approximate compatibility for strut-and-tie models is ensured (in particular the position and direction of important struts should be oriented according to linear elasticity theory).	
Eurocode 2 **5.7 Non-linear analysis**	(1) Non-linear methods of analysis may be used for both ULS and SLS, provided that equilibrium and compatibility are satisfied and an adequate non-linear behavior for materials is assumed. The analysis may be first or second order. (105) Non-linear analysis may be used provided that the model can appropriately cover all failure modes (e.g. bending, axial force, shear, compression failure affected by reduced effective concrete strength, etc.) and that the concrete tensile strength is not utilized as a primary load resisting mechanism. If one analysis is not sufficient to verify all the failure mechanisms, separate additional analyses should be carried out. The following design format should be used: - The resistance should be evaluated for different levels of appropriate actions which should be increased from their serviceability values by incremental steps, such that the value of $\gamma_G.Gk$ and $\gamma_Q.Qk$ are reached in the same step. The incrementing process should be continued until one region of the structure attains the ultimate strength, evaluated taking account of α_{CC}, or there is global failure of the structure. The corresponding load is referred to as q_{ud}. Further steps in the design format that should be used are given.	
Eurocode 2 **5.10 Prestressed members and structures**	(1)P For serviceability and fatigue calculations allowance shall be made for possible variations in prestress. Two characteristic values of the prestressing force at the serviceability limit state are estimated. These are based on the upper characteristic value and the lower characteristic value.	

5.10.9 Effects of prestressing at serviceability limit state and limit state of fatigue		
Eurocode 2 **SECTION 7 SERVICEABILITY LIMIT STATES (SLS) 7.1 General**	(1)P This section covers the common serviceability limit states. These are: - stress limitation (see 7.2) - crack control (see 7.3) - deflection control (see 7.4) Other limit states (such as vibration) may be of importance in particular structures but are not covered in this Standard. (2) In the calculation of stresses and deflections, cross-sections should be assumed to be uncracked provided that the flexural tensile stress does not exceed $f_{ct,eff}$. The value of $f_{ct,eff}$ may be taken as f_{ctm} or $f_{ctm,n}$ provided that the calculation for minimum tension reinforcement is also based on the same value. For the purposes of calculating crack widths and tension stiffening f_{ctm} should be used.	
Eurocode 2 **SECTION 7 SERVICEABILITY LIMIT STATES (SLS) 7.2 Stress limitation**	(I)P The compressive stress in the concrete shall be limited in order to avoid longitudinal cracks, micro-cracks or high levels of creep, where they could result in unacceptable effects on the function of the structure. (102) Longitudinal cracks may occur if the stress level under the characteristic combination of loads exceeds a critical value. Such cracking may lead to a reduction of durability. In the absence of other measures, such as an increase in the cover to reinforcement in the compressive zone or confinement by transverse reinforcement, it may be appropriate to limit the compressive stress to a value $k_1 f_{ck}$ in areas exposed to environments of exposure classes XD, XF and XS (see Table 4.1 of EN1992-1-1). NOTE: The value of k_1 for use in a Country may be found in its National Annex. The recommended value is 0.6. The maximum increase in the stress limit above $k_1 f_{ck}$ in the presence of confinement may also be found in a country's National Annex. The recommended maximum increase is 10%. NOTE: British National Document PD 6687: 2006 (*Background paper to the UK National Annexes to BS EN 1992-1*) gives non-contradictory complimentary information for use with EN 1992-1. In particular, when considering stress limitation in serviceability it notes: a) Stress checks in reinforced concrete members have not been required in the UK for the past 50 years or so and there has been no known adverse effect. Provided that the design has been carried out properly for ultimate limit state there will be no significant effect at serviceability in respect of longitudinal cracking. b) There has been no evidence either from research or practice that there is a correlation between high compressive stress and durability problems. (3) If the stress in the concrete under the quasi-permanent loads is less than $k_2 f_{ck}$, linear creep may be assumed. If the stress in concrete exceeds $k_2 f_{ck}$, non-linear creep should be considered (see 3.1.4)	

	NOTE: The value of k_2 for use in a Country may be found in its National Annex. The recommended value is 0.45. (4)P Tensile stresses in the reinforcement shall be limited in order to avoid inelastic strain, unacceptable cracking or deformation. (5) When structural appearance is considered, unacceptable cracking or deformation may be assumed to be avoided if, under the characteristic combination of loads, the tensile strength in the reinforcement does not exceed $k_3 f_{yk}$ **.** Where the stress is caused by an imposed deformation, the tensile strength should not exceed $k_4 f_{yk}$ **.** The mean value of the stress in prestressing tendons should not exceed $k_5 f_{yk}$ **.** NOTE: The values of k_3 , k_4 and k_5 for use in a Country may be found in its National Annex. The recommended values are 0.8, 1 and 0.75 respectively.	
Eurocode 2 **SECTION 7 SERVICEABILITY LIMIT STATES (SLS)** **7.3 Crack control** **7.3.1 General considerations**	(1)P Cracking shall be limited to an extent that will not impair the proper functioning or durability of the structure or cause its appearance to be unacceptable. (2) Cracking is normal in reinforced concrete structures subject to bending, shear, torsion or tension resulting from either direct loading or restraint or imposed deformations. (3) Cracks may also arise from other causes such as plastic shrinkage or expansive chemical reactions within the hardened concrete. Such cracks may be unacceptably large but their avoidance and control lie outside the scope of this Section. (4) Cracks may be permitted to form without any attempt to control their width, provided they do not impair the functioning of the structure. (105) A limiting calculated crack width w_{max}, taking account of the proposed function and nature of the structure and the costs of limiting cracking, should be established. Due to the random nature of the cracking phenomenon, actual crack widths cannot be predicted. However, if the crack widths calculated in accordance with the models given in this Standard are limited to the values given in Table 7.101N, the performance of the structure is unlikely to be impaired. NOTE: The value of w_{max} and the definition of decompression and its application for use in a country may be found in its National Annex. The recommended value for w_{max} and the application of the decompression limit are given in Table 7.101N. The recommended definition of decompression is noted in the text under the Table. NOTE: British National Document PD 6687-2: 2008 (*Recommendations for the design of structures to BS EN 1992-2: 2005*) gives non-contradictory complimentary information for use with EN 1992-2. In particular, it contains a Section 8 – Serviceability limit states. Under 8.2.1 it makes recommendations for the values of w_{max} and notes a lack of clarity. Under 8.2.2 it offers a simplification in crack calculation methods. Under 8.2.3 it gives guidance on calculating crack widths due to early age restraint of imposed deformations, which can arise due to early thermal contraction and shrinkage. Such effects should be taken into account in design. (6) For members with only unbonded tendons, the requirements for reinforced concrete elements apply. For members with a	

	combination of bonded and unbonded tendons, requirements for prestressed concrete members with bonded tendons apply. (7) Special measures may be necessary for members subjected to exposure class XD3. The choice of appropriate measures will depend upon the nature of the aggressive agent involved. (8) When using strut-and-tie models with the struts oriented according to the compressive stress trajectories in the uncracked state, it is possible to use the forces in the ties to obtain the corresponding steel stresses to estimate the crack width (see 5.6.4 (2). (9) Crack widths may be calculated according to 7.3.4. A simplified alternative is to limit the bar size or spacing according to 7.3.3. (110) In some cases it may be necessary to check and control shear cracking in webs. NOTE: Further information may be found in Annex QQ.	
Eurocode 2 **SECTION 7 SERVICEABILITY LIMIT STATES (SLS) 7.3 Crack control 7.3.2 Minimum reinforcement areas**	(I)P If crack control is required, a minimum amount of bonded reinforcement is required to control cracking in areas where tension is expected. The amount may be estimated from equilibrium between the tensile force in concrete just before cracking and the tensile force in reinforcement at yielding or at a lower stress if necessary to limit the crack width. (102) Unless a more rigorous calculation shows lesser areas to be adequate, the required minimum areas of reinforcement may be calculated - a procedure is given. (3) Bonded tendons in the tension zone may be assumed to contribute to crack control within a distance *5* 150 mm from the centre of the tendon. (4) In prestressed members no minimum reinforcement is required in sections where, under the characteristic combination of loads and the characteristic value of prestress, the concrete is compressed or the absolute value of the tensile stress in the concrete is below a given value.	
Eurocode 2 **SECTION 7 SERVICEABILITY LIMIT STATES (SLS) 7.3 Crack control 7.3.3 Control of cracking without direct calculation**	(101) The control of cracking without direct calculation may be performed by means of simplified methods. A recommended method is given with several sub-clauses indicating where crack control is deemed to be adequate provided relevant detailing rules have been followed.	
Eurocode 2 **SECTION 7 SERVICEABILITY LIMIT STATES (SLS) 7.3 Crack control 7.3.4 Calculation of crack widths**	(101) The evaluation of crack width may be performed using recognized methods. NOTE: Details of recognized methods for crack width control may be found in a Country's National Annex. The recommended method is that in EN 1992-1-1, 7.3.4.	
Eurocode 2 **SECTION 7 SERVICEABILITY LIMIT STATES (SLS) 7.4 Deflection**	(1)P The deformation of a member or structure shall not be such that it adversely affects its proper functioning or appearance. (2) Appropriate limiting values of deflection taking into account the nature of the structure, of the finishes, partitions and fixings and upon the function of the structure should be established.	

control **7.4.1 General considerations**		
Eurocode 2 **SECTION 7 SERVICEABILITY LIMIT STATES (SLS)** **7.4 Deflection control** **7.4.3 Checking deflections by calculation**	(I)P Where a calculation is deemed necessary, the deformations shall be calculated under load conditions which are appropriate to the purpose of the check. (2)P The calculation method adopted shall represent the true behavior of the structure under relevant actions to an accuracy appropriate to the objectives of the calculation. (3) Members which are not expected to be loaded above the level which would cause the tensile strength of the concrete to be exceeded anywhere within the member should be considered to be uncracked. Members which are expected to crack, but may not be fully cracked, will behave in a manner intermediate between the uncracked and fully cracked conditions and, for members subjected mainly to flexure, an adequate prediction of behavior is given by Expression (7.18) presented in EN 1992-1.1. (4) Deformations due to loading may be assessed using the tensile strength and modulus of elasticity of the concrete (see (5)). (5) For loads with a duration causing creep, the total deformation including creep may be calculated by using an effective modulus of elasticity for concrete according to Expression (7.20) presented in EN 1992-1.1. (6) Shrinkage curvatures may be assessed using Expression (7.21) presented in EN 1992-1.1. (7) The most rigorous method of assessing deflections using the method given in (3) above is to compute the curvatures at frequent sections along the member and then calculate the deflection by numerical integration. In most cases it will be acceptable to compute the deflection twice, assuming the whole member to be in the uncracked and fully cracked condition in turn, and then interpolate using Expression (7.1 8).	
Eurocode 2 **SECTION 8 Detailing of reinforcement and prestressing tendons — General**	No rules peculiar to the serviceability limit state are given.	
Eurocode 2 **SECTION 9 Detailing of members and particular rules** **9.1 General**	(103) Minimum areas of reinforcement are given in order to prevent a brittle failure, wide cracks and also to resist forces arising from restrained actions. NOTE: Additional rules concerning the minimum thickness of structural elements and the minimum reinforcement for all surfaces of members in bridges, with minimum bar diameter and maximum bar spacing for use in a Country may be found in its National Annex. No additional rules are recommended in this standard.	
Eurocode 2 **SECTION 10 ADDITIONAL RULES FOR PRECAST CONCRETE ELEMENTS AND STRUCTURES**	(1) For precast products in continuous production, subjected to an appropriate quality control system according to the product standards, with the concrete tensile strength tested, a statistical analysis of test results may be used as a basis for the evaluation of the tensile strength that is used for serviceability limit states verifications, as an alternative to Table 3.1. (2) Intermediate strength classes within Table 3.1 may be used.	

10.3 Materials **10.3.1 Concrete** **10.3.1.1 Strength**		
Eurocode 2 **SECTION 11 LIGHTWEIGHT AGGREGATE CONCRETE STRUCTURES** **11.7 Serviceability limit states**	(I)P The basic ratios of span/effective depth for reinforced concrete members without axial compression, given in 7.4.2, should be reduced by a factor when applied to LWAC.	
Eurocode 2 **SECTION 12 PLAIN AND LIGHTLY REINFORCED CONCRETE STRUCTURES** **12.1 General**	(4) Members using plain concrete do not preclude the provision of steel reinforcement needed to satisfy serviceability and/or durability requirements, nor reinforcement in certain parts of the members. This reinforcement may be taken into account for the verification of local ultimate limit states as well as for the checks of the serviceability limit states.	
Eurocode 2 **SECTION 12 PLAIN AND LIGHTLY REINFORCED CONCRETE STRUCTURES** **12.5 Structural analysis: ultimate limit states**	(1) Since plain concrete members have limited ductility, linear analysis with redistribution or a plastic approach to analysis, e.g. methods without an explicit check of the deformation capacity, should not be used unless their application can be justified. (2) Structural analysis may be based on the non-linear or the linear elastic theory. In the case of a non-linear analysis (e.g. fracture mechanics) a check of the deformation capacity should be carried out.	
Eurocode 2 **SECTION 12 PLAIN AND LIGHTLY REINFORCED CONCRETE STRUCTURES** **12.7 Serviceability limit states**	(1) Stresses should be checked where structural restraint is expected to occur. (2) The following measures to ensure adequate serviceability should be considered: a) with regard to crack formation: - limitation of concrete tensile stresses to acceptable values; - provision of subsidiary structural reinforcement (surface reinforcement, tying system where necessary) - provision of joints; - choice of concrete technology (e.g. appropriate concrete composition, curing); - choice of appropriate method of construction. b) with regard to limitation of deformations: - a minimum section size (see 12.9 below); - limitation of slenderness in the case of compression members. (3) Any reinforcement provided in plain concrete members, although not taken into account for load bearing purposes, should comply with 4.4.1.	
Eurocode 2 **SECTION 113 Design for the execution stages** **113.3 Verification**	(101) The verifications for the execution stage should be the same as those for the completed structure, with the following exceptions. (102) Serviceability criteria for the completed structure need not be applied to intermediate execution stages, provided that durability and final appearance of the completed structure are	

criteria **113.3.2** **Serviceability limit states**	not affected (e.g. deformations). (103) Even for bridges or elements of bridges in which the limit state of decompression is checked under the quasi-permanent or frequent combination of actions on the completed structure, tensile stresses less than $k.f_{ctm}(t)$ under the quasi-permanent combination of actions during execution are permitted. NOTE: The value of *k* to be used in a Country may be found in its National Annex. The recommended value of *k* is1.0. (104) For bridges or elements of bridges in which the limit-state of cracking is checked under frequent combination on the completed structure, the limit state of cracking should be verified under the quasi-permanent combination of actions during execution.	
Eurocode 2 **ANNEX B** (informative) **Creep and shrinkage strain** **B.100 General**	(101) This Annex may be used for calculating creep and shrinkage, including development with time. However, typical experimental values can exhibit a scatter of ± 30 % around the values of creep and shrinkage predicted in accordance with this Annex. Where greater accuracy is required due to the structural sensitivity to creep and/or shrinkage, an experimental assessment of these effects and of the development of delayed strains with time should be undertaken. Section B.104 includes guidelines for the experimental determination of creep and shrinkage coefficients.	
Eurocode 2 **Annex E** **(Informative)** **Indicative strength classes for durability** **E.I General**	(1) The choice of adequately durable concrete for corrosion protection of reinforcement and protection of concrete attack requires consideration of the composition of concrete. This may result in a higher compressive strength of the concrete than is required for structural design. The relationship between concrete strength classes and exposure classes (see Table 4.1) may be described by indicative strength classes. (2) When the chosen strength is higher than that required for structural design the value of f_{ctm} should be associated with the higher strength in the calculation of minimum reinforcement according to 7.3.2 and 9.2.1.1 and crack width control according to 7.3.3 and 7.3.4.	
Eurocode 2 **Annex F** (Informative) **Tension reinforcement expressions for in-plane stress conditions** **F.1 General**	In order to avoid unacceptable cracks for the serviceability limit state, and to ensure the required deformation capacity for the ultimate limit state, the reinforcement derived from Expressions (F.8) and (F.9) for each direction should not be more than twice and not less than half the reinforcement determined by expressions (F.2) and (F.3) or (F.5) and (F.6).	
Eurocode 2 **G.1.2 Levels of analysis**	**G.1.2 Levels of analysis** (1) For design purposes, various levels of analysis are permitted depending on conditions at both the serviceability and the ultimate limit states – more guidance is given.	

Eurocode 2 **Annex KK** (informative) **Structural effects of time dependent behavior of concrete** **KK.1 Introduction**	This Annex describes different methods of evaluating the time dependent effects of concrete behavior.	
Eurocode 2 **KK.2 General considerations**	(101) Structural effects of time dependent behavior of concrete, such as variation of deformation and/or of internal actions, shall be considered, in general, in serviceability conditions. NOTE: In particular cases (e.g. structures or structural elements sensitive to second order effects or structures in which action effects cannot be redistributed) time dependent effects may also have an influence at ULS. (102) It is noted that for higher compressive stresses, non-linear creep effects should be considered. (104) Different types of analysis and their typical applications are shown in a table. Brief outline details of some of the analysis methods are given in the sections that follow.	
Eurocode 2 **Annex QQ** (informative) **Control of shear cracks within webs**	At present, the prediction of shear cracking in webs is accompanied by large model uncertainty. Where it is considered necessary to check shear cracking, particularly for prestressed members, the reinforcement required for crack control can be determined - some detailed guidance is given.	

APPENDIX C – CONCRETE GIRDER DATABASE

C.1 Database of Existing Bridges

Strand Legend:

Legend:

- No strand at this position at the current section location
- No strand at this position at the current location but a strand is harped to this position
- A strand occupies this position at the current section location
- The strand is debonded at the current section location
- The strand is debonded between the current section and the mid-span
- The harped position of a harped strand.
- The mid-span position of a harped strand.
- The mid-span position of one strand and the harped position of another strand.
- Mild steel.

Tendon Types:

LR = Low Relaxation
SR = Stress Relieved

C.2 Prestressed Concrete I-Beams and Bulb-T's

Bridge #	Virtis BID #	Span length (ft)	t_{slab} (in)	Girder Spacing (ft)	Overhang Width (ft)	# of Girders	Skew (deg)	Materials				Dist. to Extreme Strands (in)		Harp Point (ft)	Beam Section
								P/S Tendons	f_c' (ksi)	$f_{c\,I}'$ (ksi)	$f_{c\,deck}'$ (ksi)	Bottom	Top		
18067	562	131’-0 ¼”	6	5’-3 ½”	3’-0 ½”	17	112.5	50-0.6” Gr. 270 LR	7.5	6.5	3.0	2.5	3.5	44.51	AL BT-54 Mod

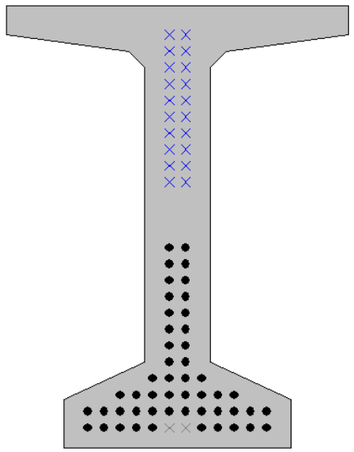

Strand Layout at Midspan

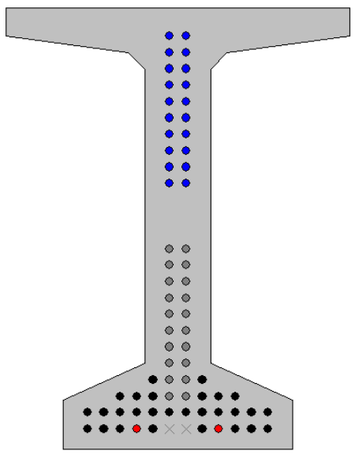

Strand Layout at 60” from Support

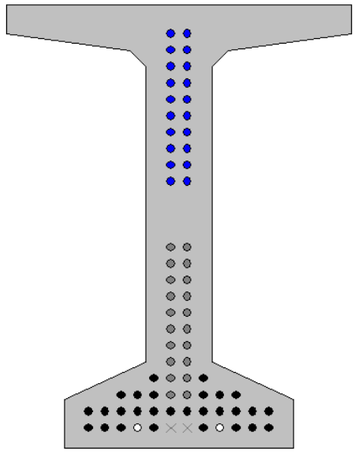

Strand Layout at Support

Strand Spacing:
Horizontal: 2”
Vertical: 2”

# of Strands: 50
Number of Harped Strands:20
CG from bottom at Midspan: 8.9”
CG from Bottom at Support: 20.0”
Debonded Strands: 2
Debonded Length: 60 inches
CG from Bottom at 60”: 18.78”

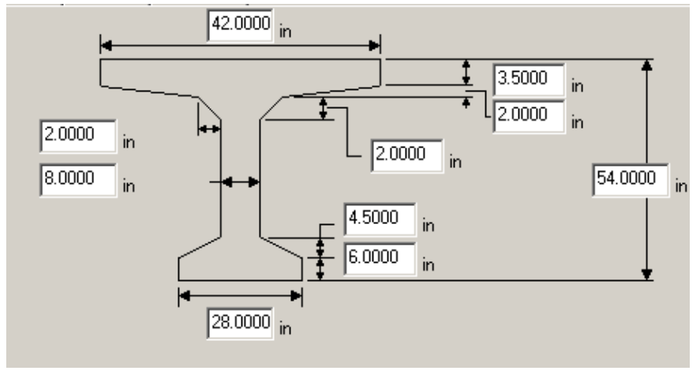

Cross-Section

Bridge #	Virtis BID #	Span length (ft)	t_{slab} (in)	Girder Spacing (ft)	Overhang Width (ft)	# of Girders	Skew (deg)	Materials				Dist. to Extreme Strands (in)		Harp Point (ft)	Beam Section
								P/S Tendons	f_c' (ksi)	$f_{c'l}$ (ksi)	$f_{c'deck}$ (ksi)	Bottom	Top		
8891	571	47'-2"	8.5	1@ 7'-10, 12@10'-8"	3'-4"	14	90	14-0.5" Gr. 270 LR	6.0	5.0	4.0	2.0	14.0	19.33	Beam Type 6

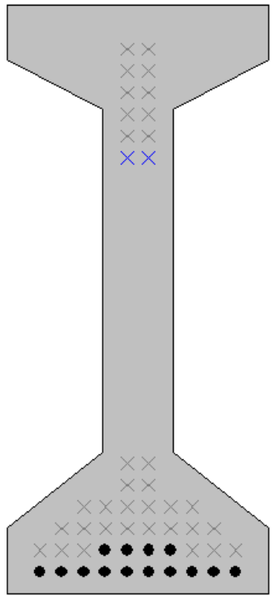

Strand Layout at Midspan

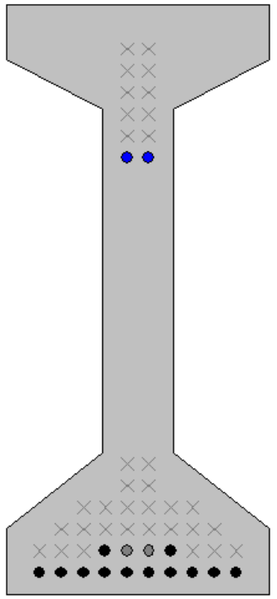

Strand Layout at Support

Strand Spacing:
Horizontal: 2"
Vertical: 2"

# of Strands: 14
Number of Harped Strands: 2
CG from bottom at Midspan: 2.57"
CG from Bottom at Support: 7.71"

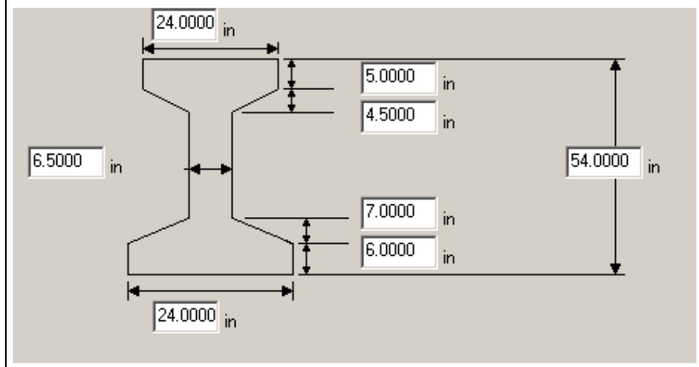

Cross-Section

Bridge #	Virtis BID #	Span length (ft)	t_{slab} (in)	Girder Spacing (ft)	Overhang Width (ft)	# of Girders	Skew (deg)	Materials				Dist. to Extreme Strands (in)		Harp Point (ft)	Beam Section
								P/S Tendons	f_c' (ksi)	$f_{c'l}$ (ksi)	$f_{c'deck}$ (ksi)	Bottom	Top		
8832	570	43'-3⅛"	8.5	10	2'-4"	16	87.5	20-0.5" Gr. 270 LR	8.0	6.0	4.0	2.0	3.0	N/A	36" I Beam

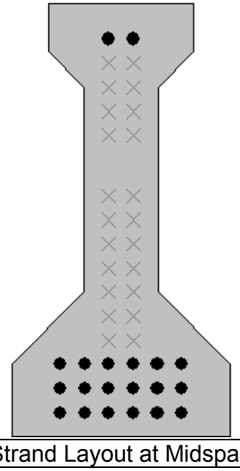

Strand Layout at Midspan

Strand Spacing:
Horizontal: 2"
Vertical: 2"

# of Strands: 20
Number of Harped Strands: 0
CG from bottom at Midspan: 6.90"

Cross-Section

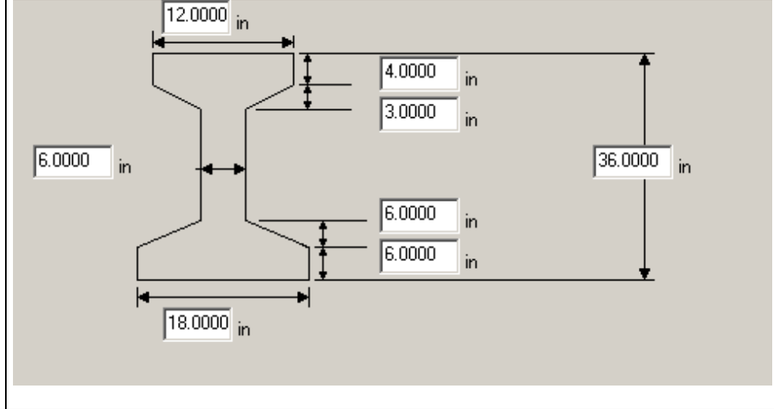

Cross-Section

Bridge #	Virtis BID #	Span length (ft)	t_{slab} (in)	Girder Spacing (ft)	Overhang Width (ft)	# of Girders	Skew (deg)	Materials				Dist. to Extreme Strands (in)		Harp Point (ft)	Beam Section
								P/S Tendons	f_c' (ksi)	$f_{c'l}$ (ksi)	$f_{c'deck}$ (ksi)	Bottom	Top		
12603	572	37'-8¾"	7.875	11'-5¾"	3'-6½"	4	90	14-0.6" Gr. 270 LR	7.25	5.5	4.0	2.0	4.0	N/A	AASHTO Type II

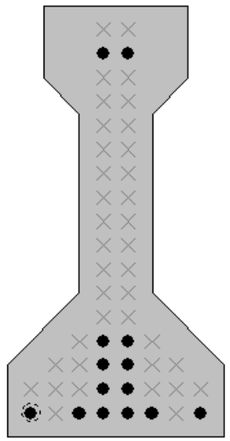

Strand Layout at Midspan

Strand Spacing:
Horizontal: 2"
Vertical: 2"

# of Strands: 14
Number of Harped Strands: 0
CG from bottom at Midspan: 8.00"

Cross-Section

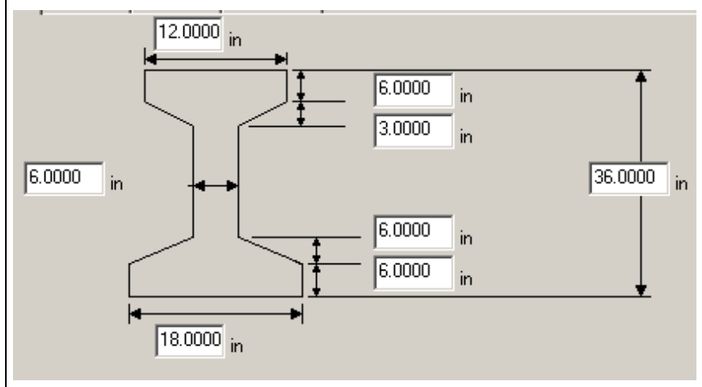

Cross-Section

Bridge #	Virtis BID #	Span length (ft)	t_{slab} (in)	Girder Spacing (ft)	Overhang Width (ft)	# of Girders	Skew (deg)	Materials				Dist. to Extreme Strands (in)		Harp Point (ft)	Beam Section
								P/S Tendons	f_c' (ksi)	$f_{c\,l}'$ (ksi)	$f_{c\,deck}'$ (ksi)	Bottom	Top		
10740	575	78'-6½"	6.25	7	3'-10½"	6	90	32-0.5" Gr. 270 LR	6.0	5.4	3.0	3.0		N/A	AASHTO Type III

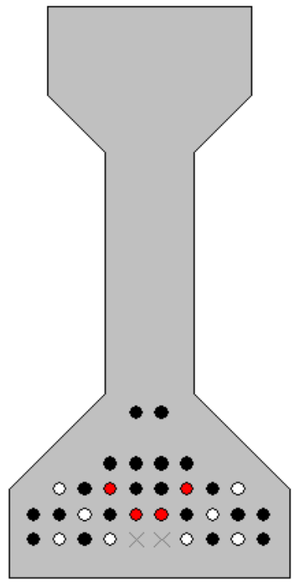

@48" from left support

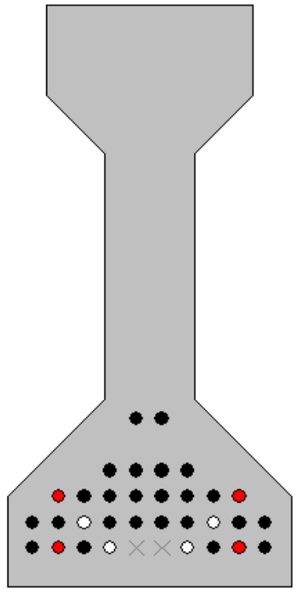

@ 120" from left support

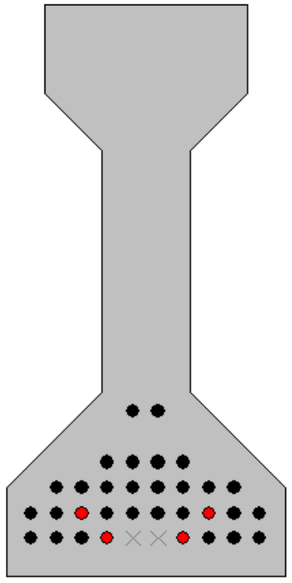

@ 168" from left support

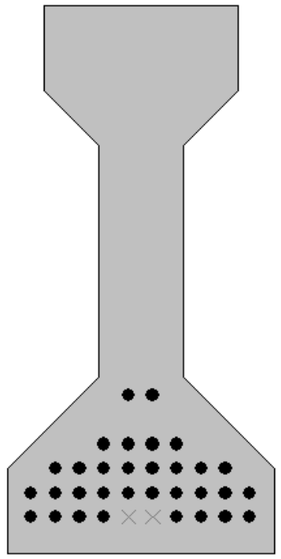

Strand Layout at Midspan

Strand Spacing:
Horizontal: 2"
Vertical: 2" (4" to top pair of strands)

# of Strands: 32
Number of Harped Strands: 0
CG from bottom at 48": 6.60"
CG from bottom at 120": 6.50"
CG from bottom at 168": 6.29"
CG from bottom at Midspan: 6.00"

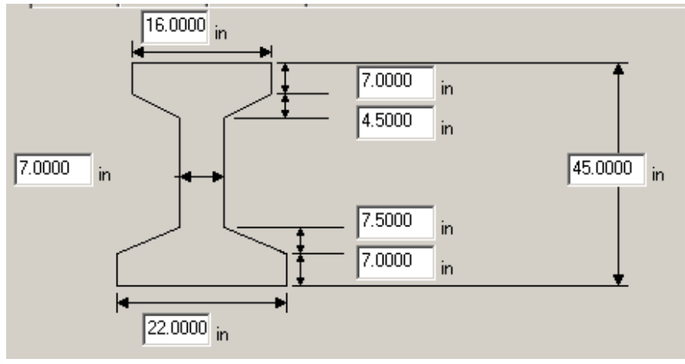

Cross-Section

Bridge #	Virtis BID #	Span length (ft)	t_{slab} (in)	Girder Spacing (ft)	Overhang Width (ft)	# of Girders	Skew (deg)	Materials				Dist. to Extreme Strands (in)		Harp Point (ft)	Beam Section
								P/S Tendons	f_c' (ksi)	f_c'$_I$ (ksi)	f_c'$_{deck}$ (ksi)	Bottom	Top		
10269	0576	78'-0"	6.25	6'-8"	3'-4 ½"	7	90	28-0.5" Gr. 270 LR	6.0	5.0	3.3	3.0	6.0	28.75	AASHTO Type III

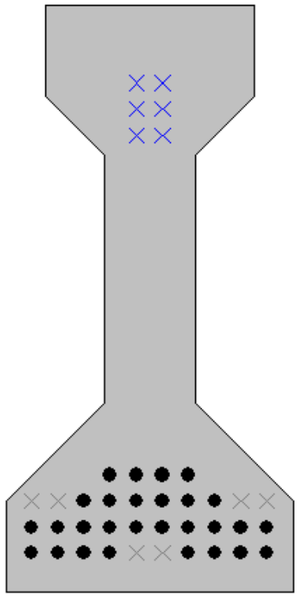

Strand Layout at Midspan

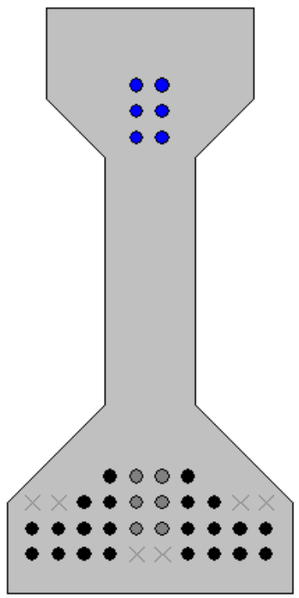

Strand Layout at Support

Strand Spacing:
Horizontal: 2"
Vertical: 2"

# of Strands: 28
Number of Harped Strands: 6
CG from bottom at Midspan: 5.43"
CG from Bottom at Support: 11.86"

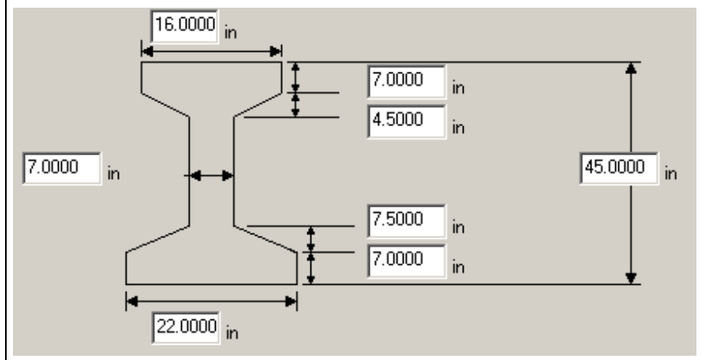

Cross-Section

Bridge #	Virtis BID #	Span length (ft)	t_{slab} (in)	Girder Spacing (ft)	Overhang Width (ft)	# of Girders	Skew (deg)	Materials				Dist. to Extreme Strands (in)		Harp Point (ft)	Beam Section
								P/S Tendons	f_c' (ksi)	$f_{c'}$ (ksi)	$f_{c'\ deck}$ (ksi)	Bottom	Top		
5624	0588	59'-4⅜"	9	7'-3"	2'-10"	21	109.9	20-0.5" Gr. 270 LR	6.0	4.5	4.0	2.0	3.0	24.15	Beam Type 4

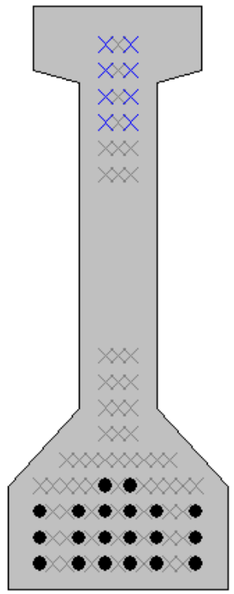

Strand Layout at Midspan

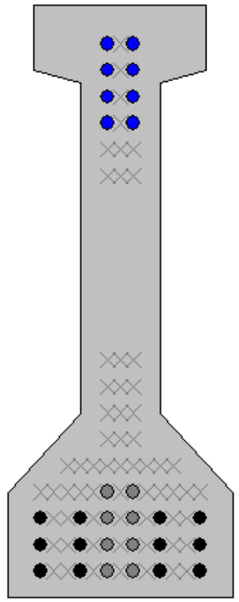

Strand Layout at Support

Strand Spacing:
Horizontal: 1"
Vertical: 2"

# of Strands: 20
Number of Harped Strands: 8
CG from bottom at Midspan: 4.40"
CG from Bottom at Support: 18.00"

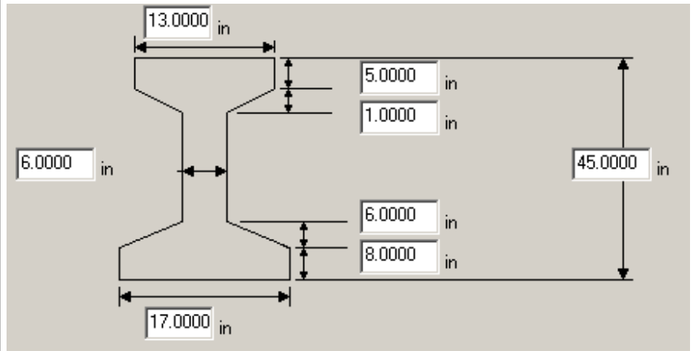

Cross-Section

Bridge #	Virtis BID #	Span length (ft)	t_{slab} (in)	Girder Spacing (ft)	Overhang Width (ft)	# of Girders	Skew (deg)	Materials				Dist. to Extreme Strands (in)		Harp Point (ft)	Beam Section
								P/S Tendons	f_c' (ksi)	$f_c'_l$ (ksi)	$f_c'_{deck}$ (ksi)	Bottom	Top		
5794	0589	72'-0"	8.5	5'-10"	2'-9"	6	100.0	20-0.6" Gr. 270 LR	9.0	7.0	4.0	2.0	3.0	29.13	Beam Type 3

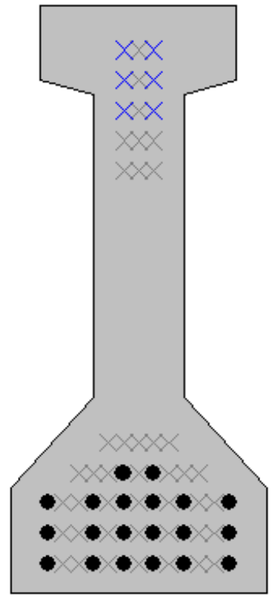

Strand Layout at Midspan

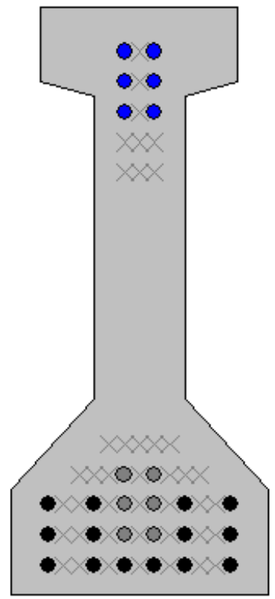

Strand Layout at Support

Strand Spacing:
Horizontal: 1"
Vertical: 2"

# of Strands: 20
Number of Harped Strands: 6
CG from bottom at Midspan: 4.40"
CG from Bottom at Support: 12.80"

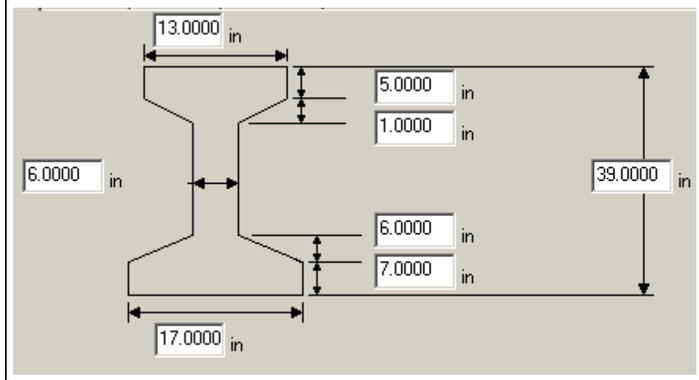

Cross-Section

Bridge #	Virtis BID #	Span length (ft)	t_{slab} (in)	Girder Spacing (ft)	Overhang Width (ft)	# of Girders	Skew (deg)	Materials				Dist. to Extreme Strands (in)		Harp Point (ft)	Beam Section
								P/S Tendons	f_c' (ksi)	$f_c'_l$ (ksi)	$f_c'_{deck}$ (ksi)	Bottom	Top		
9378	0598	101’-10”	9	10’-5”	2’-7½”	5	90	40-0.5” Gr. 270 LR	6.0	5.1	4.0	2.0	2.0	41.17	Wisconsin 70”

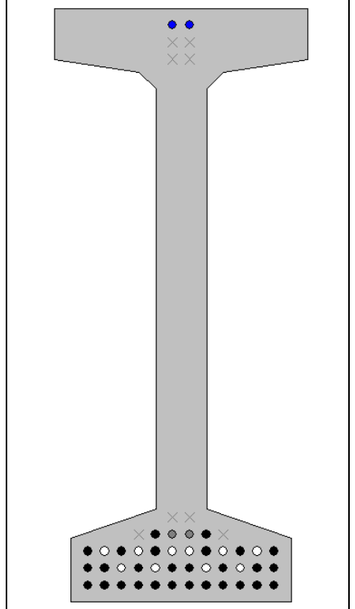

@ left support

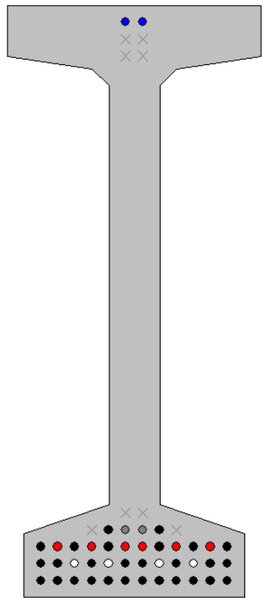

@ 78” from left support

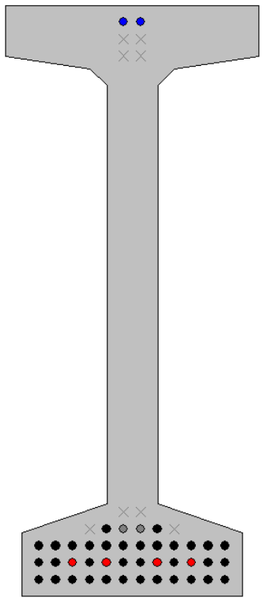

@ 318” from left support

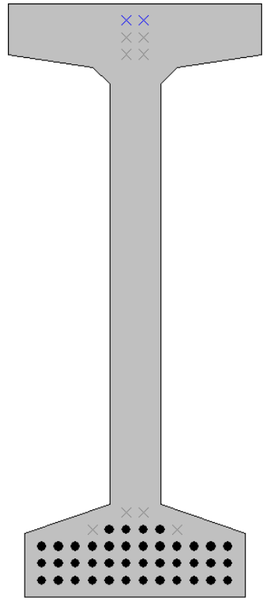

Strand Layout at Midspan

Strand Spacing:
Horizontal: 2”
Vertical: 2”

# of Strands: 40
Number of Harped Strands: 2
CG from bottom at Left Support”: 8.13”
CG from bottom at 78”: 7.50”
CG from bottom at 318”: 5.63”
CG from bottom at Midspan: 4.40”

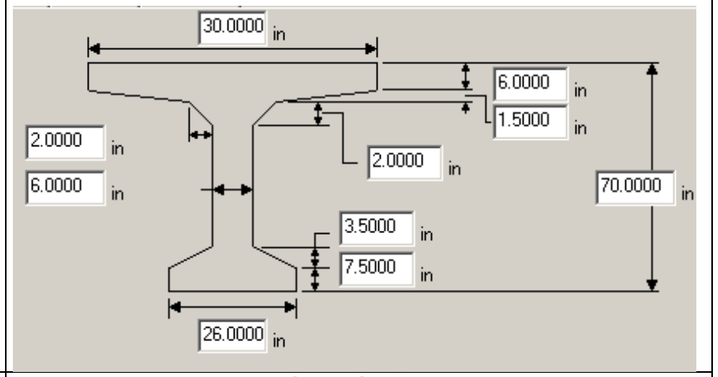

Cross-Section

Bridge #	Virtis BID #	Span length (ft)	t_{slab} (in)	Girder Spacing (ft)	Overhang Width (ft)	# of Girders	Skew (deg)	Materials				Dist. to Extreme Strands (in)		Harp Point (ft)	Beam Section
								P/S Tendons	f_c' (ksi)	$f_c'_l$ (ksi)	$f_c'_{deck}$ (ksi)	Bottom	Top		
5884	0602	90'-0"	8.5	8'-2"	3'-1"	4	110.0	38-0.5" Gr. 270 LR	7.0	5.0	4.0	2.0	4.0	27.28	Beam Type 6

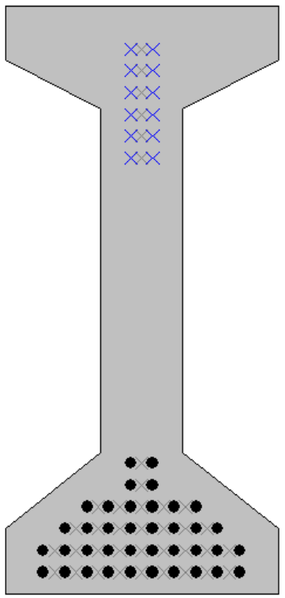

Strand Layout at Midspan

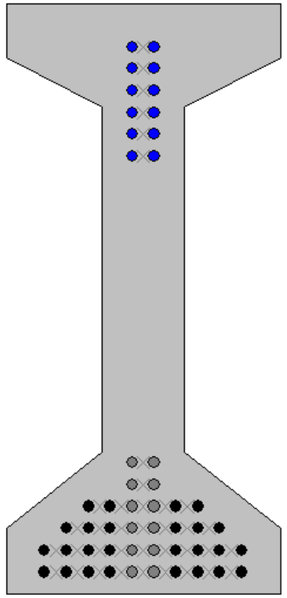

Strand Layout at Support

Strand Spacing:
Horizontal: 1"
Vertical: 2"

# of Strands: 38
Number of Harped Strands: 12
CG from bottom at Midspan: 5.26"
CG from Bottom at Support: 17.26"

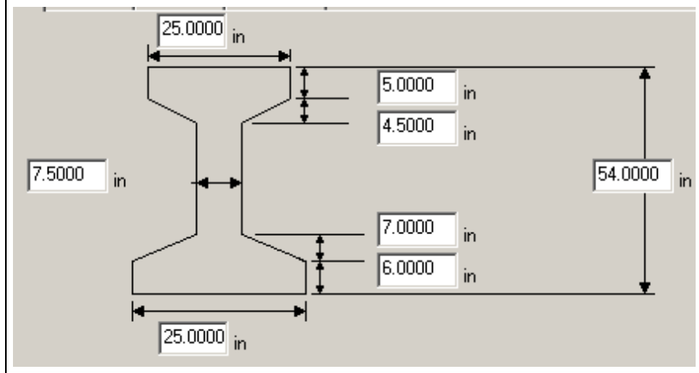

Cross-Section

Bridge #	Virtis BID #	Span length (ft)	t_{slab} (in)	Girder Spacing (ft)	Overhang Width (ft)	# of Girders	Skew (deg)	Materials				Dist. to Extreme Strands (in)		Harp Point (ft)	Beam Section
								P/S Tendons	f_c' (ksi)	f_c'$_l$ (ksi)	f_c'$_{deck}$ (ksi)	Bottom	Top		
8885	0603	90'-0"	8.5	10'-7"	3'-5½"	4	105.8	36-0.5" Gr. 270 LR	7.0	5.5	4.0	2.5	2.5	36.00	BT-63

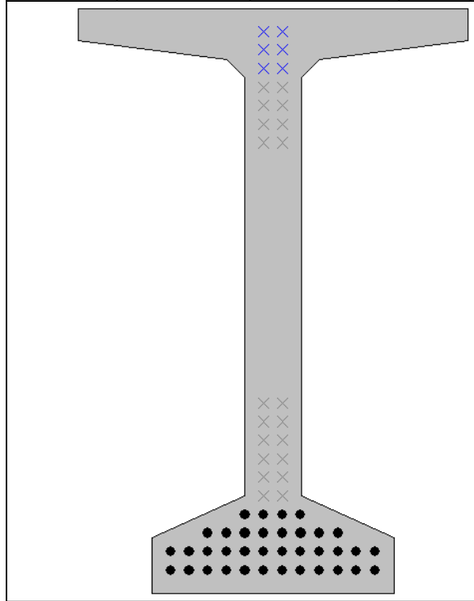

Strand Layout at Midspan

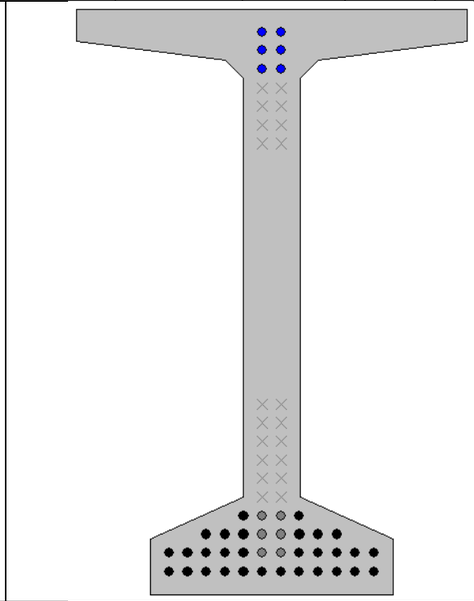

Strand Layout at Support

Strand Spacing:
Horizontal: 2"
Vertical: 2"

# of Strands: 36
Number of Harped Strands: 6
CG from bottom at Midspan: 4.72"
CG from Bottom at Support: 13.39"

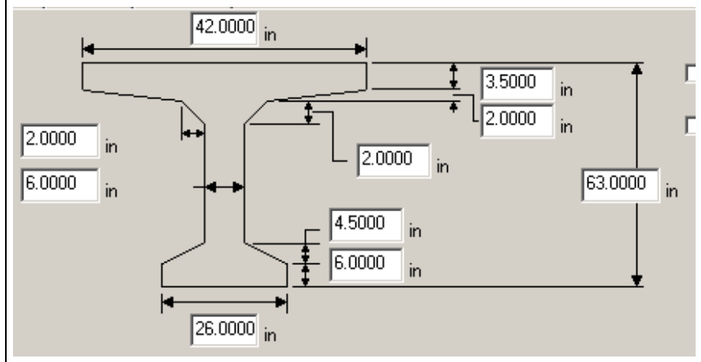

Cross-Section

Bridge #	Virtis BID #	Span length (ft)	t_{slab} (in)	Girder Spacing (ft)	Overhang Width (ft)	# of Girders	Skew (deg)	Materials				Dist. to Extreme Strands (in)		Harp Point (ft)	Beam Section
								P/S Tendons	f_c' (ksi)	$f_c'_l$ (ksi)	$f_c'_{deck}$ (ksi)	Bottom	Top		
8957	0604	98’-0”	8.5	8’-8”	3’-0”	5	90.0	26-0.6” Gr. 270 LR	8.0	6.4	4.0	2.0	4.0	39.67	Beam Type 6

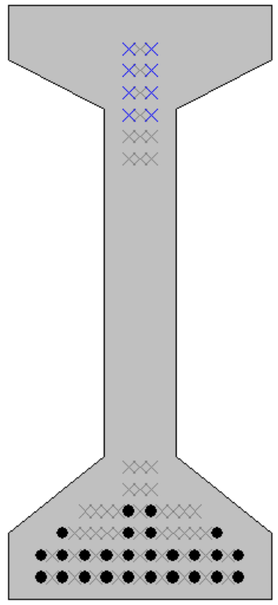

Strand Layout at Midspan

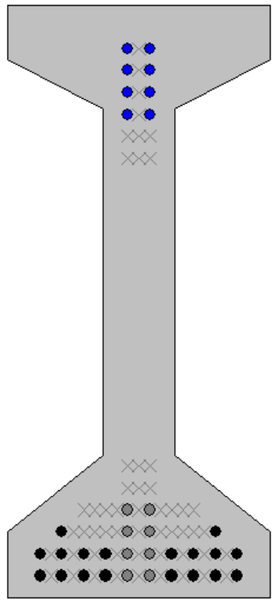

Strand Layout at Support

Strand Spacing:
Horizontal: 1”
Vertical: 2”

# of Strands: 26
Number of Harped Strands: 8
CG from bottom at Midspan: 3.85”
CG from Bottom at Support: 16.77”

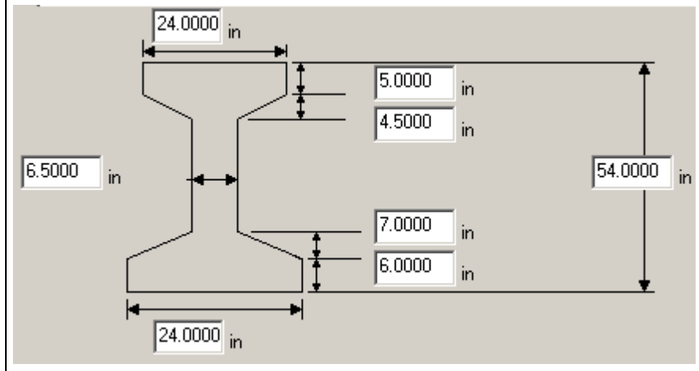

Cross-Section

Bridge #	Virtis BID #	Span length (ft)	t_{slab} (in)	Girder Spacing (ft)	Overhang Width (ft)	# of Girders	Skew (deg)	Materials				Dist. to Extreme Strands (in)		Harp Point (ft)	Beam Section
								P/S Tendons	f_c' (ksi)	$f_c'_I$ (ksi)	$f_c'_{deck}$ (ksi)	Bottom	Top		
12596	0610	96’-9⅜”	7.875	11’-1⅞”	4’-0 7/16”	4	90	50-0.6” Gr. 270 LR	10.2	7.1	4.0	2.0	2.0	N/A	AASHTO Type IV

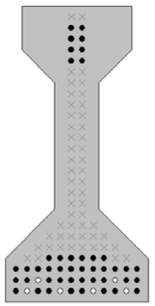

@ left support

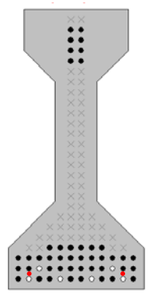

@ 102.36” from left support

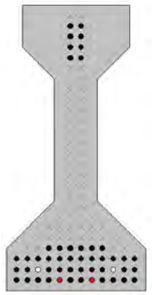

@ 133.86” from left support

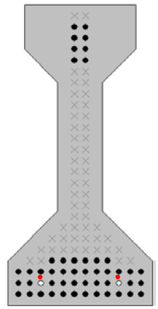

@ 157.48” from left support

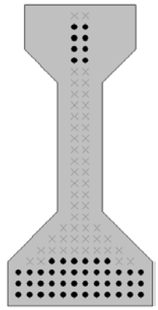

Strand Layout at Midspan

Strand Spacing:
Horizontal: 2”
Vertical: 2”

# of Strands: 50
Number of Harped Strands: 0
CG from bottom at Left Support to 102.36”: 12.55”
CG from bottom at 133.86”: 12.09”
CG from bottom at 157.48”: 11.67”
CG from bottom at Midspan: 11.36”

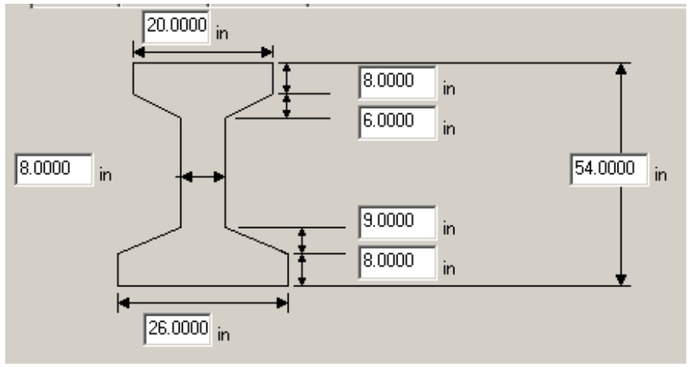

Cross-Section

Bridge #	Virtis BID #	Span length (ft)	t_{slab} (in)	Girder Spacing (ft)	Overhang Width (ft)	# of Girders	Skew (deg)	Materials				Dist. to Extreme Strands (in)		Harp Point (ft)	Beam Section
								P/S Tendons	f_c' (ksi)	$f_c'_l$ (ksi)	$f_c'_{deck}$ (ksi)	Bottom	Top		
10803	0611	138'-3"	6.25	6'-0"	3'-4½"	7	90.0	46-0.5" Gr. 270 LR	7.0	6.0	4.0	2.5	3.5	54.75	BT-72

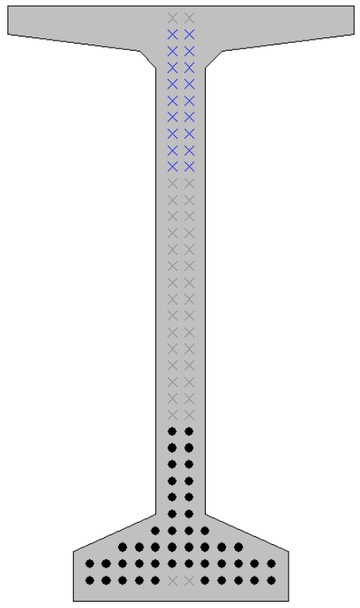

Strand Layout at Midspan

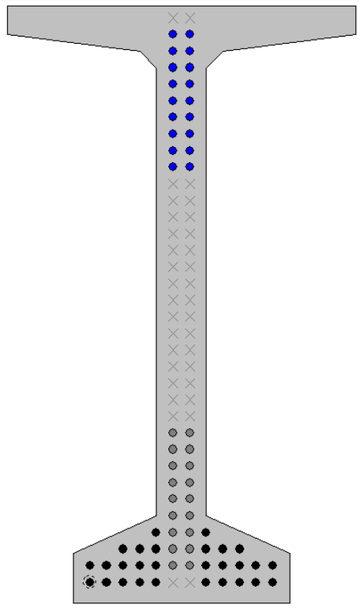

Strand Layout at Support

Strand Spacing:
Horizontal: 2"
Vertical: 2"

# of Strands: 46
Number of Harped Strands: 18
CG from bottom at Midspan: 7.63"
CG from Bottom at Support: 26.41"

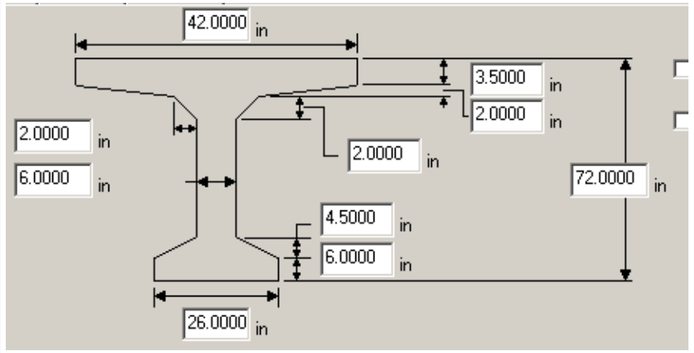

Cross-Section

Bridge #	Virtis BID #	Span length (ft)	t_{slab} (in)	Girder Spacing (ft)	Overhang Width (ft)	# of Girders	Skew (deg)	Materials				Dist. to Extreme Strands (in)		Harp Point (ft)	Beam Section
								P/S Tendons	f_c' (ksi)	$f_c'_l$ (ksi)	$f_c'_{deck}$ (ksi)	Bottom	Top		
8890	0613	143’-6”	8.5	8’-0”	2’-9”	14	92.8	48-0.6” Gr. 270 LR	8.0	6.0	4.0	2.5	3	57.90	AASHTO Type VI

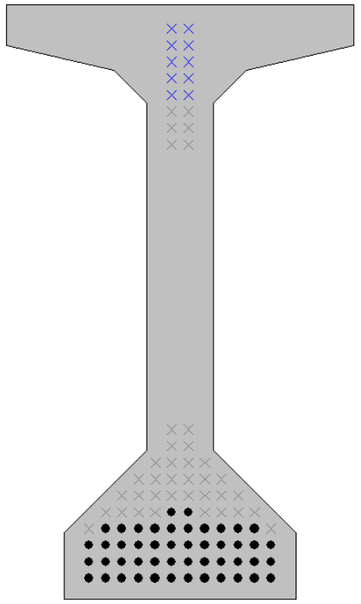

Strand Layout at Midspan

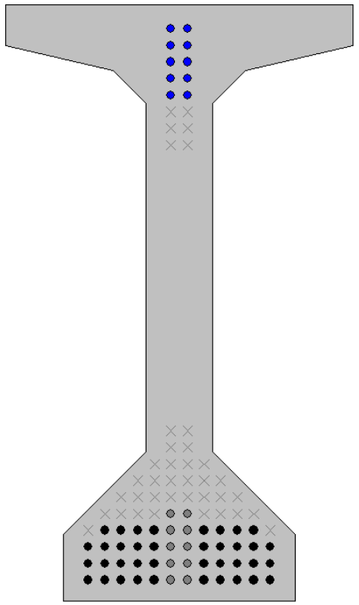

Strand Layout at Support

Strand Spacing:
Horizontal: 2”
Vertical: 2”

# of Strands: 48
Number of Harped Strands: 10
CG from bottom at Midspan: 5.58”
CG from Bottom at Support: 17.77”

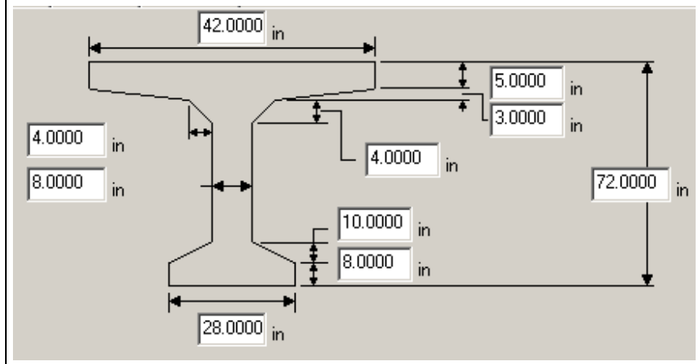

Cross-Section

Bridge #	Virtis BID #	Span length (ft)	t_{slab} (in)	Girder Spacing (ft)	Overhang Width (ft)	# of Girders	Skew (deg)	Materials				Dist. to Extreme Strands (in)		Harp Point (ft)	Beam Section
								P/S Tendons	f_c' (ksi)	f_{ci}' (ksi)	f_{cdeck}' (ksi)	Bottom	Top		
10755	0411	52’-6”	6.25	7’-0”	3’-10½”	6	90.0	24-0.5” Gr. 270 SR	6.0	5.0	3.0	3.0	9.0	N/A	AASHTO Type II

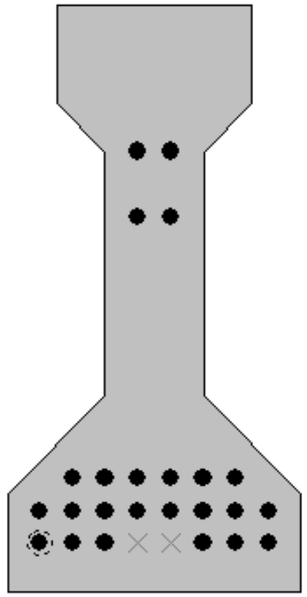

Strand Layout at Midspan

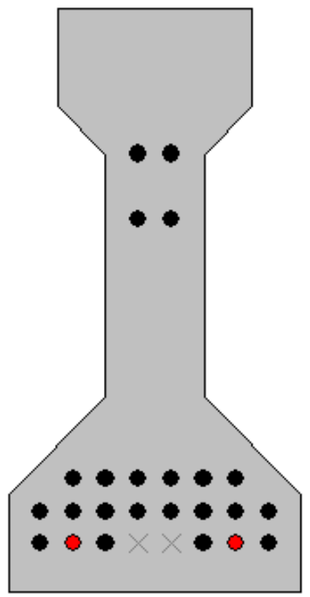

@ 60” from left support

Strand Spacing:
Horizontal: 2”
Vertical: 2”

# of Strands: 24
Number of Harped Strands: 0
CG from bottom at Midspan: 8.33”
CG from Bottom at 60”: 8.82”

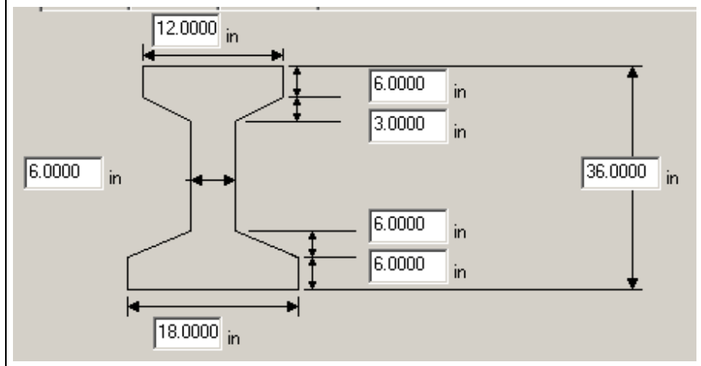

Cross-Section

Bridge #	Virtis BID #	Span length (ft)	t_{slab} (in)	Girder Spacing (ft)	Overhang Width (ft)	# of Girders	Skew (deg)	Materials				Dist. to Extreme Strands (in)		Harp Point (ft)	Beam Section
								P/S Tendons	f_c' (ksi)	$f_{c\ l}$' (ksi)	$f_{c\ deck}$' (ksi)	Bottom	Top		
3107	0416	49'-6½"	7.6875	5'-9¼"	2'-9 7/16"	6	90.0	12-0.5" Gr. 270 LR	6.1	5.1	3.5	2		N/A	36" I Beam

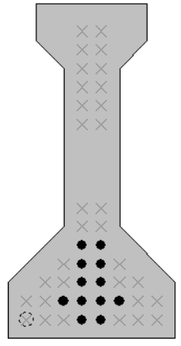

Strand Layout at Midspan

Strand Spacing:
Horizontal: 2"
Vertical: 2"

# of Strands: 12
Number of Harped Strands: 0
CG from bottom at Midspan: 5.67"

Cross-Section

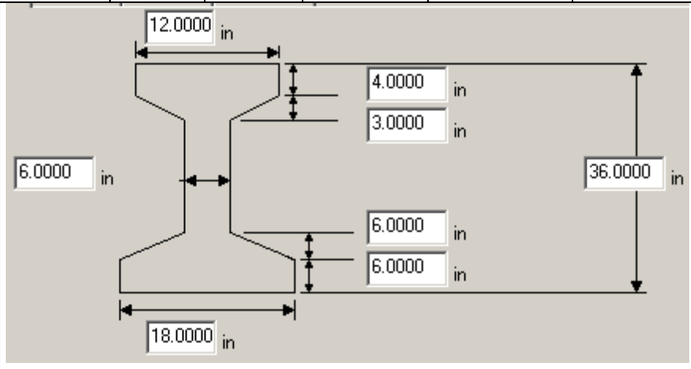

Cross-Section

Bridge #	Virtis BID #	Span length (ft)	t_{slab} (in)	Girder Spacing (ft)	Overhang Width (ft)	# of Girders	Skew (deg)	Materials				Dist. to Extreme Strands (in)		Harp Point (ft)	Beam Section
								P/S Tendons	f_c' (ksi)	f_c'$_l$ (ksi)	f_c'$_{deck}$ (ksi)	Bottom	Top		
4827	0418	50'-7"	8.5	7'-2"	3'-0"	5	125.0	18-0.5" Gr. 270 LR	6.0	4.5	4.0	2	3	20.54	Beam Type 2

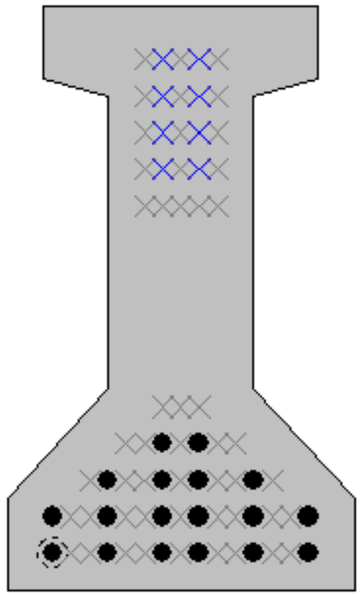

Strand Layout at Midspan

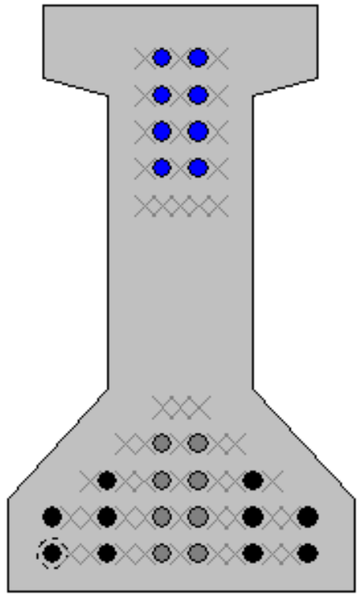

Strand Layout at Left Support

Strand Spacing:
Horizontal: 1"
Vertical: 2"

# of Strands: 18
Number of Harped Strands: 8
CG from bottom at Midspan: 4.22"
CG from bottom at Left Support: 13.56"

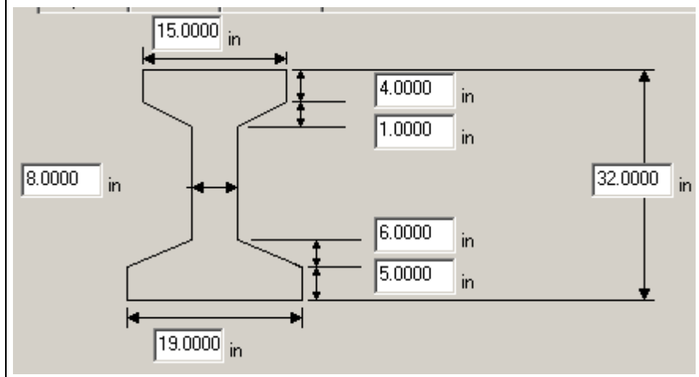

Cross-Section

Bridge #	Virtis BID #	Span length (ft)	t_{slab} (in)	Girder Spacing (ft)	Overhang Width (ft)	# of Girders	Skew (deg)	Materials				Dist. to Extreme Strands (in)		Harp Point (ft)	Beam Section
								P/S Tendons	f_c' (ksi)	$f_c'_l$ (ksi)	$f_c'_{deck}$ (ksi)	Bottom	Top		
10599	0476	62'-10"	8.0	6'-9"	3'-3"	4	90	28-0.5" Gr. 270 LR	7.0	6.5	4.0	3.0	13.0	N/A	AASHTO Type II

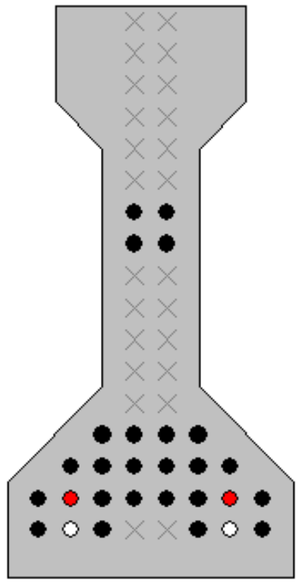

@ 66.75" from left support

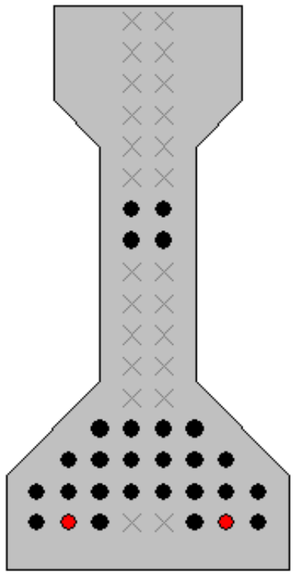

@ 138.75" from left support

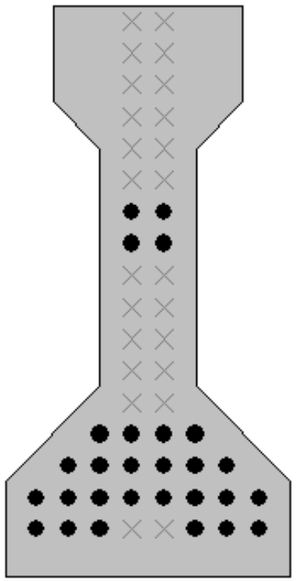

Strand Layout at Midspan

Strand Spacing:
Horizontal: 2"
Vertical: 2"

# of Strands: 28
Number of Harped Strands: 0
CG from bottom at 66.75": 8.67"
CG from bottom at 138.75": 8.38"
CG from bottom at Midspan: 8.0"

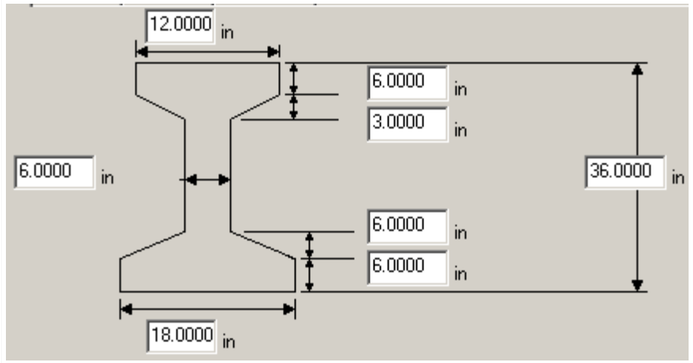

Cross-Section

Bridge #	Virtis BID #	Span length (ft)	t_{slab} (in)	Girder Spacing (ft)	Overhang Width (ft)	# of Girders	Skew (deg)	Materials				Dist. to Extreme Strands (in)		Harp Point (ft)	Beam Section
								P/S Tendons	f_c' (ksi)	$f_c'_l$ (ksi)	$f_c'_{deck}$ (ksi)	Bottom	Top		
12589	0478	73'-2 ½"	9.0	8'-9"	3'-0"	5	90	30-0.5" Gr. 270 LR	6.0	4.8	4.0	2.0	4.0	29.58	AASHTO Type IV

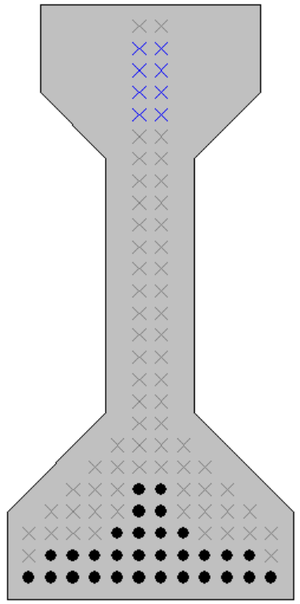

Strand Layout at Midspan

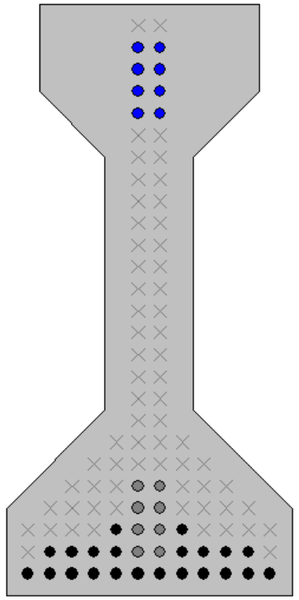

Strand Layout at Left Support

Strand Spacing:
Horizontal: 2"
Vertical: 2"

# of Strands: 30
Number of Harped Strands: 8
CG from bottom at Midspan: 4.13"
CG from bottom at Left Support: 14.80"

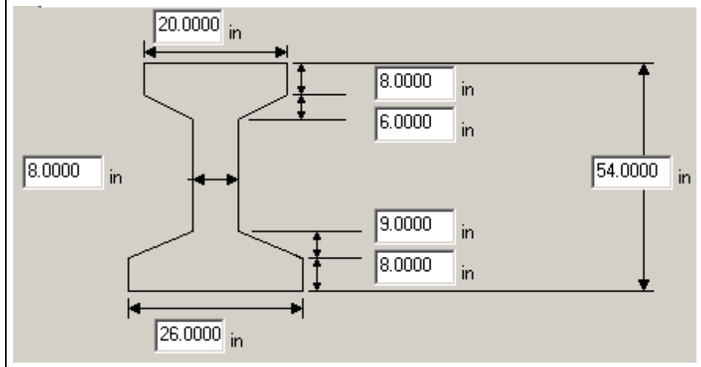

Cross-Section

Bridge #	Virtis BID #	Span length (ft)	t_{slab} (in)	Girder Spacing (ft)	Overhang Width (ft)	# of Girders	Skew (deg)	Materials				Dist. to Extreme Strands (in)		Harp Point (ft)	Beam Section
								P/S Tendons	f_c' (ksi)	$f_{c\ l}'$ (ksi)	$f_{c\ deck}'$ (ksi)	Bottom	Top		
5840	0489	85’-0”	8.5	9’-0”	3’-4”	5	70.0	30-0.5” Gr. 270 LR	7.5	5.25	4.0	2.0	4.0	34.47	Beam Type 6

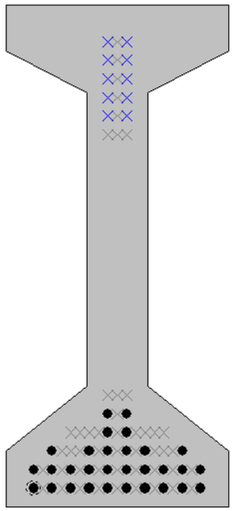

Strand Layout at Midspan

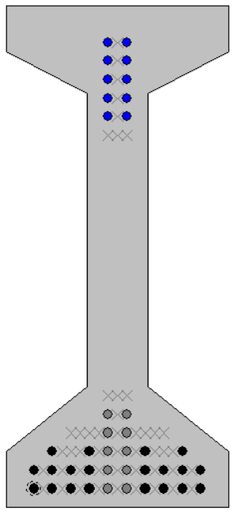

Strand Layout at Left Support

Strand Spacing:
Horizontal: 1”
Vertical: 2”

# of Strands: 30
Number of Harped Strands: 10
CG from bottom at Midspan: 4.40”
CG from bottom at Left Support: 17.73”

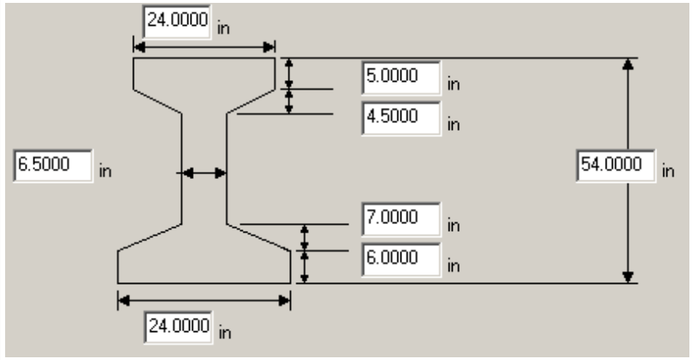

Cross-Section

Bridge #	Virtis BID #	Span length (ft)	t_{slab} (in)	Girder Spacing (ft)	Overhang Width (ft)	# of Girders	Skew (deg)	Materials				Dist. to Extreme Strands (in)		Harp Point (ft)	Beam Section
								P/S Tendons	f_c' (ksi)	f_{ci}' (ksi)	f_{cdeck}' (ksi)	Bottom	Top		
8330	0491	76’-4 ½”	8.5	8’-8”	3’-0”	5	75.5	28-0.5” Gr. 270 LR	6.0	4.5	4.0	2	4	31.14	Beam Type 6

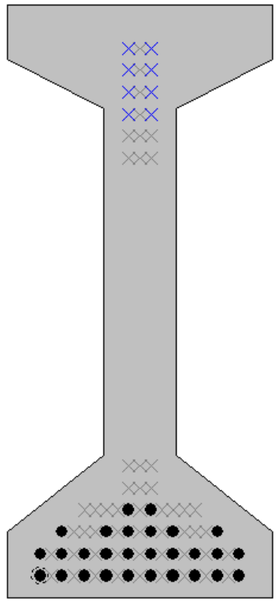

Strand Layout at Midspan

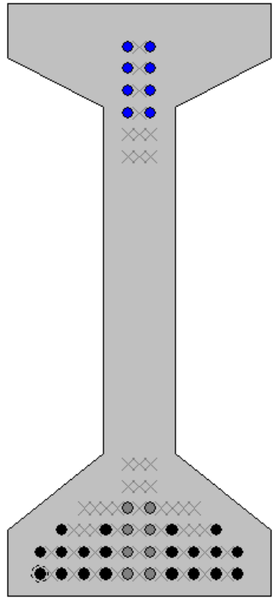

Strand Layout at Left Support

Strand Spacing:
Horizontal: 1”
Vertical: 2”

# of Strands: 28
Number of Harped Strands: 8
CG from bottom at Midspan: 4.00”
CG from bottom at Left Support: 16.00”

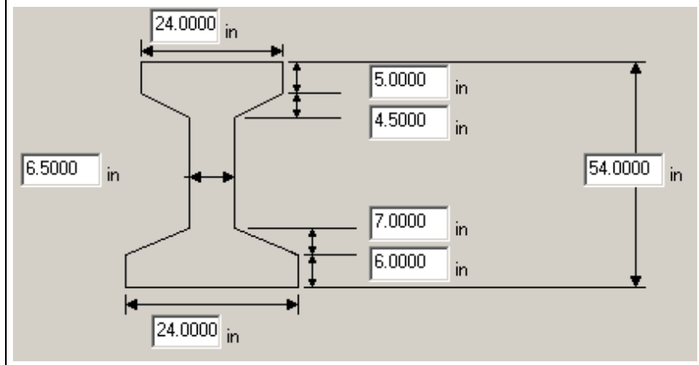

Cross-Section

Bridge #	Virtis BID #	Span length (ft)	t_{slab} (in)	Girder Spacing (ft)	Overhang Width (ft)	# of Girders	Skew (deg)	Materials				Dist. to Extreme Strands (in)		Harp Point (ft)	Beam Section
								P/S Tendons	f_c' (ksi)	f_{ci}' (ksi)	$f_{c\ deck}'$ (ksi)	Bottom	Top		
82	0498	82’-9”	8.75	10’-4”	3’-6”	4	105.0	34-0.5” Gr. 270 LR	5.0	4.8	4.5	2.0	2.0	33.38	MN Type 63

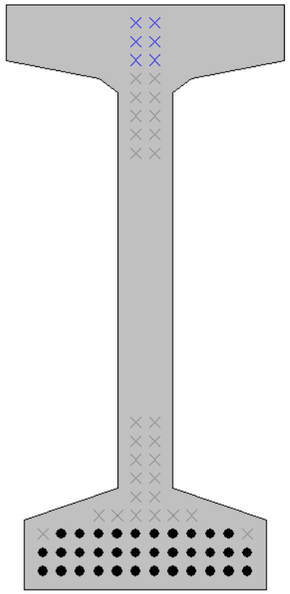

Strand Layout at Midspan

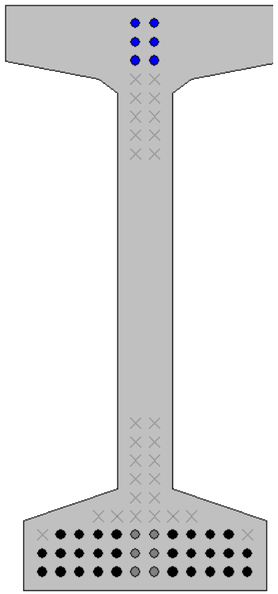

Strand Layout at Left Support

Strand Spacing:
Horizontal: 2”
Vertical: 2”

# of Strands: 34
Number of Harped Strands: 6
CG from bottom at Midspan: 3.88”
CG from bottom at Left Support: 13.59”

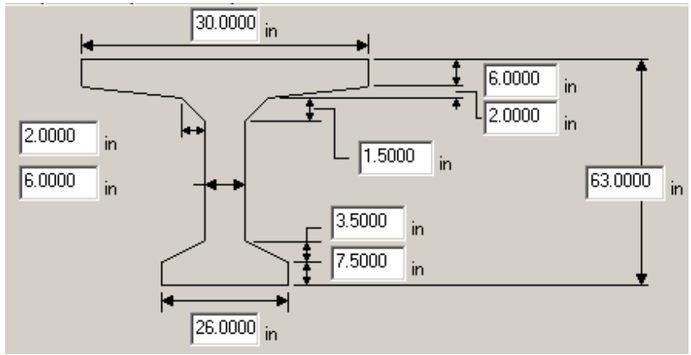

Cross-Section

Bridge #	Virtis BID #	Span length (ft)	t_{slab} (in)	Girder Spacing (ft)	Overhang Width (ft)	# of Girders	Skew (deg)	Materials				Dist. to Extreme Strands (in)		Harp Point (ft)	Beam Section
								P/S Tendons	f_c' (ksi)	$f_c'_l$ (ksi)	$f_c'_{deck}$ (ksi)	Bottom	Top		
4794	0497	66'-8"	8.5	3@7'-4", 7@9'-4"	3'-7"	11	90	33-0.5" Gr. 270 LR	10.0	7.0	6.0	2	3	27.92	Beam Type 4

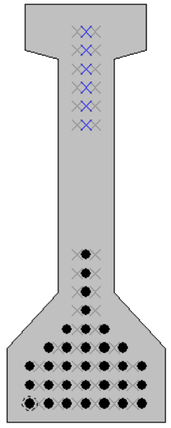

Strand Layout at Midspan

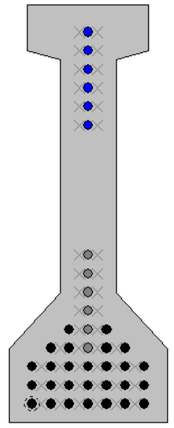

Strand Layout at Left Support

Strand Spacing:
Horizontal: 1"
Vertical: 2"

# of Strands: 33
Number of Harped Strands: 6
CG from bottom at Midspan: 6.48"
CG from bottom at Left Support: 10.85"

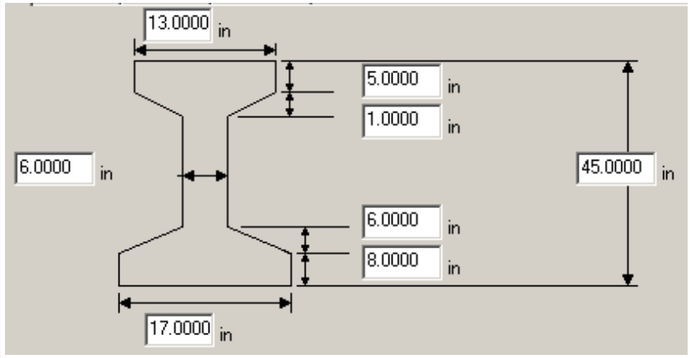

Cross-Section

Bridge #	Virtis BID #	Span length (ft)	t_{slab} (in)	Girder Spacing (ft)	Overhang Width (ft)	# of Girders	Skew (deg)	Materials				Dist. to Extreme Strands (in)		Harp Point (ft)	Beam Section
								P/S Tendons	f_c' (ksi)	$f_{c'\,l}$ (ksi)	$f_{c'\,deck}$ (ksi)	Bottom	Top		
12610	0539	108'-6⅜"	8.0	8@7'-1 ½", 4@6'-11"	3'-2 ½" (L) 3'-0½" (R)	13	90.0	52-0.5" Gr. 270 LR	7.0	5.4	4.0	2.0	4.0	44.85	AASHTO Type IV

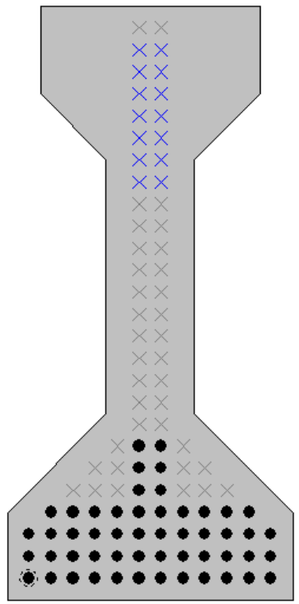

Strand Layout at Midspan

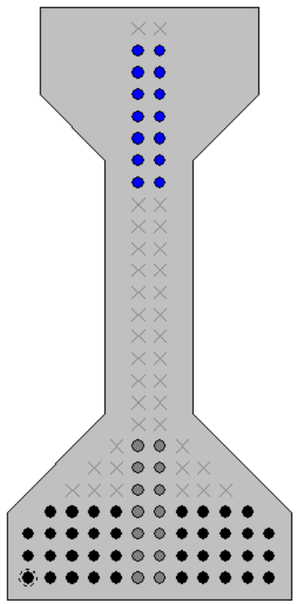

Strand Layout at Left Support

Strand Spacing:
Horizontal: 2"
Vertical: 2"

# of Strands: 52
Number of Harped Strands: 14
CG from bottom at Midspan: 5.69"
CG from bottom at Left Support: 15.38"

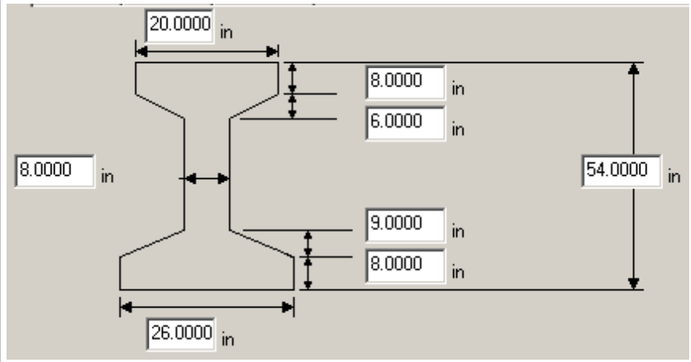

Cross-Section

Bridge #	Virtis BID #	Span length (ft)	t_{slab} (in)	Girder Spacing (ft)	Overhang Width (ft)	# of Girders	Skew (deg)	Materials				Dist. to Extreme Strands (in)		Harp Point (ft)	Beam Section
								P/S Tendons	f_c' (ksi)	$f_c'_l$ (ksi)	$f_c'_{deck}$ (ksi)	Bottom	Top		
11938	0545	116’-6¼”	7	7’ – 3 ¾”	3’-9”	8	117.9	46-0.5” Gr. 270 LR	7.0	6.0	3.0	2.5	2.5	47.64	BT-63

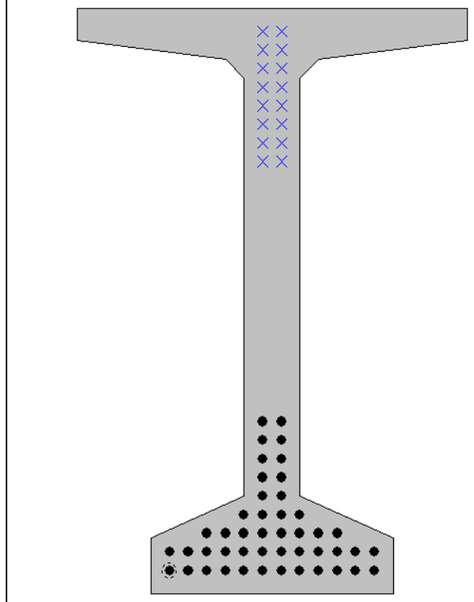

Strand Layout at Midspan

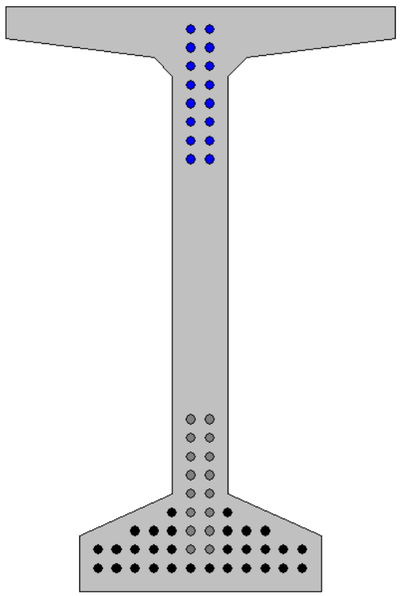

Strand Layout at Left Support

Strand Spacing:
Horizontal: 2”
Vertical: 2”

# of Strands: 46
Number of Harped Strands: 16
CG from bottom at Midspan: 6.85”
CG from bottom at Left Support: 21.46”

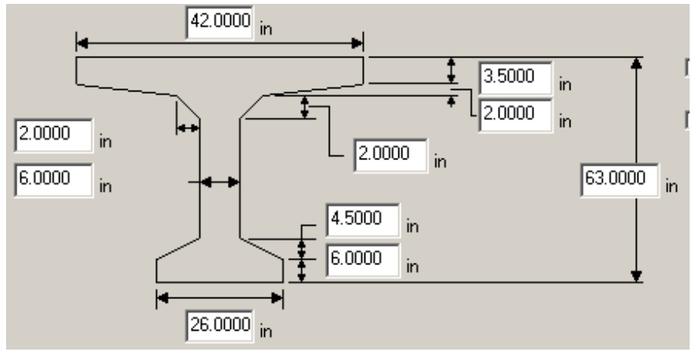

Cross-Section

Bridge #	Virtis BID #	Span length (ft)	t_{slab} (in)	Girder Spacing (ft)	Overhang Width (ft)	# of Girders	Skew (deg)	Materials				Dist. to Extreme Strands (in)		Harp Point (ft)	Beam Section
								P/S Tendons	f_c' (ksi)	$f_c'_l$ (ksi)	$f_c'_{deck}$ (ksi)	Bottom	Top		
11030	0551	136'-0"	6.25	6'-4 ½"	3'-10½"	9	90.0	50-0.5" Gr. 270 LR	7.0	6.0	3.0	2.5	3.5	48.75	BT-72

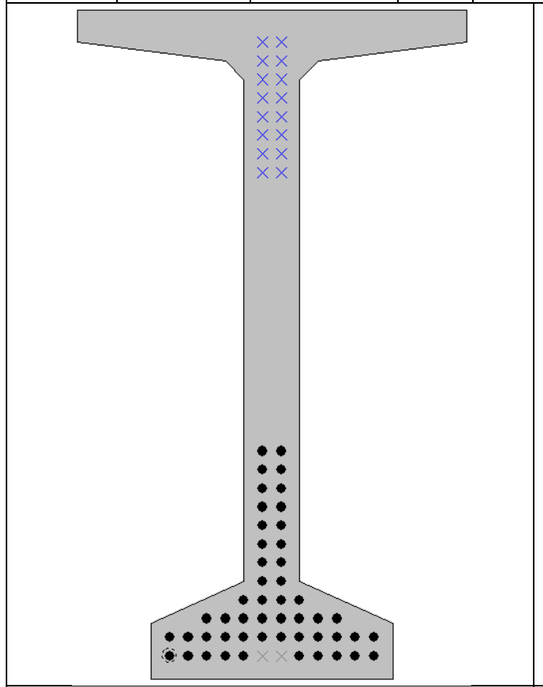

Strand Layout at Midspan

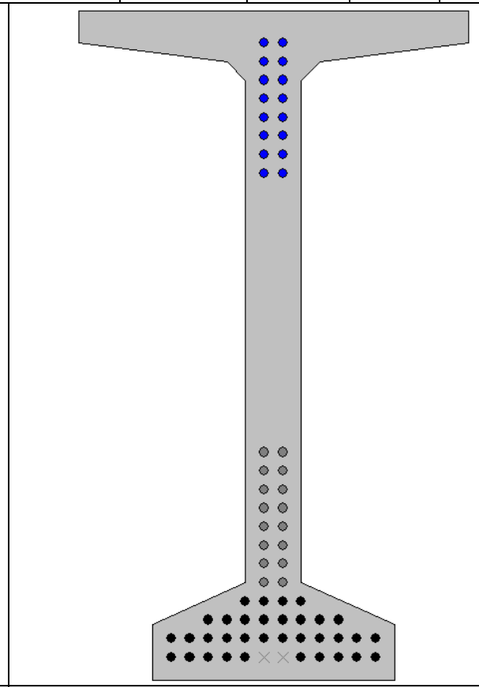

Strand Layout at Left Support

Strand Spacing:
Horizontal: 2"
Vertical: 2"

# of Strands: 50
Number of Harped Strands: 16
CG from bottom at Midspan: 8.90"
CG from bottom at Left Support: 22.98"

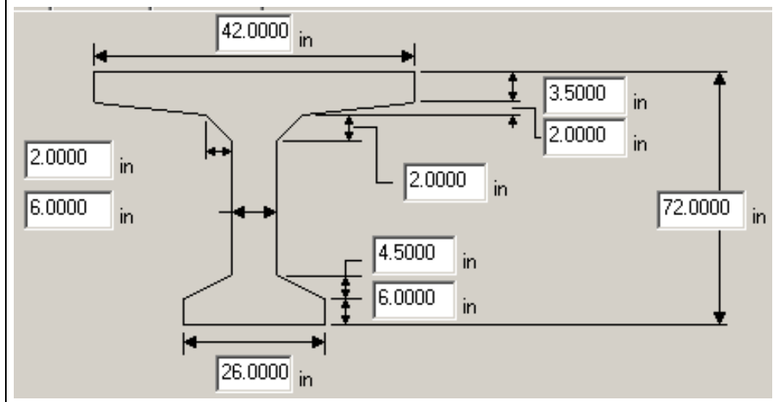

Cross-Section

Bridge #	Virtis BID #	Span length (ft)	t_{slab} (in)	Girder Spacing (ft)	Overhang Width (ft)	# of Girders	Skew (deg)	Materials				Dist. to Extreme Strands (in)		Harp Point (ft)	Beam Section
								P/S Tendons	f_c' (ksi)	$f_c'_I$ (ksi)	$f_c'_{deck}$ (ksi)	Bottom	Top		
8889	0549	90’-10¼”	8.5	10’-7”	3’-7” (L) 4’-1” (R)	4	70.6	36-0.5” Gr. 270 LR	7.0	5.5	4.0	2.5	2.5	36.74	BT-63

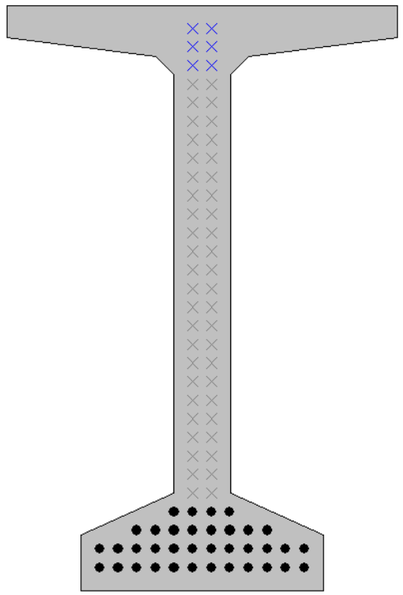

Strand Layout at Midspan

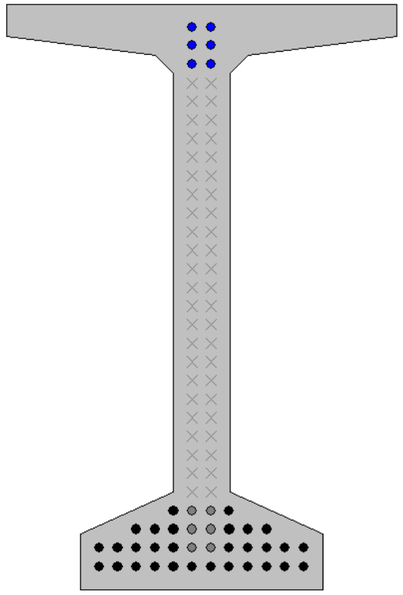

Strand Layout at Left Support

Strand Spacing:
Horizontal: 2”
Vertical: 2”

# of Strands: 36
Number of Harped Strands: 6
CG from bottom at Midspan: 4.72”
CG from bottom at Left Support: 13.39”

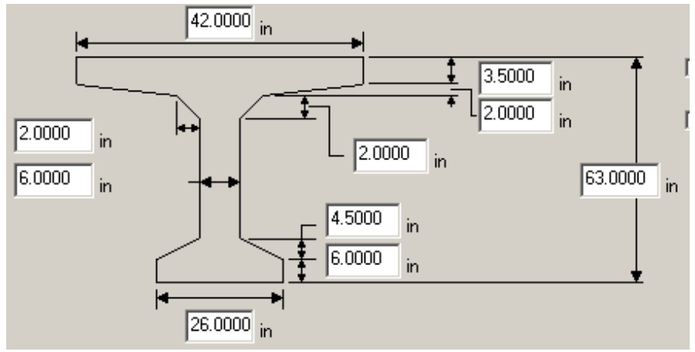

Cross-Section

Bridge #	Virtis BID #	Span length (ft)	t_{slab} (in)	Girder Spacing (ft)	Overhang Width (ft)	# of Girders	Skew (deg)	Materials				Dist. to Extreme Strands (in)		Harp Point (ft)	Beam Section
								P/S Tendons	f_c' (ksi)	$f_c'_l$ (ksi)	$f_c'_{deck}$ (ksi)	Bottom	Top		
8783	0553	141'-1¾"	8.5	7'-9"	3'-1"	8	96.9	46-0.6" Gr. 270 LR	8.0	6.0	4.0	2.0	2.0	57.78	AASHTO Type VI

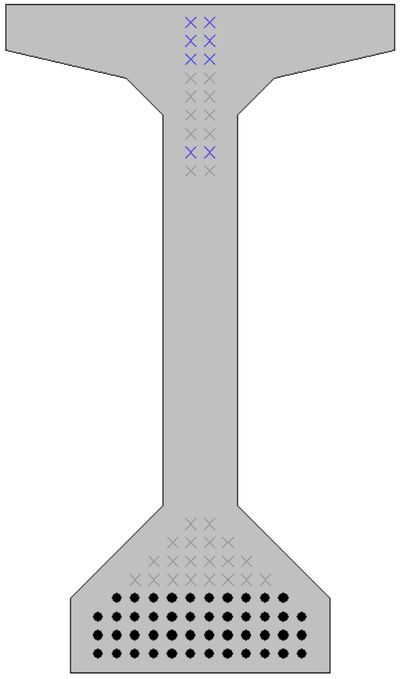

Strand Layout at Midspan

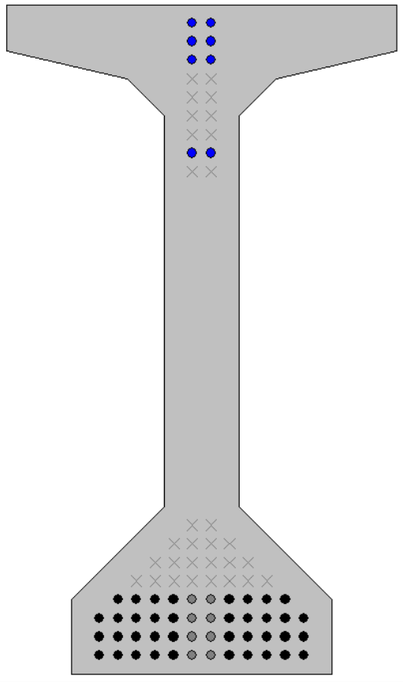

Strand Layout at Left Support

Strand Spacing:
Horizontal: 2"
Vertical: 2"

# of Strands: 46
Number of Harped Strands: 8
CG from bottom at Midspan: 4.87"
CG from bottom at Left Support: 15.30"

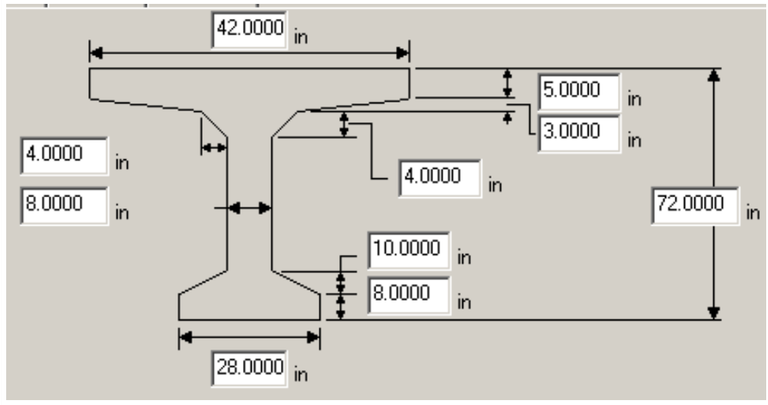

Cross-Section

Bridge #	Virtis BID #	Span length (ft)	t_{slab} (in)	Girder Spacing (ft)	Overhang Width (ft)	# of Girders	Skew (deg)	Materials				Dist. to Extreme Strands (in)		Harp Point (ft)	Beam Section
								P/S Tendons	f_c' (ksi)	f_{ci}' (ksi)	$f_{c\ deck}$' (ksi)	Bottom	Top		
15620	0561	119'-9 ¾"	9.4375	5'-4⅛"	3'-3⅜"	11	90	48-0.6" Gr. 270 LR	10.0	8.0	3.0	2.7559		N/A	Bulb Tee

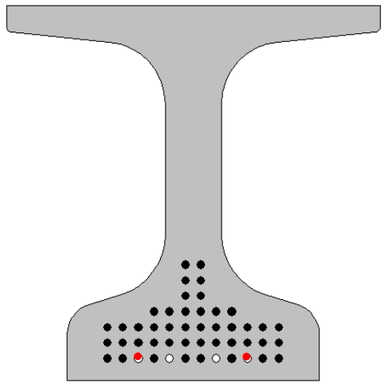

@ 51.57" from Left Support

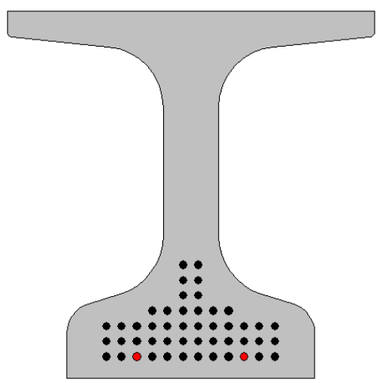

@75.20" from Left Support

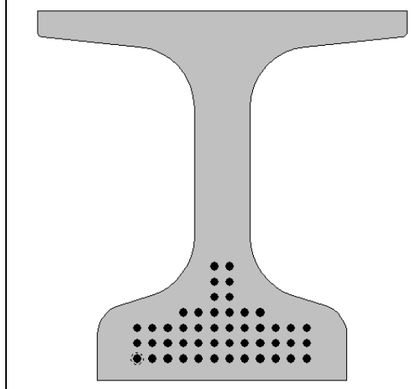

Strand Layout at Midspan

Strand Spacing:
Horizontal: 1.9685"
Vertical: 1.9685"

# of Strands: 48
Number of Harped Strands: 0
CG from bottom at 51.57": 6.51"
CG from bottom at 75.20": 6.35"
CG from bottom at Midspan: 6.20"

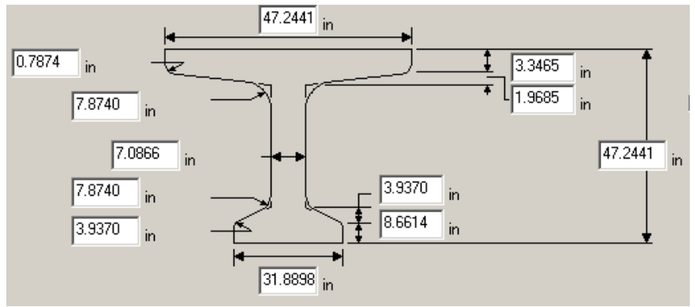

Cross-Section

C.3 Adjacent Precast Box Girders

Bridge #	Virtis BID #	Span length (ft)	t_{slab} (in)	Girder Spacing (ft)	Overhang Width (ft)	# of Girders	Skew (deg)	Materials: P/S Tendons	Materials: f_c' (ksi)	Materials: f_{ci}' (ksi)	Materials: $f_{c\,deck}'$ (ksi)	Dist. to Extreme Strands (in): Bottom	Dist. to Extreme Strands (in): Top	Harp Point (ft)	Beam Section
				3@4'-0½", 1@3'-6 ½", 2@3'-0 ½", 1@3'-6 ½", 3@4'-0 ½"				34-0.5" Gr. 270 SR				2.0		N/A	BIII-48
12807	0780	84'-0¼"	6.0		2'-4 ½"	11	48.0	28-0.5" Gr. 270 SR	6.0	4.8	3.0	2.0		N/A	BIII-36

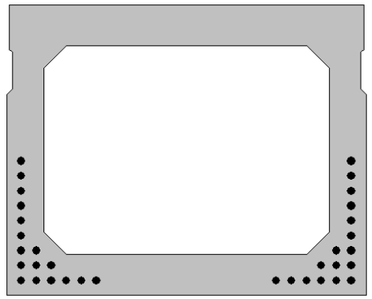

Strand Layout at Midspan

Strand Spacing:
Horizontal: 2"
Vertical: 2"

# of Strands: 34
CG from bottom at Midspan: 6.71"

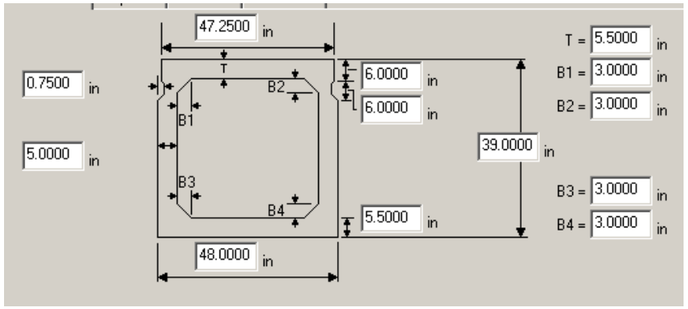

Cross-Section – BIII-48

Cross-Section – BIII-48

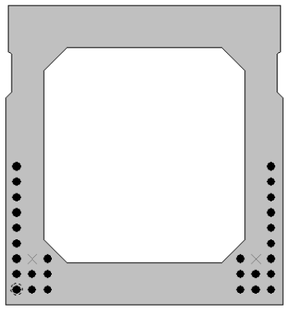

Strand Layout at Midspan

Strand Spacing:
Horizontal: 2"
Vertical: 2"

# of Strands: 28
CG from bottom at Midspan: 7.71"

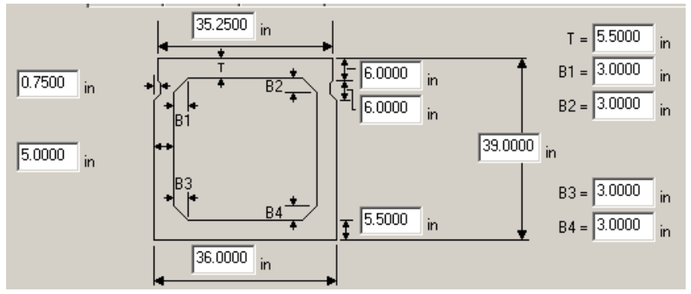

Cross-Section – BIII-36

Cross-Section – BIII-36

Bridge #	Virtis BID #	Span length (ft)	t_{slab} (in)	Girder Spacing (ft)	Overhang Width (ft)	# of Girders	Skew (deg)	Materials				Dist. to Extreme Strands (in)		Harp Point (ft)	Beam Section
								P/S Tendons	f_c' (ksi)	f_{ci}' (ksi)	$f_{c\,deck}$' (ksi)	Bottom	Top		
13788	0781	83'-0"	6.0	4'-0½"	2'-5"	9	56.8	32-0.5" Gr. 270 SR	6.0	4.8	3.0	2.0		N/A	BIV-48

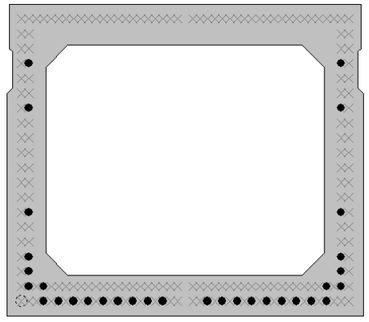

Strand Layout at Midspan

Strand Spacing:
Horizontal: 1"
Vertical: 2"

# of Strands: 32
CG from bottom at Midspan: 7.25"

Strand Layout at Left Support

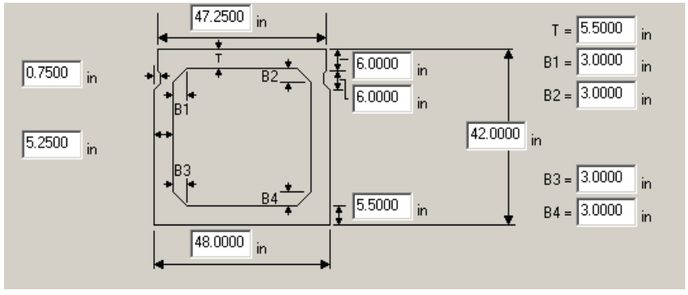

Cross-Section

Bridge #	Virtis BID #	Span length (ft)	t_{slab} (in)	Girder Spacing (ft)	Overhang Width (ft)	# of Girders	Skew (deg)	Materials				Dist. to Extreme Strands (in)		Harp Point (ft)	Beam Section
								P/S Tendons	f_c' (ksi)	$f_c'_l$ (ksi)	$f_c'_{deck}$ (ksi)	Bottom	Top		
15238	0782	73'-9⅞"	5.875	1@3'-6⅜", 9@4'-0⅜", 1@3'-6⅜"	1'-11 15/16"	12	90.0	34-0.5" Gr. 270 SR	6.5	5.2	3.0	1.9685	5.118	N/A	BII-48
								26-0.5" Gr. 270 SR				1.9685	5.118	N/A	BII-36

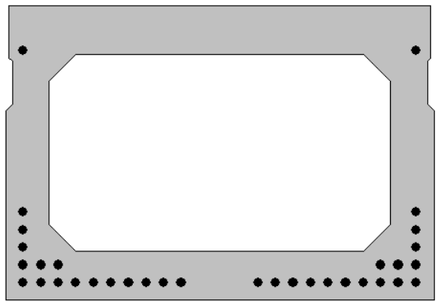

Strand Layout at Midspan

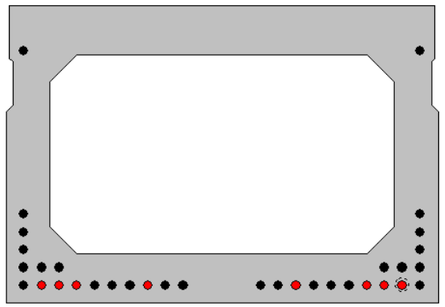

@94.49" from Left Support

Strand Spacing:
Horizontal: 1.9685"
Vertical: 1.9685"

# of Strands: 34
CG from bottom at 94.49": 5.78"
CG from bottom at Midspan: 4.89"

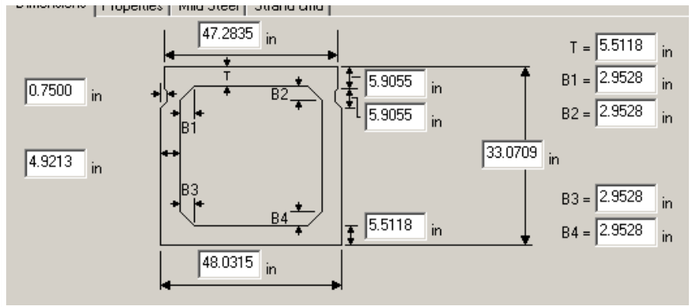

Cross-Section – BII-48

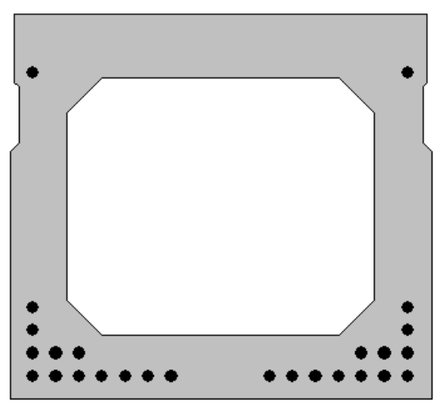

Strand Layout at Midspan

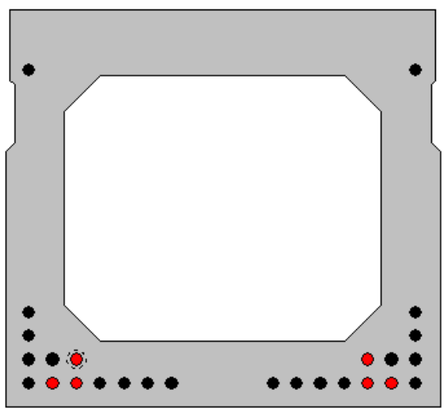

@94.49" from Left Support

Strand Spacing:
Horizontal: 1.9685"
Vertical: 1.9685"

# of Strands: 26
CG from bottom at 94.49": 5.94"
CG from bottom at Midspan: 5.18"

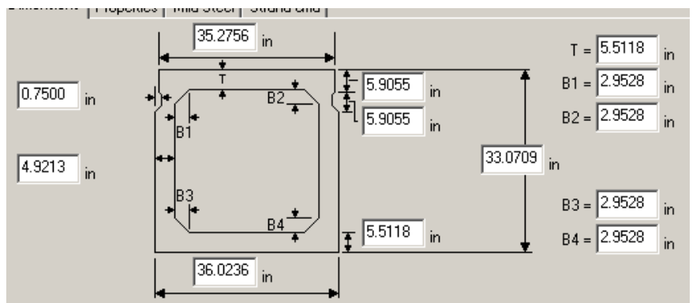

Cross-Section – BII-36

Bridge #	Virtis BID #	Span length (ft)	t_{slab} (in)	Girder Spacing (ft)	Overhang Width (ft)	# of Girders	Skew (deg)	Materials				Dist. to Extreme Strands (in)		Harp Point (ft)	Beam Section
								P/S Tendons	f_c' (ksi)	$f_c'_I$ (ksi)	$f_{c\ deck}'$ (ksi)	Bottom	Top		
				1@3'-6⅜", 9@4'-0⅜", 1@3'-6⅜"				34-0.5" Gr. 270 SR				1.9685	5.118	N/A	BII-48
15238	0782	73'-9⅞"	5.875		1'-11 15/16"	12	90.0	26-0.5" Gr. 270 SR	6.5	5.2	3.0	1.9685	5.118	N/A	BII-36
Strand Layout at Midspan				Cross-Section – BII-36								Cross-Section – BII-36			

Bridge #	Virtis BID #	Span length (ft)	t_{slab} (in)	Girder Spacing (ft)	Overhang Width (ft)	# of Girders	Skew (deg)	Materials				Dist. to Extreme Strands (in)		Harp Point (ft)	Beam Section
								P/S Tendons	f_c' (ksi)	$f_c'_I$ (ksi)	$f_{c\ deck}'$ (ksi)	Bottom	Top		
9314	0783	83'-8"	6.0	3'-1½"	1'-6"	16	90.0	22-0.6" Gr. 270 LR	5.2	5.0	4.0	2		N/A	27x36 Box Beam

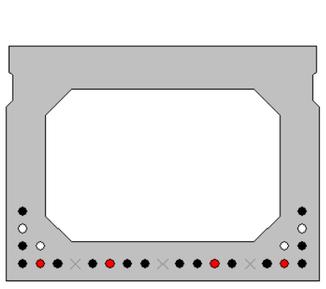

@ left support to 96" from left support

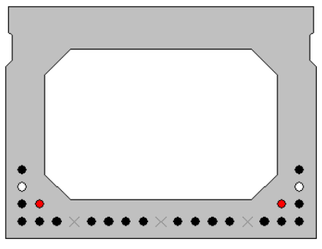

@ 156" from left support

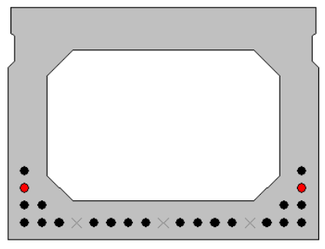

@ 240" from left support

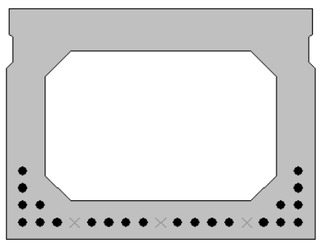

Strand Layout at Midspan

Strand Spacing:
Horizontal: 2"
Vertical: 2"

# of Strands: 22
CG from bottom at Left Support to 96": 3.14"
CG from bottom at 156": 2.89"
CG from bottom at 240": 3.00"
CG from bottom at Midspan: 3.27"

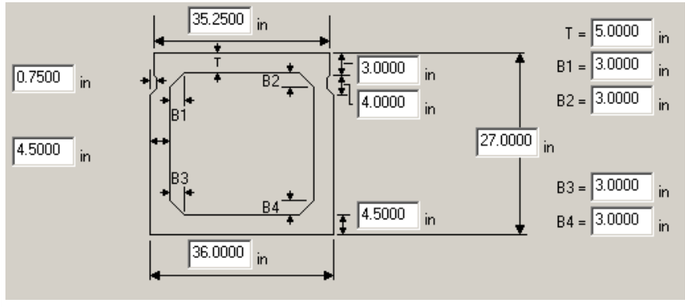

Cross-Section (Interior)

Bridge #	Virtis BID #	Span length (ft)	t_{slab} (in)	Girder Spacing (ft)	Overhang Width (ft)	# of Girders	Skew (deg)	Materials				Dist. to Extreme Strands (in)		Harp Point (ft)	Beam Section
								P/S Tendons	f_c' (ksi)	$f_c'_I$ (ksi)	$f_c'_{deck}$ (ksi)	Bottom	Top		
9314	0783	83’-8”	6.0	3’-1½”	1’-6”	16	90.0	22-0.6” Gr. 270 LR	5.2	5.0	4.0	2		N/A	27x36 Box Beam

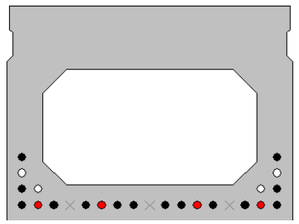	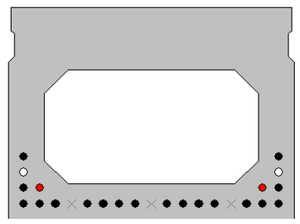	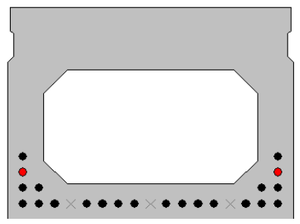	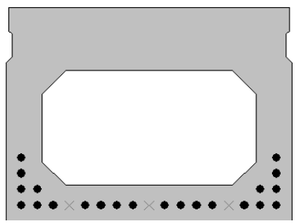	Strand Spacing: Horizontal: 2” Vertical: 2” # of Strands: 22 CG from bottom at Left Support to 96”: 3.14” CG from bottom at 156”: 2.89” CG from bottom at 240”: 3.00” CG from bottom at Midspan: 3.27” 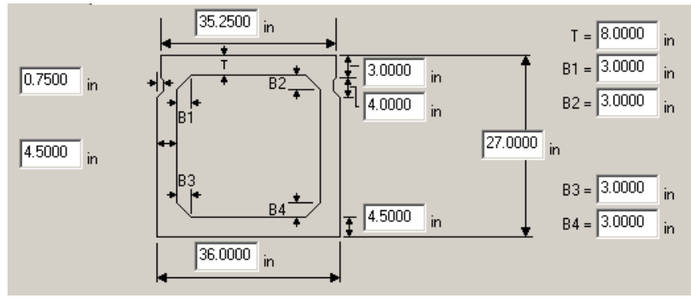
@ left support to 96” from left support	@ 156” from left support	@ 240” from left support	Strand Layout at Midspan	Cross-Section (Exterior)

Bridge #	Virtis BID #	Span length (ft)	t_{slab} (in)	Girder Spacing (ft)	Overhang Width (ft)	# of Girders	Skew (deg)	Materials				Dist. to Extreme Strands (in)		Harp Point (ft)	Beam Section
								P/S Tendons	f_c' (ksi)	f_{ci}' (ksi)	$f_{c\,deck}$' (ksi)	Bottom	Top		
17075	0785	107'-0"	6.0	4'-0"	2'-7½"	10	90	44-0.5" Gr. 270 SR	6.0	4.8	3.3	2.0		N/A	BIV-48

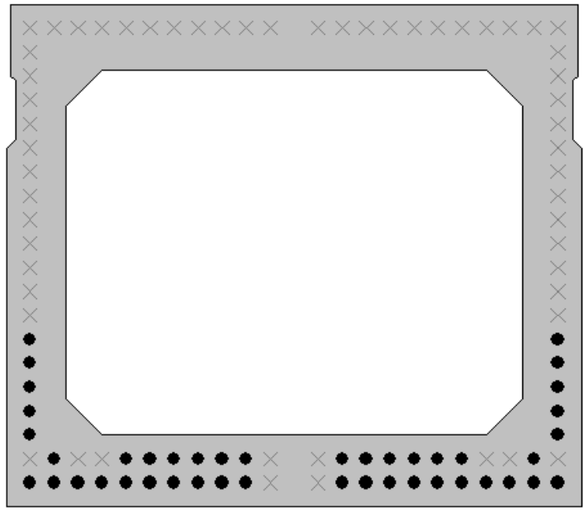

Strand Layout at Midspan

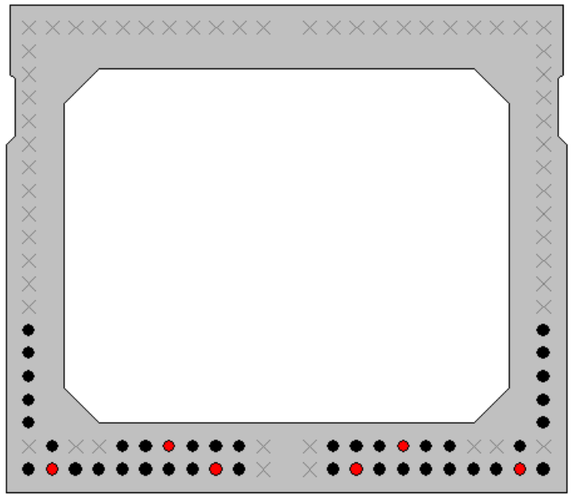

Strand Layout at Left Support to 138"

Strand Spacing:
Horizontal: 2"
Vertical: 2"

# of Strands: 44
CG from bottom at left support to 138": 4.74"
CG from bottom at Midspan: 4.45"

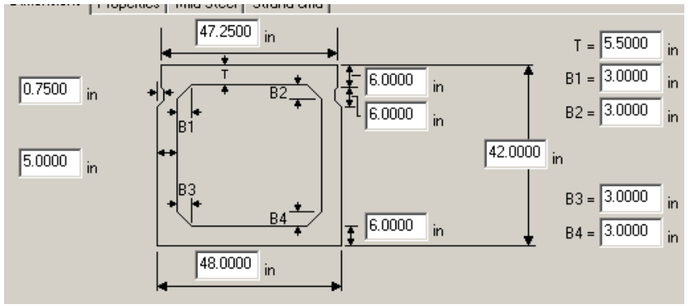

Cross-Section

Bridge #	Virtis BID #	Span length (ft)	t_{slab} (in)	Girder Spacing (ft)	Overhang Width (ft)	# of Girders	Skew (deg)	Materials				Dist. to Extreme Strands (in)		Harp Point (ft)	Beam Section
								P/S Tendons	f_c' (ksi)	f_{ci}' (ksi)	$f_{c\,deck}$' (ksi)	Bottom	Top		
17175	0786	88'-9"	6.0	1@4'-0", 1@3'-6", 2@3'-0", 1@3'-6", 1@4'-0"	2'-6"	7	90.0	44-0.5" Gr. 270 SR	6.0	4.8	3.0	2.0	7.0	N/A	BII-48
								38-0.5" Gr. 270 SR				2	7.0	N/A	BII-36

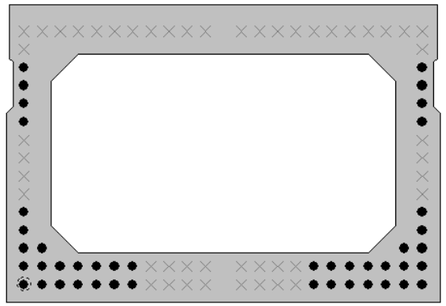

Strand Spacing:
Horizontal: 2"
Vertical: 2"

# of Strands: 44
CG from bottom at Midspan: 7.45"

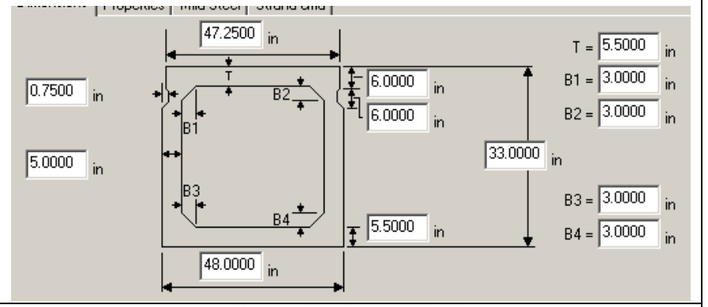

Strand Layout at Midspan – 4'Box | Cross-Section – BII 48 | Cross-Section – BII 48

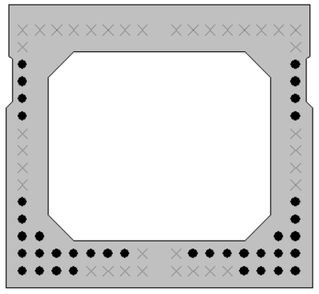

Strand Spacing:
Horizontal: 2"
Vertical: 2"

# of Strands: 38
CG from bottom at Midspan: 8.32"

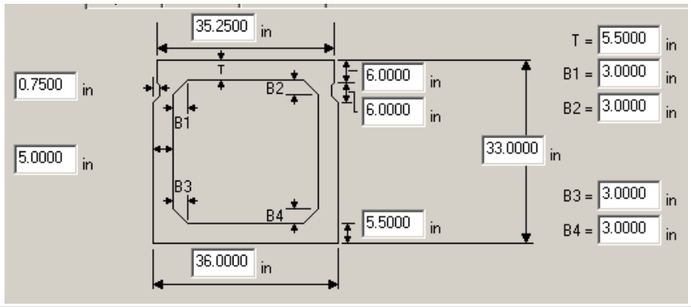

Strand Layout at Midspan -3' Interior Box | Cross-Section – BII-36 | Cross-Section – BII-36

Bridge #	Virtis BID #	Span length (ft)	t_{slab} (in)	Girder Spacing (ft)	Overhang Width (ft)	# of Girders	Skew (deg)	Materials				Dist. to Extreme Strands (in)		Harp Point (ft)	Beam Section
								P/S Tendons	f_c' (ksi)	$f_c'_I$ (ksi)	f_c'$_{deck}$ (ksi)	Bottom	Top		
13805	0681	52'-6"	3.5	4'-0 11/16"	2'-0" (L), 1'-11 3/16" (R)	7	75	24-0.5" Gr. 270 SR	5.0	4.0	3.0	2.0	3.0	N/A	BI-48

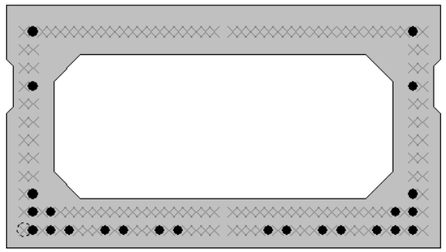

Strand Layout at Midspan

Strand Spacing:
Horizontal: 1"
Vertical: 2"

# of Strands: 24
CG from bottom at Midspan: 5.83"

Cross-Section

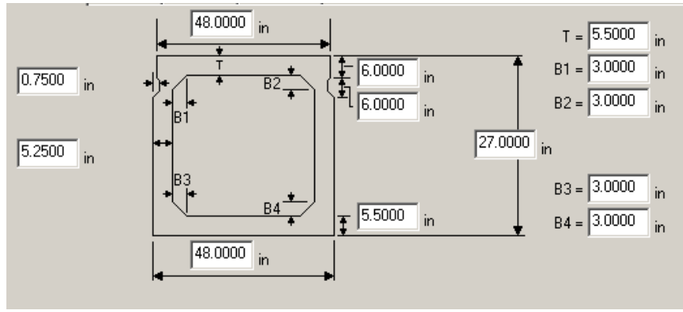

Cross-Section

Bridge #	Virtis BID #	Span length (ft)	t_{slab} (in)	Girder Spacing (ft)	Overhang Width (ft)	# of Girders	Skew (deg)	Materials				Dist. to Extreme Strands (in)		Harp Point (ft)	Beam Section
								P/S Tendons	f_c' (ksi)	$f_c'_I$ (ksi)	f_c'$_{deck}$ (ksi)	Bottom	Top		
14246	0684	52'-0"	6.0	4'-0½"	2'-4¼"	8	90.0	24-0.5" Gr. 270 SR	5.0	4.0	3.0	2.0	3.0	N/A	BI-48

Strand Layout at Midspan

Strand Spacing:
Horizontal: 2"
Vertical: 2"

# of Strands: 24
CG from bottom at Midspan: 7.50"

Cross-Section

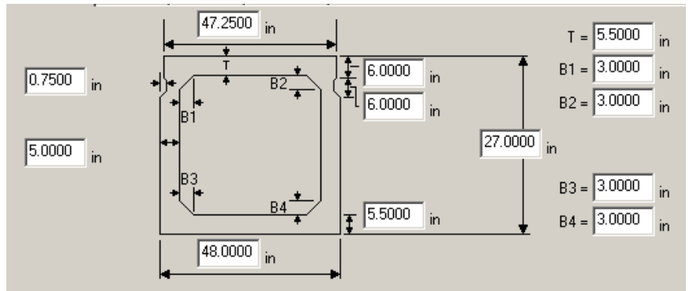

Cross-Section

Bridge #	Virtis BID #	Span length (ft)	t_{slab} (in)	Girder Spacing (ft)	Overhang Width (ft)	# of Girders	Skew (deg)	Materials				Dist. to Extreme Strands (in)		Harp Point (ft)	Beam Section
								P/S Tendons	f_c' (ksi)	$f_{c'l}$ (ksi)	$f_{c'deck}$ (ksi)	Bottom	Top		
9180	0690	44'-8⅜"	5.875	3'-1 ½"	1'-6"	27	78.6	13-0.6" Gr. 270 LR	5.0	4.0	4.0	1.9685		N/A	MDOT 535x915

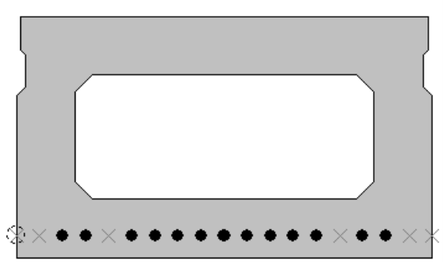

Strand Layout at Midspan

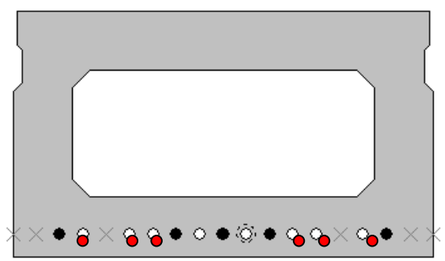

Strand layout at 59.055"

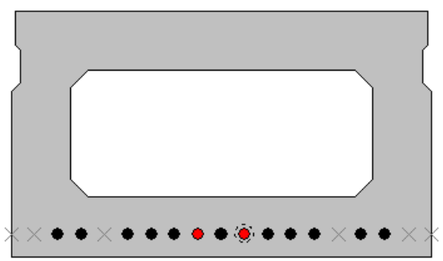

Strand layout at 98.425"

Strand Spacing:
Horizontal: 2"

# of Strands: 13
CG from bottom at left support: 1.97"
CG from bottom at 98.425": 1.97"
CG from bottom at Midspan: 1.97"

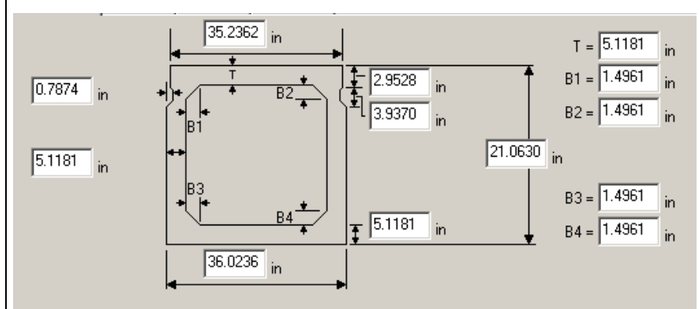

Cross-Section

Bridge #	Virtis BID #	Span length (ft)	t_{slab} (in)	Girder Spacing (ft)	Overhang Width (ft)	# of Girders	Skew (deg)	Materials				Dist. to Extreme Strands (in)		Harp Point (ft)	Beam Section
								P/S Tendons	f_c' (ksi)	f_{ci}' (ksi)	$f_{c\,deck}$' (ksi)	Bottom	Top		
				1@4'-0", 4@3'-6", 1@4'-0"				24-0.5" Gr. 270 SR				1.9685		N/A	4' Box
17042	0693	50'-0⅜"	5.875		2'-5 7/16"	7	57.0	20-0.5" Gr. 270 SR	6.0	4.8	3.0	1.9685	5.118	N/A	3' Box

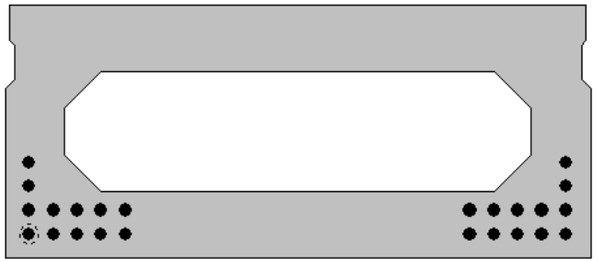

Strand Spacing:
Horizontal: 1.9685"
Vertical: 1.9685"

# of Strands: 24
CG from bottom at Midspan: 3.61"

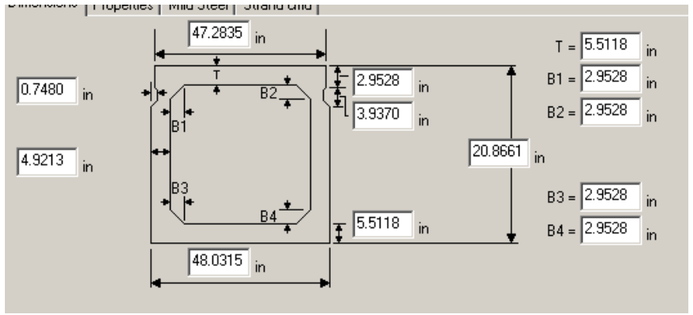

Strand Layout at Midspan – 4'Box | Cross-Section – 4' Box | Cross-Section – 4' Box

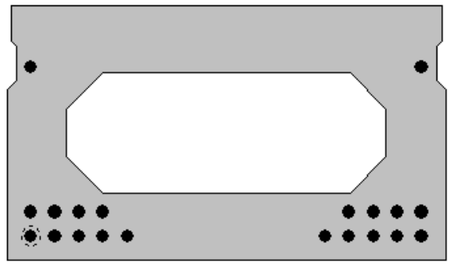

Strand Spacing:
Horizontal: 1.9685"
Vertical: 1.9685"

# of Strands: 20
CG from bottom at Midspan: 4.13"

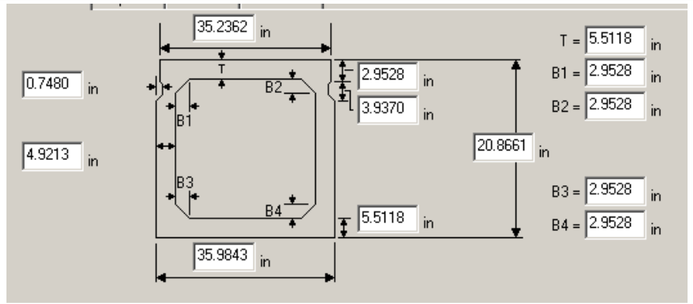

Strand Layout at Midspan -3' Interior Box | Cross-Section – 3' Box | Cross-Section – 3' Box

Bridge #	Virtis BID #	Span length (ft)	t_{slab} (in)	Girder Spacing (ft)	Overhang Width (ft)	# of Girders	Skew (deg)	Materials				Dist. to Extreme Strands (in)		Harp Point (ft)	Beam Section
								P/S Tendons	f_c' (ksi)	f_c'$_I$ (ksi)	f_c'$_{deck}$ (ksi)	Bottom	Top		
9191	0736	72'-6"	6.0	3'-1 11/16"	1'-7 ½"	15	60.0	20-0.5" Gr. 270 LR	5.5	4.0	4.0	2.0		N/A	27x36 Box Beam

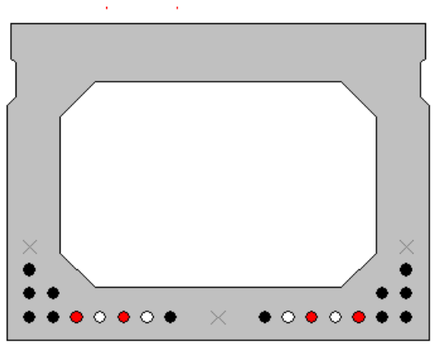

@ 66.00" from left support

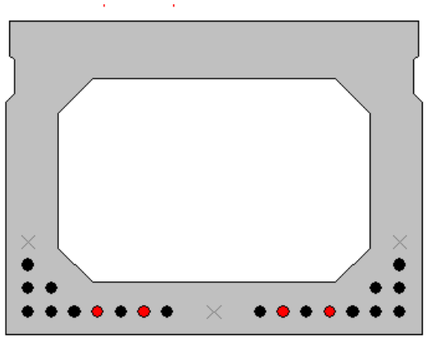

@ 114" from left support

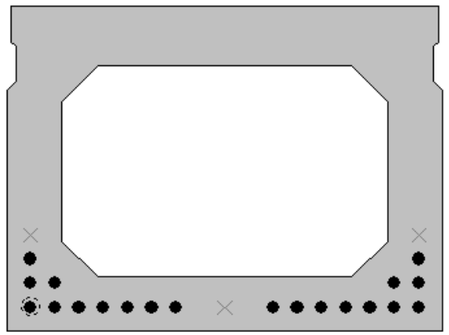

Strand Layout at Midspan

Strand Spacing:
Horizontal: 2"
Vertical: 2"

# of Strands: 20
CG from bottom at 66.00": 3.33"
CG from bottom at 114": 3.00"
CG from bottom at Midspan: 2.80"

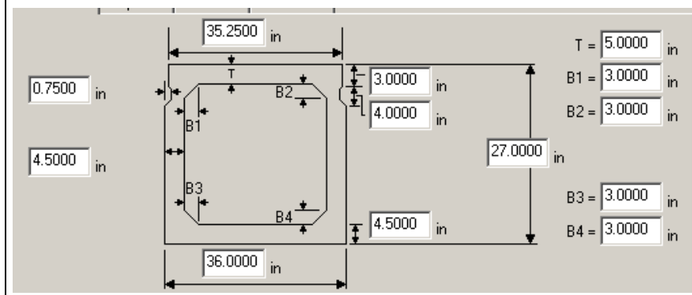

Cross-Section

Bridge #	Virtis BID #	Span length (ft)	t_{slab} (in)	Girder Spacing (ft)	Overhang Width (ft)	# of Girders	Skew (deg)	Materials				Dist. to Extreme Strands (in)		Harp Point (ft)	Beam Section
								P/S Tendons	f_c' (ksi)	f_{ci}' (ksi)	$f_{c\,deck}$' (ksi)	Bottom	Top		
16799	0737	84'-0"	0.0	4'-0"	2'-1 ½"	5	90.0	38-0.5" Gr. 270 LR	5.0	4.0	3.3	2.0		N/A	

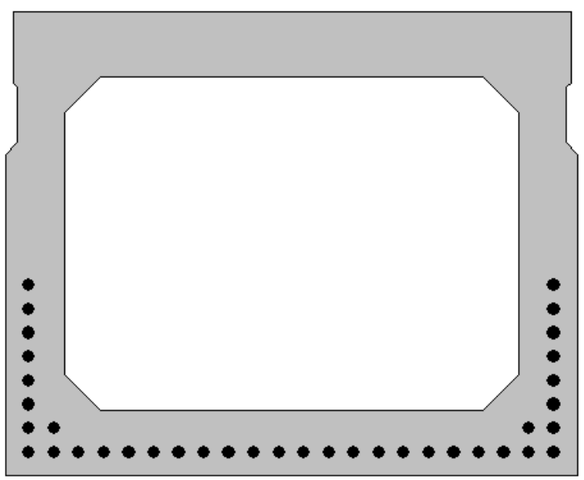

Strand Layout at Midspan

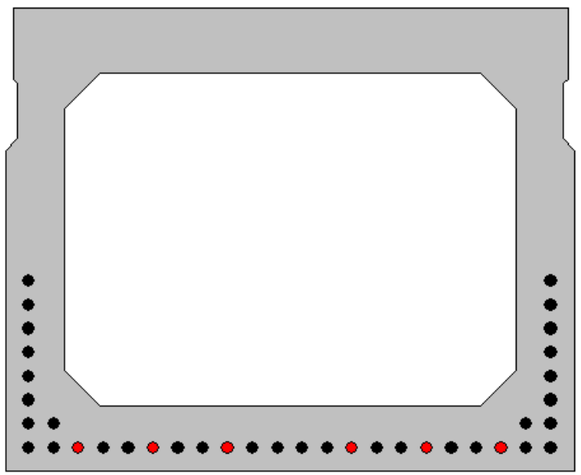

Strand layout at Support to 13.25"

Strand Spacing:
Horizontal: 2.0952"
Vertical: 2"

# of Strands: 38
CG from bottom at left support: 5.63"
CG from bottom at Midspan: 5.05"

Interior:

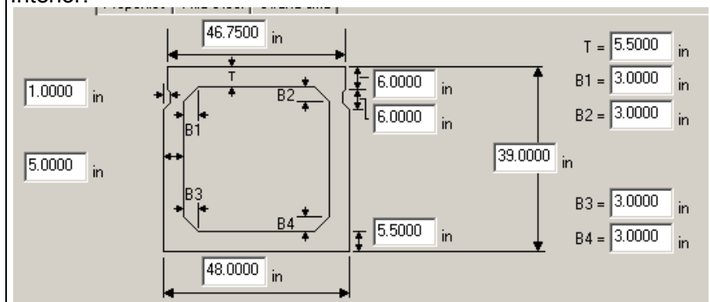

Exterior:

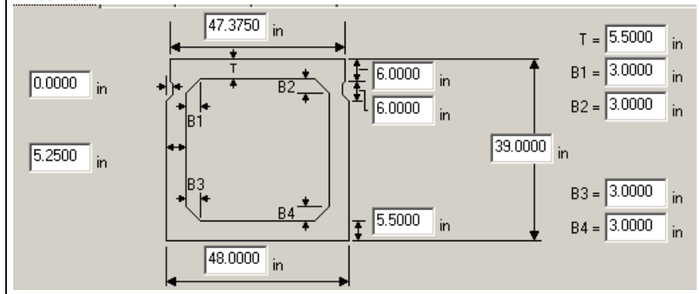

Cross-Section

Bridge #	Virtis BID #	Span length (ft)	t_{slab} (in)	Girder Spacing (ft)	Overhang Width (ft)	# of Girders	Skew (deg)	Materials				Dist. to Extreme Strands (in)		Harp Point (ft)	Beam Section
								P/S Tendons	f_c' (ksi)	f_{ci}' (ksi)	$f_{c\,deck}$' (ksi)	Bottom	Top		
14987	0738	73'-0"	6.0	3@4'-0¾", 1@4'-7¼"	2'-3" (L) 2'-6" (R)	5	99.7	34-0.5" Gr. 270 SR	5.0	4.0	3.3	2.0	8	N/A	BIV-48

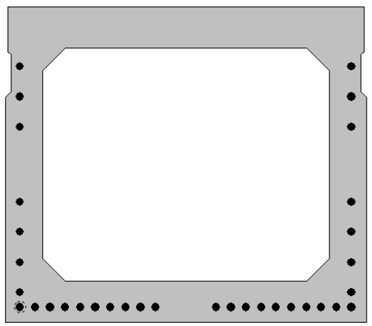

Strand Layout at Midspan

Strand Spacing:
Horizontal: 2"
Vertical: 2", 4"

# of Strands: 34
CG from bottom at Midspan: 8.82"

Cross-Section

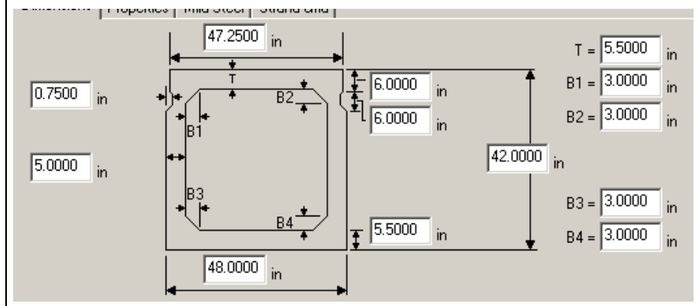

Cross-Section

Bridge #	Virtis BID #	Span length (ft)	t_{slab} (in)	Girder Spacing (ft)	Overhang Width (ft)	# of Girders	Skew (deg)	Materials				Dist. to Extreme Strands (in)		Harp Point (ft)	Beam Section
								P/S Tendons	f_c' (ksi)	$f_c'_I$ (ksi)	$f_c'_{deck}$ (ksi)	Bottom	Top		
12809	0739	82'-0"	6.0	3@4'-0 ½",1@ 3'-6 ½", 2@3'-0 ½", 1@3'-6 ½", 3@4'-0 ½"	2'-4 ¾"	11	90.0	28-0.5" Gr. 270 SR	5.0	4.0	3.0	2.0		N/A	BII-36
								36-0.5" Gr. 270 SR				2.0		N/A	BII-48

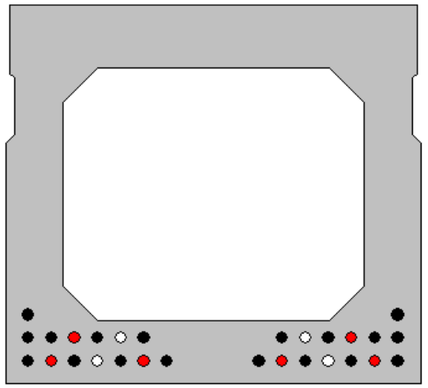

Strand Layout at 72" from Left Support

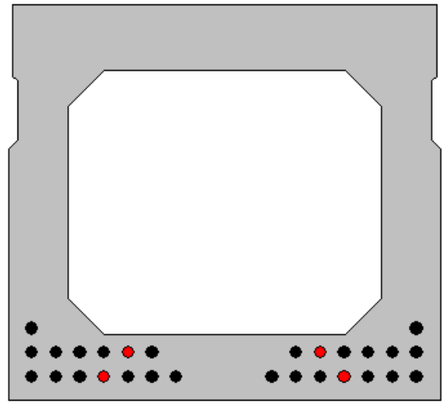

Strand Layout at 120" from Left Support

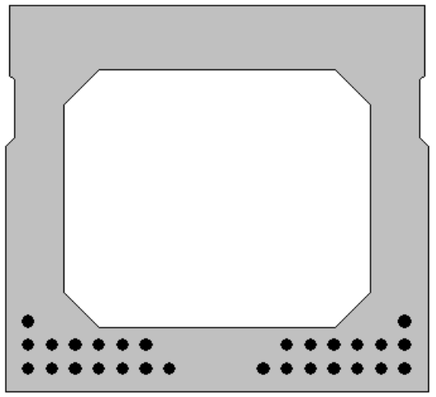

Strand Layout at Midspan- BII-36

Strand Spacing:
Horizontal: 2"
Vertical: 2"
# of Strands: 28
CG from bottom at 72": 3.33"
CG from bottom at 120": 3.17"
CG from bottom at Midspan: 3.14"

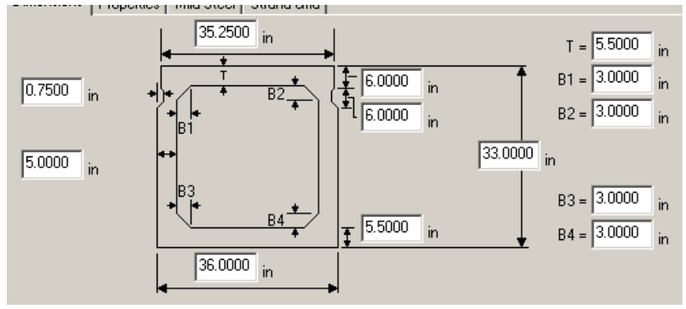

Cross-Section – BII-36

Strand Spacing:
Horizontal: 2"
Vertical: 2", 8"
# of Strands: 36

CG from bottom at 72": 3.38"
CG from bottom at 144": 3.33"
CG from bottom at Midspan: 3.33"

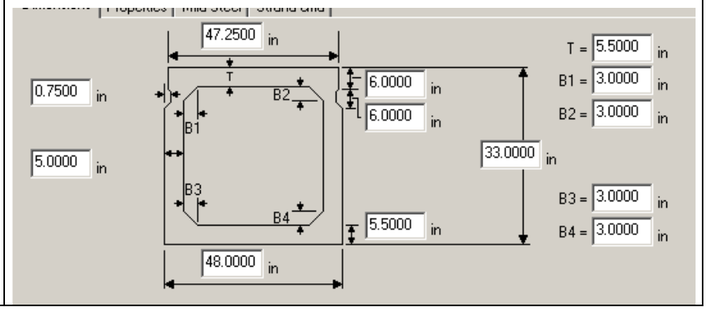

Bridge #	Virtis BID #	Span length (ft)	t_{slab} (in)	Girder Spacing (ft)	Overhang Width (ft)	# of Girders	Skew (deg)	Materials				Dist. to Extreme Strands (in)		Harp Point (ft)	Beam Section
								P/S Tendons	f_c' (ksi)	f_{ci}' (ksi)	$f_{c\,deck}'$ (ksi)	Bottom	Top		
12809	0739	82’-0”	6.0	3@4’-0 ½”,1@ 3’-6 ½”, 2@3’-0 ½”, 1@3’-6 ½”, 3@4’-0 ½”	2’-4 ¾”	11	90.0	28-0.5” Gr. 270 SR	5.0	4.0	3.0	2.0		N/A	BII-36
								36-0.5” Gr. 270 SR				2.0		N/A	BII-48

Strand Layout at 72” from Left Support	Strand Layout at 144” from Left Support	Strand Layout at Midspan - BII-48	Cross-Section – BII-48

Bridge #	Virtis BID #	Span length (ft)	t_{slab} (in)	Girder Spacing (ft)	Overhang Width (ft)	# of Girders	Skew (deg)	Materials				Dist. to Extreme Strands (in)		Harp Point (ft)	Beam Section
								P/S Tendons	f_c' (ksi)	f_{ci}' (ksi)	$f_{c\,deck}'$ (ksi)	Bottom	Top		
12952	0741	79’-11 ½”	8.25	1@4’-0½”, 10@3’-6½”, 1@4’-0½”	2’-4”	13	59.8	42-0.5” Gr. 270 LR	6.0	4.8	3.0	2.0	2.0	N/A	BIV-48
								30-0.5” Gr. 270 LR				2.0	2.0	N/A	BIV-36

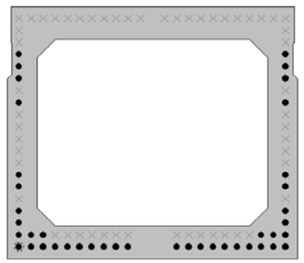

Strand Spacing:
Horizontal: 2”
Vertical: 2”

# of Strands: 42
CG from bottom at Midspan: 9.24”

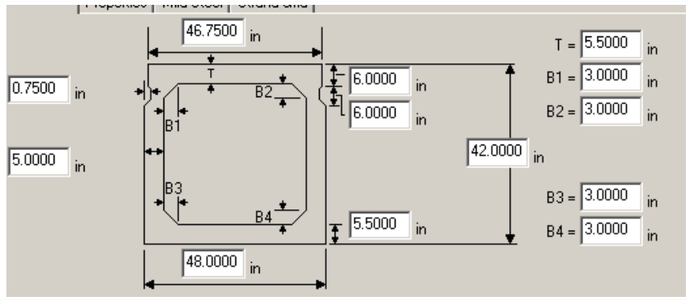

Strand Layout at Midspan – BIV-48	Cross-Section – BIV-48	Cross-Section – BIV-48

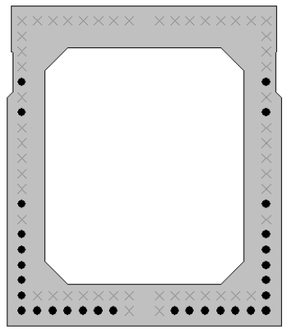

Strand Spacing:
Horizontal: 2”
Vertical: 2”

# of Strands: 30
CG from bottom at Midspan: 8.67”

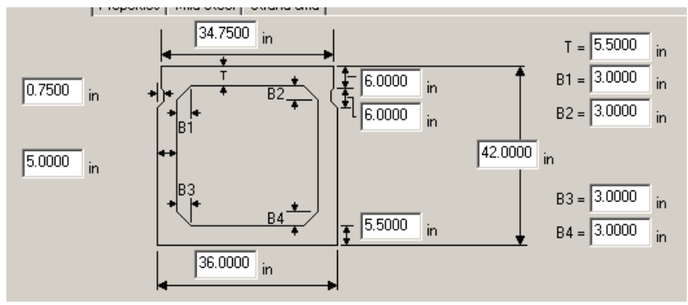

Strand Layout at Midspan - BIV-36	Cross-Section – BIV-36	Cross-Section – BIV-36

Bridge #	Virtis BID #	Span length (ft)	t_{slab} (in)	Girder Spacing (ft)	Overhang Width (ft)	# of Girders	Skew (deg)	Materials				Dist. to Extreme Strands (in)		Harp Point (ft)	Beam Section
								P/S Tendons	f_c' (ksi)	f_{ci}' (ksi)	$f_{c\,deck}$' (ksi)	Bottom	Top		
17143	0742	70'-0"	6.0	1@4'-0", 2@3'-6", 1@4'-0"	2'-6"	5	90	30-0.5" Gr. 270 SR	5.0	4.0	3.0	2.0	7.0	N/A	BIII-48
								26-0.5" Gr. 270 SR				2.0	7.0	N/A	BIII-36

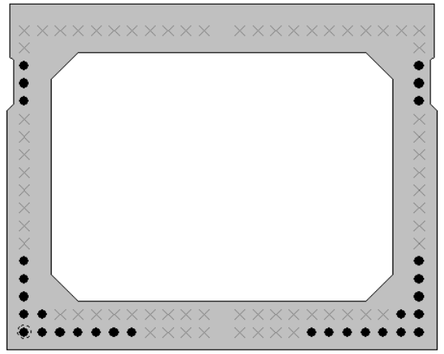

Strand Layout at Midspan – 4'Box

Strand Spacing:
Horizontal: 2"
Vertical: 2"

# of Strands: 30
CG from bottom at Midspan: 9.07"

Cross-Section – BIII-48

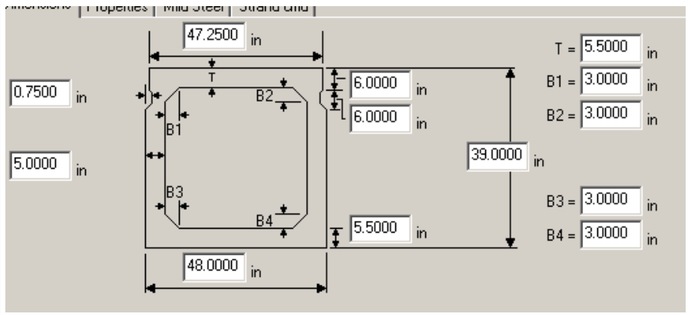

Cross-Section – BIII-48

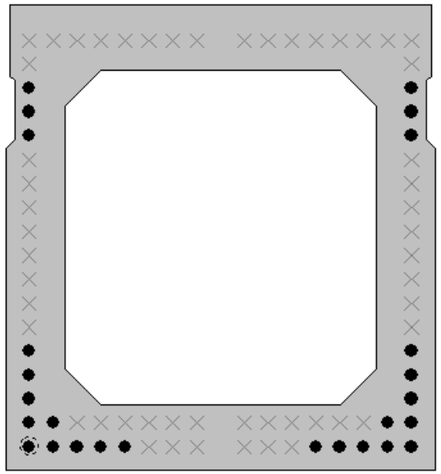

Strand Layout at Midspan

Strand Spacing:
Horizontal: 2"
Vertical: 2"

# of Strands: 26
CG from bottom at Midspan: 10.15"

Cross-Section – BIII-36

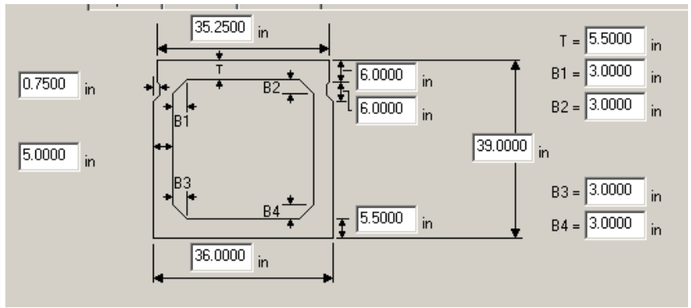

Cross-Section – BIII-36

Bridge #	Virtis BID #	Span length (ft)	t_{slab} (in)	Girder Spacing (ft)	Overhang Width (ft)	# of Girders	Skew (deg)	Materials				Dist. to Extreme Strands (in)		Harp Point (ft)	Beam Section
								P/S Tendons	f_c' (ksi)	f_{ci}' (ksi)	$f_{c\,deck}$' (ksi)	Bottom	Top		
9181	0743	60'-4⅜"	5.875	3'-1⅝"	1'-7⅛"	15	90.0	21-0.5" Gr. 270 LR	6.5	5.0	4.0	1.9685		N/A	MDOT 535x915

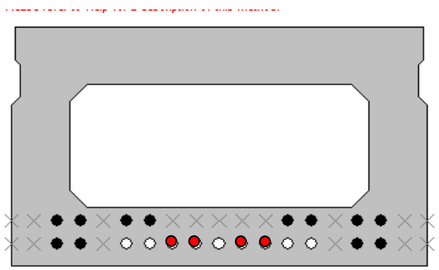

@ 36.02" from left support

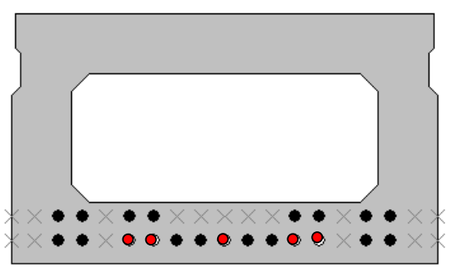

@ 72.05" from left support

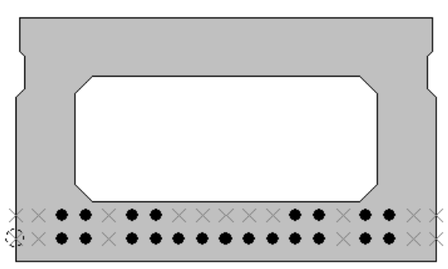

Strand Layout at Midspan

Strand Spacing:
Horizontal: 2"
Vertical: 2.0079"

# of Strands: 21
CG from bottom at 36.02": 3.31"
CG from bottom at 72.05": 2.97"
CG from bottom at Midspan: 2.73"

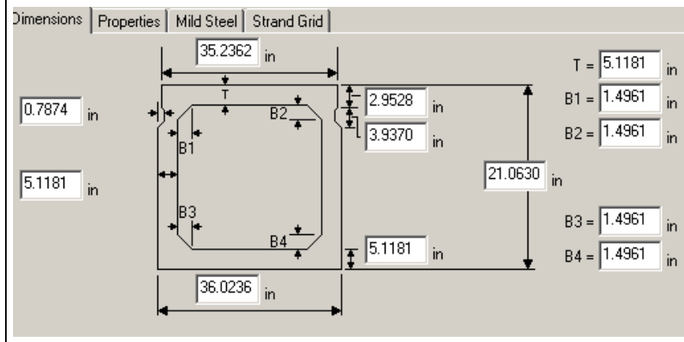

Cross-Section

Bridge #	Virtis BID #	Span length (ft)	t_{slab} (in)	Girder Spacing (ft)	Overhang Width (ft)	# of Girders	Skew (deg)	Materials				Dist. to Extreme Strands (in)		Harp Point (ft)	Beam Section
								P/S Tendons	f_c' (ksi)	f_{ci}' (ksi)	$f_{c\,deck}'$ (ksi)	Bottom	Top		
9071	0745	83'-7⅝"	5.875	3'-1⅜"	1'-6⅛"	15	120.0	16-0.6" Gr. 270 LR	5.0	3.5	4.0	2.0		N/A	MDOT 840x915

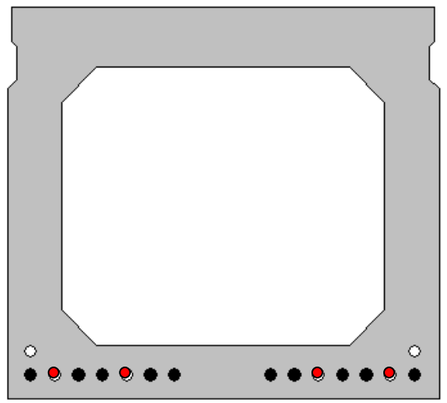

@ 157.5" from left support

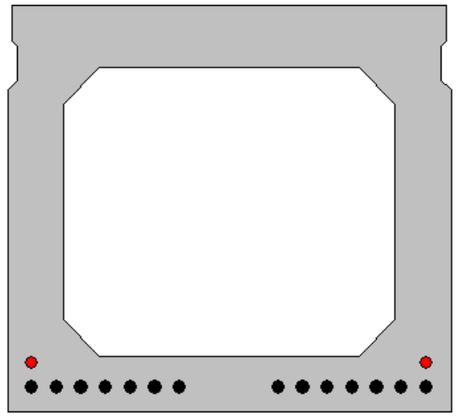

@ 248.0" from left support

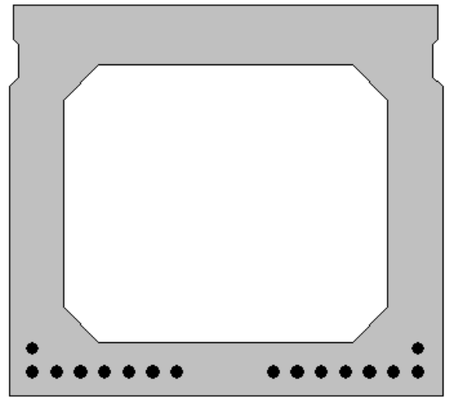

Strand Layout at Midspan

Strand Spacing:
Horizontal: 2"
Vertical: 2"

# of Strands: 16
CG from bottom at 157.5": 2.00"
CG from bottom at 248": 2.00"
CG from bottom at Midspan: 2.25"

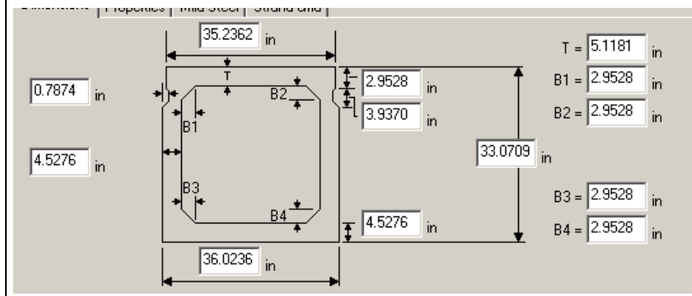

Cross-Section

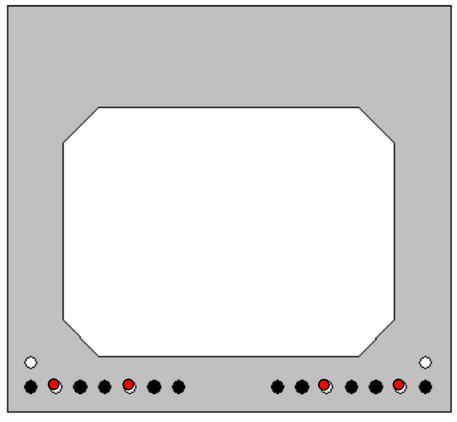

@ 157.5" from left support

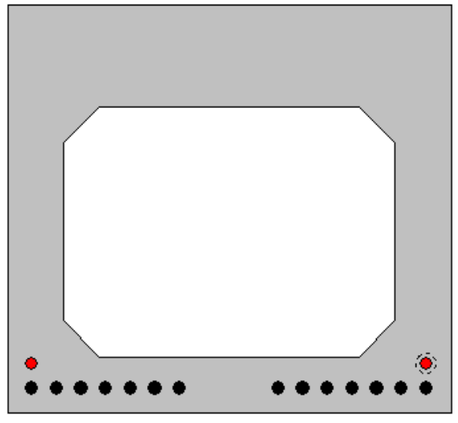

@ 248.0" from left support

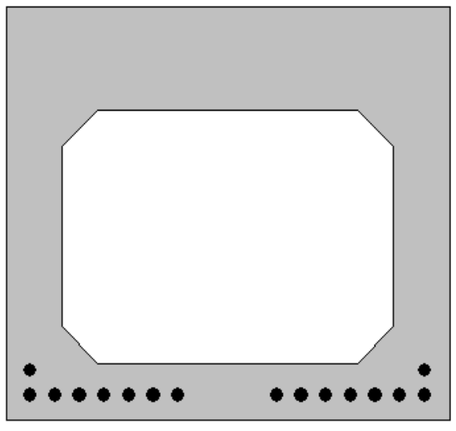

Strand Layout at Midspan

Strand Spacing:
Horizontal: 2"
Vertical: 2"

# of Strands: 16
CG from bottom at 157.5": 2.00"
CG from bottom at 248": 2.25"
CG from bottom at Midspan: 2.25"

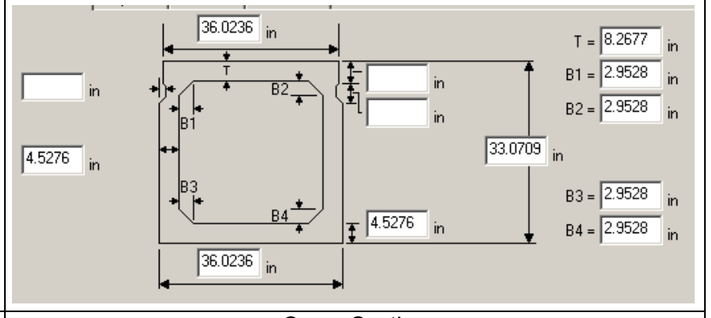

Cross-Section

Bridge #	Virtis BID #	Span length (ft)	t_{slab} (in)	Girder Spacing (ft)	Overhang Width (ft)	# of Girders	Skew (deg)	Materials				Dist. to Extreme Strands (in)		Harp Point (ft)	Beam Section
								P/S Tendons	f_c' (ksi)	f_c'$_l$ (ksi)	f_c'$_{deck}$ (ksi)	Bottom	Top		
9167	0746	75'-6¾"	5.875	4'-1½"	2'-1⅝"	12	120.0	22-0.6" Gr. 270 LR	5.0	4.0	4.0	1.9685		N/A	MDOT 685x1220

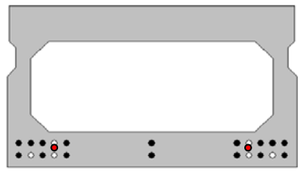

@ 63.0" from left support

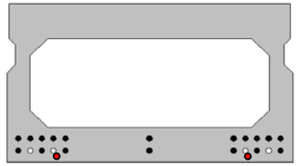

@ 118.11" from left support

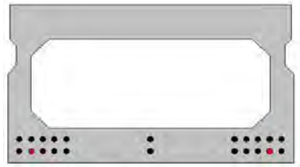

@ 185.04" from left support

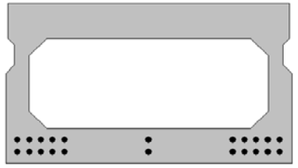

Strand Layout at Midspan

Strand Spacing:
Horizontal: 1.9685"
Vertical: 2.0079"

# of Strands: 22
CG from bottom at 63.0": 3.10"
CG from bottom at 118.125": 3.20"
CG from bottom at 185.04": 3.07"
CG from bottom at Midspan: 2.97"

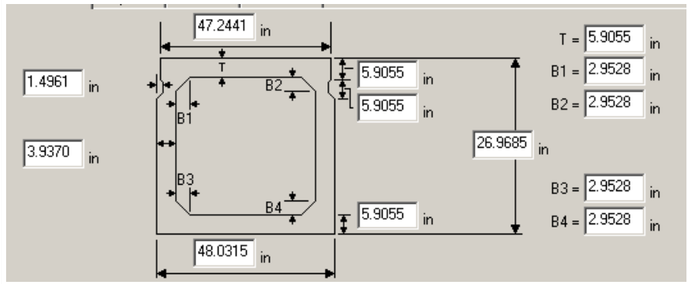

Cross-Section - Interior

Bridge #	Virtis BID #	Span length (ft)	t_{slab} (in)	Girder Spacing (ft)	Overhang Width (ft)	# of Girders	Skew (deg)	Materials				Dist. to Extreme Strands (in)		Harp Point (ft)	Beam Section
								P/S Tendons	f_c' (ksi)	$f_c'_l$ (ksi)	$f_c'_{deck}$ (ksi)	Bottom	Top		
9167	0746	75'-6¾"	5.875	4'-1½"	2'-1⅝"	12	120.0	22-0.6" Gr. 270 LR	5.0	4.0	4.0	1.9685		N/A	MDOT 685x1220

@ 63.0" from left support	@ 118.11" from left support	@ 185.04" from left support	Strand Layout at Midspan	Cross-Section - Exterior

Strand Spacing:
Horizontal: 1.9685"
Vertical: 2.0079"

# of Strands: 22
CG from bottom at 63.0": 3.10"
CG from bottom at 118.11": 3.20"
CG from bottom at 185.04": 3.07"
CG from bottom at Midspan: 2.97"

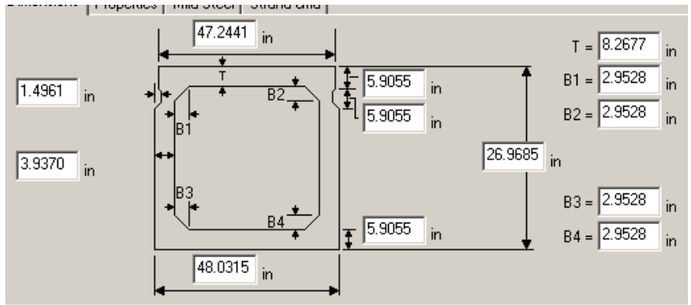

Bridge #	Virtis BID #	Span length (ft)	t_{slab} (in)	Girder Spacing (ft)	Overhang Width (ft)	# of Girders	Skew (deg)	Materials				Dist. to Extreme Strands (in)		Harp Point (ft)	Beam Section
								P/S Tendons	f_c' (ksi)	$f_c'_l$ (ksi)	$f_c'_{deck}$ (ksi)	Bottom	Top		
17008	0747	82'-6⅛"	6.25	4'-0"	2'-6"	8	115.0	38-0.5" Gr. 270 SR	7.0	5.6	3.0	1.9685		N/A	AASHTO BII-1220

Strand Spacing:
Horizontal: 1.9685"
Vertical: 1.9685"

# of Strands: 38
CG from bottom at Midspan: 6.11"

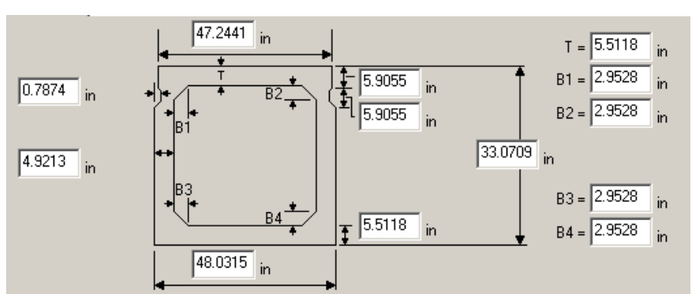

Strand Layout at Midspan	Cross-Section	Cross-Section

Bridge #	Virtis BID #	Span length (ft)	t_{slab} (in)	Girder Spacing (ft)	Overhang Width (ft)	# of Girders	Skew (deg)	Materials				Dist. to Extreme Strands (in)		Harp Point (ft)	Beam Section
								P/S Tendons	f_c' (ksi)	f_c'$_I$ (ksi)	$f_{c\,deck}$' (ksi)	Bottom	Top		
5125	0748	66'-0"	5.5	1@3'-6", 7@4'-0",1@3'-6", 2@3'-0", 1@3'-6", 7@4'-0", 1@3'-6"	1'-6"	22	108.0	24-0.5" Gr. 270 LR	6.0	4.5	4.0	2.0	3.0	N/A	36"x33" Box Girder
								26-0.5" Gr. 270 LR				2.0	3.0		48"x33" Box Girder

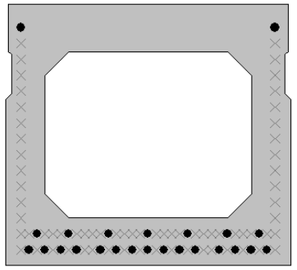

Strand Spacing:
Horizontal: 1"
Vertical: 2"

# of Strands: 24
CG from bottom at Midspan: 4.92"

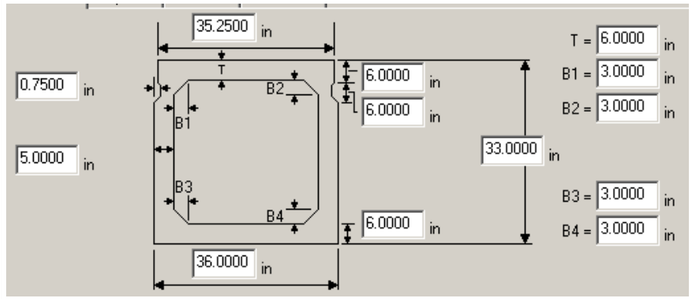

Strand Layout at Midspan | Cross-Section | Cross-Section – 36"x33" Box Girder

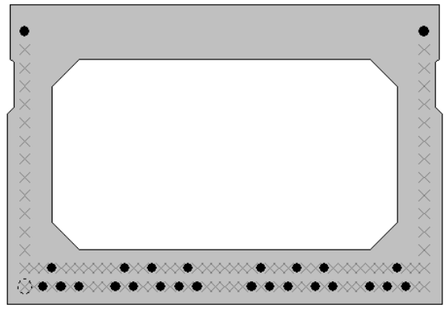

Strand Spacing:
Horizontal: 1"
Vertical: 2"

# of Strands: 26
CG from bottom at Midspan: 4.77"

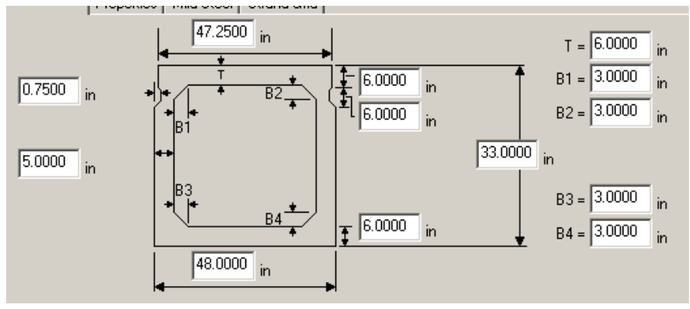

Strand Layout at Midspan | Cross-Section | Cross-Section – 48"x33" Box Girder

Bridge #	Virtis BID #	Span length (ft)	t_{slab} (in)	Girder Spacing (ft)	Overhang Width (ft)	# of Girders	Skew (deg)	Materials				Dist. to Extreme Strands (in)		Harp Point (ft)	Beam Section
								P/S Tendons	f_c' (ksi)	f_{ci}' (ksi)	$f_{c\,deck}$' (ksi)	Bottom	Top		
13118	0749	69'-2¾"	5.875	1@3'-7 3/16", 2@3'-1 3/16", 1@3'-7 ¼", 2@4'1 3/16", 1@3'-7 ¼", 2@3'-1 3/16", 1@3'-7 3/16"	2'-3 15/16"	11	60.0	18-0.6" Gr. 270 LR	10.2	8.0	3.0	1.9685	4.9213	N/A	AASHTO BI-915
								19-0.6" Gr. 270 LR				1.9685	4.9213	N/A	AASHTO BI-1220

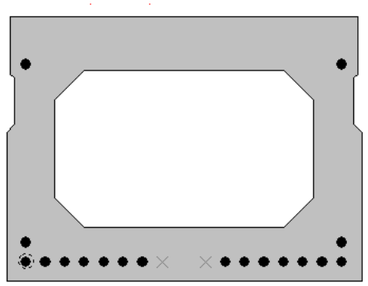

Strand Layout at Midspan

Strand Spacing:
Horizontal: 1.9685"
Vertical: 1.9685"

# of Strands: 18
CG from bottom at Midspan: 4.42"

Cross-Section

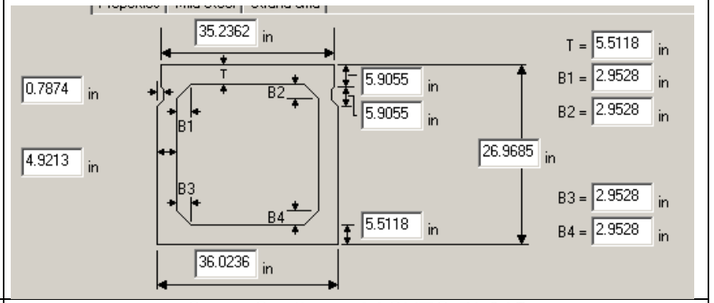

Cross-Section – AASHTO BI-915

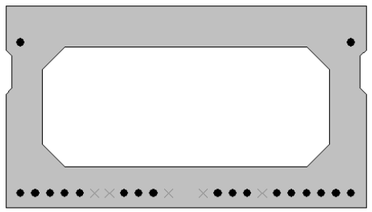

Strand Layout at Midspan

Strand Spacing:
Horizontal: 1.9685"
Vertical: 1.9685"

# of Strands: 19
CG from bottom at Midspan: 4.08"

Cross-Section

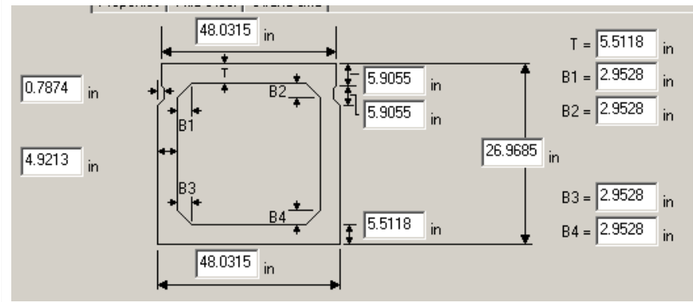

Cross-Section – AASHTO BI-1220

Bridge #	Virtis BID #	Span length (ft)	t_{slab} (in)	Girder Spacing (ft)	Overhang Width (ft)	# of Girders	Skew (deg)	Materials				Dist. to Extreme Strands (in)		Harp Point (ft)	Beam Section
								P/S Tendons	f_c' (ksi)	f_{ci}' (ksi)	$f_{c\,deck}'$ (ksi)	Bottom	Top		
5911	0750	59’-5”	5.5	3’-0”	1’-6”	50	125	14-0.5” Gr. 270 LR	5.0	4.0	4.0	1.75		N/A	27x36 Box

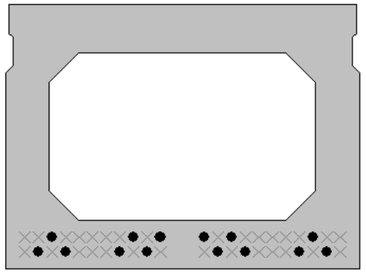

Strand Layout at Midspan

Strand Spacing:
Horizontal: 1.375”
Vertical: 1.5”

# of Strands: 14
CG from bottom at Midspan: 2.39”

Cross-Section

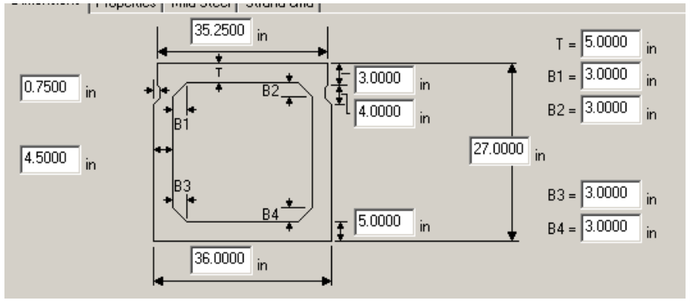

Cross-Section – 27x36 Box

Bridge #	Virtis BID #	Span length (ft)	t_{slab} (in)	Girder Spacing (ft)	Overhang Width (ft)	# of Girders	Skew (deg)	Materials				Dist. to Extreme Strands (in)		Harp Point (ft)	Beam Section
								P/S Tendons	f_c' (ksi)	f_{ci}' (ksi)	$f_{c\,deck}'$ (ksi)	Bottom	Top		
3805	0751	59’-0½”	0.0	3’-0”	1’-6”	14	90.0	15-0.5” Gr. 270 LR	5.0	4.0	3.5	1.75		N/A	27”x36” IDOT Beam

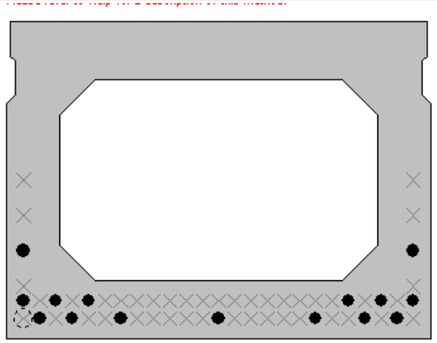

Strand Layout at Midspan

Strand Spacing:
Horizontal: 1.375”, 3”
Vertical: 1.5”, 1.25”, 3”

# of Strands: 15
CG from bottom at Midspan: 3.12”

Cross-Section

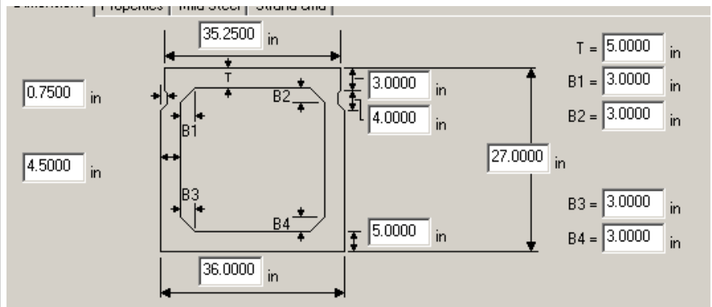

Cross-Section – 27”x36” IDOT Beam

Bridge #	Virtis BID #	Span length (ft)	t_{slab} (in)	Girder Spacing (ft)	Overhang Width (ft)	# of Girders	Skew (deg)	Materials				Dist. to Extreme Strands (in)		Harp Point (ft)	Beam Section
								P/S Tendons	f_c' (ksi)	f_{ci}' (ksi)	$f_{c\,deck}$' (ksi)	Bottom	Top		
3819	0752	74'-10½"	0.0	3'-0"	1'-6"	11	128.8	18-0.5" Gr. 270 LR	5.0	4.0	3.5	1.75		N/A	33"x36" Box Beam

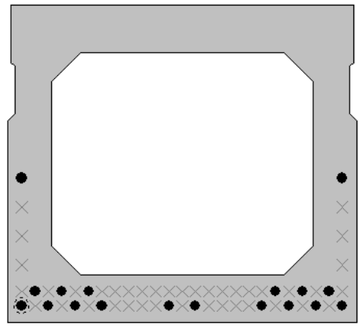

Strand Layout at Midspan

Strand Spacing:
Horizontal: 1.375", 3"
Vertical: 1.5", 2.75", 3"

# of Strands: 18
CG from bottom at Midspan: 3.72"

Cross-Section

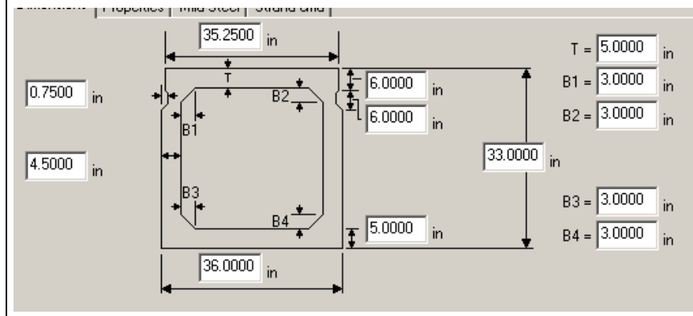

Cross-Section

Bridge #	Virtis BID #	Span length (ft)	t_{slab} (in)	Girder Spacing (ft)	Overhang Width (ft)	# of Girders	Skew (deg)	Materials				Dist. to Extreme Strands (in)		Harp Point (ft)	Beam Section
								P/S Tendons	f_c' (ksi)	f_{ci}' (ksi)	$f_{c\,deck}$' (ksi)	Bottom	Top		
9240	0763	97'-11"	6.0	3'-1 ½"	1'-6"	25	90.0	28-0.5" Gr. 270 LR	5.5	3.6	4.0	2.0		N/A	33"x36" MDOT Beam

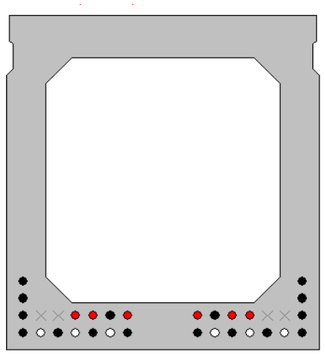

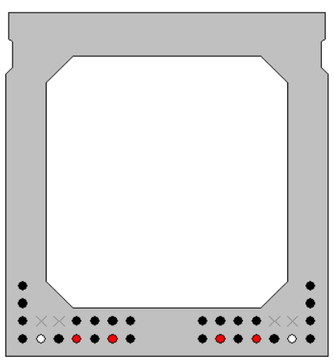

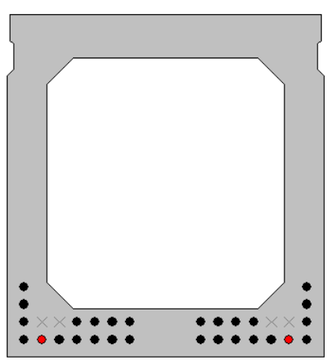

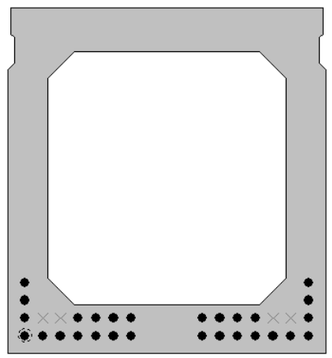

Strand Spacing:
Horizontal: 2"
Vertical: 2"

# of Strands: 28
CG from bottom at Left Support to 132": 3.75"
CG from bottom at 252": 3.82"
CG from bottom at 312": 3.54"
CG from bottom at Midspan: 3.43"

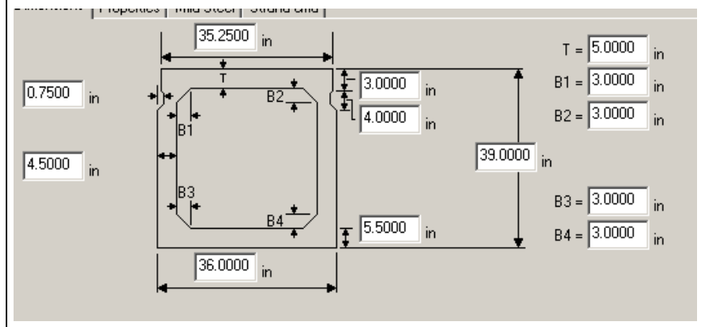

@ left support to 132” from left support	@ 252” from left support	@ 312” from left support	Strand Layout at Midspan	Cross-Section

Bridge #	Virtis BID #	Span length (ft)	t_{slab} (in)	Girder Spacing (ft)	Overhang Width (ft)	# of Girders	Skew (deg)	Materials				Dist. to Extreme Strands (in)		Harp Point (ft)	Beam Section
								P/S Tendons	f_c’ (ksi)	f_{ci}’ (ksi)	f_c’ deck (ksi)	Bottom	Top		
9103	0764	111’-2⅝”	5.875	4’-1⅝”	2’-1 ½”	16	100.8	25-0.6” Gr. 270 LR	5.0	3.5	4.0	2.0		N/A	MDOT 1220x1220

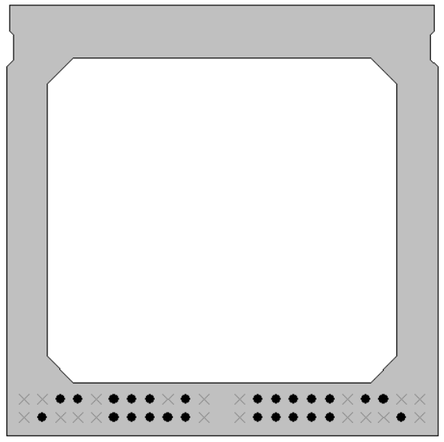

Strand Layout at Midspan

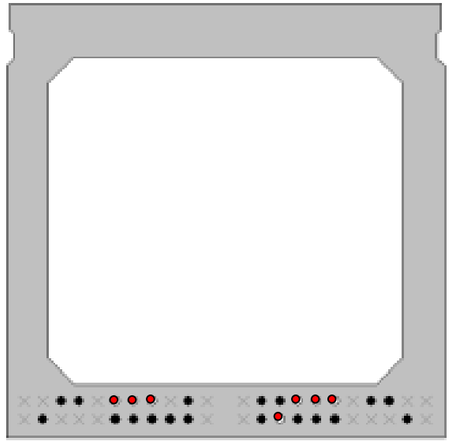

Strand layout at Support to 157.48”

Strand Spacing:
Horizontal: 2”
Vertical: 2”

# of Strands: 25
CG from bottom at left support: 2.78”
CG from bottom at Midspan: 3.04”

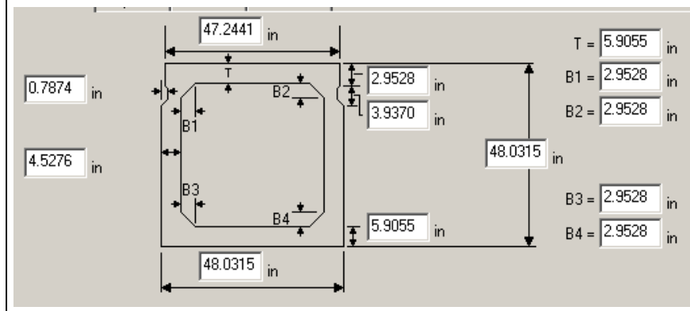

Cross-Section - Interior

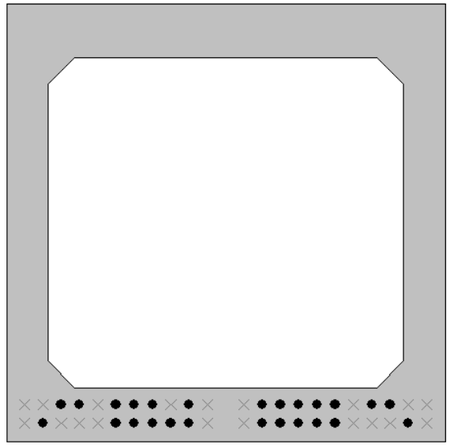	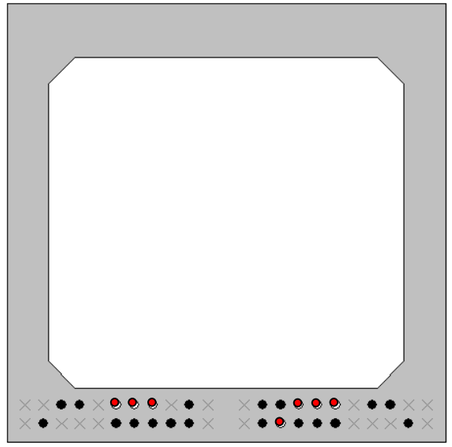	Strand Spacing: Horizontal: 2” Vertical: 2” # of Strands: 25 CG from bottom at left support: 2.78” CG from bottom at Midspan: 3.04” 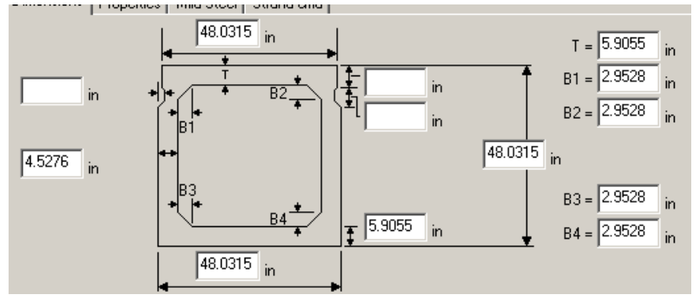
Strand Layout at Midspan	Strand layout at Support to 157.5”	Cross-Section - Exterior

Bridge #	Virtis BID #	Span length (ft)	t_{slab} (in)	Girder Spacing (ft)	Overhang Width (ft)	# of Girders	Skew (deg)	Materials				Dist. to Extreme Strands (in)		Harp Point (ft)	Beam Section
								P/S Tendons	f_c’ (ksi)	$f_{c'i}$ (ksi)	$f_{c'}$ deck (ksi)	Bottom	Top		
9228	0765	110’-5¼”	5.875	4’-2 13/16”	2’-1 ½”	11	72.2	24-0.6” Gr. 270 LR	6.1	4.6	4.0	1.9685		N/A	MDOT 1220x1220

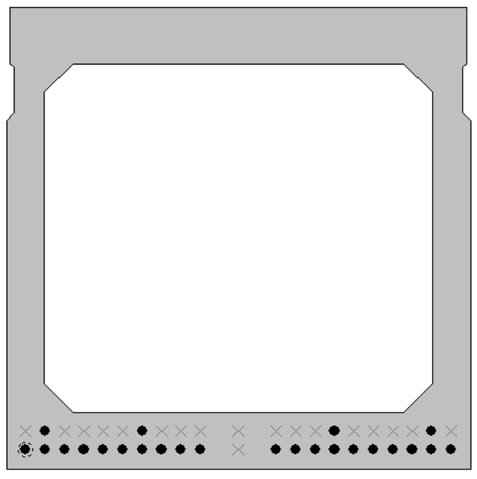	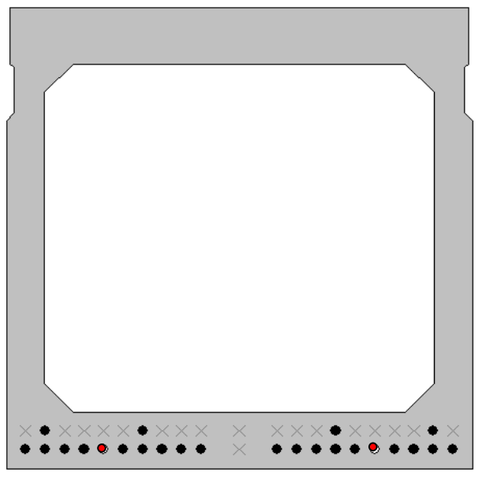	Strand Spacing: Horizontal: 2.0079” Vertical: 1.9685” # of Strands: 24 CG from bottom at left support: 2.33” CG from bottom at Midspan: 2.30” 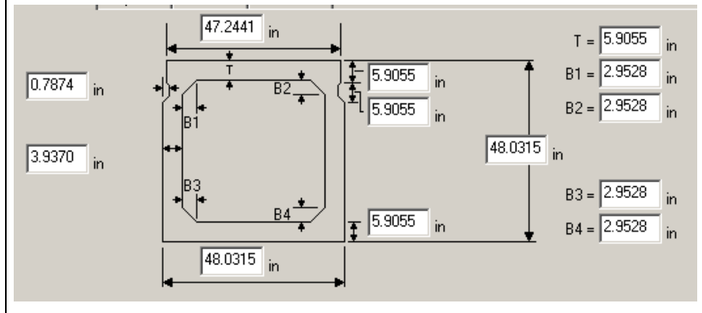
Strand Layout at Midspan	Strand layout at Support to 19.685”	Cross-Section

Bridge #	Virtis BID #	Span length (ft)	t_{slab} (in)	Girder Spacing (ft)	Overhang Width (ft)	# of Girders	Skew (deg)	Materials				Dist. to Extreme Strands (in)		Harp Point (ft)	Beam Section
								P/S Tendons	f_c' (ksi)	$f_{c'l}$ (ksi)	$f_{c'deck}$ (ksi)	Bottom	Top		
14070	0766	115'-0"	0.0	3'-1 3/16"	1'-6"	11	60.0	42-0.5" Gr. 270 LR	7.5	5.5		2.0	4.5	N/A	36"x45" Beam

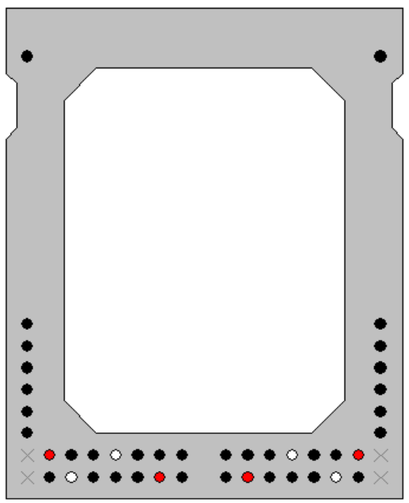

@ 36" from left support

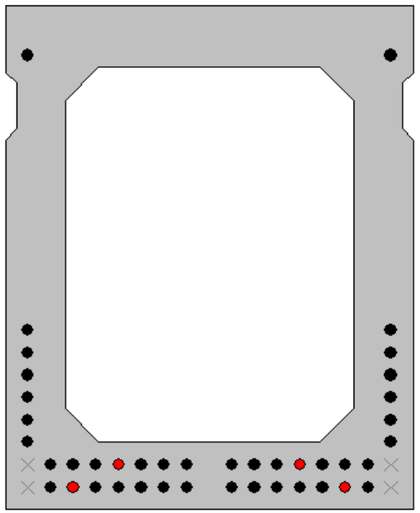

@ 72" from left support

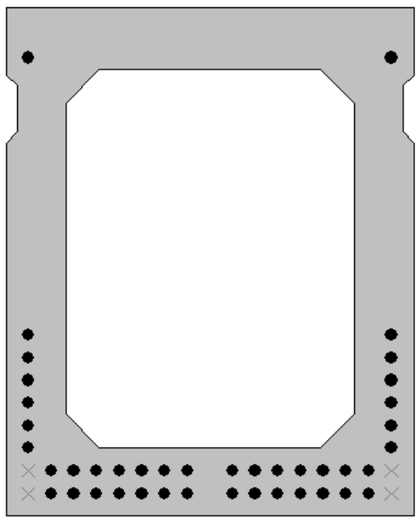

Strand Layout at Midspan

Strand Spacing:
Horizontal: 2"
Vertical: 2"

# of Strands: 42
CG from bottom at 36": 8.03"
CG from bottom at 72": 7.50"
CG from bottom at Midspan: 7.07"

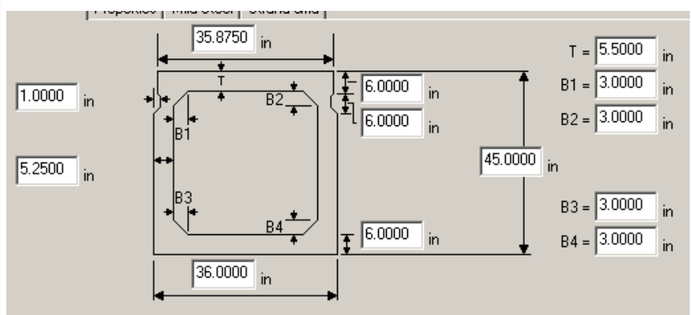

Cross-Section

Bridge #	Virtis BID #	Span length (ft)	t_{slab} (in)	Girder Spacing (ft)	Overhang Width (ft)	# of Girders	Skew (deg)	Materials				Dist. to Extreme Strands (in)		Harp Point (ft)	Beam Section
								P/S Tendons	f_c' (ksi)	$f_{c'l}$ (ksi)	$f_{c'deck}$ (ksi)	Bottom	Top		
16538	0767	101'-8½"	5.875	4'-0¾"	2'-4"	9	90.0	38-0.5" Gr. 270 LR	7.25	5.1	3.0	1.9685		N/A	AASHTO BIV-48 mod

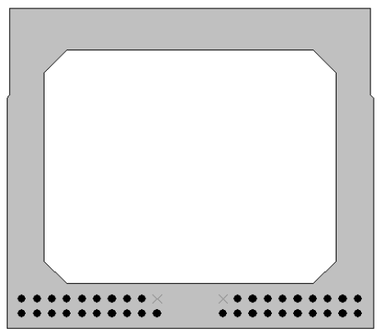

Strand Layout at Midspan

Strand Spacing:
Horizontal: 1.9685"
Vertical: 1.9685"

# of Strands: 38
CG from bottom at Midspan: 2.90"

Cross-Section

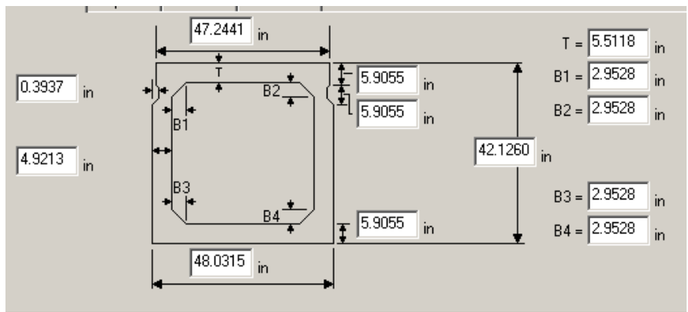

Cross-Section

C.4 Spread Precast Box Girders

Bridge #	Virtis BID #	Span length (ft)	t_{slab} (in)	Girder Spacing (ft)	Overhang Width (ft)	# of Girders	Skew (deg)	Materials				Dist. to Extreme Strands (in)		Harp Point (ft)	Beam Section
								P/S Tendons	f_c' (ksi)	f_{ci}' (ksi)	$f_{c\,deck}'$ (ksi)	Bottom	Top		
9310	0774	51’-11 ⅝”	9.0	5’-11⅝”	2’-2¼”	12	90.0	20-0.6” Gr. 270 LR	6.0	5.5	4.0	2.0		N/A	21x36 Box Beam

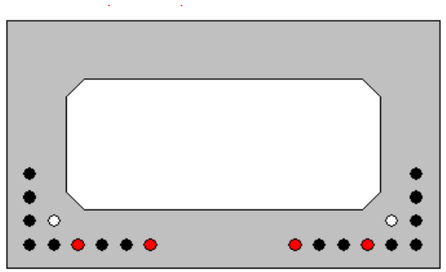

@ 118.1” from left support

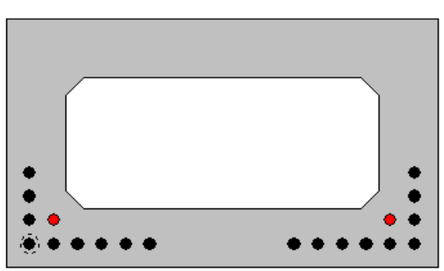

@ 196.85” from left support

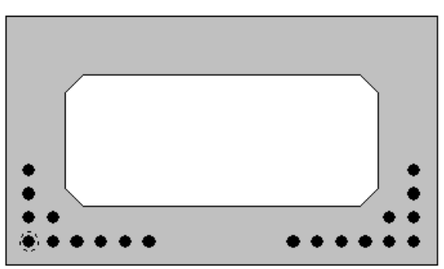

Strand Layout at Midspan

Strand Spacing:
Horizontal: 2”
Vertical: 2”

# of Strands: 20
CG from bottom at 118.1”: 3.71”
CG from bottom at 196.85”: 3.33”
CG from bottom at Midspan: 3.40”

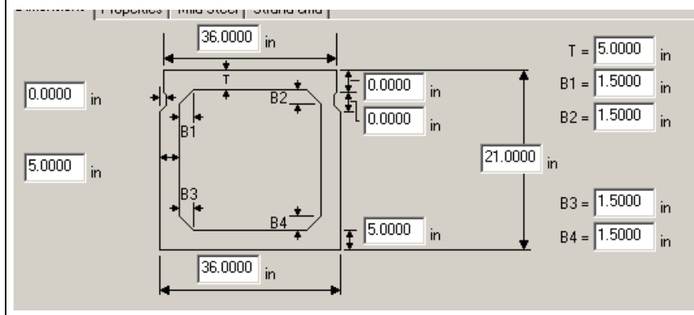

Cross-Section

Bridge #	Virtis BID #	Span length (ft)	t_{slab} (in)	Girder Spacing (ft)	Overhang Width (ft)	# of Girders	Skew (deg)	Materials				Dist. to Extreme Strands (in)		Harp Point (ft)	Beam Section
								P/S Tendons	f_c' (ksi)	f_{ci}' (ksi)	$f_{c\,deck}$' (ksi)	Bottom	Top		
9384	0622	44'-1 ½"	9.0	6'-7¼"	3'-3⅜"	10	89.4	14-0.6" Gr. 270 LR	6.1	4.6	4.0	2		N/A	21x36 Box Beam

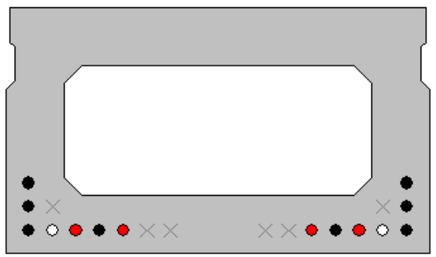

@ 59.0" from left support

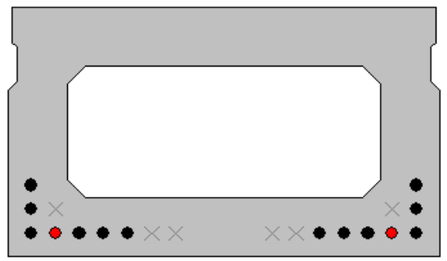

@86.6" from left support

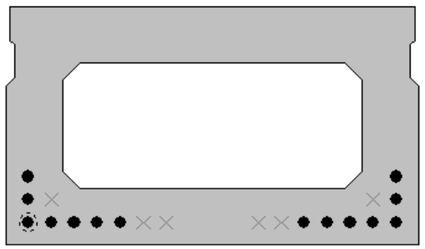

Strand Layout at Midspan

Strand Spacing:
Horizontal: 2"
Vertical: 2"

# of Strands: 14
CG from bottom at 59.0": 3.50"
CG from bottom at 86.6": 3.00"
CG from bottom at Midspan: 2.86"

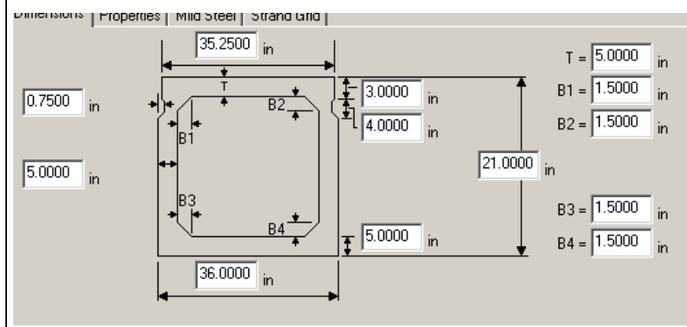

Cross-Section

Bridge #	Virtis BID #	Span length (ft)	t_{slab} (in)	Girder Spacing (ft)	Overhang Width (ft)	# of Girders	Skew (deg)	Materials				Dist. to Extreme Strands (in)		Harp Point (ft)	Beam Section
								P/S Tendons	f_c' (ksi)	f_{ci}' (ksi)	$f_{c\,deck}$' (ksi)	Bottom	Top		
9380	0629	32'-1"	9.0	9'-1 3/16"	2'-6"	10	85.6	12-0.5" Gr. 270 LR	5.0	3.0	4.0	2.0		N/A	21x36 Box Beam

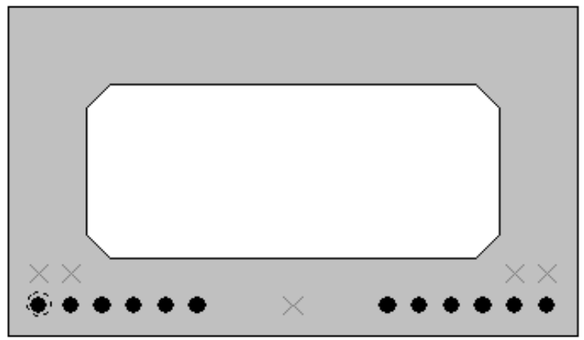

Strand Layout at Midspan

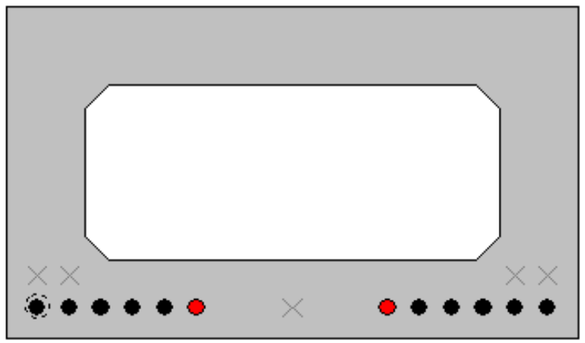

Strand layout at Support to 36.0"

Strand Spacing:
Horizontal: 2"
Vertical: 2"

# of Strands: 12
CG from bottom at left support: 2.00"
CG from bottom at Midspan: 2.00"

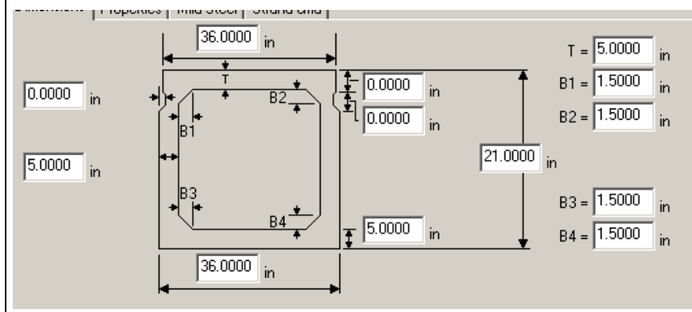

Cross-Section

Bridge #	Virtis BID #	Span length (ft)	t_{slab} (in)	Girder Spacing (ft)	Overhang Width (ft)	# of Girders	Skew (deg)	Materials				Dist. to Extreme Strands (in)		Harp Point (ft)	Beam Section
								P/S Tendons	f_c' (ksi)	f_{ci}' (ksi)	$f_{c\,deck}$' (ksi)	Bottom	Top		
17338	0675	49'-0"	8.5	8'-0"	4'-0"	4	135	18-0.5" Gr. 270 SR	5.0	4.0	3.0	2.0		N/A	AASHTO BII-48

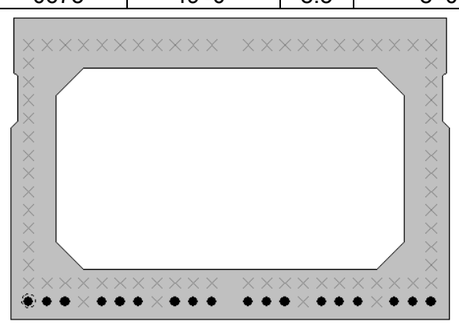

Strand Layout at Midspan

Strand Spacing:
Horizontal: 2"
Vertical: 2"

# of Strands: 18
CG from bottom at Midspan: 2.00"

Cross-Section

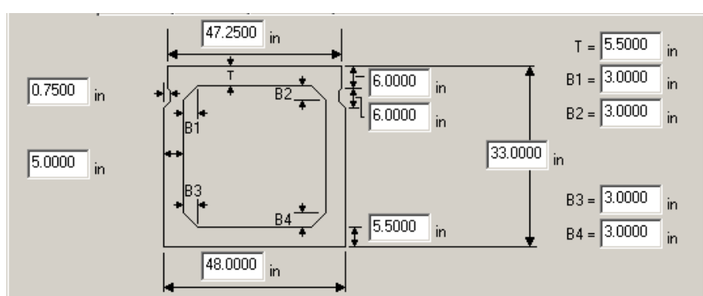

Cross-Section

Bridge #	Virtis BID #	Span length (ft)	t_{slab} (in)	Girder Spacing (ft)	Overhang Width (ft)	# of Girders	Skew (deg)	Materials				Dist. to Extreme Strands (in)		Harp Point (ft)	Beam Section
								P/S Tendons	f_c' (ksi)	$f_c'_l$ (ksi)	f_c' deck (ksi)	Bottom	Top		
9282	0679	36’-3⅝”	9.0	7’-10”	3’-0” (L), 4’-0” (R)	12	67.3	16-0.5” Gr. 270 LR	5.0	4.0	4.0	2		N/A	17”x36” Box Beam

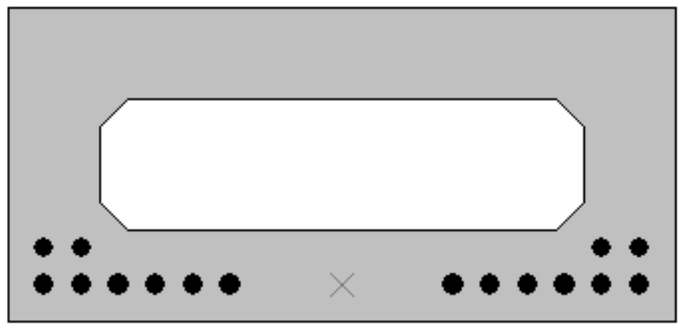

Strand Layout at Midspan

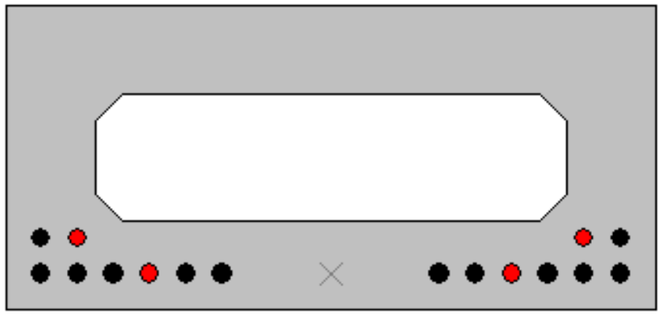

Strand layout at Support to 120.0”

Strand Spacing:
Horizontal: 2”
Vertical: 2”

# of Strands: 16
CG from bottom at left support to 120”: 2.33”
CG from bottom at Midspan: 2.50”

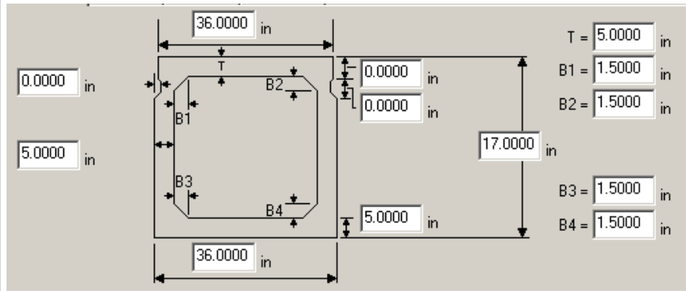

Cross-Section

Bridge #	Virtis BID #	Span length (ft)	t_{slab} (in)	Girder Spacing (ft)	Overhang Width (ft)	# of Girders	Skew (deg)	Materials				Dist. to Extreme Strands (in)		Harp Point (ft)	Beam Section
								P/S Tendons	f_c' (ksi)	f_{ci}' (ksi)	$f_{c\ deck}$' (ksi)	Bottom	Top		
9192	0686	38'-8"	9.0	3@6'-6 11/16" 5@9'-10"	3'-9 ½"	9	80	18-0.5" Gr. 270 LR	5.5	4.4	4.0	2.0		N/A	21"x36" Box Beam

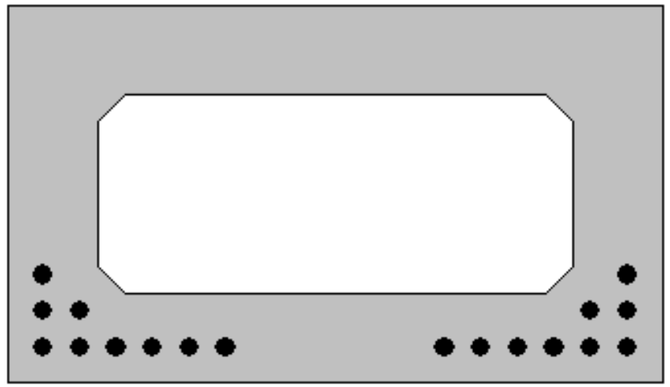

Strand Layout at Midspan

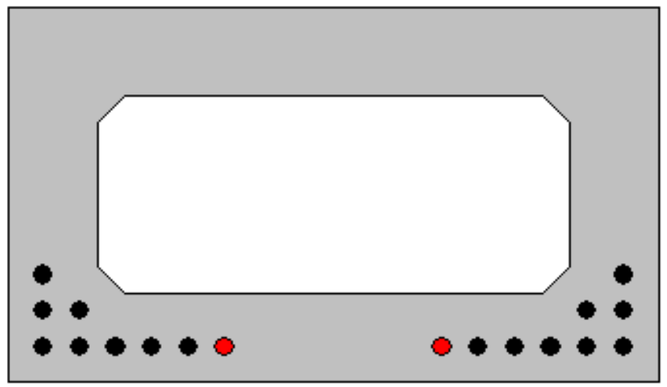

Strand Layout at Support to 24"

Strand Spacing:
Horizontal: 2"
Vertical: 2"

# of Strands: 18
CG from bottom at Support to 24": 3.00"
CG from bottom at Midspan: 2.89"

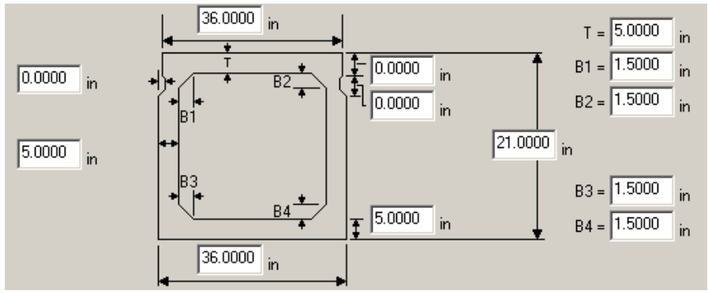

Cross-Section – 21"x36" Box Beam

Bridge #	Virtis BID #	Span length (ft)	t_{slab} (in)	Girder Spacing (ft)	Overhang Width (ft)	# of Girders	Skew (deg)	Materials				Dist. to Extreme Strands (in)		Harp Point (ft)	Beam Section
								P/S Tendons	f_c' (ksi)	f_{ci}' (ksi)	$f_{c\,deck}$' (ksi)	Bottom	Top		
9286	0695	50'-8"	9.0	8'-0 ½"	3'-2⅛"	6	90	20-0.6" Gr. 270 LR	6.0	5.0	4.0	2.0	2.5	N/A	27"x36" Box Beam

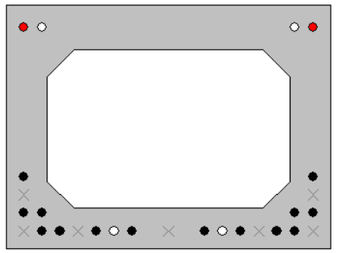	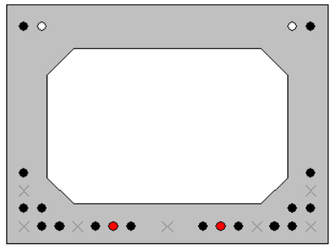	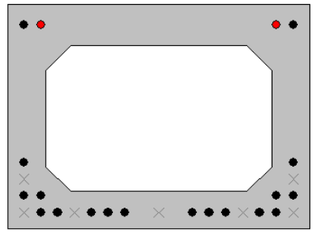	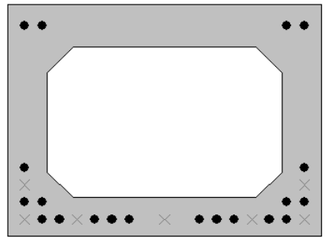	Strand Spacing: Horizontal: 2" Vertical: 2" # of Strands: 20 CG from bottom at 0.5" from LS: 3.43" CG from bottom at 48" from LS: 6.06" CG from bottom at 140" from LS: 5.61" CG from bottom at Midspan: 7.50" 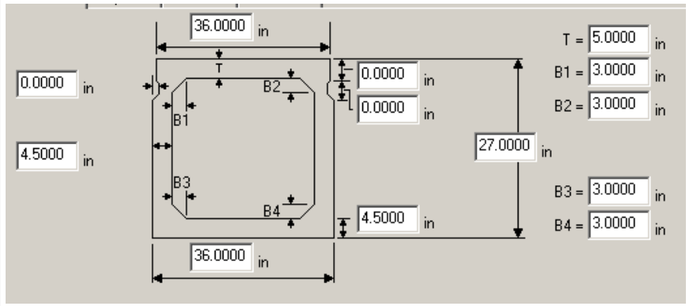
@ 0.5" from left support	@ 48" from left support	@ 140.0" from left support	Strand Layout at Midspan	Cross-Section

Bridge #	Virtis BID #	Span length (ft)	t_{slab} (in)	Girder Spacing (ft)	Overhang Width (ft)	# of Girders	Skew (deg)	Materials				Dist. to Extreme Strands (in)		Harp Point (ft)	Beam Section
								P/S Tendons	f_c' (ksi)	$f_{c'i}$ (ksi)	$f_{c'}$ deck (ksi)	Bottom	Top		
9368	0707	71'-3"	9.0	7'-4 ½"	2'-11½"	5	97.4	30-0.5" Gr. 270 LR	6.3	4.9	4.0	2.0		N/A	33"x36" Box Beam

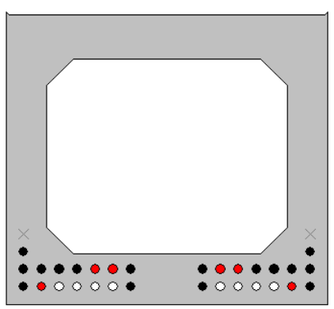

@ 63" from left support

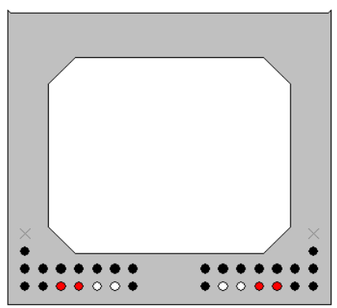

@ 102" from left support

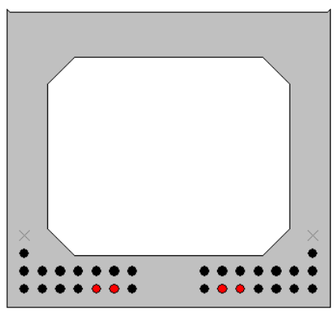

@ 147.0" from left support

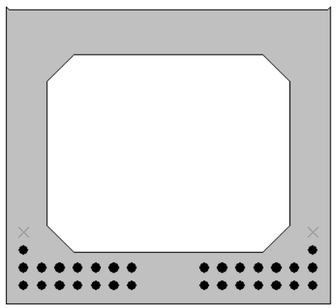

Strand Layout at Midspan

Strand Spacing:
Horizontal: 2"
Vertical: 2"

# of Strands: 30
CG from bottom at 63" from LS: 3.75"
CG from bottom at 102" from LS: 3.64"
CG from bottom at 147" from LS: 3.38"
CG from bottom at Midspan: 3.20"

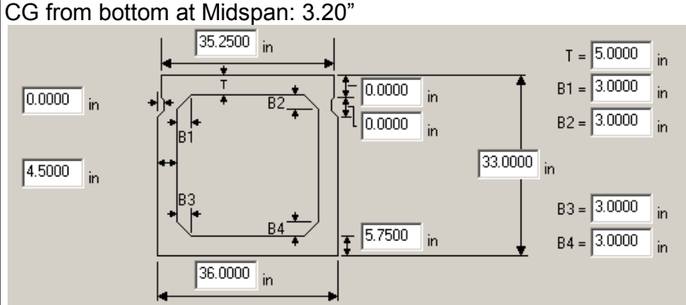

Cross-Section

Bridge #	Virtis BID #	Span length (ft)	t_{slab} (in)	Girder Spacing (ft)	Overhang Width (ft)	# of Girders	Skew (deg)	Materials				Dist. to Extreme Strands (in)		Harp Point (ft)	Beam Section
								P/S Tendons	f_c' (ksi)	f_{ci}' (ksi)	$f_{c\,deck}$' (ksi)	Bottom	Top		
9328	0740	57'-3¼"	9.0	6'-11"	3'-3⅜"	6	90.0	26-0.5" Gr. 270 LR	6.5	5.3	4.0	2		N/A	27x36 Box Beam

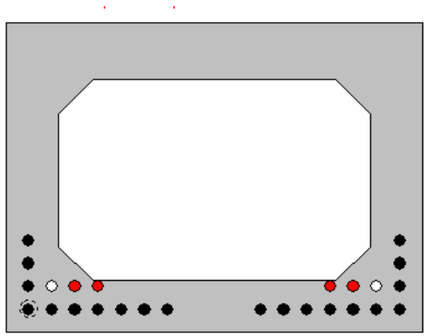

@ 36.0" from left support

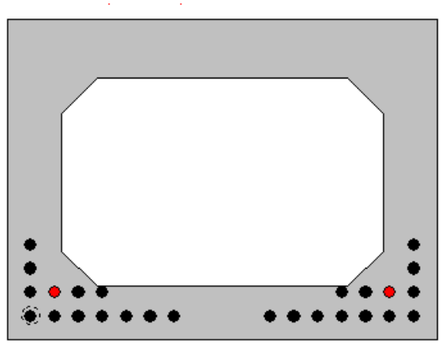

@ 114.0" from left support

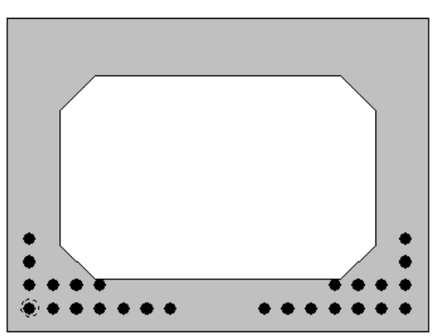

Strand Layout at Midspan

Strand Spacing:
Horizontal: 2"
Vertical: 2"

# of Strands: 26
CG from bottom at 36.0": 3.20"
CG from bottom at 114.0": 3.33"
CG from bottom at Midspan: 3.38"

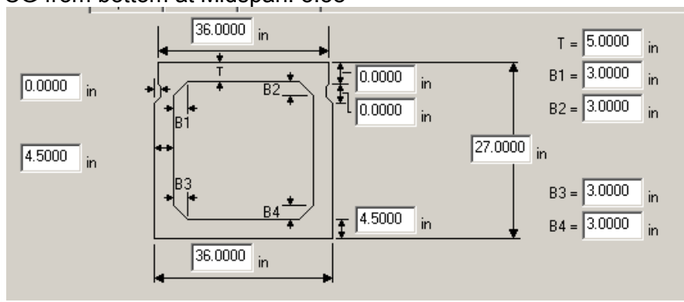

Cross-Section

Bridge #	Virtis BID #	Span length (ft)	t_{slab} (in)	Girder Spacing (ft)	Overhang Width (ft)	# of Girders	Skew (deg)	Materials				Dist. to Extreme Strands (in)		Harp Point (ft)	Beam Section
								P/S Tendons	f_c' (ksi)	f_{ci}' (ksi)	$f_{c\,deck}$' (ksi)	Bottom	Top		
9376	0744	53'-4¼"	9.0	7'-4⅝"	3'-5 5/16"	12	90.0	15-0.6" Gr. 270 LR	7.0	6.2	4.0	2		N/A	27x36 Box Beam

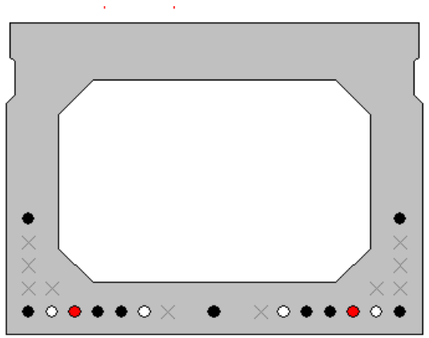

@ 72.0" from left support

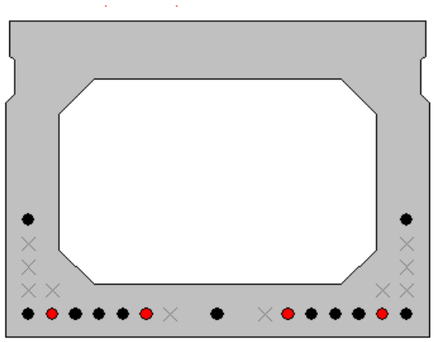

@ 108.0" from left support

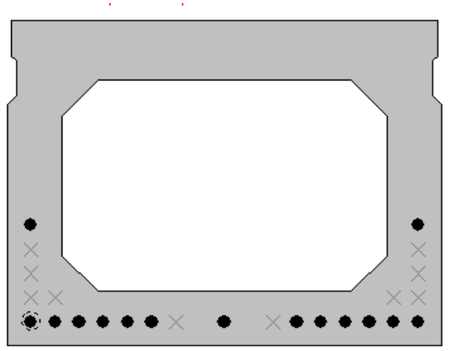

Strand Layout at Midspan

Strand Spacing:
Horizontal: 2"
Vertical: 2"

# of Strands: 15
CG from bottom at 72.0": 3.78"
CG from bottom at 108.0": 3.45"
CG from bottom at Midspan: 3.07"

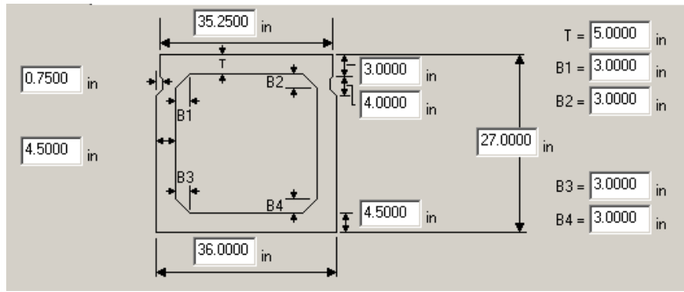

Cross-Section

Bridge #	Virtis BID #	Span length (ft)	t_{slab} (in)	Girder Spacing (ft)	Overhang Width (ft)	# of Girders	Skew (deg)	Materials				Dist. to Extreme Strands (in)		Harp Point (ft)	Beam Section
								P/S Tendons	f_c' (ksi)	f_{ci}' (ksi)	$f_{c\,deck}$' (ksi)	Bottom	Top		
3577	0222003	38'-7"	7.5	6'-8⅜"	4'-0 7/16"	4	101.3	27-0.4375" Gr. 248 SR	5.0	4.0	3.5	1.75		N/A	27"x36" IDOT Beam

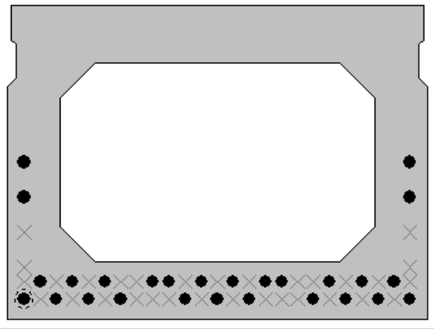

Strand Layout at Midspan

Strand Spacing:
Horizontal: 1.375", 3"
Vertical: 1.5", 1.25", 3"

# of Strands: 27
CG from bottom at Midspan: 3.94"

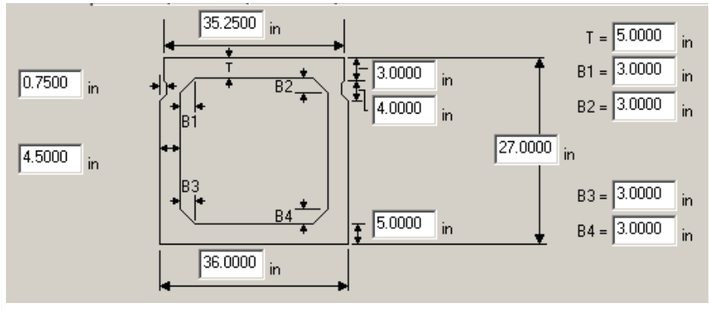

Cross-Section

Bridge #	Virtis BID #	Span length (ft)	t_{slab} (in)	Girder Spacing (ft)	Overhang Width (ft)	# of Girders	Skew (deg)	Materials				Dist. to Extreme Strands (in)		Harp Point (ft)	Beam Section
								P/S Tendons	f_c' (ksi)	$f_c'_I$ (ksi)	$f_{c\,deck}'$ (ksi)	Bottom	Top		
3754	0980015	53’-7 ¼”	7.0	1@6’-6”, 7@6’ 2 9/16”, 2@6’-0”	1’-6”	11	151.7	30 (or 28) -0.4375” Gr. 248 SR	5.0	4.0	3.5	1.75		N/A	33x36 IDOT Beam

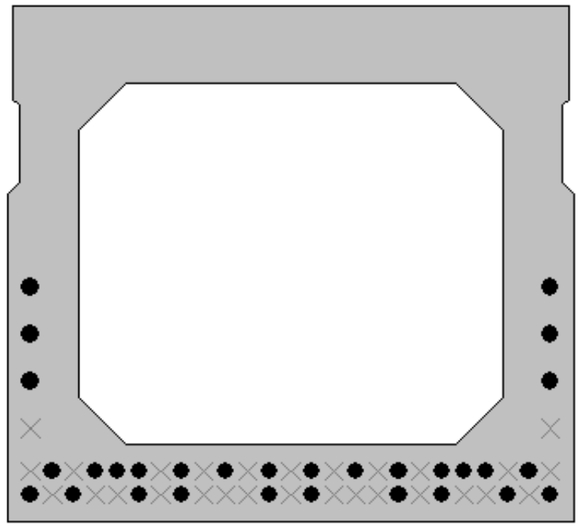

Strand Layout at Midspan

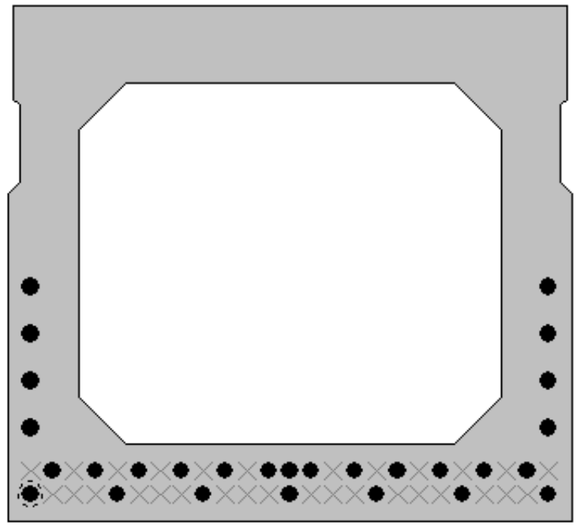

Strand Spacing:
Horizontal: 1.375”, 3”
Vertical: 1.5”, 2.75”, 3”

All girders except far left and two far right:
# of Strands: 30
CG from bottom at Midspan: 4.50”

Far left and two far right girders:
# of Strands: 28
CG from bottom at Midspan: 4.95”

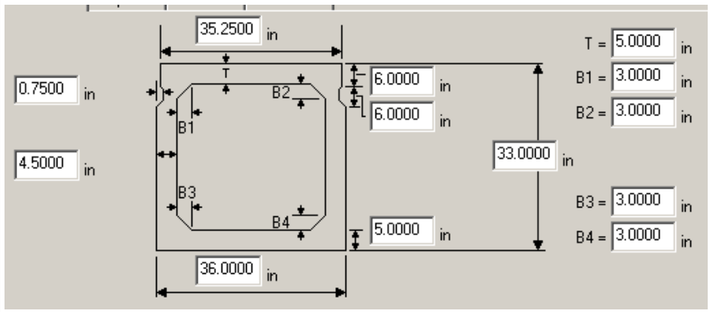

Cross-Section

Bridge #	Virtis BID #	Span length (ft)	t_{slab} (in)	Girder Spacing (ft)	Overhang Width (ft)	# of Girders	Skew (deg)	Materials				Dist. to Extreme Strands (in)		Harp Point (ft)	Beam Section
								P/S Tendons	f_c' (ksi)	f_{ci}' (ksi)	$f_{c\,deck}$' (ksi)	Bottom	Top		
8875	A8029	38'-0"	8.5	11'-3"	3'-1½"	12	96.4	23-0.5" Gr. 270 LR	8.0	5.0	4.0	1.75		N/A	27x48 Box Beam

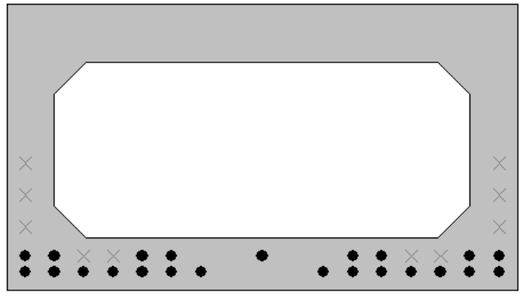

Strand Layout at Midspan

Strand Spacing:
Horizontal: 2.75"
Vertical: 1.5", 2.75", 3"

# of Strands: 23
CG from bottom at Midspan: 2.34"

Cross-Section

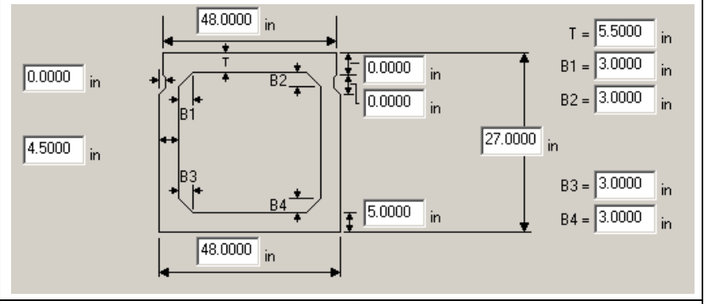

Cross-Section

Bridge #	Virtis BID #	Span length (ft)	t_{slab} (in)	Girder Spacing (ft)	Overhang Width (ft)	# of Girders	Skew (deg)	Materials				Dist. to Extreme Strands (in)		Harp Point (ft)	Beam Section
								P/S Tendons	f_c' (ksi)	f_{ci}' (ksi)	$f_{c\,deck}$' (ksi)	Bottom	Top		
12870	2219470	77'-6"	8.5	6'-6"	2'-0"	5	105.0	30-0.5" Gr. 270 SR	6.0	4.8	3.0	2.0		N/A	36x48 Box Beam

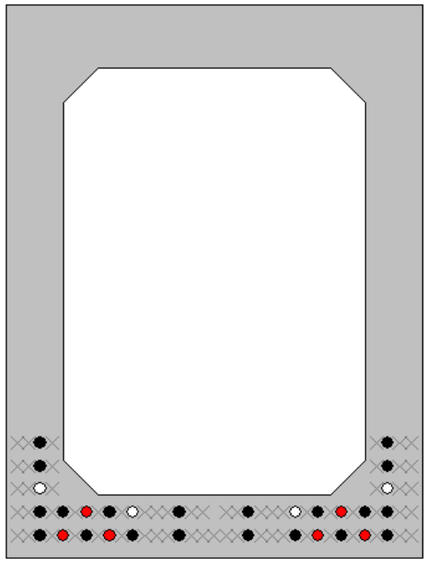

@ 120.0" from left support

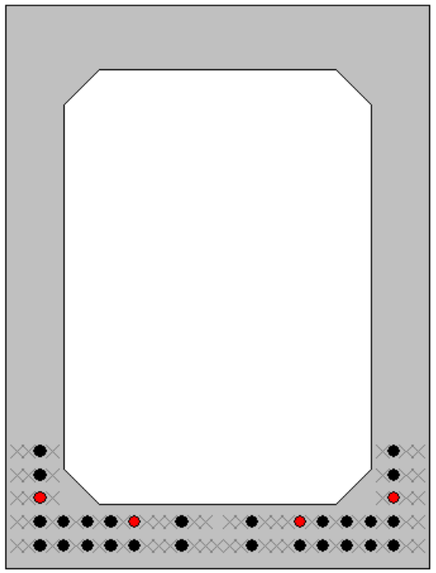

@ 144.0" from left support

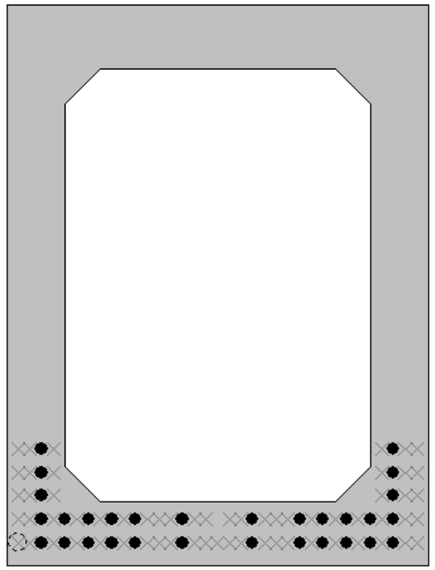

Strand Layout at Midspan

Strand Spacing:
Horizontal: 1"
Vertical: 2"

# of Strands: 30
CG from bottom at 120.0": 4.20"
CG from bottom at 144.0": 3.85"
CG from bottom at Midspan: 4.00"

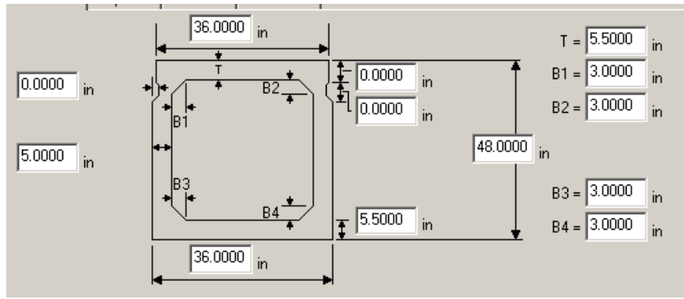

Cross-Section

Bridge #	Virtis BID #	Span length (ft)	t_{slab} (in)	Girder Spacing (ft)	Overhang Width (ft)	# of Girders	Skew (deg)	Materials				Dist. to Extreme Strands (in)		Harp Point (ft)	Beam Section
								P/S Tendons	f_c' (ksi)	$f_c'_I$ (ksi)	$f_c'_{deck}$ (ksi)	Bottom	Top		
14969	1023430	78’-8⅞”	9.4375	7’-10⅝”	4’-5 5/16” (L), 4’-11 3/16” (R)	7	90.0	48-0.5” Gr. 270 LR	6.5	4.5	3.0	1.9685		N/A	AASHTO BIV-48

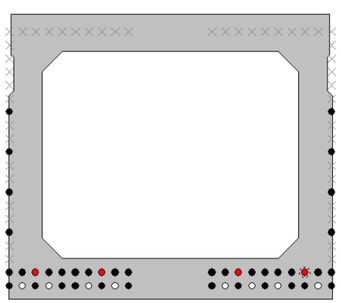

@ 98.4” from left support

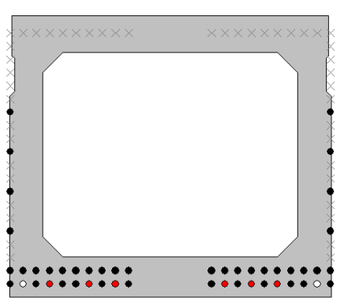

@ 141.75” from left support

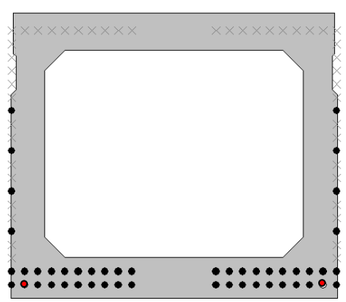

@ 216.5” from left support

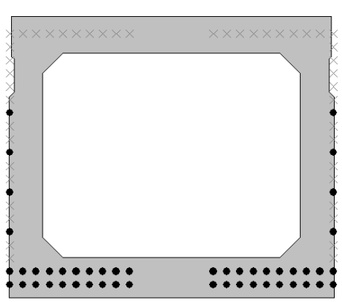

Strand Layout at Midspan

Strand Spacing:
Horizontal: 1.9685”
Vertical: 1.9685”

# of Strands: 48
CG from bottom at 98.4” from LS: 6.69”
CG from bottom at 141.75” from LS: 6.30”
CG from bottom at 216.5” from LS: 5.73”
CG from bottom at Midspan: 5.58”

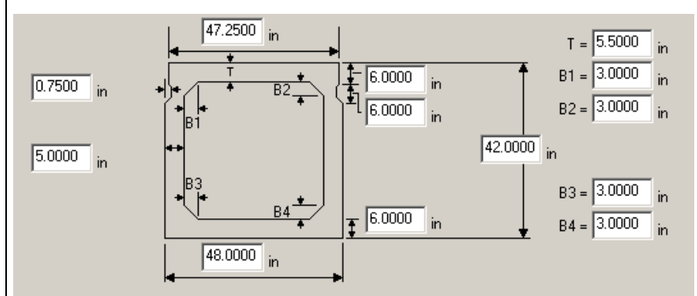

Cross-Section

Bridge #	Virtis BID #	Span length (ft)	t_{slab} (in)	Girder Spacing (ft)	Overhang Width (ft)	# of Girders	Skew (deg)	Materials				Dist. to Extreme Strands (in)		Harp Point (ft)	Beam Section
								P/S Tendons	f_c' (ksi)	$f_c'_I$ (ksi)	$f_c'_{deck}$ (ksi)	Bottom	Top		
16293	BID_2751	57’-3 ¼”	9.4375	8’-10 5/16”	4’-1⅝”	7	96.0	26-0.6” Gr. 270 LR	10.2	7.1	3.0	2.2441	4.252	N/A	1220x1220 Box Beam

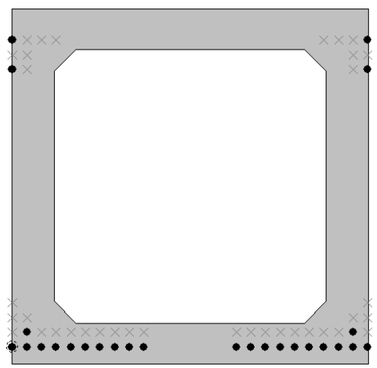

Strand Spacing:
Horizontal: 1.9685”
Vertical: 2”

# of Strands: 26
CG from bottom at Midspan: 8.48”

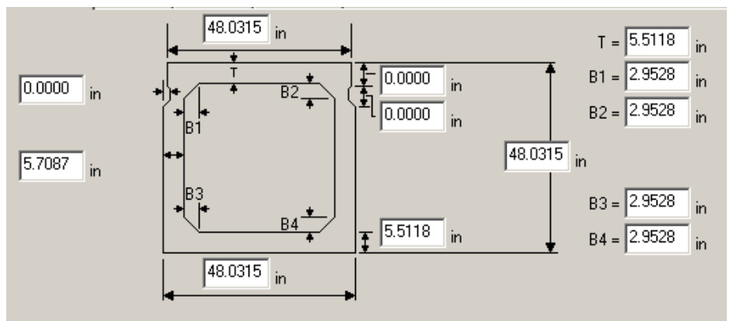

Strand Layout at Midspan	Cross-Section	Cross-Section

Bridge #	Virtis BID #	Span length (ft)	t_{slab} (in)	Girder Spacing (ft)	Overhang Width (ft)	# of Girders	Skew (deg)	Materials				Dist. to Extreme Strands (in)		Harp Point (ft)	Beam Section
								P/S Tendons	f_c' (ksi)	$f_{c'_l}$ (ksi)	$f_{c'}$ deck (ksi)	Bottom	Top		
16366	2223270	60'-4⅝"	9.4375	6'-7"	4'-0 1/16"	6	102.4	38-0.5" Gr. 270 LR	7.5	6.0	3.0	1.9685		N/A	Based on AASHTO BI-48

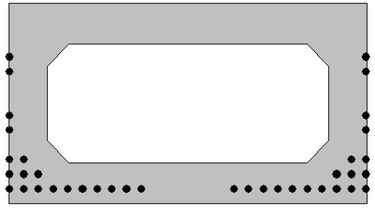

Strand Spacing:
Horizontal: 1.9685"
Vertical: 1.9685", 3.937", 1.9685", 5.9055", 1.9685"

# of Strands: 38
CG from bottom at Midspan: 5.39"

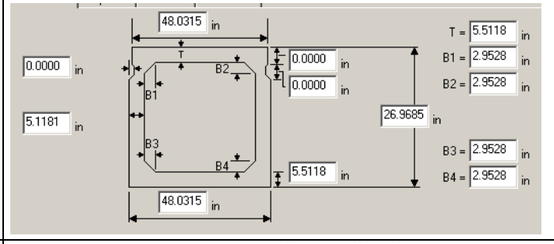

Strand Layout at Midspan	Cross-Section	Cross-Section

Bridge #	Virtis BID #	Span length (ft)	t_{slab} (in)	Girder Spacing (ft)	Overhang Width (ft)	# of Girders	Skew (deg)	Materials				Dist. to Extreme Strands (in)		Harp Point (ft)	Beam Section
								P/S Tendons	f_c' (ksi)	$f_{c'I}$ (ksi)	$f_{c'deck}$ (ksi)	Bottom	Top		
17240	3300870	51’-6”	8.5	8’-0”	4’-0”	4	90.0	24 (or 26)-0.5” Gr. 270 SR	6.0	4.8	3.0	2.0		N/A	AASHTO BII-48

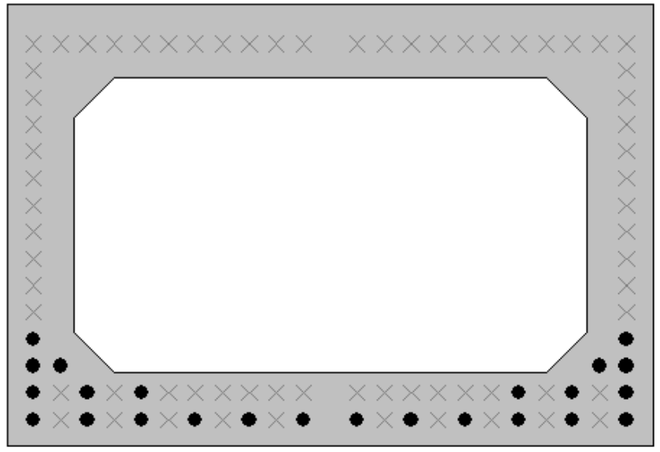

Strand Layout at Midspan – Interior Girder

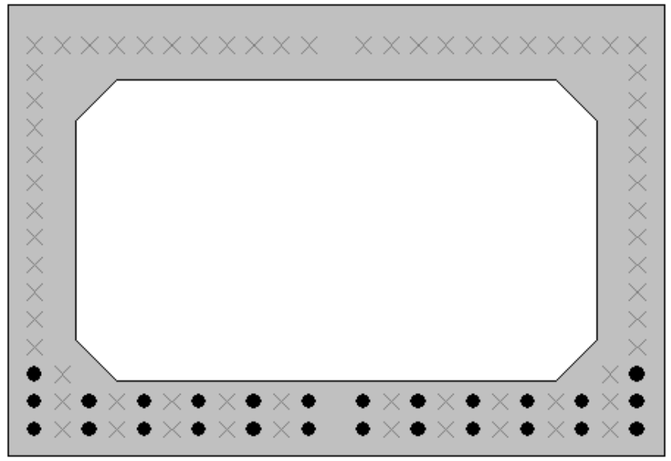

Strand Layout at Midspan – Exterior Girder

Strand Spacing:
Horizontal: 2.0”
Vertical: 2.0”

Interior:
# of Strands: 24
CG from bottom at Midspan: 3.67”

Exterior:
# of Strands: 26
CG from bottom at Midspan: 3.23”

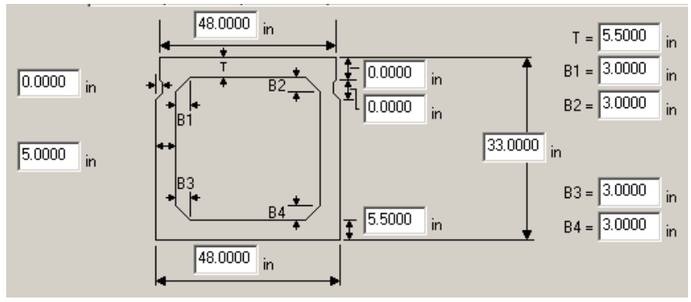

Cross-Section

Bridge #	Virtis BID #	Span length (ft)	t_{slab} (in)	Girder Spacing (ft)	Overhang Width (ft)	# of Girders	Skew (deg)	Materials				Dist. to Extreme Strands (in)		Harp Point (ft)	Beam Section
								P/S Tendons	f_c' (ksi)	$f_c'_I$ (ksi)	$f_c'_{deck}$ (ksi)	Bottom	Top		
9090	13113081000S053	66'-0½"	9.0	7'-1"	3'-5"	9	68.6	20-0.6" Gr. 270 LR	5.3 5.6	5.3 5.6	4.0	2.0		N/A	MDOT 33" Box Beam (Int) MDOT 33" Box Beam (Ext)

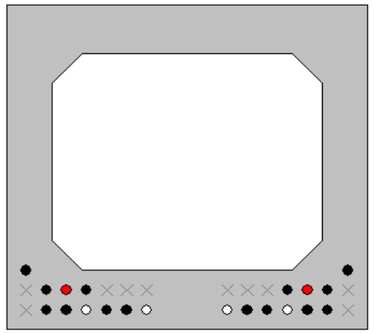

@ 60.0" from left support

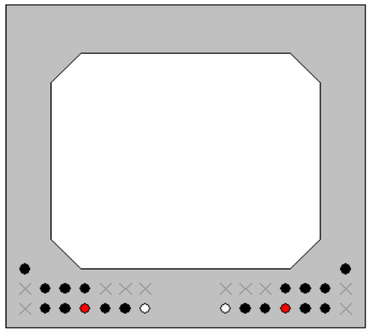

@ 84.0" from left support

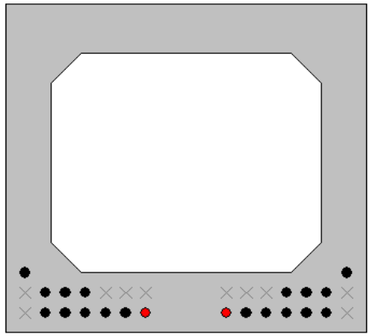

@ 174.0" from left support

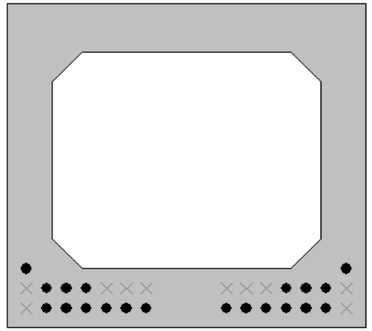

Strand Layout at Midspan

Strand Spacing:
Horizontal: 2"
Vertical: 2"

# of Strands: 20
Interior:
CG from bottom at 60.0" from LS: 3.14"
CG from bottom at 84.0" from LS: 3.25"
CG from bottom at 174.0" from LS: 3.11"
CG from bottom at Midspan: 3.00"

Exterior:
CG from bottom at 54.0" from LS: 3.14"
CG from bottom at 78.0" from LS: 3.25"
CG from bottom at 114.0" from LS: 3.11"
CG from bottom at Midspan: 3.00"

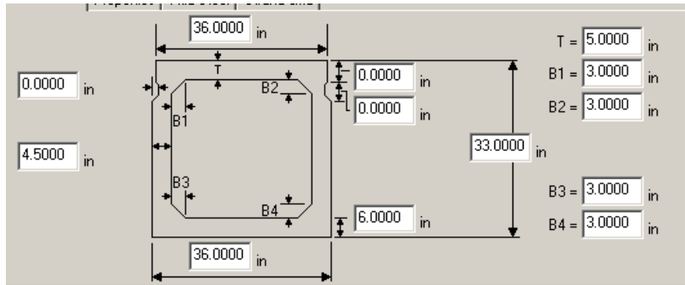

Cross-Section

Bridge #	Virtis BID #	Span length (ft)	t_{slab} (in)	Girder Spacing (ft)	Overhang Width (ft)	# of Girders	Skew (deg)	Materials				Dist. to Extreme Strands (in)		Harp Point (ft)	Beam Section
								P/S Tendons	f_c' (ksi)	f_{ci}' (ksi)	$f_{c\,deck}'$ (ksi)	Bottom	Top		
9091	13113081000S054	66'-2½"	9.0	7'-1"	3'-5"	9	68.3	20-0.6" Gr. 270 LR	5.3 5.5	5.3 5.5	4.0	2.0		N/A	MDOT 33" Box Beam (Int.) MDOT 33" Box Beam (Ext.)

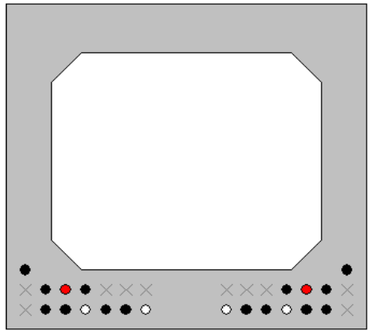

@ 60.0" from left support

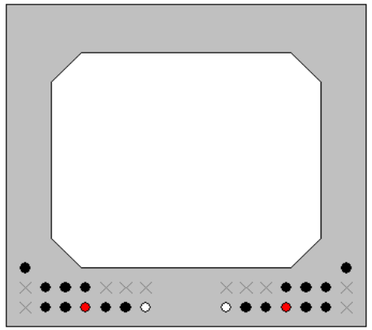

@ 84.0" from left support

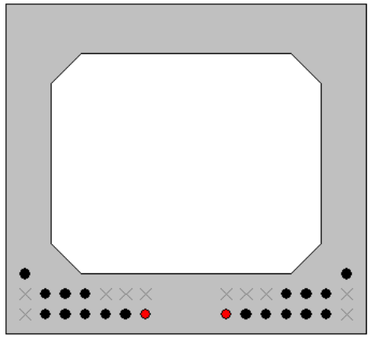

@ 174.0" from left support

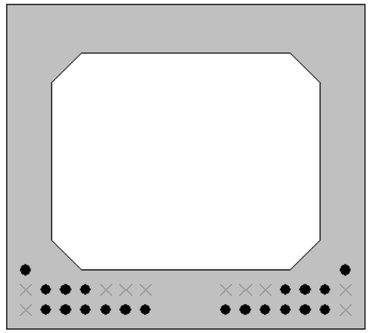

Strand Layout at Midspan

Strand Spacing:
Horizontal: 2"
Vertical: 2"

# of Strands: 20

Interior:
CG from bottom at 60.0" from LS: 3.14"
CG from bottom at 84.0" from LS: 3.25"
CG from bottom at 174.0" from LS: 3.11"
CG from bottom at Midspan: 3.00"

Exterior:
CG from bottom at 54.0" from LS: 3.14"
CG from bottom at 78.0" from LS: 3.25"
CG from bottom at 132.0" from LS: 3.11"
CG from bottom at Midspan: 3.00"

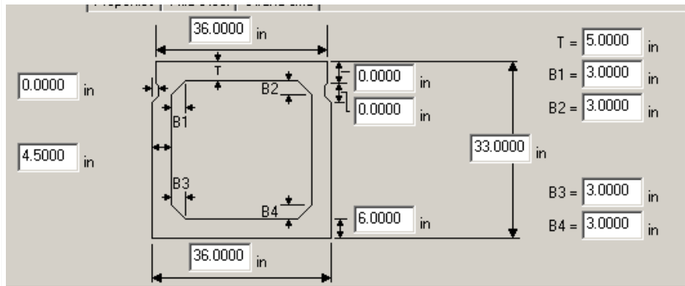

Cross-Section

Bridge #	Virtis BID #	Span length (ft)	t_{slab} (in)	Girder Spacing (ft)	Overhang Width (ft)	# of Girders	Skew (deg)	Materials				Dist. to Extreme Strands (in)		Harp Point (ft)	Beam Section
								P/S Tendons	f_c' (ksi)	f_{ci}' (ksi)	$f_{c\,deck}$' (ksi)	Bottom	Top		
9128	29129011000S140	33'-8⅜"	9.0625	7'-5⅞"	3'-1¼"	8	90.0	4-0.6" Gr. 270 LR	6.0	4.5	4.0	2.28		N/A	1525 Box Beam

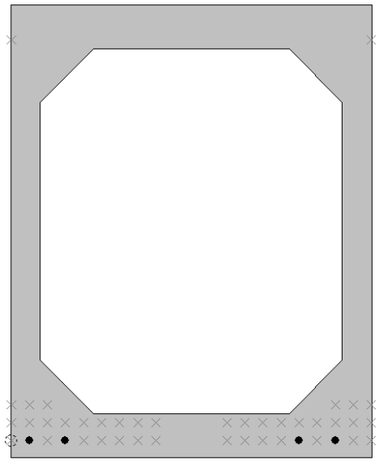

Strand Layout at Midspan

Strand Spacing:
Horizontal: 2.402"
Vertical: 2.402"

# of Strands: 4
CG from bottom at Midspan: 2.28"

Cross-Section

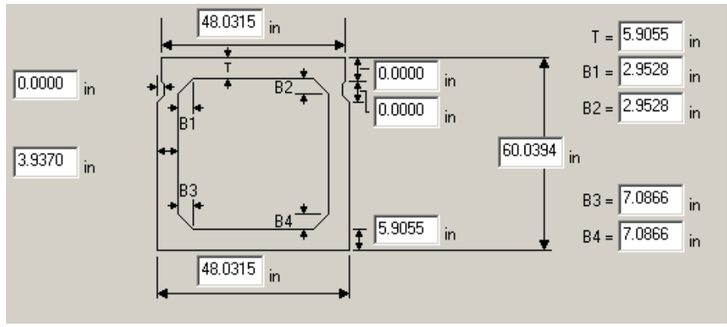

Cross-Section

Bridge #	Virtis BID #	Span length (ft)	t_{slab} (in)	Girder Spacing (ft)	Overhang Width (ft)	# of Girders	Skew (deg)	Materials				Dist. to Extreme Strands (in)		Harp Point (ft)	Beam Section
								P/S Tendons	f_c' (ksi)	f_{ci}' (ksi)	$f_{c\,deck}'$ (ksi)	Bottom	Top		
									5.8	5.3					17” Box Beam (A)
									5.6	5.2					17” Box Beam (B and C)
									5.2	5.1					17” Box Beam (D)
									5.0	4.9					17” Box Beam (E thru K)
9217	45145071000B010	42’-3½”	9.25	3@6’-2 ½”, 7@5’-8⅛”	3’-3”	11	90.0	16-0.6” Gr. 270 LR	5.9	5.3	4.0	2.0	2.5	N/A	17” Box Beam (L)

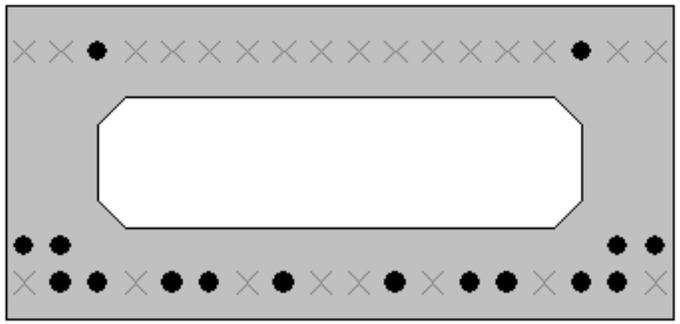

Strand Layout at Midspan (All girders)

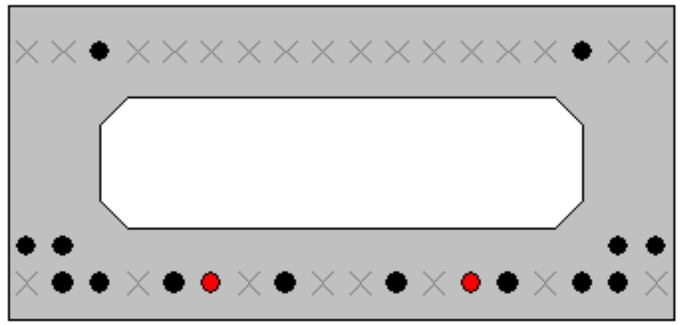

Strand Layout at Support to 96” (E thru K), 54” (B thru D)

Strand Spacing:
Horizontal: 2”
Vertical: 2”

Beams: (A) is far left girder, (L) is far right girder

# of Strands: 16
Girders: A and L
CG from bottom at Midspan: 4.06”

Girders: B, C, D
CG from bottom at Support to 54”: 4.36”
CG from bottom at Midspan: 4.06”

Girders: E thru K
CG from bottom at Support to 96”: 4.36”
CG from bottom at Midspan: 4.06”

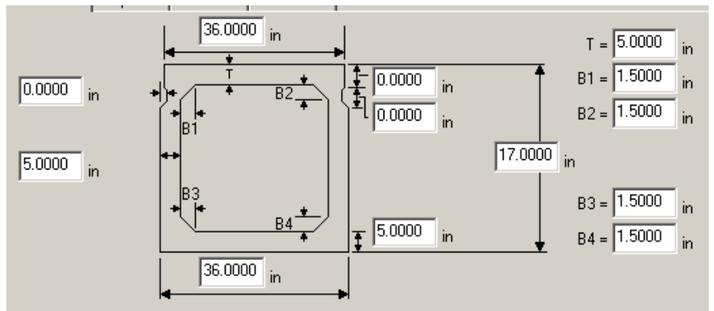

Cross-Section

Bridge #	Virtis BID #	Span length (ft)	t_{slab} (in)	Girder Spacing (ft)	Overhang Width (ft)	# of Girders	Skew (deg)	Materials				Dist. to Extreme Strands (in)		Harp Point (ft)	Beam Section
								P/S Tendons	f_c' (ksi)	$f_c'_I$ (ksi)	$f_c'_{deck}$ (ksi)	Bottom	Top		
9219	16116032000B030	53'-2"	9.0	5'-3"	2'-7½"	9	90.0	16-0.6" Gr. 270 LR	5.7	5.6	4.0	2.0		N/A	MDOT 21" Box Beam

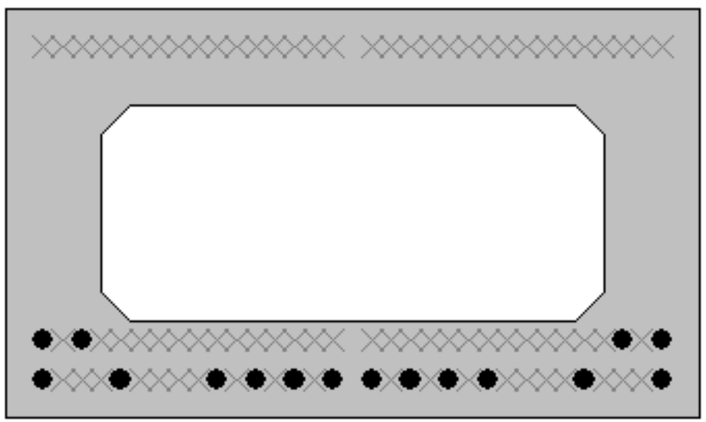

Strand Layout at Midspan

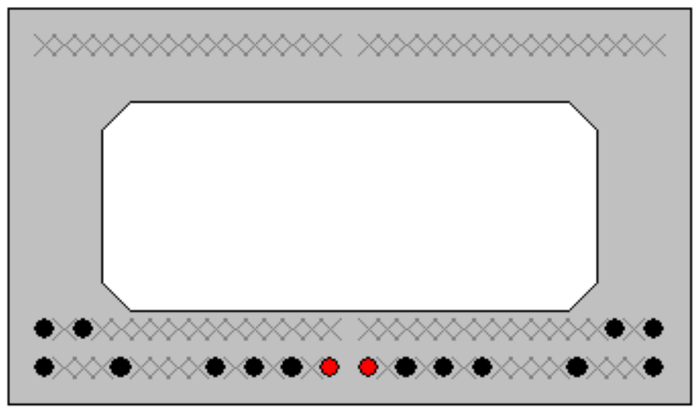

Strand Layout at Support to 72"

Strand Spacing:
Horizontal: 1"
Vertical: 2"

# of Strands: 16
CG from bottom at Support to 72": 2.57"
CG from bottom at Midspan: 2.50"

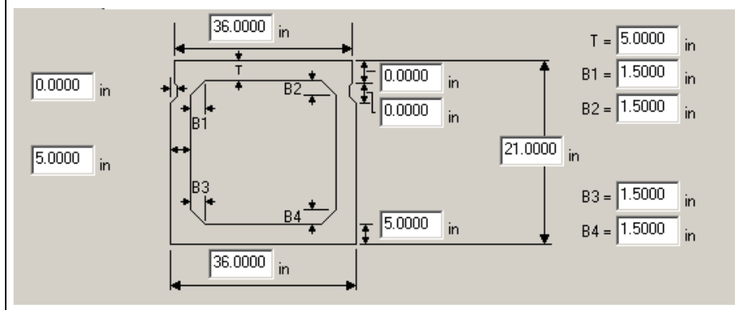

Cross-Section

Bridge #	Virtis BID #	Span length (ft)	t_{slab} (in)	Girder Spacing (ft)	Overhang Width (ft)	# of Girders	Skew (deg)	Materials				Dist. to Extreme Strands (in)		Harp Point (ft)	Beam Section
								P/S Tendons	f_c' (ksi)	$f_c'_I$ (ksi)	$f_c'_{deck}$ (ksi)	Bottom	Top		
9243	82182041000S020	73’-4”	9.0	6’-2”	2’-3¾”	13	90.0	21-0.6” Gr. 270 LR	7.0	6.0	4.0	2.0		N/A	33”x36” Box Beam

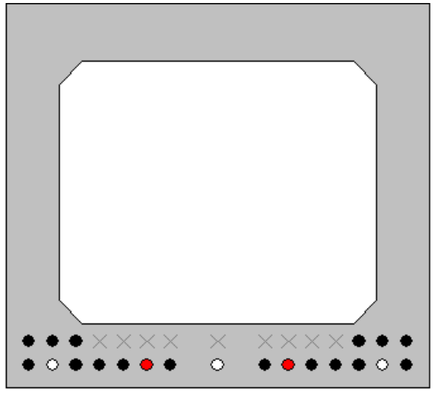

@ 24.0” from left support

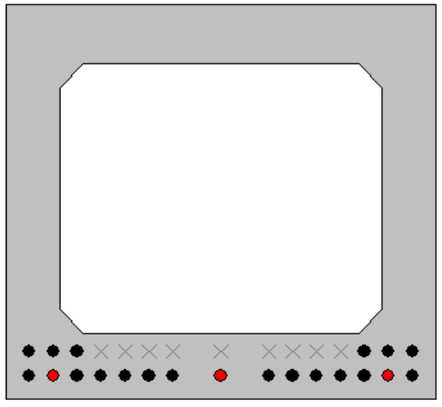

@ 48.0” from left support

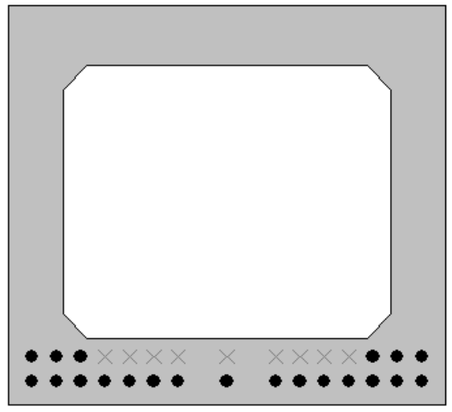

Strand Layout at Midspan

Strand Spacing:
Horizontal: 2”
Vertical: 2”

# of Strands: 21
CG from bottom at 24.0”: 2.75”
CG from bottom at 48.0”: 2.67”
CG from bottom at Midspan: 2.57”

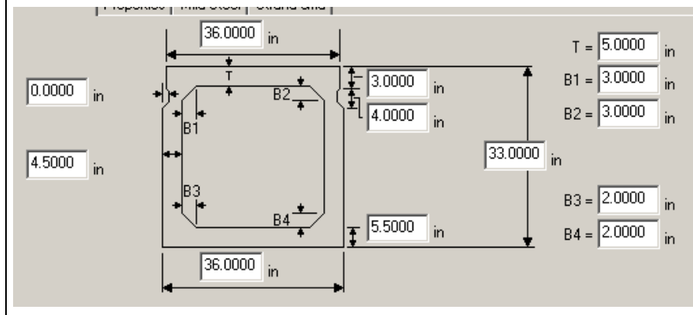

Cross-Section

Bridge #	Virtis BID #	Span length (ft)	t_{slab} (in)	Girder Spacing (ft)	Overhang Width (ft)	# of Girders	Skew (deg)	Materials				Dist. to Extreme Strands (in)		Harp Point (ft)	Beam Section
								P/S Tendons	f_c' (ksi)	$f_c'_I$ (ksi)	$f_c'_{deck}$ (ksi)	Bottom	Top		
9248	02102041000B020	37’-9”	9.0	8’-0”	3’-2½”	6	90.0	18-0.6” Gr. 270 LR	6.0	5.0	4.0	2.0	3.0	N/A	21” Box Beam

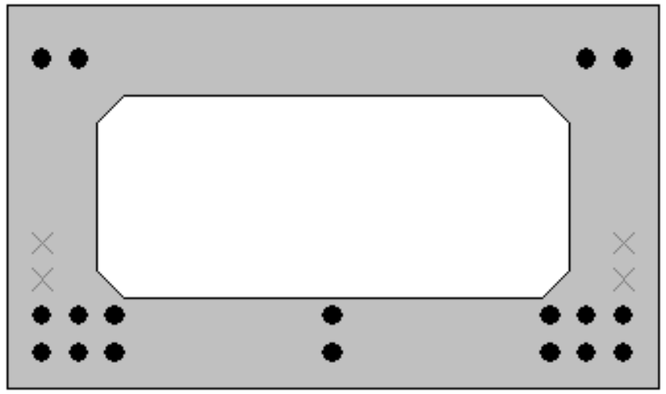	Strand Spacing: Horizontal: 2.0”, Vertical: 2.0”, 10.0” # of Strands: 18 CG from bottom at Midspan: 6.33”	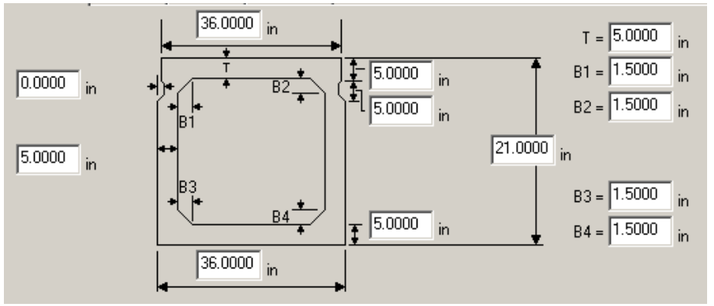
Strand Layout at Midspan	Cross-Section	Cross-Section

Bridge #	Virtis BID #	Span length (ft)	t_{slab} (in)	Girder Spacing (ft)	Overhang Width (ft)	# of Girders	Skew (deg)	Materials				Dist. to Extreme Strands (in)		Harp Point (ft)	Beam Section
								P/S Tendons	f_c’ (ksi)	f_c’$_I$ (ksi)	f_c’ $_{deck}$ (ksi)	Bottom	Top		
9284	33133082000B030	31’-6¾”	9.0625	6’-7⅞”	2’-5½”	10	90.0	9-0.6” Gr. 270 LR	5.0	3.0	4.0	2.0		N/A	17”x36” Box Beam

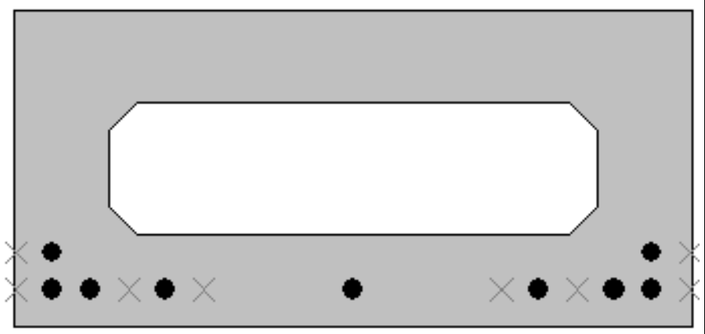	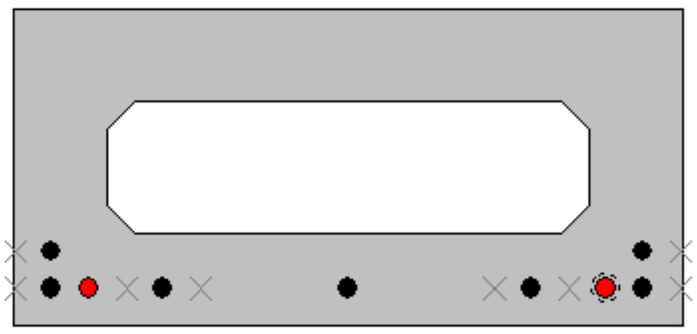	Strand Spacing: Horizontal: 2” Vertical: 2” # of Strands: 9 CG from bottom at Support to 78.74”: 2.57” CG from bottom at Midspan: 2.44” 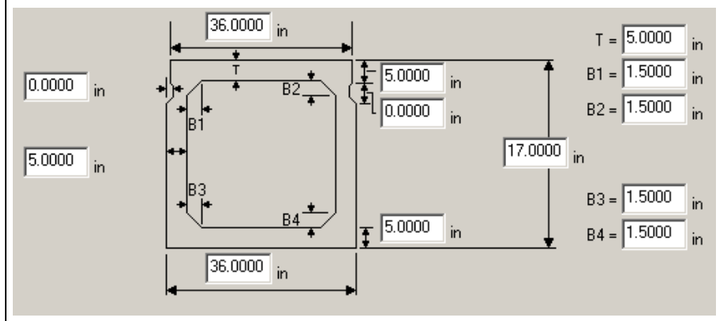
Strand Layout at Midspan	Strand Layout at Support to 78.74”	Cross-Section

Bridge #	Virtis BID #	Span length (ft)	t_{slab} (in)	Girder Spacing (ft)	Overhang Width (ft)	# of Girders	Skew (deg)	Materials				Dist. to Extreme Strands (in)		Harp Point (ft)	Beam Section
								P/S Tendons	f_c' (ksi)	$f_c'_I$ (ksi)	$f_c'_{deck}$ (ksi)	Bottom	Top		
1150	550A0490001	70'-7"	8.25	8'-6"	3'-8"	3	28	39-0.5" Gr. 270 LR	6.5	6.0	3.0	2.0	3.0	N/A	33"x36" Box Beam

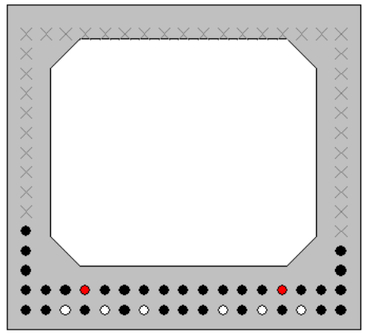

@ 36" from left support

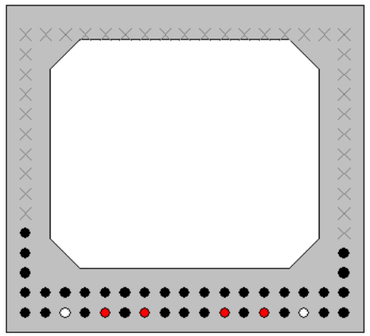

@ 72" from left support

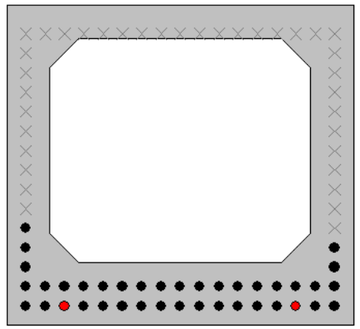

@ 108" from left support

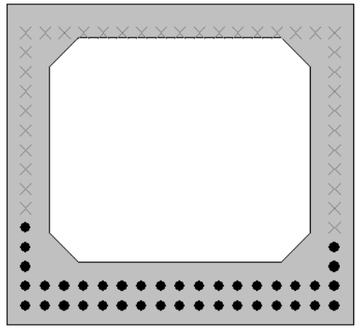

Strand Layout at Midspan

Strand Spacing:
Horizontal: 2"
Vertical: 2"

# of Strands: 39
CG from bottom at 62.99": 2.33"
CG from bottom at 36": 3.87"
CG from bottom at 72": 3.88"
CG from bottom at 108": 3.68"
CG from bottom at Midspan: 3.59"

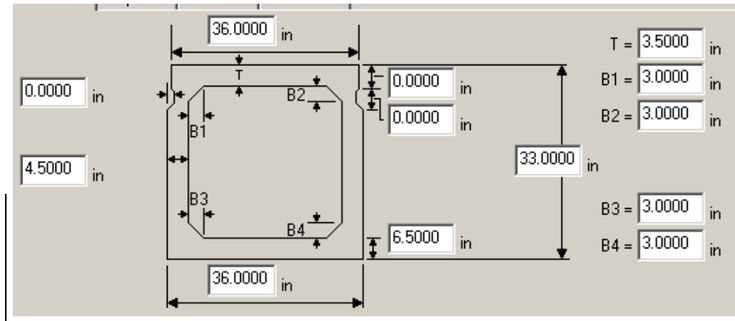

Cross-Section

Bridge #	Virtis BID #	Span length (ft)	t_{slab} (in)	Girder Spacing (ft)	Overhang Width (ft)	# of Girders	Skew (deg)	Materials				Dist. to Extreme Strands (in)		Harp Point (ft)	Beam Section
								P/S Tendons	f_c' (ksi)	$f_c'_l$ (ksi)	$f_{c\,deck}'$ (ksi)	Bottom	Top		
9324	141140410000B010	42'-4"	9.0	10'-6"	2'-7½"	5	90.0	20-0.5" Gr. 270 LR	5.5	4.4	4.0	2.0		N/A	27"x36" Box Beam

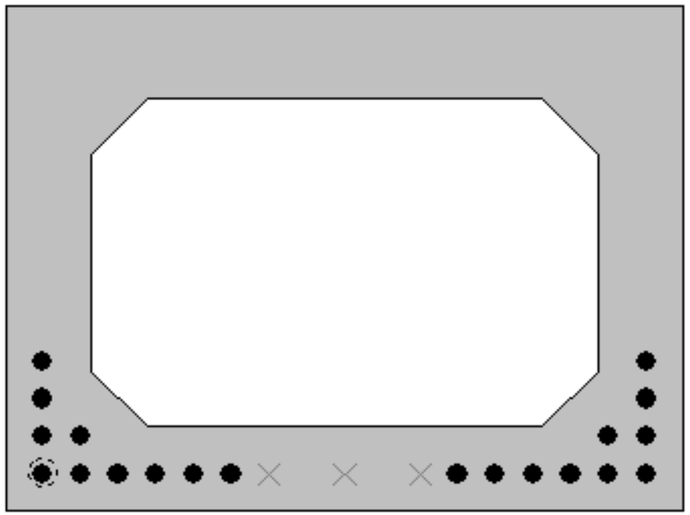

Strand Layout at Midspan

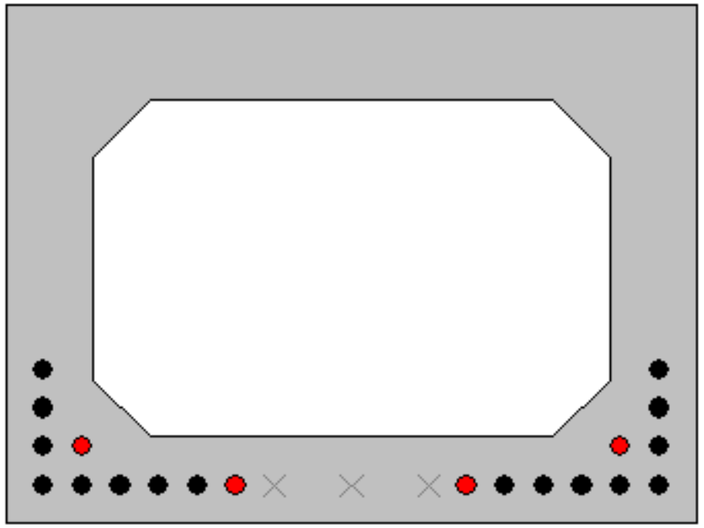

Strand Layout at Support to 66.0"

Strand Spacing:
Horizontal: 2"
Vertical: 2"

# of Strands: 20
CG from bottom at Support to 66.0": 3.50"
CG from bottom at Midspan: 3.40"

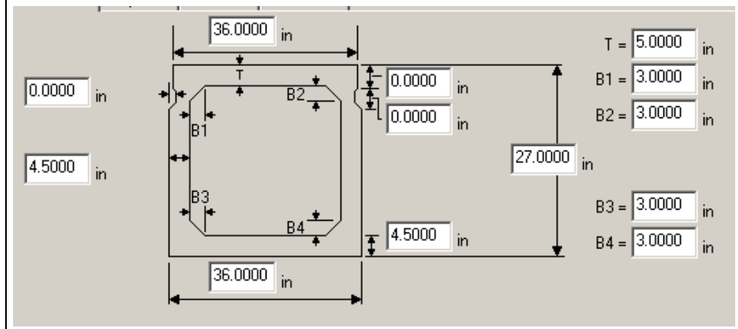

Cross-Section

Bridge #	Virtis BID #	Span length (ft)	t_{slab} (in)	Girder Spacing (ft)	Overhang Width (ft)	# of Girders	Skew (deg)	Materials				Dist. to Extreme Strands (in)		Harp Point (ft)	Beam Section
								P/S Tendons	f_c' (ksi)	$f_{c\,l}'$ (ksi)	$f_{c\,deck}'$ (ksi)	Bottom	Top		
9349	72172041000B010	48’-8”	9.0	7’-0”	3’-6”	6	90.0	22-0.5” Gr. 270 LR	6.0	4.9	4.0	2.0		N/A	21”x36” Box Beam

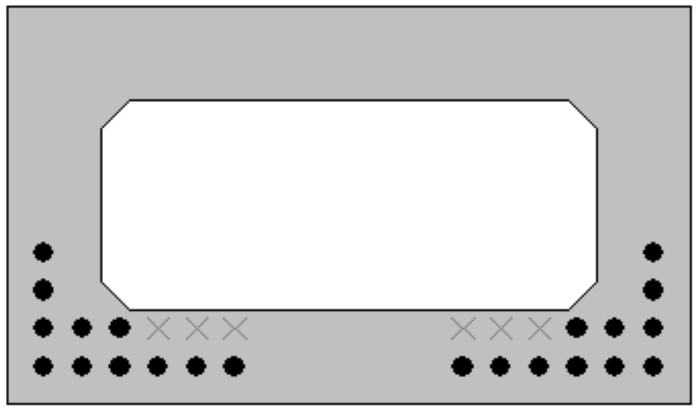

Strand Layout at Midspan

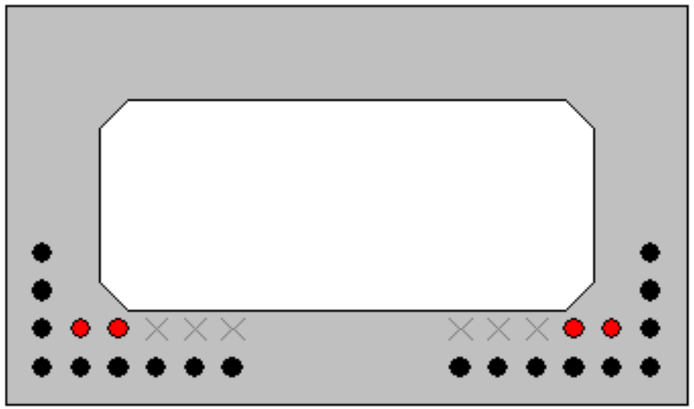

Strand Layout at Support to 66.0”

Strand Spacing:
Horizontal: 2”
Vertical: 2”

# of Strands: 22
CG from bottom at Support to 66.0”: 3.33”
CG from bottom at Midspan: 3.45”

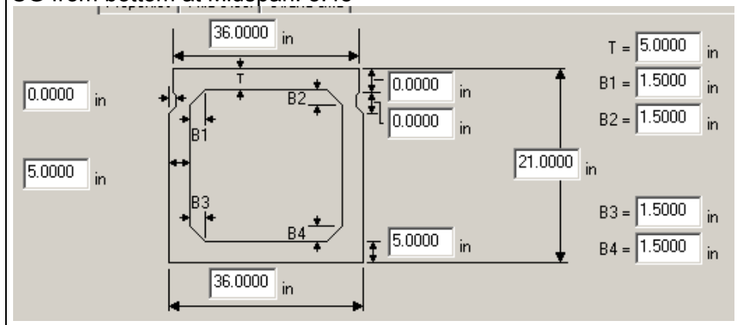

Cross-Section

Bridge #	Virtis BID #	Span length (ft)	t_{slab} (in)	Girder Spacing (ft)	Overhang Width (ft)	# of Girders	Skew (deg)	Materials				Dist. to Extreme Strands (in)		Harp Point (ft)	Beam Section
								P/S Tendons	f_c' (ksi)	f_c'$_I$ (ksi)	f_c'$_{deck}$ (ksi)	Bottom	Top		
9355	38138111000R021	75'-2⅜"	9.0625	7'-11"	3'-6"	6	109.6	26-0.6" Gr. 270 LR	7.0	6.2	4.0	2.0	2.75	N/A	39"x36" Box Beam

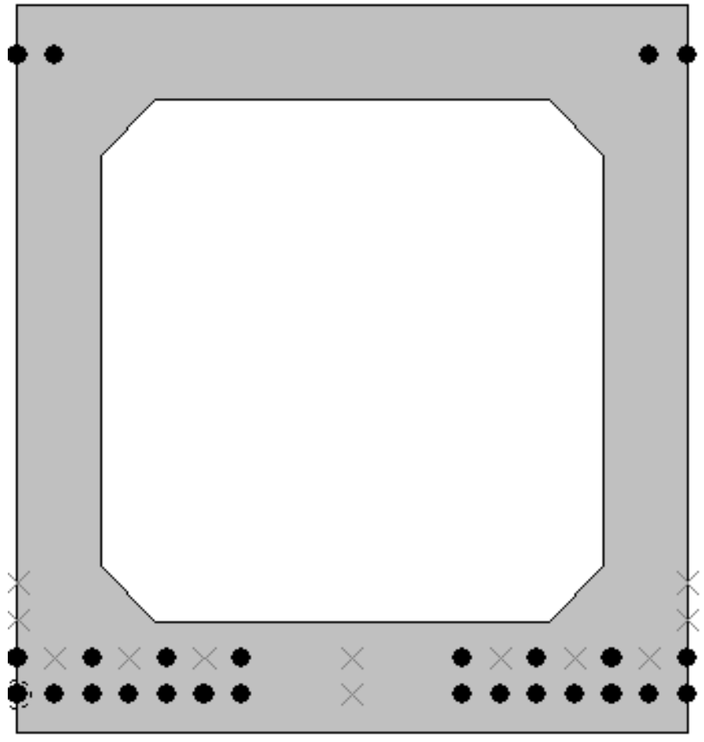

Strand Layout at Midspan

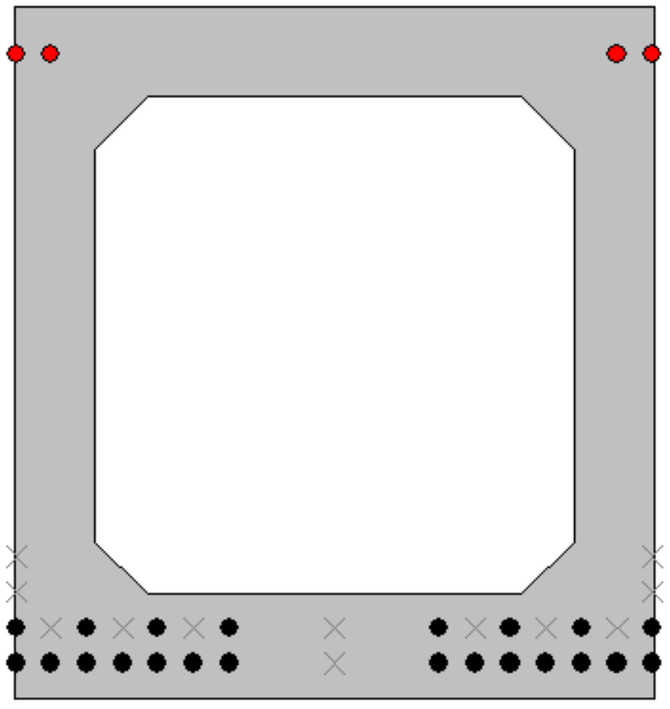

Strand Layout at Support to 225.60"

Strand Spacing:
Horizontal: 2"
Vertical: 2"

# of Strands: 26
CG from bottom at Support to 225.60": 2.73"
CG from bottom at Midspan: 7.88"

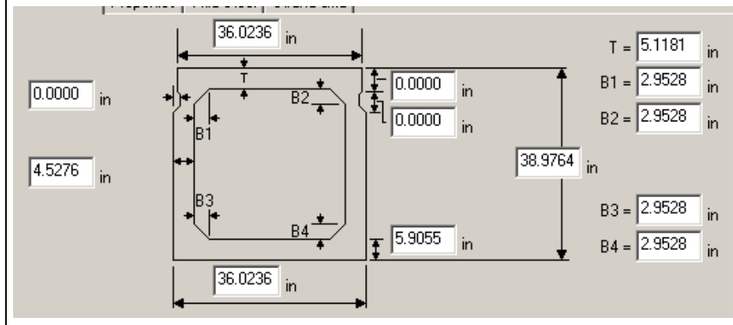

Cross-Section

Bridge #	Virtis BID #	Span length (ft)	t_{slab} (in)	Girder Spacing (ft)	Overhang Width (ft)	# of Girders	Skew (deg)	Materials				Dist. to Extreme Strands (in)		Harp Point (ft)	Beam Section
								P/S Tendons	f_c' (ksi)	f_{ci}' (ksi)	$f_{c\,deck}'$ (ksi)	Bottom	Top		
9356	38138111000R022	75’-2⅜”	9.0625	7’-11”	3’-6”	6	109.6	26-0.6” Gr. 270 LR	7.0	6.2	4.0	2.0	2.75	N/A	39”x36” Box Beam

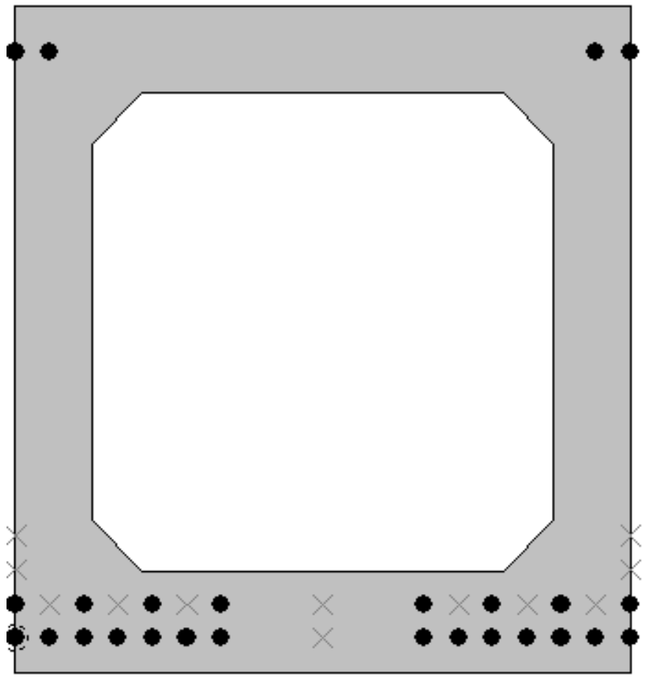

Strand Layout at Midspan

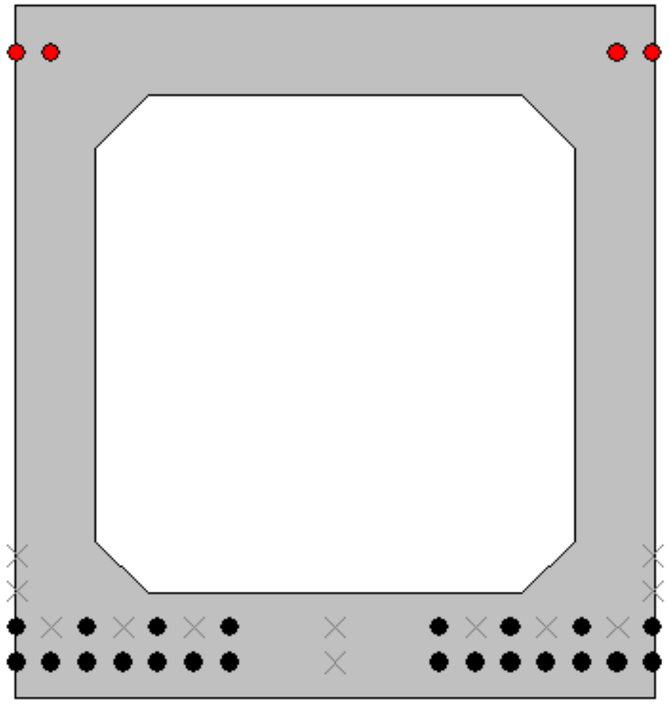

Strand Layout at Support to 213.04”

Strand Spacing:
Horizontal: 2”
Vertical: 2”

# of Strands: 26
CG from bottom at Support to 213.04”: 2.73”
CG from bottom at Midspan: 7.88”

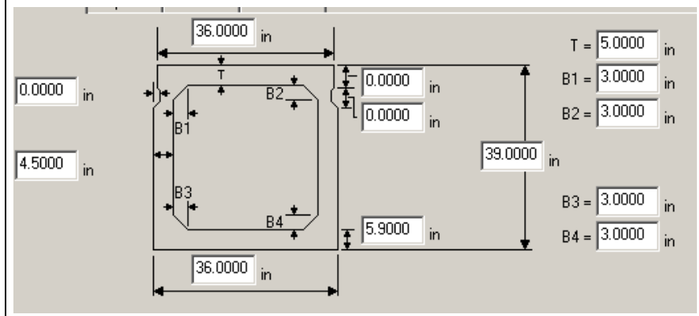

Cross-Section

Bridge #	Virtis BID #	Span length (ft)	t_{slab} (in)	Girder Spacing (ft)	Overhang Width (ft)	# of Girders	Skew (deg)	Materials				Dist. to Extreme Strands (in)		Harp Point (ft)	Beam Section
								P/S Tendons	f_c' (ksi)	f_{ci}' (ksi)	$f_{c\,deck}'$ (ksi)	Bottom	Top		
9361	47147065000R033	65’-9½”	9.0	6’-0”	2’-7½”	11	137.2	30-0.5” Gr. 270 LR	6.5	5.5	4.0	2.0		N/A	27”x36” Box Beam

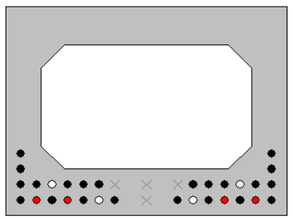	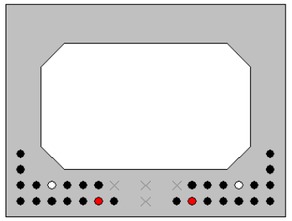	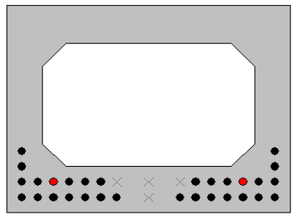	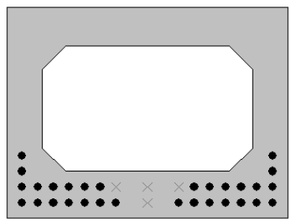	Strand Spacing: Horizontal: 2” Vertical: 2” # of Strands: 30 CG from bottom at 18.0” from LS: 3.82” CG from bottom at 79.2” from LS: 3.54” CG from bottom at 150.0” from LS: 3.43” CG from bottom at Midspan: 3.47” 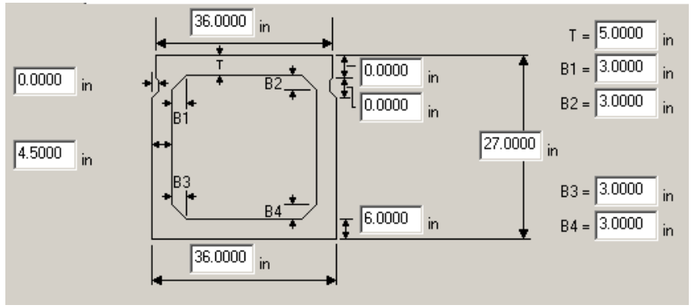
@ 18.0” from left support	@ 79.2” from left support	@ 150.0” from left support	Strand Layout at Midspan	Cross-Section

Bridge #	Virtis BID #	Span length (ft)	t_{slab} (in)	Girder Spacing (ft)	Overhang Width (ft)	# of Girders	Skew (deg)	Materials				Dist. to Extreme Strands (in)		Harp Point (ft)	Beam Section
								P/S Tendons	f_c' (ksi)	$f_{c'_l}$ (ksi)	$f_{c'\,deck}$ (ksi)	Bottom	Top		
9369	11111015000R033	51’-3⅞”	9.0	6’-6”	3’-4½”	10	115.7	14-0.6” Gr. 270 LR	5.4	4.5	4.0	2.0		N/A	27”x36” Box Beam

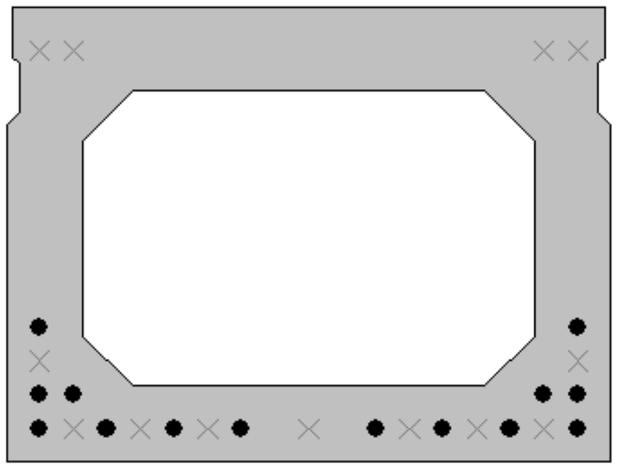

Strand Layout at Midspan

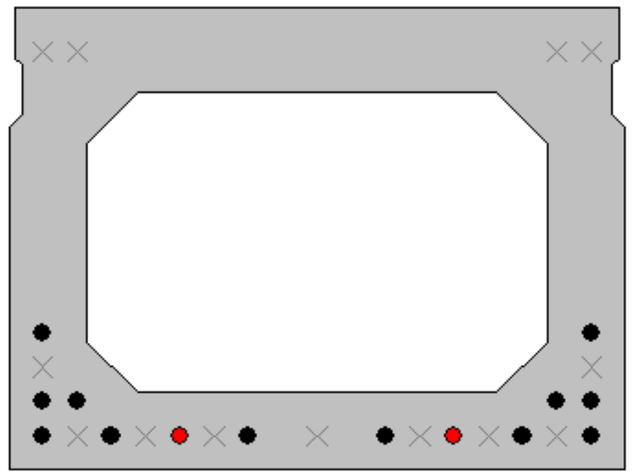

Strand Layout at Support to 48.0”

Strand Spacing:
Horizontal: 2”
Vertical: 2”

# of Strands: 14
CG from bottom at Support to 48.0”: 3.67”
CG from bottom at Midspan: 3.43”

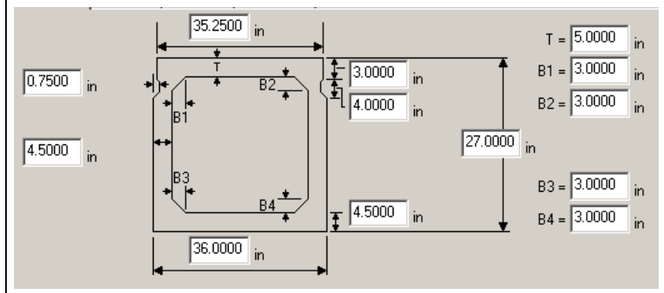

Cross-Section

Bridge #	Virtis BID #	Span length (ft)	t_{slab} (in)	Girder Spacing (ft)	Overhang Width (ft)	# of Girders	Skew (deg)	Materials				Dist. to Extreme Strands (in)		Harp Point (ft)	Beam Section
								P/S Tendons	f_c' (ksi)	$f_{c\,l}'$ (ksi)	$f_{c\,deck}'$ (ksi)	Bottom	Top		
9370	11111015000R034	51’-3⅞”	9.0	6’-5”	3’-4”	12	115.7	14-0.6” Gr. 270 LR	5.2	4.4	4.0	2.0		N/A	27”x36” Box Beam

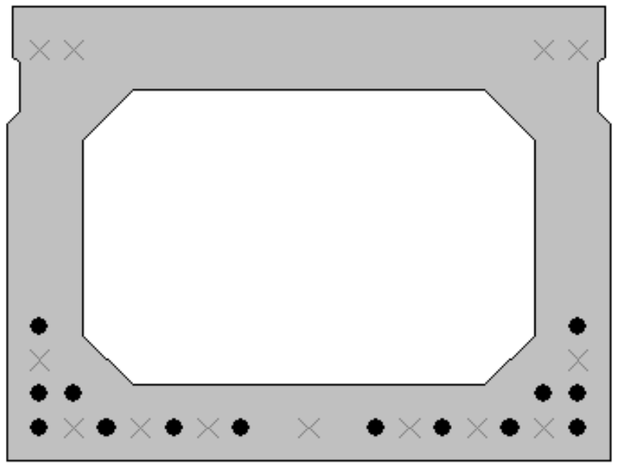

Strand Layout at Midspan

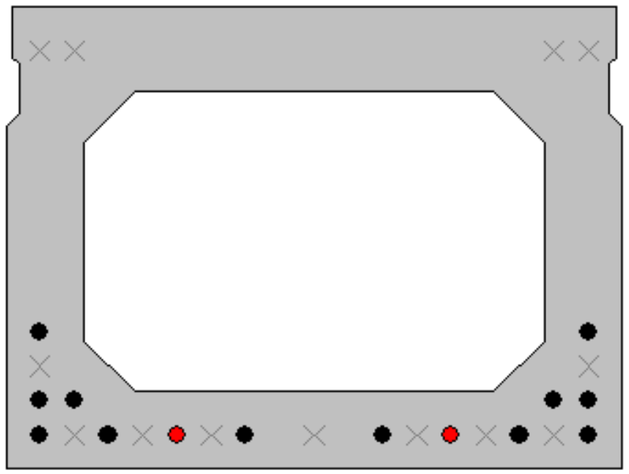

Strand Layout at Support to 54.0”

Strand Spacing:
Horizontal: 2”
Vertical: 2”

# of Strands: 14
CG from bottom at Support to 54.0”: 3.67”
CG from bottom at Midspan: 3.43”

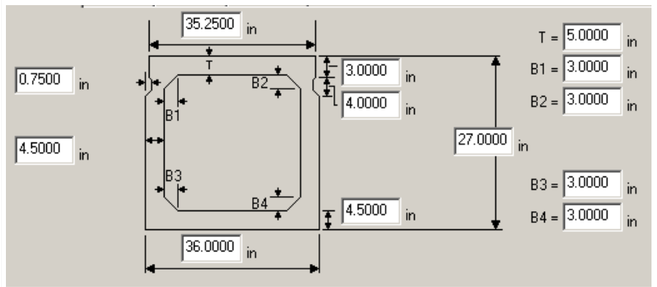

Cross-Section

Bridge #	Virtis BID #	Span length (ft)	t_{slab} (in)	Girder Spacing (ft)	Overhang Width (ft)	# of Girders	Skew (deg)	Materials				Dist. to Extreme Strands (in)		Harp Point (ft)	Beam Section
								P/S Tendons	f_c' (ksi)	f_{ci}' (ksi)	$f_{c\,deck}'$ (ksi)	Bottom	Top		
9383	71171073000B010	46’-9⅞”	9.0	10’-7”	2’-6”	5	45.0	16-0.6” Gr. 270 LR	6.0	5.0	4.0	2.0		N/A	27”x36” Box Beam

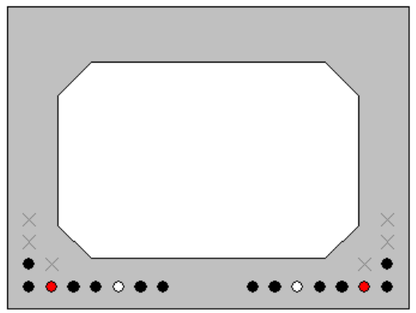

@ 24.0” from left support

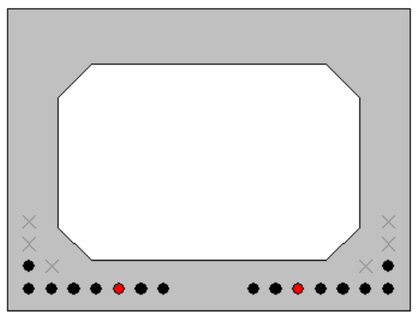

@ 72.0” from left support

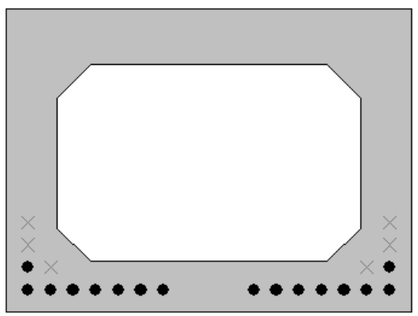

Strand Layout at Midspan

Strand Spacing:
Horizontal: 2”
Vertical: 2”

# of Strands: 16
CG from bottom at 24.0”: 2.33”
CG from bottom at 72.0”: 2.29”
CG from bottom at Midspan: 2.25”

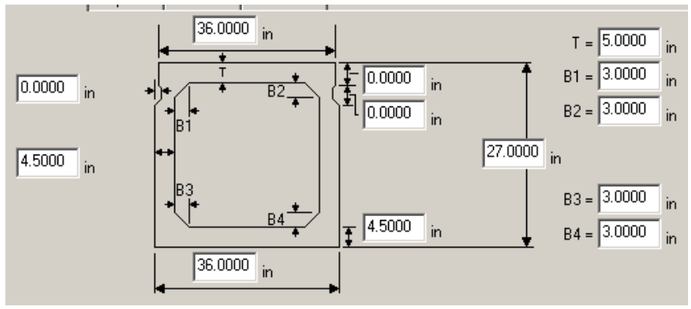

Cross-Section

Bridge #	Virtis BID #	Span length (ft)	t_{slab} (in)	Girder Spacing (ft)	Overhang Width (ft)	# of Girders	Skew (deg)	Materials				Dist. to Extreme Strands (in)		Harp Point (ft)	Beam Section
								P/S Tendons	f_c' (ksi)	$f_{c\,l}'$ ksi)	$f_{c\,deck}'$ (ksi)	Bottom	Top		
9394	25125031000S010	66'-10⅞"	9.0	7'-6"	4'-1½"	11	59.8	34-0.5" Gr. 270 LR	6.0	5.0	4.0	2		N/A	27"x48" Box Beam

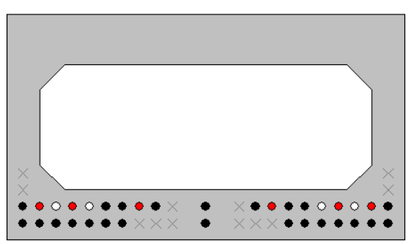

@ 54.0" from left support

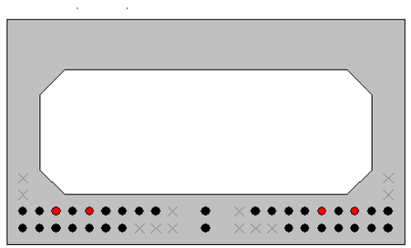

@ 96.0" from left support

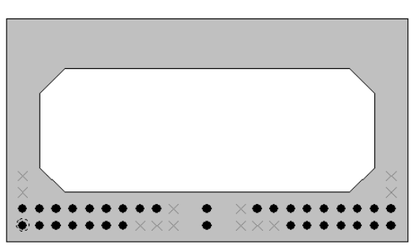

Strand Layout at Midspan

Strand Spacing:
Horizontal: 2"
Vertical: 2"

# of Strands: 34
CG from bottom at 54.0": 2.75"
CG from bottom at 96.0": 3.00"
CG from bottom at Midspan: 3.12"

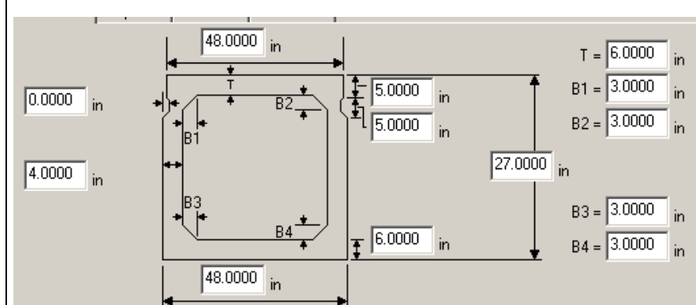

Cross-Section

Bridge #	Virtis BID #	Span length (ft)	t_{slab} (in)	Girder Spacing (ft)	Overhang Width (ft)	# of Girders	Skew (deg)	Materials				Dist. to Extreme Strands (in)		Harp Point (ft)	Beam Section
								P/S Tendons	f_c' (ksi)	$f_{c'_i}$ (ksi)	$f_{c'_{deck}}$ (ksi)	Bottom	Top		
1150	550A0490001	70'-7"	8.25	8'-6"	3'-8"	3	118.0	39-0.5" Gr. 270 LR	6.5	6.0	3.0	2.0		N/A	33"x36" Box Beam

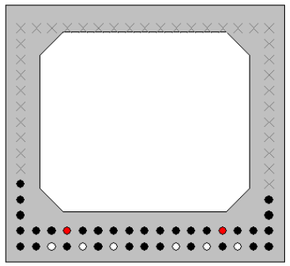

@ 36.0" from left support

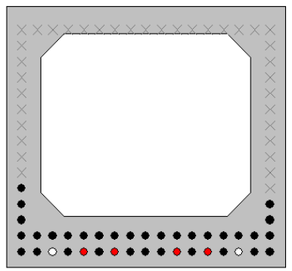

@ 72.0" from left support

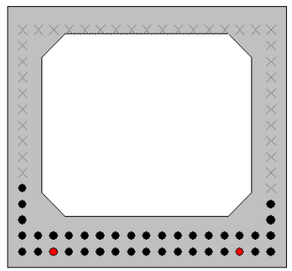

@ 108.0" from left support

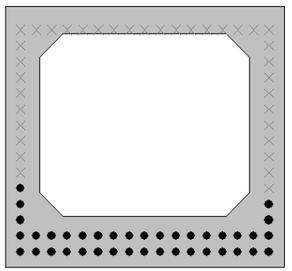

Strand Layout at Midspan

Strand Spacing:
Horizontal: 2"
Vertical: 2"

# of Strands: 39
CG from bottom at 36.0" from LS: 3.87"
CG from bottom at 72.0" from LS: 3.88"
CG from bottom at 108.0" from LS: 3.68"
CG from bottom at Midspan: 3.59"

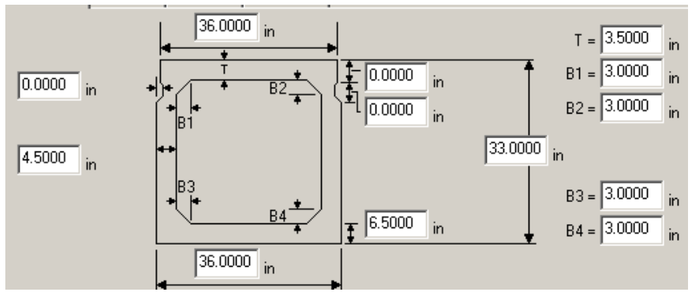

Cross-Section

C.5 ASBI Box Girders

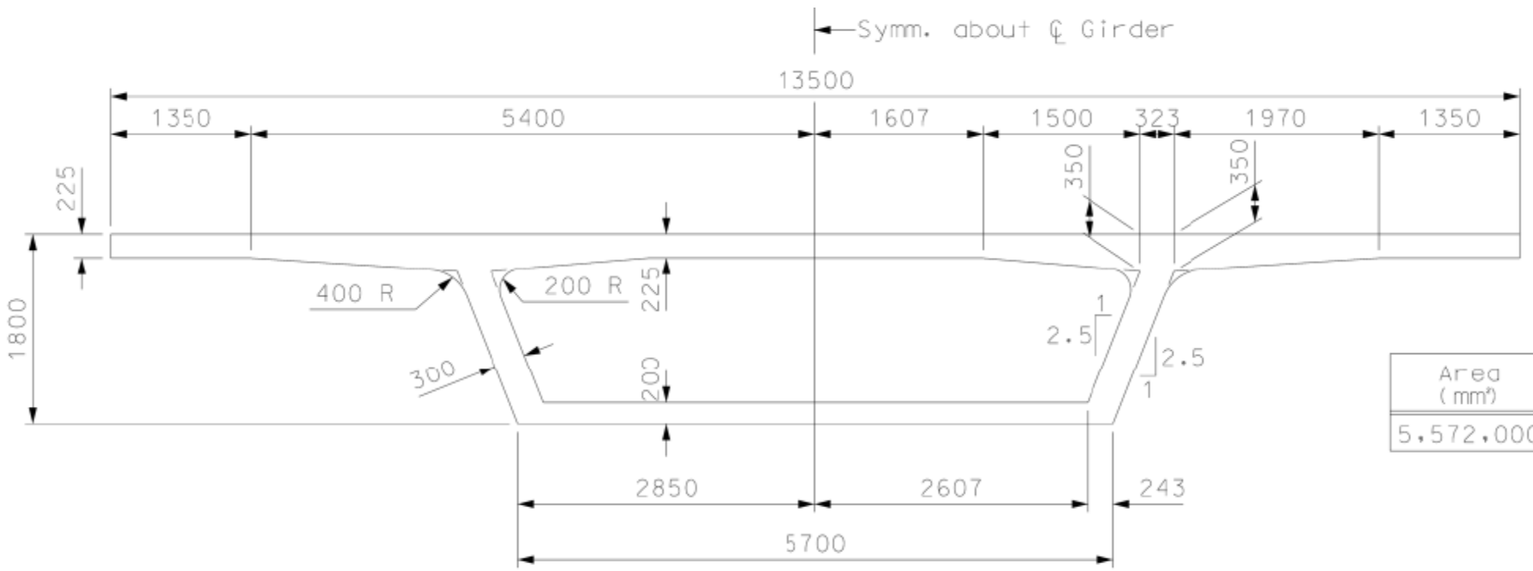

Area (mm²)	Wt/3000 mm (Kn)	Ix (m⁴)	Yt (mm)
5,572,000	408	2412	584

ASBI Box Section 1800-2

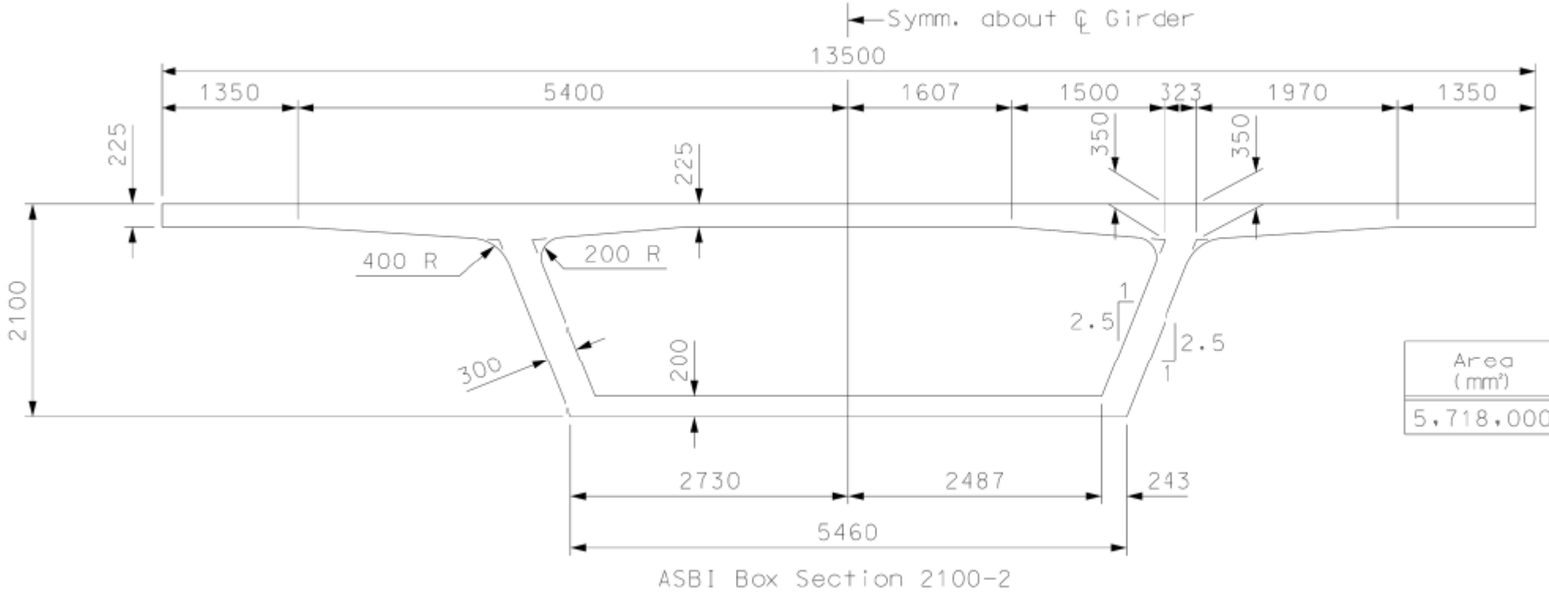

Area (mm²)	Wt/3000 mm (Kn)	Ix (m⁴)	Yt (mm)
5,718,000	419	3414	672

ASBI Box Section 2100-2

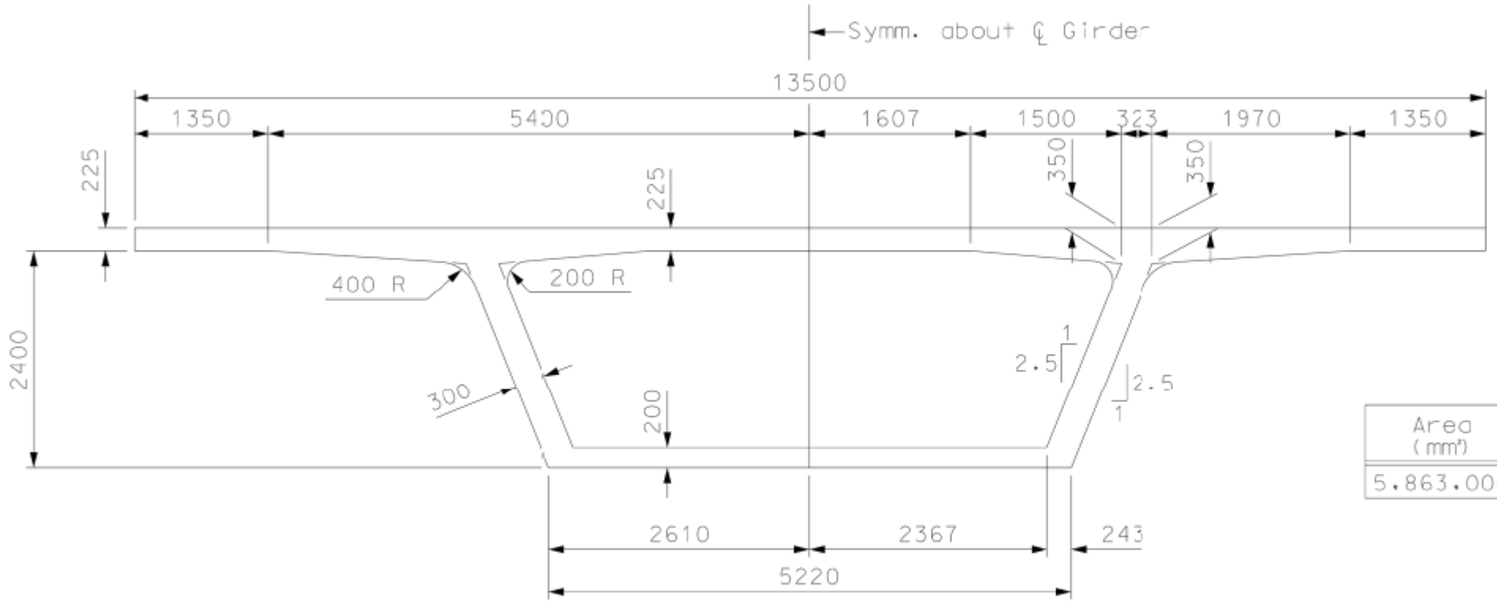

ASBI Box Section 2400-2

Area (mm²)	Wt/3000 mm (Kn)	Ix (m⁴)	Yt (mm)
5.863.000	429	4591	761

APPENDIX D – CALIBRATION OF SERVICE III LIMIT STATE

Table of Contents

List of Tables

List of Figures

D.1 Calibration Process

This section summarized the calibration procedure utilized in this study. The RT proposed the following general procedure for the calibration of Service III limit state.

1) Formulate the limit state function and identify basic variables.
2) Identify and select representative structural types and design cases.
3) Determine load and resistance parameters for the selected design cases.
4) Develop models for load and resistance.
5) Calculate the reliability indices for current design code and current practice.
6) Review the results and select the target reliability index β_T.
7) Select new potential load and resistance factors or Revise the provisions.
8) Calculate reliability index.

In order to achieve a specified and uniform target reliability index for each limit state, a detailed calibration process will be performed. Figure D-1 shows the flowchart of the calibration process.

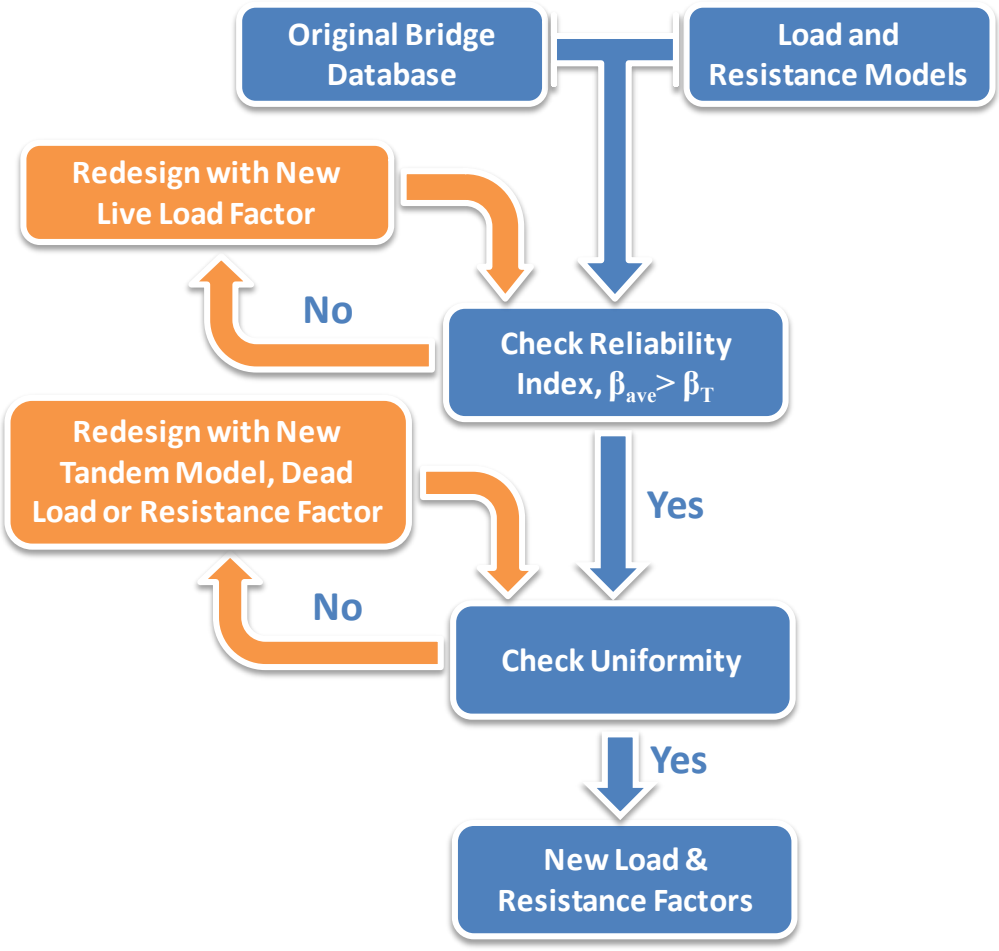

Figure D-1- Calibration process for Service III limit state

D.2 Simulated Bridge databases, Bridge characteristics

The following sections summarized the bridge databases developed by the research team that used in the calibration and investigation in this study. The majority of the girder section types, includes I girder, adjacent box girder, and spread box girder was included in the bridge databases with the span lengths ranging from 30 ft. to 160 ft. Furthermore, compressive strength of 6ksi, 8ksi, and 10ksi was employed in the design to represent the low, medium and high compressive strength that might be observed in current designs. In addition, live load factor of 0.8 and 1.0 were used in the design.

D.2.1 I Girder Bridges

Table D-1 Design Outcomes of I Girder Bridges Designed with Compressive Strength of 6ksi, Live Load Factor of 0.8 and Tensile Stress Limit of $0.0948\sqrt{f'_c}$.

Cases	Section Type	Span Length (ft.)	Spacing (ft.)	Aps (in^2)	# of Strands
1	AASHTO I	30	6	1.224	8
2	AASHTO I	30	8	1.53	10
3	AASHTO I	30	10	1.836	12
4	AASHTO I	30	12	2.142	14
5	AASHTO II	60	6	2.754	18
6	AASHTO III	60	8	2.754	18
7	AASHTO III	60	10	3.366	22
8	AASHTO III	60	12	3.672	24
9	AASHTO III	80	6	3.978	26
10	AASHTO III	80	8	4.896	32
11	AASHTO IV	80	10	4.59	30
12	AASHTO IV	80	12	5.508	36
13	AASHTO IV	100	6	5.508	36
14	AASHTO IV	100	8	6.426	42
15	AASHTO V	100	10	6.426	42
16	AASHTO V	100	12	7.344	48
17	AASHTO V	120	6	7.038	46
18	AASHTO V	120	8	8.262	54
19	AASHTO VI	120	10	8.262	54
20	AASHTO VI	120	12	9.486	62
21	AASHTO VI	140	6	8.568	56
22	AASHTO VI	140	8	10.098	66
23	AASHTO VI	140	10	-	-
24	F.I.B.-96	160	6	8.246	38
25	F.I.B.-96	160	8	9.548	44
26	F.I.B.-96	160	10	10.85	50

Table D-2 Design Outcomes of I Girder Bridges Designed with Compressive Strength of 6ksi, Live Load Factor of 0.8 and Tensile Stress Limit of $0.158\sqrt{f'_c}$.

Cases	Section Type	Span Length (ft.)	Spacing (ft.)	Aps (in^2)	# of Strands
1	AASHTO I	30	6	1.224	8
2	AASHTO I	30	8	1.53	10
3	AASHTO I	30	10	1.53	10
4	AASHTO I	30	12	1.836	12
5	AASHTO II	60	6	2.448	16
6	AASHTO III	60	8	2.448	16
7	AASHTO III	60	10	3.06	20
8	AASHTO III	60	12	3.366	22
9	AASHTO III	80	6	3.672	24
10	AASHTO IV	80	8	3.978	26
11	AASHTO IV	80	10	4.284	28
12	AASHTO IV	80	12	4.896	32
13	AASHTO IV	100	6	5.202	34
14	AASHTO IV	100	8	6.12	40
15	AASHTO V	100	10	5.814	38
16	AASHTO V	100	12	6.732	44
17	AASHTO V	120	6	6.426	42
18	AASHTO V	120	8	7.65	50
19	AASHTO VI	120	10	7.65	50
20	AASHTO VI	120	12	8.874	58
21	AASHTO VI	140	6	7.956	52
22	AASHTO VI	140	8	9.792	64
23	AASHTO VI	140	10	-	-
24	F.I.B.-96	160	6	7.378	34
25	F.I.B.-96	160	8	8.68	40
26	F.I.B.-96	160	10	10.416	48

Table D-3 Design Outcomes of I Girder Bridges Designed with Compressive Strength of 6ksi, Live Load Factor of 0.8 and Tensile Stress Limit of $0.19\sqrt{f'_c}$.

Cases	Section Type	Span Length (ft.)	Spacing (ft.)	Aps (in^2)	# of Strands
1	AASHTO I	30	6	1.224	8
2	AASHTO I	30	8	1.53	10
3	AASHTO I	30	10	1.836	12
4	AASHTO I	30	12	2.142	14
5	AASHTO II	60	6	2.448	16
6	AASHTO III	60	8	2.142	14
7	AASHTO III	60	10	2.754	18
8	AASHTO III	60	12	3.366	22
9	AASHTO III	80	6	3.366	22
10	AASHTO III	80	8	4.59	30
11	AASHTO IV	80	10	4.284	28
12	AASHTO IV	80	12	4.896	32
13	AASHTO IV	100	6	4.896	32
14	AASHTO IV	100	8	6.12	40
15	AASHTO V	100	10	5.814	38
16	AASHTO V	100	12	6.732	44
17	AASHTO V	120	6	6.12	40
18	AASHTO V	120	8	7.65	50
19	AASHTO VI	120	10	7.344	48
20	AASHTO VI	120	12	8.568	56
21	AASHTO VI	140	6	7.65	50
22	AASHTO VI	140	8	9.18	60
23	AASHTO VI	140	10	-	-
24	F.I.B.-96	160	6	7.378	34
25	F.I.B.-96	160	8	8.68	40
26	F.I.B.-96	160	10	9.982	46

Table D-4 Design Outcomes of I Girder Bridges Designed with Compressive Strength of 6ksi, Live Load Factor of 0.8 and Tensile Stress Limit of $0.253\sqrt{f'_c}$.

Cases	Section Type	Span Length (ft.)	Spacing (ft.)	Aps (in^2)	# of Strands
1	AASHTO I	30	6	1.224	8
2	AASHTO I	30	8	1.224	8
3	AASHTO I	30	10	1.53	10
4	AASHTO I	30	12	1.836	12
5	AASHTO II	60	6	2.142	14
6	AASHTO III	60	8	2.142	14
7	AASHTO III	60	10	2.448	16
8	AASHTO III	60	12	3.06	20
9	AASHTO III	80	6	3.366	22
10	AASHTO IV	80	8	3.366	22
11	AASHTO IV	80	10	3.978	26
12	AASHTO IV	80	12	4.59	30
13	AASHTO IV	100	6	4.59	30
14	AASHTO IV	100	8	5.814	38
15	AASHTO V	100	10	5.202	34
16	AASHTO V	100	12	6.12	40
17	AASHTO V	120	6	5.814	38
18	AASHTO V	120	8	7.038	46
19	AASHTO VI	120	10	7.038	46
20	AASHTO VI	120	12	7.956	52
21	AASHTO VI	140	6	7.344	48
22	AASHTO VI	140	8	8.874	58
23	AASHTO VI	140	10	10.404	68
24	F.I.B.-96	160	6	6.944	32
25	F.I.B.-96	160	8	7.812	36
26	F.I.B.-96	160	10	9.114	42

Table D-5 Design Outcomes of I Girder Bridges Designed with Compressive Strength of 6ksi, Live Load Factor of 1.0 and Tensile Stress Limit of $0.0948\sqrt{f'_c}$.

Cases	Section Type	Span Length (ft.)	Spacing (ft.)	Aps (in^2)	# of Strands
1	AASHTO I	30	6	1.224	8
2	AASHTO I	30	8	1.53	10
3	AASHTO I	30	10	1.836	12
4	AASHTO I	30	12	2.142	14
5	AASHTO II	60	6	3.06	20
6	AASHTO III	60	8	3.06	20
7	AASHTO III	60	10	3.672	24
8	AASHTO III	60	12	4.284	28
9	AASHTO III	80	6	4.284	28
10	AASHTO IV	80	8	4.59	30
11	AASHTO IV	80	10	5.202	34
12	AASHTO IV	80	12	6.12	40
13	AASHTO IV	100	6	6.12	40
14	AASHTO V	100	8	6.12	40
15	AASHTO V	100	10	7.038	46
16	AASHTO V	100	12	7.956	52
17	AASHTO V	120	6	7.65	50
18	AASHTO VI	120	8	7.65	50
19	AASHTO VI	120	10	8.874	58
20	AASHTO VI	120	12	-	-
21	AASHTO VI	140	6	9.18	60
22	AASHTO VI	140	8	-	-
23	AASHTO VI	140	10	-	-
24	F.I.B.-96	160	6	8.68	40
25	F.I.B.-96	160	8	10.416	48
26	F.I.B.-96	160	10	11.718	54

Table D-6 Design Outcomes of I Girder Bridges Designed with Compressive Strength of 6ksi, Live Load Factor of 1.0 and Tensile Stress Limit of $0.158\sqrt{f'_c}$.

Cases	Section Type	Span Length (ft.)	Spacing (ft.)	Aps (in^2)	# of Strands
1	AASHTO I	30	6	1.224	8
2	AASHTO I	30	8	1.53	10
3	AASHTO I	30	10	1.836	12
4	AASHTO I	30	12	2.448	16
5	AASHTO II	60	6	2.754	18
6	AASHTO III	60	8	2.754	18
7	AASHTO III	60	10	3.366	22
8	AASHTO III	60	12	3.978	26
9	AASHTO III	80	6	3.978	26
10	AASHTO IV	80	8	4.284	28
11	AASHTO IV	80	10	4.896	32
12	AASHTO IV	80	12	5.814	38
13	AASHTO IV	100	6	5.508	36
14	AASHTO IV	100	8	7.038	46
15	AASHTO V	100	10	6.732	44
16	AASHTO V	100	12	7.65	50
17	AASHTO V	120	6	7.038	46
18	AASHTO V	120	8	8.568	56
19	AASHTO VI	120	10	8.568	56
20	AASHTO VI	120	12	-	-
21	AASHTO VI	140	6	8.874	58
22	AASHTO VI	140	8	-	-
23	AASHTO VI	140	10	-	-
24	F.I.B.-96	160	6	8.246	38
25	F.I.B.-96	160	8	9.548	44
26	F.I.B.-96	160	10	11.284	52

Table D-7 Design Outcomes of I Girder Bridges Designed with Compressive Strength of 6ksi, Live Load Factor of 1.0 and Tensile Stress Limit of $0.19\sqrt{f'_c}$.

Cases	Section Type	Span Length (ft.)	Spacing (ft.)	Aps (in^2)	# of Strands
1	AASHTO I	30	6	1.224	8
2	AASHTO I	30	8	1.53	10
3	AASHTO I	30	10	1.836	12
4	AASHTO I	30	12	2.448	16
5	AASHTO II	60	6	2.754	18
6	AASHTO III	60	8	2.448	16
7	AASHTO III	60	10	3.366	22
8	AASHTO III	60	12	3.978	26
9	AASHTO III	80	6	3.978	26
10	AASHTO IV	80	8	3.978	26
11	AASHTO IV	80	10	4.59	30
12	AASHTO IV	80	12	5.508	36
13	AASHTO IV	100	6	5.508	36
14	AASHTO IV	100	8	6.732	44
15	AASHTO V	100	10	6.426	42
16	AASHTO V	100	12	7.344	48
17	AASHTO V	120	6	6.732	44
18	AASHTO V	120	8	8.262	54
19	AASHTO VI	120	10	8.262	54
20	AASHTO VI	120	12	9.486	62
21	AASHTO VI	140	6	8.568	56
22	AASHTO VI	140	8	10.404	68
23	AASHTO VI	140	10	-	-
24	F.I.B.-96	160	6	7.812	36
25	F.I.B.-96	160	8	9.548	44
26	F.I.B.-96	160	10	10.85	50

Table D-8 Design Outcomes of I Girder Bridges Designed with Compressive Strength of 6ksi, Live Load Factor of 1.0 and Tensile Stress Limit of $0.253\sqrt{f'_c}$.

Cases	Section Type	Span Length (ft.)	Spacing (ft.)	Aps (in^2)	# of Strands
1	AASHTO I	30	6	1.224	8
2	AASHTO I	30	8	1.224	8
3	AASHTO I	30	10	1.53	10
4	AASHTO I	30	12	1.836	12
5	AASHTO II	60	6	2.448	16
6	AASHTO III	60	8	2.448	16
7	AASHTO III	60	10	3.06	20
8	AASHTO III	60	12	3.672	24
9	AASHTO III	80	6	3.672	24
10	AASHTO IV	80	8	3.672	24
11	AASHTO IV	80	10	4.284	28
12	AASHTO IV	80	12	5.202	34
13	AASHTO IV	100	6	5.202	34
14	AASHTO IV	100	8	6.426	42
15	AASHTO V	100	10	5.814	38
16	AASHTO V	100	12	7.038	46
17	AASHTO V	120	6	6.426	42
18	AASHTO V	120	8	7.956	52
19	AASHTO VI	120	10	7.65	50
20	AASHTO VI	120	12	8.874	58
21	AASHTO VI	140	6	7.956	52
22	AASHTO VI	140	8	9.792	64
23	AASHTO VI	140	10	-	-
24	F.I.B.-96	160	6	7.378	34
25	F.I.B.-96	160	8	8.68	40
26	F.I.B.-96	160	10	10.416	48

Table D-9 Design Outcomes of I Girder Bridges Designed with Compressive Strength of 8ksi, Live Load Factor of 0.8 and Tensile Stress Limit of $0.0948\sqrt{f'_c}$.

Cases	Section Type	Span Length (ft.)	Spacing (ft.)	Aps (in^2)	# of Strands
1	AASHTO I	30	6	1.224	8
2	AASHTO I	30	8	1.53	10
3	AASHTO I	30	10	1.836	12
4	AASHTO I	30	12	1.836	12
5	AASHTO II	60	6	2.448	16
6	AASHTO II	60	8	3.366	22
7	AASHTO III	60	10	3.06	20
8	AASHTO III	60	12	3.672	24
9	AASHTO III	80	6	3.672	24
10	AASHTO III	80	8	4.59	30
11	AASHTO III	80	10	5.508	36
12	AASHTO IV	80	12	5.202	34
13	AASHTO III	100	6	6.12	40
14	AASHTO IV	100	8	6.426	42
15	AASHTO IV	100	10	7.344	48
16	AASHTO V	100	12	7.038	46
17	AASHTO IV	120	6	7.956	52
18	AASHTO V	120	8	7.956	52
19	AASHTO V	120	10	9.18	60
20	AASHTO VI	120	12	8.874	58
21	AASHTO VI	140	6	8.262	54
22	AASHTO VI	140	8	9.792	64
23	AASHTO VI	140	10	11.322	74
24	F.I.B.-96	160	6	7.812	36
25	F.I.B.-96	160	8	9.114	42
26	F.I.B.-96	160	10	10.416	48

Table D-10 Design Outcomes of I Girder Bridges Designed with Compressive Strength of 8ksi, Live Load Factor of 0.8 and Tensile Stress Limit of $0.158\sqrt{f'_c}$.

Cases	Section Type	Span Length (ft.)	Spacing (ft.)	Aps (in^2)	# of Strands
1	AASHTO I	30	6	1.224	8
2	AASHTO I	30	8	1.53	10
3	AASHTO I	30	10	1.836	12
4	AASHTO I	30	12	2.295	15
5	AASHTO II	60	6	2.448	16
6	AASHTO II	60	8	3.672	24
7	AASHTO III	60	10	3.06	20
8	AASHTO III	60	12	3.672	24
9	AASHTO III	80	6	3.366	22
10	AASHTO III	80	8	4.284	28
11	AASHTO III	80	10	5.202	34
12	AASHTO IV	80	12	4.896	32
13	AASHTO III	100	6	5.814	38
14	AASHTO IV	100	8	5.814	38
15	AASHTO IV	100	10	7.038	46
16	AASHTO V	100	12	6.426	42
17	AASHTO IV	120	6	7.344	48
18	AASHTO V	120	8	7.344	48
19	AASHTO V	120	10	8.568	56
20	AASHTO VI	120	12	8.262	54
21	AASHTO VI	140	6	7.65	50
22	AASHTO VI	140	8	9.18	60
23	AASHTO VI	140	10	10.71	70
24	F.I.B.-96	160	6	7.378	34
25	F.I.B.-96	160	8	8.68	40
26	F.I.B.-96	160	10	9.548	44

Table D-11 Design Outcomes of I Girder Bridges Designed with Compressive Strength of 8ksi, Live Load Factor of 0.8 and Tensile Stress Limit of $0.19\sqrt{f'_c}$.

Cases	Section Type	Span Length (ft.)	Spacing (ft.)	Aps (in^2)	# of Strands
1	AASHTO I	30	6	1.224	8
2	AASHTO I	30	8	1.53	10
3	AASHTO I	30	10	1.836	12
4	AASHTO I	30	12	2.295	15
5	AASHTO II	60	6	2.448	16
6	AASHTO II	60	8	3.06	20
7	AASHTO III	60	10	3.06	20
8	AASHTO III	60	12	3.672	24
9	AASHTO III	80	6	3.366	22
10	AASHTO III	80	8	4.284	28
11	AASHTO III	80	10	4.896	32
12	AASHTO IV	80	12	4.896	32
13	AASHTO III	100	6	5.814	38
14	AASHTO IV	100	8	5.814	38
15	AASHTO IV	100	10	6.732	44
16	AASHTO V	100	12	6.426	42
17	AASHTO IV	120	6	7.344	48
18	AASHTO V	120	8	7.344	48
19	AASHTO V	120	10	8.262	54
20	AASHTO VI	120	12	8.262	54
21	AASHTO VI	140	6	7.344	48
22	AASHTO VI	140	8	8.874	58
23	AASHTO VI	140	10	10.404	68
24	F.I.B.-96	160	6	6.944	32
25	F.I.B.-96	160	8	8.246	38
26	F.I.B.-96	160	10	9.548	44

Table D-12 Design Outcomes of I Girder Bridges Designed with Compressive Strength of 8ksi, Live Load Factor of 0.8 and Tensile Stress Limit of $0.253\sqrt{f'_c}$.

Cases	Section Type	Span Length (ft.)	Spacing (ft.)	Aps (in^2)	# of Strands
1	AASHTO I	30	6	1.224	8
2	AASHTO I	30	8	1.53	10
3	AASHTO I	30	10	1.836	12
4	AASHTO I	30	12	2.142	14
5	AASHTO II	60	6	2.142	14
6	AASHTO II	60	8	2.754	18
7	AASHTO III	60	10	2.448	16
8	AASHTO III	60	12	3.06	20
9	AASHTO III	80	6	3.06	20
10	AASHTO III	80	8	3.978	26
11	AASHTO III	80	10	4.59	30
12	AASHTO IV	80	12	4.284	28
13	AASHTO III	100	6	5.202	34
14	AASHTO IV	100	8	5.202	34
15	AASHTO IV	100	10	6.426	42
16	AASHTO V	100	12	5.814	38
17	AASHTO IV	120	6	6.732	44
18	AASHTO V	120	8	6.732	44
19	AASHTO V	120	10	7.956	52
20	AASHTO VI	120	12	7.65	50
21	AASHTO VI	140	6	6.732	44
22	AASHTO VI	140	8	8.262	54
23	AASHTO VI	140	10	9.792	64
24	F.I.B.-96	160	6	6.51	30
25	F.I.B.-96	160	8	7.378	34
26	F.I.B.-96	160	10	8.68	40

Table D-13 Design Outcomes of I Girder Bridges Designed with Compressive Strength of 8ksi, Live Load Factor of 1.0 and Tensile Stress Limit of $0.0948\sqrt{f'_c}$.

Cases	Section Type	Span Length (ft.)	Spacing (ft.)	Aps (in^2)	# of Strands
1	AASHTO I	30	6	1.224	8
2	AASHTO I	30	8	1.53	10
3	AASHTO I	30	10	1.836	12
4	AASHTO I	30	12	2.295	15
5	AASHTO II	60	6	3.06	20
6	AASHTO II	60	8	3.978	26
7	AASHTO III	60	10	3.366	22
8	AASHTO III	60	12	4.284	28
9	AASHTO III	80	6	4.284	28
10	AASHTO III	80	8	5.202	34
11	AASHTO III	80	10	6.12	40
12	AASHTO IV	80	12	5.814	38
13	AASHTO III	100	6	7.038	46
14	AASHTO IV	100	8	7.038	46
15	AASHTO IV	100	10	8.262	54
16	AASHTO V	100	12	7.65	50
17	AASHTO IV	120	6	8.874	58
18	AASHTO V	120	8	8.874	58
19	AASHTO V	120	10	10.404	68
20	AASHTO VI	120	12	9.792	64
21	AASHTO VI	140	6	8.874	58
22	AASHTO VI	140	8	10.71	70
23	AASHTO VI	140	10	12.852	84
24	F.I.B.-96	160	6	8.246	38
25	F.I.B.-96	160	8	10.199	47
26	F.I.B.-96	160	10	11.284	52

Table D-14 Design Outcomes of I Girder Bridges Designed with Compressive Strength of 8ksi, Live Load Factor of 1.0 and Tensile Stress Limit of $0.158\sqrt{f'_c}$.

Cases	Section Type	Span Length (ft.)	Spacing (ft.)	Aps (in^2)	# of Strands
1	AASHTO I	30	6	1.224	8
2	AASHTO I	30	8	1.53	10
3	AASHTO I	30	10	1.836	12
4	AASHTO I	30	12	2.295	15
5	AASHTO II	60	6	2.754	18
6	AASHTO II	60	8	3.672	24
7	AASHTO III	60	10	3.06	20
8	AASHTO III	60	12	3.672	24
9	AASHTO III	80	6	3.978	26
10	AASHTO III	80	8	4.896	32
11	AASHTO III	80	10	5.814	38
12	AASHTO IV	80	12	5.508	36
13	AASHTO III	100	6	6.732	44
14	AASHTO IV	100	8	6.426	42
15	AASHTO IV	100	10	7.65	50
16	AASHTO V	100	12	7.344	48
17	AASHTO IV	120	6	8.262	54
18	AASHTO V	120	8	8.262	54
19	AASHTO V	120	10	9.486	62
20	AASHTO VI	120	12	9.18	60
21	AASHTO VI	140	6	8.262	54
22	AASHTO VI	140	8	10.098	66
23	AASHTO VI	140	10	11.628	76
24	F.I.B.-96	160	6	7.812	36
25	F.I.B.-96	160	8	9.114	42
26	F.I.B.-96	160	10	10.416	48

Table D-15 Design Outcomes of I Girder Bridges Designed with Compressive Strength of 8ksi, Live Load Factor of 1.0 and Tensile Stress Limit of $0.19\sqrt{f'_c}$.

Cases	Section Type	Span Length (ft.)	Spacing (ft.)	Aps (in^2)	# of Strands
1	AASHTO I	30	6	1.224	8
2	AASHTO I	30	8	1.53	10
3	AASHTO I	30	10	1.836	12
4	AASHTO I	30	12	2.295	15
5	AASHTO II	60	6	2.448	16
6	AASHTO II	60	8	3.366	22
7	AASHTO III	60	10	3.06	20
8	AASHTO III	60	12	3.672	24
9	AASHTO III	80	6	3.672	24
10	AASHTO III	80	8	4.59	30
11	AASHTO III	80	10	5.814	38
12	AASHTO IV	80	12	5.202	34
13	AASHTO III	100	6	6.426	42
14	AASHTO IV	100	8	6.426	42
15	AASHTO IV	100	10	7.65	50
16	AASHTO V	100	12	7.038	46
17	AASHTO IV	120	6	7.956	52
18	AASHTO V	120	8	7.956	52
19	AASHTO V	120	10	9.18	60
20	AASHTO VI	120	12	8.874	58
21	AASHTO VI	140	6	7.956	52
22	AASHTO VI	140	8	9.792	64
23	AASHTO VI	140	10	11.322	74
24	F.I.B.-96	160	6	7.378	34
25	F.I.B.-96	160	8	8.68	40
26	F.I.B.-96	160	10	10.416	48

Table D-16 Design Outcomes of I Girder Bridges Designed with Compressive Strength of 8ksi, Live Load Factor of 1.0 and Tensile Stress Limit of $0.253\sqrt{f'_c}$.

Cases	Section Type	Span Length (ft.)	Spacing (ft.)	Aps (in^2)	# of Strands
1	AASHTO I	30	6	1.224	8
2	AASHTO I	30	8	1.53	10
3	AASHTO I	30	10	1.836	12
4	AASHTO I	30	12	2.295	15
5	AASHTO II	60	6	2.448	16
6	AASHTO II	60	8	3.366	22
7	AASHTO III	60	10	3.06	20
8	AASHTO III	60	12	3.672	24
9	AASHTO III	80	6	3.366	22
10	AASHTO III	80	8	4.284	28
11	AASHTO III	80	10	5.202	34
12	AASHTO IV	80	12	4.896	32
13	AASHTO III	100	6	6.12	40
14	AASHTO IV	100	8	5.814	38
15	AASHTO IV	100	10	7.038	46
16	AASHTO V	100	12	6.426	42
17	AASHTO IV	120	6	7.65	50
18	AASHTO V	120	8	7.344	48
19	AASHTO V	120	10	8.874	58
20	AASHTO VI	120	12	8.568	56
21	AASHTO VI	140	6	7.344	48
22	AASHTO VI	140	8	9.18	60
23	AASHTO VI	140	10	10.71	70
24	F.I.B.-96	160	6	6.944	32
25	F.I.B.-96	160	8	8.246	38
26	F.I.B.-96	160	10	9.548	44

Table D-17 Design Outcomes of I Girder Bridges Designed with Compressive Strength of 10 ksi, Live Load Factor of 0.8 and Tensile Stress Limit of $0.0948\sqrt{f'_c}$.

Cases	Section Type	Span Length (ft.)	Spacing (ft.)	Aps (in^2)	# of Strands
1	AASHTO I	30	6	1.224	8
2	AASHTO I	30	8	1.53	10
3	AASHTO I	30	10	1.53	10
4	AASHTO I	30	12	1.836	12
5	AASHTO II	60	6	2.448	16
6	AASHTO II	60	8	3.366	22
7	AASHTO III	60	10	3.06	20
8	AASHTO III	60	12	3.672	24
9	AASHTO III	80	6	3.672	24
10	AASHTO III	80	8	4.59	30
11	AASHTO III	80	10	5.202	34
12	AASHTO IV	80	12	5.202	34
13	AASHTO III	100	6	6.12	40
14	AASHTO IV	100	8	6.12	40
15	AASHTO IV	100	10	7.038	46
16	AASHTO V	100	12	6.732	44
17	AASHTO IV	120	6	7.65	50
18	AASHTO V	120	8	7.65	50
19	AASHTO V	120	10	8.874	58
20	AASHTO VI	120	12	8.568	56
21	AASHTO VI	140	6	7.956	52
22	AASHTO VI	140	8	9.486	62
23	AASHTO VI	140	10	11.016	72
24	F.I.B.-96	160	6	7.812	36
25	F.I.B.-96	160	8	8.68	40
26	F.I.B.-96	160	10	9.982	46

Table D-18 Design Outcomes of I Girder Bridges Designed with Compressive Strength of 10 ksi, Live Load Factor of 0.8 and Tensile Stress Limit of $0.158\sqrt{f'_c}$.

Cases	Section Type	Span Length (ft.)	Spacing (ft.)	Aps (in^2)	# of Strands
1	AASHTO I	30	6	0.918	6
2	AASHTO I	30	8	1.224	8
3	AASHTO I	30	10	1.224	8
4	AASHTO I	30	12	1.53	10
5	AASHTO II	60	6	2.142	14
6	AASHTO II	60	8	3.06	20
7	AASHTO III	60	10	2.754	18
8	AASHTO III	60	12	3.366	22
9	AASHTO III	80	6	3.366	22
10	AASHTO III	80	8	4.284	28
11	AASHTO III	80	10	4.896	32
12	AASHTO IV	80	12	4.59	30
13	AASHTO III	100	6	5.508	36
14	AASHTO IV	100	8	5.814	38
15	AASHTO IV	100	10	6.732	44
16	AASHTO V	100	12	6.426	42
17	AASHTO IV	120	6	7.344	48
18	AASHTO V	120	8	7.038	46
19	AASHTO V	120	10	8.262	54
20	AASHTO VI	120	12	8.262	54
21	AASHTO VI	140	6	7.344	48
22	AASHTO VI	140	8	8.874	58
23	AASHTO VI	140	10	10.098	66
24	F.I.B.-96	160	6	6.944	32
25	F.I.B.-96	160	8	8.246	38
26	F.I.B.-96	160	10	9.548	44

Table D-19 Design Outcomes of I Girder Bridges Designed with Compressive Strength of 10 ksi, Live Load Factor of 0.8 and Tensile Stress Limit of $0.19\sqrt{f'_c}$.

Cases	Section Type	Span Length (ft.)	Spacing (ft.)	Aps (in^2)	# of Strands
1	AASHTO I	30	6	1.224	8
2	AASHTO I	30	8	1.53	10
3	AASHTO I	30	10	1.836	12
4	AASHTO I	30	12	2.142	14
5	AASHTO II	60	6	2.142	14
6	AASHTO II	60	8	2.754	18
7	AASHTO III	60	10	2.448	16
8	AASHTO III	60	12	3.06	20
9	AASHTO III	80	6	3.366	22
10	AASHTO III	80	8	3.978	26
11	AASHTO III	80	10	4.896	32
12	AASHTO IV	80	12	4.59	30
13	AASHTO III	100	6	5.508	36
14	AASHTO IV	100	8	5.508	36
15	AASHTO IV	100	10	6.426	42
16	AASHTO V	100	12	6.12	40
17	AASHTO IV	120	6	7.038	46
18	AASHTO V	120	8	7.038	46
19	AASHTO V	120	10	7.956	52
20	AASHTO VI	120	12	7.956	52
21	AASHTO VI	140	6	7.038	46
22	AASHTO VI	140	8	8.568	56
23	AASHTO VI	140	10	9.792	64
24	F.I.B.-96	160	6	6.944	32
25	F.I.B.-96	160	8	8.246	38
26	F.I.B.-96	160	10	9.114	42

Table D-20 Design Outcomes of I Girder Bridges Designed with Compressive Strength of 10 ksi, Live Load Factor of 0.8 and Tensile Stress Limit of $0.253\sqrt{f'_c}$.

Cases	Section Type	Span Length (ft.)	Spacing (ft.)	Aps (in^2)	# of Strands
1	AASHTO I	30	6	0.918	6
2	AASHTO I	30	8	1.224	8
3	AASHTO I	30	10	1.224	8
4	AASHTO I	30	12	1.836	12
5	AASHTO II	60	6	2.142	14
6	AASHTO II	60	8	2.754	18
7	AASHTO III	60	10	2.142	14
8	AASHTO III	60	12	2.754	18
9	AASHTO III	80	6	3.06	20
10	AASHTO III	80	8	3.672	24
11	AASHTO III	80	10	4.59	30
12	AASHTO IV	80	12	3.978	26
13	AASHTO III	100	6	5.202	34
14	AASHTO IV	100	8	5.202	34
15	AASHTO IV	100	10	6.12	40
16	AASHTO V	100	12	5.508	36
17	AASHTO IV	120	6	6.426	42
18	AASHTO V	120	8	6.426	42
19	AASHTO V	120	10	7.65	50
20	AASHTO VI	120	12	7.344	48
21	AASHTO VI	140	6	6.426	42
22	AASHTO VI	140	8	7.956	52
23	AASHTO VI	140	10	9.18	60
24	F.I.B.-96	160	6	6.076	28
25	F.I.B.-96	160	8	7.378	34
26	F.I.B.-96	160	10	8.246	38

Table D-21 Design Outcomes of I Girder Bridges Designed with Compressive Strength of 10 ksi, Live Load Factor of 1.0 and Tensile Stress Limit of $0.0948\sqrt{f'_c}$.

Cases	Section Type	Span Length (ft.)	Spacing (ft.)	Aps (in^2)	# of Strands
1	AASHTO I	30	6	1.224	8
2	AASHTO I	30	8	1.53	10
3	AASHTO I	30	10	1.836	12
4	AASHTO I	30	12	2.142	14
5	AASHTO II	60	6	3.06	20
6	AASHTO II	60	8	3.978	26
7	AASHTO III	60	10	3.366	22
8	AASHTO III	60	12	3.978	26
9	AASHTO III	80	6	3.978	26
10	AASHTO III	80	8	4.896	32
11	AASHTO III	80	10	6.12	40
12	AASHTO IV	80	12	5.814	38
13	AASHTO III	100	6	6.732	44
14	AASHTO IV	100	8	6.732	44
15	AASHTO IV	100	10	7.956	52
16	AASHTO V	100	12	7.65	50
17	AASHTO IV	120	6	8.568	56
18	AASHTO V	120	8	8.568	56
19	AASHTO V	120	10	10.098	66
20	AASHTO VI	120	12	9.486	62
21	AASHTO VI	140	6	8.568	56
22	AASHTO VI	140	8	10.404	68
23	AASHTO VI	140	10	11.934	78
24	F.I.B.-96	160	6	8.246	38
25	F.I.B.-96	160	8	9.548	44
26	F.I.B.-96	160	10	10.85	50

Table D-22 Design Outcomes of I Girder Bridges Designed with Compressive Strength of 10 ksi, Live Load Factor of 1.0 and Tensile Stress Limit of $0.158\sqrt{f'_c}$.

Cases	Section Type	Span Length (ft.)	Spacing (ft.)	Aps (in^2)	# of Strands
1	AASHTO I	30	6	1.224	8
2	AASHTO I	30	8	1.53	10
3	AASHTO I	30	10	1.53	10
4	AASHTO I	30	12	2.142	14
5	AASHTO II	60	6	2.754	18
6	AASHTO II	60	8	3.672	24
7	AASHTO III	60	10	3.06	20
8	AASHTO III	60	12	3.672	24
9	AASHTO III	80	6	3.672	24
10	AASHTO III	80	8	4.59	30
11	AASHTO III	80	10	5.508	36
12	AASHTO IV	80	12	5.202	34
13	AASHTO III	100	6	6.426	42
14	AASHTO IV	100	8	6.426	42
15	AASHTO IV	100	10	7.65	50
16	AASHTO V	100	12	7.038	46
17	AASHTO IV	120	6	7.956	52
18	AASHTO V	120	8	7.956	52
19	AASHTO V	120	10	9.18	60
20	AASHTO VI	120	12	8.874	58
21	AASHTO VI	140	6	7.956	52
22	AASHTO VI	140	8	9.486	62
23	AASHTO VI	140	10	11.322	74
24	F.I.B.-96	160	6	7.812	36
25	F.I.B.-96	160	8	9.114	42
26	F.I.B.-96	160	10	10.416	48

Table D-23 Design Outcomes of I Girder Bridges Designed with Compressive Strength of 10 ksi, Live Load Factor of 1.0 and Tensile Stress Limit of $0.19\sqrt{f'_c}$.

Cases	Section Type	Span Length (ft.)	Spacing (ft.)	Aps (in^2)	# of Strands
1	AASHTO I	30	6	1.224	8
2	AASHTO I	30	8	1.53	10
3	AASHTO I	30	10	1.53	10
4	AASHTO I	30	12	1.836	12
5	AASHTO II	60	6	2.448	16
6	AASHTO II	60	8	3.366	22
7	AASHTO III	60	10	2.754	18
8	AASHTO III	60	12	3.672	24
9	AASHTO III	80	6	3.672	24
10	AASHTO III	80	8	4.59	30
11	AASHTO III	80	10	5.508	36
12	AASHTO IV	80	12	5.202	34
13	AASHTO III	100	6	6.12	40
14	AASHTO IV	100	8	6.12	40
15	AASHTO IV	100	10	7.344	48
16	AASHTO V	100	12	6.732	44
17	AASHTO IV	120	6	7.65	50
18	AASHTO V	120	8	7.65	50
19	AASHTO V	120	10	8.874	58
20	AASHTO VI	120	12	8.568	56
21	AASHTO VI	140	6	7.65	50
22	AASHTO VI	140	8	9.18	60
23	AASHTO VI	140	10	11.016	72
24	F.I.B.-96	160	6	7.378	34
25	F.I.B.-96	160	8	8.68	40
26	F.I.B.-96	160	10	9.982	46

Table D-24 Design Outcomes of I Girder Bridges Designed with Compressive Strength of 10 ksi, Live Load Factor of 1.0 and Tensile Stress Limit of $0.253\sqrt{f'_c}$.

Cases	Section Type	Span Length (ft.)	Spacing (ft.)	Aps (in^2)	# of Strands
1	AASHTO I	30	6	1.224	8
2	AASHTO I	30	8	1.53	10
3	AASHTO I	30	10	1.53	10
4	AASHTO I	30	12	1.836	12
5	AASHTO II	60	6	2.448	16
6	AASHTO II	60	8	3.06	20
7	AASHTO III	60	10	2.754	18
8	AASHTO III	60	12	3.366	22
9	AASHTO III	80	6	3.366	22
10	AASHTO III	80	8	4.284	28
11	AASHTO III	80	10	5.202	34
12	AASHTO IV	80	12	4.59	30
13	AASHTO III	100	6	5.814	38
14	AASHTO IV	100	8	5.814	38
15	AASHTO IV	100	10	6.732	44
16	AASHTO V	100	12	6.426	42
17	AASHTO IV	120	6	7.344	48
18	AASHTO V	120	8	7.038	46
19	AASHTO V	120	10	8.262	54
20	AASHTO VI	120	12	8.262	54
21	AASHTO VI	140	6	7.038	46
22	AASHTO VI	140	8	8.874	58
23	AASHTO VI	140	10	10.404	68
24	F.I.B.-96	160	6	6.51	30
25	F.I.B.-96	160	8	8.246	38
26	F.I.B.-96	160	10	9.114	42

D.2.2 Adjacent Box Girder Bridges

Table D-25 Design Outcomes of Adjacent Box Girder Bridges Designed with Compressive Strength of 6 ksi, Live Load Factor of 0.8 and Tensile Stress Limit of $0.0948\sqrt{f'_c}$.

Cases	Section Type	Span Length (ft.)	Spacing (ft.)	Aps (in^2)	# of Strands
1	BI-36	30	3	1.224	8
2	BI-48	30	4	1.224	8
3	BI-36	60	3	2.754	18
4	BI-48	60	4	3.366	22
5	BII-36	80	3	3.672	24
6	BI-48	80	4	5.508	36
7	BIII-36	100	3	4.896	32
8	BII-48	100	4	7.038	46
9	BIV-36	120	3	6.732	44
10	BIII-48	120	4	8.874	58

Table D-26 Design Outcomes of Adjacent Box Girder Bridges Designed with Compressive Strength of 6 ksi, Live Load Factor of 0.8 and Tensile Stress Limit of $0.158\sqrt{f'_c}$.

Cases	Section Type	Span Length (ft.)	Spacing (ft.)	Aps (in^2)	# of Strands
1	BI-36	30	3	0.918	6
2	BI-48	30	4	0.918	6
3	BI-36	60	3	2.448	16
4	BI-48	60	4	3.06	20
5	BII-36	80	3	3.366	22
6	BI-48	80	4	5.202	34
7	BIII-36	100	3	4.59	30
8	BII-48	100	4	6.426	42
9	BIV-36	120	3	6.12	40
10	BIII-48	120	4	8.262	54

Table D-27 Design Outcomes of Adjacent Box Girder Bridges Designed with Compressive Strength of 6 ksi, Live Load Factor of 0.8 and Tensile Stress Limit of $0.19\sqrt{f'_c}$.

Cases	Section Type	Span Length (ft.)	Spacing (ft.)	Aps (in^2)	# of Strands
1	BI-36	30	3	0.918	6
2	BI-48	30	4	0.918	6
3	BI-36	60	3	2.448	16
4	BI-48	60	4	2.754	18
5	BII-36	80	3	3.366	22
6	BI-48	80	4	5.508	36
7	BIII-36	100	3	4.284	28
8	BII-48	100	4	6.426	42
9	BIV-36	120	3	6.12	40
10	BIII-48	120	4	7.956	52

Table D-28 Design Outcomes of Adjacent Box Girder Bridges Designed with Compressive Strength of 6 ksi, Live Load Factor of 0.8 and Tensile Stress Limit of $0.253\sqrt{f'_c}$.

Cases	Section Type	Span Length (ft.)	Spacing (ft.)	Aps (in^2)	# of Strands
1	BI-36	30	3	0.612	4
2	BI-48	30	4	0.612	4
3	BI-36	60	3	2.142	14
4	BI-48	60	4	2.754	18
5	BII-36	80	3	3.06	20
6	BI-48	80	4	4.896	32
7	BIII-36	100	3	3.978	26
8	BII-48	100	4	6.12	40
9	BIV-36	120	3	5.814	38
10	BIII-48	120	4	7.344	48

Table D-29 Design Outcomes of Adjacent Box Girder Bridges Designed with Compressive Strength of 6 ksi, Live Load Factor of 1.0 and Tensile Stress Limit of $0.0948\sqrt{f'_c}$.

Cases	Section Type	Span Length (ft.)	Spacing (ft.)	Aps (in^2)	# of Strands
1	BI-36	30	3	1.224	8
2	BI-48	30	4	1.224	8
3	BI-36	60	3	2.754	18
4	BI-48	60	4	3.366	22
5	BII-36	80	3	3.978	26
6	BI-48	80	4	5.814	38
7	BIII-36	100	3	4.896	32
8	BII-48	100	4	7.344	48
9	BIV-36	120	3	7.344	48
10	BIII-48	120	4	-	-

Table D-30 Design Outcomes of Adjacent Box Girder Bridges Designed with Compressive Strength of 6 ksi, Live Load Factor of 1.0 and Tensile Stress Limit of $0.158\sqrt{f'_c}$.

Cases	Section Type	Span Length (ft.)	Spacing (ft.)	Aps (in^2)	# of Strands
1	BI-36	30	3	0.918	6
2	BI-48	30	4	1.224	8
3	BI-36	60	3	2.754	18
4	BI-48	60	4	3.06	20
5	BII-36	80	3	3.672	24
6	BI-48	80	4	5.508	36
7	BIII-36	100	3	4.896	32
8	BII-48	100	4	7.038	46
9	BIV-36	120	3	6.732	44
10	BIII-48	120	4	8.874	58

Table D-31 Design Outcomes of Adjacent Box Girder Bridges Designed with Compressive Strength of 6 ksi, Live Load Factor of 1.0 and Tensile Stress Limit of $0.19\sqrt{f'_c}$.

Cases	Section Type	Span Length (ft.)	Spacing (ft.)	Aps (in^2)	# of Strands
1	BI-36	30	3	0.918	6
2	BI-48	30	4	0.918	6
3	BI-36	60	3	2.448	16
4	BI-48	60	4	3.06	20
5	BII-36	80	3	3.366	22
6	BI-48	80	4	5.508	36
7	BIII-36	100	3	4.59	30
8	BII-48	100	4	6.732	44
9	BIV-36	120	3	6.426	42
10	BIII-48	120	4	8.568	56

Table D-32 Design Outcomes of Adjacent Box Girder Bridges Designed with Compressive Strength of 6 ksi, Live Load Factor of 1.0 and Tensile Stress Limit of $0.253\sqrt{f'_c}$.

Cases	Section Type	Span Length (ft.)	Spacing (ft.)	Aps (in^2)	# of Strands
1	BI-36	30	3	0.918	6
2	BI-48	30	4	0.612	4
3	BI-36	60	3	2.448	16
4	BI-48	60	4	2.754	18
5	BII-36	80	3	3.366	22
6	BI-48	80	4	5.202	34
7	BIII-36	100	3	4.284	28
8	BII-48	100	4	6.426	42
9	BIV-36	120	3	6.12	40
10	BIII-48	120	4	7.956	52

Table D-33 Design Outcomes of Adjacent Box Girder Bridges Designed with Compressive Strength of 8 ksi, Live Load Factor of 0.8 and Tensile Stress Limit of $0.0948\sqrt{f'_c}$.

Cases	Section Type	Span Length (ft.)	Spacing (ft.)	Aps (in^2)	# of Strands
1	BI-36	30	3	1.224	8
2	BI-48	30	4	1.224	8
3	BI-36	60	3	2.754	18
4	BI-48	60	4	3.06	20
5	BII-36	80	3	3.672	24
6	BI-48	80	4	5.202	34
7	BIII-36	100	3	4.59	30
8	BII-48	100	4	6.732	44
9	BIV-36	120	3	6.426	42
10	BIII-48	120	4	8.262	54

Table D-34 Design Outcomes of Adjacent Box Girder Bridges Designed with Compressive Strength of 8 ksi, Live Load Factor of 0.8 and Tensile Stress Limit of $0.158\sqrt{f'_c}$.

Cases	Section Type	Span Length (ft.)	Spacing (ft.)	Aps (in^2)	# of Strands
1	BI-36	30	3	0.918	6
2	BI-48	30	4	0.918	6
3	BI-36	60	3	2.448	16
4	BI-48	60	4	2.754	18
5	BII-36	80	3	3.366	22
6	BI-48	80	4	4.896	32
7	BIII-36	100	3	4.284	28
8	BII-48	100	4	6.12	40
9	BIV-36	120	3	5.814	38
10	BIII-48	120	4	7.65	50

Table D-35 Design Outcomes of Adjacent Box Girder Bridges Designed with Compressive Strength of 8 ksi, Live Load Factor of 0.8 and Tensile Stress Limit of $0.19\sqrt{f'_c}$.

Cases	Section Type	Span Length (ft.)	Spacing (ft.)	Aps (in^2)	# of Strands
1	BI-36	30	3	0.918	6
2	BI-48	30	4	0.918	6
3	BI-36	60	3	2.448	16
4	BI-48	60	4	2.754	18
5	BII-36	80	3	3.06	20
6	BI-48	80	4	4.896	32
7	BIII-36	100	3	4.284	28
8	BII-48	100	4	6.12	40
9	BIV-36	120	3	5.814	38
10	BIII-48	120	4	7.344	48

Table D-36 Design Outcomes of Adjacent Box Girder Bridges Designed with Compressive Strength of 8 ksi, Live Load Factor of 0.8 and Tensile Stress Limit of $0.253\sqrt{f'_c}$.

Cases	Section Type	Span Length (ft.)	Spacing (ft.)	Aps (in^2)	# of Strands
1	BI-36	30	3	0.612	4
2	BI-48	30	4	0.612	4
3	BI-36	60	3	2.142	14
4	BI-48	60	4	2.448	16
5	BII-36	80	3	3.06	20
6	BI-48	80	4	4.59	30
7	BIII-36	100	3	3.978	26
8	BII-48	100	4	5.814	38
9	BIV-36	120	3	5.508	36
10	BIII-48	120	4	7.038	46

Table D-37 Design Outcomes of Adjacent Box Girder Bridges Designed with Compressive Strength of 8 ksi, Live Load Factor of 1.0 and Tensile Stress Limit of $0.0948\sqrt{f'_c}$.

Cases	Section Type	Span Length (ft.)	Spacing (ft.)	Aps (in^2)	# of Strands
1	BI-36	30	3	1.224	8
2	BI-48	30	4	1.53	10
3	BI-36	60	3	2.754	18
4	BI-48	60	4	3.366	22
5	BII-36	80	3	3.672	24
6	BI-48	80	4	5.814	38
7	BIII-36	100	3	4.896	32
8	BII-48	100	4	7.038	46
9	BIV-36	120	3	6.732	44
10	BIII-48	120	4	8.874	58

Table D-38 Design Outcomes of Adjacent Box Girder Bridges Designed with Compressive Strength of 8 ksi, Live Load Factor of 1.0 and Tensile Stress Limit of $0.158\sqrt{f'_c}$.

Cases	Section Type	Span Length (ft.)	Spacing (ft.)	Aps (in^2)	# of Strands
1	BI-36	30	3	0.918	6
2	BI-48	30	4	0.918	6
3	BI-36	60	3	2.448	16
4	BI-48	60	4	3.06	20
5	BII-36	80	3	3.366	22
6	BI-48	80	4	5.508	36
7	BIII-36	100	3	4.59	30
8	BII-48	100	4	6.732	44
9	BIV-36	120	3	6.12	40
10	BIII-48	120	4	8.262	54

Table D-39 Design Outcomes of Adjacent Box Girder Bridges Designed with Compressive Strength of 8 ksi, Live Load Factor of 1.0 and Tensile Stress Limit of $0.19\sqrt{f'_c}$.

Cases	Section Type	Span Length (ft.)	Spacing (ft.)	Aps (in^2)	# of Strands
1	BI-36	30	3	0.918	6
2	BI-48	30	4	0.918	6
3	BI-36	60	3	2.448	16
4	BI-48	60	4	3.06	20
5	BII-36	80	3	3.366	22
6	BI-48	80	4	5.202	34
7	BIII-36	100	3	4.284	28
8	BII-48	100	4	6.426	42
9	BIV-36	120	3	6.12	40
10	BIII-48	120	4	7.956	52

Table D-40 Design Outcomes of Adjacent Box Girder Bridges Designed with Compressive Strength of 8 ksi, Live Load Factor of 1.0 and Tensile Stress Limit of $0.253\sqrt{f'_c}$.

Cases	Section Type	Span Length (ft.)	Spacing (ft.)	Aps (in^2)	# of Strands
1	BI-36	30	3	0.612	4
2	BI-48	30	4	0.612	4
3	BI-36	60	3	2.142	14
4	BI-48	60	4	2.754	18
5	BII-36	80	3	3.06	20
6	BI-48	80	4	4.896	32
7	BIII-36	100	3	3.978	26
8	BII-48	100	4	6.12	40
9	BIV-36	120	3	5.814	38
10	BIII-48	120	4	7.344	48

D.2.3 Spread Box Girder Bridges

Table D-41 Design Outcomes of Spread Box Girder Bridges Designed with Compressive Strength of 6ksi, Live Load Factor of 0.8 and Tensile Stress Limit of $0.0948\sqrt{f'_c}$.

Cases	Section Type	Span Length (ft.)	Spacing (ft.)	Aps (in^2)	# of Strands
1	BI-36	30	6	1.53	10
2	BI-36	30	8	1.836	12
3	BI-36	30	10	1.836	12
4	BI-36	30	12	2.142	14
5	BI-36	60	6	4.284	28
6	BI-36	60	8	4.896	32
7	BI-36	60	10	4.59	30
8	BI-48	60	12	5.202	34
9	BI-48	80	6	5.814	38
10	BII-48	80	8	5.814	38
11	BII-48	80	10	6.426	42
12	BIII-48	80	12	7.038	46
13	BIII-48	100	6	7.344	48
14	BIII-48	100	8	-	-
15	BIV-48	100	10	-	-

Table D-42 Design Outcomes of Spread Box Girder Bridges Designed with Compressive Strength of 6ksi, Live Load Factor of 0.8 and Tensile Stress Limit of $0.158\sqrt{f'_c}$.

Cases	Section Type	Span Length (ft.)	Spacing (ft.)	Aps (in^2)	# of Strands
1	BI-36	30	6	1.224	8
2	BI-36	30	8	1.53	10
3	BI-36	30	10	1.836	12
4	BI-36	30	12	1.836	12
5	BI-36	60	6	3.978	26
6	BI-36	60	8	4.896	32
7	BI-36	60	10	4.284	28
8	BI-48	60	12	4.896	32
9	BI-48	80	6	5.508	36
10	BII-48	80	8	5.508	36
11	BII-48	80	10	6.12	40
12	BIII-48	80	12	6.426	42
13	BIII-48	100	6	7.038	46
14	BIII-48	100	8	-	-
15	BIV-48	100	10	-	-

Table D-43 Design Outcomes of Spread Box Girder Bridges Designed with Compressive Strength of 6ksi, Live Load Factor of 0.8 and Tensile Stress Limit of $0.19\sqrt{f'_c}$.

Cases	Section Type	Span Length (ft.)	Spacing (ft.)	Aps (in^2)	# of Strands
1	BI-36	30	6	1.224	8
2	BI-36	30	8	1.53	10
3	BI-36	30	10	1.53	10
4	BI-36	30	12	1.836	12
5	BI-36	60	6	3.672	24
6	BI-36	60	8	4.59	30
7	BI-36	60	10	3.978	26
8	BI-48	60	12	4.59	30
9	BI-48	80	6	5.202	34
10	BII-48	80	8	5.202	34
11	BII-48	80	10	6.12	40
12	BIII-48	80	12	6.426	42
13	BIII-48	100	6	7.038	46
14	BIII-48	100	8	-	-
15	BIV-48	100	10	-	-

Table D-44 Design Outcomes of Spread Box Girder Bridges Designed with Compressive Strength of 6ksi, Live Load Factor of 0.8 and Tensile Stress Limit of $0.253\sqrt{f'_c}$.

Cases	Section Type	Span Length (ft.)	Spacing (ft.)	Aps (in^2)	# of Strands
1	BI-36	30	6	1.224	8
2	BI-36	30	8	1.224	8
3	BI-36	30	10	1.53	10
4	BI-36	30	12	1.53	10
5	BI-36	60	6	3.672	24
6	BI-36	60	8	4.284	28
7	BII-36	60	10	3.978	26
8	BII-48	60	12	4.284	28
9	BII-48	80	6	4.896	32
10	BIII-48	80	8	4.896	32
11	BIII-48	80	10	5.814	38
12	BIV-48	80	12	5.814	38
13	BIII-48	100	6	6.426	42
14	BIII-48	100	8	-	-
15	BIV-48	100	10	-	-

Table D-45 Design Outcomes of Spread Box Girder Bridges Designed with Compressive Strength of 6ksi, Live Load Factor of 1.0 and Tensile Stress Limit of $0.0948\sqrt{f'_c}$.

Cases	Section Type	Span Length (ft.)	Spacing (ft.)	Aps (in^2)	# of Strands
1	BI-36	30	6	1.53	10
2	BI-36	30	8	1.836	12
3	BI-36	30	10	2.142	14
4	BI-36	30	12	2.448	16
5	BI-36	60	6	4.59	30
6	BII-36	60	8	4.284	28
7	BII-36	60	10	4.896	32
8	BII-48	60	12	5.814	38
9	BII-48	80	6	6.12	40
10	BIII-48	80	8	6.12	40
11	BIV-48	80	10	6.732	44
12	BIV-48	80	12	7.65	50
13	BIV-48	100	6	7.344	48
14	BIII-48	100	8	-	-
15	BIV-48	100	10	-	-

Table D-46 Design Outcomes of Spread Box Girder Bridges Designed with Compressive Strength of 6ksi, Live Load Factor of 1.0 and Tensile Stress Limit of $0.158\sqrt{f'_c}$.

Cases	Section Type	Span Length (ft.)	Spacing (ft.)	Aps (in^2)	# of Strands
1	BI-36	30	6	1.53	10
2	BI-36	30	8	1.836	12
3	BI-36	30	10	1.836	12
4	BI-36	30	12	2.142	14
5	BI-36	60	6	4.284	28
6	BII-36	60	8	3.978	26
7	BII-36	60	10	4.59	30
8	BII-48	60	12	5.508	36
9	BII-48	80	6	5.814	38
10	BIII-48	80	8	5.814	38
11	BIII-48	80	10	6.732	44
12	BIV-48	80	12	7.038	46
13	BIII-48	100	6	7.65	50
14	BIII-48	100	8	-	-
15	BIV-48	100	10	-	-

Table D-47 Design Outcomes of Spread Box Girder Bridges Designed with Compressive Strength of 6ksi, Live Load Factor of 1.0 and Tensile Stress Limit of $0.19\sqrt{f'_c}$.

Cases	Section Type	Span Length (ft.)	Spacing (ft.)	Aps (in^2)	# of Strands
1	BI-36	30	6	1.53	10
2	BI-36	30	8	1.53	10
3	BI-36	30	10	1.836	12
4	BI-36	30	12	2.142	14
5	BI-36	60	6	4.284	28
6	BI-36	60	8	5.202	34
7	BII-36	60	10	4.59	30
8	BII-48	60	12	5.202	34
9	BII-48	80	6	5.814	38
10	BIII-48	80	8	5.814	38
11	BIII-48	80	10	6.732	44
12	BIV-48	80	12	7.038	46
13	BIII-48	100	6	7.65	50
14	BIII-48	100	8	-	-
15	BIV-48	100	10	-	-

Table D-48 Design Outcomes of Spread Box Girder Bridges Designed with Compressive Strength of 6ksi, Live Load Factor of 1.0 and Tensile Stress Limit of $0.253\sqrt{f'_c}$.

Cases	Section Type	Span Length (ft.)	Spacing (ft.)	Aps (in^2)	# of Strands
1	BI-36	30	6	1.224	8
2	BI-36	30	8	1.53	10
3	BI-36	30	10	1.53	10
4	BI-36	30	12	1.836	12
5	BI-36	60	6	3.978	26
6	BI-36	60	8	4.896	32
7	BII-36	60	10	4.284	28
8	BII-48	60	12	4.896	32
9	BII-48	80	6	5.508	36
10	BIII-48	80	8	5.508	36
11	BIII-48	80	10	6.426	42
12	BIV-48	80	12	7.038	46
13	BIII-48	100	6	7.038	46
14	BIII-48	100	8	-	-
15	BIV-48	100	10	-	-

Table D-49 Design Outcomes of Spread Box Girder Bridges Designed with Compressive Strength of 8ksi, Live Load Factor of 0.8 and Tensile Stress Limit of $0.0948\sqrt{f'_c}$.

Cases	Section Type	Span Length (ft.)	Spacing (ft.)	Aps (in^2)	# of Strands
1	BI-36	30	6	1.53	10
2	BI-36	30	8	1.836	12
3	BI-36	30	10	1.836	12
4	BI-36	30	12	2.142	14
5	BI-36	60	6	3.978	26
6	BI-36	60	8	4.896	32
7	BI-36	60	10	5.508	36
8	BI-48	60	12	6.426	42
9	BI-48	80	6	7.038	46
10	BII-48	80	8	6.732	44
11	BII-48	80	10	7.65	50
12	BIII-48	80	12	7.038	46
13	BIII-48	100	6	7.344	48
14	BIII-48	100	8	9.18	60
15	BIV-48	100	10	10.404	68

Table D-50 Design Outcomes of Spread Box Girder Bridges Designed with Compressive Strength of 8ksi, Live Load Factor of 0.8 and Tensile Stress Limit of $0.158\sqrt{f'_c}$.

Cases	Section Type	Span Length (ft.)	Spacing (ft.)	Aps (in^2)	# of Strands
1	BI-36	30	6	1.224	8
2	BI-36	30	8	1.53	10
3	BI-36	30	10	1.836	12
4	BI-36	30	12	1.836	12
5	BI-36	60	6	3.672	24
6	BI-36	60	8	4.59	30
7	BI-36	60	10	5.202	34
8	BI-48	60	12	5.814	38
9	BI-48	80	6	6.732	44
10	BII-48	80	8	6.12	40
11	BII-48	80	10	7.344	48
12	BIII-48	80	12	6.732	44
13	BIII-48	100	6	7.038	46
14	BIII-48	100	8	8.262	54
15	BIV-48	100	10	9.18	60

Table D-51 Design Outcomes of Spread Box Girder Bridges Designed with Compressive Strength of 8ksi, Live Load Factor of 0.8 and Tensile Stress Limit of $0.19\sqrt{f'_c}$.

Cases	Section Type	Span Length (ft.)	Spacing (ft.)	Aps (in^2)	# of Strands
1	BI-36	30	6	1.224	8
2	BI-36	30	8	1.53	10
3	BI-36	30	10	1.53	10
4	BI-36	30	12	1.836	12
5	BI-36	60	6	3.672	24
6	BI-36	60	8	4.284	28
7	BI-36	60	10	5.202	34
8	BI-48	60	12	5.814	38
9	BI-48	80	6	6.426	42
10	BII-48	80	8	6.12	40
11	BII-48	80	10	7.038	46
12	BIII-48	80	12	6.732	44
13	BIII-48	100	6	6.732	44
14	BIII-48	100	8	7.956	52
15	BIV-48	100	10	8.568	56

Table D-52 Design Outcomes of Spread Box Girder Bridges Designed with Compressive Strength of 8ksi, Live Load Factor of 0.8 and Tensile Stress Limit of $0.253\sqrt{f'_c}$.

Cases	Section Type	Span Length (ft.)	Spacing (ft.)	Aps (in^2)	# of Strands
1	BI-36	30	6	0.918	6
2	BI-36	30	8	1.224	8
3	BI-36	30	10	1.53	10
4	BI-36	30	12	1.53	10
5	BI-36	60	6	3.366	22
6	BI-36	60	8	4.284	28
7	BI-36	60	10	4.896	32
8	BI-48	60	12	5.508	36
9	BI-48	80	6	6.12	40
10	BII-48	80	8	5.814	38
11	BII-48	80	10	6.732	44
12	BIII-48	80	12	6.12	40
13	BIII-48	100	6	6.426	42
14	BIII-48	100	8	7.65	50
15	BIV-48	100	10	7.956	52

Table D-53 Design Outcomes of Spread Box Girder Bridges Designed with Compressive Strength of 8ksi, Live Load Factor of 1.0 and Tensile Stress Limit of $0.0948\sqrt{f'_c}$.

Cases	Section Type	Span Length (ft.)	Spacing (ft.)	Aps (in^2)	# of Strands
1	BI-36	30	6	1.53	10
2	BI-36	30	8	1.836	12
3	BI-36	30	10	2.142	14
4	BI-36	30	12	2.142	14
5	BI-36	60	6	4.284	28
6	BI-36	60	8	5.202	34
7	BI-36	60	10	6.426	42
8	BI-48	60	12	7.038	46
9	BI-48	80	6	7.65	50
10	BII-48	80	8	7.344	48
11	BII-48	80	10	8.874	58
12	BIII-48	80	12	7.956	52
13	BIII-48	100	6	7.956	52
14	BIII-48	100	8	-	-
15	BIV-48	100	10	-	-

Table D-54 Design Outcomes of Spread Box Girder Bridges Designed with Compressive Strength of 8ksi, Live Load Factor of 1.0 and Tensile Stress Limit of $0.158\sqrt{f'_c}$.

Cases	Section Type	Span Length (ft.)	Spacing (ft.)	Aps (in^2)	# of Strands
1	BI-36	30	6	1.53	10
2	BI-36	30	8	1.53	10
3	BI-36	30	10	1.836	12
4	BI-36	30	12	2.142	14
5	BI-36	60	6	4.284	28
6	BI-36	60	8	4.896	32
7	BI-36	60	10	5.814	38
8	BI-48	60	12	6.732	44
9	BI-48	80	6	7.344	48
10	BII-48	80	8	6.732	44
11	BII-48	80	10	7.956	52
12	BIII-48	80	12	7.344	48
13	BIII-48	100	6	7.344	48
14	BIII-48	100	8	9.792	64
15	BIV-48	100	10	-	-

Table D-55 Design Outcomes of Spread Box Girder Bridges Designed with Compressive Strength of 8ksi, Live Load Factor of 1.0 and Tensile Stress Limit of $0.19\sqrt{f'_c}$.

Cases	Section Type	Span Length (ft.)	Spacing (ft.)	Aps (in^2)	# of Strands
1	BI-36	30	6	1.224	8
2	BI-36	30	8	1.53	10
3	BI-36	30	10	1.836	12
4	BI-36	30	12	1.836	12
5	BI-36	60	6	3.978	26
6	BI-36	60	8	4.896	32
7	BI-36	60	10	5.814	38
8	BI-48	60	12	6.426	42
9	BI-48	80	6	7.038	46
10	BII-48	80	8	6.732	44
11	BII-48	80	10	7.956	52
12	BIII-48	80	12	7.344	48
13	BIII-48	100	6	7.038	46
14	BIII-48	100	8	9.18	60
15	BIV-48	100	10	-	-

Table D-56 Design Outcomes of Spread Box Girder Bridges Designed with Compressive Strength of 8ksi, Live Load Factor of 1.0 and Tensile Stress Limit of $0.253\sqrt{f'_c}$.

Cases	Section Type	Span Length (ft.)	Spacing (ft.)	Aps (in^2)	# of Strands
1	BI-36	30	6	1.224	8
2	BI-36	30	8	1.224	8
3	BI-36	30	10	1.53	10
4	BI-36	30	12	1.836	12
5	BI-36	60	6	3.672	24
6	BI-36	60	8	4.59	30
7	BI-36	60	10	5.508	36
8	BI-48	60	12	6.12	40
9	BI-48	80	6	6.732	44
10	BII-48	80	8	6.426	42
11	BII-48	80	10	7.344	48
12	BIII-48	80	12	6.732	44
13	BIII-48	100	6	6.732	44
14	BIII-48	100	8	8.568	56
15	BIV-48	100	10	8.874	58

Table D-57 Design Outcomes of Spread Box Girder Bridges Designed with Compressive Strength of 10ksi, Live Load Factor of 0.8 and Tensile Stress Limit of $0.0948\sqrt{f'_c}$.

Cases	Section Type	Span Length (ft.)	Spacing (ft.)	Aps (in^2)	# of Strands
1	BI-36	30	6	1.53	10
2	BI-36	30	8	1.53	10
3	BI-36	30	10	1.836	12
4	BI-36	30	12	2.142	14
5	BI-36	60	6	3.978	26
6	BI-36	60	8	4.59	30
7	BI-36	60	10	5.508	36
8	BI-48	60	12	6.12	40
9	BI-48	80	6	6.732	44
10	BII-48	80	8	6.426	42
11	BII-48	80	10	7.344	48
12	BIII-48	80	12	7.038	46
13	BIII-48	100	6	7.038	46
14	BIII-48	100	8	8.568	56
15	BIV-48	100	10	9.486	62

Table D-58 Design Outcomes of Spread Box Girder Bridges Designed with Compressive Strength of 10ksi, Live Load Factor of 0.8 and Tensile Stress Limit of $0.158\sqrt{f'_c}$.

Cases	Section Type	Span Length (ft.)	Spacing (ft.)	Aps (in^2)	# of Strands
1	BI-36	30	6	1.224	8
2	BI-36	30	8	1.53	10
3	BI-36	30	10	1.53	10
4	BI-36	30	12	1.836	12
5	BI-36	60	6	3.672	24
6	BI-36	60	8	4.284	28
7	BI-36	60	10	5.202	34
8	BI-48	60	12	5.814	38
9	BI-48	80	6	6.426	42
10	BII-48	80	8	6.12	40
11	BII-48	80	10	7.038	46
12	BIII-48	80	12	6.426	42
13	BIII-48	100	6	6.732	44
14	BIII-48	100	8	7.956	52
15	BIV-48	100	10	8.568	56

Table D-59 Design Outcomes of Spread Box Girder Bridges Designed with Compressive Strength of 10ksi, Live Load Factor of 0.8 and Tensile Stress Limit of $0.19\sqrt{f'_c}$.

Cases	Section Type	Span Length (ft.)	Spacing (ft.)	Aps (in^2)	# of Strands
1	BI-36	30	6	1.224	8
2	BI-36	30	8	1.224	8
3	BI-36	30	10	1.53	10
4	BI-36	30	12	1.836	12
5	BI-36	60	6	3.672	24
6	BI-36	60	8	4.284	28
7	BI-36	60	10	4.896	32
8	BI-48	60	12	5.508	36
9	BI-48	80	6	6.426	42
10	BII-48	80	8	5.814	38
11	BII-48	80	10	6.732	44
12	BIII-48	80	12	6.426	42
13	BIII-48	100	6	6.732	44
14	BIII-48	100	8	7.65	50
15	BIV-48	100	10	8.262	54

Table D-60 Design Outcomes of Spread Box Girder Bridges Designed with Compressive Strength of 10ksi, Live Load Factor of 0.8 and Tensile Stress Limit of $0.253\sqrt{f'_c}$.

Cases	Section Type	Span Length (ft.)	Spacing (ft.)	Aps (in^2)	# of Strands
1	BI-36	30	6	0.918	6
2	BI-36	30	8	1.224	8
3	BI-36	30	10	1.224	8
4	BI-36	30	12	1.53	10
5	BI-36	60	6	3.366	22
6	BI-36	60	8	3.978	26
7	BI-36	60	10	4.59	30
8	BI-48	60	12	5.202	34
9	BI-48	80	6	5.814	38
10	BII-48	80	8	5.508	36
11	BII-48	80	10	6.426	42
12	BIII-48	80	12	5.814	38
13	BIII-48	100	6	6.12	40
14	BIII-48	100	8	7.344	48
15	BIV-48	100	10	7.65	50

Table D-61 Design Outcomes of Spread Box Girder Bridges Designed with Compressive Strength of 10ksi, Live Load Factor of 1.0 and Tensile Stress Limit of $0.0948\sqrt{f'_c}$.

Cases	Section Type	Span Length (ft.)	Spacing (ft.)	Aps (in^2)	# of Strands
1	BI-36	30	6	1.53	10
2	BI-36	30	8	1.836	12
3	BI-36	30	10	2.142	14
4	BI-36	30	12	2.142	14
5	BI-36	60	6	4.284	28
6	BI-36	60	8	5.202	34
7	BI-36	60	10	6.12	40
8	BI-48	60	12	6.732	44
9	BI-48	80	6	7.344	48
10	BII-48	80	8	7.038	46
11	BII-48	80	10	8.262	54
12	BIII-48	80	12	7.65	50
13	BIII-48	100	6	7.65	50
14	BIII-48	100	8	-	-
15	BIV-48	100	10	-	-

Table D-62 Design Outcomes of Spread Box Girder Bridges Designed with Compressive Strength of 10ksi, Live Load Factor of 1.0 and Tensile Stress Limit of $0.158\sqrt{f'_c}$.

Cases	Section Type	Span Length (ft.)	Spacing (ft.)	Aps (in^2)	# of Strands
1	BI-36	30	6	1.53	10
2	BI-36	30	8	1.53	10
3	BI-36	30	10	1.836	12
4	BI-36	30	12	2.142	14
5	BI-36	60	6	3.978	26
6	BI-36	60	8	4.896	32
7	BI-36	60	10	5.814	38
8	BI-48	60	12	6.426	42
9	BI-48	80	6	7.038	46
10	BII-48	80	8	6.732	44
11	BII-48	80	10	7.65	50
12	BIII-48	80	12	7.344	48
13	BIII-48	100	6	7.344	48
14	BIII-48	100	8	8.874	58
15	BIV-48	100	10	10.098	66

Table D-63 Design Outcomes of Spread Box Girder Bridges Designed with Compressive Strength of 10ksi, Live Load Factor of 1.0 and Tensile Stress Limit of $0.19\sqrt{f'_c}$.

Cases	Section Type	Span Length (ft.)	Spacing (ft.)	Aps (in^2)	# of Strands
1	BI-36	30	6	1.224	8
2	BI-36	30	8	1.53	10
3	BI-36	30	10	1.836	12
4	BI-36	30	12	1.836	12
5	BI-36	60	6	3.978	26
6	BI-36	60	8	4.59	30
7	BI-36	60	10	5.508	36
8	BI-48	60	12	6.12	40
9	BI-48	80	6	6.732	44
10	BII-48	80	8	6.426	42
11	BII-48	80	10	7.65	50
12	BIII-48	80	12	7.038	46
13	BIII-48	100	6	7.038	46
14	BIII-48	100	8	8.568	56
15	BIV-48	100	10	9.486	62

Table D-64 Design Outcomes of Spread Box Girder Bridges Designed with Compressive Strength of 10ksi, Live Load Factor of 1.0 and Tensile Stress Limit of $0.253\sqrt{f'_c}$.

Cases	Section Type	Span Length (ft.)	Spacing (ft.)	Aps (in^2)	# of Strands
1	BI-36	30	6	0.918	6
2	BI-36	30	8	1.224	8
3	BI-36	30	10	1.53	10
4	BI-36	30	12	1.53	10
5	BI-36	60	6	3.672	24
6	BI-36	60	8	4.59	30
7	BI-36	60	10	5.202	34
8	BI-48	60	12	5.814	38
9	BI-48	80	6	6.426	42
10	BII-48	80	8	6.12	40
11	BII-48	80	10	7.038	46
12	BIII-48	80	12	6.426	42
13	BIII-48	100	6	6.732	44
14	BIII-48	100	8	7.956	52
15	BIV-48	100	10	8.568	56

D.2.4 PCI ASBI Box Girder Bridge

Table D-65 Design Outcomes of Spread Box Girder Bridges Designed with Compressive Strength of 8ksi, Live Load Factor of 0.8 and Tensile Stress Limit of $0.0948\sqrt{f'_c}$.

Cases	Section Type	Span Length (ft.)	Aps (in^2)	# of Strands
1	1800-2	100	7.344	48
2	1800-2	120	10.71	70
3	1800-2	140	14.076	92
4	2100-2	160	21.266	98
5	2400-2	180	22.568	104
6	2400-2	200	27.342	126

Table D-66 Design Outcomes of Spread Box Girder Bridges Designed with Compressive Strength of 8ksi, Live Load Factor of 0.8 and Tensile Stress Limit of $0.158\sqrt{f'_c}$.

Cases	Section Type	Span Length (ft.)	Aps (in^2)	# of Strands
1	1800-2	100	5.814	38
2	1800-2	120	9.18	60
3	1800-2	140	12.546	82
4	2100-2	160	19.096	88
5	2400-2	180	20.398	94
6	2400-2	200	25.172	116

Table D-67 Design Outcomes of Spread Box Girder Bridges Designed with Compressive Strength of 8ksi, Live Load Factor of 0.8 and Tensile Stress Limit of $0.19\sqrt{f'_c}$.

Cases	Section Type	Span Length (ft.)	Aps (in^2)	# of Strands
1	1800-2	100	5.202	34
2	1800-2	120	8.568	56
3	1800-2	140	11.934	78
4	2100-2	160	17.794	82
5	2400-2	180	19.096	88
6	2400-2	200	24.304	112

Table D-68 Design Outcomes of Spread Box Girder Bridges Designed with Compressive Strength of 8ksi, Live Load Factor of 0.8 and Tensile Stress Limit of $0.253\sqrt{f'_c}$.

Cases	Section Type	Span Length (ft.)	Aps (in^2)	# of Strands
1	1800-2	100	3.978	26
2	1800-2	120	7.344	48
3	1800-2	140	10.404	68
4	2100-2	160	16.058	74
5	2400-2	180	16.926	78
6	2400-2	200	22.134	102

D.3 Application of the Calibration Process to I-Girders and Bulb-Tees

D.3.1 Effect of changing design specifications (old losses, new losses)

Depending on the environmental exposure conditions, both the AASHTO Standard Specifications and the AASHTO LRFD Specifications allow designing prestressed components for maximum concrete tensile stress of $f_t = 0.0948\sqrt{f'_c}$ or $f_t = 0.19\sqrt{f'_c}$. When either specifications are applied without owner's exceptions, most bridges are designed for $f_t = 0.19\sqrt{f'_c}$ with a small number of bridges in coastal areas designed for $f_t = 0.0948\sqrt{f'_c}$. This makes it likely that the reliability indices calculated for existing bridges are for bridges designed for maximum concrete tensile stress of $f_t = 0.19\sqrt{f'_c}$. As indicated earlier, based on the dates of construction, it is likely that all bridges considered were designed using the prestressing loss provisions method that existed in both the AASHTO Standard Specifications and in the pre-2005 AASHTO LRFD.

To study the effect of the maximum concrete tensile stress ($f_t = 0.0948\sqrt{f'_c}$ or $f_t = 0.19\sqrt{f'_c}$) and the method of calculating the prestressing losses on the reliability index, a group of simulated I-girder bridges was designed for four cases:

Case 1: AASHTO LRFD with maximum concrete tensile stress of $f_t = 0.0948\sqrt{f'_c}$ and pre-2005 prestress loss method

Case 2: AASHTO LRFD with maximum concrete tensile stress of $f_t = 0.0948\sqrt{f'_c}$ and current (2012) prestress loss method

Case 3: AASHTO LRFD with maximum concrete tensile stress of $f_t = 0.19\sqrt{f'_c}$ and pre-2005 prestress loss method

Case 4: AASHTO LRFD with maximum concrete tensile stress of $f_t = 0.19\sqrt{f'_c}$ and current (2012) prestress loss method

The smallest possible AASHTO girder size was used for each simulated bridge. Comparing Case 1 to Case 2 and Case 3 to Case 4 shows the effect of changing the prestressing loss method. Results from Case 1 generally indicate the inherent reliability of existing bridges designed for severe environmental conditions ($f_t = 0.0948\sqrt{f_c'}$) and results from Case 3 indicate the inherent reliability of existing bridges designed for normal environmental conditions ($f_t = 0.19\sqrt{f_c'}$).

Table D-69 and Table D-70 show the results for I-girder bridges designed for Maximum concrete tensile stress $f_t = 0.0948\sqrt{f_c'}$ (Case 1 and Case 2) and $f_t = 0.19\sqrt{f_c'}$ (Case 3 and Case 4) for I –girder bridges for ADTT 5000.

Table D-69 Summary Information of Bridges Designed using AASHTO I-Girders with ADTT 5000 and $f_t = 0.0948\sqrt{f'_c}$

Cases	Section Type	Span Length (ft.)	Spacing (ft.)	Case 1 Designed Using Old Loss Method			Case 2 Designed Using New Loss Method		
				Decomp.	Max. Tensile	Max. Crack	Decomp.	Max. Tensile	Max. Crack
1	AASHTO I	30	6	1.05	1.49	2.92	1.03	1.51	2.55
2	AASHTO I	30	8	0.9	0.94	2.41	0.93	1	2.32
3	AASHTO I	30	10	1.16	1.68	2.87	1.28	1.67	2.82
4	AASHTO I	30	12	1.28	1.67	2.91	0.63	0.97	2.29
Average for 30 ft. Span				**1.10**	**1.45**	**2.78**	**0.97**	**1.29**	**2.50**
5	AASHTO II	60	6	0.66	1.01	3.35	0.23	0.61	2.47
6	AASHTO II	60	8	—	—	—	0.73	1.04	2.42
7	AASHTO III	60	10	1.22	1.62	3.01	0.43	0.76	1.97
8	AASHTO III	60	12	1.57	1.96	3.68	0.73	0.99	2.51
Average for 60 ft. Span				**1.15**	**1.53**	**3.35**	**0.53**	**0.85**	**2.34**
9	AASHTO III	80	6	1.35	1.66	4.1	0.61	0.92	3.07
10	AASHTO III	80	8	1.8	2.14	5.23	0.82	1.13	3.64
11	AASHTO III	80	10	—	—	—	0.90	1.19	2.93
12	AASHTO IV	80	12	2.2	2.49	5.11	0.83	1.17	3.32
Average for 80 ft. Span				**1.78**	**2.10**	**4.81**	**0.79**	**1.10**	**3.24**
13	AASHTO III	100	6	—	—	—	1.45	1.85	3.51
14	AASHTO IV	100	8	1.86	2	3.86	1.33	1.43	3.44
15	AASHTO IV	100	10	—	—	—	1.33	1.65	3.37
16	AASHTO V	100	12	1.68	1.99	4.08	0.93	1.24	3.33
Average for 100 ft. Span				**1.77**	**2.00**	**3.97**	**1.26**	**1.54**	**3.41**
17	AASHTO IV	120	6	—	—	—	1.32	1.76	3.81
18	AASHTO V	120	8	1.54	2.05	3.65	0.92	1.4	3.14
19	AASHTO V	120	10	—	—	—	0.95	1.46	3.02
20	AASHTO VI	120	12	1.82	2.26	3.88	0.9	1.35	3.38
Average for 120 ft. Span				**1.68**	**2.16**	**3.77**	**1.02**	**1.49**	**3.34**
21	AASHTO VI	140	6	1.48	1.99	3.91	0.86	1.36	2.32
22	AASHTO VI	140	8	—	—	—	0.99	1.47	2.79
23	AASHTO VI	140	10	—	—	—	1.05	1.53	3.22
24	—	140	12	—	—	—	—	—	—
Average for 140 ft. Span				**1.48**	**1.99**	**3.91**	**0.97**	**1.45**	**2.78**
Average for All Spans				**1.44**	**1.80**	**3.66**	**0.92**	**1.28**	**2.94**

Table D-70 Summary Information of Bridges Designed using AASHTO I-Girders with ADTT 5000 and $f_t = 0.19\sqrt{f_c'}$

Cases	Section Type	Span Length (ft.)	Spacing (ft.)	Case 3			Case 4		
				Designed Using Old Loss Method			Designed Using New Loss Method		
				Decomp.	Max. Tensile	Max. Crack	Decomp.	Max. Tensile	Max. Crack
1	AASHTO I	30	6	1	1.55	2.39	0.97	1.55	2.46
2	AASHTO I	30	8	0.94	0.92	2.35	0.91	1.00	2.16
3	AASHTO I	30	10	1.29	1.66	2.91	1.18	1.66	2.79
4	AASHTO I	30	12	1.3	1.72	3.02	1.26	1.70	2.91
Average for 30 ft. Span				1.13	1.46	2.67	1.08	1.48	2.58
5	AASHTO II	60	6	0.74	1.13	3.11	0.18	0.58	2.41
6	AASHTO II	60	8	1.04	1.39	2.82	0.28	0.66	1.91
7	AASHTO III	60	10	0.42	0.79	2.05	0.42	0.78	2.07
8	AASHTO III	60	12	0.66	1.00	2.5	0.68	0.96	2.53
Average for 60 ft. Span				0.72	1.08	2.62	0.39	0.75	2.23
9	AASHTO III	80	6	0.56	0.97	3.13	0.13	0.51	2.53
10	AASHTO III	80	8	1.06	1.46	3.43	0.42	0.78	3.2
11	AASHTO III	80	10	1.58	1.84	3.65	0.37	0.65	2.72
12	AASHTO IV	80	12	0.83	1.15	3.72	0.51	0.87	3.11
Average for 80 ft. Span				1.01	1.36	3.48	0.36	0.70	2.89
13	AASHTO III	100	6	—	—	—	0.82	1.23	3.44
14	AASHTO IV	100	8	1.31	1.42	3.6	0.69	0.76	2.76
15	AASHTO IV	100	10	1.8	1.98	3.67	0.75	1.04	3.12
16	AASHTO V	100	12	1.08	1.37	3.43	0.4	0.72	2.55
Average for 100 ft. Span				1.40	1.59	3.57	0.67	0.94	2.97
17	AASHTO IV	120	6	1.53	1.98	3.71	0.7	1.28	3.1
18	AASHTO V	120	8	0.9	1.30	3.31	0.46	0.85	2.55
19	AASHTO V	120	10	1.25	1.65	3.35	0.26	0.78	2.68
20	AASHTO VI	120	12	1.19	1.66	3.37	0.47	0.91	2.69
Average for 120 ft. Span				1.22	1.65	3.44	0.47	0.96	2.76
21	AASHTO VI	140	6	0.84	1.41	3.23	0.28	0.82	2.41
22	AASHTO VI	140	8	1.22	1.68	3.3	0.53	0.98	3.04
23	AASHTO VI	140	10	—	—	—	0.62	1.08	2.46
24	—	140	12	—	—	—	—	—	—
Average for 140 ft. Span				1.03	1.55	3.27	0.48	0.96	2.64
Average for All Spans				**1.07**	**1.43**	**3.15**	0.58	0.96	2.68

Using the current prestress loss method resulted in smaller number of strands than the old loss method. As shown in Table D-69 and Table D-70, this resulted in lower reliability index for bridges designed using the new (current) prestress loss method.

With most bridges on the system designed using the old prestress loss method, the reliability indices corresponding to bridges designed using the old loss method (Case 1 and Case 3) are considered to better represent the inherent reliability of existing bridges designed for severe exposure conditions (Case 1) and normal exposure conditions (Case 3).

D.3.2 Reliability indices of existing and redesigned bridges

As specified in the AASHTO LRFD Bridge Design Specifications (2012), the service limit state is the limit state to restrict stress, deformation, and crack width under regular service conditions. The service III limit state is mainly related to the tension in prestressed concrete superstructures with the objective of crack control and to the principal tension in the webs of segmental concrete girders. According to the proposed calibration procedure, there are three limit states corresponding to the tension level at the bottom of the P/C girder that would need to be calibrated: (1) Decompression limit state, (2) Maximum allowable tensile stress limit state, and (3) Maximum allowable crack width limit state.

In this section, following the proposed calibration procedure, the reliability indices of the following bridges databases were investigated:

1- Existing bridges from NCHRP 12-78 bridge database.
2- NCHRP 12-78 bridges redesigned using new losses provisions (AASHTO Specifications 2012) and tensile stress limit of $0.0948\sqrt{f'_c}$.
3- NCHRP 12-78 bridges redesigned using new losses provisions (AASHTO Specifications 2012) and tensile stress limit of $0.19\sqrt{f'_c}$.
4- NCHRP 12-78 bridges redesigned using new losses provisions (AASHTO Specifications 2012) and tensile stress limit of $0.253\sqrt{f'_c}$.

D.3.2.1 Evaluation of Existing Bridges (NCHRP 12-78 Bridge Database)

Following the proposed calibration procedure, the RT evaluated the reliability levels of existing bridges. These existing bridges are taken from the NCHRP 12-78 bridge database, which include 30 I-girder bridges, 36 spread box girder bridges, and 31 adjacent box girder bridges. Among these existing bridges, Most of the bridges were designed before 2005, some of the bridges were designed over 70 years ago (e.g. Spread Box Girder Bridge #9349 was built on 1935). In Comparison with current design, the load distribution factors, impact factor, losses calculation, etc. might be different when the existing bridges have been designed, these differences might result in more conservative design.

Table D-71 through Table D-73 shows a summary of the information for a total of these 97 existing bridges.

Table D-71 Summary of NCHRP 12-78 I-Girder Bridge

Bridge Name	Section Type	Girder Spacing (ft.)	Span Length (ft.)	Aps (in^2)	# of Strands
82	MN type 63	10.33	82.75	5.20	34
3107	36" I BEAM	5.77	49.54	1.84	12
4794	BEAM Type 4	9.33	66.67	5.05	33
4827	BEAM Type 2	7.17	50.58	2.75	18
5624	BEAM Type 4	7.25	59.37	3.06	20
5794	BEAM Type 3	5.83	72.00	4.34	20
5840	BEAM Type 6	9.00	85.00	4.59	30
5884	BEAM Type 6	8.17	90.01	5.81	38
8330	BEAM Type 6	8.67	76.38	4.28	28
8783	AASHTO VI	7.75	143.15	9.98	46
8832	36" I BEAM	10.00	43.26	3.06	20
8885	BT-63	10.58	90.01	5.51	36
8889	BT-63	10.58	90.85	5.51	36
8890	AASHTO VI	8.00	143.50	10.42	48
8891	BEAM Type 6	9.25	47.17	2.14	14
8957	BEAM Type 6	8.67	98.00	5.64	26
9378	Wisconsin Girder	10.42	101.83	6.12	40
10269	AASHTO III	6.67	78.00	4.28	28
10599	AASHTO II	6.75	62.83	4.28	28
10740	AASHTO III	7.00	78.55	4.90	32
10755	AASHTO II	7.00	52.50	3.67	24
10803	BT-72	6.00	138.25	7.68	46
11030	BT-72	6.38	136.00	7.65	50
11938	BT-63	7.31	116.52	7.68	46
12589	AASHTO IV	8.75	73.21	4.59	30
12596	AASHTO IV	11.15	96.79	10.85	50
12603	AASHTO II	11.48	37.73	3.04	14
12610	AASHTO IV	7.13	108.53	7.96	52
15620	Bulb-Tee	5.35	119.82	10.42	48
18067	AL BT-54 Mod.	5.29	131.02	10.85	50

Table D-72 Summary of NCHRP 12-78 Spread Box Girder Bridge

Bridge Name	Section Type	Girder Spacing (ft.)	Span Length (ft.)	Aps (in^2)	# of Strands
1150	33" x 36" Box	8.50	70.58	5.97	39
3577	27"x36" IDOT	6.70	38.58	2.92	27
3754	33"x36" IDOT	6.36	53.61	3.24	30
8875	27"x48" P/S Box	11.25	38.00	3.52	23
9090	MDOT 33" Box	7.08	66.04	4.34	20
9091	MDOT 33" Box	7.08	66.20	4.34	20
9128	1525 Box	7.49	33.69	0.87	4
9192	21" x 36" Box	9.83	38.67	2.75	18
9217	17" Box	6.21	42.30	3.47	16
9219	MDOT 21" Box	5.25	53.17	3.47	16
9243	33in x 36in Box	6.17	73.33	4.56	21
9248	21 in Box Beam	8.00	37.75	3.91	18
9282	17" x 36" Box	7.83	36.30	2.45	16
9284	17" x 36" Box	6.66	31.56	1.95	9
9286	27" x 36" Box	8.04	50.67	4.34	20
9310	21" x 36" Box	5.97	51.97	4.34	20
9324	27" x 36" Box	10.50	42.33	3.06	20
9328	27" x 36" Box	6.92	57.27	3.98	26
9349	21" x 36" Box	7.00	48.67	3.37	22
9355	39" x 36" Box	7.92	75.20	5.64	26
9356	39" x 36" Box	7.92	75.20	5.64	26
9361	27" x 36" Box	6.00	65.79	4.59	30
9368	33" x 36" Box	7.38	71.25	4.59	30
9369	27" x 36" Box	6.50	51.32	3.04	14
9370	27" x 36" Box	6.42	51.32	3.04	14
9376	27" x 36" Box	7.38	53.35	3.26	15
9380	21" x 36" Box	9.10	32.09	1.84	12
9383	27" x 36" Box	10.58	46.82	3.47	16
9384	21" x 36" Box	6.60	44.13	3.04	14
9394	27x 48 in Box	7.50	66.91	5.20	34
12870	36" x 48"	6.50	77.50	4.59	30
14969	BIV-48	7.88	78.74	7.34	48
16293	1220 x 1220 box	8.86	57.27	5.64	26
16366	Beams B1-B6	6.58	60.38	5.81	38
17240	BII-48	8.00	51.50	3.67	24
17338	BII-48	8.00	49.00	2.75	18

Table D-73 Summary of NCHRP 12-78 Adjacent Box Girder Bridge

Bridge Name	Section Type	Girder Spacing (ft.)	Span Length (ft.)	Aps (in^2)	# of Strands
3805	27"x36" IDOT	3.00	59.04	2.30	15
3819	33"x36" IDOT	3.00	74.88	2.60	17
5125	48"x33" P/S Box	4.00	66.00	3.98	26
5911	36"x27"P/S Box	3.00	59.42	2.14	14
9071	MDOT 840 x 915 Box	3.12	83.64	3.47	16
9103	MDOT 1220 x 1220 Box	4.13	111.21	5.43	25
9167	685mm x 1220mm Box	4.13	75.56	4.77	22
9180	MDOT 535 x 915 Box	3.13	44.70	2.82	13
9181	MDOT 535 x 915 Box	3.13	60.37	3.21	21
9191	27" x 36" Box	3.14	72.50	3.06	20
9228	1220mm x 1220 mm Box	4.23	110.44	5.21	24
9240	33in x 36in Box	3.13	97.92	4.28	28
9314	27" x 36" Box	3.13	83.67	4.77	22
12807	BII-48	4.04	84.00	5.20	34
12809	BII-48	4.04	82.00	5.20	34
12952	BIV-48 modified	3.79	79.96	6.43	42
13118- interior 915	AASHTO BI-915	3.35	69.23	3.87	18
13118-Interior 1220	AASHTO BI-1220	3.85	69.23	4.09	19
13788	BIV-48	4.04	83.00	4.90	32
13805	BI-48	4.06	52.50	3.67	24
14070	B 3' 45"	3.10	115.00	6.43	42
14246	BI-48	4.04	52.00	3.67	24
14987	BIV-48	4.06	73.00	5.20	34
15238	BII-48, 1.220 m Wide	4.04	73.82	5.20	34
16538	ps bx	4.06	101.71	5.81	38
16799	PS Shape 1-Interior	4.00	84.00	5.85	38
17008	AASHTO BII-1220	4.00	82.51	5.81	38
17042	4' PS Box	3.75	50.03	3.67	24
17075	BIV-48Modified	4.00	107.00	6.73	44
17143	BIII-48	3.75	70.00	4.59	30
17175	BII-48	3.75	88.75	6.73	44

The reliability analysis results for existing bridges are shown in Table D-74. Table D-75 shows the probability of exceedance for existing bridges for various conditions.

Table D-74 Summary of Reliability Indices for Existing Bridges

Performance Levels		Existing Bridges (NCHRP 12-78) (Reliability Index β), 1 Year			
		ADTT=1000	ADTT=2500	ADTT=5000	ADTT=10000
Decompression		0.95	0.85	0.74	0.61
Max.Tensile Stress Limit	$0.0948\sqrt{f'_c}$	1.15	1.01	0.94	0.82
	$0.19\sqrt{f'_c}$	1.24	1.14	1.05	0.95
	$0.253\sqrt{f'_c}$	1.4	1.27	1.19	1.07
Maximum Crack Width	.008 in	2.29	2.21	1.99	1.85
	.012 in	2.65	2.6	2.37	2.22
	.016 in	3.06	2.89	2.69	2.56

Table D-75 Summary of Probability of Exceedance for Existing Bridges

Performance Levels		Existing Bridges (NCHRP 12-78) (Reliability Index β), 1 Year			
		ADTT=1000	ADTT=2500	ADTT=5000	ADTT=10000
Decompression		1539/10000	1814/10000	2119/10000	2546/10000
Max.Tensile Stress Limit	$0.0948\sqrt{f'_c}$	1251/10000	1562/10000	1736/10000	2061/10000
	$0.19\sqrt{f'_c}$	1075/10000	1271/10000	1469/10000	1711/10000
	$0.253\sqrt{f'_c}$	808/10000	1020/10000	1170/10000	1423/10000
Maximum Crack Width	.008 in	110/10000	136/10000	233/10000	322/10000
	.012 in	40/10000	47/10000	89/10000	132/10000
	.016 in	11/10000	19/10000	36/10000	52/10000

D.3.2.2 Evaluation of redesigned bridges using new loss provisions and tensile stress limit of $3\sqrt{f'_c}$

The reliability analysis results for existing bridges are shown in Table D-76. Table D-77 shows the probability of exceedance for existing bridges for various conditions.

Table D-76 Summary of Reliability Indices for redesigned bridges using new losses provisions and tensile stress limit of $0.0948\sqrt{f'_c}$

Performance Levels		Existing Bridges (NCHRP 12-78) (Reliability Index β), 1 Year			
		ADTT=1000	ADTT=2500	ADTT=5000	ADTT=10000
Decompression		0.94	0.84	0.74	0.56
Max.Tensile Stress Limit	$0.0948\sqrt{f'_c}$	1.18	1.03	0.88	0.74
	$0.19\sqrt{f'_c}$	1.29	1.14	1	0.86
	$0.253\sqrt{f'_c}$	1.36	1.2	1.05	0.9
Maximum Crack Width	.008 in	2.33	2.18	2.04	1.89
	.012 in	2.76	2.6	2.45	2.3
	.016 in	3.14	2.99	2.84	2.69

Table D-77 Summary of Probability of Exceedance for redesigned bridges using new losses provisions and tensile stress limit of $0.0948\sqrt{f'_c}$

Performance Levels		Existing Bridges (NCHRP 12-78) (Reliability Index β), 1 Year			
		ADTT=1000	ADTT=2500	ADTT=5000	ADTT=10000
Decompression		1736/10000	2005/10000	2296/10000	2877/10000
Max.Tensile Stress Limit	$0.0948\sqrt{f'_c}$	1190/10000	1515/10000	1894/10000	2296/10000
	$0.19\sqrt{f'_c}$	985/10000	1271/10000	1587/10000	1949/10000
	$0.253\sqrt{f'_c}$	869/10000	1151/10000	1469/10000	1841/10000
Maximum Crack Width	.008 in	99/10000	146/10000	207/10000	294/10000
	.012 in	29/10000	47/10000	71/10000	107/10000
	.016 in	8/10000	14/10000	23/10000	36/10000

D.3.2.3 Evaluation of redesigned bridges using new losses provisions and tensile stress limit of $6\sqrt{f'_c}$

The reliability analysis results for existing bridges are shown in Table D-78. Table D-79 shows the probability of exceedance for existing bridges for various conditions.

Table D-78 Summary of Reliability Indices for redesigned bridges using new losses provisions and tensile stress limit of $0.19\sqrt{f'_c}$

Performance Levels		Existing Bridges (NCHRP 12-78) (Reliability Index β), 1 Year			
		ADTT=1000	ADTT=2500	ADTT=5000	ADTT=10000
Decompression		0.86	0.75	0.64	0.45
Max.Tensile Stress Limit	$0.0948\sqrt{f'_c}$	1.08	0.94	0.79	0.64
	$0.19\sqrt{f'_c}$	1.19	1.04	0.9	0.75
	$0.253\sqrt{f'_c}$	1.25	1.1	0.95	0.8
Maximum Crack Width	.008 in	2.21	2.06	1.9	1.75
	.012 in	2.62	2.47	2.32	2.17
	.016 in	3.03	2.88	2.73	2.58

Table D-79 Summary of Probability of Exceedance for redesigned bridges using new losses provisions and tensile stress limit of $0.19\sqrt{f'_c}$

Performance Levels		Existing Bridges (NCHRP 12-78) (Reliability Index β), 1 Year			
		ADTT=1000	ADTT=2500	ADTT=5000	ADTT=10000
Decompression		1949/10000	2266/10000	2611/10000	3264/10000
Max.Tensile Stress Limit	$0.0948\sqrt{f'_c}$	1401/10000	1736/10000	2148/10000	2611/10000
	$0.19\sqrt{f'_c}$	1170/10000	1492/10000	1841/10000	2266/10000
	$0.253\sqrt{f'_c}$	1056/10000	1357/10000	1711/10000	2119/10000
Maximum Crack Width	.008 in	136/10000	197/10000	287/10000	401/10000
	.012 in	44/10000	68/10000	102/10000	150/10000
	.016 in	12/10000	20/10000	32/10000	49/10000

D.3.2.4 Evaluation of redesigned bridges using new losses provisions and tensile stress limit of $0.253\sqrt{f'_c}$

The reliability analysis results for existing bridges are shown in Table D-80. Table D-81 shows the probability of exceedance for existing bridges for various conditions.

Table D-80 Summary of Reliability Indices for redesigned bridges using new losses provisions and tensile stress limit of $0.253\sqrt{f'_c}$

Performance Levels		Existing Bridges (NCHRP 12-78) (Reliability Index β), 1 Year			
		ADTT=1000	ADTT=2500	ADTT=5000	ADTT=10000
Decompression		0.82	0.73	0.62	0.44
Max.Tensile Stress Limit	$0.0948\sqrt{f'_c}$	1.05	0.9	0.75	0.6
	$0.19\sqrt{f'_c}$	1.16	1.01	0.86	0.71
	$0.253\sqrt{f'_c}$	1.23	1.08	0.93	0.78
Maximum Crack Width	.008 in	2.19	2.04	1.89	1.73
	.012 in	2.61	2.46	2.3	2.15
	.016 in	3	2.85	2.7	2.55

Table D-81 Summary of Probability of Exceedance for redesigned bridges using new losses provisions and tensile stress limit of $0.253\sqrt{f'_c}$

Performance Levels		Existing Bridges (NCHRP 12-78) (Reliability Index β), 1 Year			
		ADTT=1000	ADTT=2500	ADTT=5000	ADTT=10000
Decompression		2061/10000	2327/10000	2676/10000	3300/10000
Max.Tensile Stress Limit	$0.0948\sqrt{f'_c}$	1469/10000	1841/10000	2266/10000	2743/10000
	$0.19\sqrt{f'_c}$	1230/10000	1562/10000	1949/10000	2389/10000
	$0.253\sqrt{f'_c}$	1093/10000	1401/10000	1762/10000	2177/10000
Maximum Crack Width	.008 in	143/10000	207/10000	294/10000	418/10000
	.012 in	45/10000	69/10000	107/10000	158/10000
	.016 in	13/10000	22/10000	35/10000	54/10000

D.3.3 Selection of Target Reliability indices

The target reliability indices for the serviceability limit states from various codes were discussed in the project's interim report. The European Code selected a target reliability index for irreversible service limit state equal to 2.9 and 1.5 for a 1-year and 50 years period, respectively, whereas the ISO 2394-1998 specified target reliability indices for reversible and irreversible limit states as 0 and 1.5 for life time duration, respectively. These are general values that do not take into account the specific nature of the limit state being considered, the limiting criteria, the inherent reliability of existing structures or the load used for calibration relative to the load used for design. For example, for prestressed concrete members the limiting criteria may be decompression, a calculated concrete tensile stress of a certain magnitude, or, a crack opening to a certain width. For a given girder, the reliability index will vary depending on the criteria and the limiting

value. Limited contacts with individuals, who contributed to the development of the European Code indicate that the reliability indices listed for service limit states were not supported by research, rather they were based on general consensus.

The proposed target reliability indices used herein were selected based on the calculated average values of the reliability levels of existing bridges and previous practices with some consideration given to experiences from other Codes (European Code and ISO 2394 Document). Return period of 1 year was selected due to the fact that the live load statistics were developed based on 1 year of reliable WIM data from various WIM sites. Furthermore, since only 3 out of 32 WIM sites have the ADTT larger than 5000 and only 1 out of 32 WIM sites have the ADTT larger than 8000, the average reliability indices for ADTT equals to 5000 were used to represent the reliability levels of existing bridges.

Table D-82 shows the target reliability indices selected in this study. For example, the European Code specified target reliability indices for irreversible limit states as 2.9 for 1-year reference period. For ADTT of 5000, the reliability index of existing bridges, simulated bridges designed for severe environments, and simulated bridges designed for normal environments, at the Maximum Crack Width performance level is around 2.69, 3.55 and 3.15, respectively (See Table D-82). Therefore, a target reliability index of 3.30 and 3.10 was selected for Maximum Crack Width performance level for bridges designed for severe environments and bridges designed for normal environments, respectively. The reliability index of 3.0 means that 13 out of 10000 bridges will have a crack width at the bottom of the girder exceeding 0.016 inch in one year.

Table D-82 Reliability Indices for Existing Bridges (Return Period of 1 Year) with One Lane Loaded (ADTT 5000)

Performance Level	Reliability Index				
	Average β for Existing Bridges in the NCHRP 12-78	β for Simulated bridges designed for $f_t = 3\sqrt{f'_c}$ and old loss method	β for Simulated bridges designed for $f_t = 6\sqrt{f'_c}$ and old loss method	Proposed Target β for bridges in severe environment	Proposed Target β for bridges in normal or benign environment
Decompression	0.74	1.44	1.07	1.20	1.00
Maximum Allowable Tensile Stress of $f_t = 6\sqrt{f'_c}$	1.05	1.82	1.43	1.50	1.25
Maximum Allowable Crack Width of 0.016 in	2.69	3.55	3.15	3.30	3.10

D.3.4 Reliability indices of girders designed for various design criteria (I Girders)

D.3.4.1 Calibration for ADTT=1000

D.3.4.1.1 Bridges Designed for Maximum Concrete Tensile Stress of $f_t = 0.0948\sqrt{f_c'}$

In this section, the calibration process for a selected bridge database (shown in Table D-83) is performed for ADTT equal to 1000 and normal exposure condition. 0.6" diameter strands were used in the design for Florida I Beam (FIB) while 0.5" diameter strands were used in other designs. This rule is valid throughout this report. Please note that the allowable maximum crack width of 0.016 in is applied for maximum allowable crack width limit state and a compressive strength of concrete of 8 ksi is used for all the designed girders in this section and throughout the report.

Table D-83 Summary Information of Bridges Designed with γLL=0.8

($f_t = 0.0948\sqrt{f_c'}$ **)**

Cases	Section Type	Span Length (ft.)	Spacing (ft.)	Aps (in^2)	# of Strands
1	AASHTO I	30	6	1.224	8
2	AASHTO I	30	8	1.53	10
3	AASHTO I	30	10	1.836	12
4	AASHTO I	30	12	2.142	14
5	AASHTO II	60	6	2.448	16
6	AASHTO II	60	8	3.366	22
7	AASHTO III	60	10	3.06	20
8	AASHTO III	60	12	3.672	24
9	AASHTO III	80	6	3.672	24
10	AASHTO III	80	8	4.59	30
11	AASHTO III	80	10	5.508	36
12	AASHTO IV	80	12	5.202	34
13	AASHTO III	100	6	6.12	40
14	AASHTO IV	100	8	6.426	42
15	AASHTO IV	100	10	7.344	48
16	AASHTO V	100	12	7.038	46
17	AASHTO IV	120	6	7.956	52
18	AASHTO V	120	8	7.956	52
19	AASHTO V	120	10	9.18	60
20	AASHTO VI	120	12	8.874	58
21	AASHTO VI	140	6	8.262	54
22	AASHTO VI	140	8	9.792	64
23	AASHTO VI	140	10	11.322	74
24	AASHTO VI	140	12	-	-
25	FIB-96	160	6	7.812	36
26	FIB-96	160	8	9.114	42
27	FIB-96	160	10	10.416	48
28	FIB-96	160	12	-	-

Step 1: Calculate the reliability level of designs according to AASHTO LRFD Specifications (2010) (Figure D-2~Figure D-4)

Figure D-2 through Figure D-4 show the reliability indices for the bridges designed using AASHTO type girders according to AASHTO LRFD specifications (2010). It is observed that the average reliability index for decompression limit state, maximum allowable tensile stress limit state and maximum allowable crack width limit state is 1.05, 1.41, and 3.16, respectively, which satisfy the proposed target reliability index of 1.0 for decompression limit state. However, a larger live load factor will be used to estimate the effect of changing live load factor on reliability level of structure.

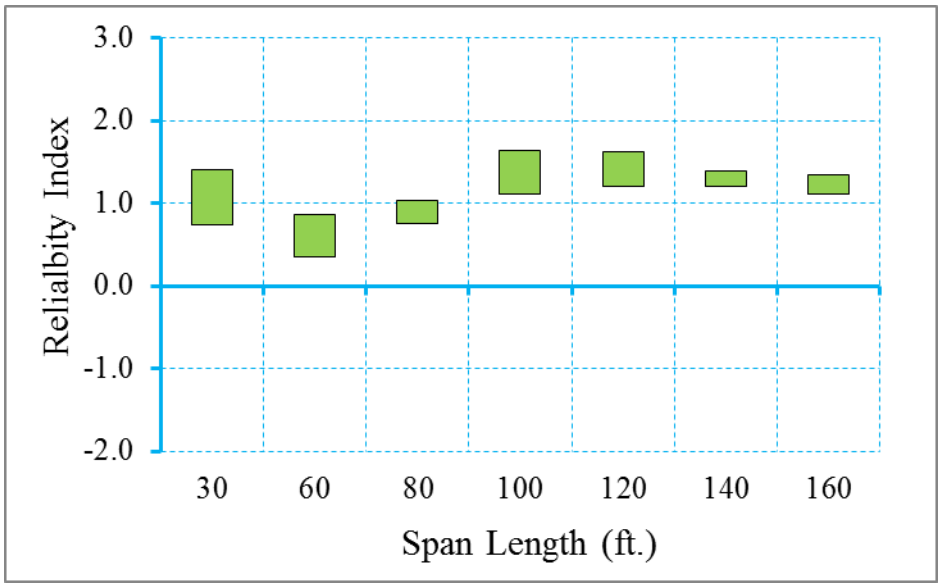

Figure D-2 Reliability Indices for Bridges at Decompression Limit State (ADTT=1000), γLL=0.8 ($f_t = 0.0948\sqrt{f_c'}$)

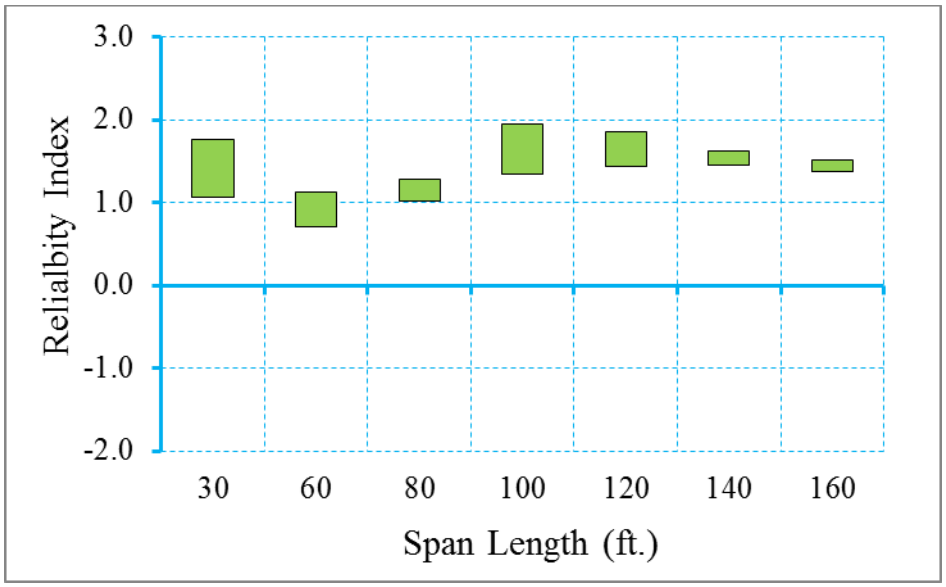

Figure D-3 Reliability Indices for Bridges at Maximum Allowable Tensile Stress Limit State (ADTT=1000), γLL=0.8 ($f_t = 0.0948\sqrt{f_c'}$)

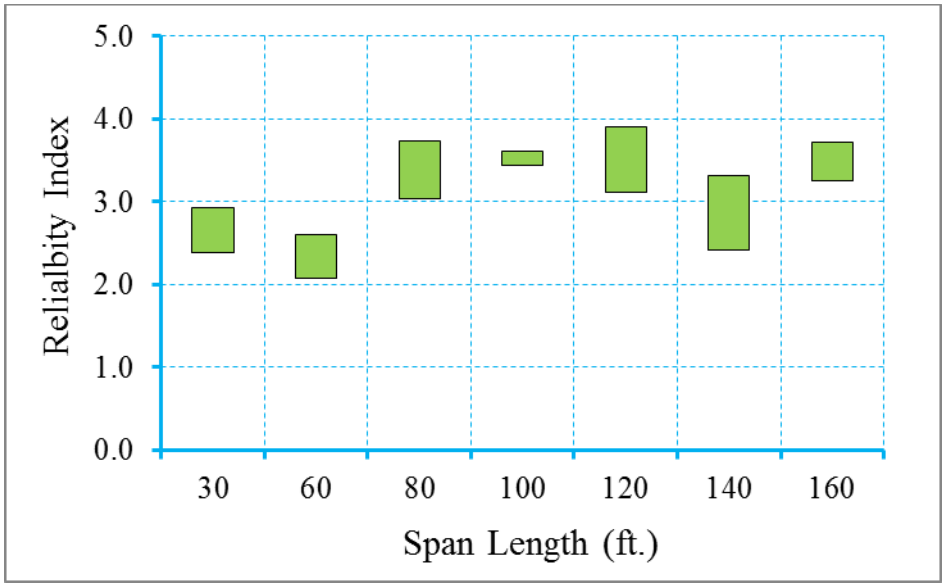

Figure D-4 Reliability Indices for Bridges at Maximum Allowable Crack Width Limit State (ADTT=1000), γLL=0.8 ($f_t = 0.0948\sqrt{f_c'}$)

Step 2: Redesign the bridges with live load factor of 1.0 (Figure D-5~Figure D-7)

Since the reliability level of the original bridge database is below the target reliability level at decompression limit state and maximum allowable tensile stress limit state, the bridges have been redesigned using a live load factor of 1.0. Please note that only the live load factor of Service III limit state is increased from 0.8 to 1.0, dead load

and resistance factors were kept the same during the redesign. Table D-84 shows the design outcomes of the redesigned bridges.

Figure D-5 though Figure D-7 shows the reliability indices for the redesigned bridges using live load factor of 1.0. It is observed the average reliability index of decompression limit state, maximum allowable tensile stress limit state and maximum allowable crack width limit state is 1.42, 1.79, and 3.36, respectively.

Table D-84 Summary Information of Bridges Designed with γLL=1.0

($f_t = 0.0948\sqrt{f_c'}$)

	Section Type	Span Length (ft.)	Spacing (ft.)	Aps (in^2)	# of Strands
1	AASHTO I	30	6	1.224	8
2	AASHTO I	30	8	1.53	10
3	AASHTO I	30	10	1.836	12
4	AASHTO I	30	12	2.142	14
5	AASHTO II	60	6	3.06	20
6	AASHTO II	60	8	3.978	26
7	AASHTO III	60	10	3.366	22
8	AASHTO III	60	12	4.284	28
9	AASHTO III	80	6	4.284	28
10	AASHTO III	80	8	5.202	34
11	AASHTO III	80	10	6.12	40
12	AASHTO IV	80	12	5.814	38
13	AASHTO III	100	6	7.038	46
14	AASHTO IV	100	8	7.038	46
15	AASHTO IV	100	10	8.262	54
16	AASHTO V	100	12	7.65	50
17	AASHTO IV	120	6	8.874	58
18	AASHTO V	120	8	8.874	58
19	AASHTO V	120	10	10.404	68
20	AASHTO VI	120	12	9.792	64
21	AASHTO VI	140	6	8.874	58
22	AASHTO VI	140	8	10.71	70
23	AASHTO VI	140	10	-	-
24	AASHTO VI	140	12	-	-
25	FIB-96	160	6	8.246	38
26	FIB-96	160	8	10.416	48
27	FIB-96	160	10	11.284	52
28	FIB-96	160	12	-	-

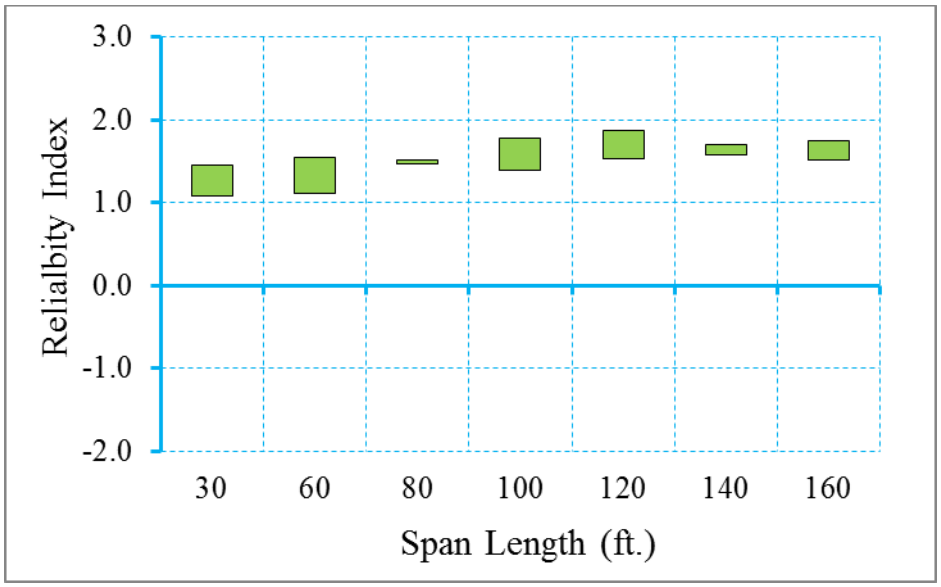

Figure D-5 Reliability Indices for Bridges at Decompression Limit State (ADTT=1000), γLL=1.0 ($f_t = 0.0948\sqrt{f_c'}$)

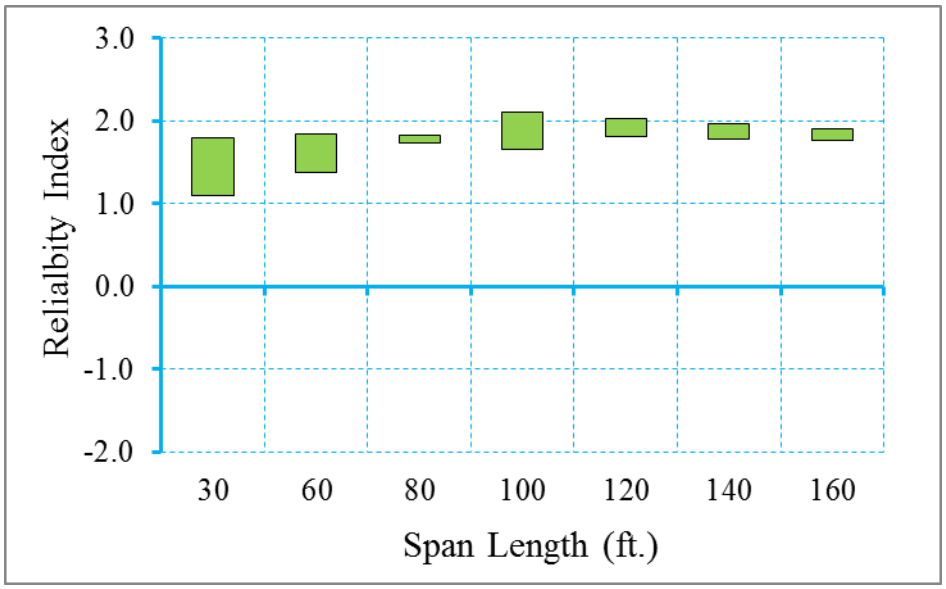

Figure D-6 Reliability Indices for Bridges at Maximum Tensile Stress Limit State (ADTT=1000), γLL=1.0 ($f_t = 0.0948\sqrt{f_c'}$)

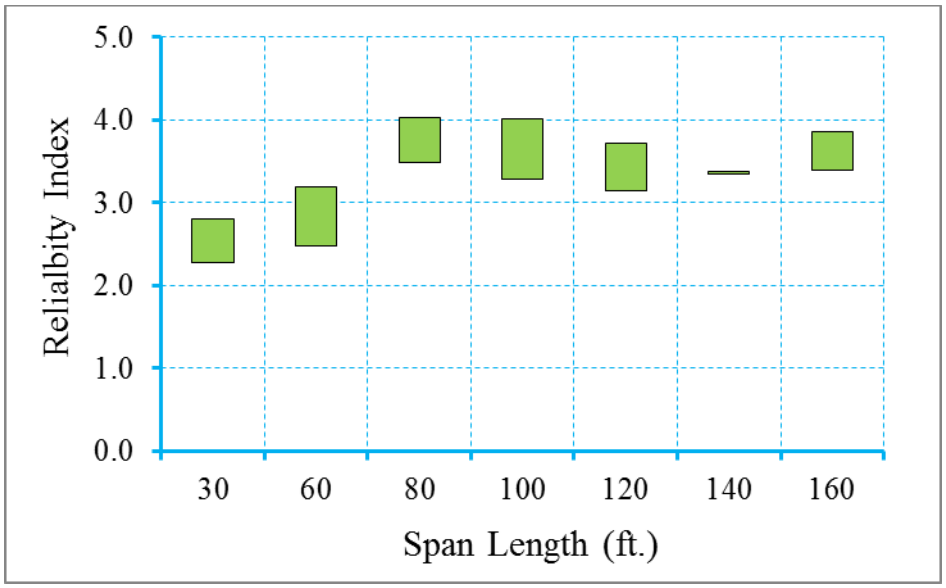

Figure D-7 Reliability Indices for Bridges at Maximum Crack Width Limit State (ADTT=1000), γLL=1.0 ($f_t = 0.0948\sqrt{f_c'}$)

Step 3: Propose new live load, dead load, and/or resistance factors

Based on the calibration process shown in step 1 through step 3, it is observed that the uniform target reliability index can be achieved using a live load factor of 1.0. Therefore, for ADTT equal to 1000 and maximum concrete tensile stress of $f_t = 0.0948\sqrt{f_c'}$, a new live load factor of 1.0 is proposed.

D.3.4.1.2 Bridges Designed for Maximum Concrete Tensile Stress of $f_t = 0.158\sqrt{f_c'}$

In this section, the calibration process for a selected bridge database (shown in Table D-85) is performed for ADTT equal to 1000 and normal exposure condition. 0.6" diameter strands were used in the design for Florida I Beam (FIB) while 0.5" diameter strands were used in other designs. Please note that the allowable maximum crack width of 0.016 in is applied for maximum allowable crack width limit state and a compressive strength of concrete of 8 ksi is used for all the designed girders in this section and throughout the report.

Table D-85 Summary Information of Bridges Designed with γLL=0.8 ($f_t = 0.158\sqrt{f_c'}$)

	Section Type	Span Length (ft.)	Spacing (ft.)	Aps (in^2)	# of Strands
1	AASHTO I	30	6	1.224	8
2	AASHTO I	30	8	1.53	10
3	AASHTO I	30	10	1.836	12
4	AASHTO I	30	12	2.142	14
5	AASHTO II	60	6	2.448	16
6	AASHTO II	60	8	3.672	24
7	AASHTO III	60	10	3.06	20
8	AASHTO III	60	12	3.672	24
9	AASHTO III	80	6	3.366	22
10	AASHTO III	80	8	4.284	28
11	AASHTO III	80	10	5.202	34
12	AASHTO IV	80	12	4.896	32
13	AASHTO III	100	6	5.814	38
14	AASHTO IV	100	8	5.814	38
15	AASHTO IV	100	10	7.038	46
16	AASHTO V	100	12	6.426	42
17	AASHTO IV	120	6	7.344	48
18	AASHTO V	120	8	7.344	48
19	AASHTO V	120	10	8.568	56
20	AASHTO VI	120	12	8.262	54
21	AASHTO VI	140	6	7.65	50
22	AASHTO VI	140	8	9.18	60
23	AASHTO VI	140	10	10.71	70
24	AASHTO VI	140	12	-	-
25	FIB-96	160	6	7.378	34
26	FIB-96	160	8	8.246	38
27	FIB-96	160	10	9.548	44
28	FIB-96	160	12	-	-

Step 1: Calculate the reliability level of designs according to AASHTO LRFD Specifications (2010) (Figure D-8~Figure D-10)

Figure D-8 through Figure D-10 show the reliability indices for the bridges designed using AASHTO type girders according to AASHTO LRFD specifications (2010). It is observed that the average reliability index for decompression limit state, maximum allowable tensile stress limit state and maximum allowable crack width limit state is 0.97, 1.31, and 2.99, respectively. Live load factor of 1.0 will be used in next step.

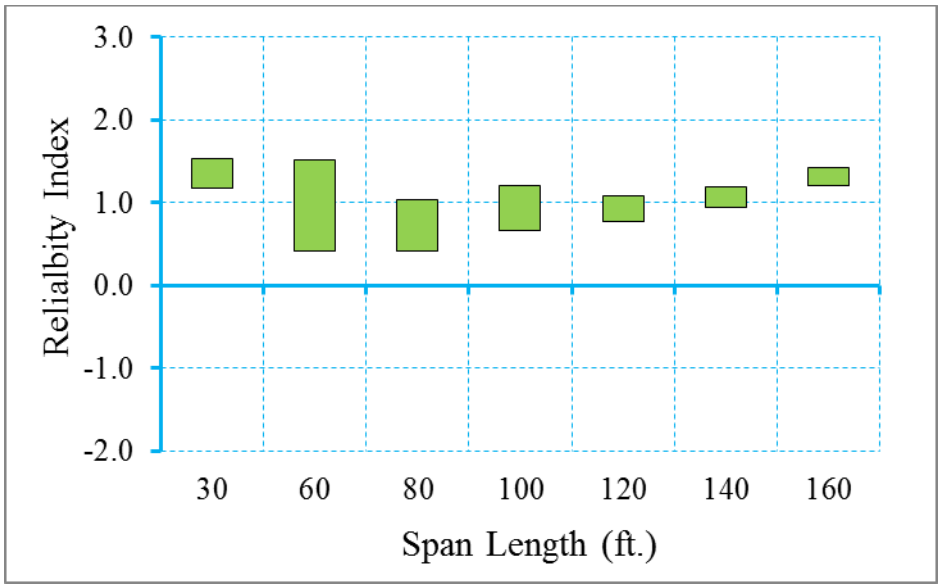

Figure D-8 Reliability Indices for Bridges at Decompression Limit State (ADTT=1000), γLL=0.8 ($f_t = 0.158\sqrt{f'_c}$)

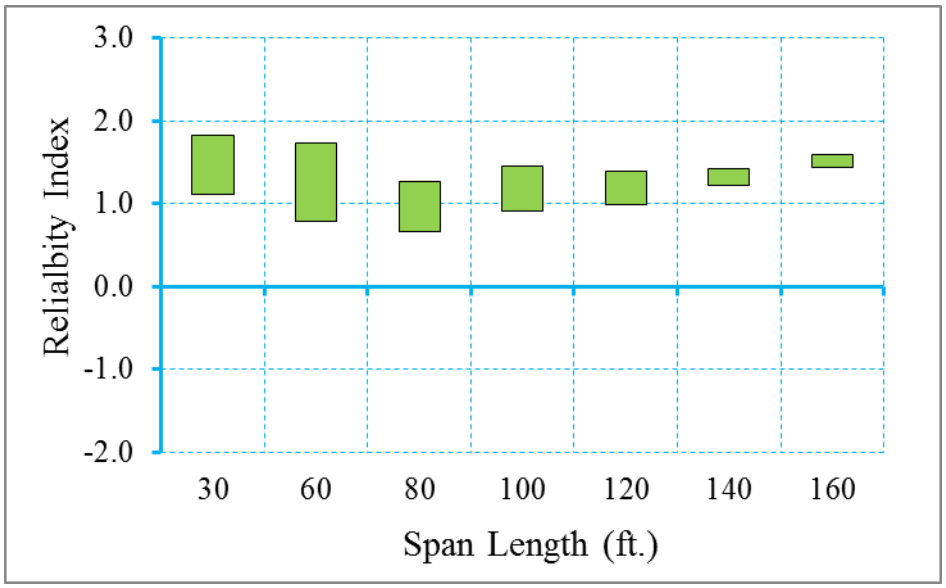

Figure D-9 Reliability Indices for Bridges at Maximum Allowable Tensile Stress Limit State (ADTT=1000), γLL=0.8 ($f_t = 0.158\sqrt{f'_c}$)

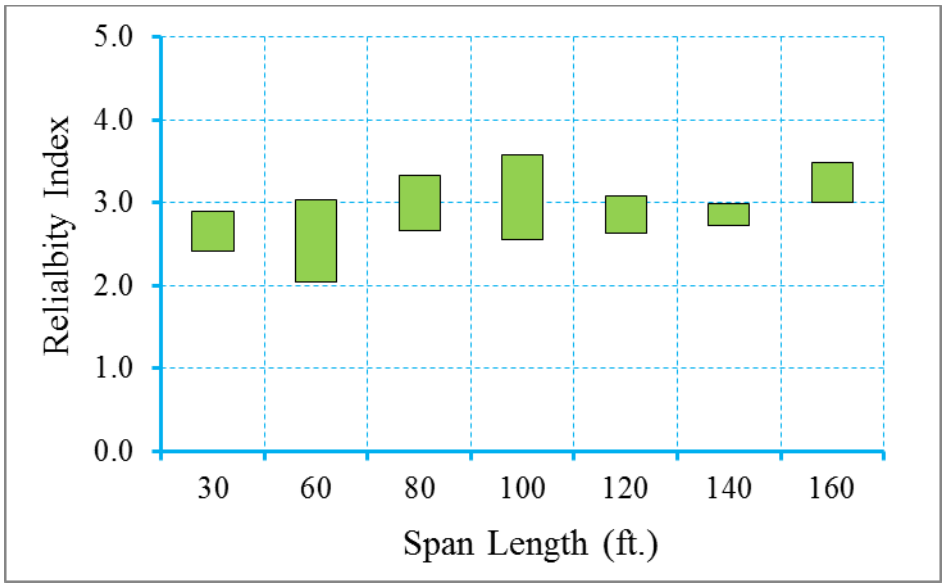

Figure D-10 Reliability Indices for Bridges at Maximum Allowable Crack Width Limit State (ADTT=1000), γLL=0.8 ($f_t = 0.158\sqrt{f_c'}$)

Step 2: Redesign the bridges with live load factor of 1.0 (Figure D-11~Figure D-13)

Since the reliability level of the original bridge database is below the target reliability level at decompression limit state and maximum allowable tensile stress limit state, the bridges have been redesigned using a live load factor of 1.0. Please note that only the live load factor of Service III limit state is increased from 0.8 to 1.0, dead load and resistance factors were kept the same during the redesign. Table D-86 shows the design outcomes of the redesigned bridges.

Figure D-11 though Figure D-13 show the reliability indices for the redesigned bridges using live load factor of 1.0. It is observed that the average reliability index of decompression limit state, maximum allowable tensile stress limit state and maximum allowable crack width limit state is 1.16, 1.55, and 3.32, respectively.

Table D-86 Summary Information of Bridges Designed with γLL=1.0 ($f_t = 0.158\sqrt{f_c'}$)

	Section Type	Span Length (ft.)	Spacing (ft.)	Aps (in^2)	# of Strands
1	AASHTO I	30	6	1.224	8
2	AASHTO I	30	8	1.53	10
3	AASHTO I	30	10	1.836	12
4	AASHTO I	30	12	2.142	14
5	AASHTO II	60	6	2.754	18
6	AASHTO II	60	8	3.672	24
7	AASHTO III	60	10	3.06	20
8	AASHTO III	60	12	3.672	24
9	AASHTO III	80	6	3.978	26
10	AASHTO III	80	8	4.896	32
11	AASHTO III	80	10	5.814	38
12	AASHTO IV	80	12	5.508	36
13	AASHTO III	100	6	6.732	44
14	AASHTO IV	100	8	6.426	42
15	AASHTO IV	100	10	7.65	50
16	AASHTO V	100	12	7.344	48
17	AASHTO IV	120	6	8.262	54
18	AASHTO V	120	8	8.262	54
19	AASHTO V	120	10	9.486	62
20	AASHTO VI	120	12	9.18	60
21	AASHTO VI	140	6	8.262	54
22	AASHTO VI	140	8	10.098	66
23	AASHTO VI	140	10	-	-
24	AASHTO VI	140	12	-	-
25	FIB-96	160	6	7.812	36
26	FIB-96	160	8	9.114	42
27	FIB-96	160	10	10.416	48
28	FIB-96	160	12	-	-

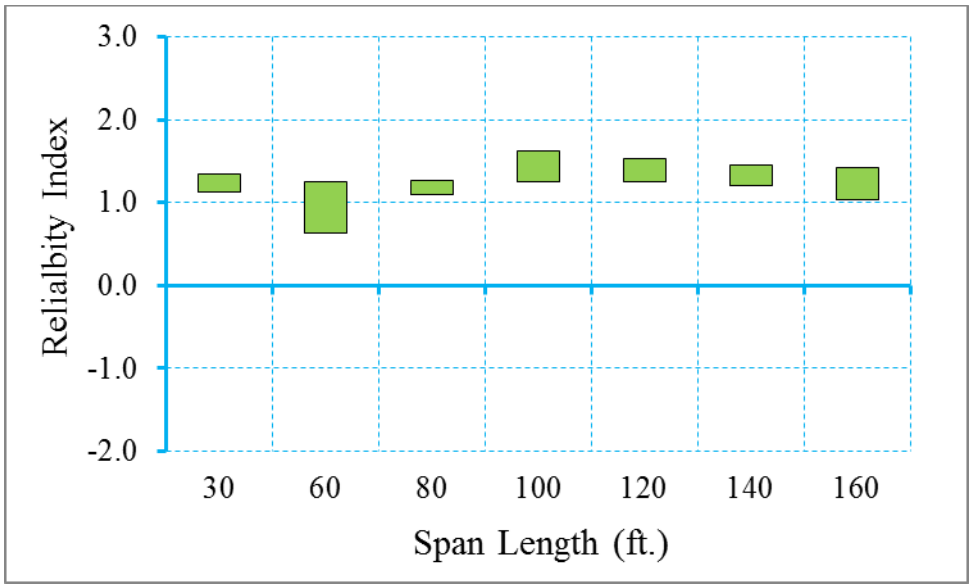

Figure D-11 Reliability Indices for Bridges at Decompression Limit State (ADTT=1000) , γLL=1.0 ($f_t = 0.158\sqrt{f'_c}$)

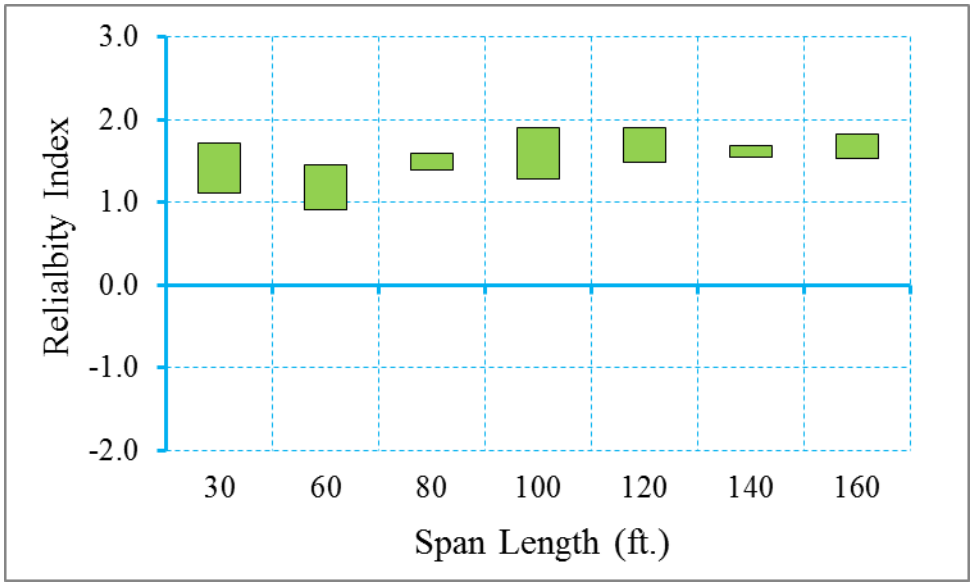

Figure D-12 Reliability Indices for Bridges at Maximum Tensile Stress Limit State (ADTT=1000), γLL=1.0 ($f_t = 0.158\sqrt{f'_c}$)

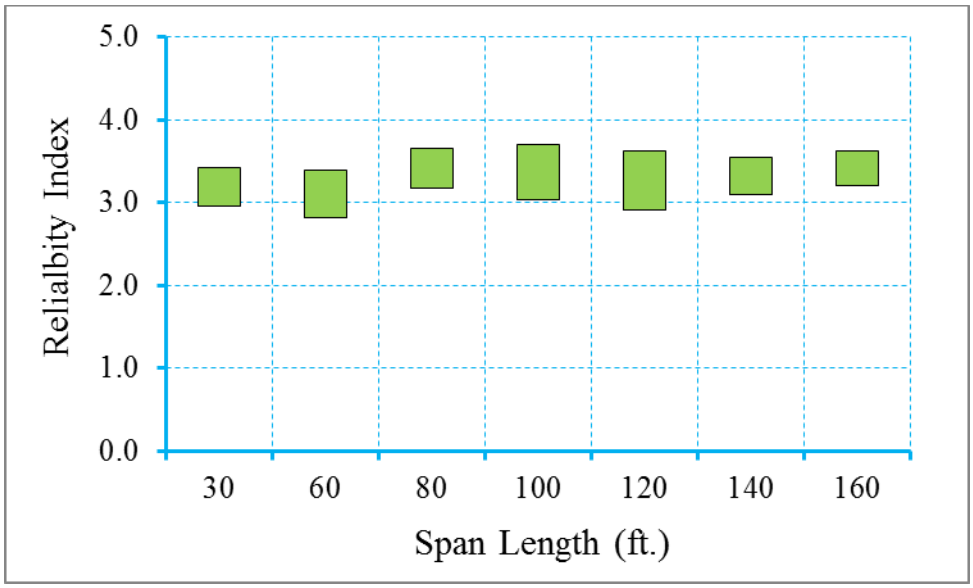

Figure D-13 Reliability Indices for Bridges at Maximum Crack Width Limit State (ADTT=1000), γLL=1.0 ($f_t = 0.158\sqrt{f_c'}$)

Step 3: Propose new live load, dead load, and/or resistance factors

Based on the calibration process shown in step 1 through step 3, it is observed that the uniform target reliability index can be achieved using a live load factor of 1.0. Therefore, for ADTT equal to 1000 and maximum concrete tensile stress of $f_t = 0.158\sqrt{f_c'}$, a new live load factor of 1.0 is proposed.

D.3.4.1.3 Bridges Designed for Maximum Concrete Tensile Stress of $f_t = 0.19\sqrt{f_c'}$

In this section, the calibration process for a selected bridge database (shown in Table D-87) is performed for ADTT equal to 1000 and normal exposure condition. 0.6" diameter strands were used in the design for Florida I Beam (FIB) while 0.5" diameter were used in other designs. This rule is valid throughout this report. Please note that the allowable maximum crack width of 0.016 in is applied for maximum allowable crack width limit state and a compressive strength of concrete of 8 ksi is used for all the designed girders in this section and throughout the report.

Table D-87 Summary Information of Bridges Designed with γLL=0.8 ($f_t = 0.19\sqrt{f_c'}$)

	Section Type	Span Length (ft.)	Spacing (ft.)	Aps (in^2)	# of Strands
1	AASHTO I	30	6	1.224	8
2	AASHTO I	30	8	1.53	10
3	AASHTO I	30	10	1.836	12
4	AASHTO I	30	12	2.142	14
5	AASHTO II	60	6	2.448	16
6	AASHTO II	60	8	3.06	20
7	AASHTO III	60	10	3.06	20
8	AASHTO III	60	12	3.672	24
9	AASHTO III	80	6	3.366	22
10	AASHTO III	80	8	4.284	28
11	AASHTO III	80	10	4.896	32
12	AASHTO IV	80	12	4.896	32
13	AASHTO III	100	6	5.814	38
14	AASHTO IV	100	8	5.814	38
15	AASHTO IV	100	10	6.732	44
16	AASHTO V	100	12	6.426	42
17	AASHTO IV	120	6	7.344	48
18	AASHTO V	120	8	7.344	48
19	AASHTO V	120	10	8.262	54
20	AASHTO VI	120	12	8.262	54
21	AASHTO VI	140	6	7.344	48
22	AASHTO VI	140	8	8.874	58
23	AASHTO VI	140	10	10.404	68
24	AASHTO VI	140	12	-	-
25	FIB-96	160	6	6.944	32
26	FIB-96	160	8	8.246	38
27	FIB-96	160	10	9.548	44
28	FIB-96	160	12	-	-

Step 1: Calculate the reliability level of designs according to AASHTO LRFD Specifications (2010) (Figure D-14~Figure D-16)

Figure D-14 through Figure D-16 show the reliability indices for the bridges designed using AASHTO type girders according to AASHTO LRFD specifications (2010). It is observed that the average reliability index for decompression limit state, maximum allowable tensile stress limit state and maximum allowable crack width limit state is 0.84, 1.27, and 2.92, respectively. Since the reliability indices are lower than target reliability index, live load factor of 1.0 will be used in next step.

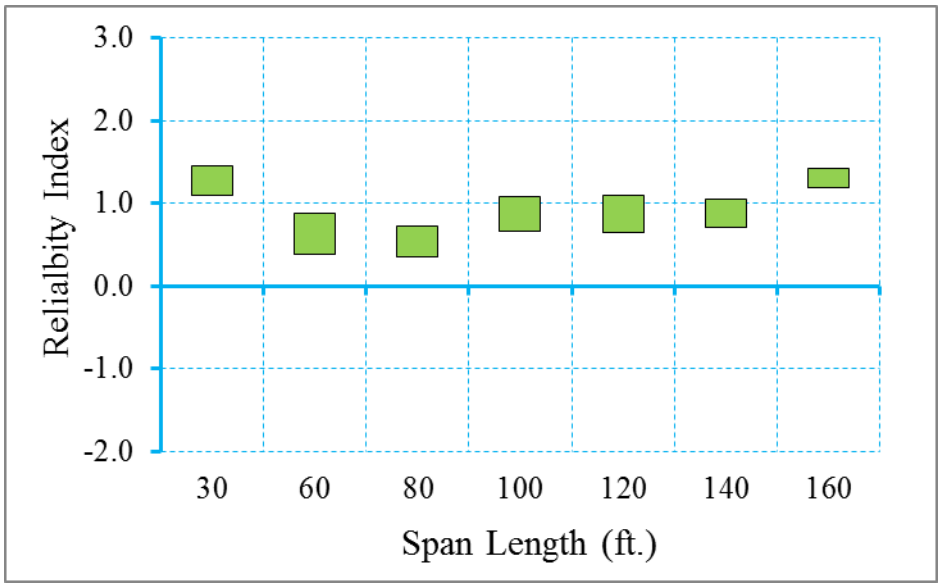

Figure D-14 Reliability Indices for Bridges at Decompression Limit State (ADTT=1000), γLL=0.8 ($f_t = 0.19\sqrt{f_c'}$)

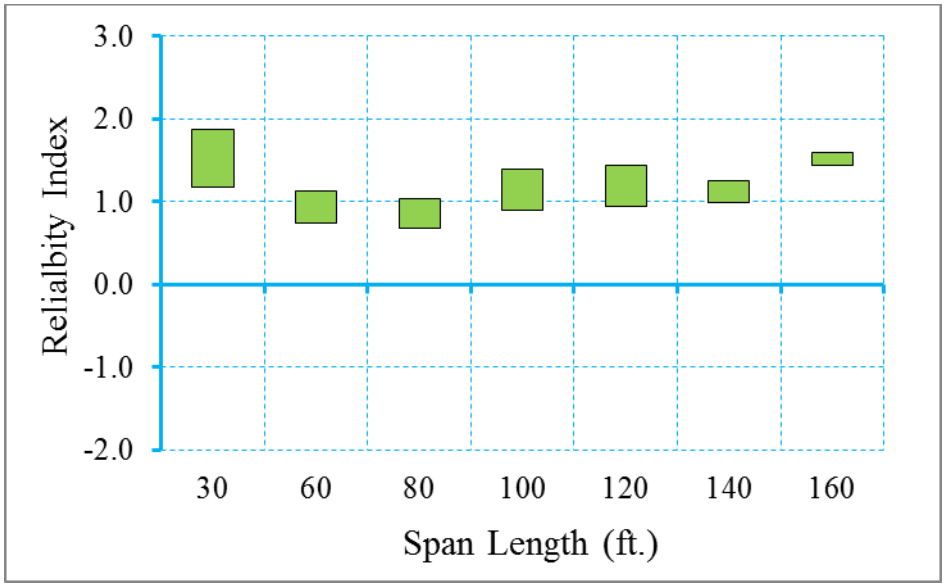

Figure D-15 Reliability Indices for Bridges at Maximum Allowable Tensile Stress Limit State (ADTT=1000), γLL=0.8 ($f_t = 0.19\sqrt{f_c'}$)

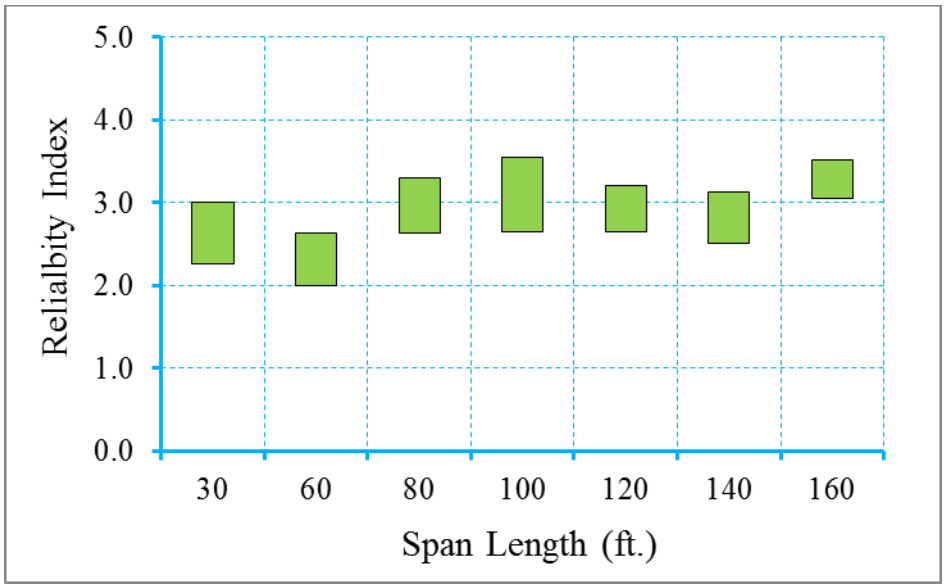

Figure D-16 Reliability Indices for Bridges at Maximum Allowable Crack Width Limit State (ADTT=1000), γLL=0.8 ($f_t = 0.19\sqrt{f_c'}$)

Step 2: Redesign the bridges with live load factor of 1.0 (Figure D-17~Figure D-19)

Since the reliability level of the original bridge database is below the target reliability level at decompression limit state and maximum allowable tensile stress limit state, the bridges have been redesigned using a live load factor of 1.0. Please note that only the live load factor of Service III limit state is increased from 0.8 to 1.0, dead load and resistance factors were kept the same during the redesign. Table D-88 shows the design outcomes of the redesigned bridges.

Figure D-17 though Figure D-19 show the reliability indices for the redesigned bridges using live load factor of 1.0. It is observed that the average reliability index of decompression limit state, maximum allowable tensile stress limit state and maximum allowable crack width limit state is 1.11, 1.53, and 3.25, respectively.

Table D-88 Summary Information of Bridges Designed with γLL=1.0 ($f_t = 0.19\sqrt{f_c'}$)

	Section Type	Span Length (ft.)	Spacing (ft.)	Aps (in^2)	# of Strands
1	AASHTO I	30	6	1.224	8
2	AASHTO I	30	8	1.53	10
3	AASHTO I	30	10	1.836	12
4	AASHTO I	30	12	2.142	14
5	AASHTO II	60	6	2.448	16
6	AASHTO II	60	8	3.366	22
7	AASHTO III	60	10	3.06	20
8	AASHTO III	60	12	3.672	24
9	AASHTO III	80	6	3.672	24
10	AASHTO III	80	8	4.59	30
11	AASHTO III	80	10	5.814	38
12	AASHTO IV	80	12	5.202	34
13	AASHTO III	100	6	6.426	42
14	AASHTO IV	100	8	6.426	42
15	AASHTO IV	100	10	7.65	50
16	AASHTO V	100	12	7.038	46
17	AASHTO IV	120	6	7.956	52
18	AASHTO V	120	8	7.956	52
19	AASHTO V	120	10	9.18	60
20	AASHTO VI	120	12	8.874	58
21	AASHTO VI	140	6	7.956	52
22	AASHTO VI	140	8	9.792	64
23	AASHTO VI	140	10	11.322	74
24	AASHTO VI	140	12	-	-
25	FIB-96	160	6	7.378	34
26	FIB-96	160	8	8.68	40
27	FIB-96	160	10	10.416	48
28	FIB-96	160	12	-	-

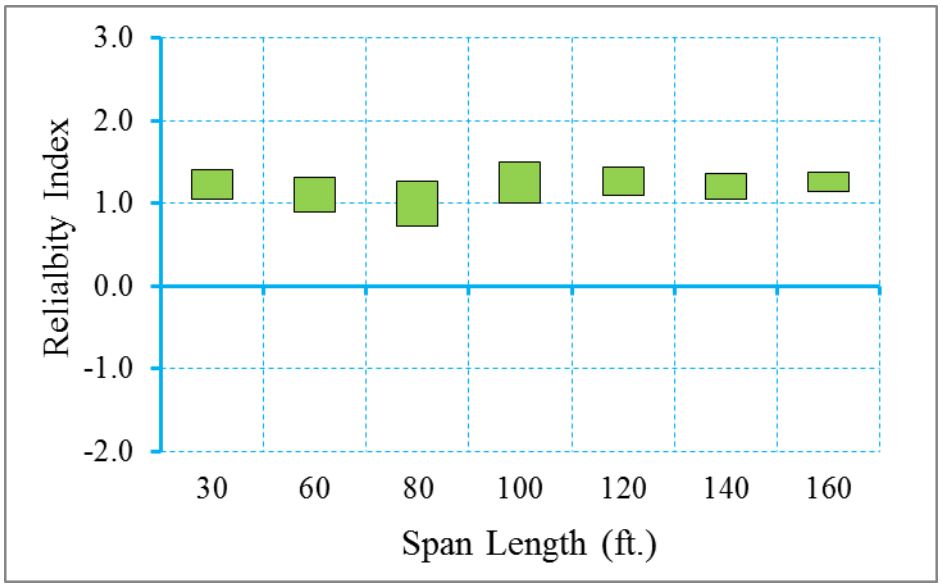

Figure D-17 Reliability Indices for Bridges at Decompression Limit State (ADTT=1000) , γLL=1.0 ($f_t = 0.19\sqrt{f_c'}$)

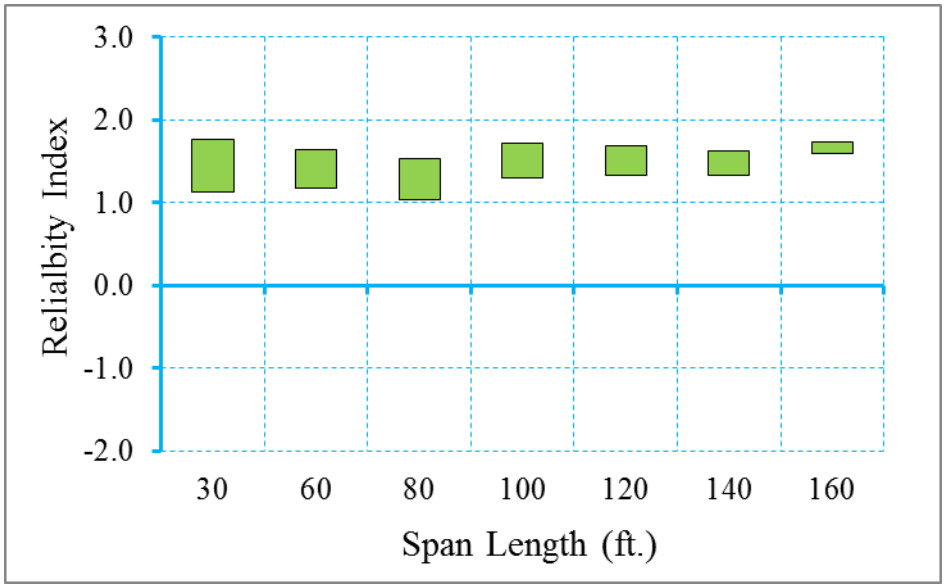

Figure D-18 Reliability Indices for Bridges at Maximum Tensile Stress Limit State (ADTT=1000), γLL=1.0 ($f_t = 0.19\sqrt{f_c'}$)

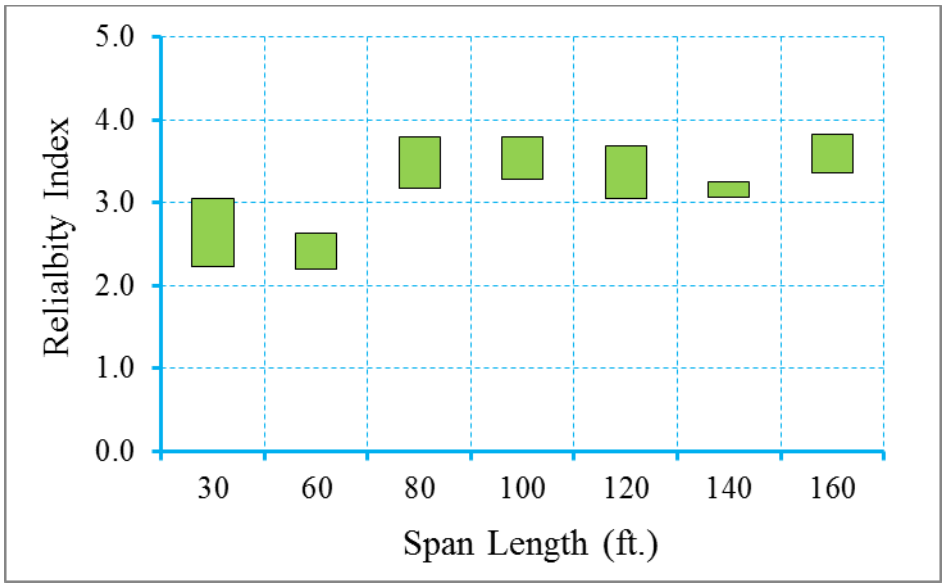

Figure D-19 Reliability Indices for Bridges at Maximum Crack Width Limit State (ADTT=1000), γLL=1.0 ($f_t = 0.19\sqrt{f_c'}$)

Step 3: Propose new live load, dead load, and/or resistance factors

Based on the calibration process shown in step 1 through step 3, it is observed that the uniform target reliability index can be achieved using a live load factor of 1.0. Therefore, for ADTT equal to 1000 and maximum concrete tensile stress of $f_t = 0.19\sqrt{f_c'}$, a new live load factor of 1.0 is proposed.

D.3.4.1.4 Bridges Designed for Maximum Concrete Tensile Stress of $f_t = 0.253\sqrt{f_c'}$

In this section, the calibration for a selected bridge database (shown in Table D-89) is performed for a scenario of ADTT equal to 1000 and severe exposure conditions. Please note that the maximum allowable crack width is specified as 0.016 in for maximum allowable crack width limit state.

Step 1: Calculate the reliability level of designs according to AASHTO LRFD Specifications (2010) (Figure D-20~Figure D-22)

Figure D-20 through Figure D-22 show the reliability indices for the bridges designed using AASHTO type girders according to AASHTO LRFD specifications (2010) under severe exposure conditions. It is observed that the average reliability index for decompression limit state, maximum allowable tensile stress limit state and maximum allowable crack width limit state is 0.2, 0.55, and 2.83, respectively, which is higher than proposed target reliability index. However, live load factor of 1.0 will be used to estimate the effect of changing live load factor on reliability level.

Table D-89 Summary Information of Bridges Designed with γLL=0.8 ($f_t = 0.253\sqrt{f_c'}$)

	Section Type	Span Length (ft.)	Spacing (ft.)	Aps (in^2)	# of Strands
1	AASHTO I	30	6	1.224	8
2	AASHTO I	30	8	1.53	10
3	AASHTO I	30	10	1.836	12
4	AASHTO I	30	12	2.142	14
5	AASHTO II	60	6	2.142	14
6	AASHTO II	60	8	2.754	18
7	AASHTO III	60	10	2.448	16
8	AASHTO III	60	12	3.06	20
9	AASHTO III	80	6	3.06	20
10	AASHTO III	80	8	3.978	26
11	AASHTO III	80	10	4.59	30
12	AASHTO IV	80	12	4.284	28
13	AASHTO III	100	6	5.202	34
14	AASHTO IV	100	8	5.202	34
15	AASHTO IV	100	10	6.426	42
16	AASHTO V	100	12	5.814	38
17	AASHTO IV	120	6	6.732	44
18	AASHTO V	120	8	6.732	44
19	AASHTO V	120	10	7.956	52
20	AASHTO VI	120	12	7.65	50
21	AASHTO VI	140	6	6.732	44
22	AASHTO VI	140	8	8.262	54
23	AASHTO VI	140	10	9.792	64
24	AASHTO VI	140	12	-	-
25	FIB-96	160	6	6.51	30
26	FIB-96	160	8	7.378	34
27	FIB-96	160	10	8.68	40
28	FIB-96	160	12	-	-

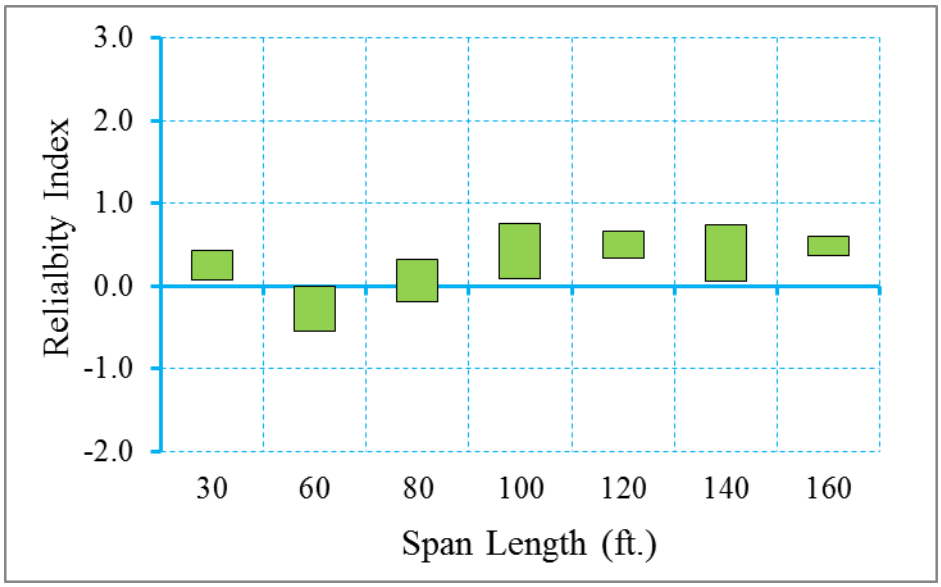

Figure D-20 Reliability Indices for Bridges at Decompression Limit State (ADTT=1000), γLL=0.8 ($f_t = 0.253\sqrt{f_c'}$)

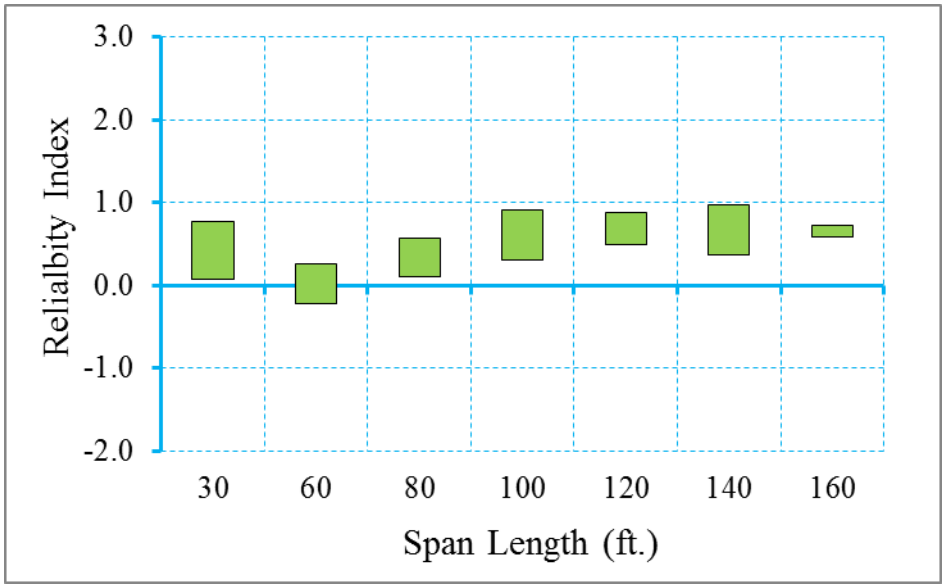

Figure D-21 Reliability Indices for Bridges at Maximum Allowable Tensile Stress Limit State (ADTT=1000), γLL=0.8 ($f_t = 0.253\sqrt{f_c'}$)

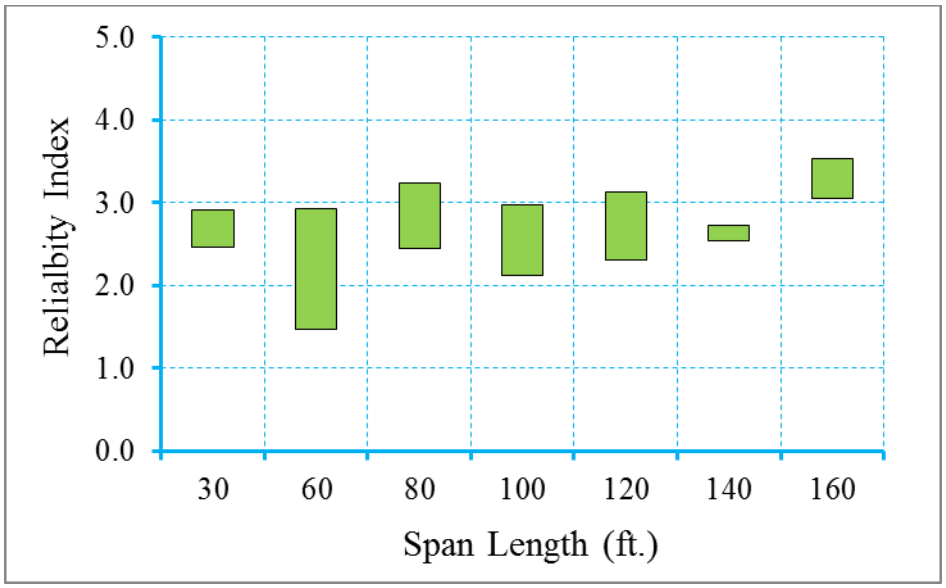

Figure D-22 Reliability Indices for Bridges at Maximum Allowable Crack Width Limit State (ADTT=1000), γLL=0.8 ($f_t = 0.253\sqrt{f_c'}$)

Step 2: Redesign the bridges with live load factor of 1.0 (Figure D-23~Figure D-25)

In this step, the bridges were redesigned using a live load factor of 1.0. Please note that only the live load factor of Service III limit state is increased from 0.8 to 1.0, dead load and resistance factors were kept the same during the redesign. Table D-90 shows the design outcomes of the redesigned bridges.

Figure D-23 though Figure D-25 show the reliability indices for the redesigned bridges using a live load factor of 1.0. It is observed that the average reliability index for the decompression limit state, the maximum allowable tensile stress limit state and the maximum allowable crack width limit state is 0.93, 1.29, and 3.03, respectively.

Table D-90 Summary Information of Bridges Designed with γLL=1.0 ($f_t = 0.253\sqrt{f_c'}$)

	Section Type	Span Length (ft.)	Spacing (ft.)	Aps (in^2)	# of Strands
1	AASHTO I	30	6	1.224	8
2	AASHTO I	30	8	1.53	10
3	AASHTO I	30	10	1.836	12
4	AASHTO I	30	12	2.142	14
5	AASHTO II	60	6	2.142	14
6	AASHTO II	60	8	2.754	18
7	AASHTO III	60	10	2.448	16
8	AASHTO III	60	12	3.06	20
9	AASHTO III	80	6	3.06	20
10	AASHTO III	80	8	3.978	26
11	AASHTO III	80	10	4.59	30
12	AASHTO IV	80	12	4.284	28
13	AASHTO III	100	6	5.202	34
14	AASHTO IV	100	8	5.202	34
15	AASHTO IV	100	10	6.426	42
16	AASHTO V	100	12	5.814	38
17	AASHTO IV	120	6	6.732	44
18	AASHTO V	120	8	6.732	44
19	AASHTO V	120	10	7.956	52
20	AASHTO VI	120	12	7.65	50
21	AASHTO VI	140	6	6.732	44
22	AASHTO VI	140	8	8.262	54
23	AASHTO VI	140	10	9.792	64
24	AASHTO VI	140	12	-	-
25	FIB-96	160	6	6.51	30
26	FIB-96	160	8	7.378	34
27	FIB-96	160	10	8.68	40
28	FIB-96	160	12	-	-

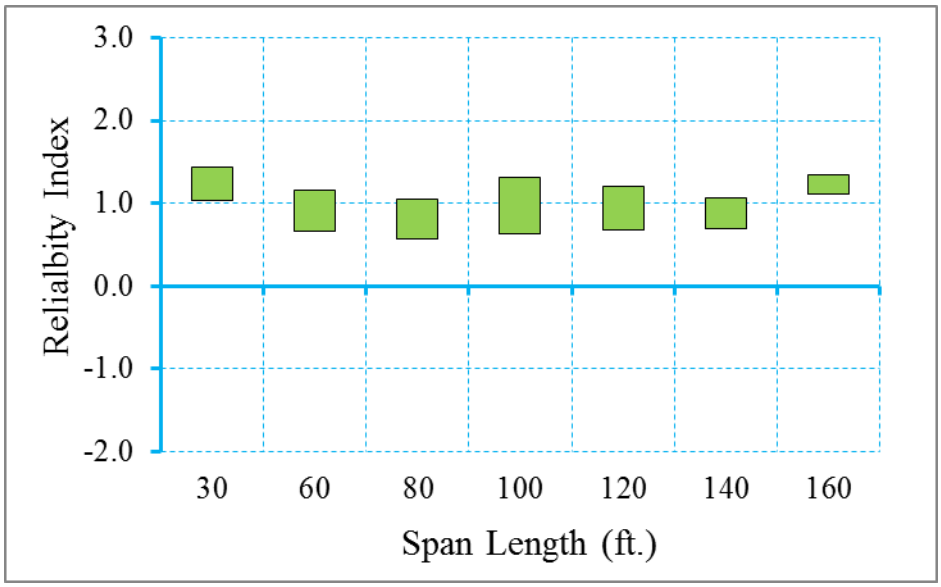

Figure D-23 Reliability Indices for Bridges at Decompression Limit State (ADTT=1000), γLL=1.0 ($f_t = 0.253\sqrt{f_c'}$)

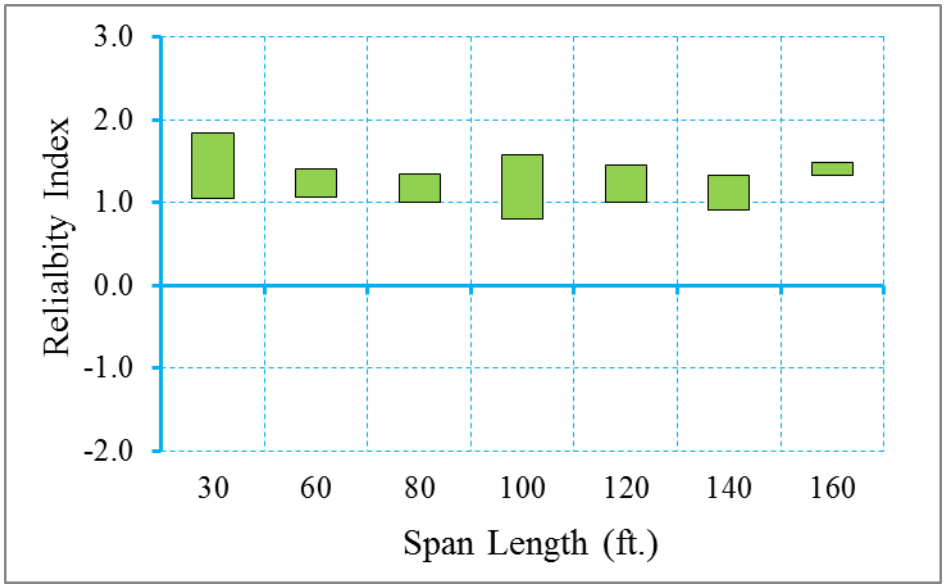

Figure D-24 Reliability Indices for Bridges at Maximum Allowable Tensile Stress Limit State (ADTT=1000), γLL=1.0 ($f_t = 0.253\sqrt{f_c'}$)

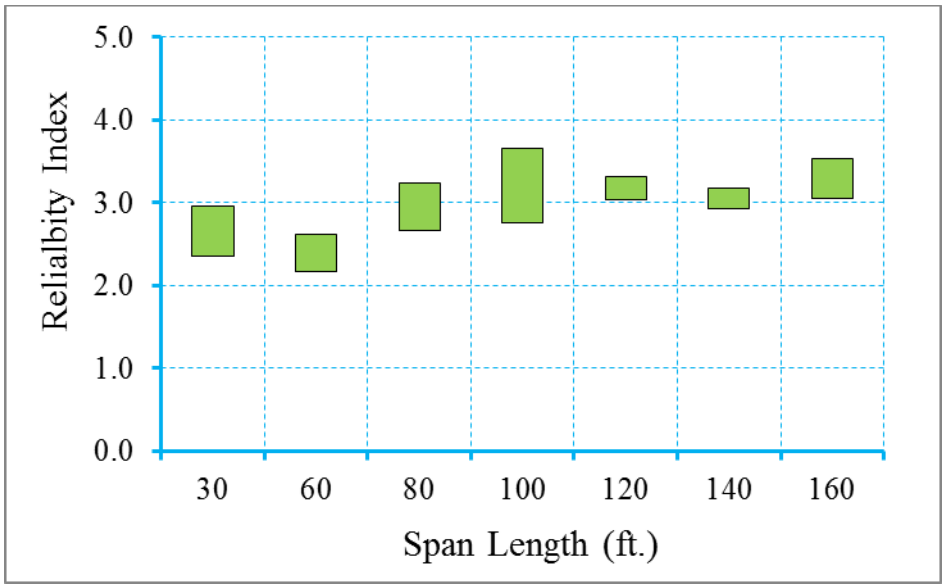

Figure D-25 Reliability Indices for Bridges at Maximum Allowable Crack Width Limit State (ADTT=1000), γLL=1.0 ($f_t = 0.253\sqrt{f_c'}$)

Step 3: Propose new live load, dead load, and/or resistance factors

Based on the calibration process shown in step 1 through step 3, it is observed that the uniform target reliability index can be achieved using a live load factor of 1.0. Therefore, for ADTT equal to 1000 and maximum concrete tensile stress of $f_t = 0.253\sqrt{f_c'}$, a new live load factor of 1.0 is proposed.

D.3.4.2 Calibration for ADTT=2500

D.3.4.2.1 Bridges Designed for Maximum Concrete Tensile Stress of $f_t = 0.0948\sqrt{f_c'}$

In this section, the calibration for a selected bridge database (shown in Table D-83) is performed for ADTT equal to 2500 and maximum concrete tensile stress of $f_t = 0.0948\sqrt{f_c'}$. Please note that the allowable maximum crack width of 0.016 in is applied for maximum allowable crack width limit state.

Step 1: Calculate the reliability level of designs according to AASHTO LRFD Specifications (2010) (Figure D-26~Figure D-28)

Figure D-26 through Figure D-28 show the reliability indices for the bridges designed using AASHTO type girders according to AASHTO LRFD specifications (2010). It is observed that the average reliability index for decompression limit state, maximum allowable tensile stress limit state and maximum allowable crack width limit state is 1.01, 1.35, and 3.11, respectively. Live load factor of 1.0 will be used in next step.

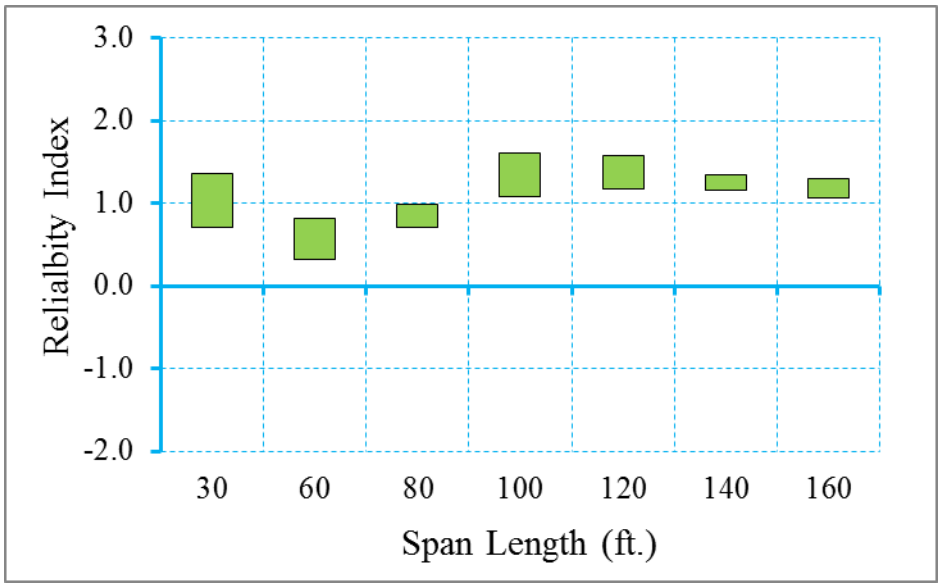

Figure D-26 Reliability Indices for Bridges at Decompression Limit State (ADTT=2500), γLL=0.8 ($f_t = 0.0948\sqrt{f'_c}$)

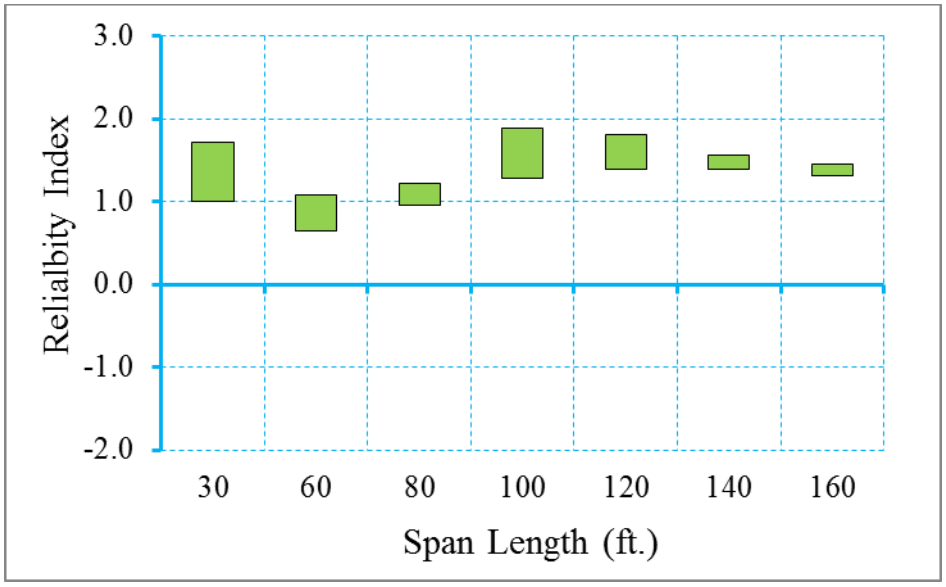

Figure D-27 Reliability Indices for Bridges at Maximum Allowable Tensile Stress Limit State (ADTT=2500), γLL=0.8 ($f_t = 0.0948\sqrt{f'_c}$)

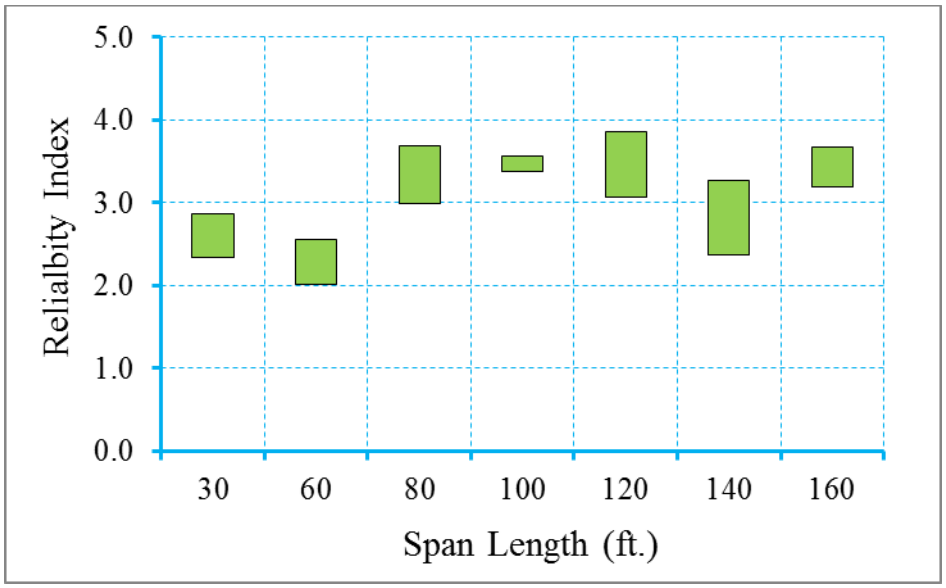

Figure D-28 Reliability Indices for Bridges at Maximum Allowable Crack Width Limit State (ADTT=2500), γLL=0.8 ($f_t = 0.0948\sqrt{f_c'}$)

Step 2: Redesign the bridges with live load factor of 1.0 (Figure D-29~Figure D-31)

Since the reliability level of the original bridge database was below the target reliability level at decompression limit state and maximum allowable tensile stress limit state, the bridges were redesigned using a live load factor of 1.0. Please note that only the live load factor of Service III limit state is increased from 0.8 to 1.0, dead load and resistance factors were kept the same during the redesign. Table D-84 shows the design outcomes of the redesigned bridges.

Figure D-29 through Figure D-31 show the reliability indices for the redesigned bridges using live load factor of 1.0. It is observed that the average reliability index of decompression limit state, maximum allowable tensile stress limit state and maximum allowable crack width limit state is 1.38, 1.75, and 3.33, respectively.

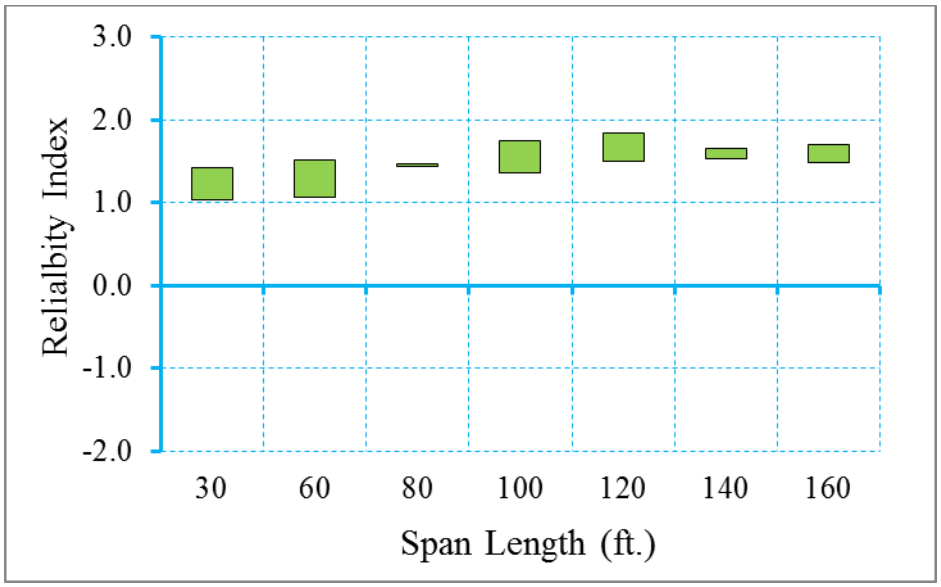

Figure D-29 Reliability Indices for Bridges at Decompression Limit State (ADTT=2500), γLL=1.0 ($f_t = 0.0948\sqrt{f_c'}$)

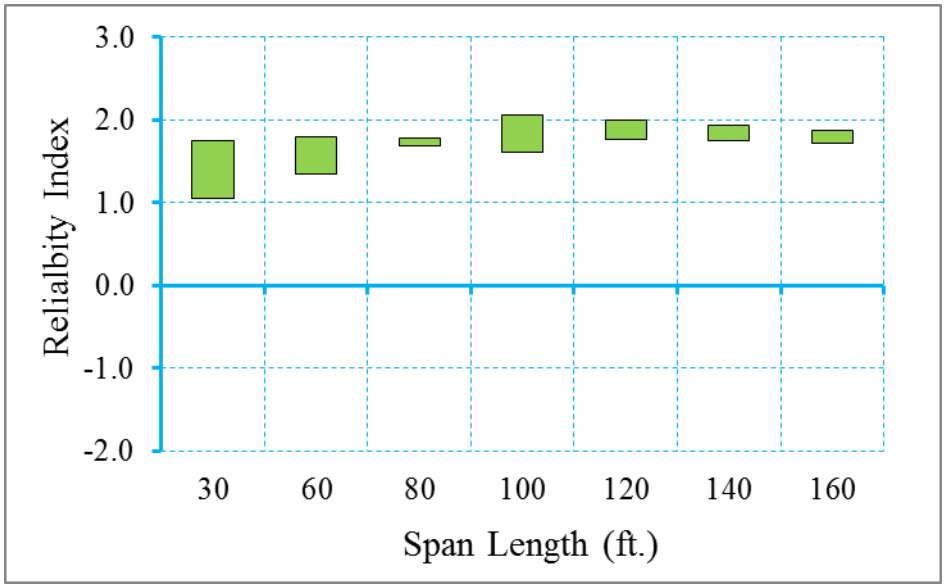

Figure D-30 Reliability Indices for Bridges at Maximum Tensile Stress Limit State (ADTT=2500), γLL=1.0 ($f_t = 0.0948\sqrt{f_c'}$)

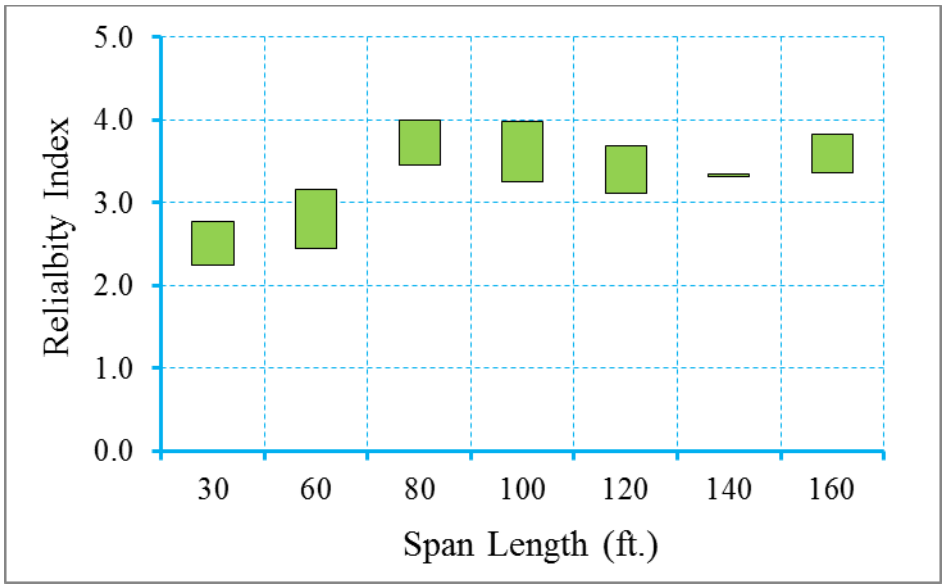

Figure D-31 Reliability Indices for Bridges at Maximum Crack Width Limit State (ADTT=2500), γLL=1.0 ($f_t = 0.0948\sqrt{f_c'}$)

Step 3: Propose new live load, dead load, and/or resistance factors

Based on the calibration process shown in step 1 through step 3, it is observed that the uniform target reliability index can be achieved using a live load factor of 1.0. Therefore, for ADTT equal to 2500 and maximum concrete tensile stress of $f_t = 0.0948\sqrt{f_c'}$, a new live load factor of 1.0 is proposed.

D.3.4.2.2 Bridges Designed for Maximum Concrete Tensile Stress of $f_t = 0.158\sqrt{f_c'}$

In this section, the calibration for a selected bridge database (shown in Table D-85) is performed for ADTT equal to 2500 and maximum concrete tensile stress of $f_t = 0.158\sqrt{f_c'}$. Please note that the allowable maximum crack width of 0.016 in is applied for maximum allowable crack width limit state.

Step 1: Calculate the reliability level of designs according to AASHTO LRFD Specifications (2010) (Figure D-32~Figure D-34)

Figure D-32 through Figure D-34 show the reliability indices for the bridges designed using AASHTO type girders according to AASHTO LRFD specifications (2010). It is observed that the average reliability index for decompression limit state, maximum allowable tensile stress limit state and maximum allowable crack width limit state is 0.83, 1.19, and 2.96, respectively, which does not satisfy the proposed target reliability index of 1.0 for decompression limit state. Therefore, a larger live load factor will be used to modify the original design in order to improve the reliability level of the bridges.

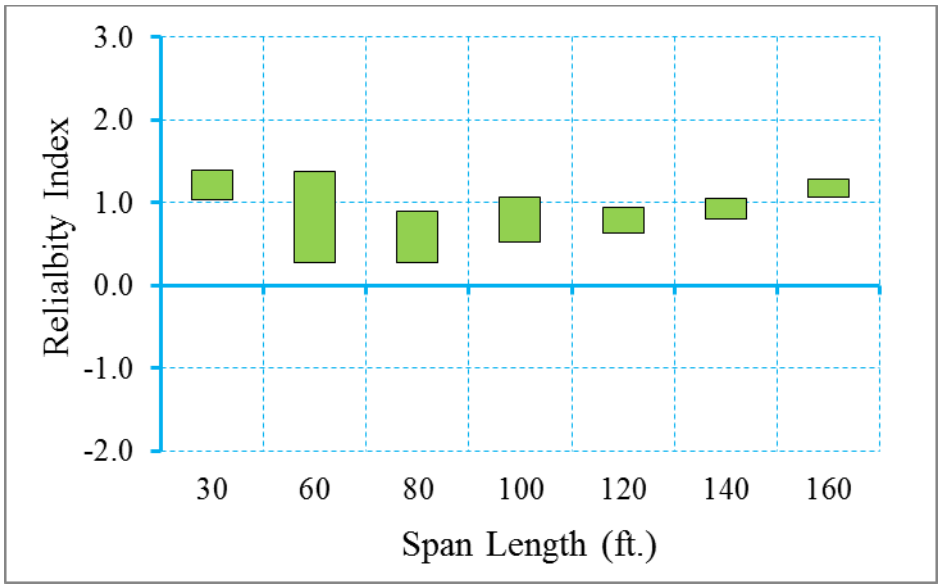

Figure D-32 Reliability Indices for Bridges at Decompression Limit State (ADTT=2500), γLL=0.8 ($f_t = 0.158\sqrt{f'_c}$)

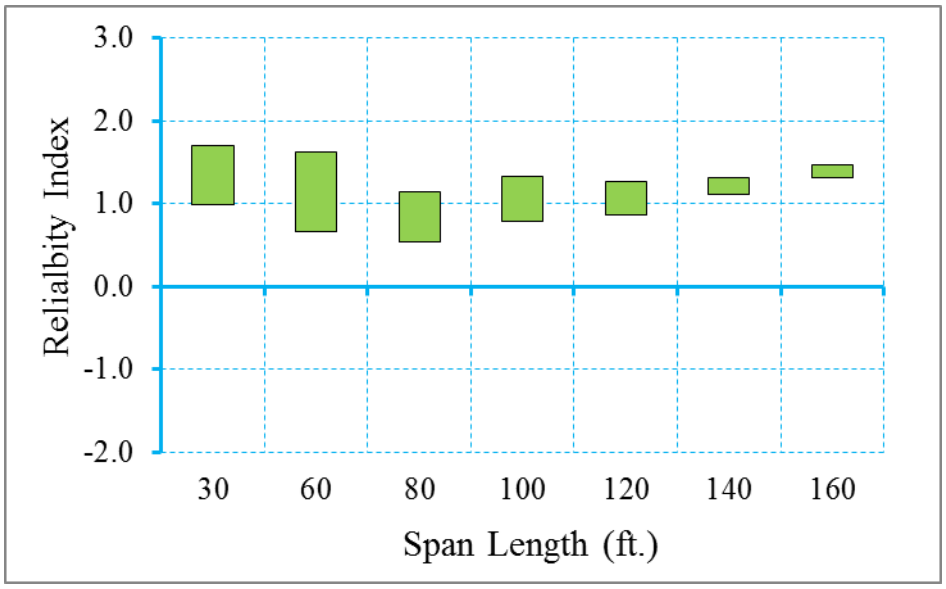

Figure D-33 Reliability Indices for Bridges at Maximum Allowable Tensile Stress Limit State (ADTT=2500), γLL=0.8 ($f_t = 0.158\sqrt{f'_c}$)

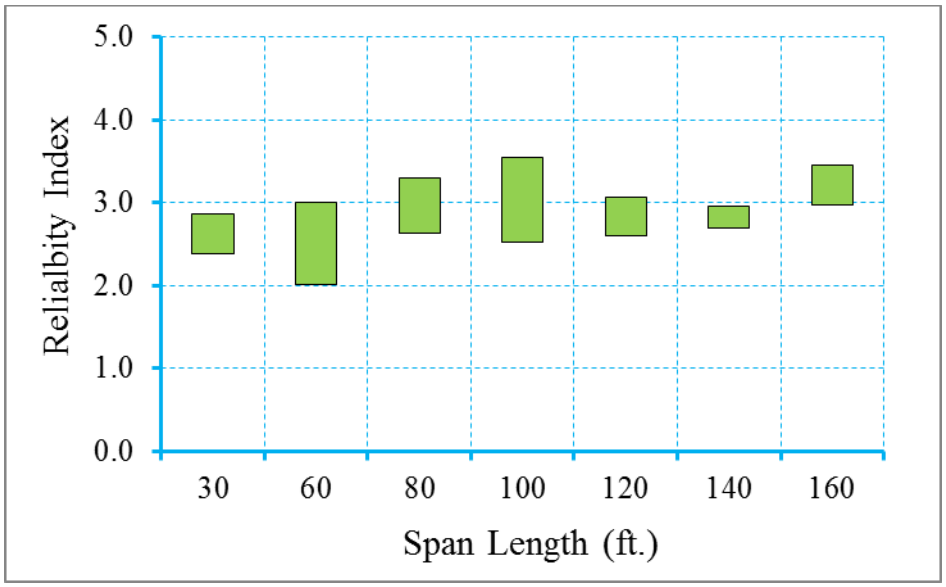

Figure D-34 Reliability Indices for Bridges at Maximum Allowable Crack Width Limit State (ADTT=2500), γLL=0.8 ($f_t = 0.158\sqrt{f_c'}$)

Step 2: Redesign the bridges with live load factor of 1.0 (Figure D-35~Figure D-37)

Since the reliability level of the original bridge database was below the target reliability level at decompression limit state and maximum allowable tensile stress limit state, the bridges were redesigned using a live load factor of 1.0. Please note that only the live load factor of Service III limit state is increased from 0.8 to 1.0, dead load and resistance factors were kept the same during the redesign. Table D-86 shows the design outcomes of the redesigned bridges.

Figure D-35 through Figure D-37 show the reliability indices for the redesigned bridges using live load factor of 1.0. It is observed that the average reliability index of decompression limit state, maximum allowable tensile stress limit state and maximum allowable crack width limit state is 1.12, 1.50, and 3.29, respectively.

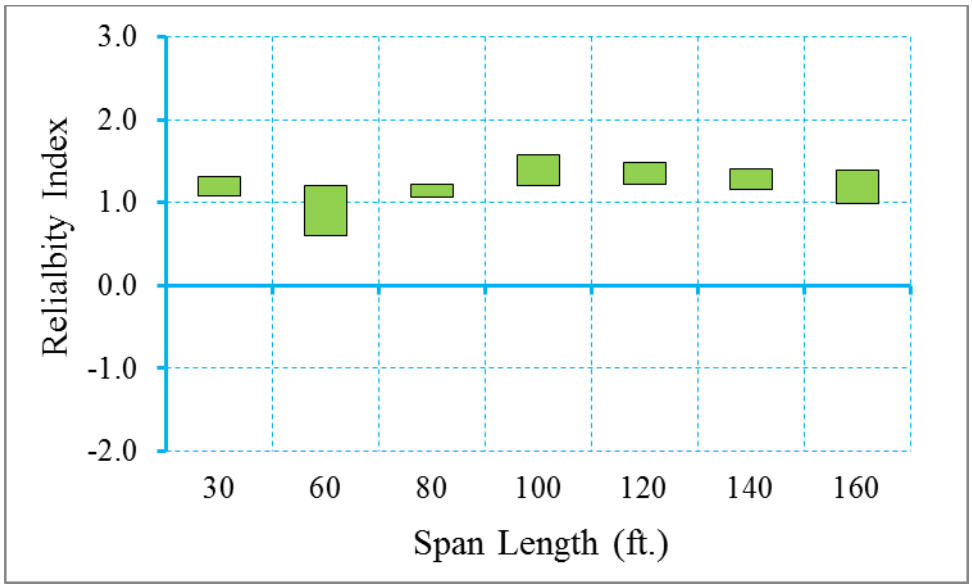

Figure D-35 Reliability Indices for Bridges at Decompression Limit State (ADTT=2500) , γLL=1.0 ($f_t = 0.158\sqrt{f'_c}$)

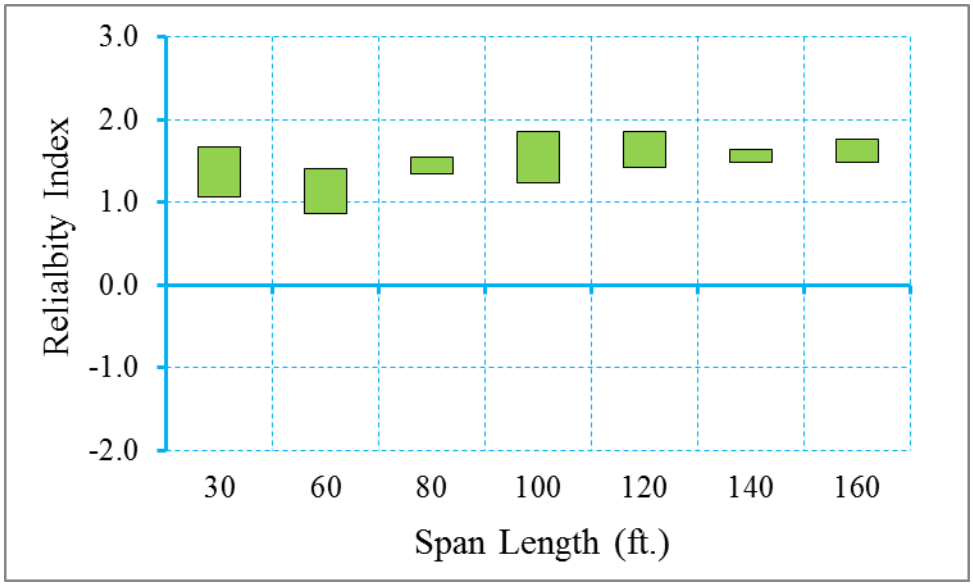

Figure D-36 Reliability Indices for Bridges at Maximum Tensile Stress Limit State (ADTT=2500), γLL=1.0 ($f_t = 0.158\sqrt{f'_c}$)

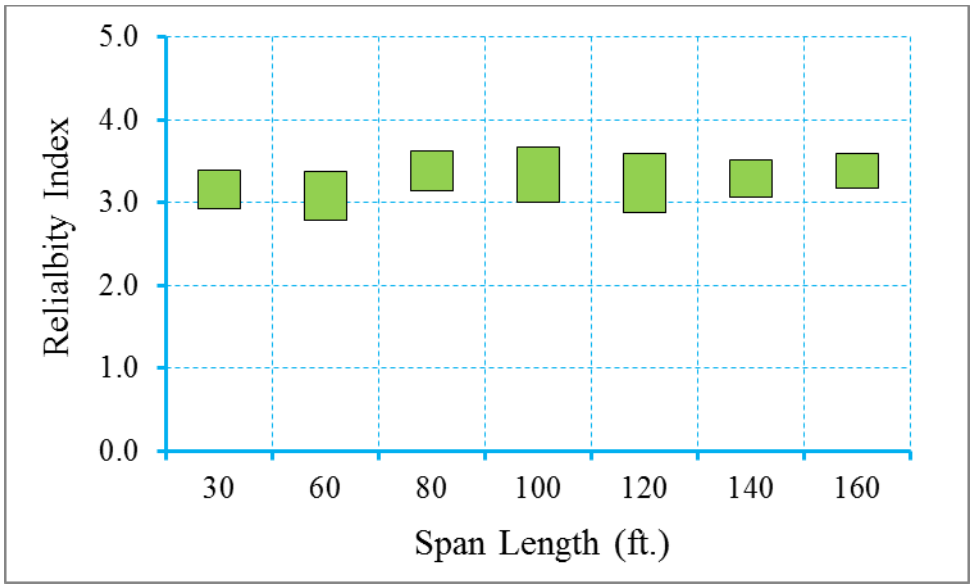

Figure D-37 Reliability Indices for Bridges at Maximum Crack Width Limit State (ADTT=2500), γLL=1.0 ($f_t = 0.158\sqrt{f_c'}$)

Step 3: Propose new live load, dead load, and/or resistance factors

Based on the calibration process shown in step 1 through step 3, it is observed that the uniform target reliability index can be achieved using a live load factor of 1.0. Therefore, for ADTT equal to 2500 and maximum concrete tensile stress of $f_t = 0.158\sqrt{f_c'}$, a new live load factor of 1.0 is proposed.

D.3.4.2.3 Bridges Designed for Maximum Concrete Tensile Stress of $f_t = 0.19\sqrt{f_c'}$

In this section, the calibration for a selected bridge database (shown in Table D-87) is performed for ADTT equal to 2500 and maximum concrete tensile stress of $f_t = 0.19\sqrt{f_c'}$. Please note that the allowable maximum crack width of 0.016 in is applied for maximum allowable crack width limit state.

Step 1: Calculate the reliability level of designs according to AASHTO LRFD Specifications (2010) (Figure D-38~Figure D-40)

Figure D-38 through Figure D-40 show the reliability indices for the bridges designed using AASHTO type girders according to AASHTO LRFD specifications (2010). It is observed that the average reliability index for decompression limit state, maximum allowable tensile stress limit state and maximum allowable crack width limit state is 0.7, 1.15, and 2.87, respectively, which does not satisfy the proposed target reliability index of 1.0 for decompression limit state and 1.25 for maximum allowable tensile stress limit state. Therefore, a larger live load factor will be used to modify the original design in order to improve the reliability level of the bridges.

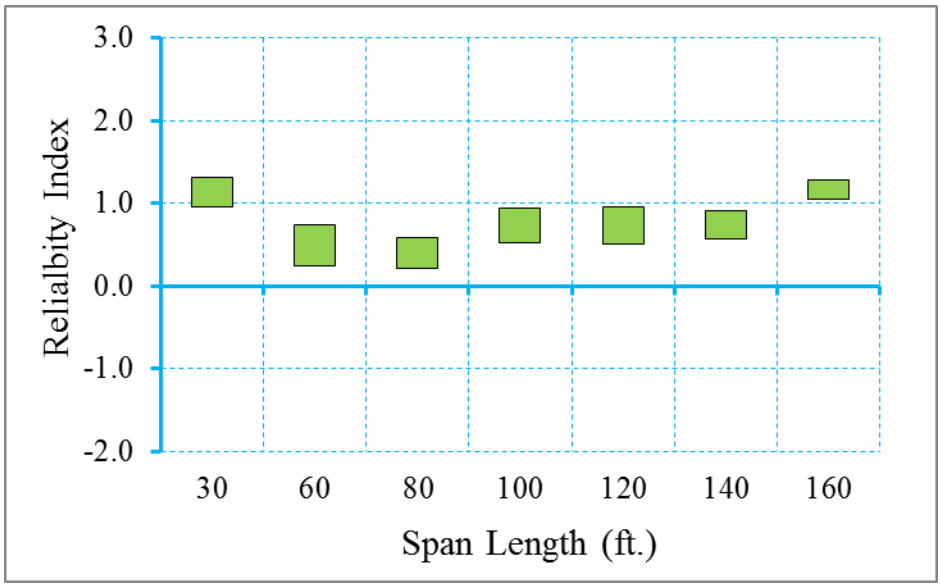

Figure D-38 Reliability Indices for Bridges at Decompression Limit State (ADTT=2500), γLL=0.8 ($f_t = 0.19\sqrt{f'_c}$)

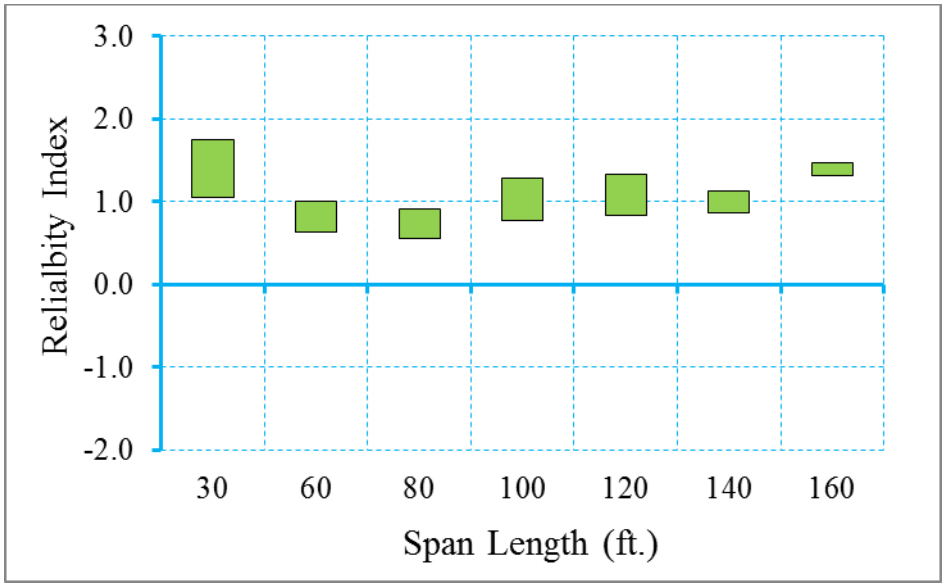

Figure D-39 Reliability Indices for Bridges at Maximum Allowable Tensile Stress Limit State (ADTT=2500), γLL=0.8 ($f_t = 0.19\sqrt{f'_c}$)

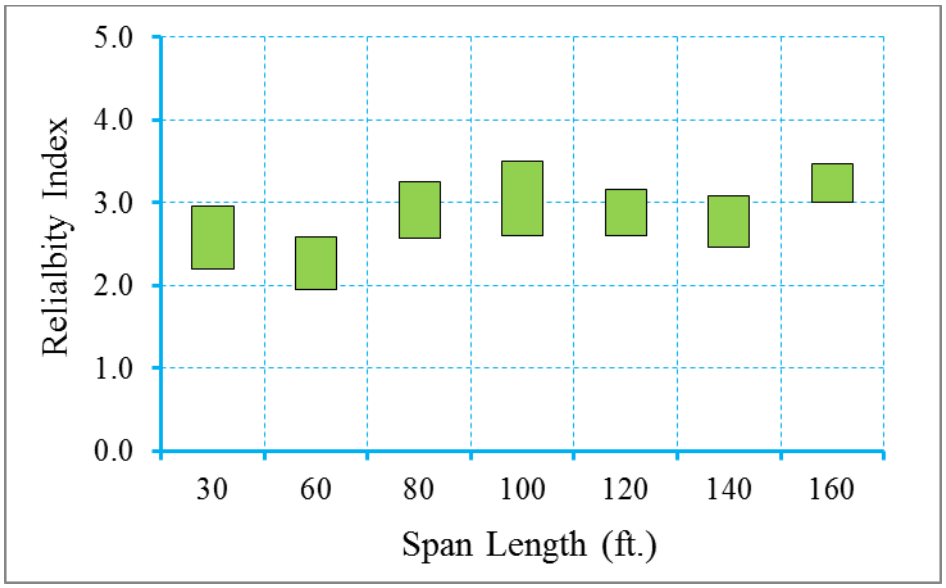

Figure D-40 Reliability Indices for Bridges at Maximum Allowable Crack Width Limit State (ADTT=2500), γLL=0.8 ($f_t = 0.19\sqrt{f_c'}$)

Step 2: Redesign the bridges with live load factor of 1.0 (Figure D-41~Figure D-43)

Since the reliability level of the original bridge database was below the target reliability level at decompression limit state and maximum allowable tensile stress limit state, the bridges were redesigned using a live load factor of 1.0. Please note that only the live load factor of Service III limit state is increased from 0.8 to 1.0, dead load and resistance factors were kept the same during the redesign. Table D-88 shows the design outcomes of the redesigned bridges.

Figure D-41 through Figure D-43 show the reliability indices for the redesigned bridges using live load factor of 1.0. It is observed that the average reliability index of decompression limit state, maximum allowable tensile stress limit state and maximum allowable crack width limit state is 1.04, 1.46, and 3.17, respectively.

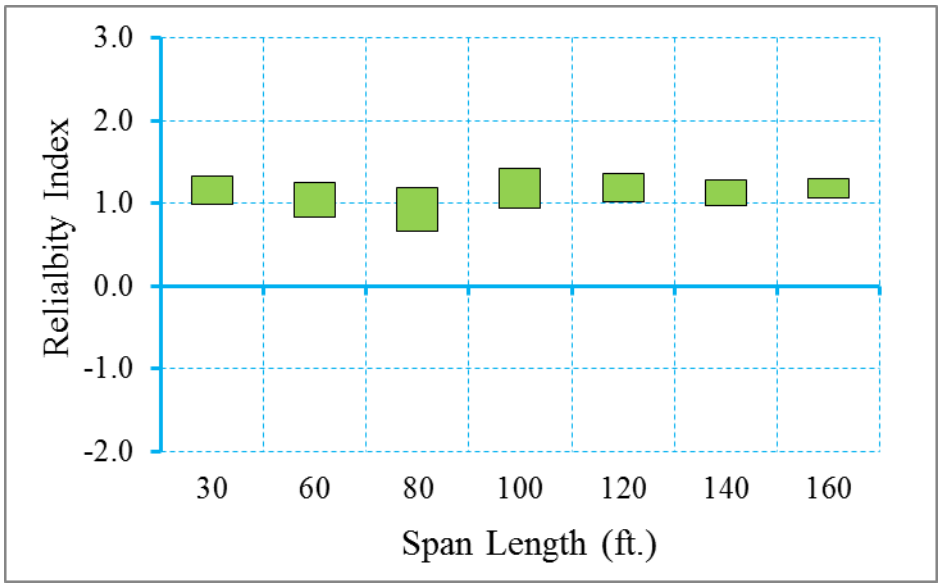

Figure D-41 Reliability Indices for Bridges at Decompression Limit State (ADTT=2500) , γLL=1.0 ($f_t = 0.19\sqrt{f_c'}$)

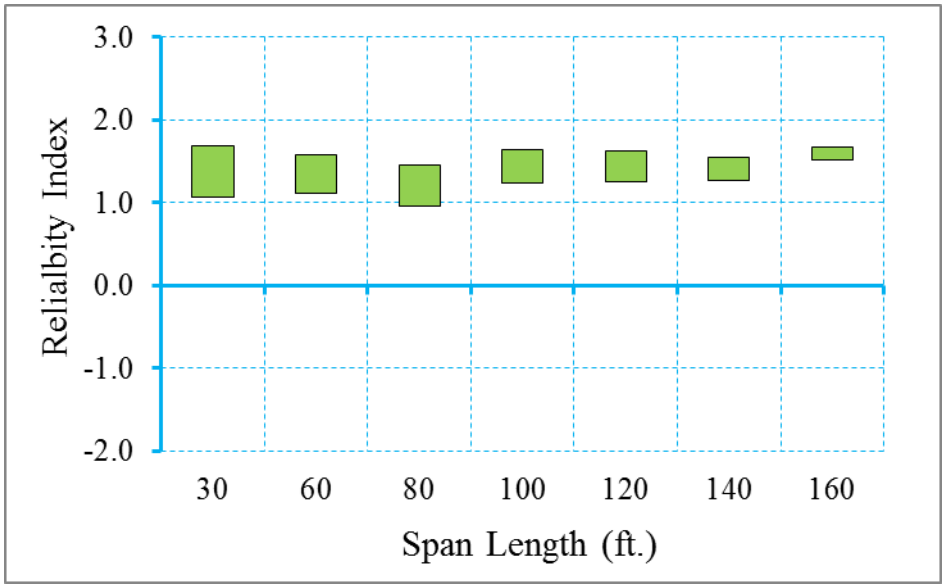

Figure D-42 Reliability Indices for Bridges at Maximum Tensile Stress Limit State (ADTT=2500), γLL=1.0 ($f_t = 0.19\sqrt{f_c'}$)

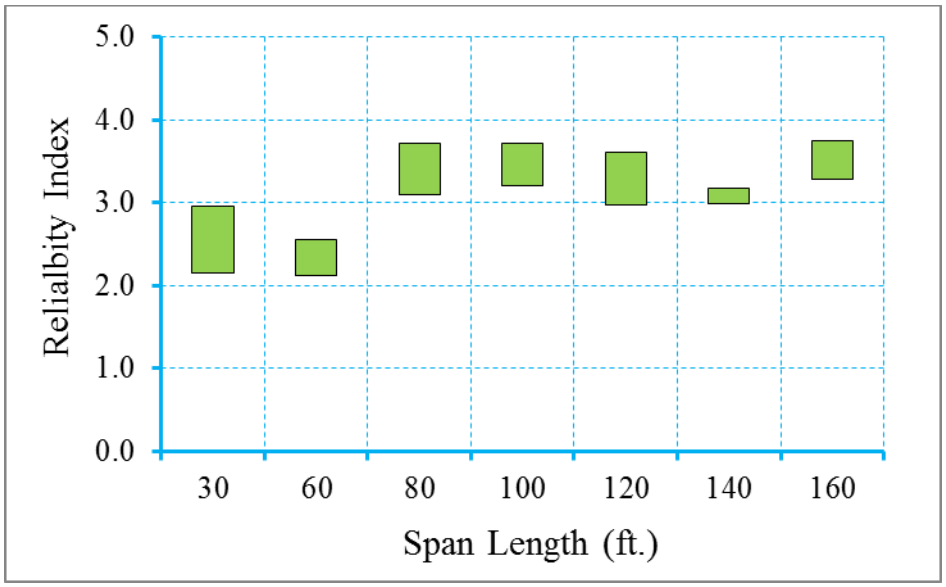

Figure D-43 Reliability Indices for Bridges at Maximum Crack Width Limit State (ADTT=2500), γLL=1.0 ($f_t = 0.19\sqrt{f_c'}$)

Step 4: Propose new live load, dead load, and/or resistance factors

Based on the calibration process shown in step 1 through step 3, it is observed that the uniform target reliability index can be achieved using a live load factor of 1.0. Therefore, for ADTT equal to 2500 and maximum concrete tensile stress of $f_t = 0.19\sqrt{f_c'}$, a new live load factor of 1.0 is proposed.

D.3.4.2.4 Bridges Designed for Maximum Concrete Tensile Stress of $f_t = 0.253\sqrt{f_c'}$

In this section, the calibration for a selected bridge database (shown in Table D-89) is performed for ADTT equal to 2500 and maximum concrete tensile stress of $f_t = 0.253\sqrt{f_c'}$. Please note that the allowable maximum crack width of 0.016 in is applied for maximum allowable crack width limit state.

Step 1: Calculate the reliability level of designs according to AASHTO LRFD Specifications (2010) (Figure D-44~Figure D-46)

Figure D-44 through Figure D-46 show the reliability indices for the bridges designed using AASHTO type girders according to AASHTO LRFD specifications (2010). It is observed that the average reliability index for decompression limit state, maximum allowable tensile stress limit state and maximum allowable crack width limit state is 0.08, 0.49, and 2.77, respectively, which does not satisfy the proposed target reliability index of 1.0 for decompression limit state and 1.25 for maximum allowable tensile stress limit state. Therefore, a larger live load factor will be used to modify the original design in order to improve the reliability level of the bridges.

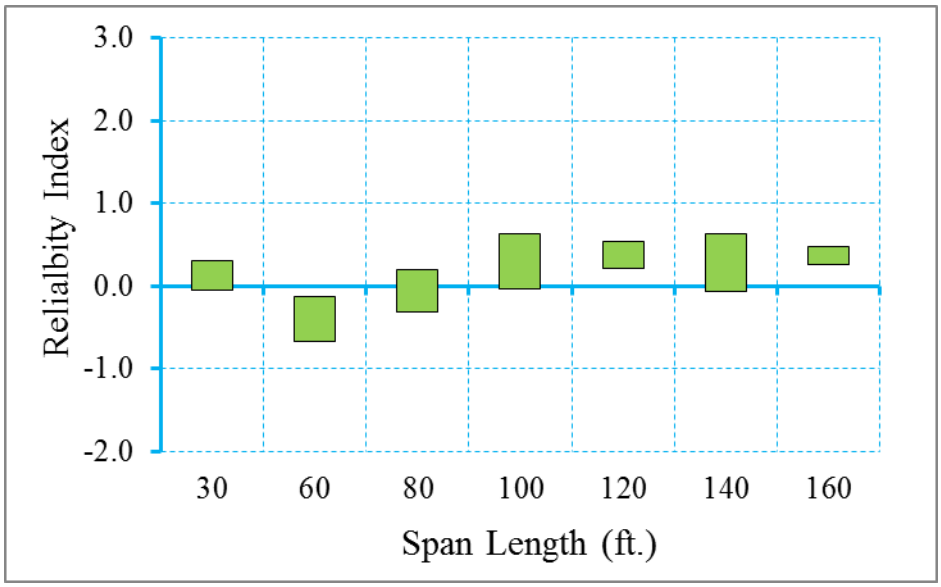

Figure D-44 Reliability Indices for Bridges at Decompression Limit State (ADTT=2500), γLL=0.8 ($f_t = 0.253\sqrt{f'_c}$)

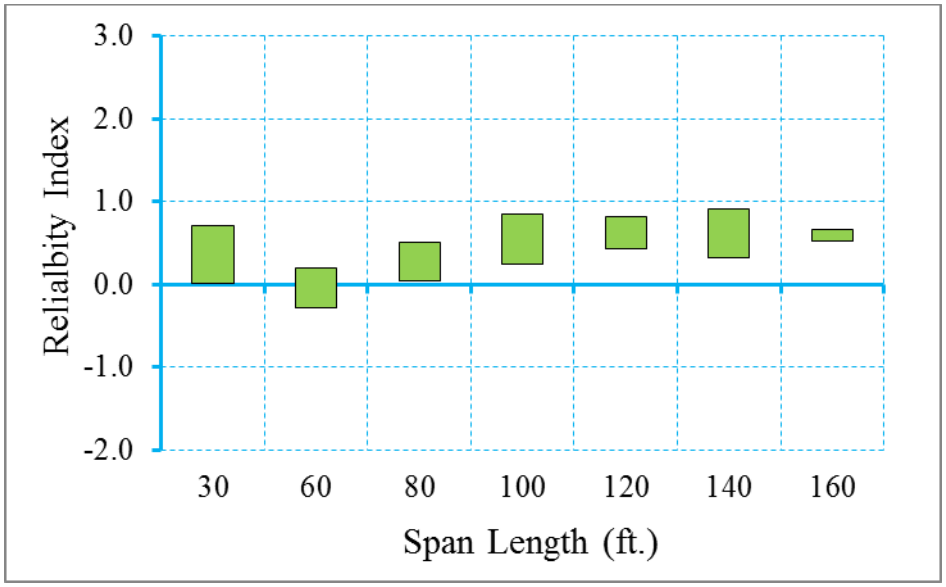

Figure D-45 Reliability Indices for Bridges at Maximum Allowable Tensile Stress Limit State (ADTT=2500), γLL=0.8 ($f_t = 0.253\sqrt{f'_c}$)

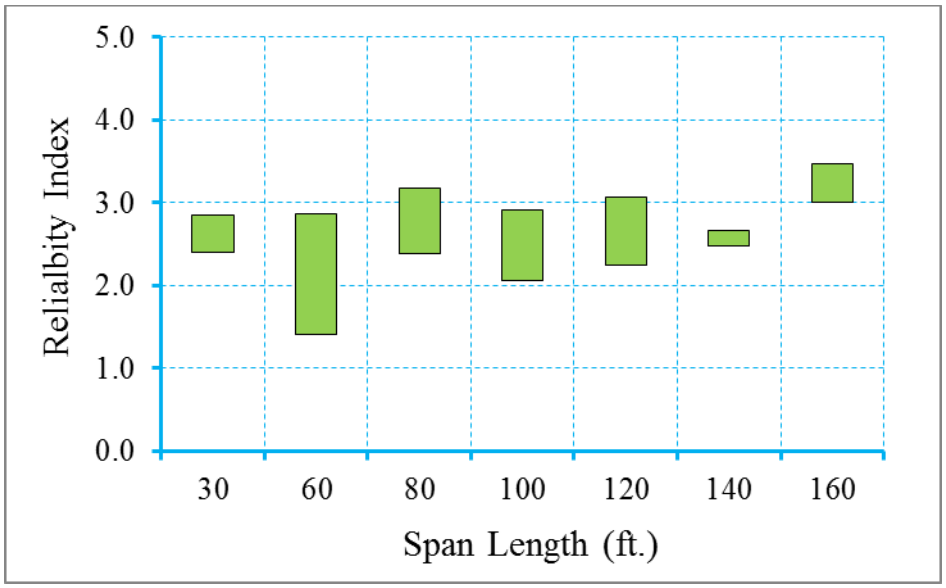

Figure D-46 Reliability Indices for Bridges at Maximum Allowable Crack Width Limit State (ADTT=2500), γLL=0.8 ($f_t = 0.253\sqrt{f_c'}$)

Step 2: Redesign the bridges with live load factor of 1.0 (Figure D-47~Figure D-49)

Since the reliability level of the original bridge database was below the target reliability level at decompression limit state and maximum allowable tensile stress limit state, the bridges were redesigned using a live load factor of 1.0. Please note that only the live load factor of Service III limit state is increased from 0.8 to 1.0, dead load and resistance factors were kept the same during the redesign. Table D-90 shows the design outcomes of the redesigned bridges.

Figure D-47 through Figure D-49 show the reliability indices for the redesigned bridges using live load factor of 1.0. It is observed that the average reliability index of decompression limit state, maximum allowable tensile stress limit state and maximum allowable crack width limit state is 0.89, 1.27, and 2.95, respectively.

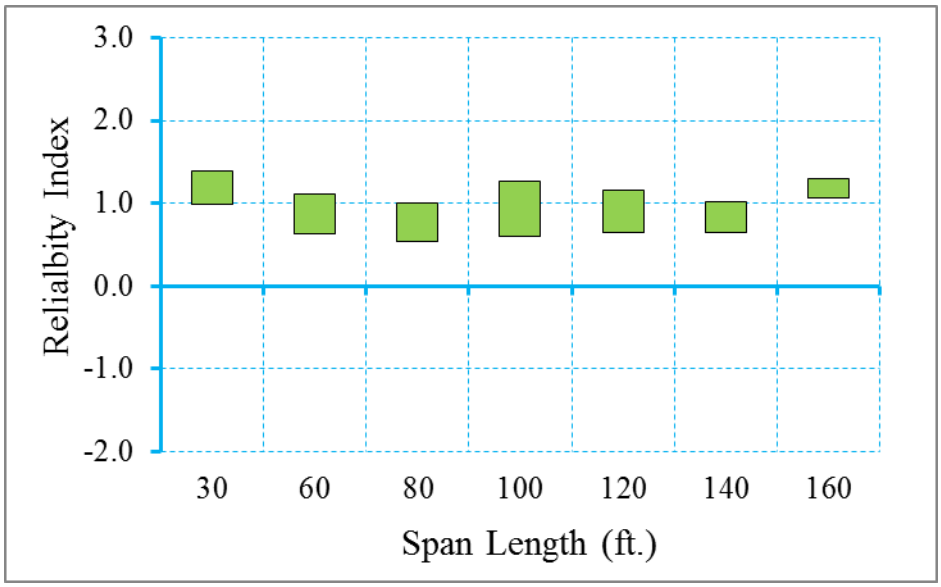

Figure D-47 Reliability Indices for Bridges at Decompression Limit State (ADTT=2500) , γLL=1.0 ($f_t = 0.253\sqrt{f_c'}$)

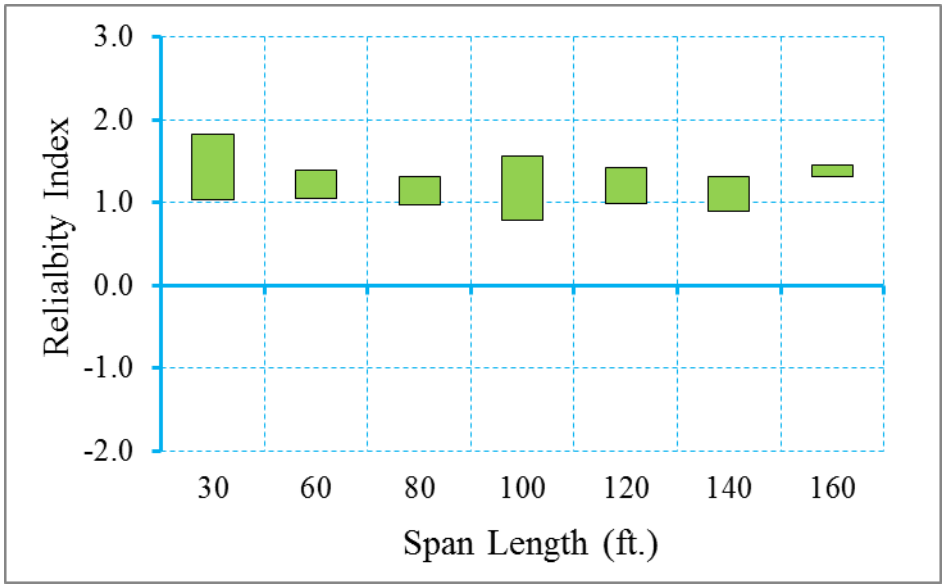

Figure D-48 Reliability Indices for Bridges at Maximum Tensile Stress Limit State (ADTT=2500), γLL=1.0 ($f_t = 0.253\sqrt{f_c'}$)

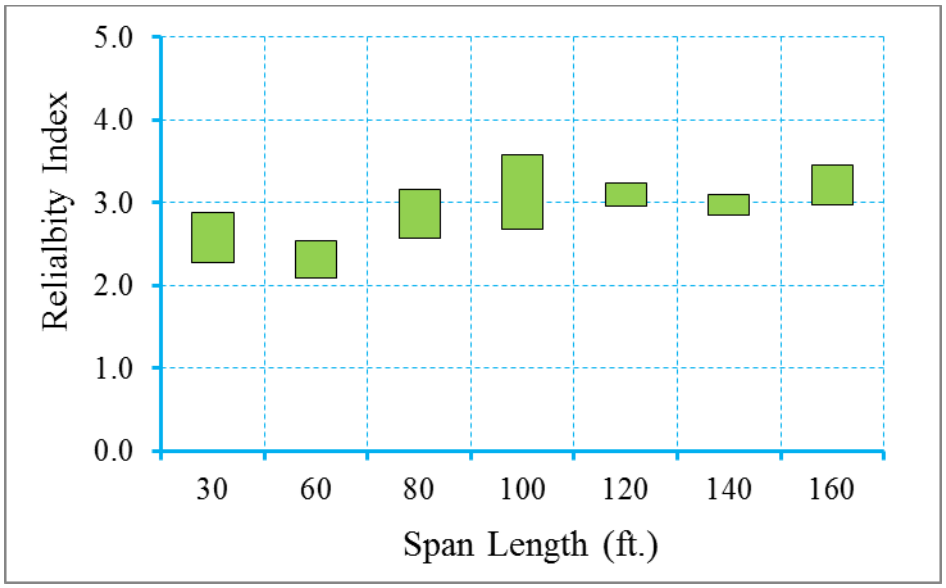

Figure D-49 Reliability Indices for Bridges at Maximum Crack Width Limit State (ADTT=2500), γLL=1.0 ($f_t = 0.253\sqrt{f_c'}$)

Step 4: Propose new live load, dead load, and/or resistance factors

Based on the calibration process shown in step 1 through step 3, it is observed that the uniform target reliability index can be achieved using a live load factor of 1.0. Therefore, for ADTT equal to 2500 and maximum concrete tensile stress of $f_t = 0.253\sqrt{f_c'}$, a new live load factor of 1.0 is proposed.

D.3.4.3 Calibration Procedure for ADTT=5000

D.3.4.3.1 Bridges Designed for Maximum Concrete Tensile Stress of $f_t = 0.0948\sqrt{f_c'}$

In this section, the calibration for a selected bridge database (shown in Table D-83) is performed for ADTT equal to 5000 and maximum concrete tensile stress of $f_t = 0.0948\sqrt{f_c'}$. Please note that the allowable maximum crack width of 0.016 in is applied for maximum allowable crack width limit state.

Step 1: Calculate the reliability level of designs according to AASHTO LRFD Specifications (2010) (Figure D-50~Figure D-52)

Figure D-50 through Figure D-52 show the reliability indices for the bridges designed using AASHTO type girders according to AASHTO LRFD specifications (2010). It is observed that the average reliability index for decompression limit state, maximum allowable tensile stress limit state and maximum allowable crack width limit state is 0.97, 1.31, and 3.06, respectively. The live load factor of 1.0 will be used in the next step

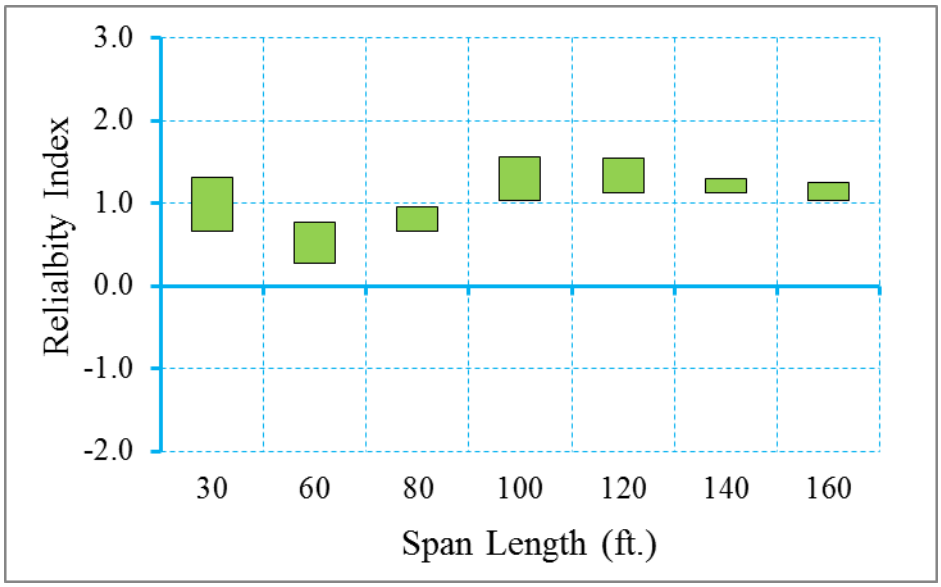

Figure D-50 Reliability Indices for Bridges at Decompression Limit State (ADTT=5000), γLL=0.8 ($f_t = 0.0948\sqrt{f'_c}$)

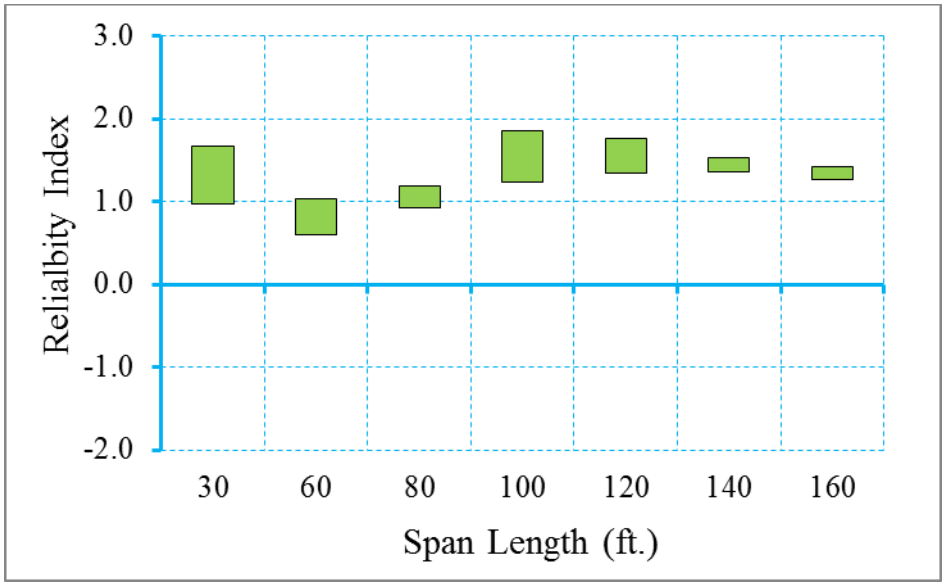

Figure D-51 Reliability Indices for Bridges at Maximum Allowable Tensile Stress Limit State (ADTT=5000), γLL=0.8 ($f_t = 0.0948\sqrt{f'_c}$)

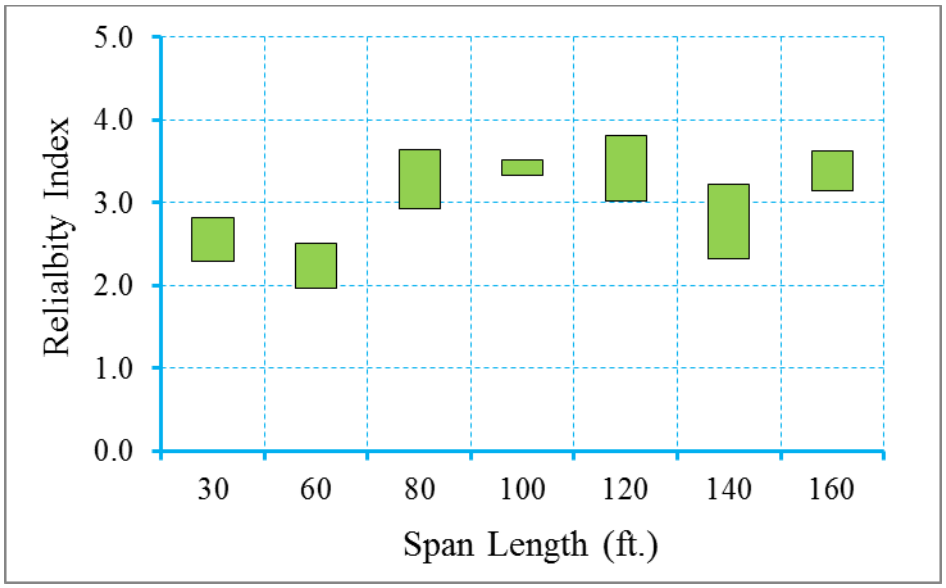

Figure D-52 Reliability Indices for Bridges at Maximum Allowable Crack Width Limit State (ADTT=5000), γLL=0.8 ($f_t = 0.0948\sqrt{f_c'}$)

Step 2: Redesign the bridges with live load factor of 1.0 (Figure D-53~Figure D-55)

Since the reliability level of the original bridge database was below the target reliability level at decompression limit state and maximum allowable tensile stress limit state, the bridges were redesigned using a live load factor of 1.0. Please note that only the live load factor of Service III limit state is increased from 0.8 to 1.0, dead load and resistance factors were kept the same during the redesign. Table D-84 shows the design outcomes of the redesigned bridges.

Figure D-53 through Figure D-55 show the reliability indices for the redesigned bridges using live load factor of 1.0. It is observed that the average reliability index of decompression limit state, maximum allowable tensile stress limit state and maximum allowable crack width limit state is 1.33, 1.7, and 3.32, respectively.

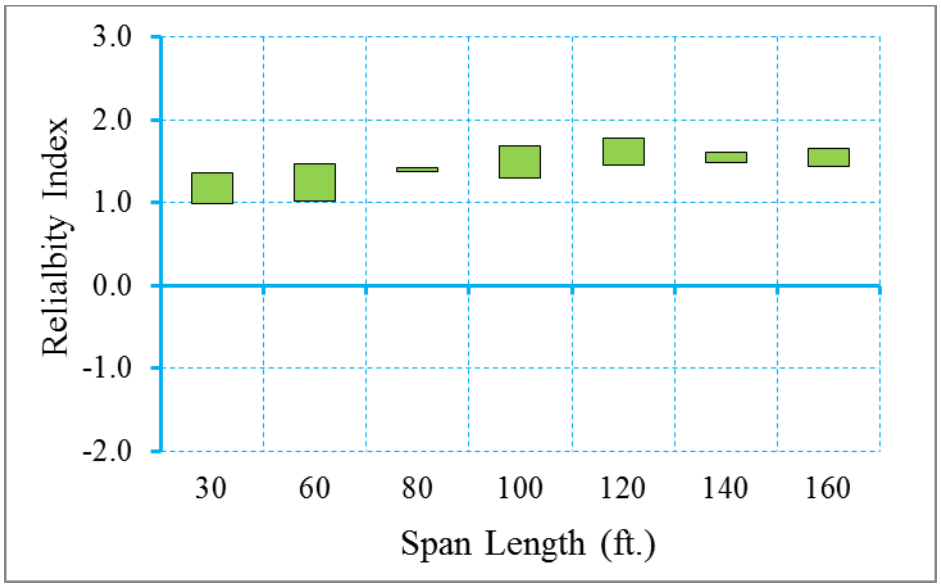

Figure D-53 Reliability Indices for Bridges at Decompression Limit State (ADTT=5000), γLL=1.0 ($f_t = 0.0948\sqrt{f_c'}$)

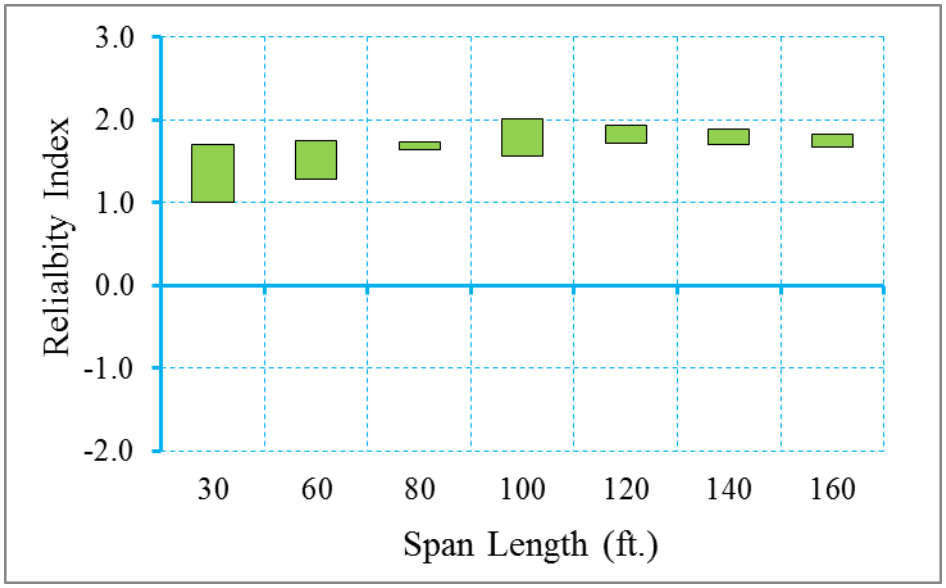

Figure D-54 Reliability Indices for Bridges at Maximum Tensile Stress Limit State (ADTT=5000), γLL=1.0 ($f_t = 0.0948\sqrt{f_c'}$)

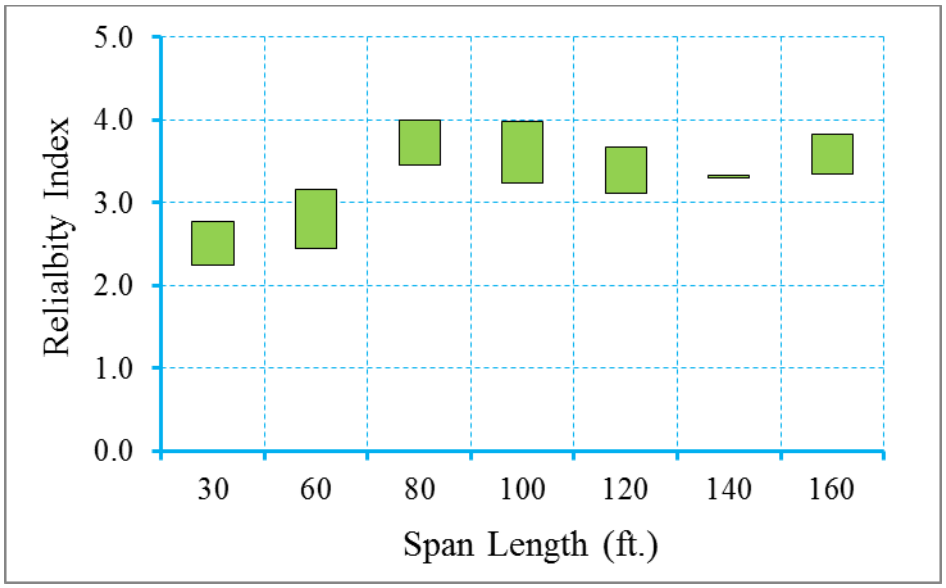

Figure D-55 Reliability Indices for Bridges at Maximum Crack Width Limit State (ADTT=5000), γLL=1.0 ($f_t = 0.0948\sqrt{f_c'}$)

Step 4: Propose new live load, dead load, and/or resistance factors

Based on the calibration process shown in step 1 through step 3, it is observed that the uniform target reliability index can be achieved using a live load factor of 1.0. Therefore, for ADTT equal to 5000 and maximum concrete tensile stress of $f_t = 0.0948\sqrt{f_c'}$, a new live load factor of 1.0 is proposed.

D.3.4.3.2 Bridges Designed for Maximum Concrete Tensile Stress of $f_t = 0.158\sqrt{f_c'}$

In this section, the calibration for a selected bridge database (shown in Table D-85) is performed for ADTT equal to 5000 and maximum concrete tensile stress of $f_t = 0.158\sqrt{f_c'}$. Please note that the allowable maximum crack width of 0.016 in is applied for maximum allowable crack width limit state.

Step 1: Calculate the reliability level of designs according to AASHTO LRFD Specifications (2010) (Figure D-56~Figure D-58)

Figure D-56 through Figure D-58 show the reliability indices for the bridges designed using AASHTO type girders according to AASHTO LRFD specifications (2010). It is observed that the average reliability index for decompression limit state, maximum allowable tensile stress limit state and maximum allowable crack width limit state is 0.80, 1.14, and 2.91, respectively, which does not satisfy the proposed target reliability index of 1.0 for decompression limit state and 1.25 for maximum allowable tensile stress limit state. Therefore, a larger live load factor will be used to modify the original design in order to improve the reliability level of the bridges.

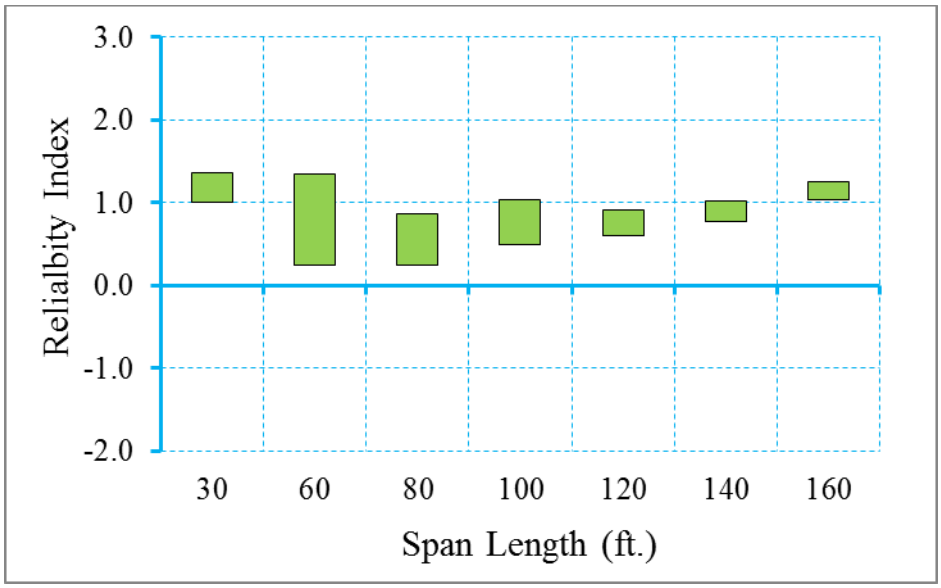

Figure D-56 Reliability Indices for Bridges at Decompression Limit State (ADTT=5000), γLL=0.8 ($f_t = 0.158\sqrt{f'_c}$)

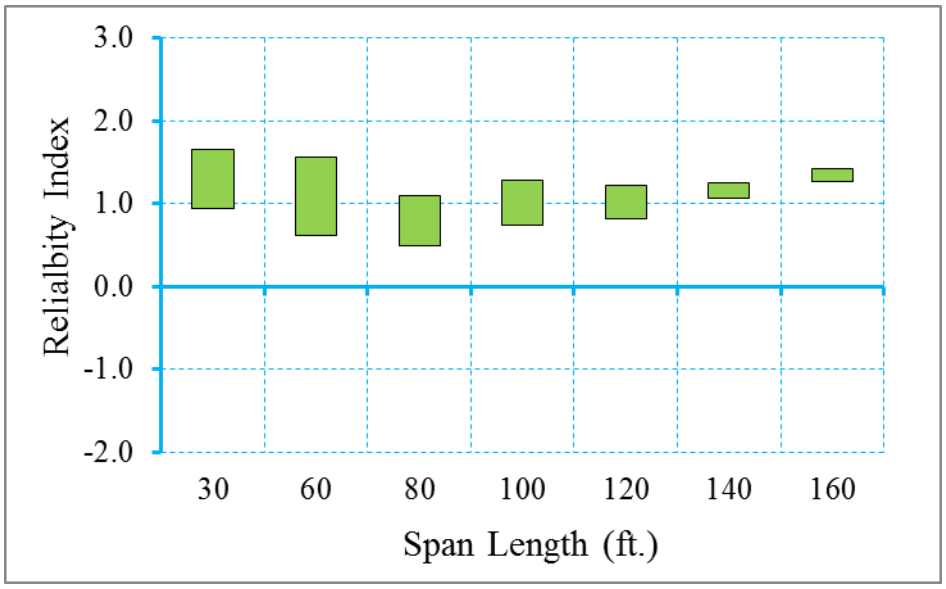

Figure D-57 Reliability Indices for Bridges at Maximum Allowable Tensile Stress Limit State (ADTT=5000), γLL=0.8 ($f_t = 0.158\sqrt{f'_c}$)

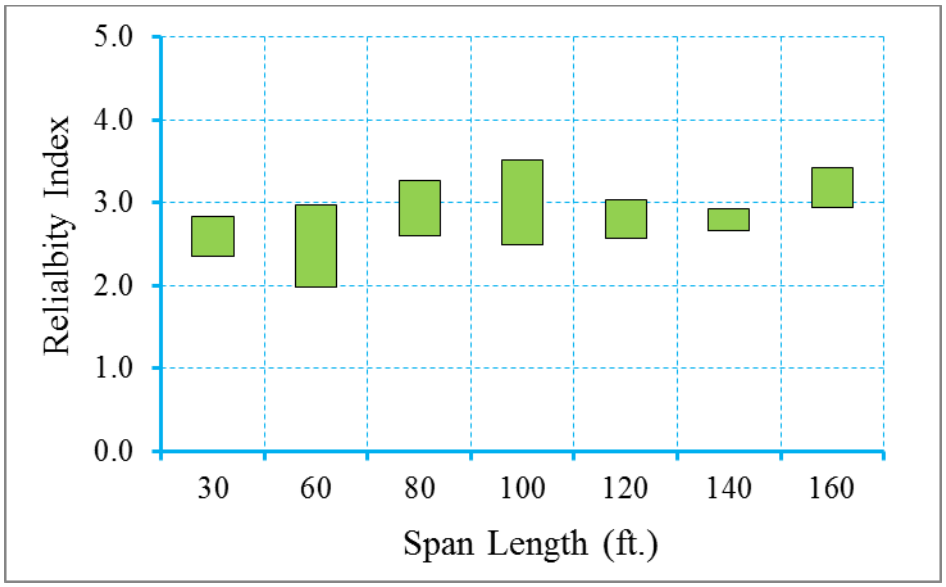

Figure D-58 Reliability Indices for Bridges at Maximum Allowable Crack Width Limit State (ADTT=5000), γLL=0.8 ($f_t = 0.158\sqrt{f_c'}$)

Step 2: Redesign the bridges with live load factor of 1.0 (Figure D-59~Figure D-61)

Since the reliability level of the original bridge database was below the target reliability level at decompression limit state and maximum allowable tensile stress limit state, the bridges were redesigned using a live load factor of 1.0. Please note that only the live load factor of Service III limit state is increased from 0.8 to 1.0, dead load and resistance factors were kept the same during the redesign. Table D-86 shows the design outcomes of the redesigned bridges.

Figure D-59 through Figure D-61 show the reliability indices for the redesigned bridges using live load factor of 1.0. It is observed that the average reliability index of decompression limit state, maximum allowable tensile stress limit state and maximum allowable crack width limit state is 1.07, 1.44, and 3.26, respectively.

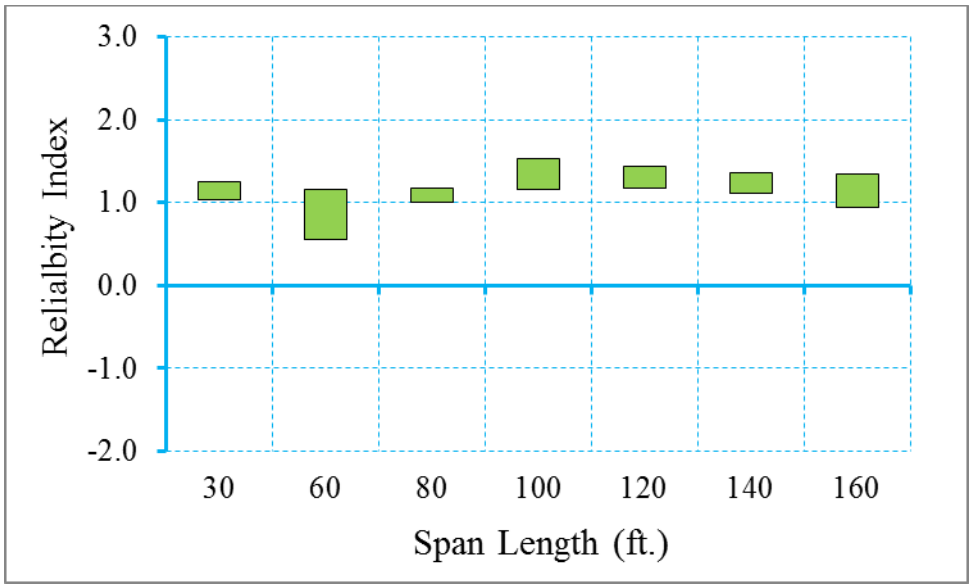

Figure D-59 Reliability Indices for Bridges at Decompression Limit State (ADTT=5000), γLL=1.0 ($f_t = 0.158\sqrt{f'_c}$)

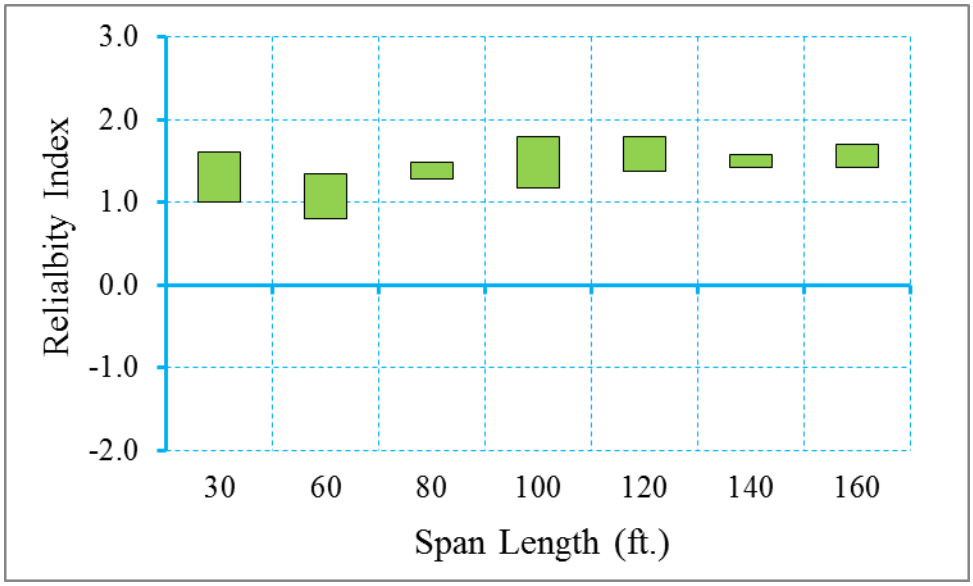

Figure D-60 Reliability Indices for Bridges at Maximum Tensile Stress Limit State (ADTT=5000), γLL=1.0 ($f_t = 0.158\sqrt{f'_c}$)

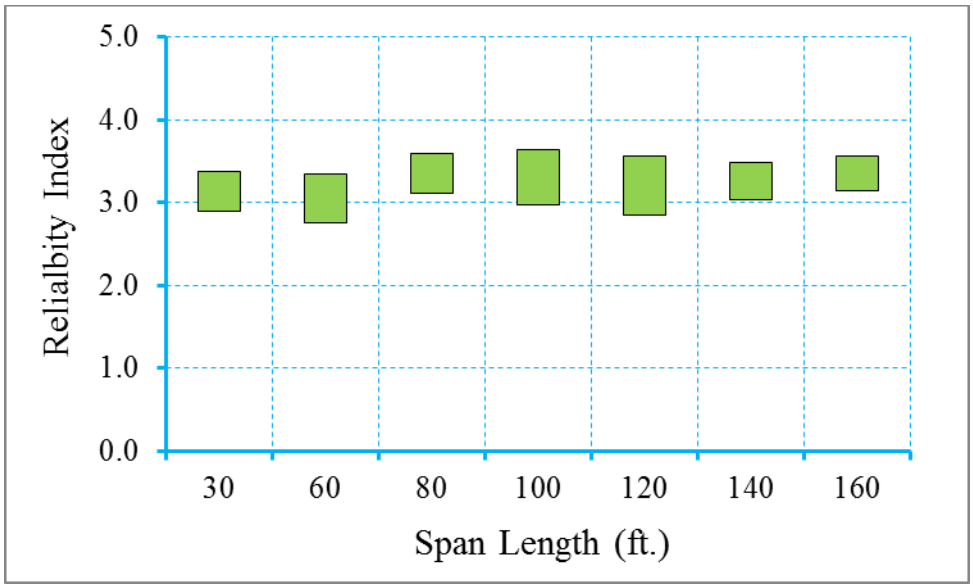

Figure D-61 Reliability Indices for Bridges at Maximum Crack Width Limit State (ADTT=5000), γLL=1.0 ($f_t = 0.158\sqrt{f_c'}$)

Step 4: Propose new live load, dead load, and/or resistance factors

Based on the calibration process shown in step 1 through step 3, it is observed that the uniform target reliability index can be achieved using a live load factor of 1.0. Therefore, for ADTT equal to 5000 and maximum concrete tensile stress of $f_t = 0.158\sqrt{f_c'}$, a new live load factor of 1.0 is proposed.

D.3.4.3.3 Bridges Designed for Maximum Concrete Tensile Stress of $f_t = 0.19\sqrt{f_c'}$

In this section, the calibration for a selected bridge database (shown in Table D-87) is performed for ADTT equal to 5000 and maximum concrete tensile stress of $f_t = 0.19\sqrt{f_c'}$. Please note that the allowable maximum crack width of 0.016 in is applied for maximum allowable crack width limit state.

Step 1: Calculate the reliability level of designs according to AASHTO LRFD Specifications (2010) (Figure D-62~Figure D-64)

Figure D-62 through Figure D-64 show the reliability indices for the bridges designed using AASHTO type girders according to AASHTO LRFD specifications (2010). It is observed that the average reliability index for decompression limit state, maximum allowable tensile stress limit state and maximum allowable crack width limit state is 0.68, 1.1, and 2.82, respectively, which does not satisfy the proposed target reliability index of 1.0 for decompression limit state and 1.25 for maximum allowable tensile stress limit state. Therefore, a larger live load factor will be used to modify the original design in order to improve the reliability level of the bridges.

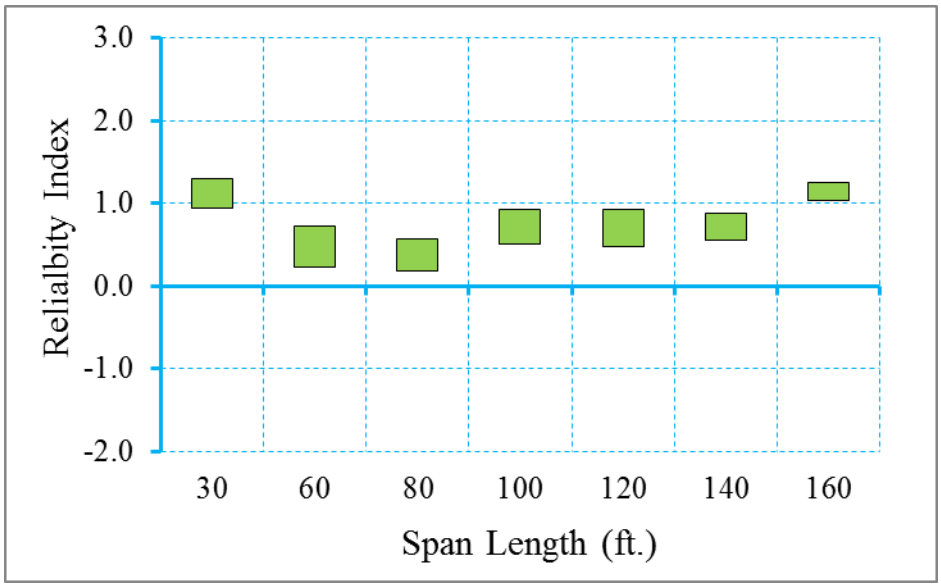

Figure D-62 Reliability Indices for Bridges at Decompression Limit State (ADTT=5000), γLL=0.8 ($f_t = 0.19\sqrt{f_c'}$)

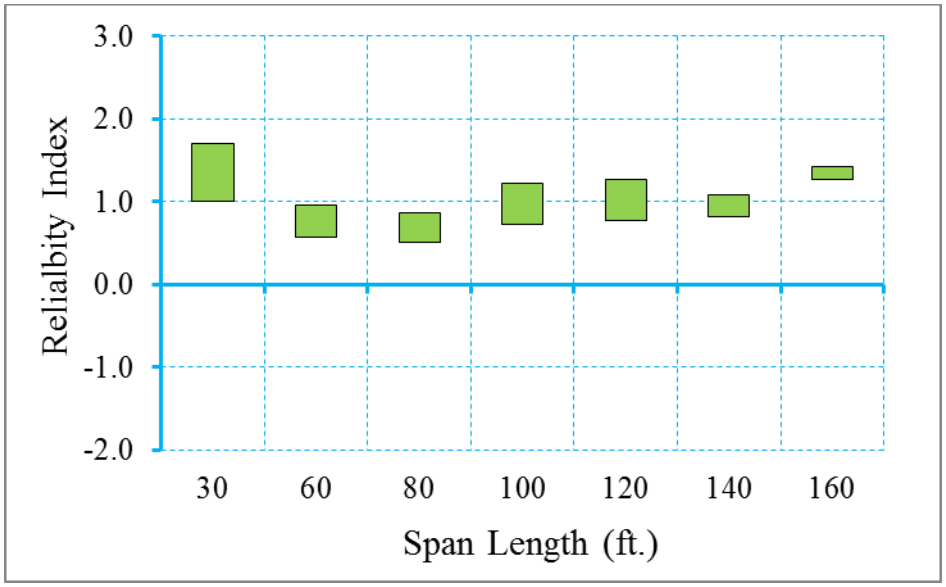

Figure D-63 Reliability Indices for Bridges at Maximum Allowable Tensile Stress Limit State (ADTT=5000), γLL=0.8 ($f_t = 0.19\sqrt{f_c'}$)

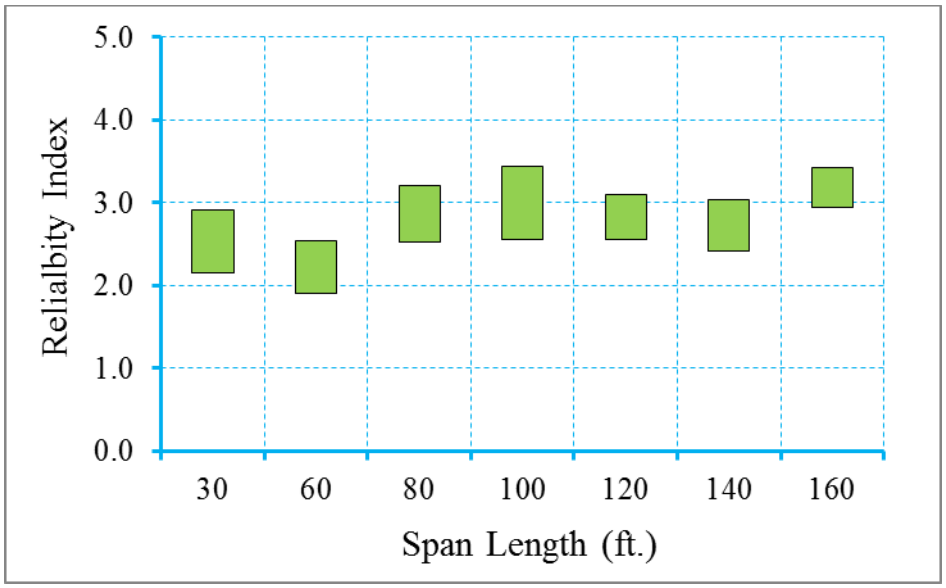

Figure D-64 Reliability Indices for Bridges at Maximum Allowable Crack Width Limit State (ADTT=5000), γLL=0.8 ($f_t = 0.19\sqrt{f_c'}$)

Step 2: Redesign the bridges with live load factor of 1.0 (Figure D-65~Figure D-67)

Since the reliability level of the original bridge database was below the target reliability level at decompression limit state and maximum allowable tensile stress limit state, the bridges were redesigned using a live load factor of 1.0. Please note that only the live load factor of Service III limit state is increased from 0.8 to 1.0, dead load and resistance factors were kept the same during the redesign. Table D-88 shows the design outcomes of the redesigned bridges.

Figure D-65 through Figure D-67 show the reliability indices for the redesigned bridges using live load factor of 1.0. It is observed that the average reliability index of decompression limit state, maximum allowable tensile stress limit state and maximum allowable crack width limit state is 1.00, 1.41, and 3.14, respectively.

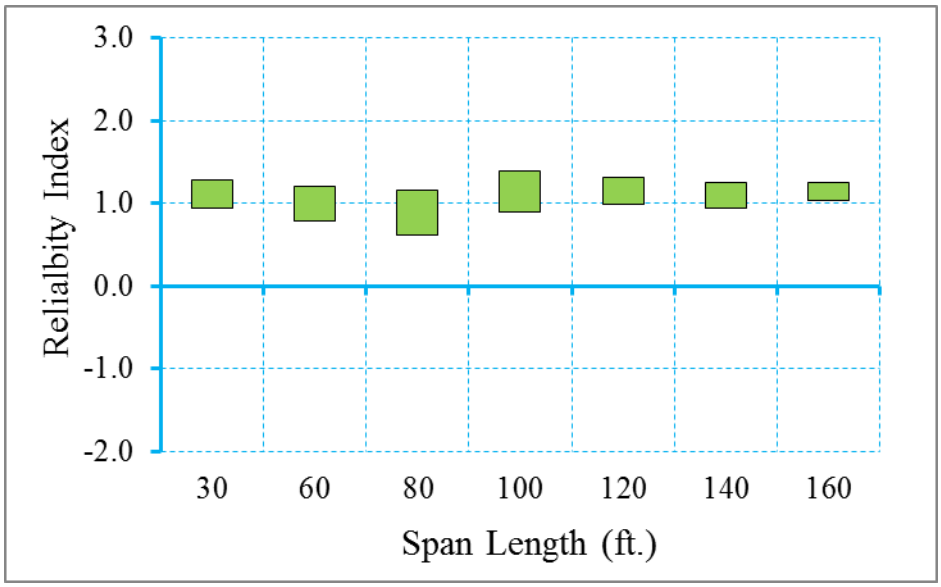

Figure D-65 Reliability Indices for Bridges at Decompression Limit State (ADTT=5000), γLL=1.0 ($f_t = 0.19\sqrt{f_c'}$)

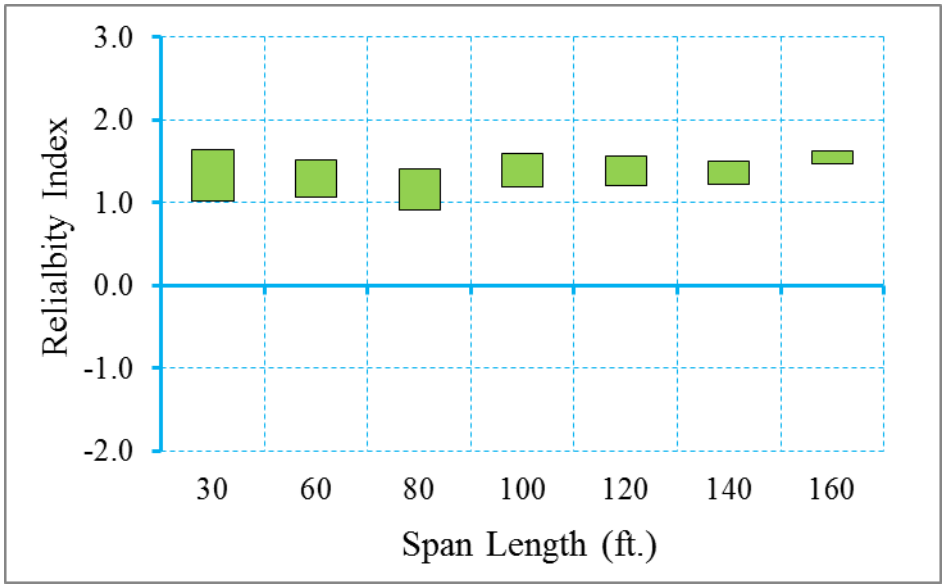

Figure D-66 Reliability Indices for Bridges at Maximum Tensile Stress Limit State (ADTT=5000), γLL=1.0 ($f_t = 0.19\sqrt{f_c'}$)

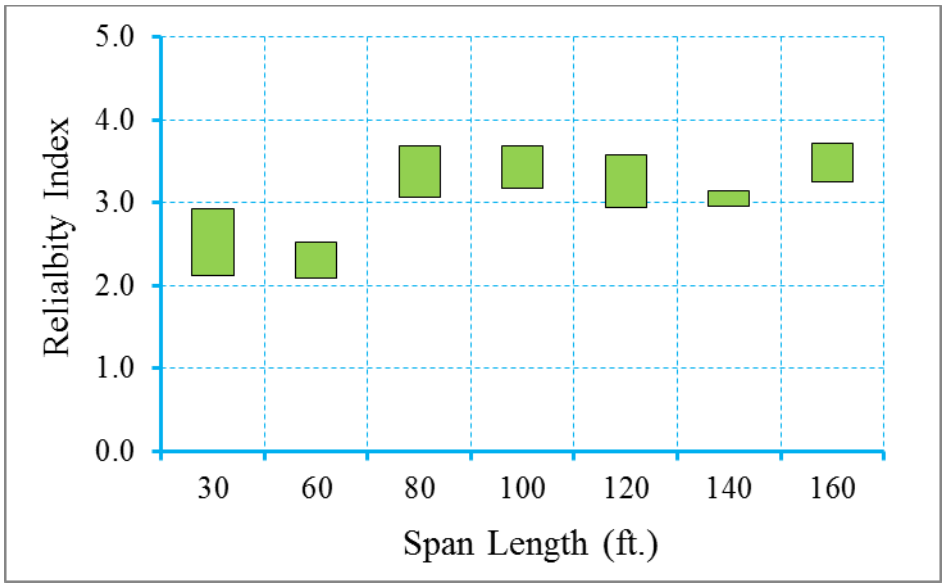

Figure D-67 Reliability Indices for Bridges at Maximum Crack Width Limit State (ADTT=5000), γLL=1.0 ($f_t = 0.19\sqrt{f_c'}$)

Step 4: Propose new live load, dead load, and/or resistance factors

Based on the calibration process shown in step 1 through step 3, it is observed that the uniform target reliability index can be achieved using a live load factor of 1.0. Therefore, for ADTT equal to 5000 and maximum concrete tensile stress of $f_t = 0.19\sqrt{f_c'}$, a new live load factor of 1.0 is proposed.

D.3.4.3.4 Bridges Designed for Maximum Concrete Tensile Stress of $f_t = 0.253\sqrt{f_c'}$

In this section, the calibration for a selected bridge database (shown in Table D-89) is performed for ADTT equal to 5000 and maximum concrete tensile stress of $f_t = 0.253\sqrt{f_c'}$. Please note that the allowable maximum crack width of 0.016 in is applied for maximum allowable crack width limit state.

Step 1: Calculate the reliability level of designs according to AASHTO LRFD Specifications (2010) (Figure D-68~Figure D-70)

Figure D-68 through Figure D-70 show the reliability indices for the bridges designed using AASHTO type girders according to AASHTO LRFD specifications (2010). It is observed that the average reliability index for decompression limit state, maximum allowable tensile stress limit state and maximum allowable crack width limit state is 0.06, 0.44, and 2.72, respectively, which does not satisfy the proposed target reliability index of 1.0 for decompression limit state and 1.25 for maximum allowable tensile stress limit state. Therefore, a larger live load factor will be used to modify the original design in order to improve the reliability level of the bridges.

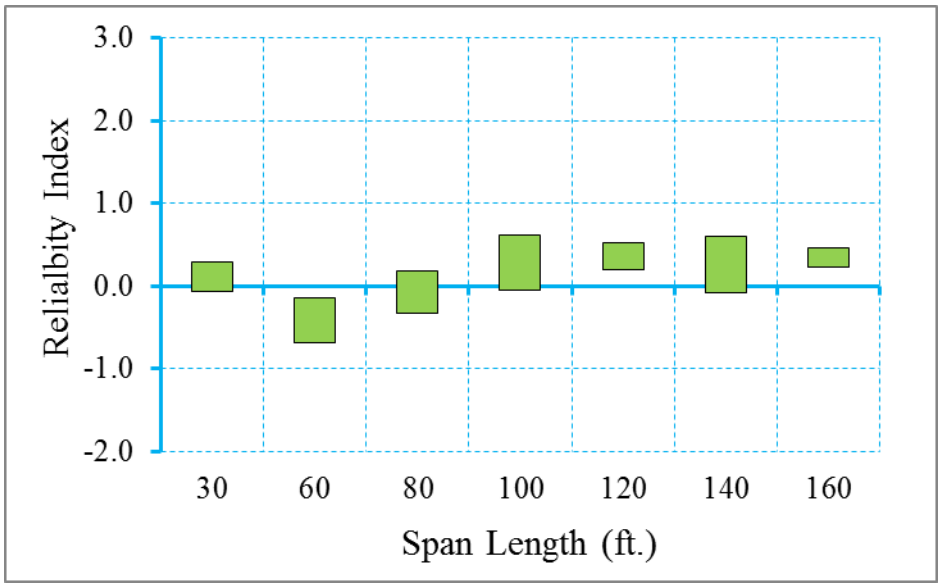

Figure D-68 Reliability Indices for Bridges at Decompression Limit State (ADTT=5000), γLL=0.8 ($f_t = 0.253\sqrt{f_c'}$)

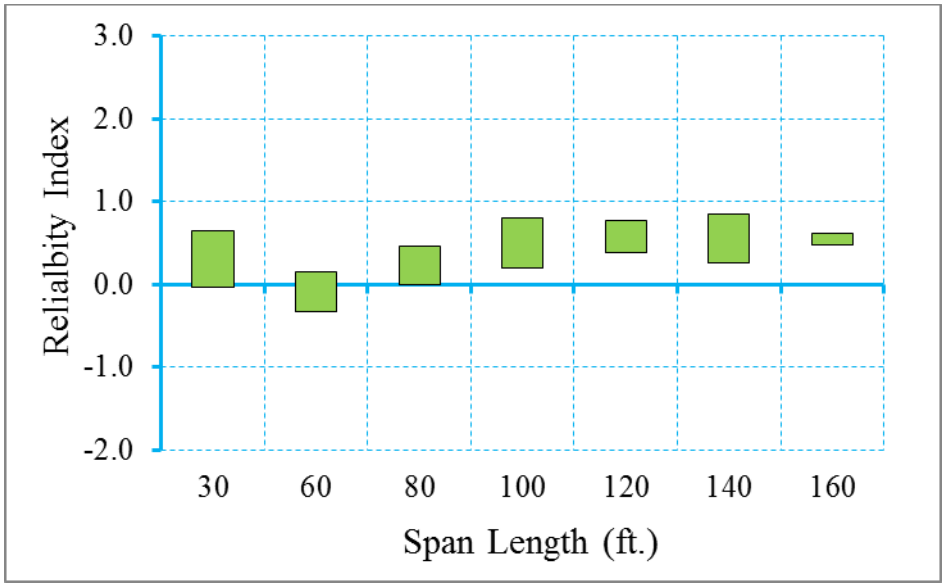

Figure D-69 Reliability Indices for Bridges at Maximum Allowable Tensile Stress Limit State (ADTT=5000), γLL=0.8 ($f_t = 0.253\sqrt{f_c'}$)

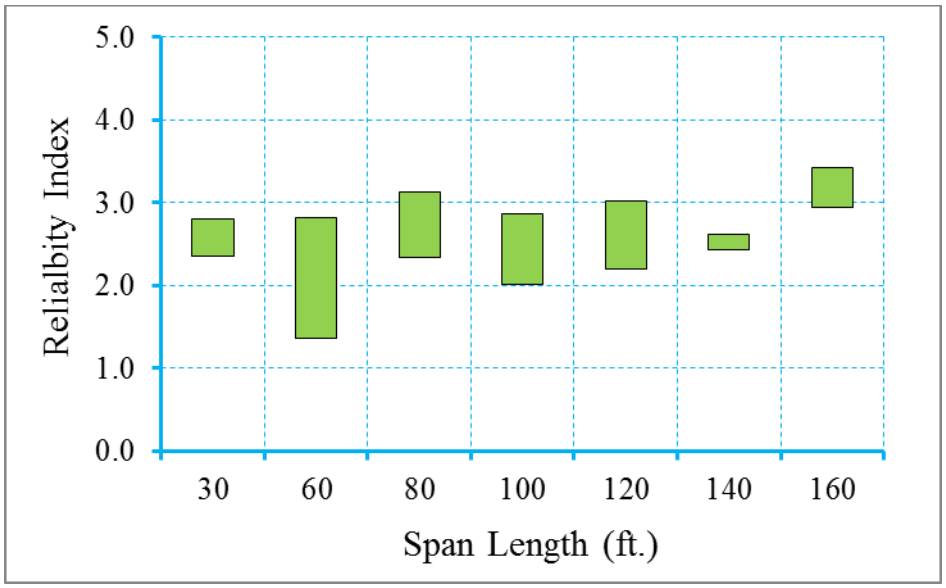

Figure D-70 Reliability Indices for Bridges at Maximum Allowable Crack Width Limit State (ADTT=5000), γLL=0.8 ($f_t = 0.253\sqrt{f_c'}$)

Step 2: Redesign the bridges with live load factor of 1.0 (Figure D-71~Figure D-73)

Since the reliability level of the original bridge database was below the target reliability level at decompression limit state and maximum allowable tensile stress limit state, the bridges were redesigned using a live load factor of 1.0. Please note that only the live load factor of Service III limit state is increased from 0.8 to 1.0, dead load and resistance factors were kept the same during the redesign. Table D-90 shows the design outcomes of the redesigned bridges.

Figure D-71 through Figure D-73 show the reliability indices for the redesigned bridges using live load factor of 1.0. It is observed that the average reliability index of decompression limit state, maximum allowable tensile stress limit state and maximum allowable crack width limit state is 0.85, 1.23, and 2.92, respectively.

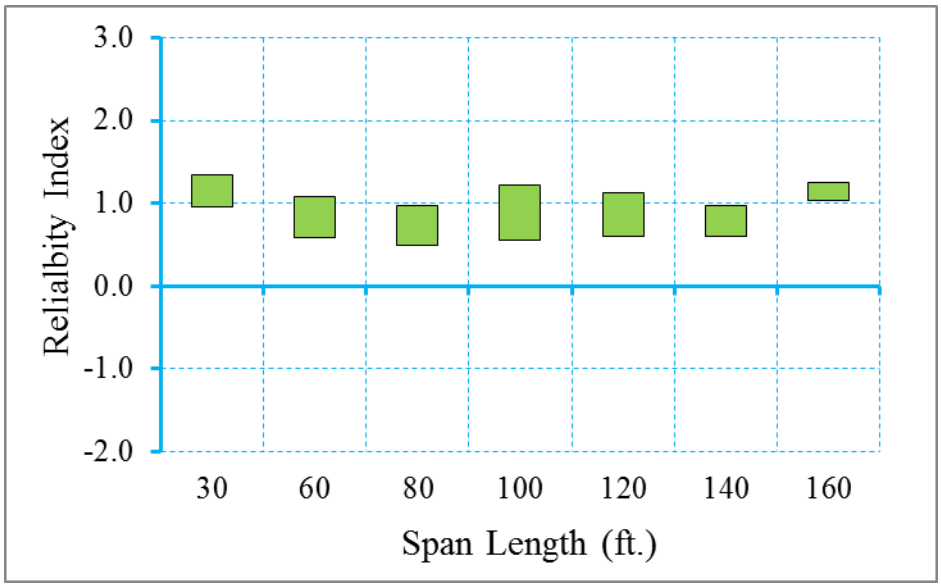

Figure D-71 Reliability Indices for Bridges at Decompression Limit State (ADTT=5000), γLL=1.0 ($f_t = 0.253\sqrt{f'_c}$)

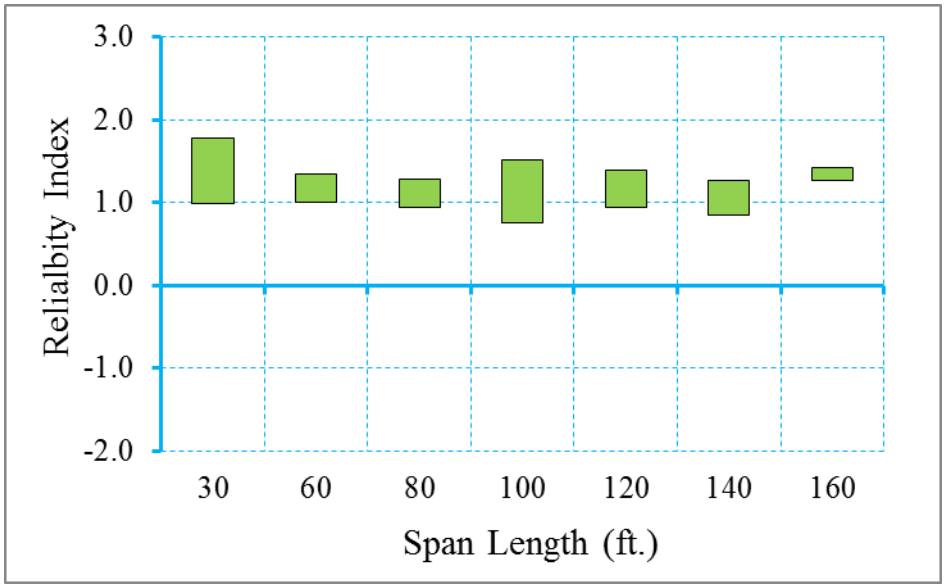

Figure D-72 Reliability Indices for Bridges at Maximum Tensile Stress Limit State (ADTT=5000), γLL=1.0 ($f_t = 0.253\sqrt{f'_c}$)

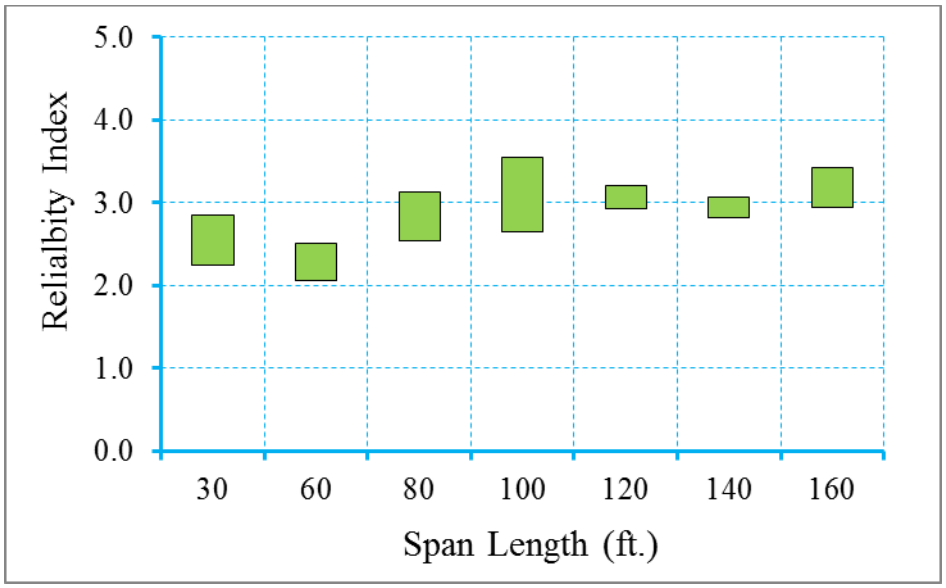

Figure D-73 Reliability Indices for Bridges at Maximum Crack Width Limit State (ADTT=5000), γLL=1.0 ($f_t = 0.253\sqrt{f_c'}$)

Step 4: Propose new live load, dead load, and/or resistance factors

Based on the calibration process shown in step 1 through step 3, it is observed that the uniform target reliability index can be achieved using a live load factor of 1.0. Therefore, for ADTT equal to 5000 and maximum concrete tensile stress of $f_t = 0.253\sqrt{f_c'}$, a new live load factor of 1.0 is proposed.

D.3.4.4 Calibration Procedure for ADTT=10000

D.3.4.4.1 Bridges Designed for Maximum Concrete Tensile Stress of $f_t = 0.0948\sqrt{f_c'}$

In this section, the calibration for a selected bridge database (shown in Table D-83) is performed for ADTT equal to 10000 and maximum concrete tensile stress of $f_t = 0.0948\sqrt{f_c'}$. Please note that the allowable maximum crack width of 0.016 in is applied for maximum allowable crack width limit state.

Step 1: Calculate the reliability level of designs according to AASHTO LRFD Specifications (2010) (Figure D-74~Figure D-76)

Figure D-74 through Figure D-76 show the reliability indices for the bridges designed using AASHTO type girders according to AASHTO LRFD specifications (2010). It is observed that the average reliability index for decompression limit state, maximum allowable tensile stress limit state and maximum allowable crack width limit state is 0.94, 1.30, and 3.00, respectively. Live load factor of 1.0 will be used in the next step.

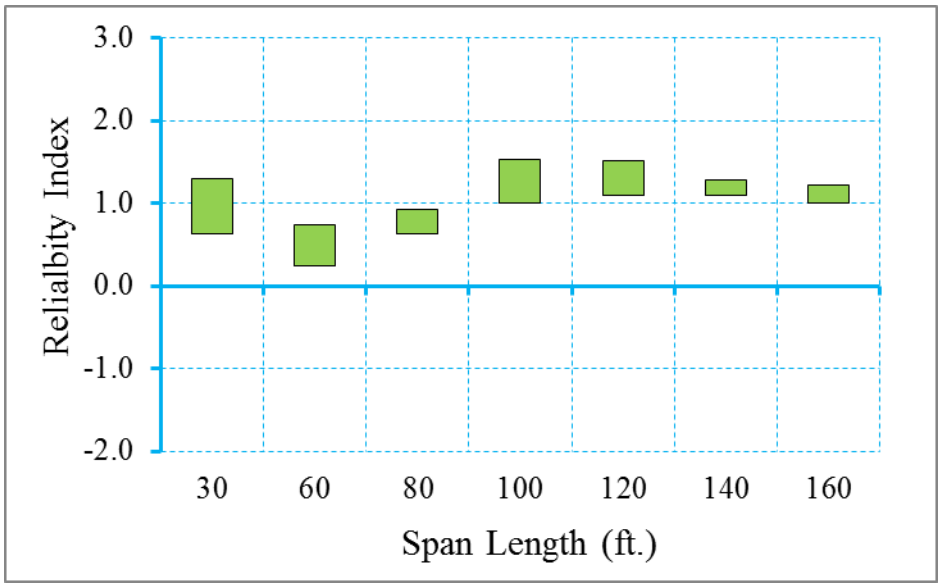

Figure D-74 Reliability Indices for Bridges at Decompression Limit State (ADTT=10000), γLL=0.8 ($f_t = 0.0948\sqrt{f_c'}$)

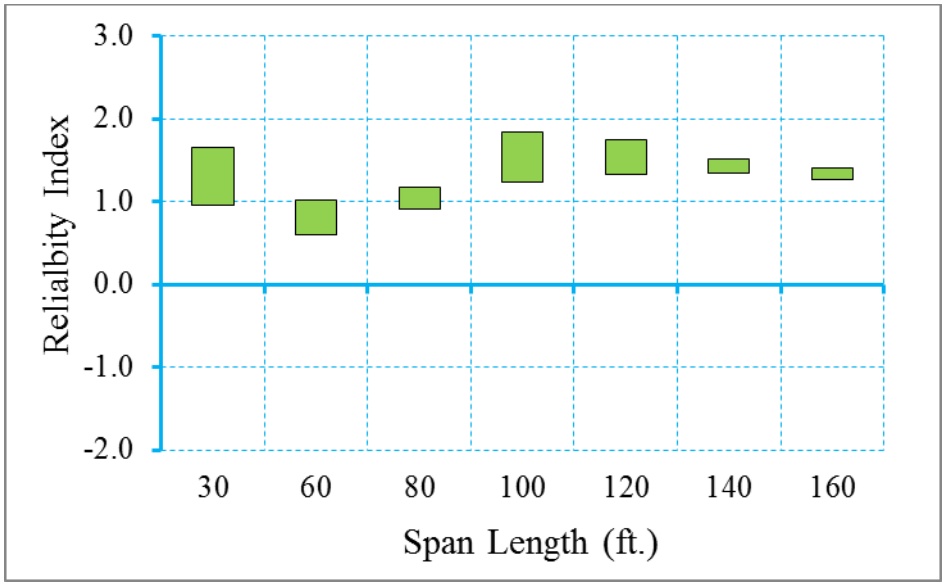

Figure D-75 Reliability Indices for Bridges at Maximum Allowable Tensile Stress Limit State (ADTT=10000), γLL=0.8 ($f_t = 0.0948\sqrt{f_c'}$)

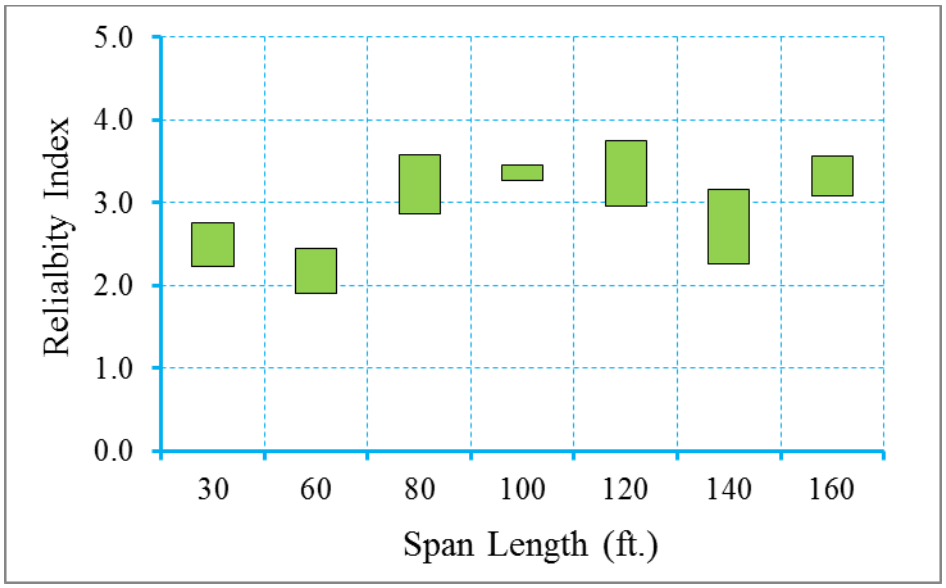

Figure D-76 Reliability Indices for Bridges at Maximum Allowable Crack Width Limit State (ADTT=10000), γLL=0.8 ($f_t = 0.0948\sqrt{f_c'}$)

Step 2: Redesign the bridges with live load factor of 1.0 (Figure D-77~Figure D-79)

Since the reliability level of the original bridge database was below the target reliability level at decompression limit state and maximum allowable tensile stress limit state, the bridges were redesigned using a live load factor of 1.0. Please note that only the live load factor of Service III limit state is increased from 0.8 to 1.0, dead load and resistance factors were kept the same during the redesign. Table D-84 shows the design outcomes of the redesigned bridges.

Figure D-77 through Figure D-79 show the reliability indices for the redesigned bridges using live load factor of 1.0. It is observed that the average reliability index of decompression limit state, maximum allowable tensile stress limit state and maximum allowable crack width limit state is 1.32, 1.66, and 3.28, respectively.

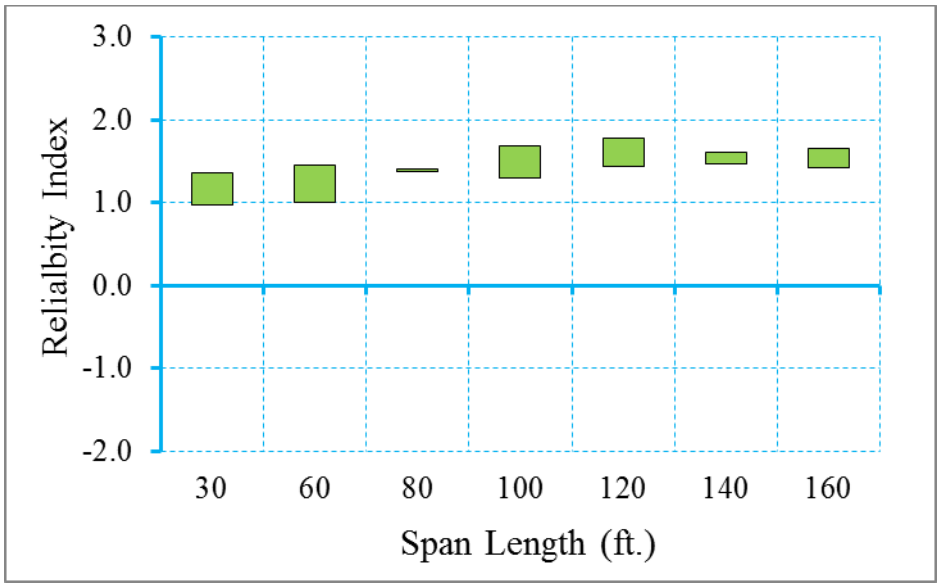

Figure D-77 Reliability Indices for Bridges at Decompression Limit State (ADTT=10000), γLL=1.0 ($f_t = 0.0948\sqrt{f_c'}$)

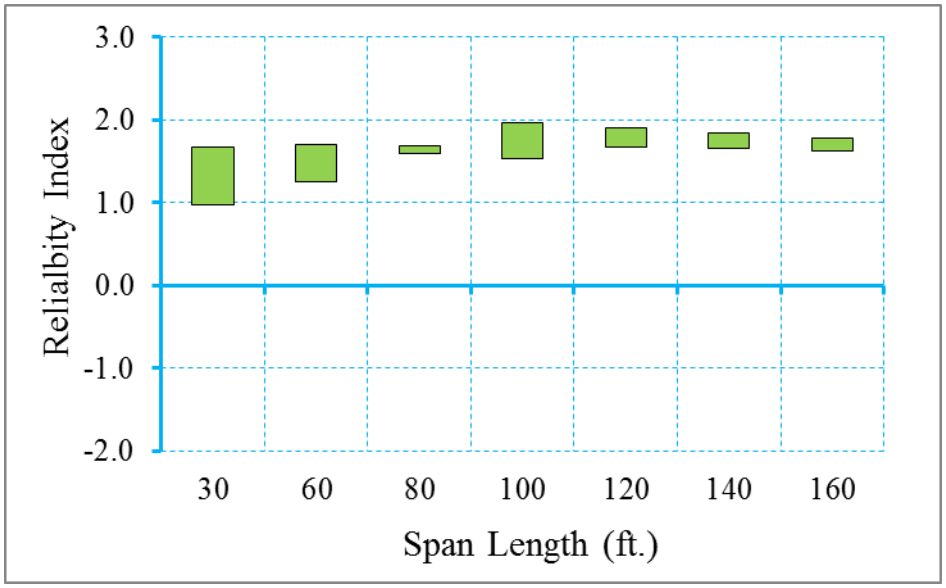

Figure D-78 Reliability Indices for Bridges at Maximum Tensile Stress Limit State (ADTT=10000), γLL=1.0 ($f_t = 0.0948\sqrt{f_c'}$)

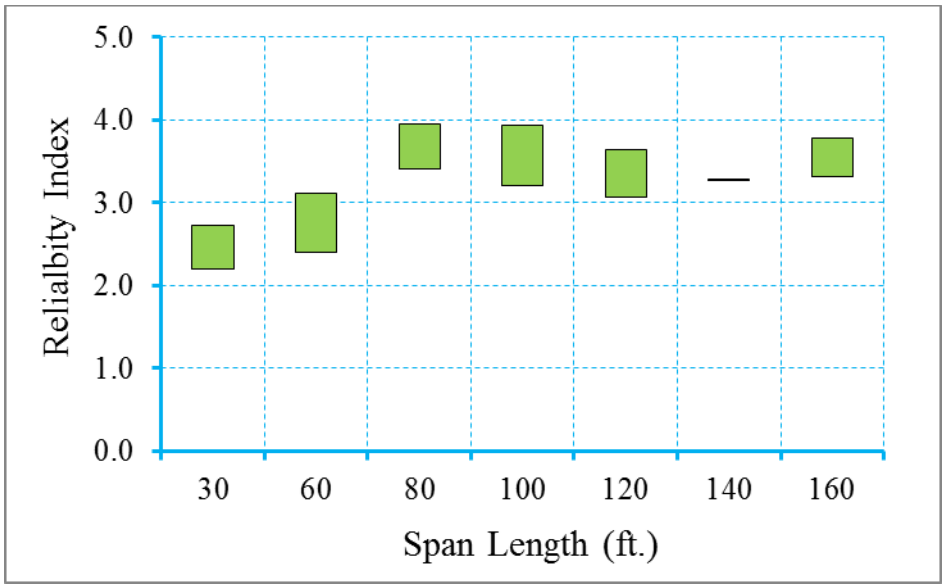

Figure D-79 Reliability Indices for Bridges at Maximum Crack Width Limit State (ADTT=10000), γLL=1.0 ($f_t = 0.0948\sqrt{f_c'}$)

Step 4: Propose new live load, dead load, and/or resistance factors

Based on the calibration process shown in step 1 through step 3, it is observed that the uniform target reliability index can be achieved using a live load factor of 1.0. Therefore, for ADTT equal to 10000 and maximum concrete tensile stress of $f_t = 0.0948\sqrt{f_c'}$, a new live load factor of 1.0 is proposed.

D.3.4.4.2 C6.4.2 Bridges Designed for Maximum Concrete Tensile Stress of $f_t = 0.158\sqrt{f_c'}$

In this section, the calibration for a selected bridge database (shown in Table D-85) is performed for ADTT equal to 10000 and maximum concrete tensile stress of $f_t = 0.158\sqrt{f_c'}$. Please note that the allowable maximum crack width of 0.016 in is applied for maximum allowable crack width limit state.

Step 1: Calculate the reliability level of designs according to AASHTO LRFD Specifications (2010) (Figure D-80~Figure D-82)

Figure D-80 through Figure D-82 show the reliability indices for the bridges designed using AASHTO type girders according to AASHTO LRFD specifications (2010). It is observed that the average reliability index for decompression limit state, maximum allowable tensile stress limit state and maximum allowable crack width limit state is 0.76, 1.11, and 2.85, respectively, which does not satisfy the proposed target reliability index of 1.0 for decompression limit state and 1.25 for maximum allowable tensile stress limit state. Therefore, a larger live load factor

will be used to modify the original design in order to improve the reliability level of the bridges.

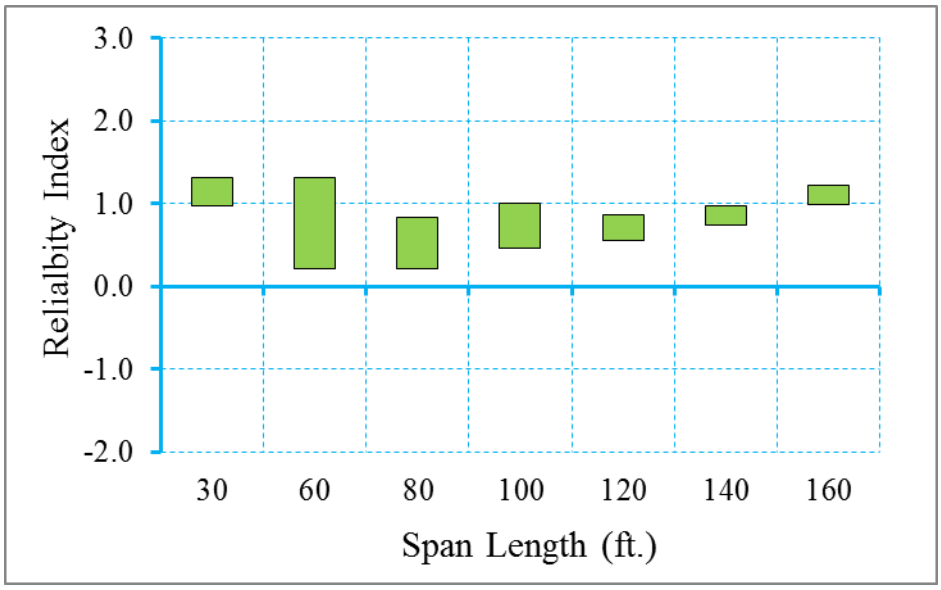

Figure D-80 Reliability Indices for Bridges at Decompression Limit State (ADTT=10000), γLL=0.8 ($f_t = 0.158\sqrt{f'_c}$)

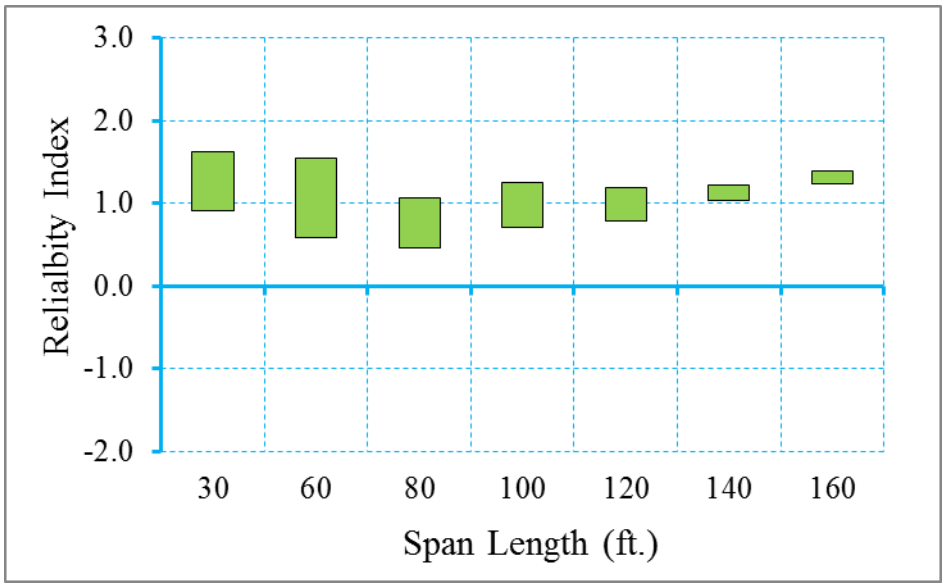

Figure D-81 Reliability Indices for Bridges at Maximum Allowable Tensile Stress Limit State (ADTT=10000), γLL=0.8 ($f_t = 0.158\sqrt{f'_c}$)

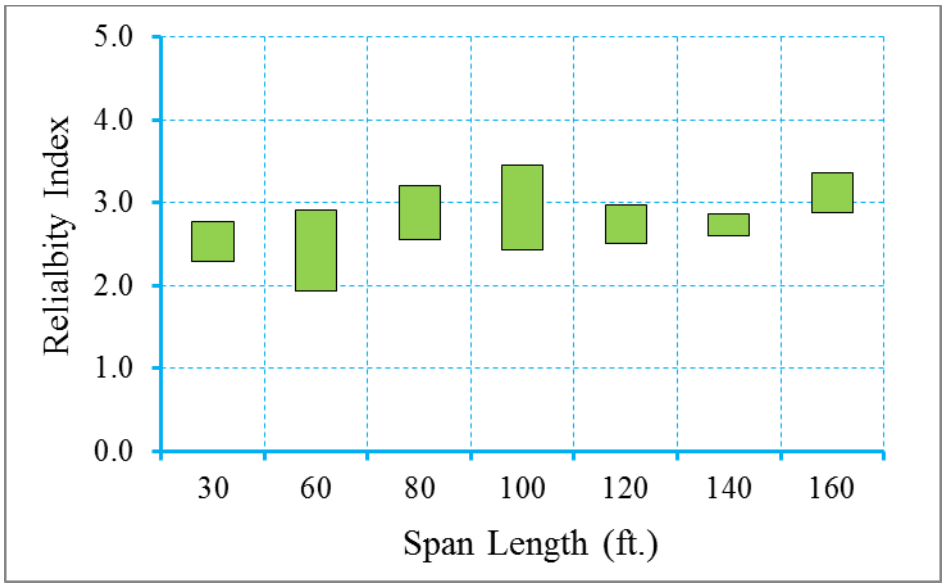

Figure D-82 Reliability Indices for Bridges at Maximum Allowable Crack Width Limit State (ADTT=10000), γLL=0.8 ($f_t = 0.158\sqrt{f_c'}$)

Step 2: Redesign the bridges with live load factor of 1.0 (Figure D-83~Figure D-85)

Since the reliability level of the original bridge database was below the target reliability level at decompression limit state and maximum allowable tensile stress limit state, the bridges were redesigned using a live load factor of 1.0. Please note that only the live load factor of Service III limit state is increased from 0.8 to 1.0, dead load and resistance factors were kept the same during the redesign. Table D-86 shows the design outcomes of the redesigned bridges.

Figure D-83 through Figure D-85 show the reliability indices for the redesigned bridges using live load factor of 1.0. It is observed that the average reliability index of decompression limit state, maximum allowable tensile stress limit state and maximum allowable crack width limit state is 1.04, 1.40, and 3.22, respectively.

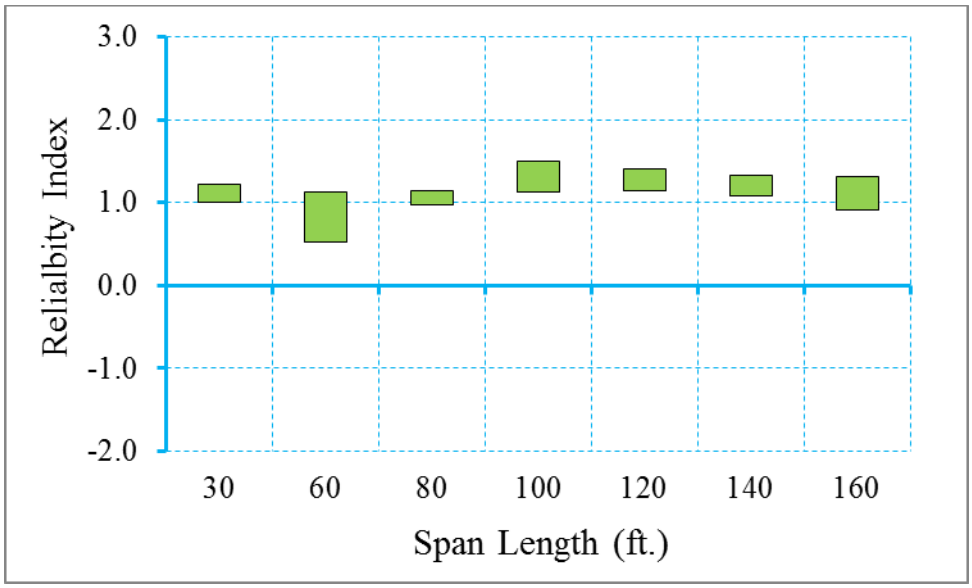

Figure D-83 Reliability Indices for Bridges at Decompression Limit State (ADTT=10000), γLL=1.0 ($f_t = 0.158\sqrt{f_c'}$)

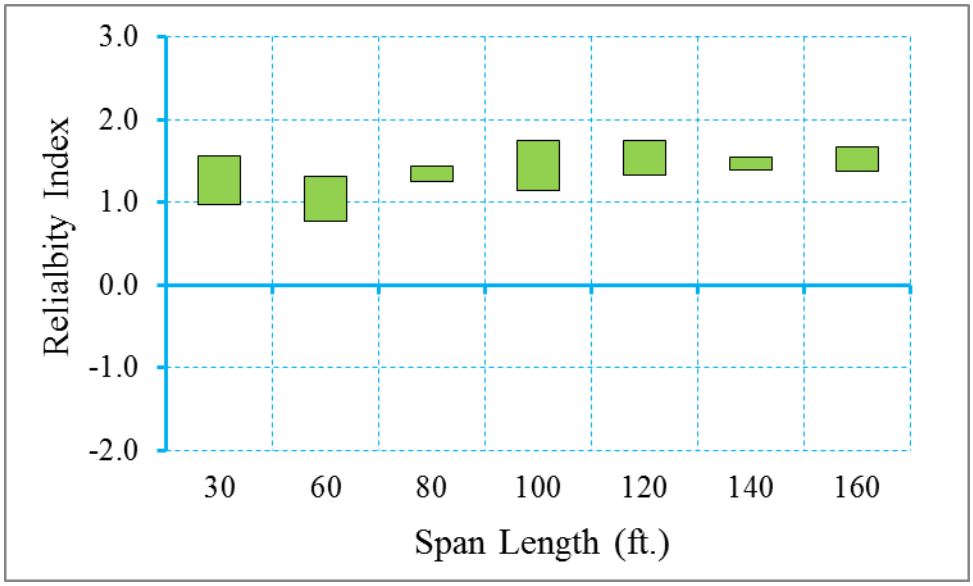

Figure D-84 Reliability Indices for Bridges at Maximum Tensile Stress Limit State (ADTT=10000), γLL=1.0 ($f_t = 0.158\sqrt{f_c'}$)

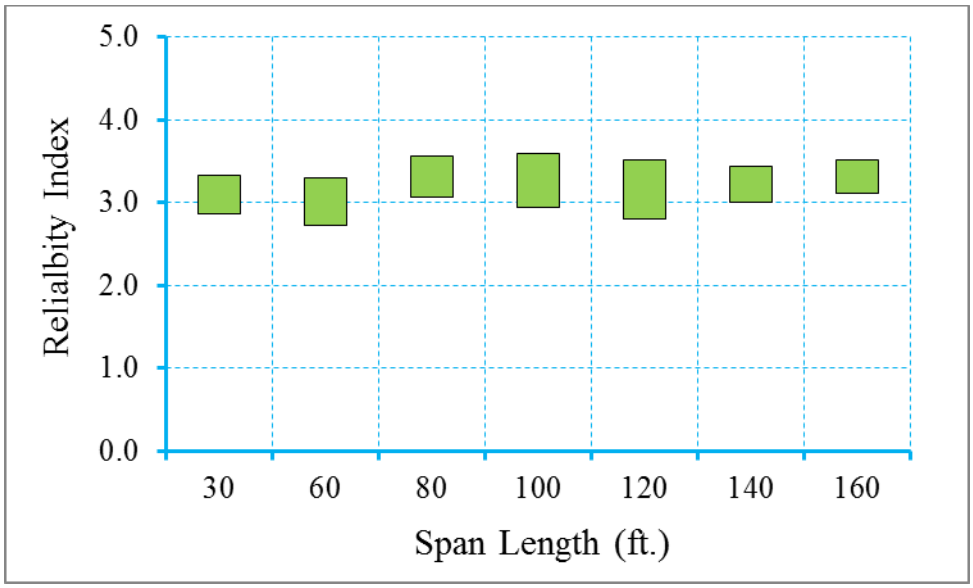

Figure D-85 Reliability Indices for Bridges at Maximum Crack Width Limit State (ADTT=10000), γLL=1.0 ($f_t = 0.158\sqrt{f_c'}$)

Step 4: Propose new live load, dead load, and/or resistance factors

Based on the calibration process shown in step 1 through step 3, it is observed that the uniform target reliability index can be achieved using a live load factor of 1.0. Therefore, for ADTT equal to 10000 and maximum concrete tensile stress of $f_t = 5\sqrt{f_c'}$, a new live load factor of 1.0 is proposed.

D.3.4.4.3 Bridges Designed for Maximum Concrete Tensile Stress of $f_t = 0.19\sqrt{f_c'}$

In this section, the calibration for a selected bridge database (shown in Table D-87) is performed for ADTT equal to 10000 and maximum concrete tensile stress of $f_t = 0.19\sqrt{f_c'}$. Please note that the allowable maximum crack width of 0.016 in is applied for maximum allowable crack width limit state.

Step 1: Calculate the reliability level of designs according to AASHTO LRFD Specifications (2010) (Figure D-86~Figure D-88)

Figure D-86 through Figure D-88 show the reliability indices for the bridges designed using AASHTO type girders according to AASHTO LRFD specifications (2010). It is observed that the average reliability index for decompression limit state, maximum allowable tensile stress limit state and maximum allowable crack width limit state is 0.64, 1.07, and 2.78, respectively, which does not satisfy the proposed target reliability index of 1.0 for decompression limit state and 1.25 for maximum allowable tensile stress limit state. Therefore, a larger live load factor will be used to modify the original design in order to improve the reliability level of the bridges.

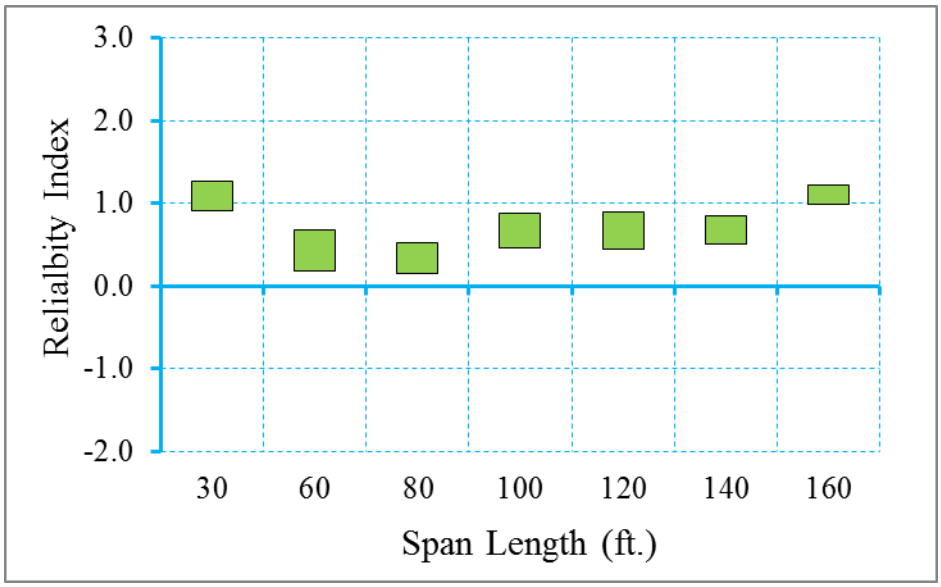

Figure D-86 Reliability Indices for Bridges at Decompression Limit State (ADTT=10000), γLL=0.8 ($f_t = 0.19\sqrt{f'_c}$)

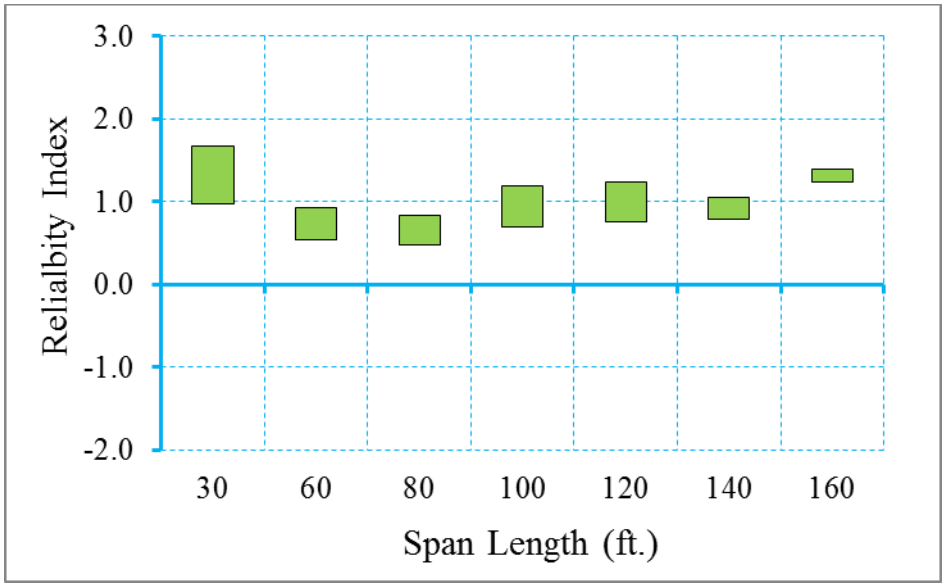

Figure D-87 Reliability Indices for Bridges at Maximum Allowable Tensile Stress Limit State (ADTT=10000), γLL=0.8 ($f_t = 0.19\sqrt{f'_c}$)

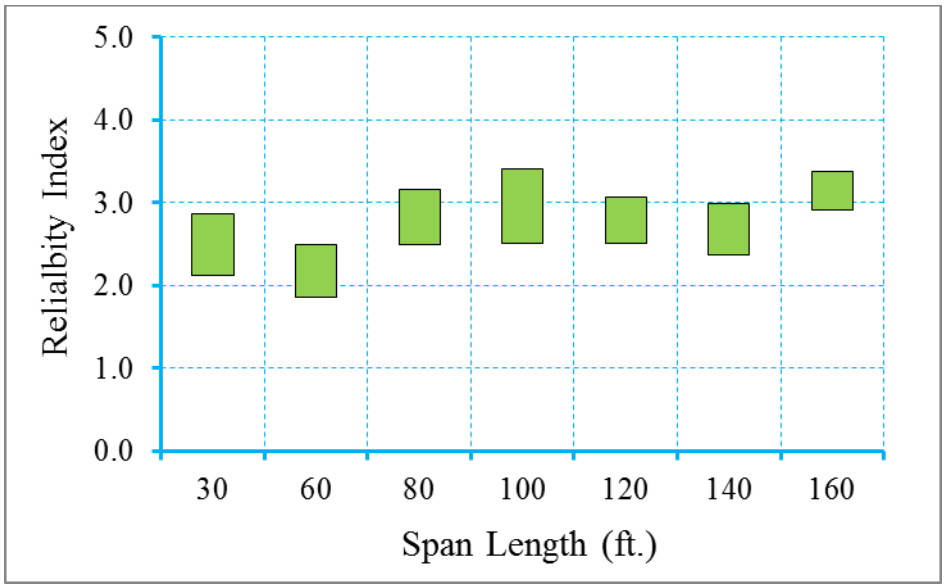

Figure D-88 Reliability Indices for Bridges at Maximum Allowable Crack Width Limit State (ADTT=10000), γLL=0.8 ($f_t = 0.19\sqrt{f_c'}$)

Step 2: Redesign the bridges with live load factor of 1.0 (Figure D-89~Figure D-91)

Since the reliability level of the original bridge database was below the target reliability level at decompression limit state and maximum allowable tensile stress limit state, the bridges were redesigned using a live load factor of 1.0. Please note that only the live load factor of Service III limit state is increased from 0.8 to 1.0, dead load and resistance factors were kept the same during the redesign. Table D-88 shows the design outcomes of the redesigned bridges.

Figure D-89 through Figure D-91 show the reliability indices for the redesigned bridges using live load factor of 1.0. It is observed that the average reliability index of decompression limit state, maximum allowable tensile stress limit state and maximum allowable crack width limit state is 0.98, 1.34, and 3.11, respectively.

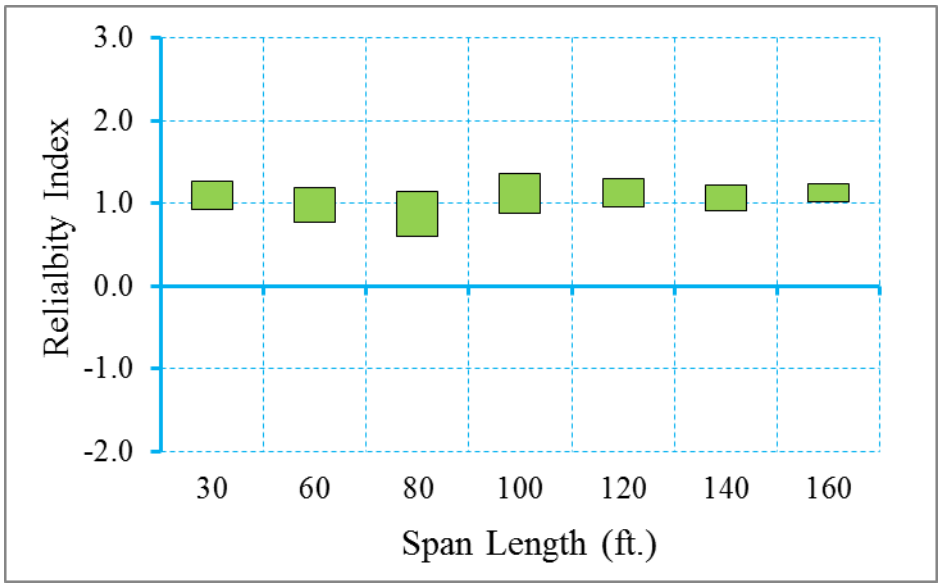

Figure D-89 Reliability Indices for Bridges at Decompression Limit State (ADTT=10000), γLL=1.0 ($f_t = 0.19\sqrt{f'_c}$)

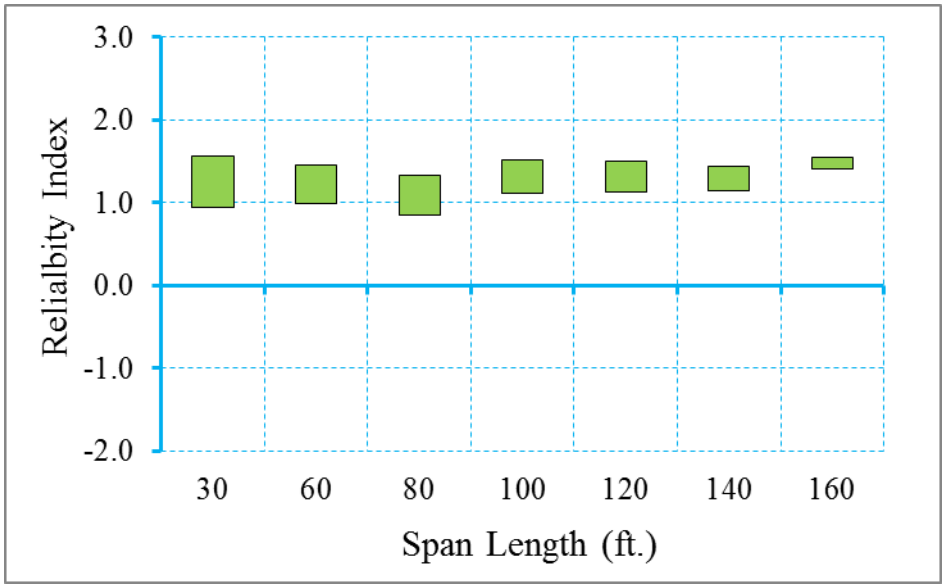

Figure D-90 Reliability Indices for Bridges at Maximum Tensile Stress Limit State (ADTT=10000), γLL=1.0 ($f_t = 0.19\sqrt{f'_c}$)

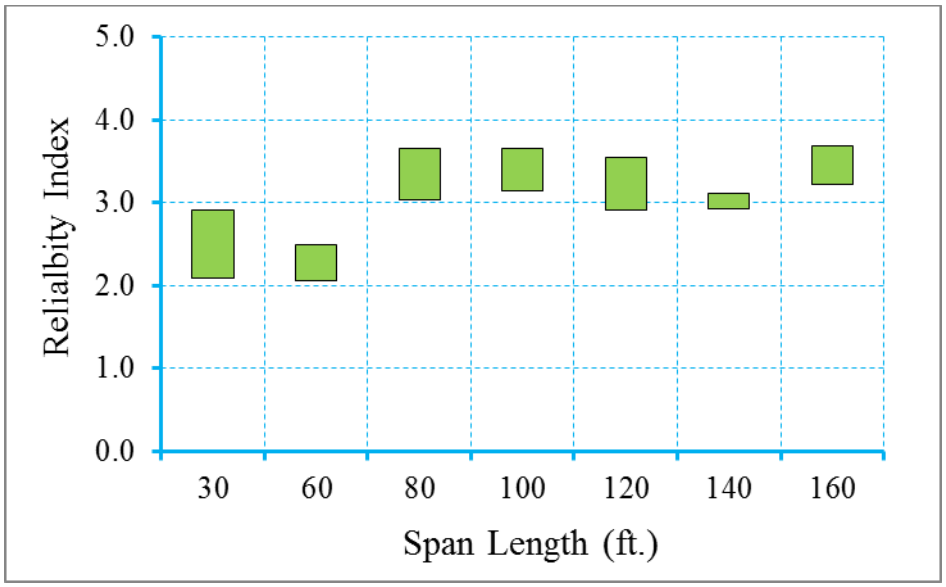

Figure D-91 Reliability Indices for Bridges at Maximum Crack Width Limit State (ADTT=10000), γLL=1.0 ($f_t = 0.19\sqrt{f_c'}$)

Step 4: Propose new live load, dead load, and/or resistance factors

Based on the calibration process shown in step 1 through step 3, it is observed that the uniform target reliability index can be achieved using a live load factor of 1.0. Therefore, for the scenario of ADTT equal to 10000 and maximum concrete tensile stress of $f_t = 0.19\sqrt{f_c'}$, a new live load factor of 1.0 is proposed.

D.3.4.4.4 Bridges Designed for Maximum Concrete Tensile Stress of $f_t = 0.253\sqrt{f_c'}$

In this section, the calibration for a selected bridge database (shown in Table D-89) is performed for ADTT equal to 10000 and maximum concrete tensile stress of $f_t = 0.253\sqrt{f_c'}$. Please note that the allowable maximum crack width of 0.016 in is applied for maximum allowable crack width limit state.

Step 1: Calculate the reliability level of designs according to AASHTO LRFD Specifications (2010) (Figure D-92~Figure D-94)

Figure D-92 through Figure D-94 show the reliability indices for the bridges designed using AASHTO type girders according to AASHTO LRFD specifications (2010). It is observed that the average reliability index for decompression limit state, maximum allowable tensile stress limit state and maximum allowable crack width limit state is 0.02, 0.41, and 2.66, respectively, which does not satisfy the proposed target reliability index of 1.0 for decompression limit state and 1.25 for maximum allowable tensile stress limit state. Therefore, a larger live load factor will be used to modify the original design in order to improve the reliability level of the bridges.

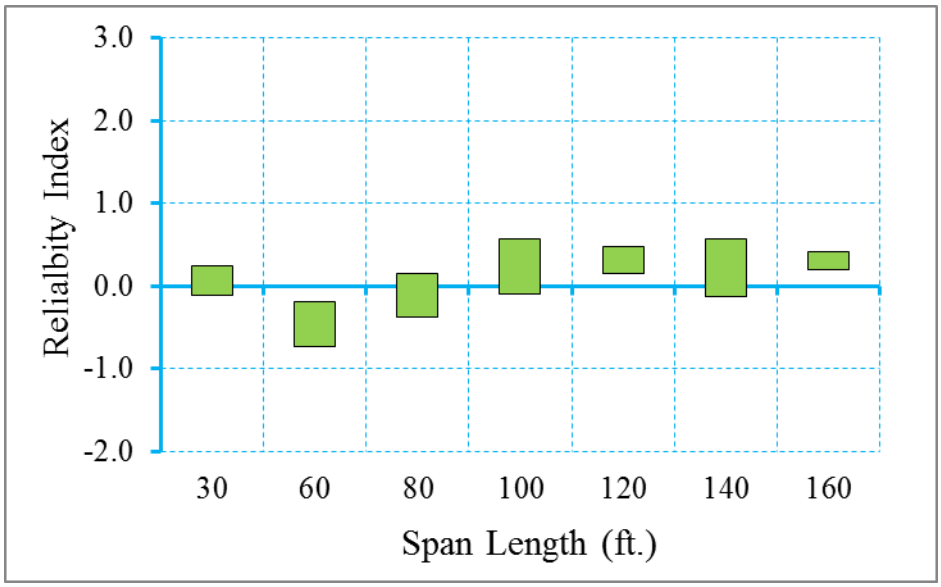

Figure D-92 Reliability Indices for Bridges at Decompression Limit State (ADTT=10000), γLL=0.8 ($f_t = 0.253\sqrt{f_c'}$)

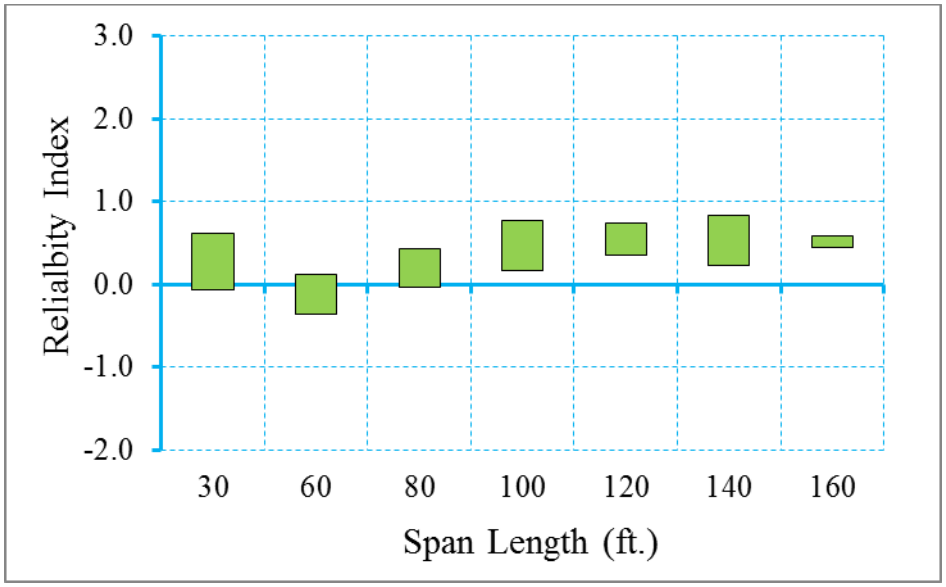

Figure D-93 Reliability Indices for Bridges at Maximum Allowable Tensile Stress Limit State (ADTT=10000), γLL=0.8 ($f_t = 0.253\sqrt{f_c'}$)

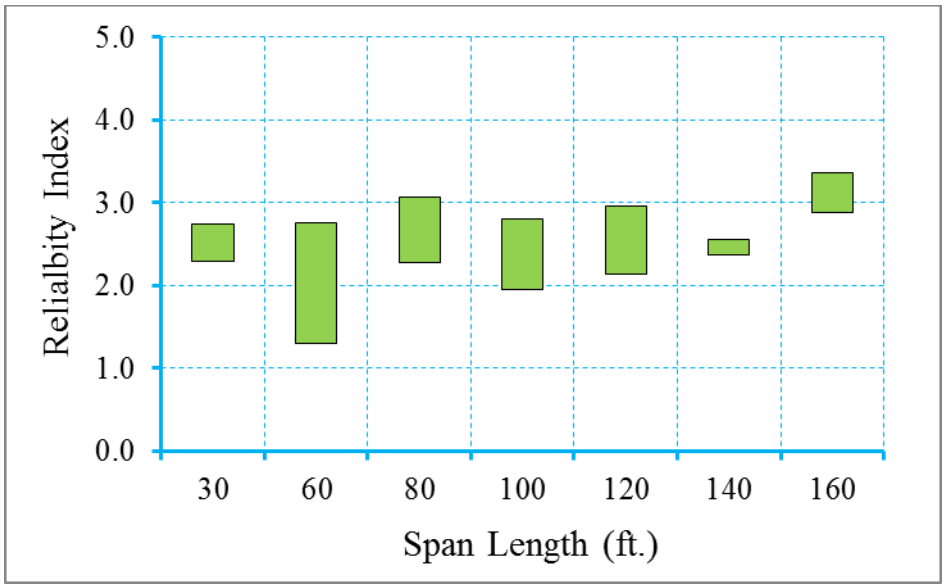

Figure D-94 Reliability Indices for Bridges at Maximum Allowable Crack Width Limit State (ADTT=10000), γLL=0.8 ($f_t = 0.253\sqrt{f_c'}$)

Step 2: Redesign the bridges with live load factor of 1.0 (Figure D-95~Figure D-97)

Since the reliability level of the original bridge database was below the target reliability level at decompression limit state and maximum allowable tensile stress limit state, the bridges were redesigned using a live load factor of 1.0. Please note that only the live load factor of Service III limit state is increased from 0.8 to 1.0, dead load and resistance factors were kept the same during the redesign. Table D-90 shows the design outcomes of the redesigned bridges.

Figure D-95 through Figure D-97 show the reliability indices for the redesigned bridges using live load factor of 1.0. It is observed that the average reliability index of decompression limit state, maximum allowable tensile stress limit state and maximum allowable crack width limit state is 0.82, 1.20, and 2.88, respectively.

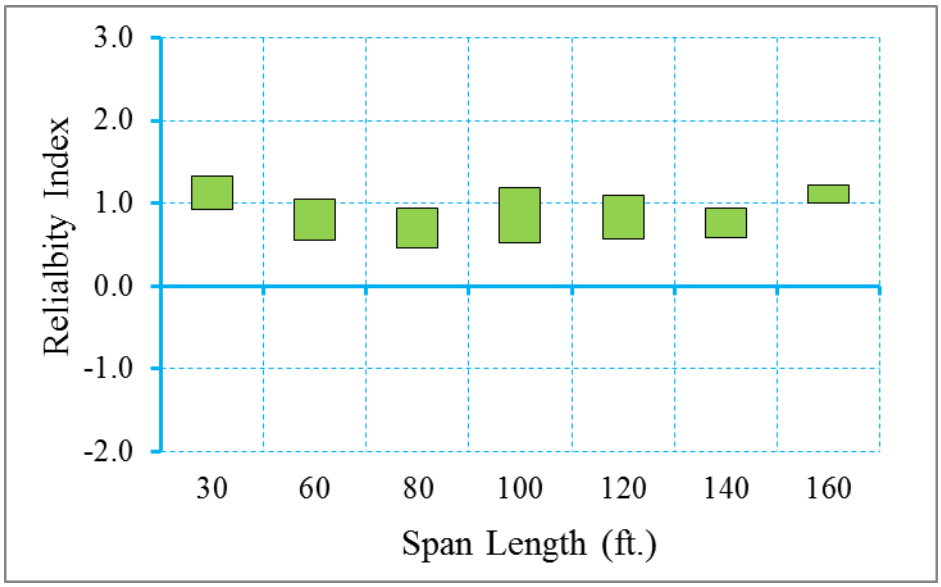

Figure D-95 Reliability Indices for Bridges at Decompression Limit State (ADTT=10000), γLL=1.0 ($f_t = 0.253\sqrt{f_c'}$)

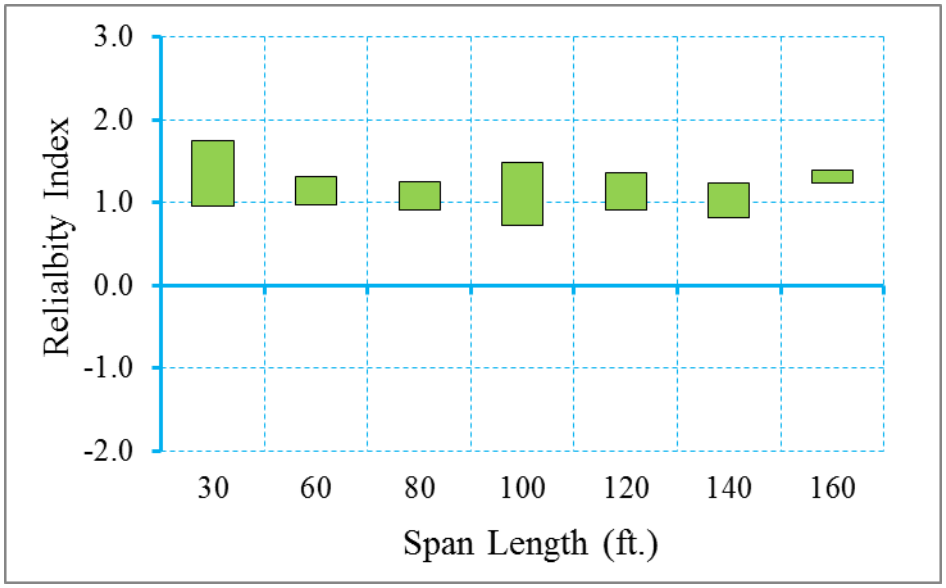

Figure D-96 Reliability Indices for Bridges at Maximum Tensile Stress Limit State (ADTT=10000), γLL=1.0 ($f_t = 0.253\sqrt{f_c'}$)

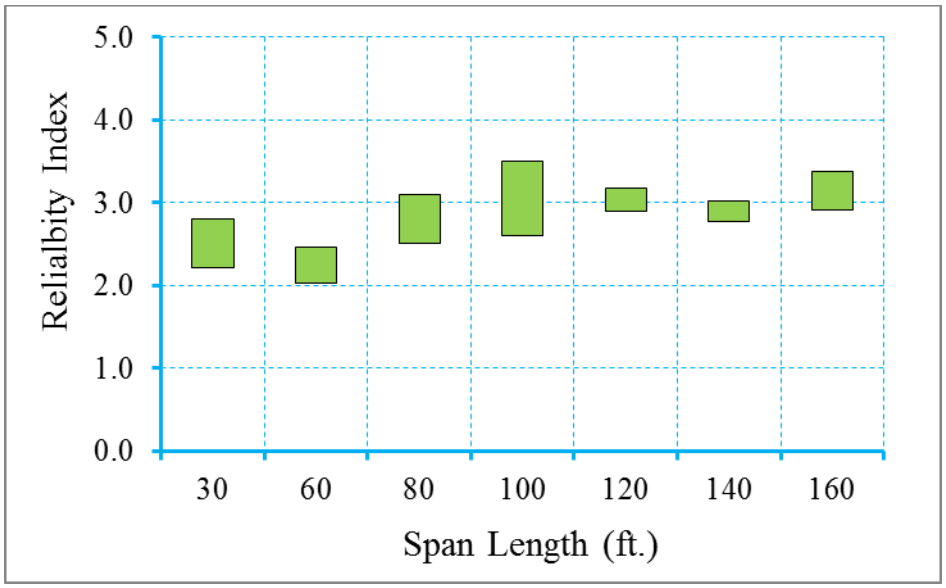

Figure D-97 Reliability Indices for Bridges at Maximum Crack Width Limit State (ADTT=10000), γLL=1.0 ($f_t = 0.253\sqrt{f_c'}$)

Step 4: Propose new live load, dead load, and/or resistance factors

Based on the calibration process shown in step 1 through step 3, it is observed that the uniform target reliability index can be achieved using a live load factor of 1.0. Therefore, for the scenario of ADTT equal to 10000 and maximum concrete tensile stress of $f_t = 0.253\sqrt{f_c'}$, a new live load factor of 1.0 is proposed.

D.4 Calibration for Other Types of Girders

D.4.1 Reliability indices of girders designed for various design criteria (Adjacent Box Girders)

In this section, the reliability analysis was performed for adjacent box girders that designed for various design criteria with compressive strength of 8000 psi. The scenario of ADTT equals to 5000 was considered in this section.

D.4.1.1 Bridges Designed for Maximum Concrete Tensile Stress of $0.0948\sqrt{f'_c}$

In this section, the calibration process for a selected bridge database (shown in Table D-91) is performed.

Table D-91 Summary Information of Bridges Designed with γLL=0.8 ($f_t = 0.0948\sqrt{f_c'}$)

Cases	Section Type	Span Length (ft.)	Spacing (ft.)	Aps (in2)	# of Strands
1	BI-36	30	3	1.224	8
2	BI-48	30	4	1.224	8
3	BI-36	60	3	2.754	18
4	BI-48	60	4	3.06	20
5	BII-36	80	3	3.672	24
6	BI-48	80	4	5.202	34
7	BIII-36	100	3	4.59	30
8	BII-48	100	4	6.732	44
9	BIV-36	120	3	6.426	42
10	BIII-48	120	4	8.262	54

Step 1: Calculate the reliability level of designs according to AASHTO LRFD Specifications (2010) (Figure D-98~Figure D-100)

Figure D-98 through Figure D-100 show the reliability indices for the bridges designed using AASHTO type girders according to AASHTO LRFD specifications (2010). It is observed that the average reliability index for decompression limit state, maximum allowable tensile stress limit state and maximum allowable crack width limit state is 1.66, 2.0, and 4.83, respectively. A larger live load factor will be used to estimate the effect of changing live load factor on reliability level of structure.

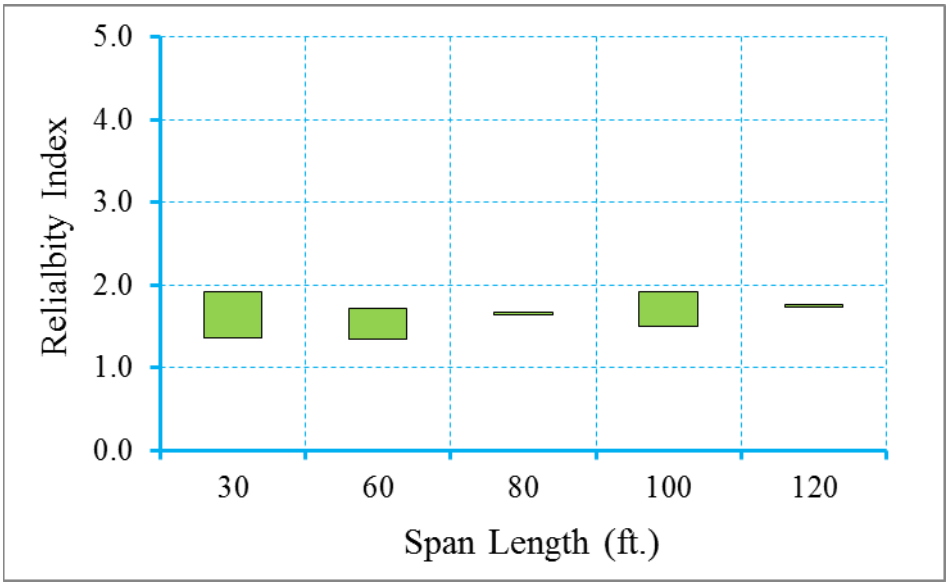

Figure D-98 Reliability Indices for Bridges at Decompression Limit State (ADTT=5000), γLL=0.8 ($f_t = 0.0948\sqrt{f_c'}$)

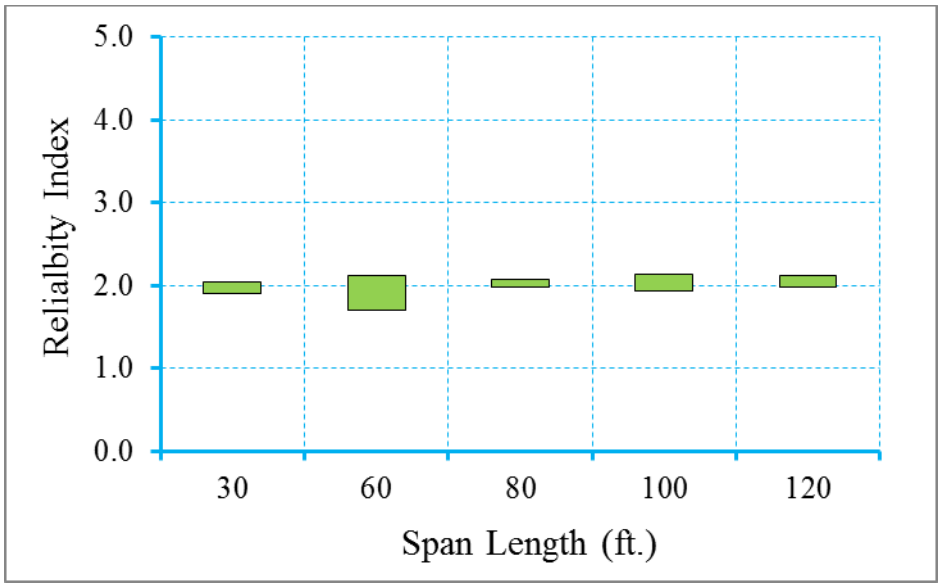

Figure D-99 Reliability Indices for Bridges at Maximum Allowable Tensile Stress Limit State (ADTT=5000), γLL=0.8 ($f_t = 0.0948\sqrt{f_c'}$)

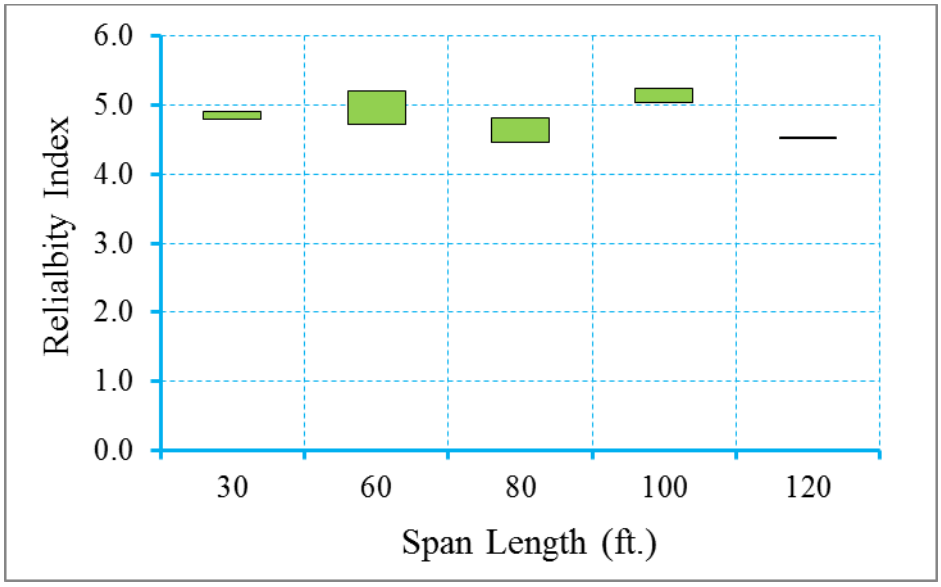

Figure D-100 Reliability Indices for Bridges at Maximum Allowable Crack Width Limit State (ADTT=5000), γLL=0.8 ($f_t = 0.0948\sqrt{f_c'}$)

Step 2: Redesign the bridges with live load factor of 1.0 (Figure D-101~Figure D-103)

In this step, the bridges have been redesigned using a live load factor of 1.0. Please note that only the live load factor of Service III limit state is increased from 0.8 to 1.0, dead load and resistance factors were kept the same during the redesign. Table D-92 shows the design outcomes of the redesigned bridges.

Figure D-101 through Figure D-103 shows the reliability indices for the redesigned bridges using live load factor of 1.0. It is observed the average reliability index of decompression limit state, maximum allowable tensile stress limit state and maximum allowable crack width limit state is 1.85, 2.18, and 4.96, respectively.

Table D-92 Summary Information of Bridges Designed with γLL=1.0 ($f_t = 0.0948\sqrt{f_c'}$)

Cases	Section Type	Span Length (ft.)	Spacing (ft.)	Aps (in2)	# of Strands
1	BI-36	30	3	1.224	8
2	BI-48	30	4	1.53	10
3	BI-36	60	3	2.754	18
4	BI-48	60	4	3.366	22
5	BII-36	80	3	3.672	24
6	BI-48	80	4	5.814	38
7	BIII-36	100	3	4.896	32
8	BII-48	100	4	7.038	46
9	BIV-36	120	3	6.732	44
10	BIII-48	120	4	8.874	58

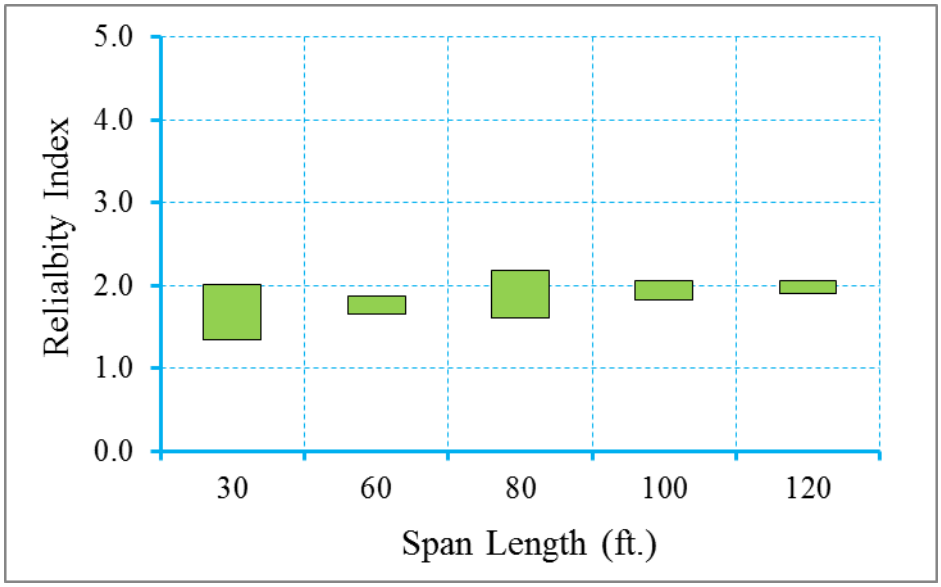

Figure D-101 Reliability Indices for Bridges at Decompression Limit State (ADTT=5000), γLL=1.0 ($f_t = 0.0948\sqrt{f_c'}$)

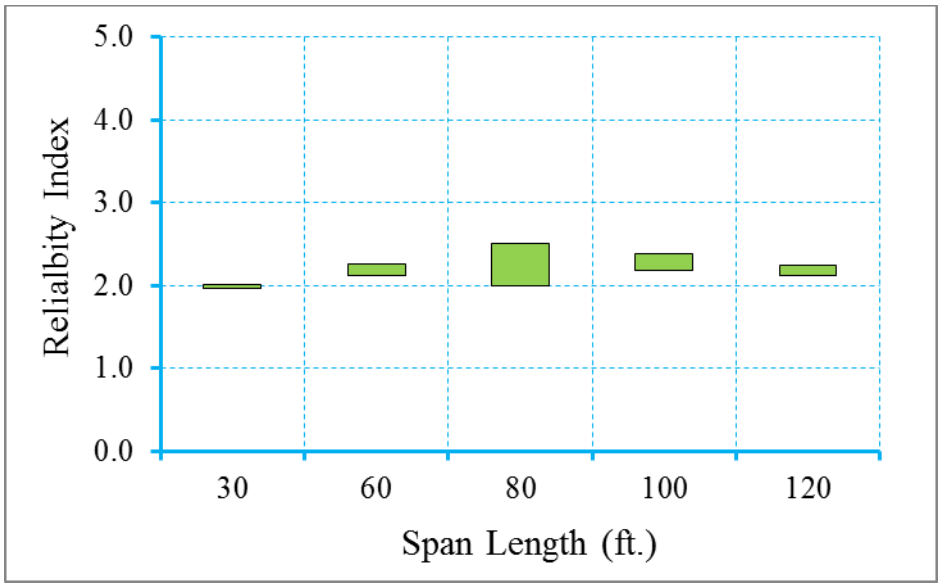

Figure D-102 Reliability Indices for Bridges at Maximum Tensile Stress Limit State (ADTT=5000), γLL=1.0 ($f_t = 0.0948\sqrt{f_c'}$)

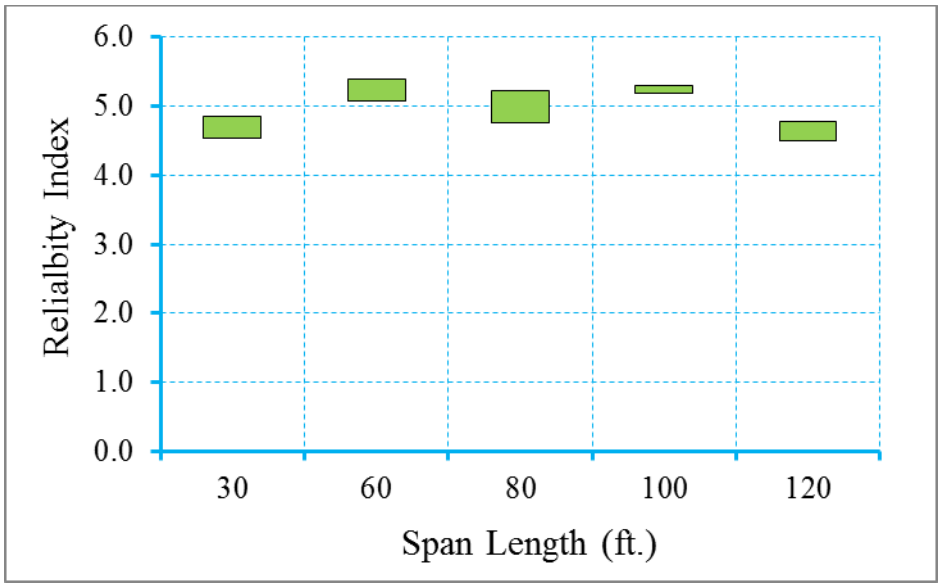

Figure D-103 Reliability Indices for Bridges at Maximum Crack Width Limit State (ADTT=5000), γLL=1.0 ($f_t = 0.0948\sqrt{f_c'}$)

Step 3: Propose new live load, dead load, and/or resistance factors

Based on the calibration process shown in step 1 through step 3, it is observed that the uniform target reliability index can be achieved using a live load factor of 1.0. Therefore, for the scenario of ADTT equal to 5000 and maximum concrete tensile stress of $f_t = 0.0948\sqrt{f_c'}$, a new live load factor of 1.0 is proposed.

D.4.1.2 C7.2 Bridges Designed for Maximum Concrete Tensile Stress of $0.158\sqrt{f'_c}$

In this section, the calibration process for a selected bridge database (shown in Table D-93) is performed.

Table D-93 Summary Information of Bridges Designed with γLL=0.8 ($f_t = 0.158\sqrt{f'_c}$)

Cases	Section Type	Span Length (ft.)	Spacing (ft.)	Aps (in2)	# of Strands
1	BI-36	30	3	0.918	6
2	BI-48	30	4	0.918	6
3	BI-36	60	3	2.448	16
4	BI-48	60	4	2.754	18
5	BII-36	80	3	3.366	22
6	BI-48	80	4	4.896	32
7	BIII-36	100	3	4.284	28
8	BII-48	100	4	6.12	40
9	BIV-36	120	3	5.814	38
10	BIII-48	120	4	7.65	50

Step 1: Calculate the reliability level of designs according to AASHTO LRFD Specifications (2010) (Figure D-104~Figure D-106)

Figure D-104 through Figure D-106 show the reliability indices for the bridges designed using AASHTO type girders according to AASHTO LRFD specifications (2010). It is observed that the average reliability index for decompression limit state, maximum allowable tensile stress limit state and maximum allowable crack width limit state is 1.12, 1.45, and 4.41, respectively. Live load factor of 1.0 will be used in next step.

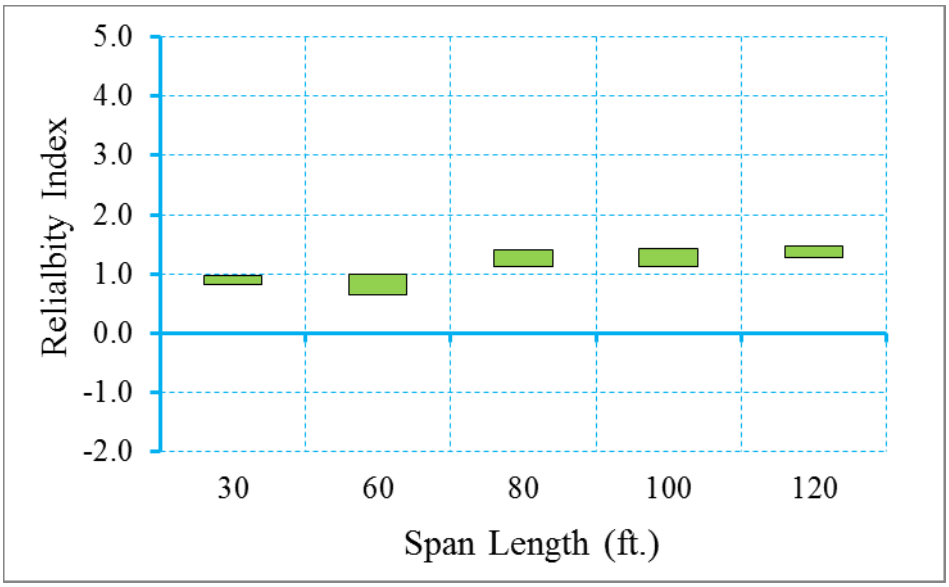

Figure D-104 Reliability Indices for Bridges at Decompression Limit State (ADTT=5000), γLL=0.8 ($f_t = 0.158\sqrt{f'_c}$)

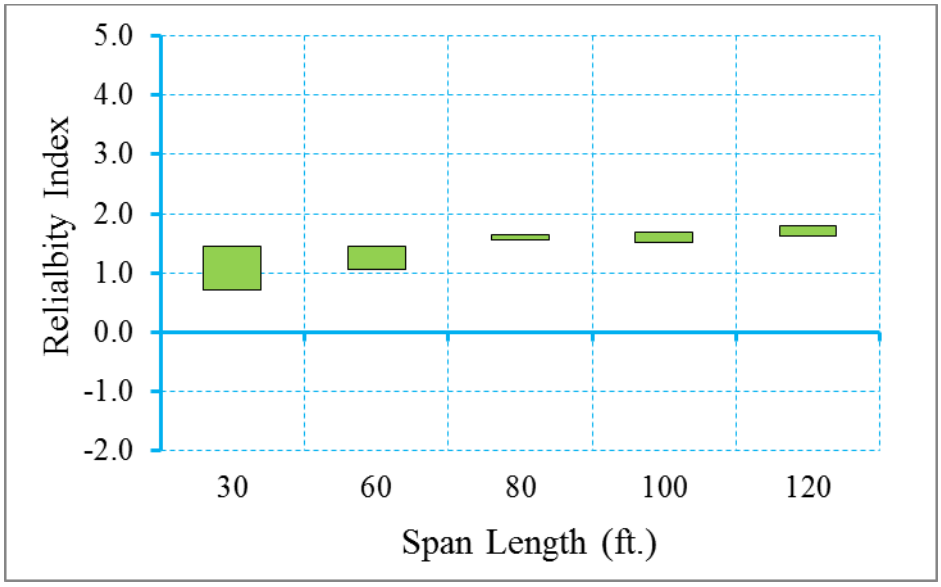

Figure D-105 Reliability Indices for Bridges at Maximum Allowable Tensile Stress Limit State (ADTT=5000), γLL=0.8 ($f_t = 0.158\sqrt{f'_c}$)

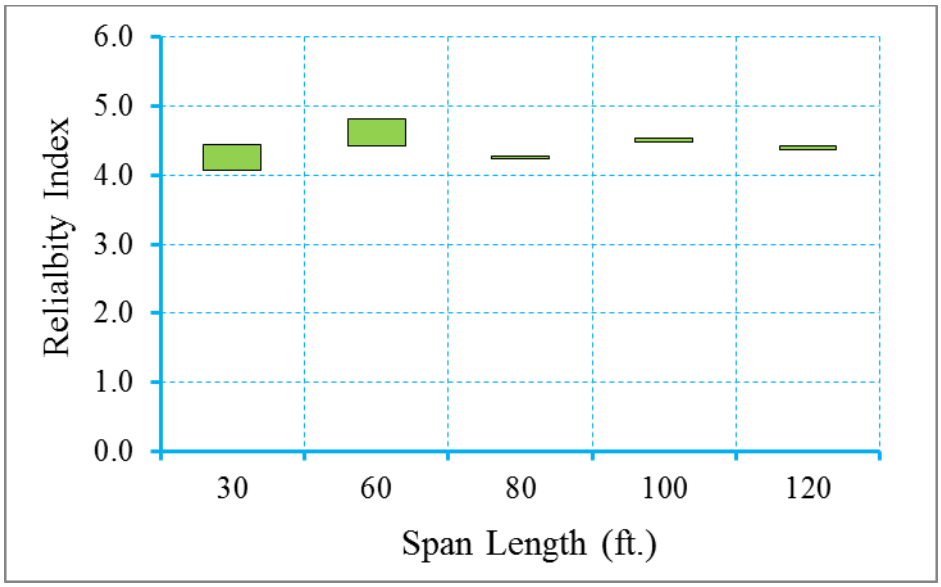

Figure D-106 Reliability Indices for Bridges at Maximum Allowable Crack Width Limit State (ADTT=5000), γLL=0.8 ($f_t = 0.158\sqrt{f_c'}$)

Step 2: Redesign the bridges with live load factor of 1.0 (Figure D-107~Figure D-109)

The bridges have been redesigned using a live load factor of 1.0. Please note that only the live load factor of Service III limit state is increased from 0.8 to 1.0, dead load and resistance factors were kept the same during the redesign. Table D-94 shows the design outcomes of the redesigned bridges.

Figure D-107 through Figure D-109 show the reliability indices for the redesigned bridges using live load factor of 1.0. It is observed that the average reliability index of decompression limit state, maximum allowable tensile stress limit state and maximum allowable crack width limit state is 1.39, 1.75, and 4.62, respectively.

Table D-94 Summary Information of Bridges Designed with γLL=1.0 ($f_t = 0.158\sqrt{f_c'}$)

Cases	Section Type	Span Length (ft.)	Spacing (ft.)	Aps (in2)	# of Strands
1	BI-36	30	3	0.918	6
2	BI-48	30	4	0.918	6
3	BI-36	60	3	2.448	16
4	BI-48	60	4	3.06	20
5	BII-36	80	3	3.366	22
6	BI-48	80	4	5.508	36
7	BIII-36	100	3	4.59	30
8	BII-48	100	4	6.732	44
9	BIV-36	120	3	6.12	40
10	BIII-48	120	4	8.262	54

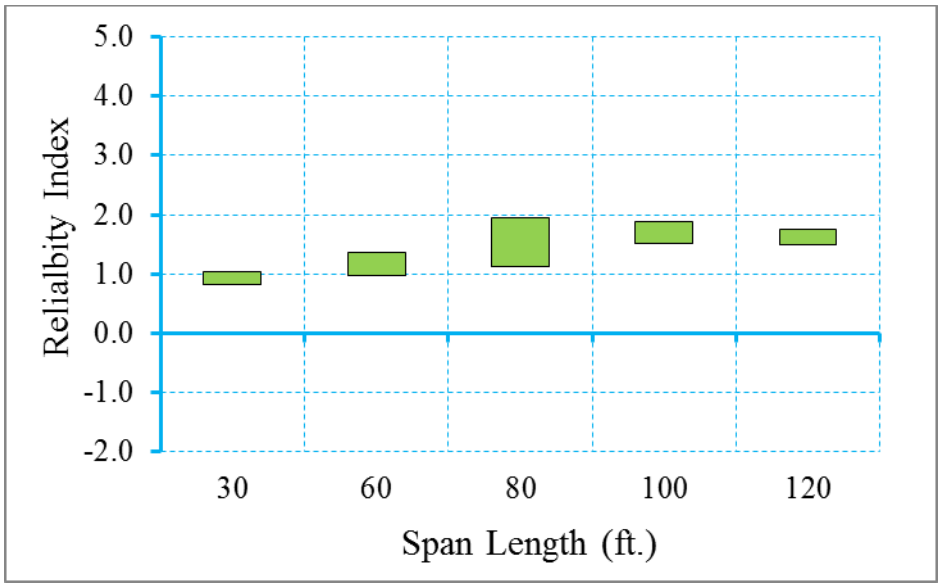

Figure D-107 Reliability Indices for Bridges at Decompression Limit State (ADTT=5000), γLL=1.0 ($f_t = 0.158\sqrt{f_c'}$)

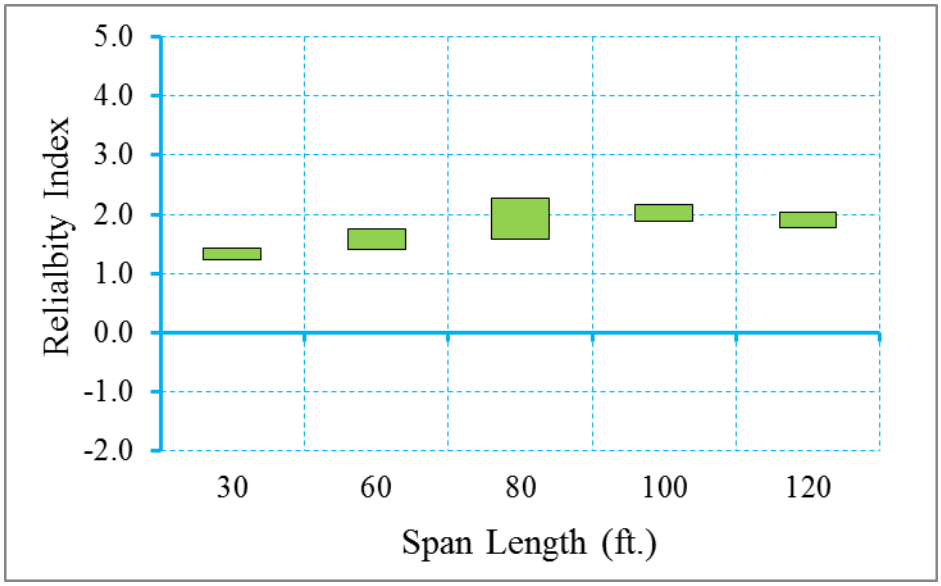

Figure D-108 Reliability Indices for Bridges at Maximum Tensile Stress Limit State (ADTT=5000), γLL=1.0 ($f_t = 0.158\sqrt{f_c'}$)

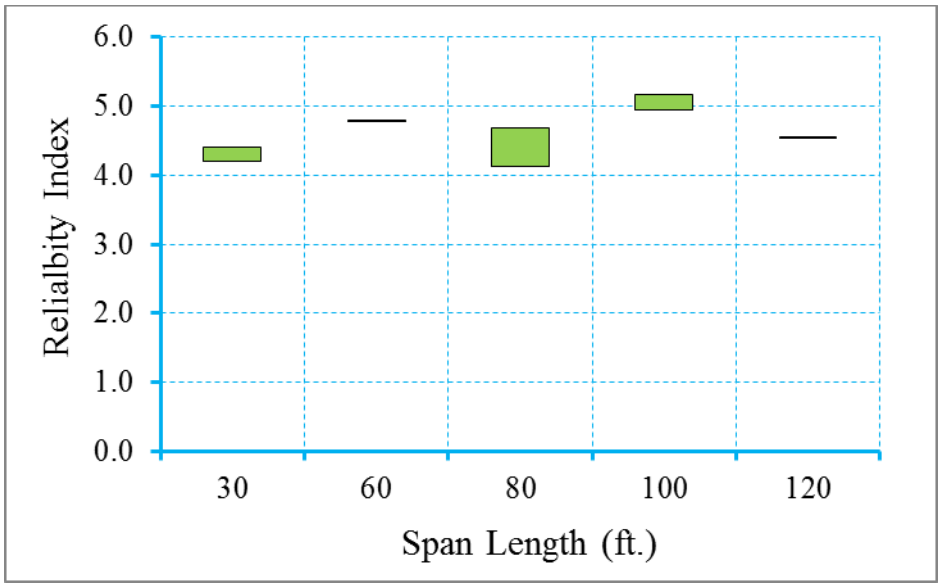

Figure D-109 Reliability Indices for Bridges at Maximum Crack Width Limit State (ADTT=5000), γLL=1.0 ($f_t = 0.158\sqrt{f'_c}$)

Step 3: Propose new live load, dead load, and/or resistance factors

Based on the calibration process shown in step 1 through step 3, it is observed that the uniform target reliability index can be achieved using a live load factor of 1.0. Therefore, for the scenario of ADTT equal to 5000 and maximum concrete tensile stress of $f_t = 0.158\sqrt{f'_c}$, a new live load factor of 1.0 is proposed.

D.4.1.3 Bridges Designed for Maximum Concrete Tensile Stress of $0.19\sqrt{f'_c}$

In this section, the calibration process for a selected bridge database (shown in Table D-95) is performed for the scenario of ADTT equal to 5000.

Table D-95 Summary Information of Bridges Designed with γLL=0.8 ($f_t = 0.19\sqrt{f'_c}$)

Cases	Section Type	Span Length(ft.)	Spacing (ft.)	Aps (in2)	# of Strands
1	BI-36	30	3	0.918	6
2	BI-48	30	4	0.918	6
3	BI-36	60	3	2.448	16
4	BI-48	60	4	2.754	18
5	BII-36	80	3	3.06	20
6	BI-48	80	4	4.896	32
7	BIII-36	100	3	4.284	28
8	BII-48	100	4	6.12	40
9	BIV-36	120	3	5.814	38
10	BIII-48	120	4	7.344	48

Step 1: Calculate the reliability level of designs according to AASHTO LRFD Specifications (2010) (Figure D-110~Figure D-112)

Figure D-110 through Figure D-112 show the reliability indices for the bridges designed using AASHTO type girders according to AASHTO LRFD specifications (2010). It is observed that the average reliability index for decompression limit state, maximum allowable tensile stress limit state and maximum allowable crack width limit state is 1.06, 1.34, and 4.37, respectively. Since the reliability indices are lower than target reliability index, live load factor of 1.0 will be used in next step.

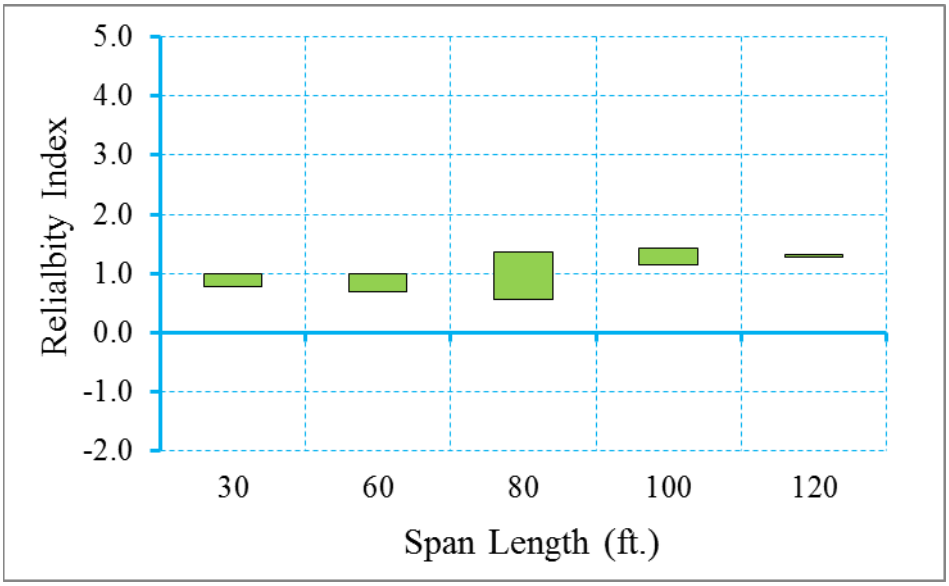

Figure D-110 Reliability Indices for Bridges at Decompression Limit State (ADTT=5000), γLL=0.8 ($f_t = 0.19\sqrt{f_c'}$)

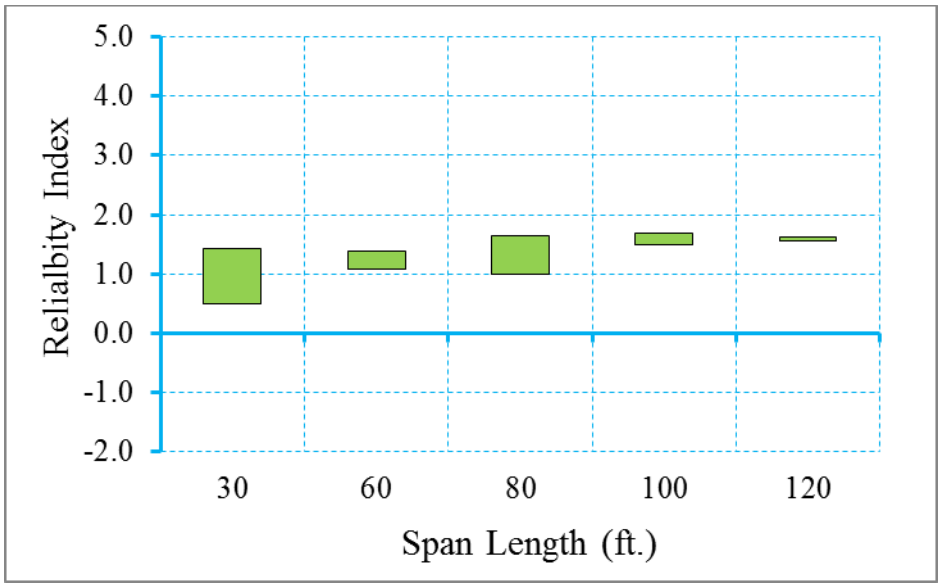

Figure D-111 Reliability Indices for Bridges at Maximum Allowable Tensile Stress Limit State (ADTT=5000), γLL=0.8 ($f_t = 0.19\sqrt{f_c'}$)

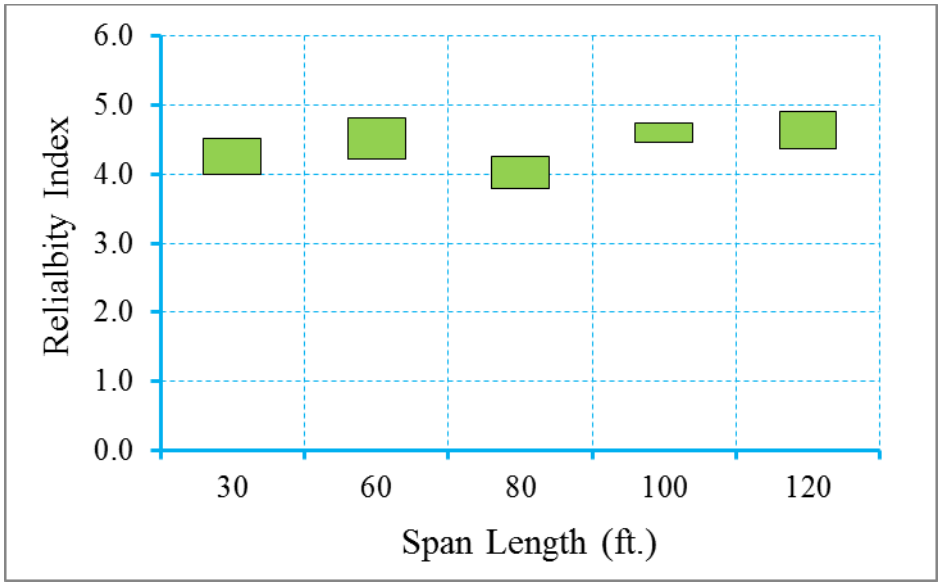

Figure D-112 Reliability Indices for Bridges at Maximum Allowable Crack Width Limit State (ADTT=5000), γLL=0.8 ($f_t = 0.19\sqrt{f_c'}$)

Step 2: Redesign the bridges with live load factor of 1.0 (Figure D-113~Figure D-115)

The bridges have been redesigned using a live load factor of 1.0. Please note that only the live load factor of Service III limit state is increased from 0.8 to 1.0, dead load and resistance factors were kept the same during the redesign. Table D-96 shows the design outcomes of the redesigned bridges.

Figure 116 through Figure 118 show the reliability indices for the redesigned bridges using live load factor of 1.0. It is observed that the average reliability index of decompression limit state, maximum allowable tensile stress limit state and maximum allowable crack width limit state is 1.31, 1.55, and 4.56, respectively.

Table D-96 Summary Information of Bridges Designed with γLL=1.0 ($f_t = 0.19\sqrt{f_c'}$)

Cases	Section Type	Span Length (ft.)	Spacing (ft.)	Aps (in2)	# of Strands
1	BI-36	30	3	0.918	6
2	BI-48	30	4	0.918	6
3	BI-36	60	3	2.448	16
4	BI-48	60	4	3.06	20
5	BII-36	80	3	3.366	22
6	BI-48	80	4	5.202	34
7	BIII-36	100	3	4.284	28
8	BII-48	100	4	6.426	42
9	BIV-36	120	3	6.12	40
10	BIII-48	120	4	7.956	52

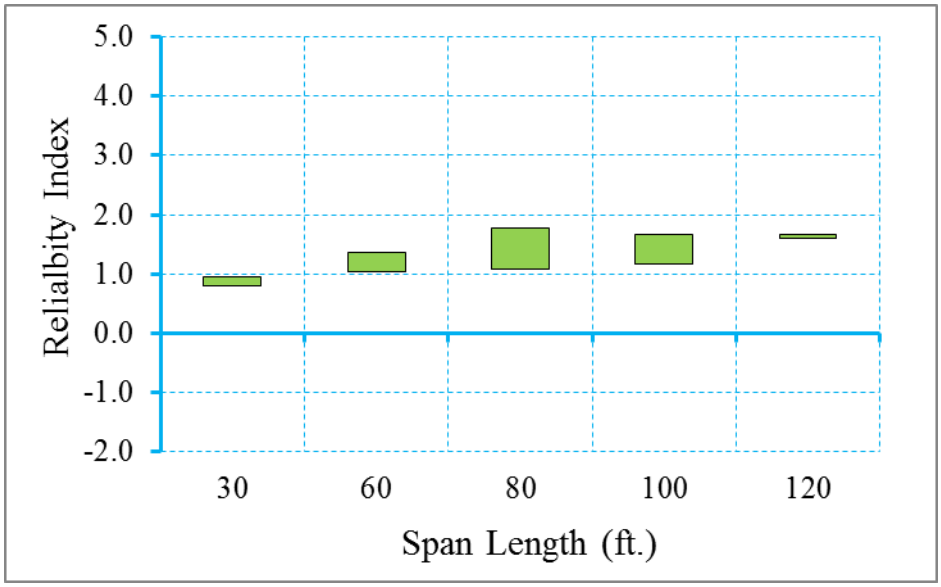

Figure D-113 Reliability Indices for Bridges at Decompression Limit State (ADTT=5000), γLL=1.0 ($f_t = 0.19\sqrt{f_c'}$)

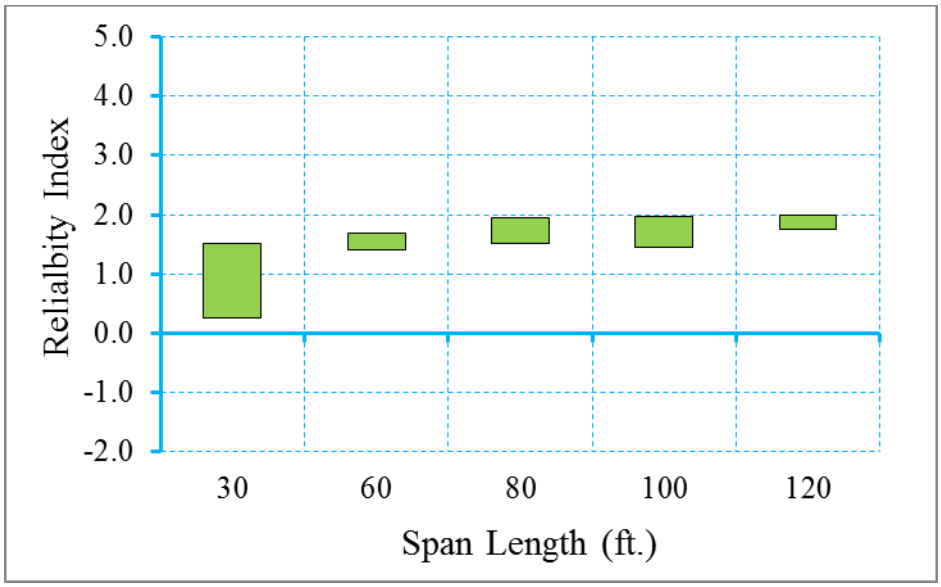

Figure D-114 Reliability Indices for Bridges at Maximum Tensile Stress Limit State (ADTT=5000), γLL=1.0 ($f_t = 0.19\sqrt{f_c'}$)

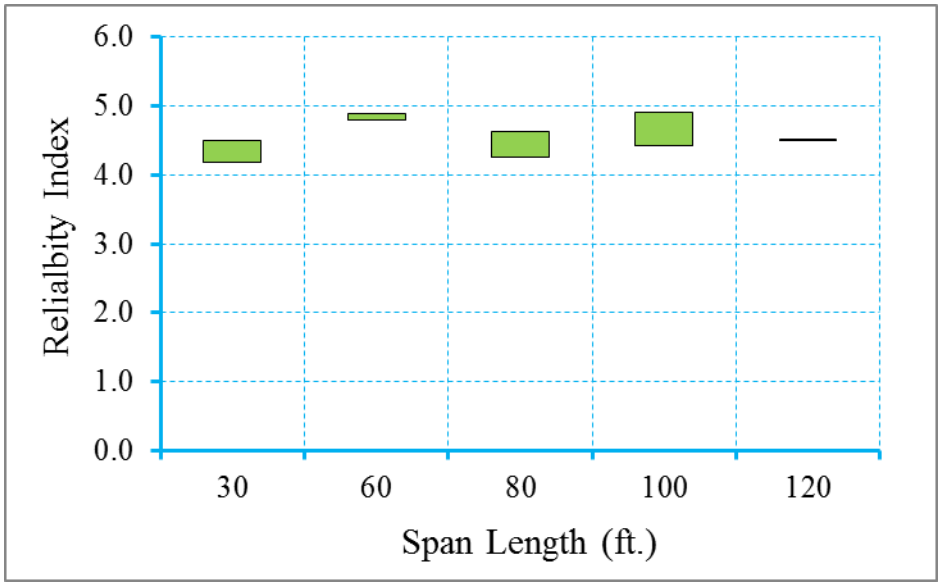

Figure D-115 Reliability Indices for Bridges at Maximum Crack Width Limit State (ADTT=5000), γLL=1.0 ($f_t = 0.19\sqrt{f_c'}$)

Step 3: Propose new live load, dead load, and/or resistance factors

Based on the calibration process shown in step 1 through step 3, it is observed that the uniform target reliability index can be achieved using a live load factor of 1.0. Therefore, for the scenario of ADTT equal to 5000 and maximum concrete tensile stress of $f_t = 0.19\sqrt{f_c'}$, a new live load factor of 1.0 is proposed.

D.4.1.4 Bridges Designed for Maximum Concrete Tensile Stress of $0.253\sqrt{f'_c}$

In this section, the calibration for a selected bridge database (shown in Table D-97) is performed for a scenario of ADTT equal to 5000. Please note that the maximum allowable crack width is specified as 0.016 in for maximum allowable crack width limit state.

Step 1: Calculate the reliability level of designs according to AASHTO LRFD Specifications (2010) (Figure D-116~Figure D-118)

Figure D-116 through Figure D-118 show the reliability indices for the bridges designed using AASHTO type girders according to AASHTO LRFD specifications (2010). It is observed that the average reliability index for decompression limit state, maximum allowable tensile stress limit state and maximum allowable crack width limit state is 0.68, 0.86, and 4.14, respectively. Live load factor of 1.0 will be used to estimate the effect of changing live load factor on reliability level.

Table D-97 Summary Information of Bridges Designed with γLL=0.8 ($f_t = 0.253\sqrt{f'_c}$)

Cases	Section Type	Span Length (ft.)	Spacing (ft.)	Aps (in2)	# of Strands
1	BI-36	30	3	0.612	4
2	BI-48	30	4	0.612	4
3	BI-36	60	3	2.142	14
4	BI-48	60	4	2.448	16
5	BII-36	80	3	3.06	20
6	BI-48	80	4	4.59	30
7	BIII-36	100	3	3.978	26
8	BII-48	100	4	5.814	38
9	BIV-36	120	3	5.508	36
10	BIII-48	120	4	7.038	46

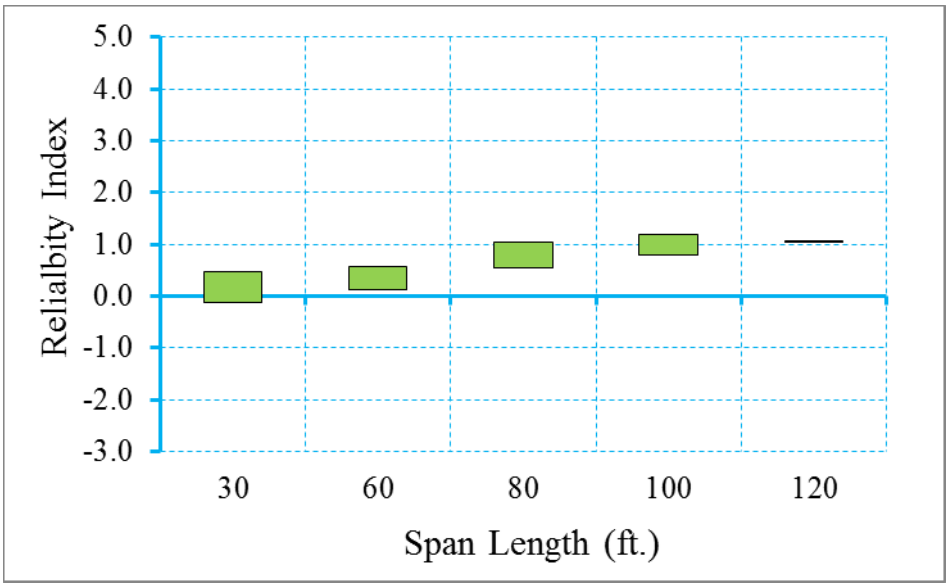

Figure D-116 Reliability Indices for Bridges at Decompression Limit State (ADTT=5000), γLL=0.8 ($f_t = 0.253\sqrt{f'_c}$)

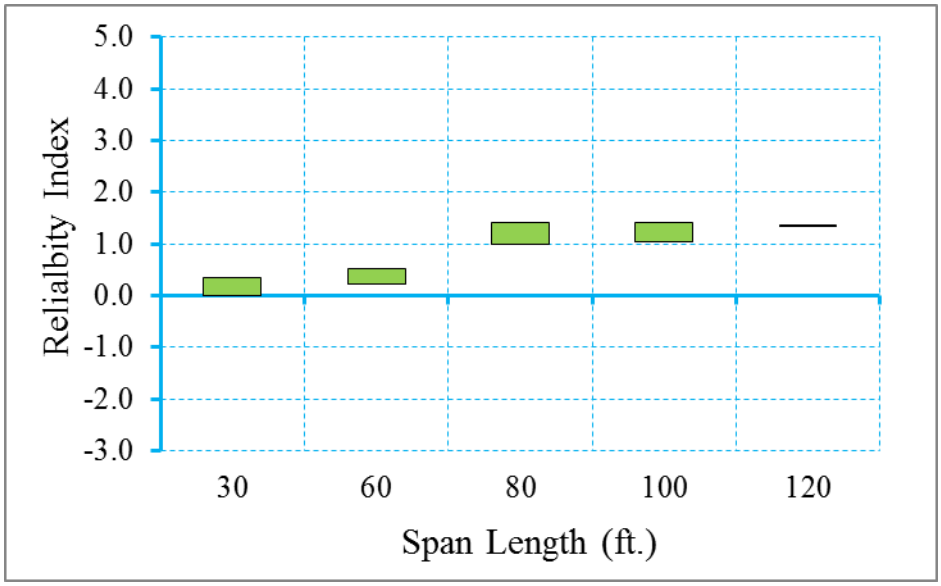

Figure D-117 Reliability Indices for Bridges at Maximum Allowable Tensile Stress Limit State (ADTT=5000), γLL=0.8 ($f_t = 0.253\sqrt{f'_c}$)

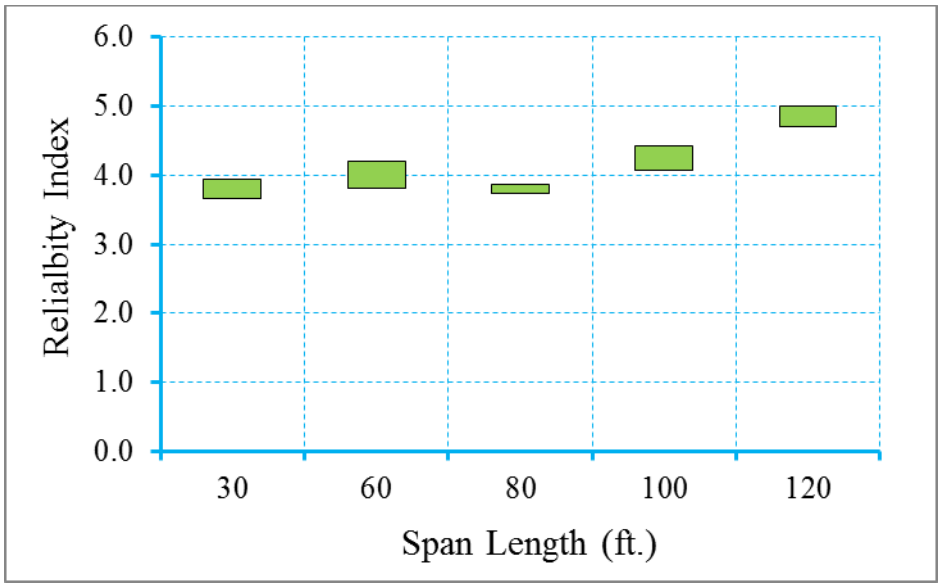

Figure D-118 Reliability Indices for Bridges at Maximum Allowable Crack Width Limit State (ADTT=5000), γLL=0.8 ($f_t = 0.253\sqrt{f_c'}$)

Step 2: Redesign the bridges with live load factor of 1.0 (Figure D-119~Figure D-121)

In this step, the bridges were redesigned using a live load factor of 1.0. Please note that only the live load factor of Service III limit state is increased from 0.8 to 1.0, dead load and resistance factors were kept the same during the redesign. Table D-98 shows the design outcomes of the redesigned bridges.

Figure D-119 through Figure D-121 show the reliability indices for the redesigned bridges using a live load factor of 1.0. It is observed that the average reliability index for the decompression limit state, the maximum allowable tensile stress limit state and the maximum allowable crack width limit state is 0.76, 1.17, and 4.18, respectively.

Table D-98 Summary Information of Bridges Designed with γLL=1.0 ($f_t = 0.253\sqrt{f_c'}$)

Cases	Section Type	Span Length (ft.)	Spacing (ft.)	Aps (in2)	# of Strands
1	BI-36	30	3	0.612	4
2	BI-48	30	4	0.612	4
3	BI-36	60	3	2.142	14
4	BI-48	60	4	2.754	18
5	BII-36	80	3	3.06	20
6	BI-48	80	4	4.896	32
7	BIII-36	100	3	3.978	26
8	BII-48	100	4	6.12	40
9	BIV-36	120	3	5.814	38
10	BIII-48	120	4	7.344	48

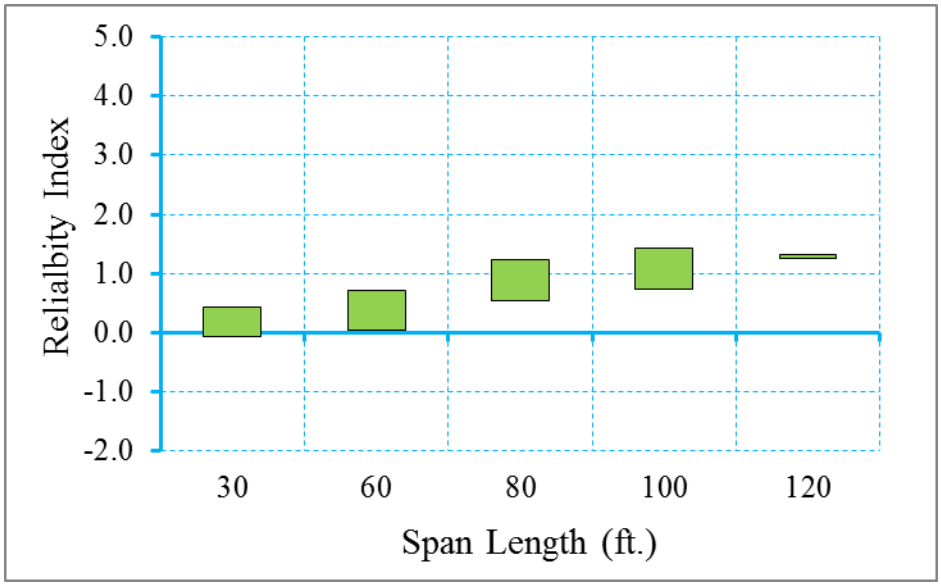

Figure D-119 Reliability Indices for Bridges at Decompression Limit State (ADTT=5000), γLL=1.0 ($f_t = 0.253\sqrt{f_c'}$)

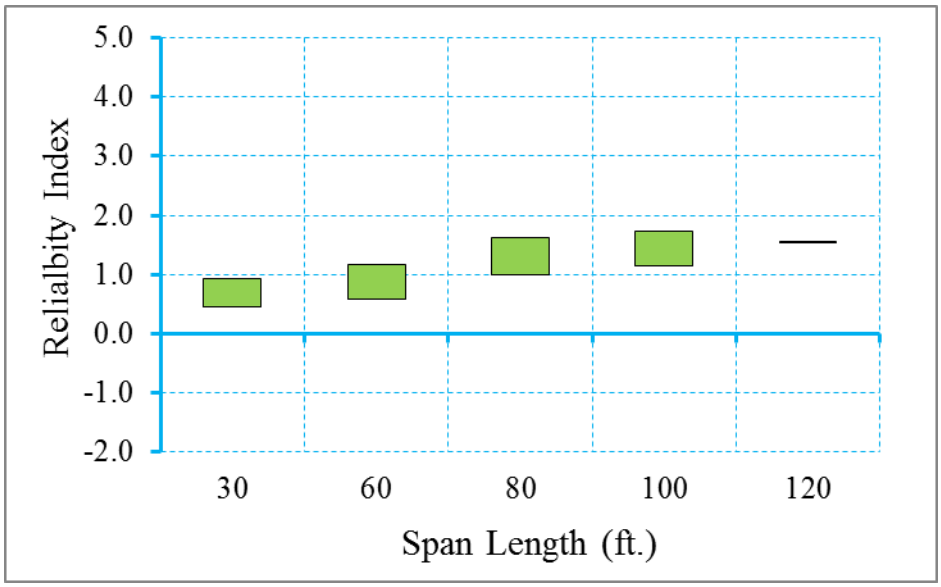

Figure D-120 Reliability Indices for Bridges at Maximum Allowable Tensile Stress Limit State (ADTT=5000), γLL=1.0 ($f_t = 0.253\sqrt{f_c'}$)

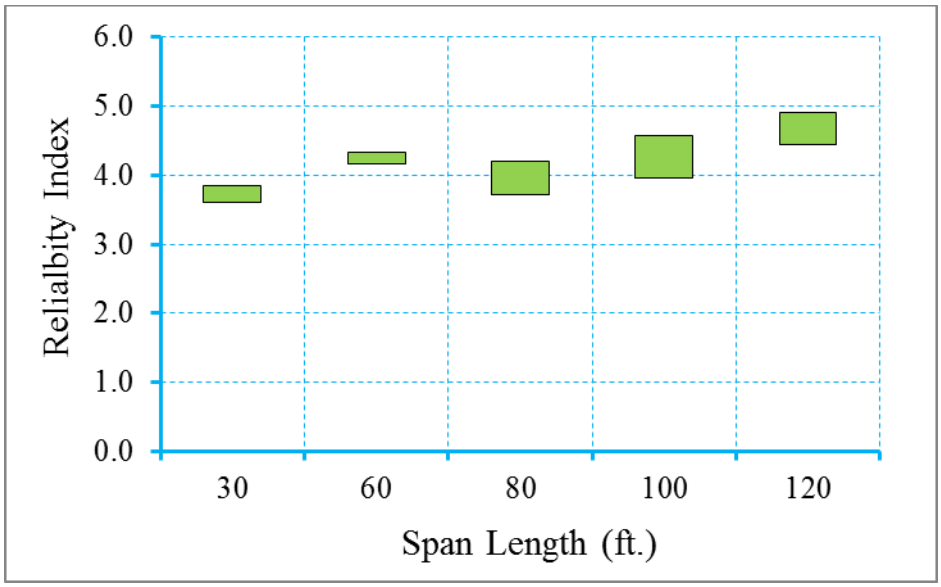

Figure D-121 Reliability Indices for Bridges at Maximum Allowable Crack Width Limit State (ADTT=5000), γLL=1.0 ($f_t = 0.253\sqrt{f_c'}$)

Step 3: Propose new live load, dead load, and/or resistance factors

Based on the calibration process shown in step 1 through step 3, it is observed that the uniform target reliability index can be achieved using a live load factor of 1.0. Therefore, for the scenario of ADTT equal to 5000 and maximum concrete tensile stress of $f_t = 0.253\sqrt{f_c'}$, a new live load factor of 1.0 is proposed.

D.4.2 Reliability indices of girders designed for various design criteria (Spread Box Girders)

In this section, the reliability analysis was performed for spread box girders that designed for various design criteria with compressive strength of 8000 psi. The scenario of ADTT equals to 5000 was considered in this section.

D.4.2.1 Bridges Designed for Maximum Concrete Tensile Stress of $0.0948\sqrt{f'_c}$

In this section, the calibration process for a selected bridge database (shown in Table D-99) is performed.

Table D-99 Summary Information of Bridges Designed with γLL=0.8

($f_t = 0.0948\sqrt{f_c'}$)

Cases	Section Type	Span Length (ft.)	Spacing (ft.)	Aps (in^2)	# of Strands
1	BI-36	30	6	1.53	10
2	BI-36	30	8	1.836	12
3	BI-36	30	10	1.836	12
4	BI-36	30	12	2.142	14
5	BI-36	60	6	3.978	26
6	BI-36	60	8	4.896	32
7	BI-36	60	10	5.508	36
8	BI-48	60	12	6.426	42
9	BI-48	80	6	7.038	46
10	BII-48	80	8	6.732	44
11	BII-48	80	10	7.65	50
12	BIII-48	80	12	7.038	46
13	BIII-48	100	6	7.344	48
14	BIII-48	100	8	9.18	60
15	BIV-48	100	10	10.404	68

Step 1: Calculate the reliability level of designs according to AASHTO LRFD Specifications (2010) (Figure D-122~Figure D-124)

Figure D-122 through Figure D-124 show the reliability indices for the bridges designed using AASHTO type girders according to AASHTO LRFD specifications (2010). It is observed that the average reliability index for decompression limit state, maximum allowable tensile stress limit state and maximum allowable crack width limit state is 1.36, 1.70, and 4.53, respectively. A larger live load factor will be used to estimate the effect of changing live load factor on reliability level of structure.

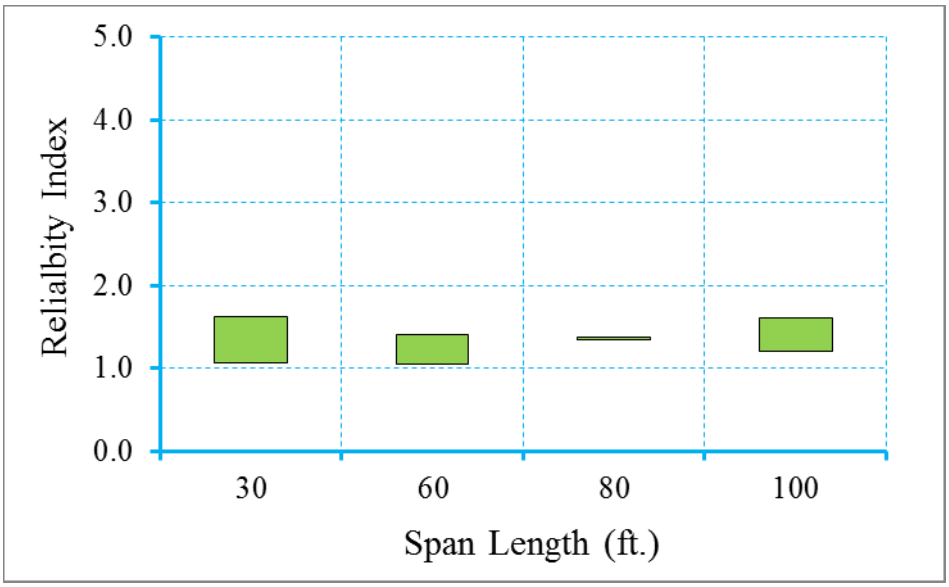

Figure D-122 Reliability Indices for Bridges at Decompression Limit State (ADTT=5000), γLL=0.8 ($f_t = 0.0948\sqrt{f'_c}$)

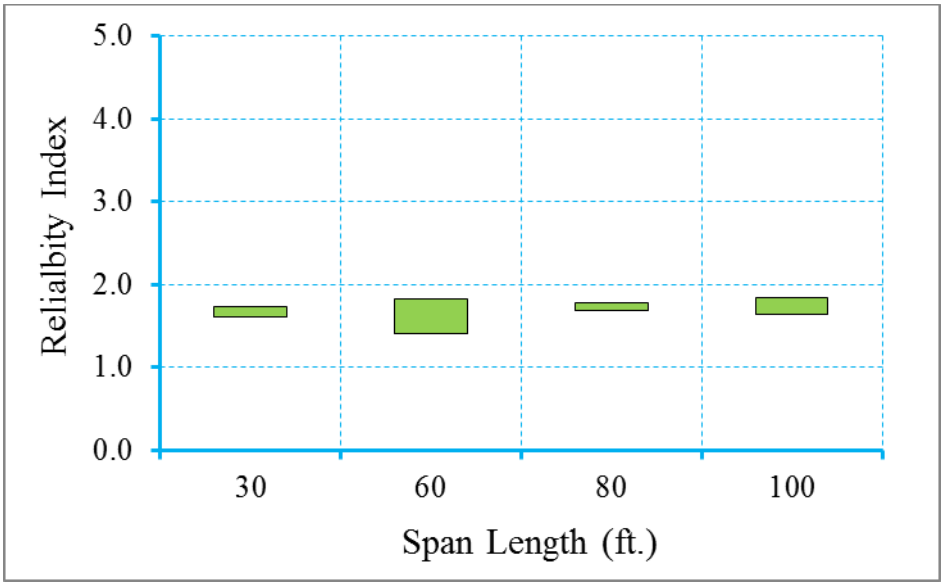

Figure D-123 Reliability Indices for Bridges at Maximum Allowable Tensile Stress Limit State (ADTT=5000), γLL=0.8 ($f_t = 0.0948\sqrt{f'_c}$)

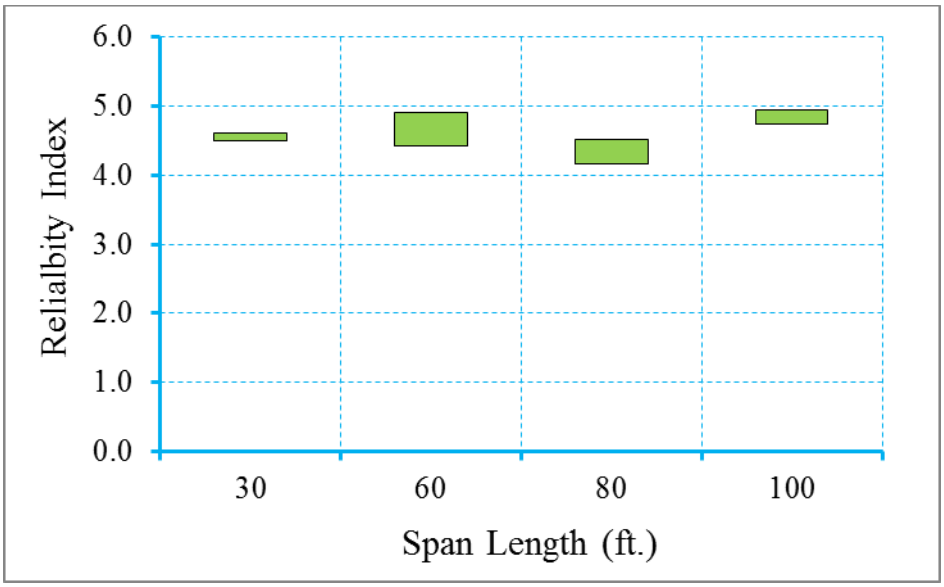

Figure D-124 Reliability Indices for Bridges at Maximum Allowable Crack Width Limit State (ADTT=5000), γLL=0.8 ($f_t = 0.0948\sqrt{f_c'}$)

Step 2: Redesign the bridges with live load factor of 1.0 (Figure D-125~Figure D-127)

In this step, the bridges have been redesigned using a live load factor of 1.0. Please note that only the live load factor of Service III limit state is increased from 0.8 to 1.0, dead load and resistance factors were kept the same during the redesign. Table D-100 shows the design outcomes of the redesigned bridges.

Figure D-125 through Figure D-127 shows the reliability indices for the redesigned bridges using live load factor of 1.0. It is observed the average reliability index of decompression limit state, maximum allowable tensile stress limit state and maximum allowable crack width limit state is 1.45, 1.78, and 4.66, respectively.

Table D-100 Summary Information of Bridges Designed with γLL=1.0

($f_t = 0.0948\sqrt{f_c'}$)

Cases	Section Type	Span Length (ft.)	Spacing (ft.)	Aps (in^2)	# of Strands
1	BI-36	30	6	1.53	10
2	BI-36	30	8	1.836	12
3	BI-36	30	10	2.142	14
4	BI-36	30	12	2.142	14
5	BI-36	60	6	4.284	28
6	BI-36	60	8	5.202	34
7	BI-36	60	10	6.426	42
8	BI-48	60	12	7.038	46
9	BI-48	80	6	7.65	50
10	BII-48	80	8	7.344	48
11	BII-48	80	10	8.874	58
12	BIII-48	80	12	7.956	52
13	BIII-48	100	6	7.956	52
14	BIII-48	100	8	-	-
15	BIV-48	100	10	-	-

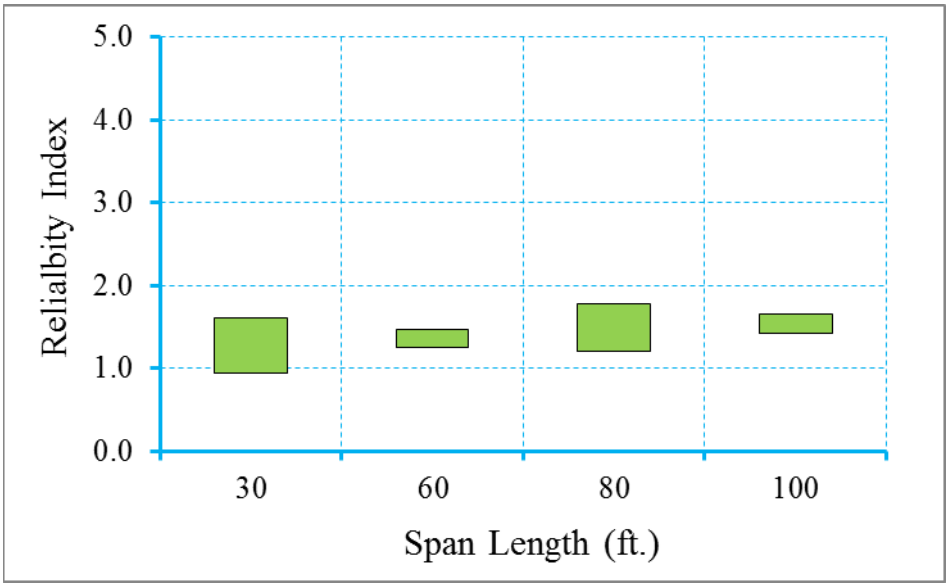

Figure D-125 Reliability Indices for Bridges at Decompression Limit State (ADTT=5000), γLL=1.0 ($f_t = 0.0948\sqrt{f_c'}$)

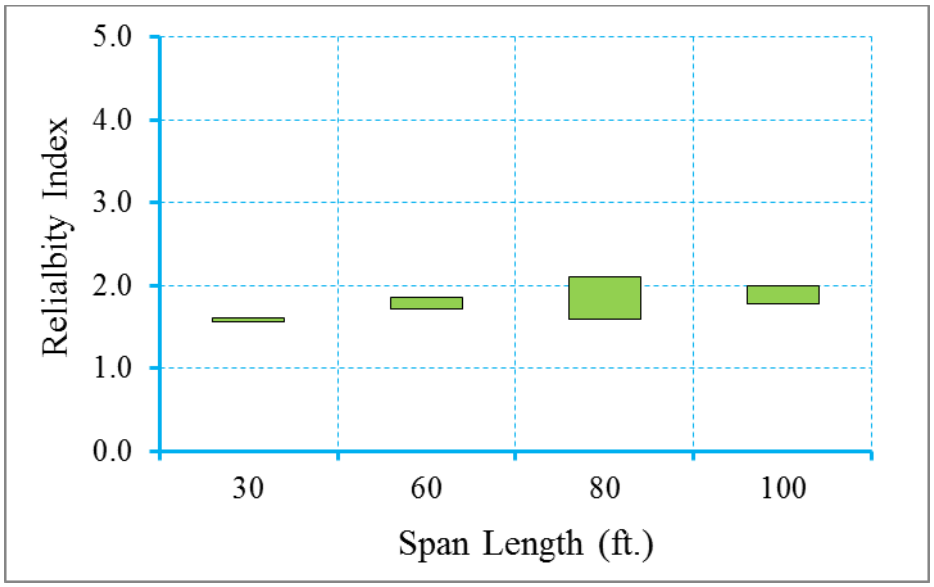

Figure D-126 Reliability Indices for Bridges at Maximum Tensile Stress Limit State (ADTT=5000), γLL=1.0 ($f_t = 0.0948\sqrt{f_c'}$)

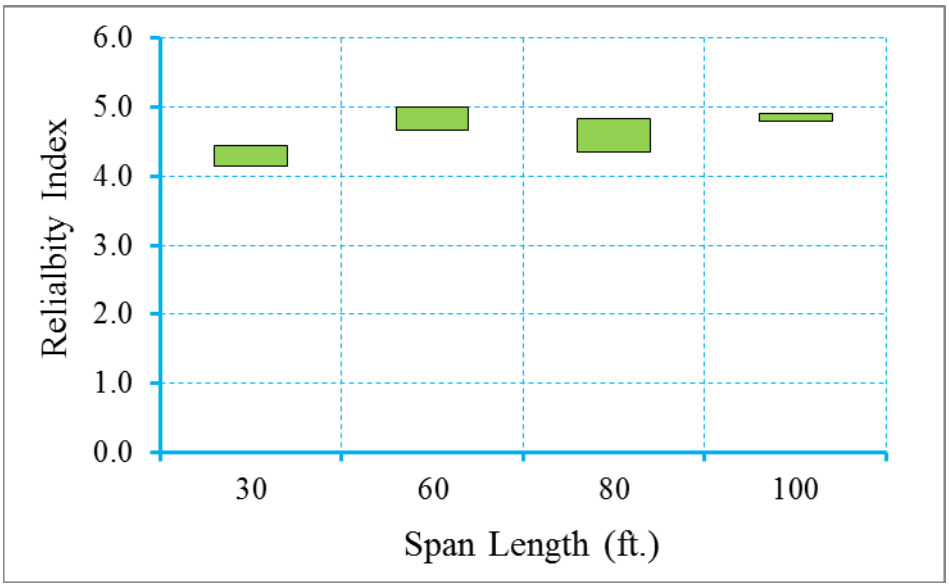

Figure D-127 Reliability Indices for Bridges at Maximum Crack Width Limit State (ADTT=5000), γLL=1.0 ($f_t = 0.0948\sqrt{f_c'}$)

Step 3: Propose new live load, dead load, and/or resistance factors

Based on the calibration process shown in step 1 through step 3, it is observed that the uniform target reliability index can be achieved using a live load factor of 1.0. Therefore, for the scenario of ADTT equal to 5000 and maximum concrete tensile stress of $f_t = 0.0948\sqrt{f_c'}$, a new live load factor of 1.0 is proposed.

D.4.2.2 Bridges Designed for Maximum Concrete Tensile Stress of $0.158\sqrt{f'_c}$

In this section, the calibration process for a selected bridge database (shown in Table D-101) is performed.

Table D-101 Summary Information of Bridges Designed with γLL=0.8

($f_t = 0.158\sqrt{f'_c}$)

Cases	Section Type	Span Length (ft.)	Spacing (ft.)	Aps (in^2)	# of Strands
1	BI-36	30	6	1.224	8
2	BI-36	30	8	1.53	10
3	BI-36	30	10	1.836	12
4	BI-36	30	12	1.836	12
5	BI-36	60	6	3.672	24
6	BI-36	60	8	4.59	30
7	BI-36	60	10	5.202	34
8	BI-48	60	12	5.814	38
9	BI-48	80	6	6.732	44
10	BII-48	80	8	6.12	40
11	BII-48	80	10	7.344	48
12	BIII-48	80	12	6.732	44
13	BIII-48	100	6	7.038	46
14	BIII-48	100	8	8.262	54
15	BIV-48	100	10	9.18	60

Step 1: Calculate the reliability level of designs according to AASHTO LRFD Specifications (2010) (Figure D-128~Figure D-130)

Figure D-128 through Figure D-130 show the reliability indices for the bridges designed using AASHTO type girders according to AASHTO LRFD specifications (2010). It is observed that the average reliability index for decompression limit state, maximum allowable tensile stress limit state and maximum allowable crack width limit state is 0.82, 1.15, and 4.11, respectively. Live load factor of 1.0 will be used in next step.

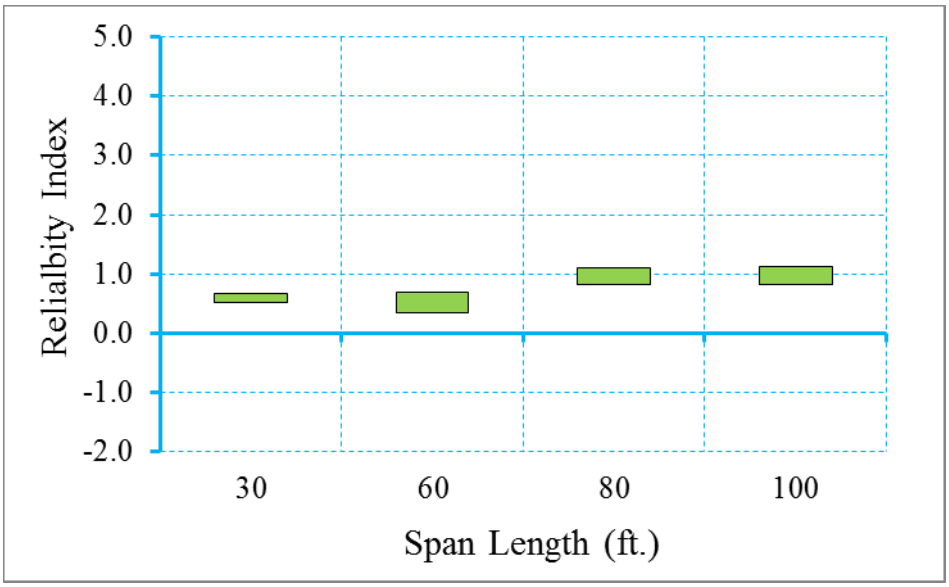

Figure D-128 Reliability Indices for Bridges at Decompression Limit State (ADTT=5000), γLL=0.8 ($f_t = 0.158\sqrt{f'_c}$)

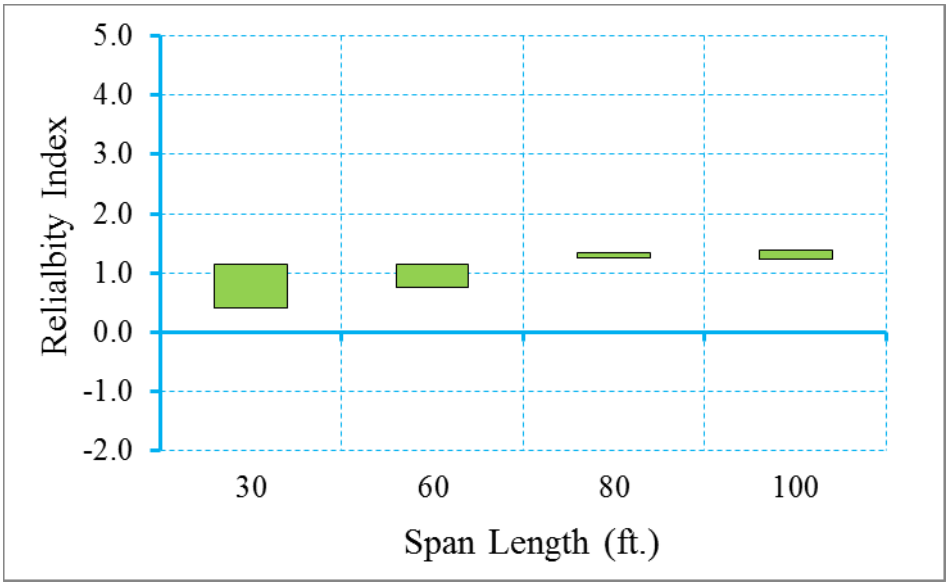

Figure D-129 Reliability Indices for Bridges at Maximum Allowable Tensile Stress Limit State (ADTT=5000), γLL=0.8 ($f_t = 0.158\sqrt{f'_c}$)

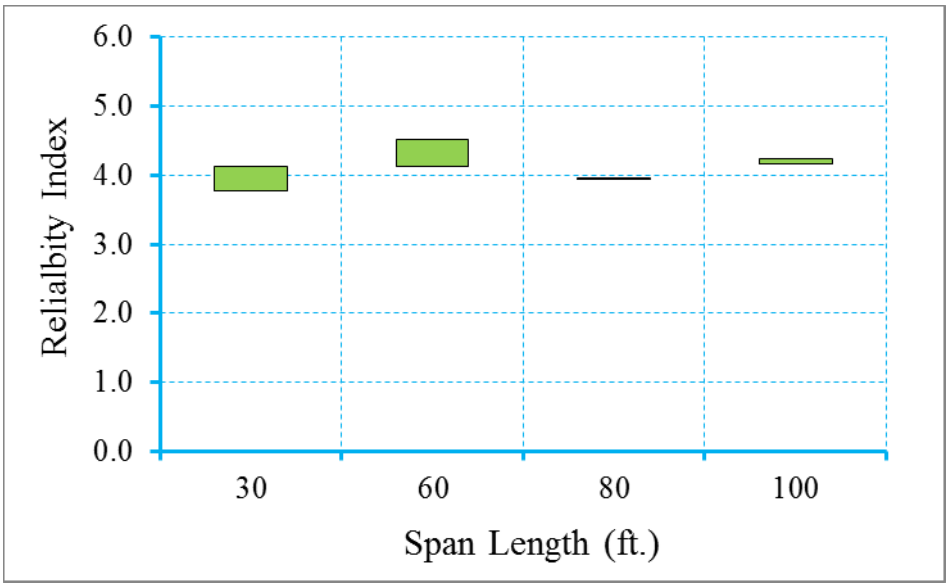

Figure D-130 Reliability Indices for Bridges at Maximum Allowable Crack Width Limit State (ADTT=5000), γLL=0.8 ($f_t = 0.158\sqrt{f_c'}$)

Step 2: Redesign the bridges with live load factor of 1.0 (Figure D-131~Figure D-133)

The bridges have been redesigned using a live load factor of 1.0. Please note that only the live load factor of Service III limit state is increased from 0.8 to 1.0, dead load and resistance factors were kept the same during the redesign. Table D-102 shows the design outcomes of the redesigned bridges.

Figure D-131 through Figure D-133 show the reliability indices for the redesigned bridges using live load factor of 1.0. It is observed that the average reliability index of decompression limit state, maximum allowable tensile stress limit state and maximum allowable crack width limit state is 1.09, 1.45, and 4.32, respectively.

Table D-102 Summary Information of Bridges Designed with γLL=1.0

($f_t = 0.158\sqrt{f_c'}$)

Cases	Section Type	Span Length (ft.)	Spacing (ft.)	Aps (in^2)	# of Strands
1	BI-36	30	6	1.53	10
2	BI-36	30	8	1.53	10
3	BI-36	30	10	1.836	12
4	BI-36	30	12	2.142	14
5	BI-36	60	6	4.284	28
6	BI-36	60	8	4.896	32
7	BI-36	60	10	5.814	38
8	BI-48	60	12	6.732	44
9	BI-48	80	6	7.344	48
10	BII-48	80	8	6.732	44
11	BII-48	80	10	7.956	52
12	BIII-48	80	12	7.344	48
13	BIII-48	100	6	7.344	48
14	BIII-48	100	8	9.792	64
15	BIV-48	100	10	-	-

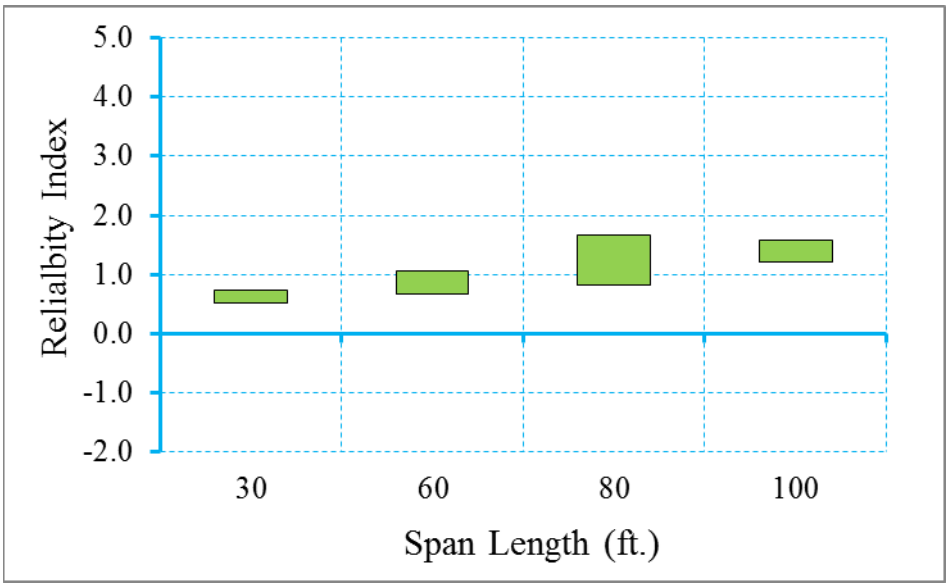

Figure D-131 Reliability Indices for Bridges at Decompression Limit State (ADTT=5000), γLL=1.0 ($f_t = 0.158\sqrt{f_c'}$)

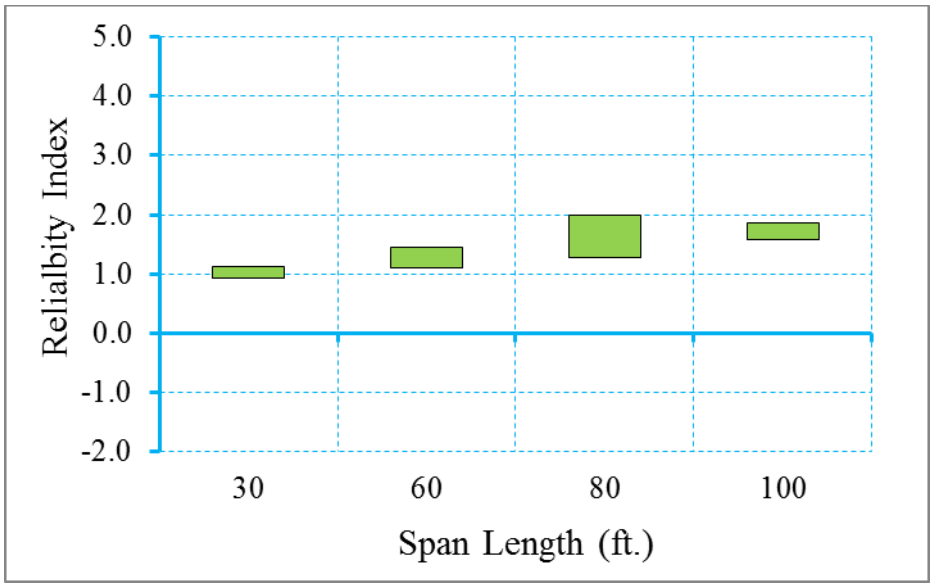

Figure D-132 Reliability Indices for Bridges at Maximum Tensile Stress Limit State (ADTT=5000), γLL=1.0 ($f_t = 0.158\sqrt{f'_c}$)

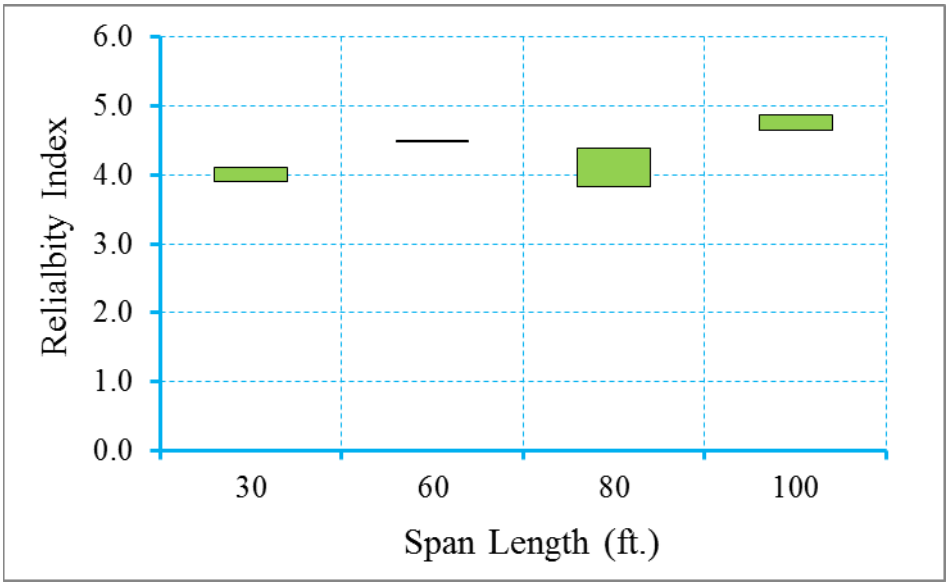

Figure D-133 Reliability Indices for Bridges at Maximum Crack Width Limit State (ADTT=5000), γLL=1.0 ($f_t = 0.158\sqrt{f'_c}$)

Step 3: Propose new live load, dead load, and/or resistance factors

Based on the calibration process shown in step 1 through step 3, it is observed that the uniform target reliability index can be achieved using a live load factor of 1.0.

Therefore, for the scenario of ADTT equal to 5000 and maximum concrete tensile stress of $f_t = 0.158\sqrt{f_c'}$, a new live load factor of 1.0 is proposed.

D.4.2.3 Bridges Designed for Maximum Concrete Tensile Stress of $0.19\sqrt{f'_c}$

In this section, the calibration process for a selected bridge database (shown in Table D-103) is performed for the scenario of ADTT equal to 5000.

Table D-103 Summary Information of Bridges Designed with γLL=0.8 ($f_t = 0.19\sqrt{f_c'}$)

Cases	Section Type	Span Length (ft.)	Spacing (ft.)	Aps (in^2)	# of Strands
1	BI-36	30	6	1.224	8
2	BI-36	30	8	1.53	10
3	BI-36	30	10	1.53	10
4	BI-36	30	12	1.836	12
5	BI-36	60	6	3.672	24
6	BI-36	60	8	4.284	28
7	BI-36	60	10	5.202	34
8	BI-48	60	12	5.814	38
9	BI-48	80	6	6.426	42
10	BII-48	80	8	6.12	40
11	BII-48	80	10	7.038	46
12	BIII-48	80	12	6.732	44
13	BIII-48	100	6	6.732	44
14	BIII-48	100	8	7.956	52
15	BIV-48	100	10	8.568	56

Step 1: Calculate the reliability level of designs according to AASHTO LRFD Specifications (2010) (Figure D-134~Figure D-136)

Figure D-134 through Figure D-136 show the reliability indices for the bridges designed using AASHTO type girders according to AASHTO LRFD specifications (2010). It is observed that the average reliability index for decompression limit state, maximum allowable tensile stress limit state and maximum allowable crack width limit state is 0.66, 0.94, and 4.01, respectively. Since the reliability indices are lower than target reliability index, live load factor of 1.0 will be used in next step.

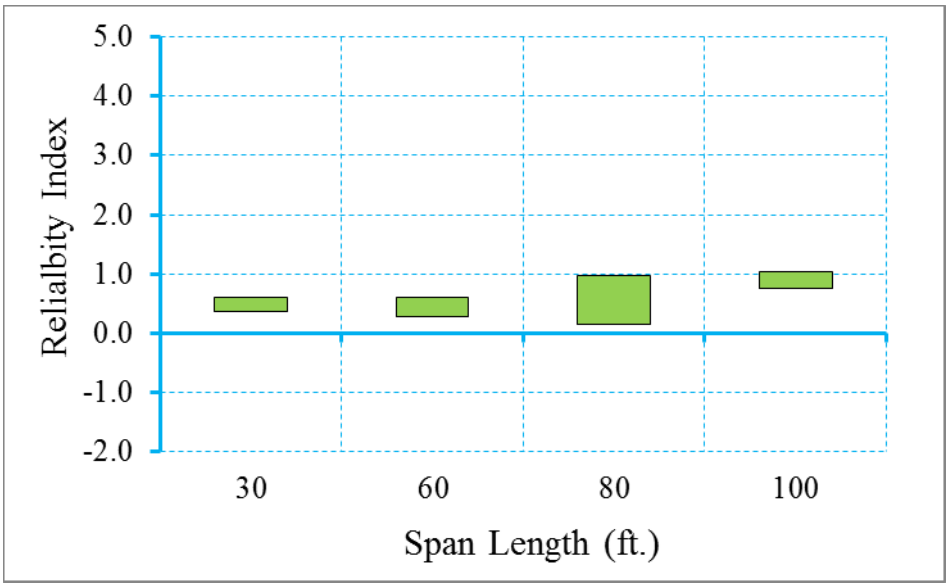

Figure D-134 Reliability Indices for Bridges at Decompression Limit State (ADTT=5000), γLL=0.8 ($f_t = 0.19\sqrt{f'_c}$)

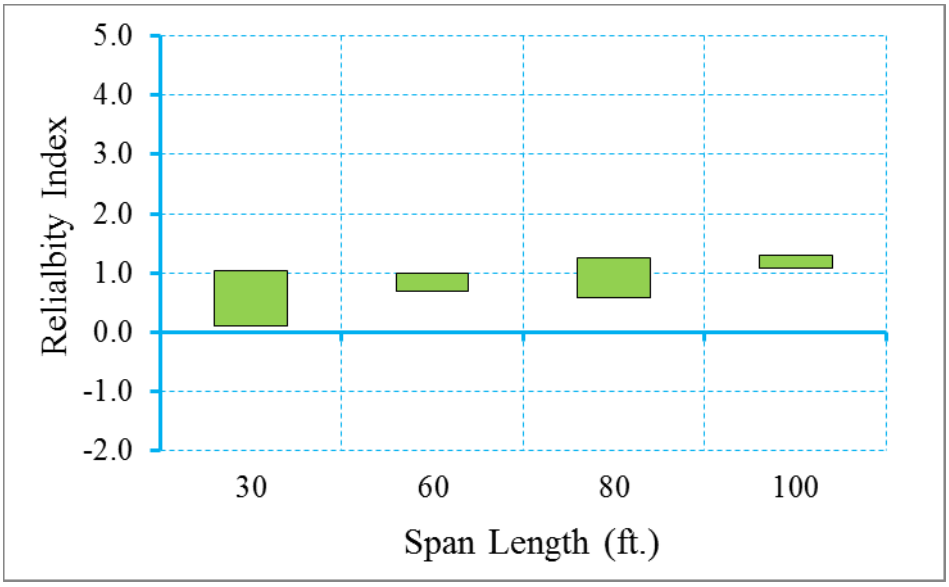

Figure D-135 Reliability Indices for Bridges at Maximum Allowable Tensile Stress Limit State (ADTT=5000), γLL=0.8 ($f_t = 0.19\sqrt{f'_c}$)

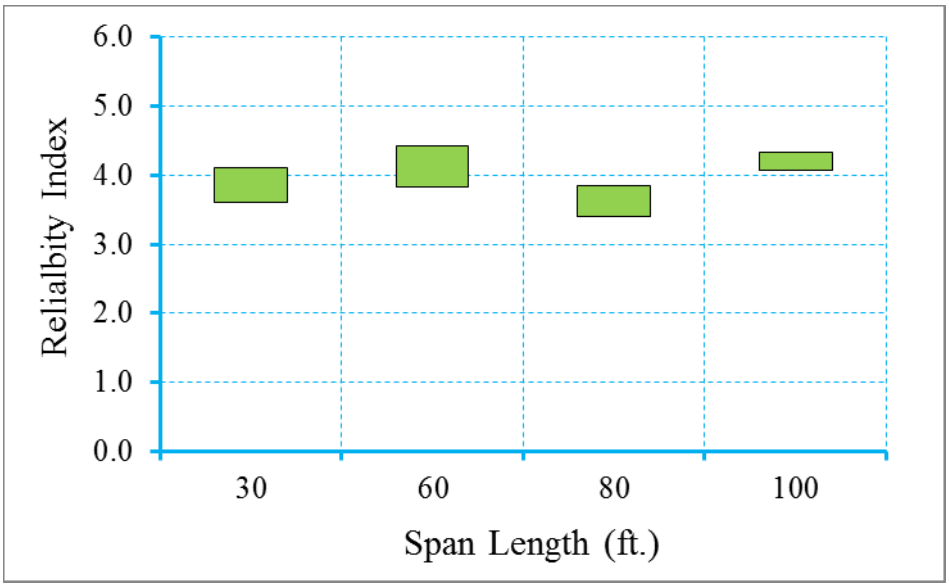

Figure D-136 Reliability Indices for Bridges at Maximum Allowable Crack Width Limit State (ADTT=5000), γLL=0.8 ($f_t = 0.19\sqrt{f_c'}$)

Step 2: Redesign the bridges with live load factor of 1.0 (Figure D-137~Figure D-139)

The bridges have been redesigned using a live load factor of 1.0. Please note that only the live load factor of Service III limit state is increased from 0.8 to 1.0, dead load and resistance factors were kept the same during the redesign. Table D-104 shows the design outcomes of the redesigned bridges.

Figure D-137 through Figure D-139 show the reliability indices for the redesigned bridges using live load factor of 1.0. It is observed that the average reliability index of decompression limit state, maximum allowable tensile stress limit state and maximum allowable crack width limit state is 1.01, 1.25, and 4.26, respectively.

Table D-104 Summary Information of Bridges Designed with γLL=1.0 ($f_t = 0.19\sqrt{f_c'}$)

Cases	Section Type	Span Length (ft.)	Spacing (ft.)	Aps (in^2)	# of Strands
1	BI-36	30	6	1.224	8
2	BI-36	30	8	1.53	10
3	BI-36	30	10	1.836	12
4	BI-36	30	12	1.836	12
5	BI-36	60	6	3.978	26
6	BI-36	60	8	4.896	32
7	BI-36	60	10	5.814	38
8	BI-48	60	12	6.426	42
9	BI-48	80	6	7.038	46
10	BII-48	80	8	6.732	44
11	BII-48	80	10	7.956	52
12	BIII-48	80	12	7.344	48
13	BIII-48	100	6	7.038	46
14	BIII-48	100	8	9.18	60
15	BIV-48	100	10	-	-

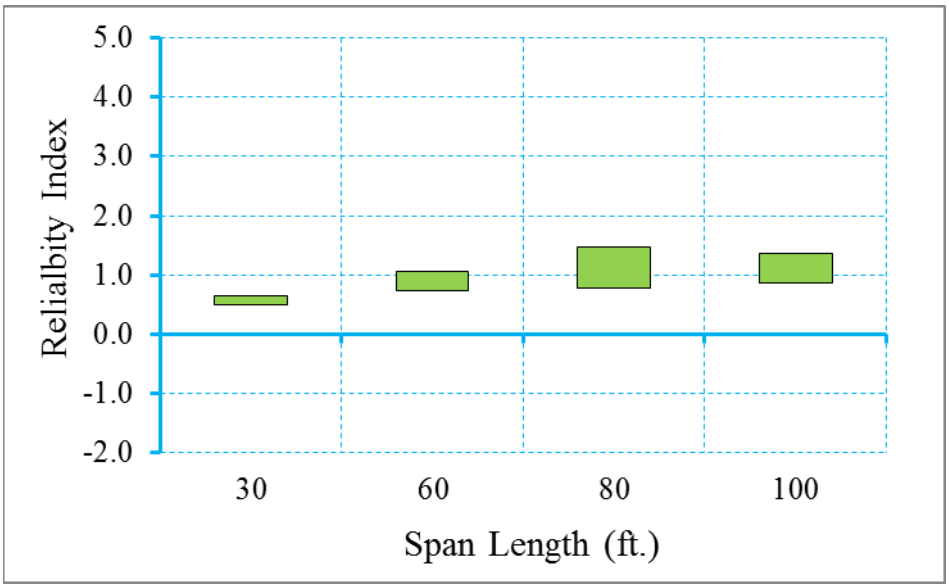

Figure D-137 Reliability Indices for Bridges at Decompression Limit State (ADTT=5000) γLL=1.0 ($f_t = 0.19\sqrt{f_c'}$)

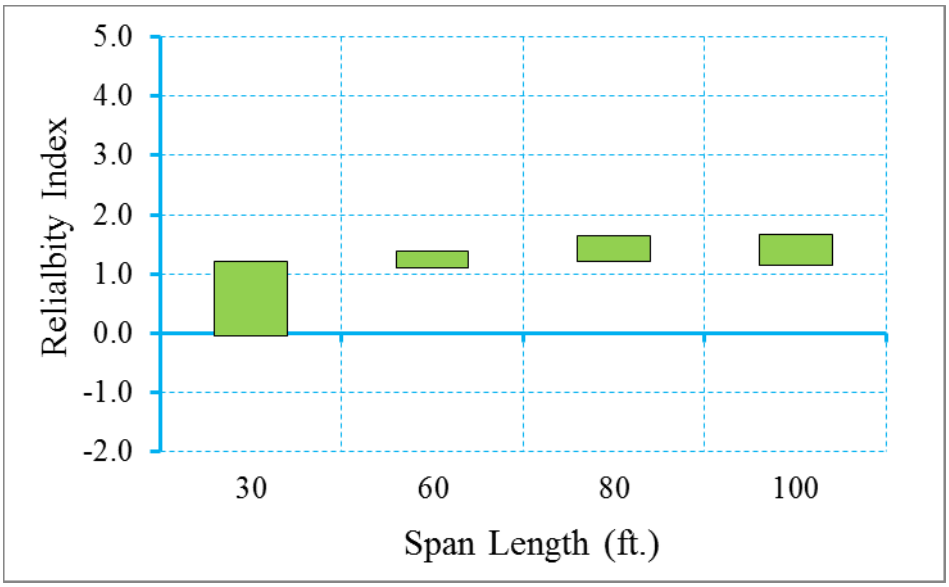

Figure D-138 Reliability Indices for Bridges at Maximum Tensile Stress Limit State (ADTT=5000), γLL=1.0 ($f_t = 0.19\sqrt{f_c'}$)

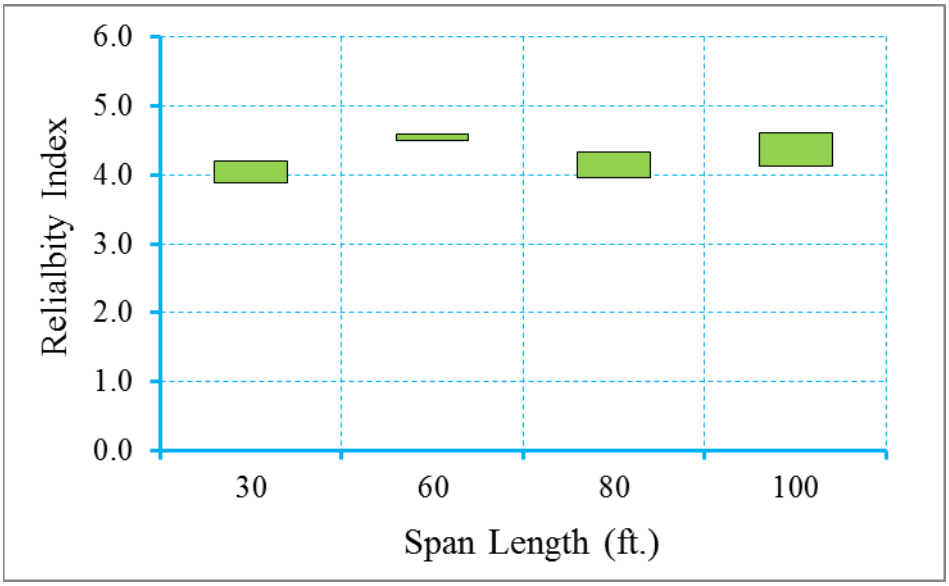

Figure D-139 Reliability Indices for Bridges at Maximum Crack Width Limit State (ADTT=5000), γLL=1.0 ($f_t = 0.19\sqrt{f_c'}$)

Step 3: Propose new live load, dead load, and/or resistance factors

Based on the calibration process shown in step 1 through step 3, it is observed that the uniform target reliability index can be achieved using a live load factor of 1.0. Therefore, for the scenario of ADTT equal to 5000 and maximum concrete tensile stress of $f_t = 0.19\sqrt{f_c'}$, a new live load factor of 1.0 is proposed.

D.4.2.4 Bridges Designed for Maximum Concrete Tensile Stress of $0.253\sqrt{f'_c}$

In this section, the calibration for a selected bridge database (shown in Table D-105) is performed for a scenario of ADTT equal to 5000. Please note that the maximum allowable crack width is specified as 0.016 in for maximum allowable crack width limit state.

Step 1: Calculate the reliability level of designs according to AASHTO LRFD Specifications (2010) (Figure D-140~Figure D-142)

Figure D-140 through Figure D-142 show the reliability indices for the bridges designed using AASHTO type girders according to AASHTO LRFD specifications (2010). It is observed that the average reliability index for decompression limit state, maximum allowable tensile stress limit state and maximum allowable crack width limit state is 0.48, 0.66, and 3.94, respectively. Live load factor of 1.0 will be used to estimate the effect of changing live load factor on reliability level.

Table D-105 Summary Information of Bridges Designed with γLL=0.8

($f_t = 0.253\sqrt{f'_c}$)

Cases	Section Type	Span Length (ft.)	Spacing (ft.)	Aps (in^2)	# of Strands
1	BI-36	30	6	0.918	6
2	BI-36	30	8	1.224	8
3	BI-36	30	10	1.53	10
4	BI-36	30	12	1.53	10
5	BI-36	60	6	3.366	22
6	BI-36	60	8	4.284	28
7	BI-36	60	10	4.896	32
8	BI-48	60	12	5.508	36
9	BI-48	80	6	6.12	40
10	BII-48	80	8	5.814	38
11	BII-48	80	10	6.732	44
12	BIII-48	80	12	6.12	40
13	BIII-48	100	6	6.426	42
14	BIII-48	100	8	7.65	50
15	BIV-48	100	10	7.956	52

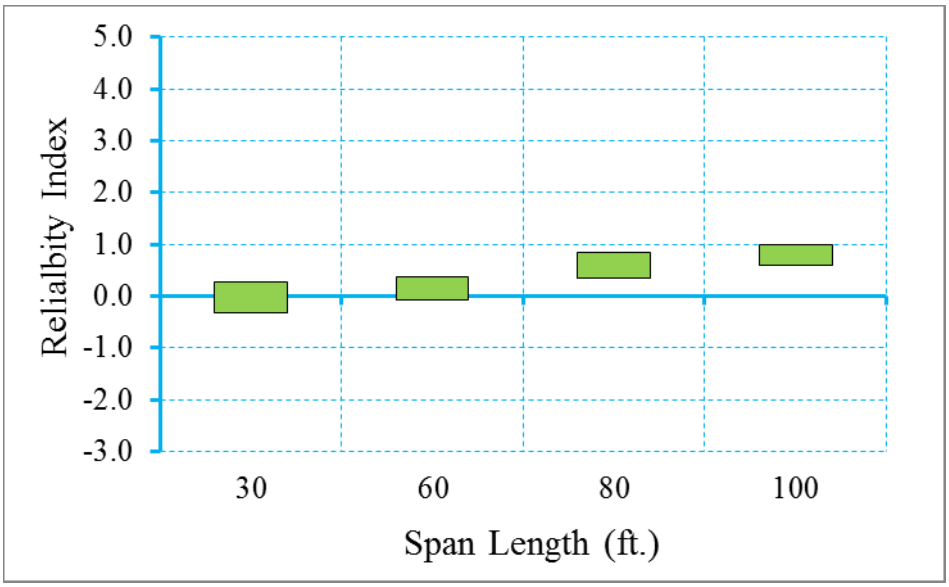

Figure D-140 Reliability Indices for Bridges at Decompression Limit State (ADTT=5000), γLL=0.8 ($f_t = 0.253\sqrt{f'_c}$)

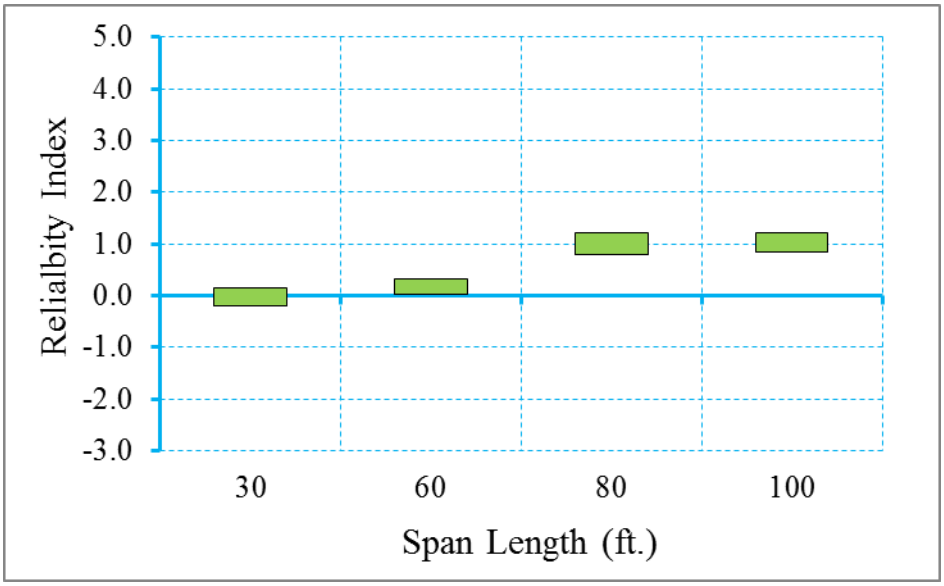

Figure D-141 Reliability Indices for Bridges at Maximum Allowable Tensile Stress Limit State (ADTT=5000), γLL=0.8 ($f_t = 0.253\sqrt{f'_c}$)

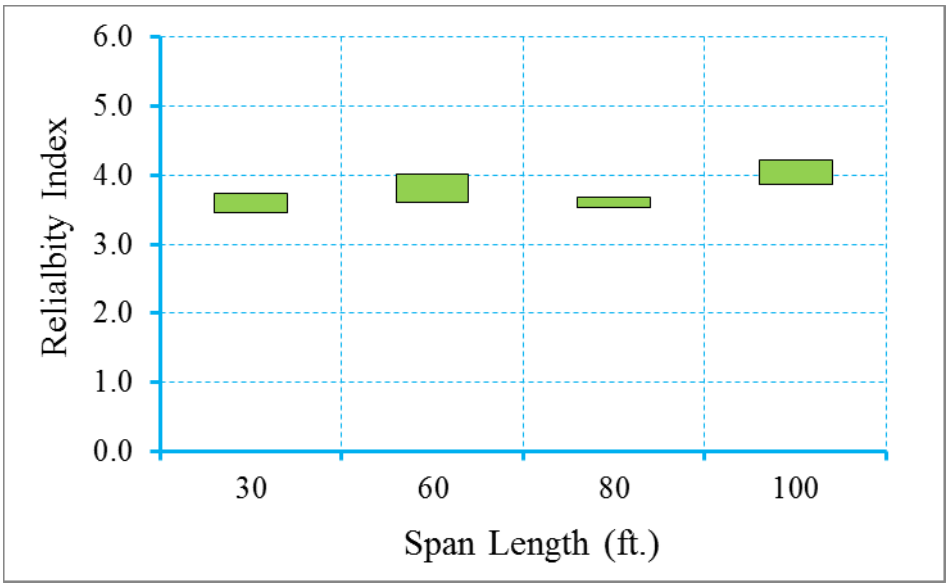

Figure D-142 Reliability Indices for Bridges at Maximum Allowable Crack Width Limit State (ADTT=5000), γLL=0.8 ($f_t = 0.253\sqrt{f_c'}$)

Step 2: Redesign the bridges with live load factor of 1.0 (Figure D-143~Figure D-145)

In this step, the bridges were redesigned using a live load factor of 1.0. Please note that only the live load factor of Service III limit state is increased from 0.8 to 1.0, dead load and resistance factors were kept the same during the redesign. Table D-106 shows the design outcomes of the redesigned bridges.

Figure D-143 through Figure D-145 show the reliability indices for the redesigned bridges using a live load factor of 1.0. It is observed that the average reliability index for the decompression limit state, the maximum allowable tensile stress limit state and the maximum allowable crack width limit state is 0.56, 0.87, and 4.08, respectively.

Table D-106 Summary Information of Bridges Designed with γLL=1.0 ($f_t = 0.253\sqrt{f_c'}$)

Cases	Section Type	Span Length (ft.)	Spacing (ft.)	Aps (in^2)	# of Strands
1	BI-36	30	6	1.224	8
2	BI-36	30	8	1.224	8
3	BI-36	30	10	1.53	10
4	BI-36	30	12	1.836	12
5	BI-36	60	6	3.672	24
6	BI-36	60	8	4.59	30
7	BI-36	60	10	5.508	36
8	BI-48	60	12	6.12	40
9	BI-48	80	6	6.732	44
10	BII-48	80	8	6.426	42
11	BII-48	80	10	7.344	48
12	BIII-48	80	12	6.732	44
13	BIII-48	100	6	6.732	44
14	BIII-48	100	8	8.568	56
15	BIV-48	100	10	8.874	58

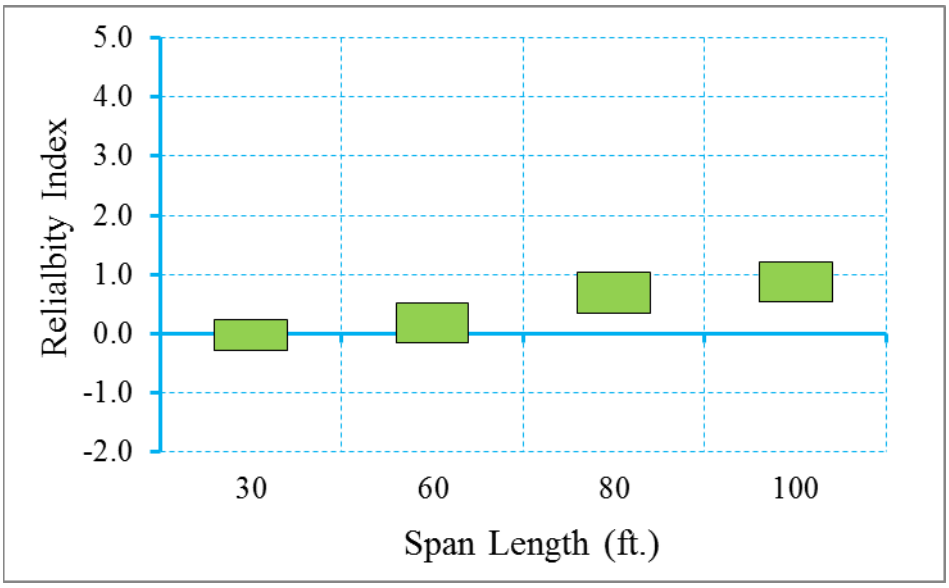

Figure D-143 Reliability Indices for Bridges at Decompression Limit State (ADTT=5000), γLL=1.0 ($f_t = 0.253\sqrt{f_c'}$)

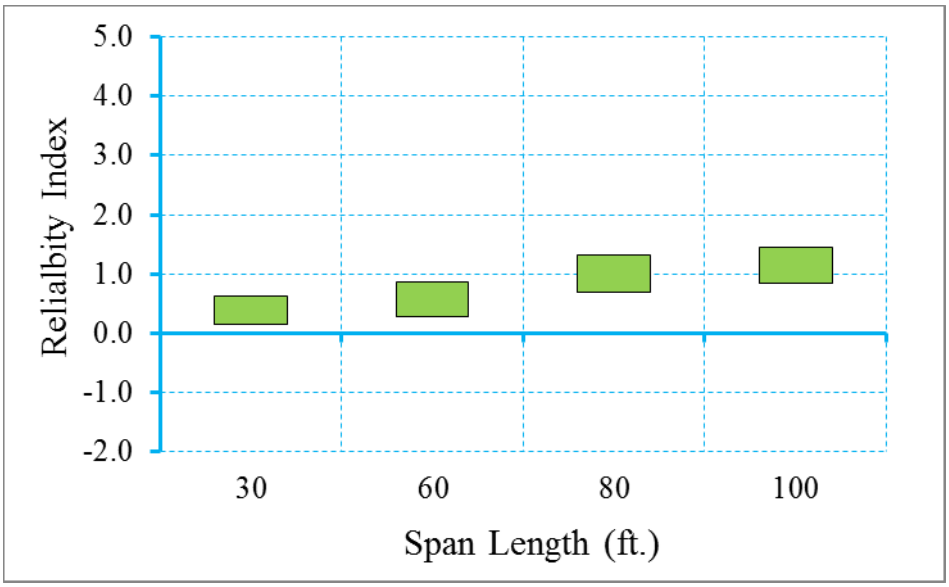

Figure D-144 Reliability Indices for Bridges at Maximum Allowable Tensile Stress Limit State (ADTT=5000), γLL=1.0 ($f_t = 0.253\sqrt{f_c'}$)

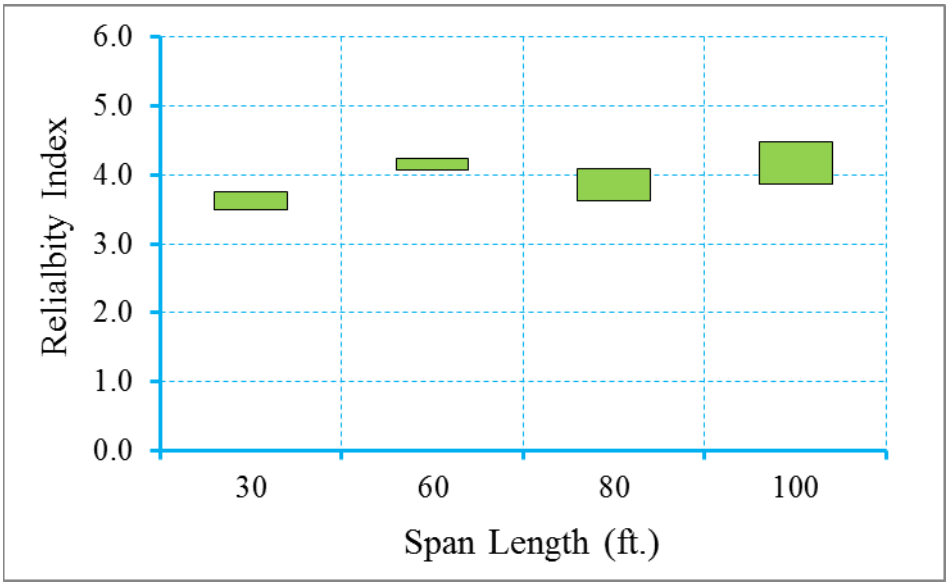

Figure D-145 Reliability Indices for Bridges at Maximum Allowable Crack Width Limit State (ADTT=5000), γLL=1.0 ($f_t = 0.253\sqrt{f_c'}$)

Step 3: Propose new live load, dead load, and/or resistance factors

Based on the calibration process shown in step 1 through step 3, it is observed that the uniform target reliability index can be achieved using a live load factor of 1.0. Therefore, for the scenario of ADTT equal to 5000 and maximum concrete tensile stress of $f_t = 0.253\sqrt{f_c'}$, a new live load factor of 1.0 is proposed.

D.4.3 Reliability indices of girders designed for various design criteria (ASBI Box Girder Bridges)

In this section, the reliability analysis was performed for adjacent box girders that designed for various design criteria with compressive strength of 8000 psi. The scenario of ADTT equals to 5000 was considered in this section.

D.4.3.1 C9.1 Bridges Designed for Maximum Concrete Tensile Stress of $0.0948\sqrt{f'_c}$

In this section, the calibration process for a selected bridge database (shown in Table D-107) is performed.

Table D-107 Summary Information of Bridges Designed with γLL=0.8

($f_t = 0.0948\sqrt{f'_c}$)

Cases	Section Type	Span Length (ft.)	Aps (in^2)	# of Strands
1	1800-2	100	7.344	48
2	1800-2	120	10.71	70
3	1800-2	140	14.076	92
4	2100-2	160	21.266	98
5	2400-2	180	22.568	104
6	2400-2	200	27.342	126

Step 1: Calculate the reliability level of designs according to AASHTO LRFD Specifications (2010) (Figure D-146~Figure D-148)

Figure D-146 through Figure D-148 show the reliability indices for the bridges designed using AASHTO type girders according to AASHTO LRFD specifications (2010). It is observed that the average reliability index for decompression limit state, maximum allowable tensile stress limit state and maximum allowable crack width limit state is 1.08, 1.42, and 3.22, respectively. A larger live load factor will be used to estimate the effect of changing live load factor on reliability level of structure.

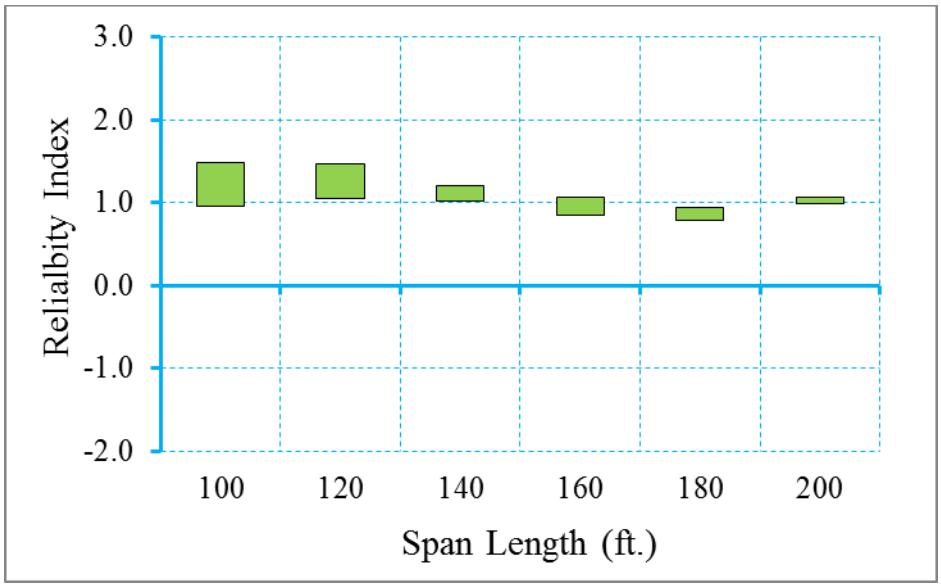

Figure D-146 Reliability Indices for Bridges at Decompression Limit State (ADTT=5000), γLL=0.8 ($f_t = 0.0948\sqrt{f_c'}$)

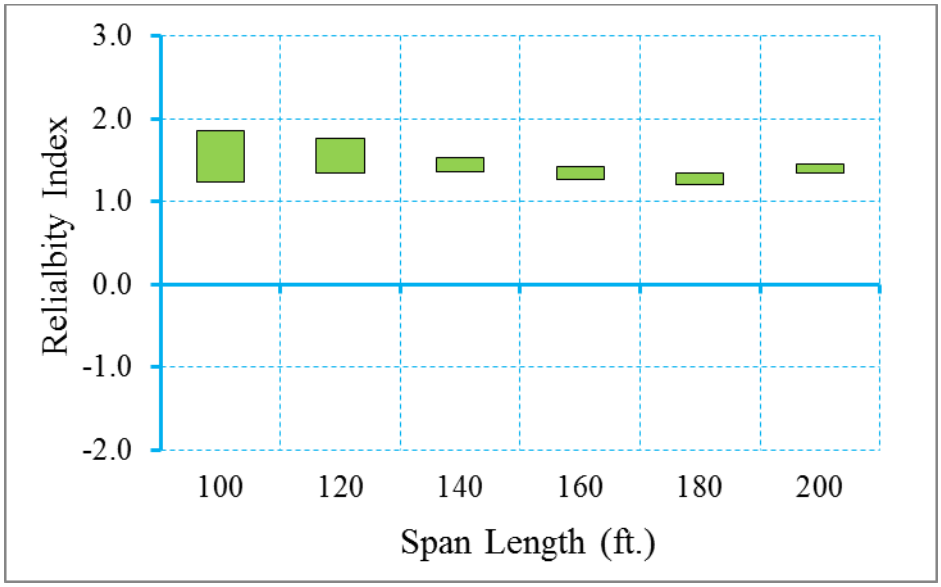

Figure D-147 Reliability Indices for Bridges at Maximum Allowable Tensile Stress Limit State (ADTT=5000), γLL=0.8 ($f_t = 0.0948\sqrt{f_c'}$)

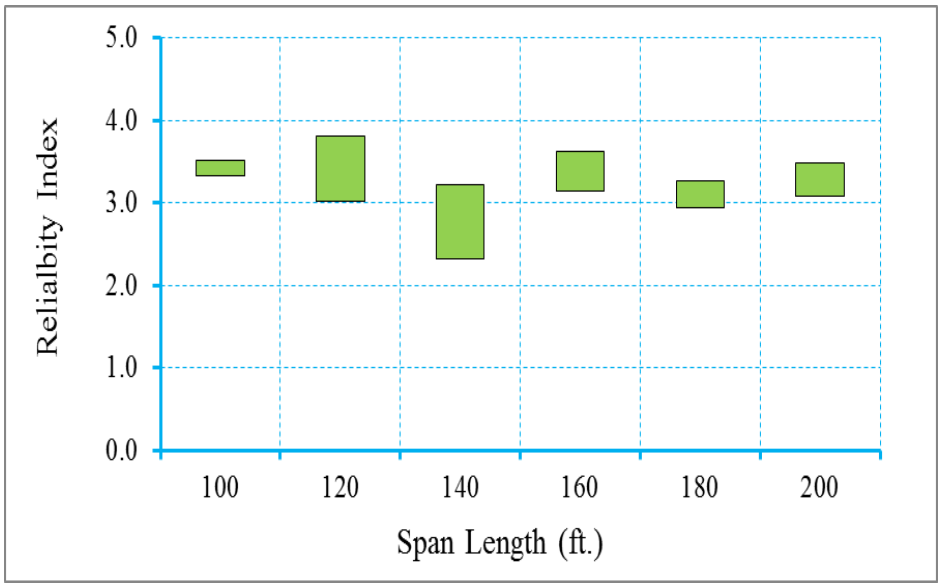

Figure D-148 Reliability Indices for Bridges at Maximum Allowable Crack Width Limit State (ADTT=5000), γLL=0.8 ($f_t = 0.0948\sqrt{f_c'}$)

Step 2: Redesign the bridges with live load factor of 1.0 (Figure D-149~Figure D-151)

In this step, the bridges have been redesigned using a live load factor of 1.0. Please note that only the live load factor of Service III limit state is increased from 0.8 to 1.0, dead load and resistance factors were kept the same during the redesign. Table D-108 shows the design outcomes of the redesigned bridges.

Figure D-149 through Figure D-151 shows the reliability indices for the redesigned bridges using live load factor of 1.0. It is observed the average reliability index of decompression limit state, maximum allowable tensile stress limit state and maximum allowable crack width limit state is 1.41, 1.77, and 3.47, respectively.

Table D-108 Summary Information of Bridges Designed with γLL=1.0 ($f_t = 0.0948\sqrt{f_c'}$)

Cases	Section Type	Span Length (ft.)	Aps (in^2)	# of Strands
1	1800-2	100	8.874	58
2	1800-2	120	10.71	70
3	1800-2	140	14.076	92
4	2100-2	160	21.266	98
5	2400-2	180	22.568	104
6	2400-2	200	27.342	126

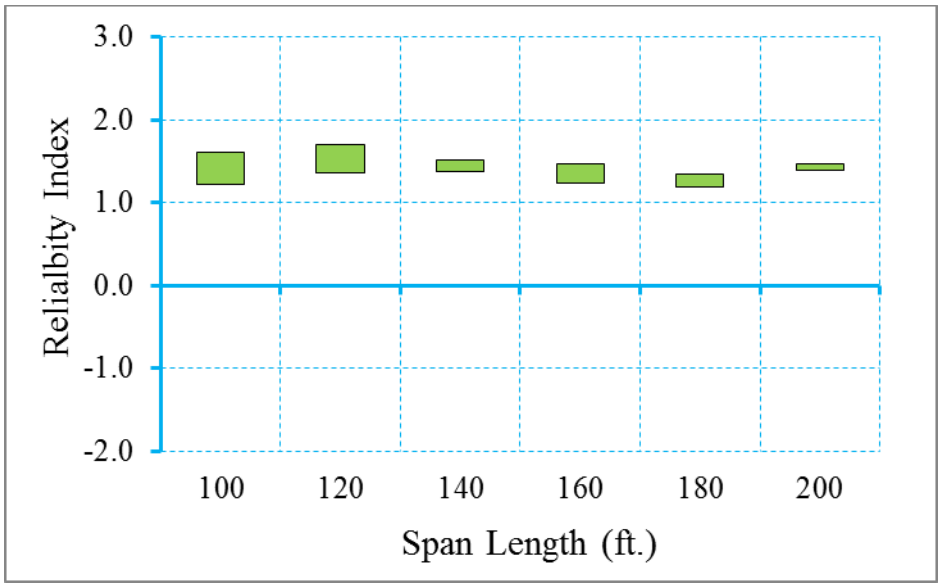

Figure D-149 Reliability Indices for Bridges at Decompression Limit State (ADTT=5000), γLL=1.0 ($f_t = 0.0948\sqrt{f_c'}$)

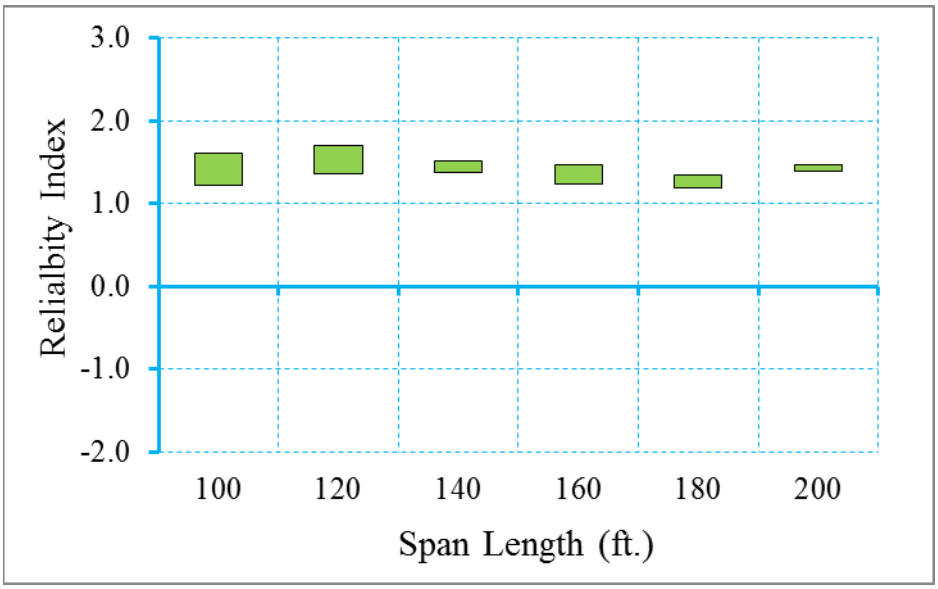

Figure D-150 Reliability Indices for Bridges at Maximum Tensile Stress Limit State (ADTT=5000), γLL=1.0 ($f_t = 0.0948\sqrt{f_c'}$)

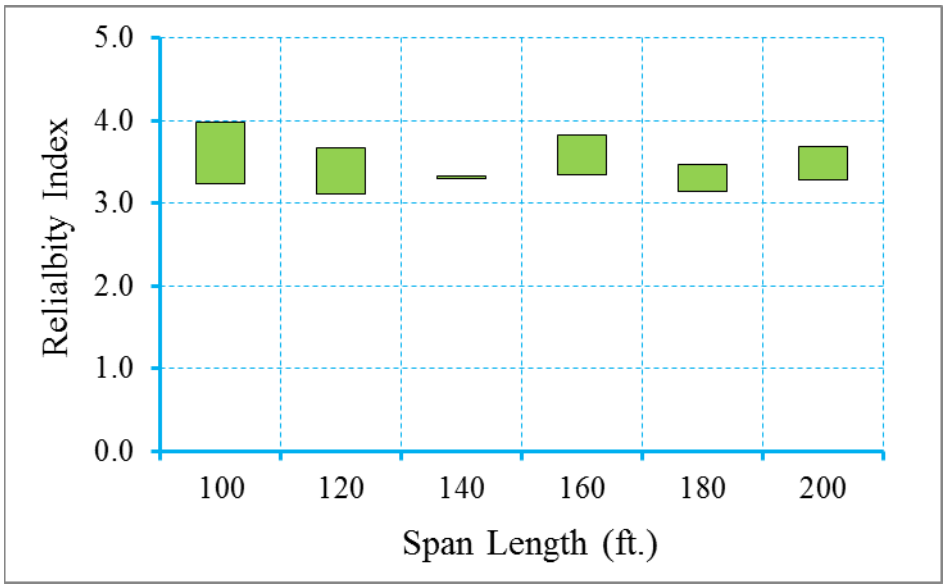

Figure D-151 Reliability Indices for Bridges at Maximum Crack Width Limit State (ADTT=5000), γLL=1.0 ($f_t = 0.0948\sqrt{f_c'}$)

Step 3: Propose new live load, dead load, and/or resistance factors

Based on the calibration process shown in step 1 through step 3, it is observed that the uniform target reliability index can be achieved using a live load factor of 1.0. Therefore, for the scenario of ADTT equal to 5000 and maximum concrete tensile stress of $f_t = 0.0948\sqrt{f_c'}$, a new live load factor of 1.0 is proposed.

D.4.3.2 Bridges Designed for Maximum Concrete Tensile Stress of $0.158\sqrt{f'_c}$

In this section, the calibration process for a selected bridge database (shown in Table D-109) is performed.

Table D-109 Summary Information of Bridges Designed with γLL=0.8 ($f_t = 0.158\sqrt{f_c'}$)

Cases	Section Type	Span Length (ft.)	Aps (in^2)	# of Strands
1	1800-2	100	5.814	38
2	1800-2	120	9.18	60
3	1800-2	140	12.546	82
4	2100-2	160	19.096	88
5	2400-2	180	20.398	94
6	2400-2	200	25.172	116

Step 1: Calculate the reliability level of designs according to AASHTO LRFD Specifications (2010) (Figure D-152~Figure D-154)

Figure D-152 through Figure D-154 show the reliability indices for the bridges designed using AASHTO type girders according to AASHTO LRFD specifications (2010). It is observed that the average reliability index for decompression limit state, maximum allowable tensile stress limit state and maximum allowable crack width limit state is 0.82, 1.18, and 2.97, respectively. Live load factor of 1.0 will be used in next step.

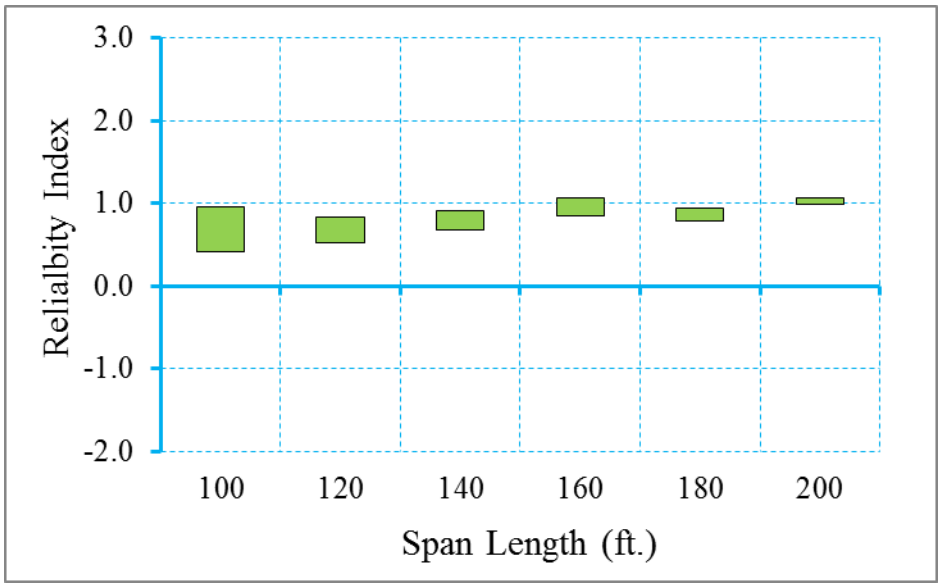

Figure D-152 Reliability Indices for Bridges at Decompression Limit State (ADTT=5000), γLL=0.8 ($f_t = 0.158\sqrt{f'_c}$)

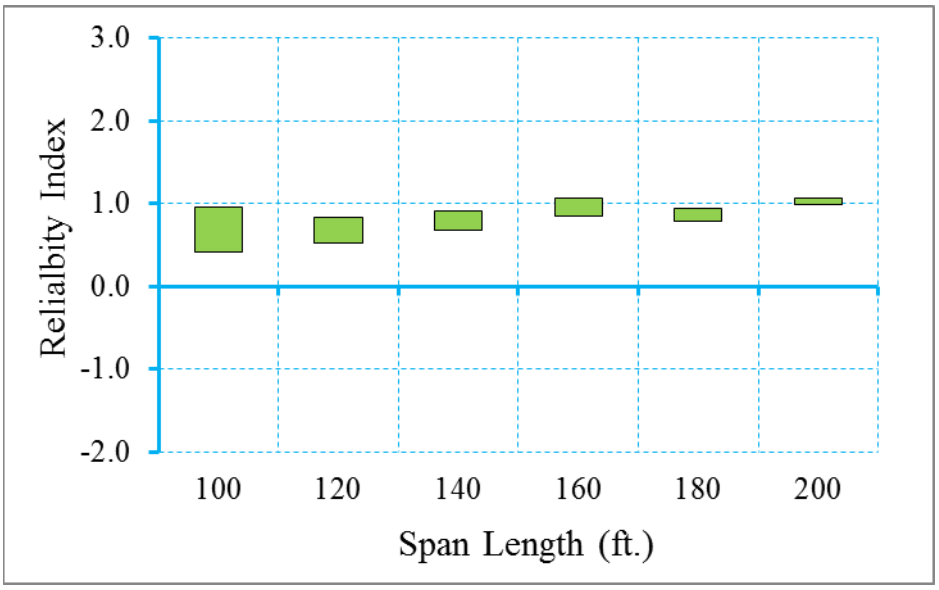

Figure D-153 Reliability Indices for Bridges at Maximum Allowable Tensile Stress Limit State (ADTT=5000), γLL=0.8 ($f_t = 0.158\sqrt{f'_c}$)

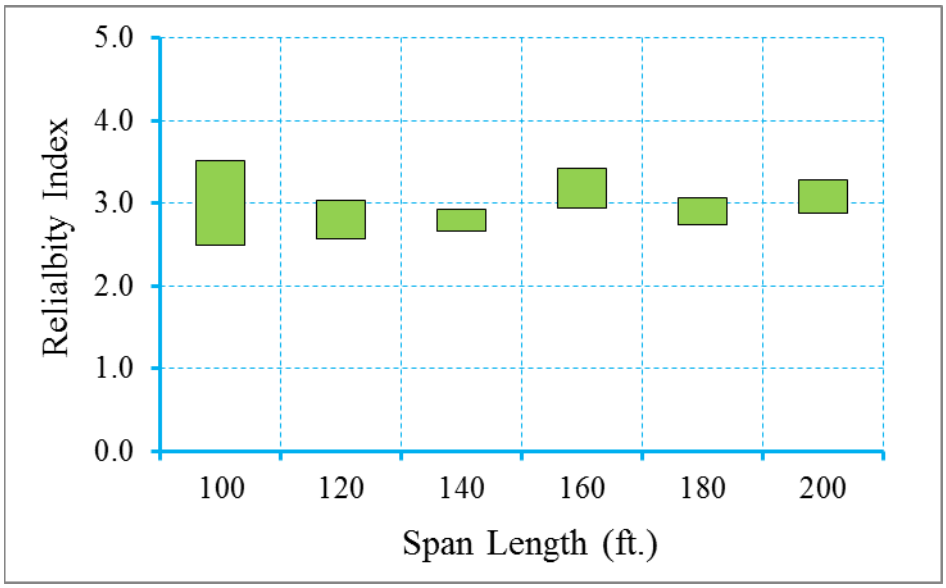

Figure D-154 Reliability Indices for Bridges at Maximum Allowable Crack Width Limit State (ADTT=5000), γLL=0.8 ($f_t = 0.158\sqrt{f_c'}$)

Step 2: Redesign the bridges with live load factor of 1.0 (Figure D-155~Figure D-157)

The bridges have been redesigned using a live load factor of 1.0. Please note that only the live load factor of Service III limit state is increased from 0.8 to 1.0, dead load and resistance factors were kept the same during the redesign. Table D-110 shows the design outcomes of the redesigned bridges.

Figure D-155 through Figure D-157 show the reliability indices for the redesigned bridges using live load factor of 1.0. It is observed that the average reliability index of decompression limit state, maximum allowable tensile stress limit state and maximum allowable crack width limit state is 1.09, 1.5, and 3.26, respectively.

Table D-110 Summary Information of Bridges Designed with γLL=1.0 ($f_t = 0.158\sqrt{f_c'}$)

Cases	Section Type	Span Length (ft.)	Aps (in^2)	# of Strands
1	1800-2	100	7.65	50
2	1800-2	120	11.628	76
3	1800-2	140	15.3	100
4	2100-2	160	23.002	106
5	2400-2	180	24.304	112
6	2400-2	200	29.946	138

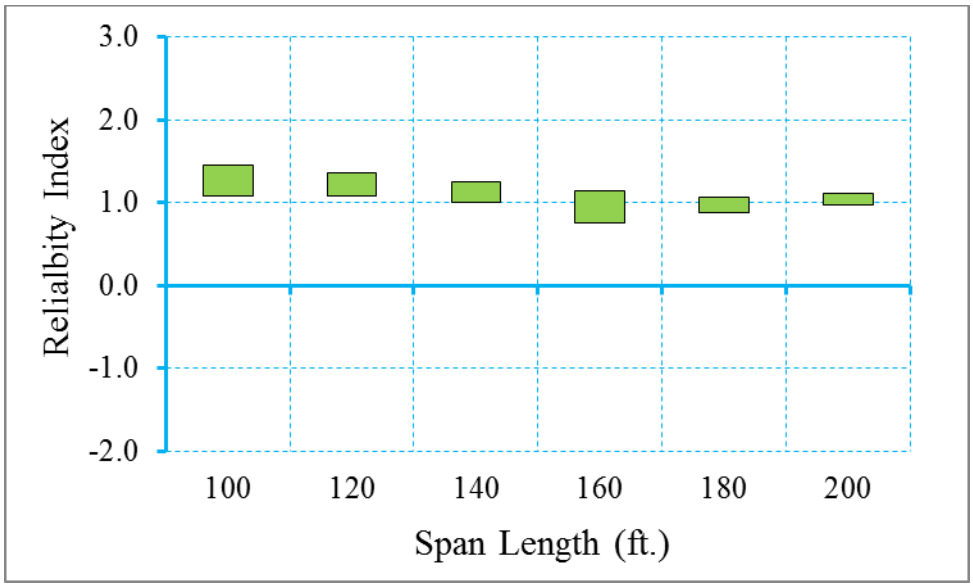

Figure D-155 Reliability Indices for Bridges at Decompression Limit State (ADTT=5000), γLL=1.0 ($f_t = 0.158\sqrt{f'_c}$)

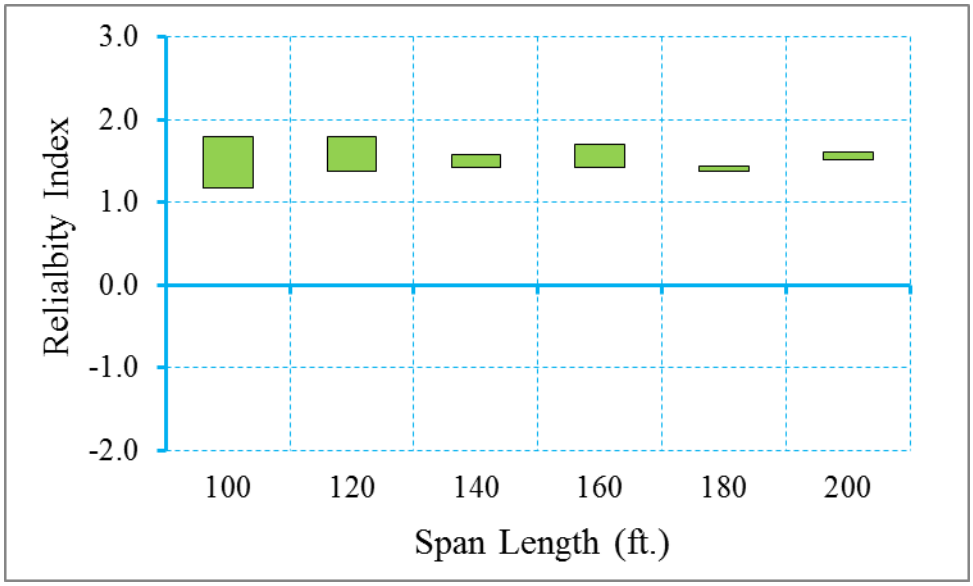

Figure D-156 Reliability Indices for Bridges at Maximum Tensile Stress Limit State (ADTT=5000), γLL=1.0 ($f_t = 0.158\sqrt{f'_c}$)

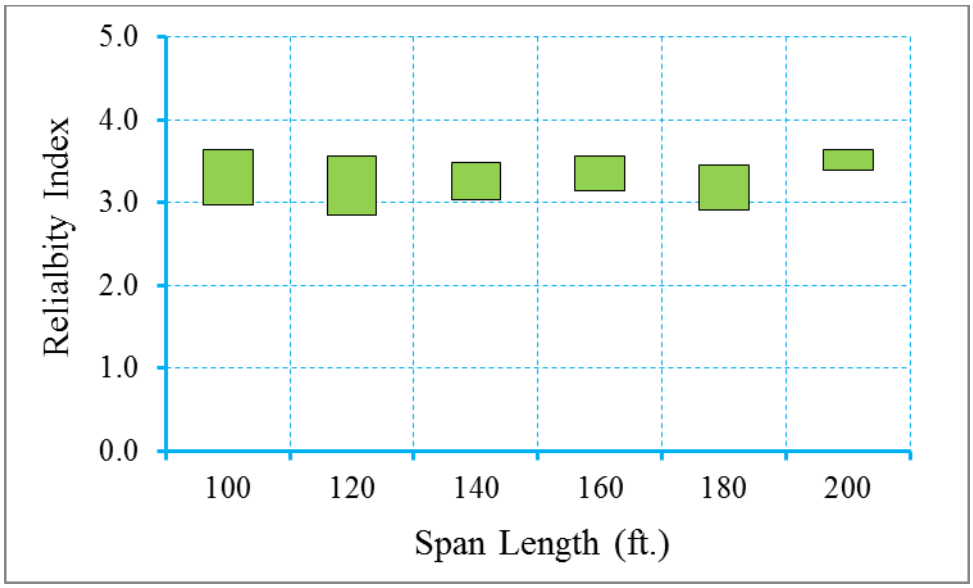

Figure D-157 Reliability Indices for Bridges at Maximum Crack Width Limit State (ADTT=5000), γLL=1.0 ($f_t = 0.158\sqrt{f'_c}$)

Step 3: Propose new live load, dead load, and/or resistance factors

Based on the calibration process shown in step 1 through step 3, it is observed that the uniform target reliability index can be achieved using a live load factor of 1.0. Therefore, for the scenario of ADTT equal to 5000 and maximum concrete tensile stress of $f_t = 0.158\sqrt{f'_c}$, a new live load factor of 1.0 is proposed.

D.4.3.3 Bridges Designed for Maximum Concrete Tensile Stress of $0.19\sqrt{f'_c}$

In this section, the calibration process for a selected bridge database (shown in Table D-111) is performed for the scenario of ADTT equal to 5000.

Table D-111 Summary Information of Bridges Designed with γLL=0.8 ($f_t = 0.19\sqrt{f'_c}$)

Cases	Section Type	Span Length (ft.)	Aps (in^2)	# of Strands
1	1800-2	100	5.202	34
2	1800-2	120	8.568	56
3	1800-2	140	11.934	78
4	2100-2	160	17.794	82
5	2400-2	180	19.096	88
6	2400-2	200	24.304	112

Step 1: Calculate the reliability level of designs according to AASHTO LRFD Specifications (2010) (Figure D-158~Figure D-160)

Figure D-158 through Figure D-160 show the reliability indices for the bridges designed using AASHTO type girders according to AASHTO LRFD specifications

(2010). It is observed that the average reliability index for decompression limit state, maximum allowable tensile stress limit state and maximum allowable crack width limit state is 0.79, 1.14, and 2.92, respectively. Since the reliability indices are lower than target reliability index, live load factor of 1.0 will be used in next step.

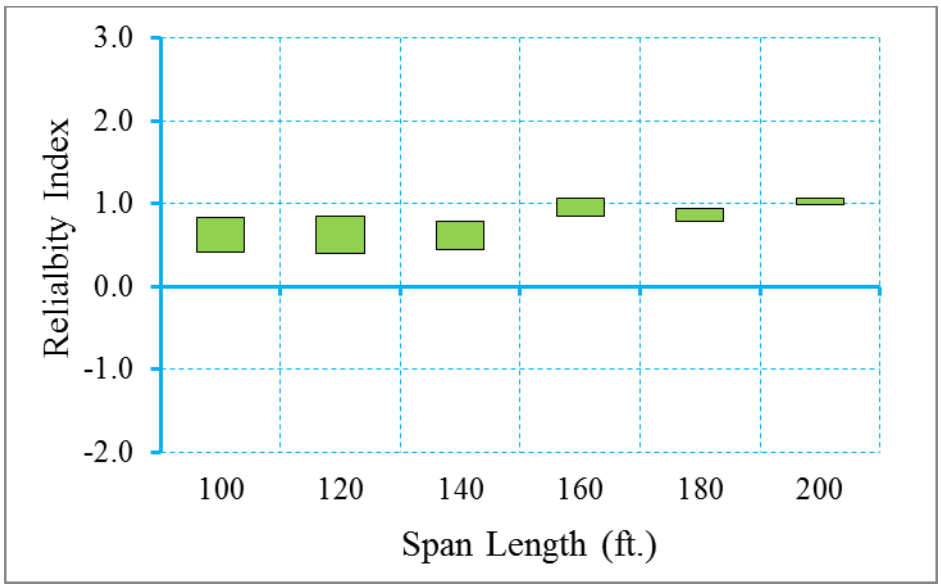

Figure D-158 Reliability Indices for Bridges at Decompression Limit State (ADTT=5000), γLL=0.8 ($f_t = 0.19\sqrt{f_c'}$)

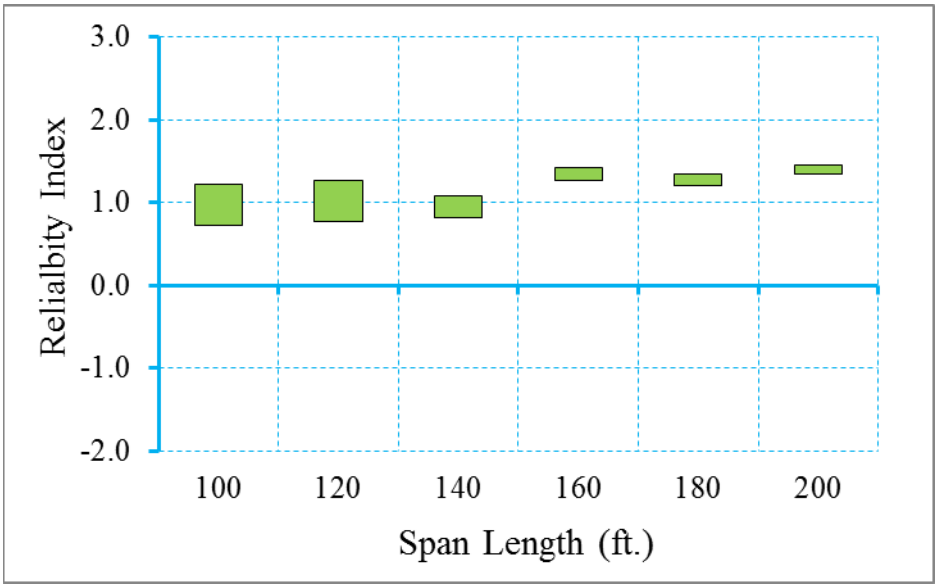

Figure D-159 Reliability Indices for Bridges at Maximum Allowable Tensile Stress Limit State (ADTT=5000), γLL=0.8 ($f_t = 0.19\sqrt{f_c'}$)

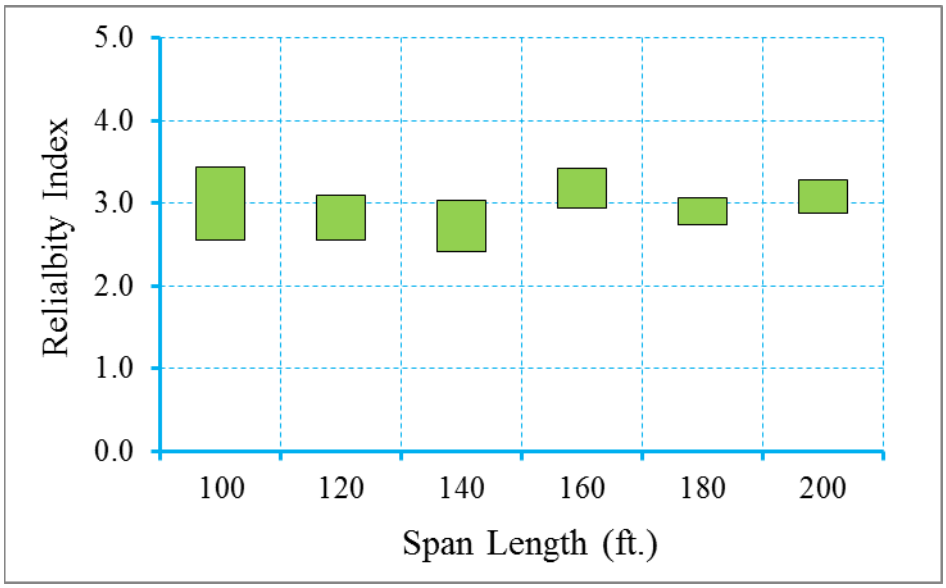

Figure D-160 Reliability Indices for Bridges at Maximum Allowable Crack Width Limit State (ADTT=5000), γLL=0.8 ($f_t = 0.19\sqrt{f_c'}$)

Step 2: Redesign the bridges with live load factor of 1.0 (Figure D-161~Figure D-163)

The bridges have been redesigned using a live load factor of 1.0. Please note that only the live load factor of Service III limit state is increased from 0.8 to 1.0, dead load and resistance factors were kept the same during the redesign. Table D-112 shows the design outcomes of the redesigned bridges.

Figure D-161 through Figure D-163 show the reliability indices for the redesigned bridges using live load factor of 1.0. It is observed that the average reliability index of decompression limit state, maximum allowable tensile stress limit state and maximum allowable crack width limit state is 1.00, 1.45, and 3.28, respectively.

Table D-112 Summary Information of Bridges Designed with γLL=1.0 ($f_t = 0.19\sqrt{f_c'}$)

Cases	Section Type	Span Length (ft.)	Aps (in^2)	# of Strands
1	1800-2	100	6.732	44
2	1800-2	120	10.71	70
3	1800-2	140	14.688	96
4	2100-2	160	21.7	100
5	2400-2	180	23.436	108
6	2400-2	200	29.078	134

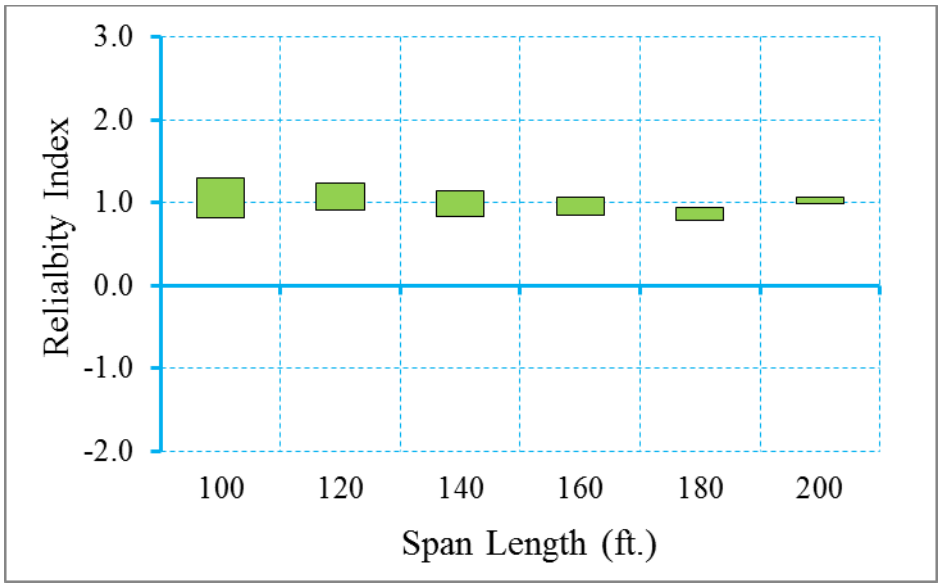

Figure D-161 Reliability Indices for Bridges at Decompression Limit State (ADTT=5000), γLL=1.0 ($f_t = 0.19\sqrt{f_c'}$)

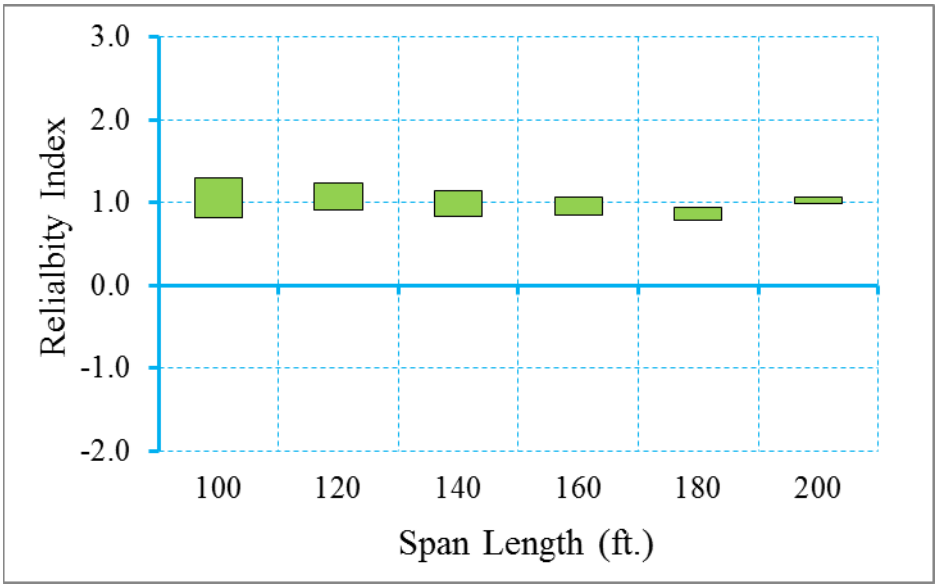

Figure D-162 Reliability Indices for Bridges at Maximum Tensile Stress Limit State (ADTT=5000), γLL=1.0 ($f_t = 0.19\sqrt{f_c'}$)

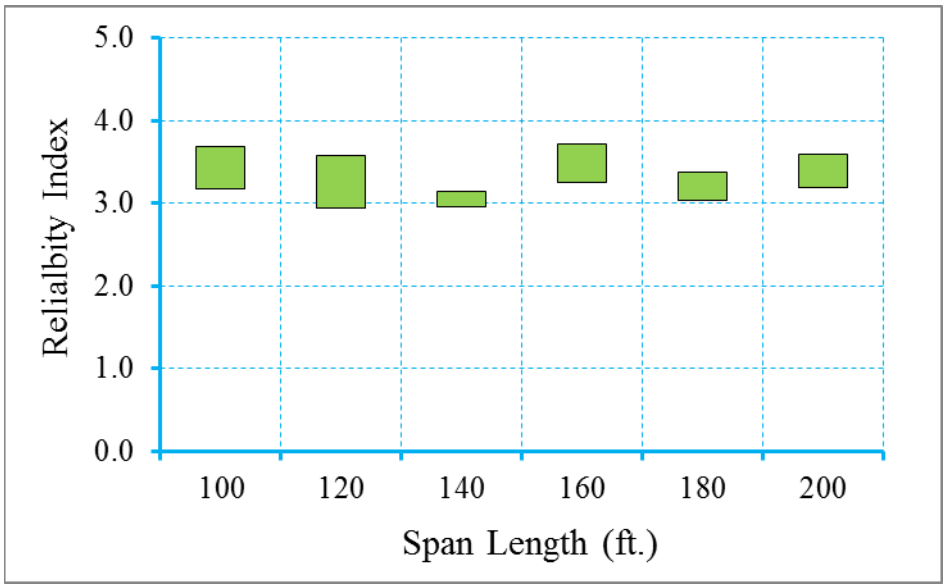

Figure D-163 Reliability Indices for Bridges at Maximum Crack Width Limit State (ADTT=5000), γLL=1.0 ($f_t = 0.19\sqrt{f_c'}$)

Step 3: Propose new live load, dead load, and/or resistance factors

Based on the calibration process shown in step 1 through step 3, it is observed that the uniform target reliability index can be achieved using a live load factor of 1.0. Therefore, for the scenario of ADTT equal to 5000 and maximum concrete tensile stress of $f_t = 0.19\sqrt{f_c'}$, a new live load factor of 1.0 is proposed.

D.4.3.4 Bridges Designed for Maximum Concrete Tensile Stress of $0.253\sqrt{f'_c}$

In this section, the calibration for a selected bridge database (shown in Table D-113) is performed for a scenario of ADTT equal to 5000. Please note that the maximum allowable crack width is specified as 0.016 in for maximum allowable crack width limit state.

Table D-113 Summary Information of Bridges Designed with γLL=0.8 ($f_t = 0.253\sqrt{f_c'}$)

Cases	Section Type	Span Length (ft.)	Aps (in^2)	# of Strands
1	1800-2	100	3.978	26
2	1800-2	120	7.344	48
3	1800-2	140	10.404	68
4	2100-2	160	16.058	74
5	2400-2	180	16.926	78
6	2400-2	200	22.134	102

Step 1: Calculate the reliability level of designs according to AASHTO LRFD Specifications (2010) (Figure D-164~Figure D-166)

Figure D-164 through Figure D-166 show the reliability indices for the bridges designed using AASHTO type girders according to AASHTO LRFD specifications (2010). It is observed that the average reliability index for decompression limit state, maximum allowable tensile stress limit state and maximum allowable crack width limit state is 0.19, 0.55, and 2.79, respectively. Live load factor of 1.0 will be used to estimate the effect of changing live load factor on reliability level.

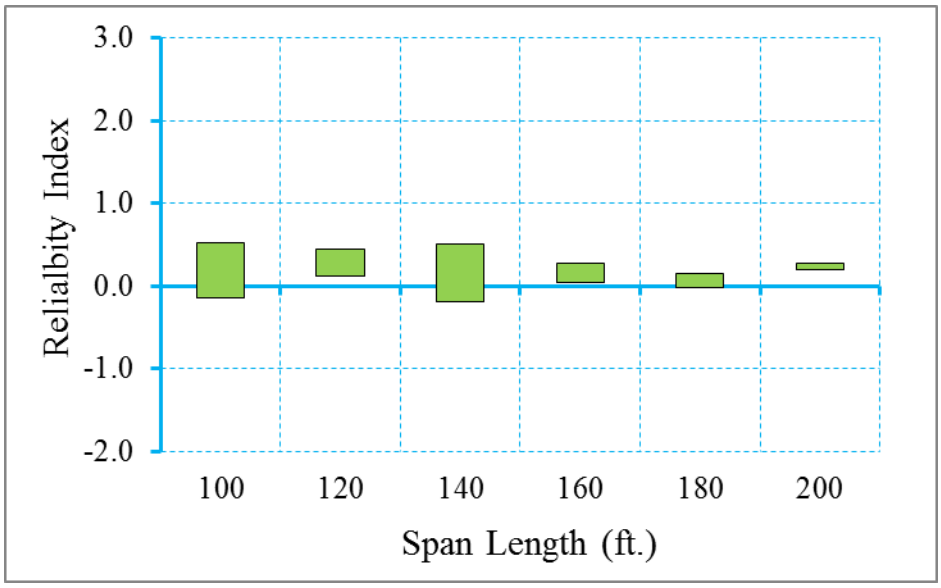

Figure D-164 Reliability Indices for Bridges at Decompression Limit State (ADTT=5000), γLL=0.8 ($f_t = 0.253\sqrt{f_c'}$)

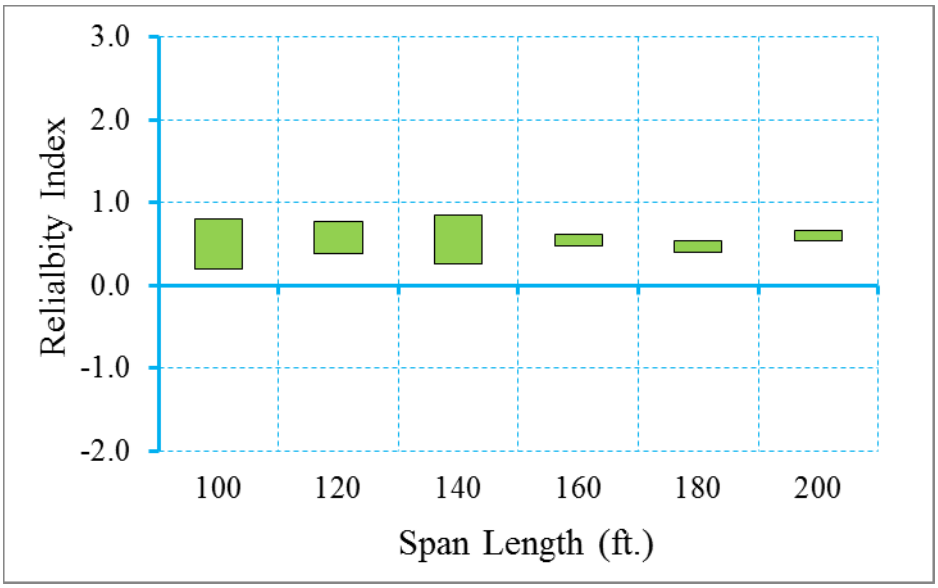

Figure D-165 Reliability Indices for Bridges at Maximum Allowable Tensile Stress Limit State (ADTT=5000), γLL=0.8 ($f_t = 0.253\sqrt{f_c'}$)

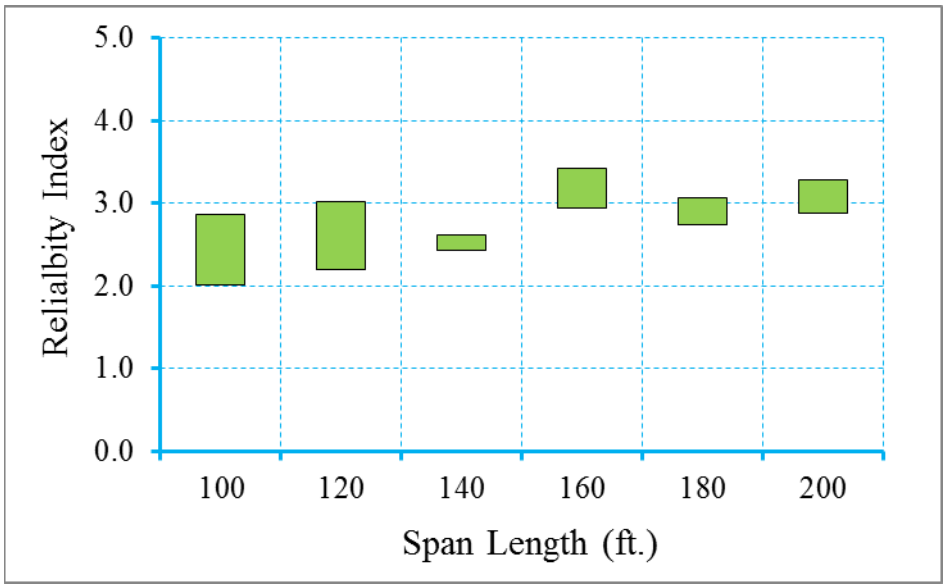

Figure D-166 Reliability Indices for Bridges at Maximum Allowable Crack Width Limit State (ADTT=5000), γLL=0.8 ($f_t = 0.253\sqrt{f_c'}$)

Step 2: Redesign the bridges with live load factor of 1.0 (Figure D-167~Figure D-169)

In this step, the bridges were redesigned using a live load factor of 1.0. Please note that only the live load factor of Service III limit state is increased from 0.8 to 1.0, dead load and resistance factors were kept the same during the redesign. Table D-114 shows the design outcomes of the redesigned bridges.

Figure D-167 through Figure D-169 show the reliability indices for the redesigned bridges using a live load factor of 1.0. It is observed that the average reliability index for the decompression limit state, the maximum allowable tensile stress limit state and the maximum allowable crack width limit state is 0.85, 1.23, and 3.04, respectively.

Table D-114 Summary Information of Bridges Designed with γLL=1.0

($f_t = 0.253\sqrt{f_c'}$)

Cases	Section Type	Span Length (ft.)	Aps (in^2)	# of Strands
1	1800-2	100	5.508	36
2	1800-2	120	9.18	60
3	1800-2	140	13.158	86
4	2100-2	160	19.964	92
5	2400-2	180	21.266	98
6	2400-2	200	26.908	124

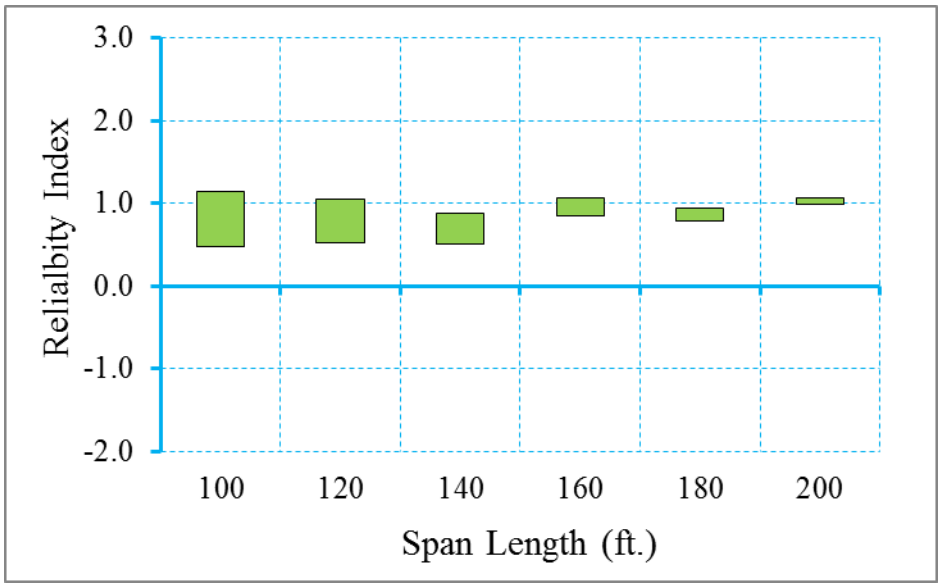

Figure D-167 Reliability Indices for Bridges at Decompression Limit State (ADTT=5000), γLL=1.0 ($f_t = 0.253\sqrt{f_c'}$)

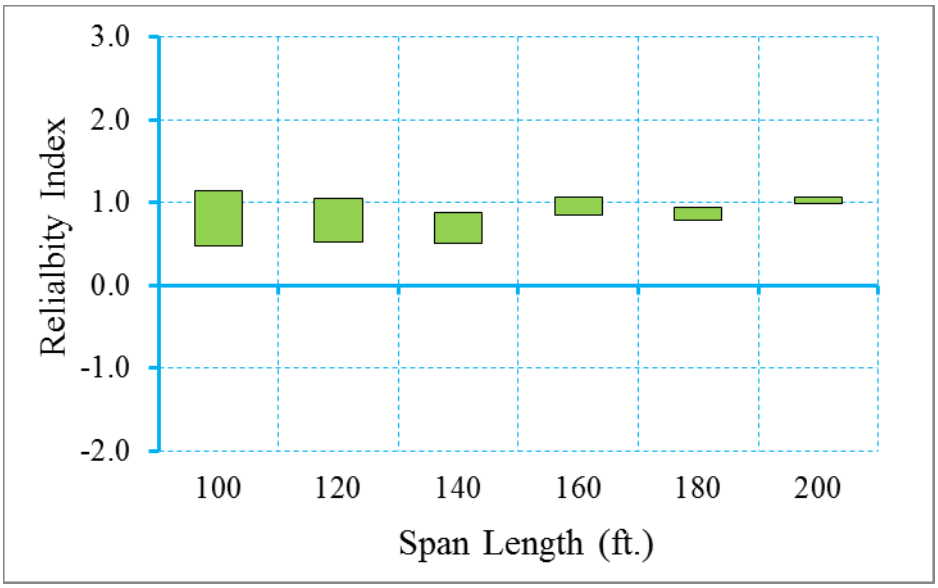

Figure D-168 Reliability Indices for Bridges at Maximum Allowable Tensile Stress Limit State (ADTT=5000), γLL=1.0 ($f_t = 0.253\sqrt{f_c'}$)

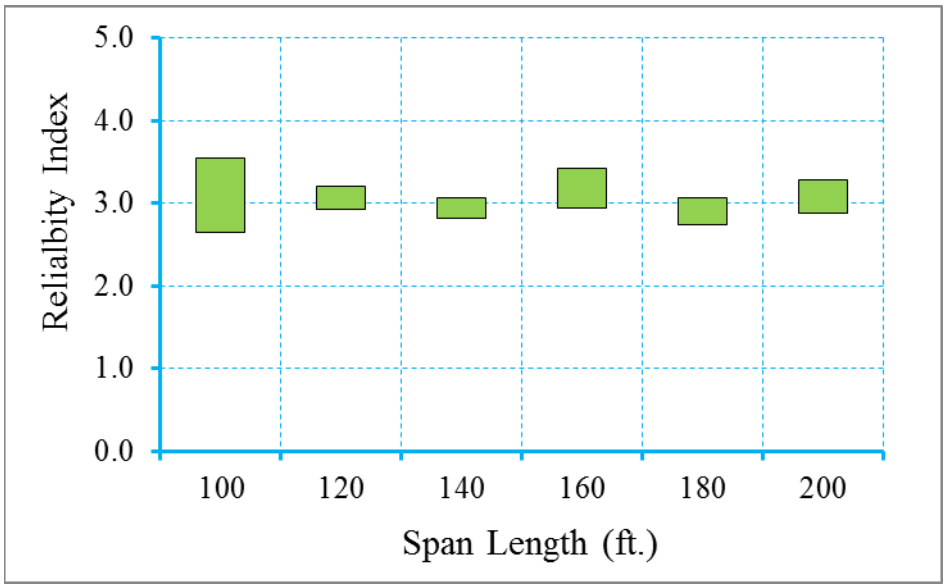

Figure D-169 Reliability Indices for Bridges at Maximum Allowable Crack Width Limit State (ADTT=5000), γLL=1.0 ($f_t = 0.253\sqrt{f_c'}$)

Step 3: Propose new live load, dead load, and/or resistance factors

Based on the calibration process shown in step 1 through step 3, it is observed that the uniform target reliability index can be achieved using a live load factor of 1.0. Therefore, for the scenario of ADTT equal to 5000 and maximum concrete tensile stress of $f_t = 0.253\sqrt{f_c'}$, a new live load factor of 1.0 is proposed.

D.5 Selection of load and resistance factors for use in the AASHTO LRFD

The detailed results presented above are summarized in Chapter 5 of the report. The proposed revisions to AASHTO LRFD are presented in Section 5.2.8 with the proposed revised specifications shown in Chapter 6. The detailed results presented above may be used by owners to revise their design requirements to fit special situations they may have.

APPENDIX E – DERIVATION OF THE RESISTANCE PREDICTION EQUATION OF PRESTRESSED CONCRETE GIRDERS

List of Figures

E.1 Derivation of the Resistance Prediction Equation of Prestressed Concrete Bridge Girders

The derivation of the resistance prediction equation for a prestressed concrete girder subjected to flexural loading is shown in this appendix. Figure E-1 shows the stress distribution diagram for a typical prestressed concrete bridge girder at various stages of loading. In this study, decompression is considered as the stress state producing a zero stress at the extreme bottom fibers of the prestressed girder.

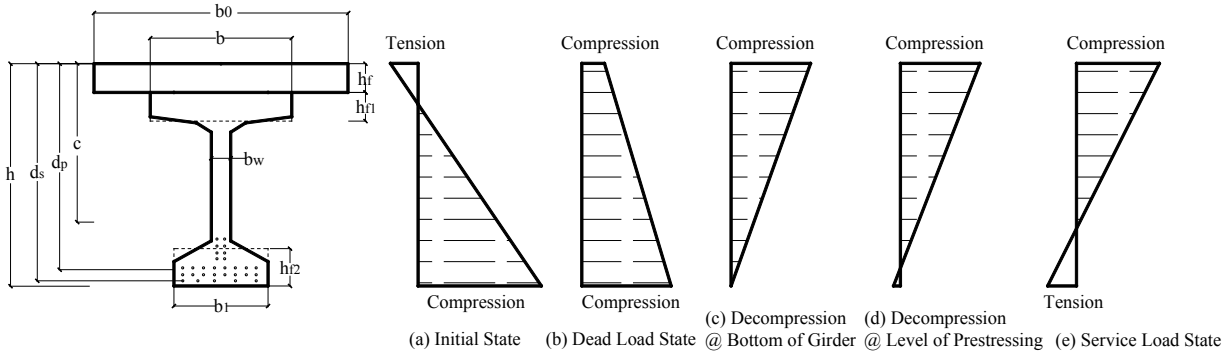

Figure E-1 Stress distribution diagrams for a typical prestressed concrete bridge girder at various stages of loading.

Using axial force equilibrium:

$$A_{ps}f_{ps} + A_s f_s = \frac{f_{ct}}{2} b_0 c - \frac{\frac{c-h_f}{2}}{c}(b_0 - b)(c-h_f)f_{ct} - \frac{\frac{c-h_f-h_{f1}}{2}}{c}(b-b_w)(c-h_f-h_{f1})f_{ct}$$

$$= \frac{f_{ct}}{2c}\left[b_0 c^2 - (c-h_f)^2(b_0-b) - (c-h_f-h_{f1})^2(b-b_w)\right] \qquad \text{(E-1)}$$

where,

A_s = area of non-prestressing steel.
A_{ps} = area of prestressing steel in tension zone.
b = prestressed beam top flange width.
b_0 = effective deck width transformed to the beam material.
b_w = web thickness.
c = depth of neutral axis from the from extreme compression fiber.
f_{ct} = calculated stress in concrete at the top fiber.
f_{ps} = calculated stress in prestressing steel.
f_s = calculated stress in non-prestressing steel.

h_f = deck thickness.

h_{f1} = top flange thickness.

The stress in the prestressing steel can be calculated as follows:

$$f_{ps} = E_{ps}\varepsilon_{ps} = E_{ps}(\varepsilon_{se} + \varepsilon_{ce}) + \frac{E_{ps}}{E_c} f_{ct}\left(\frac{d_p - c}{c}\right) \quad \text{(E-2)}$$

By rearranging Eq. (E-2), the stress in the concrete at the top fiber can be calculated as follows:

$$f_{ct} = \frac{\left[f_{ps} - E_{ps}(\varepsilon_{se} + \varepsilon_{ce})\right] E_c c}{E_{ps}(d_p - c)} \quad \text{(E-3)}$$

From strain compatibility,

$$f_s = E_s\varepsilon_s = \frac{E_s}{E_c} f_{ct}\left(\frac{d_s - c}{c}\right) \quad \text{(E-4)}$$

where, c = depth of neutral axis from the from extreme compression fiber.

d_p = the distance from extreme compression fiber to centroid of prestressing steel.

d_s = the distance from extreme compression fiber to centroid of non-prestressing steel.

E_c = modulus of elasticity of concrete.

E_{ps} = modulus of elasticity of prestressing steel.

E_s = modulus of elasticity of non-prestressing steel.

f_{ct} = stress in the concrete at the top of the beam after losses at service load.

ε_{ce} = strain in concrete at the level of prestressing steel after losses at dead load state.

ε_{ps} = strain in prestressing steel after losses at service load.

ε_s = strain in non-prestressing steel after losses at service load.

ε_{se} = strain in prestressing steel after losses at dead load state.

Substitute Eq. (E-3) and Eq. (E-4) into Eq. (E-1):

$$A_{ps} f_{ps} = \frac{\left[f_{ps} - E_{ps}(\varepsilon_{se} + \varepsilon_{ce})\right] E_c}{2E_{ps}(d_p - c)} \cdot \left[b_0 c^2 - (c - h_f)^2(b_0 - b) - (c - h_f - h_{f1})^2(b - b_w) - \frac{2A_s E_s (d_s - c)}{E_c}\right] \quad \text{(E-5)}$$

Eq. (E-5) can be simplified and rewritten as a quadratic equation with unknown c, neutral axis depth, as follows:

$$c^2+\frac{2}{b_w}\left[\frac{A_{ps}f_{ps}E_{ps}}{\left[f_{ps}-E_{ps}(\varepsilon_{se}+\varepsilon_{ce})\right]E_c}+b_0h_f+bh_{f1}-b_wh_f-b_wh_{f1}+\frac{A_sE_s}{E_c}\right]\cdot c$$
$$-\frac{2}{b_w}\left[\frac{A_{ps}f_{ps}E_{ps}}{\left[f_{ps}-E_{ps}(\varepsilon_{se}+\varepsilon_{ce})\right]E_c}-\frac{1}{2}(b-b_0)h_f{}^2+\frac{1}{2}(b-b_w)(h_f+h_{f1})^2+\frac{A_sE_sd_s}{E_c}\right]=0 \quad \text{(E-6)}$$

The moment resistance can be expressed as follows:

$$M_n=A_{ps}f_{ps}d_p+A_sf_sd_s-\frac{1}{6}f_{ct}b_0c^2+\frac{(c-h_f)^2(b_0-b)}{2c}f_{ct}\left(\frac{c+2h_f}{3}\right)$$
$$+\frac{(c-h_f-h_{f1})^2(b-b_w)}{2c}f_{ct}\left(\frac{c+2h_f+2h_{f1}}{3}\right) \quad \text{(E-7)}$$

where,

M_n = nominal moment resistance.

f_s is calculated using equation Eq. (E-3), and f_{ct} is calculated using equation Eq. (E-4).

The depth of neutral axis from the compression face, c, can be computed from Eq. (D-6)

Also, assuming linear elastic relationship in the behavior of the prestressing steel:

$$\varepsilon_{se}=\frac{f_{se}}{E_{ps}} \quad \text{(E-8)}$$

Then,

$$\varepsilon_{ce}=\frac{A_{ps}f_{se}}{E_c}\left(\frac{1}{A_c}+\frac{e_0{}^2}{I}\right)-\frac{M_De_0}{E_cI} \quad \text{(E-9)}$$

where,

A_c = area of concrete at the cross-section considered.

e_0 = eccentricity of the prestressing force with respect to the centroid of the section.

E_c = modulus of elasticity of concrete.

E_{ps} = modulus of elasticity of prestressing steel.

f_{se} = effective stress in prestressing steel after losses.

I = moment of inertia.

M_D = dead load moment.

Considering an uncracked section under service loads and plane section remains plane, the linear strain distribution diagram is as follows:

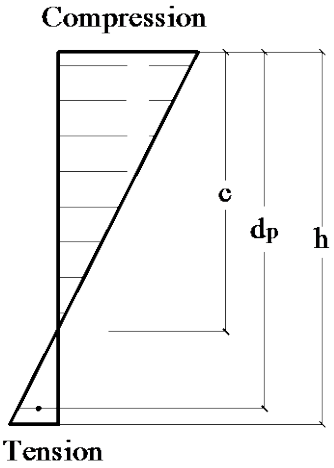

Figure E-2 Strain distribution at service loads.

From Figure E-2, the relationship between top and botom strain as follows:

$$\frac{d_p - c}{h - c} \cdot \varepsilon_c = \varepsilon_{ps} \quad \text{(E-10)}$$

$$\frac{d_p - c}{h - c} \cdot f_{cb} \frac{E_{ps}}{E_c} = \Delta f_{pt} \quad \text{(E-11)}$$

where,

E_c = elastic modulus of concrete.

Δf_{pt} = change in prestressing tendons stress between decompression and the stress in concrete at the bottom of the girder reaching f_{ct} assuming uncracked section

f_{cb} = the concrete allowable tensile stress at the bottom of the girder.

ε_c = strain in concrete at bottom fiber.

According to the current AASHTO LRFD (2012) Specifications, $f_{cb}=0.19\sqrt{f_c'}$ or $f_{cb}=0.0948\sqrt{f_c'}$, depending on the exposure conditions.

Then f_{ps} for uncracked section should be as follows:

$$f_{ps} = \Delta f_{pt} + f_{ps(M_{Dec})} \quad \text{(E-12)}$$

For the cracked section, the f_{ps} can be calculated by the following equation:

$$f_{ps} = \Delta f_{ps} + f_{ps(M_{Dec})} \quad \text{(E-13)}$$

where

$f_{ps(M_{Dec})}$ = the stress in prestressing steel at decompression

Δf_{ps} = the increase in the prestressing steel stress beyond the decompression state for cracked members.

M_{Dec} = the decompression moment.

Δf_{ps} in Eq. (D-13)can be calculated based on the equation of maximum crack width at the bottom of prestressed concrete girder. In this study, the equation below, developed by Nawy and Huang (1977) ,was used.

$$w_{\max} = 5.85 \times 10^{-5} \frac{A_t}{\beta \Sigma 0} (\Delta f_{ps}) \quad \text{(E-14)}$$

where,

A_t = area of concrete in tension.

β = ratio of distance from neutral axis of beam to concrete outside tension face to distance from neutral axis to steel reinforcement centroid.

$\sum 0$ = sum of reinforcing element circumferences.

By rearranging Eq. (D-14), Δf_{ps} can be calculated using the equation below:

$$\Delta f_{ps} = \frac{w_{\max} \cdot \beta \cdot \Sigma 0}{5.85 \times 10^{-5} \cdot A_t} \quad \text{(E-15)}$$

Δf_{pt} varies according to the maximum allowable tensile stress at the bottom of the concrete girder.

Moreover, $f_{ps(M_{Dec})}$can be calculated using the following equation:

$$f_{ps(M_{Dec})} = f_{se} + \frac{E_{ps}[M_{Dec} - M_D]}{IE_c[1 + \frac{A_{ps}E_{ps}}{E_c}(\frac{1}{A_c} + \frac{e_0^{\,2}}{I})]} \quad \text{(E-16)}$$

The decompression moment at level of prestressing strands, M_{Decp}, can be calculated using the following equation:

$$M_{Decp} = \frac{[f_{se} - \frac{M_D e_0 E_{ps}}{[I + \frac{A_{ps}E_{ps}}{E_c}(\frac{1}{A_c} + \frac{e_0^2}{I})]IE_c}]}{\frac{e_0}{I[\frac{1}{A_c} + \frac{e_0^2}{I}]A_{ps}} - \frac{e_0 E_{ps}}{[1 + \frac{A_{ps}E_{ps}}{E_c}(\frac{1}{A_c} + \frac{e_0^2}{I})]IE_c}} \quad \text{(E-17)}$$

The decompression moment at bottom fiber of concrete girder, M_{Decb}, can be calculated using the following equation:

$$M_{Decb} = \frac{[f_{se} - \frac{M_D e_0 E_{ps}}{[I + \frac{A_{ps}E_{ps}}{E_c}(\frac{1}{A_c} + \frac{e_0^2}{I})]IE_c}]}{\frac{y_b}{I[\frac{1}{A_c} + \frac{e_0 y_b}{I}]A_{ps}} - \frac{e_0 E_{ps}}{[1 + \frac{A_{ps}E_{ps}}{E_c}(\frac{1}{A_c} + \frac{e_0^2}{I})]IE_c}} \quad \text{(E-18)}$$

where,

A_c = area of concrete at the cross-section considered.
A_{ps} = the area of prestressing steel in tension zone.
e_0 = eccentricity of the prestressing force with respect to the centroid of the section at supports.
y_b = distance from centroidal axis to extreme bottom fiber
E_c = modulus of elasticity of concrete.
E_{ps} = modulus of elasticity of prestressing steel.
f_{se} = effective stress in prestressing steel after losses.
I = moment of inertia.
M_D = dead load moment.
M_{Decb} = decompression moment at the bottom of the girder.
M_{Decp} = decompression moment at the level of the prestressing strands.

APPENDIX F – COMPARISON OF CRACK WIDTH PREDICTION EQUATIONS FOR PRESTRESSED CONCRETE MEMBERS

List of Tables

List of Figures

F.1 Comparison of Crack Width Prediction Equations for Prestressed Concrete Members

This section presents a review and comparison of various prediction equations for the maximum crack width in prestressed concrete members. Test data from various sources were used in the comparisons. The equations are presented in chronological order:

1. CEB-FIP (1970) Equation

The 1970 Euro-International Committee for Concrete and International Federation for Prestressing (CEB-FIP) recommended adopting the following equation to predict the maximum crack width in partially prestressed beams:

$$w_{max} = (\Delta f_s - 4000) \times 10^{-6} \tag{F-1}$$

For static loads, the equation is:

$$w_{max} = \Delta f_s \times 10^{-6} \tag{F-2}$$

where Δf_s is the stress change in steel after decompression of concrete at the centroid of tension steel. Please note that the Δf_s in the CEB-FIP equation is in N/cm^2.

2. Nawy and Potyondy (1971) Equation

Nawy and Potyondy (1971) conducted a research program to study the flexural cracking behavior of pretensioned I and T beams. TABLE F-1 shows the geometric and mechanical properties of the prestressed beam specimens. A_s represents the area of tension reinforcement comprising both prestressing and normal steel reinforcement, A_s' represents the area of compression reinforcement, f'_c is the concrete cylinder compressive strength, and f'_t is the concrete tensile splitting strength.

Based on a regression analysis of the test data, the authors proposed Equation F-3:

$$w_{max} = 1.13 \times 10^{-6} \left(\frac{A_t}{A_s} \right)^{1/4} a_c \sqrt{\Delta f_{s1}^{\ 3}} \tag{F-3}$$

where,

- a_c = stabilized crack spacing, in.
- A_t = area of concrete in tension, in^2.
- A_s = total area of reinforcement, in^2.
- E = 27.5×10^3 ksi was used.
- f_s = stress in prestressing steel after cracking, ksi.

f_d = stress in the prestressing steel when the modulus of rupture of concrete at the extreme tensile fibers is reached, ksi.

Δf_{s1} = $\left[f_s - f_d - 3.75\right]$, ksi

TABLE F-1 Geometrical properties of the prestressed beams (Nawy and Potyondy,1971)

Beam	Section	Width *b*, in.	Depth* *d*, in.	A_s sq in.	$\rho = \frac{A_s}{bd}$ Percent	A_s' sq in.	$\rho' = \frac{A_s'}{bd}$ Percent	f'$_c$ psi	f'$_t$ psi	Slump in.
B1	T	8	8.75	0.271	0.389	-	-	4865	400	3
B2	I	6	8.90	0.271	0.518	-	-	4865	400	3
B3	T	8	8.75	0.271	.0389	-	-	4330	430	4
B4	I	6	8.90	0.271	0.518	-	-	4290	430	4
B5	I	6	8.90	0.271	0.518	-	-	4340	430	4
B6	T	8	8.75	0.271	0.389	-	-	4375	430	4
B7	T	8	8.75	0.271	0.389	-	-	4290	390	6
B8	I	6	8.90	0.271	0.518	-	-	4260	390	6
B9	I	6	8.90	0.271	0.518	-	-	4190	390	6
B10	T	8	8.75	0.271	0.389	-	-	4280	390	6
B11	T	8	8.75	0.271	0.389	-	-	4150	370	8
B12	I	6	8.90	0.271	0.518	-	-	3920	370	8
B13	I	6	8.90	0.281	0.518	-	-	3890	370	8
B14	T	8	8.75	0.271	0.389	-	-	4110	370	8
B15	T	8	8.75	0.271	0.389	0.93	1.332	3490	340	5 1/2
B16	I	6	8.90	0.271	0.518	0.33	0.631	3400	340	5 1/2
B17	I	6	8.90	0.271	0.518	0.93	1.776	3390	340	5 1/2
B18	T	8	8.75	0.271	0.389	0.33	0.473	3510	340	5 1/2
B19**	I	6	8.90	0.235	0.448	-	-	3610	385	6
B20**	I	6	8.90	0.235	0.448	-	-	3495	385	6
B21**	I	6	8.90	0.235	0.448	-	-	3430	355	6 1/2
B22**	I	6	8.90	0.235	0.448	-	-	3280	355	6 1/2
B23	I	6	8.90	0.271	0.518	-	-	4060	380	5
B24	I	6	8.90	0.271	0.518	-	-	4095	380	5
B25	I	6	8.90	0.271	0.518	-	-	3950	380	5
B26	I	6	8.90	0.271	0.518	-	-	4000	380	5

* Total depth h in each beam = 12 in.

\+ A_s includes two 3/16 in. diameter normal high strength steel wire (f_y = 96,000 psi) cage bars in addition to prestressing tendons.

** Beams B19-B22 were continuous beams and were not included in the cracking analysis

After further simplification of Equation (F-3), Nawy and Potyondy (1971) recommended the following expression:

$$w_{\max} = 1.44(\Delta f_s - 8.3) \qquad \text{(F-4)}$$

where

Δf_s is the net stress in prestressing steel, or the magnitude of tensile stress in normal steel at any crack width level. Please note the units for Δf_s in Equation (F-4) are ksi and the units for crack width are inches.

3. Bennett and Veerasubramanian (1972) Equation

Bennett and Veerasubramanian (1972) investigated the behavior of non-rectangular beams with limited prestress after flexural cracking. They tested 34 prestressed concrete beams with the following cross-sections:

- Rectangular: 12 inch deep x 6 inch wide
- I-Beam: 12 inch deep with 6 inch wide top and bottom flanges
- I-Beam: 12 inch deep with 12 inch wide top flange and 6 inch wide bottom flange
- I-Beam: 8 inch deep. A slab 24 inch wide was cast later to represent the deck

All beams were simple spans with a span length of 10 ft. Two concentrated loads spaced 6 ft. apart and centered on the span were used for loading.

- They recommended a prediction equation for the maximum crack width as follows:

$$w_{\max} = \beta_1 + \beta_2 \varepsilon_s d_c \qquad \text{(F-5)}$$

where,

d_c = clear cover over the nearest reinforcing bar to the tensile face, mm.

β_1 = a constant representing the residual crack width measured after the first cycle of loading. The value suggested for deformed bars is 0.02 mm.

β_2 = a constant depending on bond characteristics of the nonprestressed steel. The value recommended for deformed bars was 6.5.

ε_s = increase in strain in nonprestressed steel from stage of decompression of concrete at tensile face of beam, με.

Please note that this equation uses the International System of Units (SI).

4. Nawy and Huang (1977) Equation

Nawy and Huang (1977) studied crack and deflection control in pretensioned prestressed beams. They performed tests on twenty single-span and four continuous beams. Based on a detailed statistical analysis of the test data, they proposed the following equation:

$$w_{\max} = 5.85 \times 10^{-5} \frac{A_t}{\beta \Sigma 0} (\Delta f_{ps}) \qquad \text{(F-6)}$$

where, A_t = area of concrete in tension, in^2.

β = ratio of distance from neutral axis of beam to concrete outside tension face to distance from neutral axis to steel reinforcement centroid.

Δf_{ps} = increase in stress in the prestressing steel beyond decompression state, ksi.

$\sum 0$ = sum of reinforcing element circumferences, in.

Table F-2 presents a comparison of the crack widths measured from the beam tests performed by Nawy and Huang (1977) and the ones predicted using the equation developed by Nawy and Huang (1977). On average, Equation (F-6) by Nawy and Huang (1977) provides prediction results that are within 20% of the measured maximum crack width of prestressed concrete beams.

TABLE F-2 Observed vs. theoretical maximum crack width at tensile face of beam (Nawy and Huang, 1977)

Net steel stress											
30 ksi			40 ksi			60 ksi			80 ksi		
$w_{obs.}$	w_{theory}	Error %	$w_{obs.}$	w_{theory}	Error %	$w_{obs.}$	w_{theory}	Error %	$w_{obs.}$	w_{theory}	Error %
0.0111	0.0131	-15.3	0.0151	0.0175	-13.7	0.0261	0.0262	-0.4	0.04	0.0349	14.6
0.0127	0.0118	7.6	0.0204	0.0157	29.9	0.0275	0.0236	16.5	0.0409	0.0313	30.7
0.0131	0.0128	2.3	0.0166	0.0172	-3.5	0.0304	0.0256	18.8	0.0382	0.0344	11.0
0.0097	0.013	-25.4	0.0158	0.0174	-9.2	0.0226	0.0259	-12.7	0.0304	0.0347	-12.4
0.0091	0.0147	-38.1	0.0117	0.0197	-40.6	0.0205	0.0294	-30.3	0.032	0.0393	-18.6
0.0124	0.0148	-16.2	0.0181	0.0199	-9.0	0.0213	0.0297	-28.3	0.0364	0.0397	-8.3
0.0052	0.0051	2.0	0.0068	0.0069	-1.4	0.0117	0.0103	13.6	0.0188	0.0137	37.2
0.0049	0.0051	-3.9	0.0061	0.0069	-11.6	0.0111	0.0103	7.8	0.0146	0.0137	6.6
0.0051	0.0045	13.3	0.0064	0.0061	4.9	0.0107	0.009	18.9	0.0165	0.0121	36.4
0.0058	0.0045	28.9	0.0082	0.0061	34.4	0.0134	0.009	48.9	0.0185	0.0121	52.9
0.0054	0.0059	-8.5	0.0069	0.0079	-12.7	0.0112	0.0119	-5.9	0.0172	0.0158	8.9
0.0048	0.0059	-18.6	0.0076	0.0079	-3.8	0.0134	0.0119	12.6	0.0192	0.0158	21.5
0.0043	0.0046	-6.5	0.0058	0.0062	-6.5	0.0105	0.0092	14.1	0.0138	0.0123	12.2
0.0052	0.0046	13.0	0.0059	0.0062	-4.8	0.0103	0.0092	12.0	0.0145	0.0123	17.9
0.0039	0.0057	-31.6	0.0061	0.0076	-19.7	0.0115	0.0114	0.9	0.0181	0.0153	18.3
0.0038	0.0057	-33.3	0.0057	0.0076	-25.0	0.0093	0.0114	-18.4	0.016	0.0153	4.6
0.0039	0.0056	-30.4	0.006	0.0074	-18.9	0.0098	0.0112	-12.5	0.0159	0.0148	7.4
0.003	0.0056	-46.4	0.0045	0.0074	-39.2	0.0086	0.0112	-23.2	0.0147	0.0148	-0.7
0.0057	0.0061	-6.6	0.0085	0.0081	4.9	0.0129	0.0121	6.6	0.0202	0.0163	23.9
0.0034	0.0045	-24.4	0.0045	0.0059	-23.7	0.0089	0.0089	0.0	0.0139	0.0119	16.8
Average		18.6	Average		15.9	Average		15.1	Average		18.0

5. Rao and Dilger (1992) Equation

Rao and Dilger (1992) developed a detailed crack control procedure for prestressed concrete members. The authors studied the prediction equation of maximum crack width developed by various previous researchers and proposed a new equation expressed as follows:

$$w_{\max} = k_1 f_s d_c \left(A_t / A_s\right)^{0.5} \quad \text{(F-7)}$$

where,

A_t = area of concrete in tension, mm^2.

A_s = total area of reinforcement, mm^2.

d_c = concrete cover measured from surface to the center of nearest reinforcement bar, mm.

f_s = stress in steel after decompression, MPa.

k_1 = the bond coefficient defined for each combination of prestressed and nonprestressed reinforcement.

6. Eurocode 2 (2004) Provisions

Eurocode 2 (2004) provides the following provisions to calculate the crack widths:

$$w_k = s_{r,\max}\left(\varepsilon_{sm} - \varepsilon_{cm}\right) \quad \text{(F-8)}$$

where,

$s_{r,\max}$ = maximum crack spacing.

w_k = crack width.

ε_{sm} = mean strain in the reinforcement under the relevant combination of loads, including the effect of imposed deformations and taking into account the effects of tension stiffening. Only the additional tensile strain beyond the state of zero concrete strain at the same level is considered.

ε_{cm} = mean strain in the concrete between cracks.

In Equation (F-8), the quantity $\left(\varepsilon_{sm} - \varepsilon_{cm}\right)$ can be calculated from the following expression:

$$\left(\varepsilon_{sm} - \varepsilon_{cm}\right) = \frac{\sigma_s - k_t \dfrac{f_{ct,eff}}{\rho_{p,eff}}\left(1 + \alpha_e \rho_{p,eff}\right)}{E_s} \geq 0.6\frac{\sigma_s}{E_s} \quad \text{(F-9)}$$

where,

$A_{ct,eff}$ = effective area of concrete in tension surrounding the reinforcement or prestressing tendons of depth, $h_{c,ef}$, where $h_{c,ef}$ is the lesser of $2.5(h-d)$, $(h-x)/3$ or $h/2$, where h is the height of the beam, d is the effective depth of a cross section, and x is the neutral axis depth.

A_p' = area of pre or post-tensioned tendons within $A_{ct,eff}$.

A_s = area of reinforcement within $A_{ct,eff}$

E_{cm} = the secant modulus of elasticity of concrete

E_s = the design value of modulus of elasticity of reinforcing steel

$f_{ct,eff}$ = the mean value of the tensile strength of the concrete effective at the time when the cracks may first be expected to occur: $f_{ct,eff} = f_{ctm}$ or lower, ($f_{ctm}(t)$) if cracking is expected earlier than 28 days.

k_t = factor dependent on the duration of the load.

α_e = E_s / E_{cm}

$\rho_{p,eff}$ = $\left(A_s + \xi_1^2 A'_p\right) / A_{c,eff}$.

σ_s = stress in the tension reinforcement assuming a cracked section. For pretensioned members, σ_s may be replaced by $\Delta\sigma_p$, the stress variation in prestressing tendons from the state of zero strain of the concrete at the same level.

ϕ_s = largest bar diameter of reinforcing steel

ϕ_p = equivalent diameter of tendon;

ξ_1 = adjusted ratio of bond strength taking into account the different diameters of prestressing and reinforcing steel, calculated as $\sqrt{\xi \cdot \frac{\phi_s}{\phi_p}}$,

ξ = the ratio of bond strength of prestressing and reinforcing steel

$$s_{r,\max} = k_3 c + k_1 k_2 k_4 \phi / \rho_{p,eff} \quad \text{(F-10)}$$

where,

c = cover to the longitudinal reinforcement.

k_1 = coefficient that takes account of the bond properties of the bonded reinforcement.

k_2 = coefficient that takes account of the distribution of strain.

k_3 = coefficient can be found in the National Annex according to different country, the recommended value is 3.4;

k_4 = coefficient can be found in the National Annex according to different country, the recommended value is 0.425.

ϕ = bar diameter.

7. Comparison between the measured and predicted maximum crack width using various equations

Figure F-1 through Figure F-4 present a comparison of the equation developed by Nawy and Huang (1977) and four other prediction equations. Any points that fall on the 45° line plotted on the figures indicate agreement between sources. The equations used in Eurocode were not compared with the testing data since there is no sufficient information to apply this equation. Figure F-1 indicates that the equation developed by Nawy and Potyondy (1971) did not provide good prediction results compared to the measured data since it relates the

maximum crack width with the Δf_{ps} only. The equation developed by Nawy and Huang (1977) exhibited excellent correlation at low values of crack width. The predicted values are slightly different from the measured data when the loading increases, but the results were still close to the measured data.

Figure F-2 indicates the equation developed by Bennett and Veerasubramanian (1972) did not exhibit good correlation with measured results when the maximum crack width increases.

Figure F-3 indicates that the equation recommended by CEB-FIP overestimates the crack width prediction at small load. A number of beam specimens had fully prestressed tendons and the measured data did not compare well with the predicted value.

Figure F-4 indicates that the equation recommended by Rao and Dilger underestimates the crack width prediction, especially under heavy load.

In summary, based on the comparisons, the equation developed by Nawy and Huang (1977) provides the best correlation with measured data. Furthermore, this equation took the effect of bar size and steel stress into account and can be easily incorporated into the calibration procedure. The equation by Nawy and Hwang (1977) was used in the calibration of the tension in prestressed concrete when the crack width was considered.

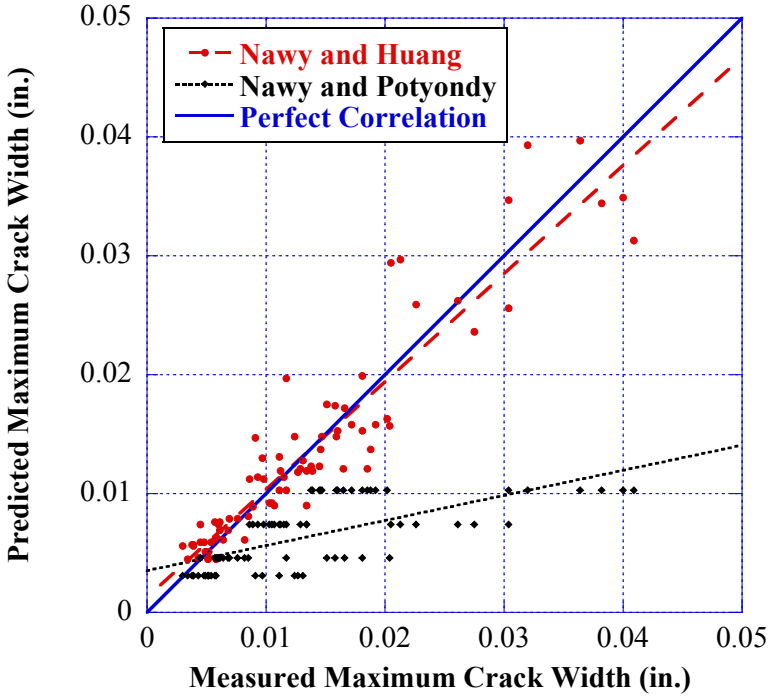

FIGURE F-1 Comparison of the measured and predicted maximum crack widths using equations developed by Nawy and Huang (1977) and Nawy and Potyondy (1971).

Figure A.6

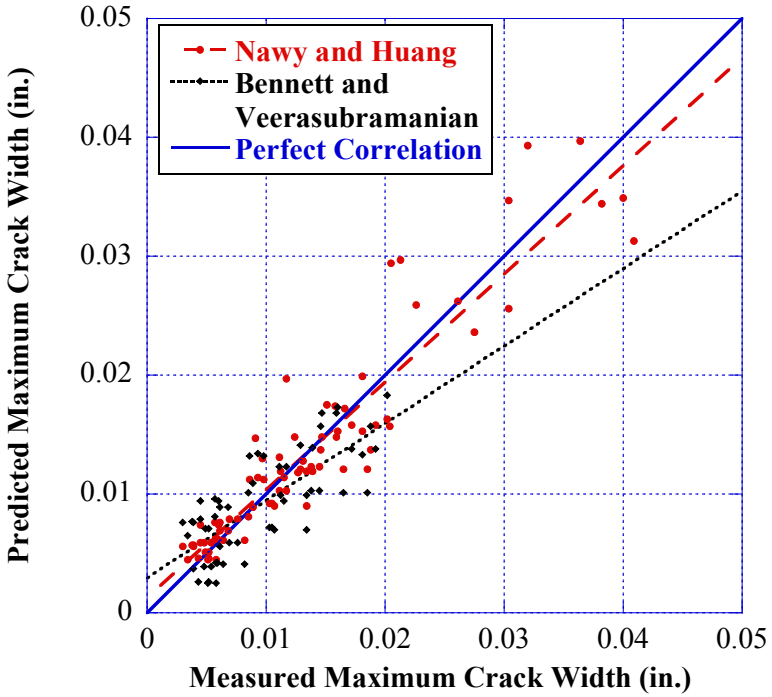

FIGURE F-2 Comparison of the measured and predicted maximum crack widths using equations developed by Nawy and Huang (1977) and Bennett and Veerasubramanian (1972).

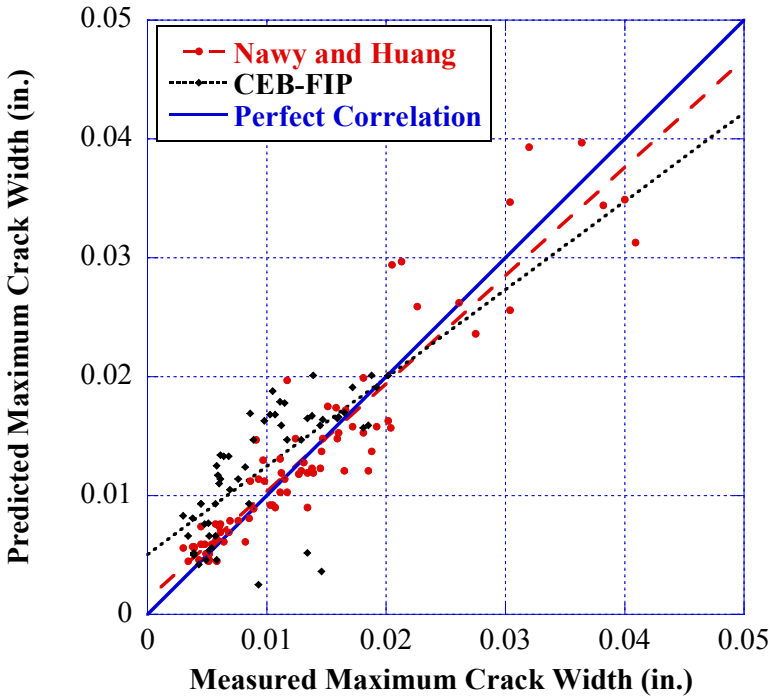

FIGURE F-3 Comparison between the measured and predicted maximum crack widths using equations developed by Nawy and Huang (1977) and CEB-FIP (1970).

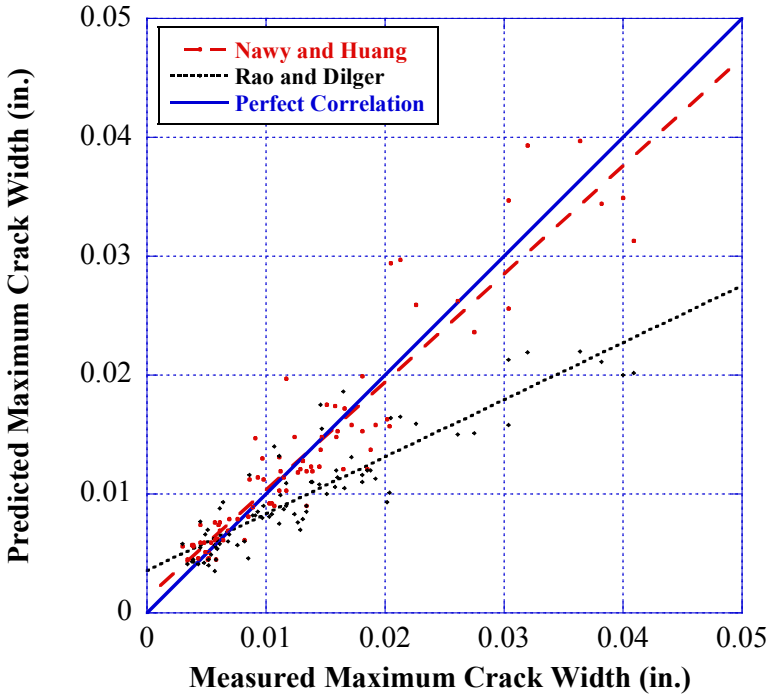

FIGURE F-4 Comparison between the measured and predicted maximum crack widths using equations developed by Nawy and Huang (1977) and Rao and Dilger (1992).

References

Bennett, E.W. and N. Veerasubramanian. September 1972. “Behavior of Nonrectangular Beams With Limited Prestress After Flexural Cracking after flexural cracking,” *ACI Journal, Proceedings*, Vol. 69, No. 9, pp. 533-542.

CEB-FIP Joint Committee. June 1970. *International recommendations for the design and construction of concrete structures*. Cement and Concrete Association, London.

European Standard EN 1992. December 2004. *Eurocode 2: Design of Concrete Structures-Part 1-1: General rules and rules for buildings*. CEN (European Committee for Standardization), 225 pp.

Nawy, E. G. and P.T. Huang. May-June 1977. “Crack and Deflection Control of Pretensioned Prestressed Beams.” *PCI Journal*, Vol. 23, No. 3, pp. 30-43.

Nawy, E. G. and J. G. Potyondy. May 1971. “Flexural Cracking Behavior of Pretensioned, Prestressed Concrete I- and T- Beams,” *ACI Journal, Proceedings*, Vol. 68, No. 5, pp. 355-360.

Rao, S. V. K. M. and W. H. Dilger. March-April 1992. “Control of Flexural Crack Width in Cracked Prestressed Concrete Members” *ACI Structural Journal*, Vol. 89, No. 2, pp 127-138.

APPENDIX G – CONCRETE FATIGUE DATABASE

List of Tables

List of Figures

Definitions:

f_min = Minimum stress (ksi)
f'c = Concrete compressive strength (ksi)
N = Cycles to failure
S_max = Maximum stress range (ksi)
S_min = Minimum stress range (ksi)
Sr = Stress range (ksi)

Table G-1 Fatigue Data for Plain Concrete in Compression [1]

S_max/f'c	S_min (ksi)	Sr (ksi)	N	Reference No.	Notes
0.75	0.6	3.9	17000	1	Group 2A; e=0in
0.75	0.6	3.9	24000	1	Group 2A; e=0in
0.75	0.6	3.9	36000	1	Group 2A; e=0in
0.75	0.6	3.9	39000	1	Group 2A; e=0in
0.75	0.6	3.9	40000	1	Group 2A; e=0in
0.75	0.6	3.9	47000	1	Group 2A; e=0in
0.75	0.6	3.9	53000	1	Group 2A; e=0in
0.75	0.6	3.9	59000	1	Group 2A; e=0in
0.75	0.6	3.9	65000	1	Group 2A; e=0in
0.75	0.6	3.9	70000	1	Group 2A; e=0in
0.725	0.6	3.75	39000	1	Group 2A; e=0in
0.725	0.6	3.75	60000	1	Group 2A; e=0in
0.725	0.6	3.75	107000	1	Group 2A; e=0in
0.725	0.6	3.75	110000	1	Group 2A; e=0in
0.725	0.6	3.75	130000	1	Group 2A; e=0in
0.725	0.6	3.75	136000	1	Group 2A; e=0in
0.725	0.6	3.75	192000	1	Group 2A; e=0in
0.725	0.6	3.75	275000	1	Group 2A; e=0in
0.7	0.6	3.6	55000	1	Group 2A; e=0in
0.7	0.6	3.6	106000	1	Group 2A; e=0in
0.7	0.6	3.6	135000	1	Group 2A; e=0in
0.7	0.6	3.6	152000	1	Group 2A; e=0in
0.7	0.6	3.6	155000	1	Group 2A; e=0in
0.7	0.6	3.6	206000	1	Group 2A; e=0in
0.7	0.6	3.6	269000	1	Group 2A; e=0in
0.7	0.6	3.6	313000	1	Group 2A; e=0in
0.7	0.6	3.6	320000	1	Group 2A; e=0in
0.7	0.6	3.6	356000	1	Group 2A; e=0in
0.7	0.6	3.6	429000	1	Group 2A; e=0in

S_max/f'c	S_min (ksi)	Sr (ksi)	N	Reference No.	Notes
0.7	0.6	3.6	492000	1	Group 2A; e=0in
0.675	0.6	3.45	159000	1	Group 2A; e=0in
0.675	0.6	3.45	256000	1	Group 2A; e=0in
0.675	0.6	3.45	270000	1	Group 2A; e=0in
0.675	0.6	3.45	655000	1	Group 2A; e=0in
0.675	0.6	3.45	779000	1	Group 2A; e=0in
0.675	0.6	3.45	970000	1	Group 2A; e=0in
0.675	0.6	3.45	1048000	1	Group 2A; e=0in
0.675	0.6	3.45	1051000	1	Group 2A; e=0in
0.675	0.6	3.45	1318000	1	Group 2A; e=0in
0.675	0.6	3.45	1661000	1	Group 2A; e=0in
0.675	0.6	3.45	2000000	1	Group 2A; e=0in
0.675	0.6	3.45	2000000	1	Group 2A; e=0in
0.9	0.6	4.8	28000	1	Group 2B; e=1in
0.9	0.6	4.8	31000	1	Group 2B; e=1in
0.9	0.6	4.8	35000	1	Group 2B; e=1in
0.9	0.6	4.8	45000	1	Group 2B; e=1in
0.9	0.6	4.8	46000	1	Group 2B; e=1in
0.9	0.6	4.8	58000	1	Group 2B; e=1in
0.9	0.6	4.8	61000	1	Group 2B; e=1in
0.9	0.6	4.8	129000	1	Group 2B; e=1in
0.875	0.6	4.65	81000	1	Group 2B; e=1in
0.875	0.6	4.65	120000	1	Group 2B; e=1in
0.875	0.6	4.65	131000	1	Group 2B; e=1in
0.875	0.6	4.65	141000	1	Group 2B; e=1in
0.875	0.6	4.65	156000	1	Group 2B; e=1in
0.875	0.6	4.65	180000	1	Group 2B; e=1in
0.875	0.6	4.65	190000	1	Group 2B; e=1in
0.875	0.6	4.65	226000	1	Group 2B; e=1in
0.875	0.6	4.65	242000	1	Group 2B; e=1in
0.875	0.6	4.65	317000	1	Group 2B; e=1in
0.875	0.6	4.65	351000	1	Group 2B; e=1in
0.875	0.6	4.65	527000	1	Group 2B; e=1in
0.85	0.6	4.5	305000	1	Group 2B; e=1in
0.85	0.6	4.5	684000	1	Group 2B; e=1in
0.85	0.6	4.5	730000	1	Group 2B; e=1in
0.85	0.6	4.5	859000	1	Group 2B; e=1in
0.85	0.6	4.5	860000	1	Group 2B; e=1in
0.85	0.6	4.5	1045000	1	Group 2B; e=1in
0.85	0.6	4.5	2105000	1	Group 2B; e=1in

S_max/f'c	S_min (ksi)	Sr (ksi)	N	Reference No.	Notes
0.85	0.6	4.5	2751000	1	Group 2B; e=1in
0.85	0.6	4.5	2000000	1	Group 2B; e=1in
0.85	0.6	4.5	16000	1	Group 2C; e=1/3in
0.85	0.6	4.5	26000	1	Group 2C; e=1/3in
0.85	0.6	4.5	35000	1	Group 2C; e=1/3in
0.85	0.6	4.5	37000	1	Group 2C; e=1/3in
0.85	0.6	4.5	46000	1	Group 2C; e=1/3in
0.85	0.6	4.5	65000	1	Group 2C; e=1/3in
0.8	0.6	4.2	108000	1	Group 2C; e=1/3in
0.8	0.6	4.2	206000	1	Group 2C; e=1/3in
0.8	0.6	4.2	224000	1	Group 2C; e=1/3in
0.8	0.6	4.2	249000	1	Group 2C; e=1/3in
0.8	0.6	4.2	270000	1	Group 2C; e=1/3in
0.8	0.6	4.2	364000	1	Group 2C; e=1/3in
0.8	0.6	4.2	542000	1	Group 2C; e=1/3in
0.8	0.6	4.2	2000000	1	Group 2C; e=1/3in
0.775	0.6	4.05	464000	1	Group 2C; e=1/3in
0.775	0.6	4.05	888000	1	Group 2C; e=1/3in
0.775	0.6	4.05	941000	1	Group 2C; e=1/3in
0.775	0.6	4.05	1198000	1	Group 2C; e=1/3in
0.775	0.6	4.05	2000000	1	Group 2C; e=1/3in

Table G-2 Concrete Fatigue Data for Reinforced Concrete [2, 3, 4, 5]

f_min	Sr	N	Reference No.	Notes/Specimen No.
5.0	39.0	216,400	2	
5.0	39.0	288,100	2	
5.0	39.0	315,600	2	
5.0	34.0	356,800	2	
15.0	34.0	406,600	2	
15.0	34.0	441,000	2	
5.0	34.0	506,100	2	
5.0	34.0	515,300	2	
5.0	29.0	626,000	2	
15.0	34.0	645,300	2	
15.0	29.0	746,000	2	
5.0	29.0	864,500	2	
5.0	29.0	920,200	2	
15.0	29.0	971,900	2	
15.0	29.0	1,232,300	2	
15.0	26.0	2,214,500	2	
15.0	24.0	3,187,500	2	
15.0	25.0	3,496,500	2	
15.0	24.0	3,702,400	2	
15.0	24.0	8,164,000	2	
4.31	39.42	6,250,000	3	Bar A-A15
24.8	22.2	5,200,000	3	Bar A-A15
4.31	34.27	3,782,000	3	Bar A-A15
12.85	31.62	3,375,000	3	Bar A-A15
4.31	38.56	3,142,800	3	Bar A-A15
4.32	38.66	2,934,000	3	Bar A-A15
12.89	34.11	2,342,000	3	Bar A-A15
4.31	42.69	2,037,000	3	Bar A-A15
12.85	36.18	1,598,000	3	Bar A-A15
4.31	39.39	1,316,000	3	Bar A-A15
4.31	38.64	1,060,000	3	Bar A-A15
12.87	35.06	964,000	3	Bar A-A15
4.31	40.2	881,000	3	Bar A-A15
4.32	41.81	750,000	3	Bar A-A15
12.87	35.06	555,000	3	Bar A-A15
4.32	40.21	526,000	3	Bar A-A15
4.31	42.69	450,000	3	Bar A-A15
12.85	34.01	435,000	3	Bar A-A15
4.31	42.69	431,000	3	Bar A-A15

f_min	Sr	N	Reference No.	Notes/Specimen No.
4.32	40.22	359,000	3	Bar A-A15
4.32	41.81	281,000	3	Bar A-A15
4.31	42.59	245,500	3	Bar A-A15
4.31	41.75	224,300	3	Bar A-A15
4.31	42.69	183,000	3	Bar A-A15
18.99	44.31	89,200	3	Bar A-A15
5.95	62.75	92,200	3	Bar A-A15
5.93	53.96	113,500	3	Bar A-A15
18.97	47.24	169,500	3	Bar A-A15
5.93	47.61	286,000	3	Bar A-A15
5.93	44.46	317,800	3	Bar A-A15
19.11	42.42	389,200	3	Bar A-A15
19.11	44.6	406,300	3	Bar A-A15
5.95	40.8	432,400	3	Bar A-A440
19.06	37.91	432,600	3	Bar A-A440
19.13	41.23	456,100	3	Bar A-A440
5.93	47.61	505,600	3	Bar A-A440
19.05	37.89	526,800	3	Bar A-A440
5.92	41.46	561,700	3	Bar A-A440
5.94	41.41	590,000	3	Bar A-A440
5.94	38.18	914,700	3	Bar A-A440
18.99	33.44	990,000	3	Bar A-A440
5.95	36.07	1,073,000	3	Bar A-A440
5.94	36.6	1,123,000	3	Bar A-A440
19.04	36.09	1,160,000	3	Bar A-A440
19.02	37.84	1,193,000	3	Bar A-A440
5.93	38.17	1,285,000	3	Bar A-A440
5.92	41.45	1,315,600	3	Bar A-A440
19.07	36.16	1,475,750	3	Bar A-A440
5.94	36.06	1,589,000	3	Bar A-A440
5.94	38.44	2,330,000	3	Bar A-A440
5.92	35.93	2,772,300	3	Bar A-A440
18.98	31.45	2,867,000	3	Bar A-A440
5.95	29.75	3,097,000	3	Bar A-A440
19.03	34.69	3,705,200	3	Bar A-A440
5.93	35.99	3,766,000	3	Bar A-A440
5.96	29.78	4,405,000	3	Bar A-A440
18.98	28.28	4,514,000	3	Bar A-A440
8.94	67.1	75,000	3	Bar A-A431
8.94	67.1	101,000	3	Bar A-A431

f_min	Sr	N	Reference No.	Notes/Specimen No.
27.14	58.48	135,000	3	Bar A-A431
26.94	58.04	137,100	3	Bar A-A431
27	48.95	152,000	3	Bar A-A431
8.99	60.72	201,100	3	Bar A-A431
27	48.95	215,000	3	Bar A-A431
26.95	49.09	216,000	3	Bar A-A431
8.94	54.7	225,100	3	Bar A-A431
9	55.03	253,000	3	Bar A-A431
26.9	49.44	301,000	3	Bar A-A431
8.94	45.61	307,600	3	Bar A-A431
26.76	49.18	474,100	3	Bar A-A431
9	45.91	512,000	3	Bar A-A431
27.12	37.18	642,300	3	Bar A-A431
27.15	40.92	702,500	3	Bar A-A431
8.36	40.85	714,200	3	Bar A-A431
26.94	40.61	1,006,000	3	Bar A-A431
26.96	37.06	1,044,000	3	Bar A-A431
8.99	40.53	1,048,000	3	Bar A-A431
26.93	40.59	1,075,000	3	Bar A-A431
26.97	37.07	1,456,000	3	Bar A-A431
26.91	36.99	1,560,000	3	Bar A-A431
8.93	40.26	2,250,000	3	Bar A-A431
8.93	40.23	4,160,000	3	Bar A-A431
27	31.56	6,654,000	3	Bar A-A431
4.85	45.68	127,500	3	Bar B-A15
14.42	38.12	259,000	3	Bar B-A15
4.83	43.09	290,000	3	Bar B-A15
4.85	36	352,000	3	Bar B-A15
14.44	35.81	372,000	3	Bar B-A15
4.83	40.69	411,000	3	Bar B-A15
14.5	33.57	477,200	3	Bar B-A15
4.84	36	504,500	3	Bar B-A15
4.84	43.4	538,200	3	Bar B-A15
14.42	33.38	568,000	3	Bar B-A15
14.46	32.3	646,000	3	Bar B-A15
4.84	40.77	661,300	3	Bar B-A15
4.85	36.13	665,000	3	Bar B-A15
4.85	34.73	887,000	3	Bar B-A15
14.44	32.25	890,400	3	Bar B-A15
14.5	31.19	1,157,300	3	Bar B-A15

f_min	Sr	N	Reference No.	Notes/Specimen No.
14.47	29.93	1,478,000	3	Bar B-A15
14.43	31.11	1,664,200	3	Bar B-A15
4.84	34.67	1,900,000	3	Bar B-A15
4.83	33.6	3,012,800	3	Bar B-A15
14.44	29.87	4,819,500	3	Bar B-A15
14.46	28.71	5,350,000	3	Bar B-A15
8.11	38.38	91,500	3	Bar B-A431
8.13	62.66	102,000	3	Bar B-A431
8.13	57.69	110,000	3	Bar B-A431
24.33	52.23	120,200	3	Bar B-A431
8.13	52.55	174,000	3	Bar B-A431
24.39	48.37	188,000	3	Bar B-A431
24.41	44.45	255,300	3	Bar B-A431
8.13	48.37	266,000	3	Bar B-A431
24.26	40.22	313,000	3	Bar B-A431
8.13	44.39	428,000	3	Bar B-A431
24.26	36.08	541,000	3	Bar B-A431
24.38	36.28	604,200	3	Bar B-A431
8.12	40.42	651,000	3	Bar B-A431
24.41	32.14	979,000	3	Bar B-A431
8.13	36.49	1,630,000	3	Bar B-A431
8.11	36.4	1,697,000	3	Bar B-A431
24.2	31.87	3,150,000	3	Bar B-A431
24.39	30.33	4,270,000	3	Bar B-A431
9.32	51.35	134,200	3	Bar C-A431
28.04	46.53	158,000	3	Bar C-A431
9.35	46.73	225,000	3	Bar C-A431
9.31	41.78	257,000	3	Bar C-A431
31.89	38.04	311,000	3	Bar C-A431
9.32	41.81	415,500	3	Bar C-A431
9.32	37.26	428,000	3	Bar C-A431
9.31	41.78	430,000	3	Bar C-A431
9.34	37.36	430,000	3	Bar C-A431
9.32	37.26	431,000	3	Bar C-A431
28.05	35.61	462,400	3	Bar C-A431
28.02	35.57	477,700	3	Bar C-A431
31.9	31.5	499,300	3	Bar C-A431
9.28	35.16	503,300	3	Bar C-A431
27.94	30.32	648,400	3	Bar C-A431
27.85	27.86	1,056,000	3	Bar C-A431

f_min	Sr	N	Reference No.	Notes/Specimen No.
9.28	33.15	1,072,000	3	Bar C-A431
9.35	31.81	1,250,000	3	Bar C-A431
28.05	26.06	2,037,000	3	Bar C-A431
9.34	29.82	2,631,000	3	Bar C-A431
5	39	216,400	3	Bar D-A15
5	39	288,000	3	Bar D-A15
5	39	315,600	3	Bar D-A15
5	34	356,800	3	Bar D-A15
15	34	365,200	3	Bar D-A15
15	34	406,600	3	Bar D-A15
5	34	435,000	3	Bar D-A15
15	34	441,000	3	Bar D-A15
5	34	506,100	3	Bar D-A15
5	34	510,000	3	Bar D-A15
5	34	515,300	3	Bar D-A15
5	29	626,600	3	Bar D-A15
15	34	645,300	3	Bar D-A15
15	29	673,000	3	Bar D-A15
15	29	746,000	3	Bar D-A15
5	29	864,500	3	Bar D-A15
15	29	888,400	3	Bar D-A15
5	29	920,200	3	Bar D-A15
15	29	971,000	3	Bar D-A15
15	29	1,030,000	3	Bar D-A15
5	34	1,120,000	3	Bar D-A15
15	29	1,232,000	3	Bar D-A15
15	26	2,214,500	3	Bar D-A15
15	24	3,187,500	3	Bar D-A15
15	25	3,496,500	3	Bar D-A15
15	24	3,702,400	3	Bar D-A15
15	24	8,164,000	3	Bar D-A15
4.6	39.7	88,900	4	44CH
4.6	39.7	129,200	4	44CV
4.7	35.5	219,800	4	40CH
4.7	35.5	334,200	4	40CV
4.7	33.5	364,000	4	38CV
4.7	31.6	507,000	4	36CH
4.7	29.5	517,000	4	34CH
4.7	29.5	575,000	4	34CH
4.7	31.5	627,300	4	36CV

f_min	Sr	N	Reference No.	Notes/Specimen No.
4.7	29.5	903,000	4	34CV
4.7	27.5	1,434,000	4	32CH
4.7	27.5	1,941,900	4	32CV
4.7	25.5	2,819,800	4	30CH
4.7	25.5	2,984,600	4	30CV
4.8	23.4	5,237,000	4	28CV
4.7	24.5	5,731,000	4	29CV
4.8	23.4	6,266,500	4	28CH
23.7	51.1	160,000	5	F75-5
22.1	49.4	248,000	5	F75-3
17.1	37.9	350,000	5	F50-7
19.3	47.3	401,000	5	F75-1
15.2	41.2	429,000	5	F60-1
21.3	40.6	604,000	5	F75-4
12.5	34.1	610,000	5	F50-1
13.6	37.8	624,000	5	F50-5
12.3	39.7	672,000	5	F60-3
15	32.4	787,000	5	F40-4
14	33.5	893,000	5	F50-3
13.5	31.9	1,063,000	5	F40-3
14.1	30.7	1,316,000	5	F50-6
16.4	28.6	1,348,000	5	F40-1
12.4	29.6	1,488,000	5	F40-2
21.5	40	1,781,000	5	F75-2
16.1	32.1	1,877,000	5	F60-2
16.4	31.9	3,004,000	5	F60-4
13.9	26.1	3,272,000	5	F50-4
12.3	27.7	3,623,000	5	F50-2

Normal probability plots for fatigue resistance data

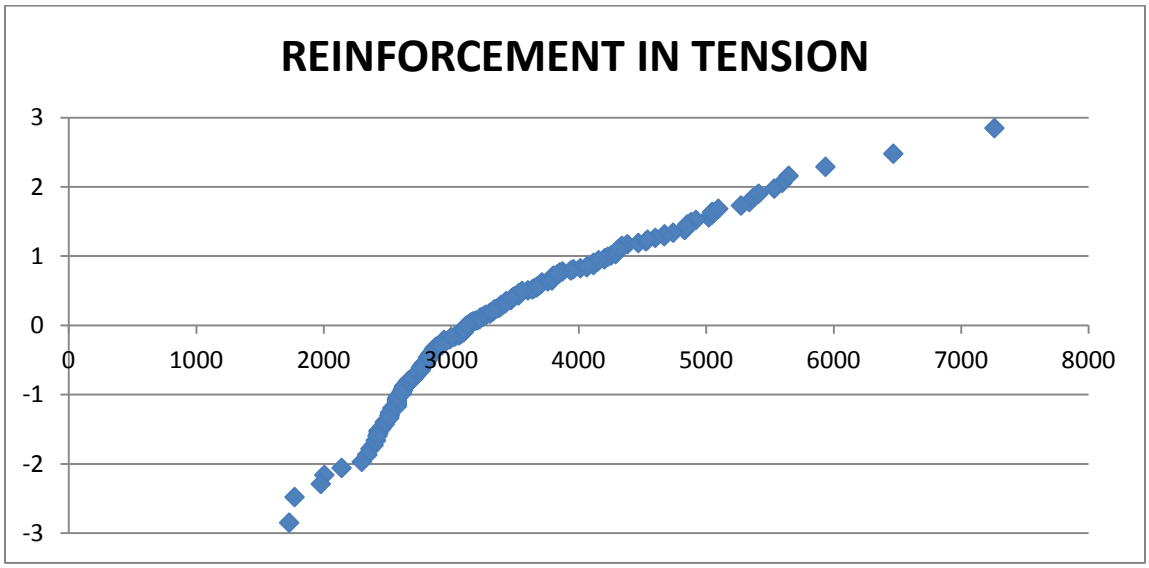

Figure G-1 Normal probability plot of fatigue resistance data for steel reinforcement in tension

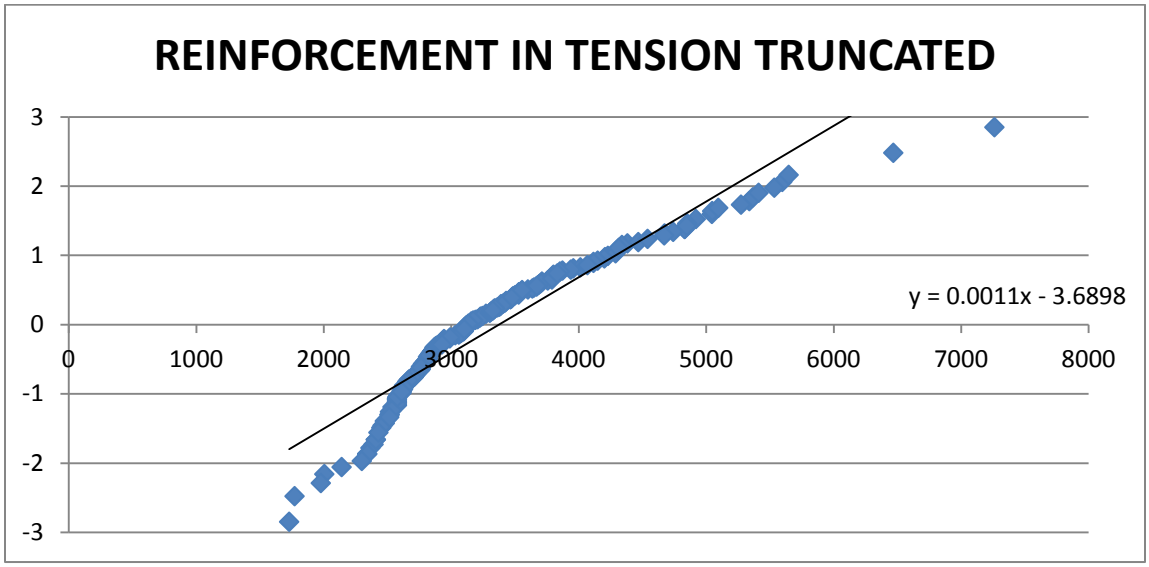

Figure G-2 Normal probability plot of truncated fatigue resistance data with best fit line for steel reinforcement in tension

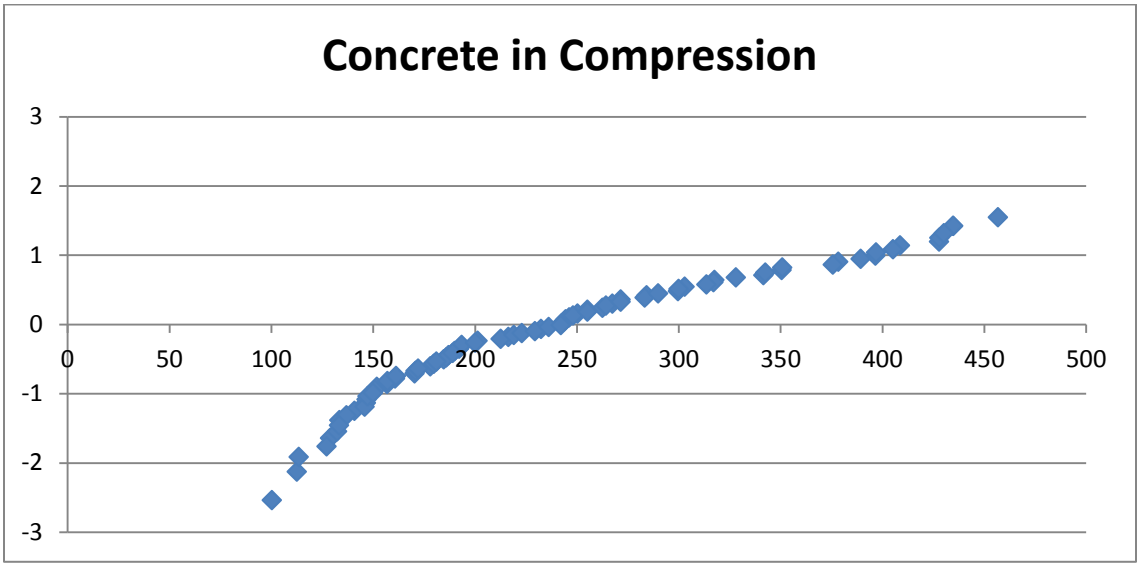

Figure G-3 Normal probability plot of fatigue resistance data for concrete in compression

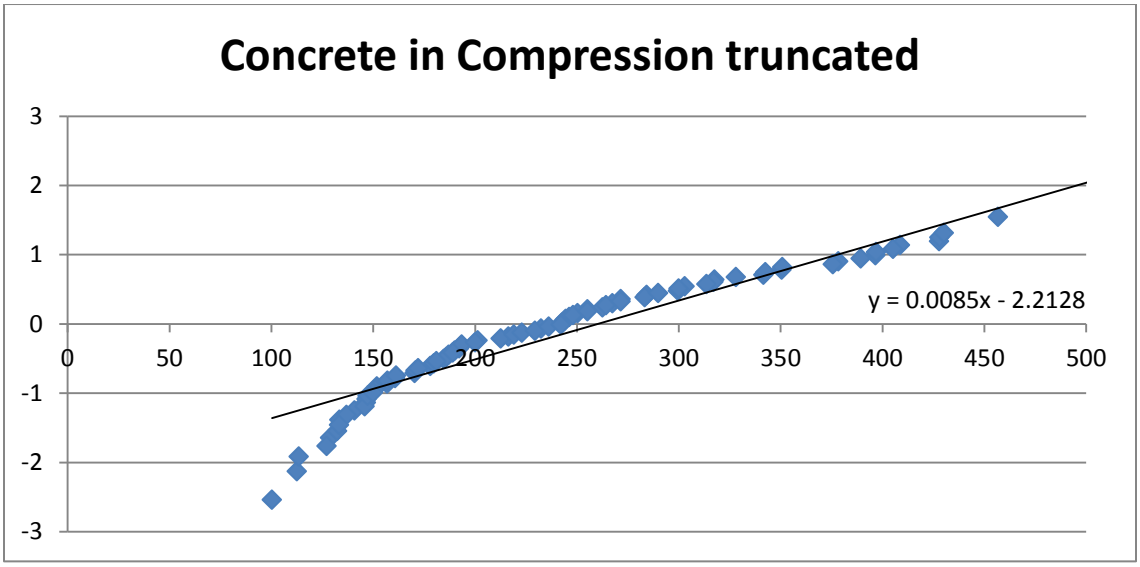

Figure G-4 Normal probability plot of truncated fatigue resistance data with best fit line for concrete in compression

References

Fisher, J. W., and I. M. Viest. 1961. "Fatigue Tests of Bridge Materials of the AASHTO Road Test." *Highway Research Board,* (Special Report No. 66), pp. 132-147.

Hanson, J. M., K. T. Burton, and E. Hognestad. 1968. “Fatigue Tests of Reinforcing Bars - Effect of Deformation Pattern.” *Journal PCA Research and Development Laboratories,* Vol. 10, No. 3, pp. 2-13.

Lash, S. 1969. "Can High-Strength Reinforcement be Used for Highway Bridges?" *First International Symposium on Concrete Bridge Design, ACI,* (SP-23), pp. 283-299.

Ople, F. S., and C. L. Hulsbos. 1966. "Probable Fatigue Life of Plain Concrete with Stress Gradient." *ACI Journal Proceedings,* Vol. 63, No. 1, pp. 59-82.

Pfister, J. F., and E. Hognestad. 1964. "High Strength Bars as Concrete Reinforcement, Part 6, Fatigue Tests." *Journal PCA Research and Development Laboratories,* Vol. 6, No. 1, pp. 65-84.